

NUTRITIONAL STRATEGIES BASED ON THE COMBINED SUPPLEMENTATION OF BIOACTIVE COMPOUNDS TO AMELIORATE OBESITY AND METABOLIC ALTERATIONS OCCURRING AT KEY STAGES OF FEMALE REPRODUCTIVE AGING

Julio Carlos Baudin Luque

ADVERTIMENT. L'accés als continguts d'aquesta tesi doctoral i la seva utilització ha de respectar els drets de la persona autora. Pot ser utilitzada per a consulta o estudi personal, així com en activitats o materials d'investigació i docència en els termes establerts a l'art. 32 del Text Refós de la Llei de Propietat Intel·lectual (RDL 1/1996). Per altres utilitzacions es requereix l'autorització prèvia i expressa de la persona autora. En qualsevol cas, en la utilització dels seus continguts caldrà indicar de forma clara el nom i cognoms de la persona autora i el títol de la tesi doctoral. No s'autoritza la seva reproducció o altres formes d'explotació efectuades amb finalitats de lucre ni la seva comunicació pública des d'un lloc aliè al servei TDX. Tampoc s'autoritza la presentació del seu contingut en una finestra o marc aliè a TDX (framing). Aquesta reserva de drets afecta tant als continguts de la tesi com als seus resums i índexs.

ADVERTENCIA. El acceso a los contenidos de esta tesis doctoral y su utilización debe respetar los derechos de la persona autora. Puede ser utilizada para consulta o estudio personal, así como en actividades o materiales de investigación y docencia en los términos establecidos en el art. 32 del Texto Refundido de la Ley de Propiedad Intelectual (RDL 1/1996). Para otros usos se requiere la autorización previa y expresa de la persona autora. En cualquier caso, en la utilización de sus contenidos se deberá indicar de forma clara el nombre y apellidos de la persona autora y el título de la tesis doctoral. No se autoriza su reproducción u otras formas de explotación efectuadas con fines lucrativos ni su comunicación pública desde un sitio ajeno al servicio TDR. Tampoco se autoriza la presentación de su contenido en una ventana o marco ajeno a TDR (framing). Esta reserva de derechos afecta tanto al contenido de la tesis como a sus resúmenes e índices.

WARNING. Access to the contents of this doctoral thesis and its use must respect the rights of the author. It can be used for reference or private study, as well as research and learning activities or materials in the terms established by the 32nd article of the Spanish Consolidated Copyright Act (RDL 1/1996). Express and previous authorization of the author is required for any other uses. In any case, when using its content, full name of the author and title of the thesis must be clearly indicated. Reproduction or other forms of for profit use or public communication from outside TDX service is not allowed. Presentation of its content in a window or frame external to TDX (framing) is not authorized either. These rights affect both the content of the thesis and its abstracts and indexes.

UNIVERSITAT ROVIRA i VIRGILI

Nutritional strategies based on the combined supplementation of bioactive compounds to ameliorate obesity and metabolic alterations occurring at key stages of female reproductive aging



Julio Carlos Baudin Luque

DOCTORAL THESIS
2024

UNIVERSITAT ROVIRA I VIRGILI
NUTRITIONAL STRATEGIES BASED ON THE COMBINED SUPPLEMENTATION OF BIOACTIVE COMPOUNDS TO AMELIORATE OBESITY AND METABOLIC ALTERATIONS OCCURRING AT KEY STAGES OF FEMALE REPRODUCTIVE AGING
Julio Carlos Baudin Luque

UNIVERSITAT ROVIRA I VIRGILI
NUTRITIONAL STRATEGIES BASED ON THE COMBINED SUPPLEMENTATION OF BIOACTIVE COMPOUNDS TO AMELIORATE OBESITY AND METABOLIC ALTERATIONS OCCURRING AT KEY STAGES OF FEMALE REPRODUCTIVE AGING
Julio Carlos Baudin Luque

Julio Carlos Baudin Luque

Nutritional strategies based on the combined supplementation of bioactive compounds to ameliorate obesity and metabolic alterations occurring at key stages of female reproductive aging

Doctoral Thesis

Directed by

Dr. Antoni Caimari Palou and Prof. Lluís Arola Ferrer



UNIVERSITAT ROVIRA i VIRGILI



URV, Department of Biochemistry and Biotechnology

Eurecat, Nutrition and Health Unit

Reus 2024

UNIVERSITAT ROVIRA I VIRGILI
NUTRITIONAL STRATEGIES BASED ON THE COMBINED SUPPLEMENTATION OF BIOACTIVE COMPOUNDS TO AMELIORATE OBESITY AND METABOLIC ALTERATIONS OCCURRING AT KEY STAGES OF FEMALE REPRODUCTIVE AGING
Julio Carlos Baudin Luque

UNIVERSITAT ROVIRA i VIRGILI

Departament de Bioquímica i Biotecnologia
Marcel·lí Domingo St, 1
Campus de Sescelades
43007, Tarragona

FEM CONSTAR que aquest treball, titulat "**Nutritional strategies based on the combined supplementation of bioactive compounds to ameliorate obesity and metabolic alterations occurring at key stages of female reproductive aging**", que presenta **Julio Carlos Baudín Luque** per a l'obtenció del títol de Doctor, ha estat realitzat sota la nostra direcció al Departament de Bioquímica i Biotecnologia d'aquesta universitat, i que compleix els requeriments per optar a la Menció Internacional.

HACEMOS CONSTAR que el presente trabajo, titulado "**Nutritional strategies based on the combined supplementation of bioactive compounds to ameliorate obesity and metabolic alterations occurring at key stages of female reproductive aging**", que presenta **Julio Carlos Baudín Luque** para la obtención del título de Doctor, ha sido realizado bajo nuestra dirección en el Departamento de Bioquímica y Biotecnología de esta universidad, y que cumple los requerimientos para optar a la Mención Internacional.

WE STATE that the present study, entitled "**Nutritional strategies based on the combined supplementation of bioactive compounds to ameliorate obesity and metabolic alterations occurring at key stages of female reproductive aging**", presented by **Julio Carlos Baudín Luque** for the award of the degree of Doctor, has been carried out under our supervision at the Department of Biochemistry and Biotechnology of this university, and fulfil the demanded requirements to get the European Mention.

Reus, 28 de Juny de 2024 / Reus, 28 de Junio de 2024 / Reus, June 28, 2024

Els directors de la tesi doctoral
Los directores de la tesis doctoral
Doctoral Thesis Supervisors

Dr. Lluís Arola Ferrer

Dr. Antoni Caimari Palou

UNIVERSITAT ROVIRA I VIRGILI
NUTRITIONAL STRATEGIES BASED ON THE COMBINED SUPPLEMENTATION OF BIOACTIVE COMPOUNDS TO AMELIORATE OBESITY AND METABOLIC ALTERATIONS OCCURRING AT KEY STAGES OF FEMALE REPRODUCTIVE AGING
Julio Carlos Baudin Luque

AGRAÏMENTS

Per on començar els agraïments, quan encara no has acabat la tesi? Doncs donant simplement les GRÀCIES i mil GRÀCIES!!! Per aquest llarg camí d'una aventura trepidant que ha suposat fer la tesis doctoral. Però això no us penseu que ho dic pel coneixement i aprenentatge que hi ha com a científic al llarg d'aquests anys, que també, sinó pel gran esforç personal i com a persona que sap (ara) el que comporta.

Ja que l'escriptura d'una tesi no sempre reflecteix la força de voluntat que hi ha darrera de cada lletra escrita a la majoria dels doctorands, per això els primers agraïments són per ells, pel suport incondicional que ens hem donat uns amb als altres, ja sigui per ajuda experimental o, encara més important, la mental! En aquest sentit, a la primera persona que hauria de donar les gràcies ¡*Cómo no*! havia de ser una dona i, coses del destí, s'havia de dir, Júlia!!! Podria dir-te mil coses però simplement diré gràcies per ser com ets, dins i fora de la feina com a persona i amiga. Gràcies al gran equip d'investigadors i, en especial, als tècnics que van estar amb mi en el dia a dia. Tampoc em vull oblidar de la resta de companys i companyes que han passat per Eurecat durant el meu camí fins arribar a aquí i han canviat de destí abans de temps, perquè al final TOTS, en certa manera, han aportat el seu granet de sorra en aquesta tesi, i a mi com investigador però sobretot com a creixement personal!

També vull dedicar unes paraules a les persones més importants en la meva vida, als meus pares, responsables de portar-me a aquest món. La meva vida no tindria sentit sense ells, això no hagués estat possible i el seu amor incondicional penso sempre transmetre'l tots els dies de la meva vida, ja que sinó no seria jo mateix. Per una altra banda, com descriure a la meva germana, per qui no presentaria la tesis el dia de demà! Que si li passes alguna

cosa, no sabria com afrontar-ho, i que no entenc com podem ser tan iguals i tan diferents al mateix temps, sobretot a l'àmbit d'oci... Que sempre estem un al costat de l'altre quan més ens necessitem encara que després poden passar mesos sense contestar-nos a un simple WhatsApp!!

Tampoc em podia deixar a l'altre adoptat a la família. Pot ser a la persona a qui més gràcies hauria de donar. Parlo del meu despistat i *pesado* preferit, d'un tal Sergio que es va deixar caure a viure amb mi a Tarragona des d'un casino de Torrelodones (història molt llarga...) i qui hauria de tenir tant dret com jo de defensar la tesis, ja que ha viscut el doctorat per doble aguantant-me aquest quatre anys cada dia fins avui. Més que un amic, és ja un segon germà! Tampoc no em puc oblidar del nostre company de vida, ¡*Larga vida al Rey Roni*!, que més que un gat és una persona, ja que a vegades es comunica millor que jo, i no es broma! A més de ser el gat més afectuós que he vist i el millor, i no ho dic perquè sigui el meu eh!

Ja que parlem d'una història llarga també hem d'incloure al germà bessó d'en Sergio, l'Àlex i el nostre canari Pablo, amb qui vam formar una família al màster, hem viscut una pandèmia junts, i van compartir el meu inici en aquesta aventura. Encara que no vivim junts ja a Tarragona, seguim i seguirem veient-nos sempre que ens sigui possible ja que el vincle que tenim es i serà únic! Qui ho diria que dos madrilenys, un canari i un tarragoní, formessin aquest vincle de per vida.

A tot Voley, a cada un de vosaltres, perquè sou la meva aleta el dia de diari, una família d'amics que et pot carregar tant l'energia com al mateix temps descarregar-te un castell i les teves energies a reserves mínimes... Gràcies per tots els moments que compartim dins i fora de la colla, el que m'aporteu com a persona i els mil castells i nous moments que ens queda per gaudir tot plegats!

Tampoc em podia deixar a la meva estimada família de Kunfu, aquells amics de tota la vida, amb els que encara que no et vegis en molt temps, sempre que ens trobem és com si fos el primer dia d'amistat.

I would like to express my appreciation to professor Adil Mardinoglu and all the members of SciLifeLab in Stockholm, Sweden, for the warm welcome and for the opportunity to do my internship with his group, SysMedicine. Special thanks to Hong Yang; thank you so much for accepting me and supporting me every day in my journey in Viking lands. To my Italian and Turkish family there, who have made me feel so well-accompanied and have forged friendships for life. I enjoyed every single moment with all of you and I am so impatient to see you again. I miss you so much.

Per acabar, però no per això menys important. Donar-les gràcies als meus directors de tesis, que no podria tenir-ne millors i sense els seus grans coneixements, seguiment, pautes i forma de treballar, no hagués arribat avui aquí!!! Primer donar les gràcies al gran professor emèrit de la URV, en Lluís Arola, brindo per la teva saviesa! Capaç de canviar-te tot el teu croquis mental en un segon i al mateix temps plasmar-te la visió de l'esquema més adient amb dues paraules, per l'esforç que ha fet conjuntament amb mi i el meu principal director de tesis, en Toni, mil gràcies.

En quant a en Toni, falten paraules i sobren tesis per donar-te les gràcies, sense ell, res d'aquest projecte que vaig començar tindria sentit. Em quedo claríssimament amb la seva forma de ser, per estar a l'altre costat als moments bons i també al dolents, ja que més que un director de tesi o director de l'àrea de Biotecnologia d'Eurecat, diria que és més un amic amb el que podré comptar amb ell el dia de demà.

Gràcies i salut a tots els que han format part d'aquesta tesis.

I aquí un proverbi d'un intent d'escriptor que en el seu dia va deixar d'escriure poesia per escriure aquest gran treball.

"Reverencia a la referencia"

Dicen que la paciencia, es la madre de la ciencia.

Pues ¡Qué gran evidencia!

Ya que ¡Tu excelencia, será la consecuencia de tu persistencia!

Con la experiencia, te darán la avenencia, de tu gran inteligencia.

Mostrando esa esencia, a la inexperta y joven audiencia, que disfrutará de tu docencia.

UNIVERSITAT ROVIRA I VIRGILI
NUTRITIONAL STRATEGIES BASED ON THE COMBINED SUPPLEMENTATION OF BIOACTIVE COMPOUNDS TO AMELIORATE OBESITY AND METABOLIC ALTERATIONS OCCURRING AT KEY STAGES OF FEMALE REPRODUCTIVE AGING
Julio Carlos Baudin Luque

TABLE OF CONTENT

SUMMARY 1

RESUM 2

ABBREVIATIONS 4

I. INTRODUCTION 7

1. Menopausal Transition and Postmenopause 8

1.1. Physiology 8

1.1.1. Menstrual cycle dynamics: Hypothalamus-Pituitary-Gonadal (HPG) axis, folliculogenesis and ovulation 9

1.1.2. Stages of Reproductive Aging Workshop (STRAW): underlying endocrine changes during menopausal transition and menopause 12

1.1.2.1. Menopausal transition: perimenopause 15

1.1.2.2. Postmenopause 19

1.2. Symptoms and health risks of menopause 20

1.2.1. Vasomotor Symptoms (VMS) 23

1.2.2. Sleep disorders 24

1.2.3. Mood changes and related disorders 25

1.2.4. Cognitive changes and related disorders 26

1.2.5. Body weight gain and obesity 27

1.2.6. Cardiovascular diseases (CVDs) 31

1.2.7. Osteoporosis 33

2. Hormone Replacement Therapy (HRT): benefits & risks 36

3. Nutritional strategies to ameliorate symptoms and metabolic disturbances related to menopause. 40

3.1. Polyphenols and phytosterols 43

3.2. Amino acid-related compounds 50

4. Biomarkers: essential indicators of the health status and their role in nutrition studies 56

4.1. Peripheral Blood Mononuclear Cells (PBMCs) as a source of omics-based biomarkers 60

II. HYPOTHESIS AND OBJECTIVES 66

III. RESULTS 72

MANUSCRIPT 1 73

MANUSCRIPT 2 124

MANUSCRIPT 3 170

MANUSCRIPT 4 218

IV. GENERAL DISCUSSION 279

V. CONCLUSIONS 299

VI. REFERENCES 302

VII. LIST OF PUBLICATIONS 336

VIII. ANNEX 338

UNIVERSITAT ROVIRA I VIRGILI
NUTRITIONAL STRATEGIES BASED ON THE COMBINED SUPPLEMENTATION OF BIOACTIVE COMPOUNDS TO AMELIORATE OBESITY AND METABOLIC ALTERATIONS OCCURRING AT KEY STAGES OF FEMALE REPRODUCTIVE AGING
Julio Carlos Baudin Luque

SUMMARY

Menopausal transition, known as perimenopause, and later, the postmenopausal state are natural biological phases in a woman's life associated with reproductive aging. These processes are characterized by senescence in the ovarian function accompanied by a decline in oestrogen production, which already occurs in perimenopause with the appearance of irregular menstrual cycles and is exacerbated during the postmenopausal state. This reproductive aging process is often accompanied by various vasomotor symptoms, such as sleep disturbances, night sweats, and hot flashes, and can be associated with an increased risk of osteoporosis and with the appearance of obesity and other cardiovascular risk factors. In this PhD thesis, we hypothesized that two multi-ingredients acting against complementary targets, one containing the natural bioactive compounds curcumin, hesperidin, and phytosterols, and the other composed of the amino acid-related compounds histidine, serine, cysteine, and carnosine can exert beneficial effects against obesity and related cardiometabolic disturbances associated with menopause. We firstly characterized the menopausal transition using ovarian-intact middle-aged rats and analyzed circulating signatures across perimenopause, identifying potential lipidomic-based biomarkers in serum during the menopausal transition. Secondly, we used ovariectomized rats, a postmenopausal model with oestrogen deficiency, and we reported, using a transcriptomics approach, that peripheral blood mononuclear cells reflected the molecular changes associated with oestrogen deficiency in the postmenopausal stage concerning alterations in immune function, stress response, bone metabolism, cholesterol metabolism, and glucose homeostasis. Finally, we revealed that the oral supplementation with the two above commented multi-ingredients ameliorated obesity and related metabolic alterations in ovariectomized rats, being these effects of a similar magnitude to those produced by the administration of oestradiol, a pharmacological treatment that simulates hormone replacement therapy that is sometimes prescribed to women during the post-menopausal state. Our findings can pave the way for using these multi-ingredient-based formulations as alternative therapies to manage menopausal-related disturbances.

RESUM

La transició menopàusica, coneguda com a perimenopausa, i, posteriorment, la postmenopausa són fases biològiques naturals en la vida de la dona associades a l'envelliment reproductiu. Aquests processos es caracteritzen per una senescència en la funció ovàrica acompanyada d'una disminució de la producció d'estrògens, que ja es produeixen en la perimenopausa amb l'aparició de cicles menstruals irregulars i s'accentuen a la postmenopausa. Aquest procés d'envelliment reproductiu sovint s'acompanya de símptomes vasomotors (alteracions del son, suors nocturnes i sufocacions), i s'associa amb un major risc d'osteoporosi, obesitat i factors de risc cardiovascular. En aquesta tesi vam hipotetitzar que dos multi-ingredients que actuen front a dianes complementàries, un que inclou curcumina, hesperidina i fitosterols, i l'altre els aminoàcids histidina, serina, cisteïna i carnosina, podien exercir efectes beneficiosos front a l'obesitat i les alteracions cardiometabòliques que poden aparèixer durant la menopausa. Inicialment, vam caracteritzar, en rates, la transició menopàusica utilitzant un model d'envelliment reproductiu natural i vam identificar en sèrum, utilitzant lipidòmica, biomarcadors potencials de transició menopàusica. En segon lloc, vam utilitzar rates ovariectomitzades, un model postmenopàusic amb deficiència d'estrògens, i vam demostrar, utilitzant transcriptòmica, que les cèl·lules mononuclears de sang perifèrica reflectien els canvis moleculars associats amb la deficiència d'estrògens pel que fa a alteracions en la funció immune, la resposta a l'estrès, el metabolisme ossi, el metabolisme del colesterol i l'homeòstasi de la glucosa. Finalment, vam revelar que la suplementació oral amb els dos multi-ingredients va atenuar l'obesitat i les alteracions metabòliques relacionades en rates ovariectomitzades, sent aquests efectes d'una magnitud similar als produïts per l'estradiol, un tractament farmacològic que simula la teràpia hormonal substitutiva que de vegades es prescriu a les dones durant la postmenopausa. Els nostres resultats poden establir les bases per utilitzar aquestes formulacions basades en multi-ingredients com a teràpies alternatives per atenuar les alteracions relacionades amb la menopausa.

UNIVERSITAT ROVIRA I VIRGILI
NUTRITIONAL STRATEGIES BASED ON THE COMBINED SUPPLEMENTATION OF BIOACTIVE COMPOUNDS TO AMELIORATE OBESITY AND METABOLIC ALTERATIONS OCCURRING AT KEY STAGES OF FEMALE REPRODUCTIVE AGING
Julio Carlos Baudin Luque

ABBREVIATIONS

µCT/MicroCT Three-dimensional microcomputed tomography
17β-E2 17β-oestradiol
8-OHdG 8-hydroxy-2'-deoxyguanosine
AAs Amino acids
AFC Antral follicle count
ALR Adiponectin-to-leptin ratio
ALSWH Australian longitudinal study on women's health
AMH Anti-müllerian hormone
AMPK AMP-activated protein kinase
ATMs Adipose tissue macrophages
BMC Bone mineral content
BMD Bone mineral density
BMI Body mass index
Cd36 Fatty acid translocase, homologue of CD36
CMA Combined metabolic activators
CRP C-reactive protein
CTX-1 Carboxy-terminal telopeptide of type I collagen
CVDs Cardiovascular diseases
DEXA Dual-energy X-ray absorptiometry
DHEA Dehydroepiandrosterone
ECM Extracellular matrix
EE Energy expenditure
ER Oestrogen receptor
Fasn Fatty acid synthase
FMP Final menstrual period
FSH Follicle-stimulating hormone
GABA Gamma-aminobutyric acid
GC-MS Gas chromatography-mass spectrometry
GLUT4 Glucose transporter 4
GnRH Gonadotropin-releasing hormone
GPA-1 Glycerol-3-phosphate acyltransferase-1
Gpx-1 Glutathione peroxidase-1
GSH Glutathione
GSSG Oxidized glutathione
HAL Histidine ammonia lyase
HDC Histidine decarboxylase
HDL-c High-density lipoprotein cholesterol
HOMA-IR Homeostasis model assessment-estimated insulin resistance
HPG Hypothalamus-pituitary-gonadal
HRT Hormone replacement therapy
IL-12 Interleukin-12
IL-18 Interleukin-18

IL-6 Interleukin-6
Insr Insulin receptor
IR Insulin resistance
IWAT Inguinal white adipose tissue
LAR Leptin-to-adiponectin ratio
LC-MS Liquid chromatography-mass spectrometry
LDL-c Low-density lipoprotein cholesterol
LH Luteinizing hormone
LPL Lipoprotein lipase
M-CSF Macrophage colony-stimulating factor
M2SH Micronized 2-S-hesperidin
MCP-1 Monocyte chemoattractant protein-1
MD Mediterranean diet
MetS Metabolic syndrome
MI Multi-ingredient
MRI Magnetic resonance imaging
MWAT Mesenteric white adipose tissue
NAFLD Non-alcoholic fatty liver disease
NEFAs Nonesterified fatty acids
NGS Next-generation sequencing
NIH National Institutes of Health
NMR Nuclear Magnetic Resonance
OC Osteocalcin
OGTT Oral glucose tolerance test
OPG Osteoprotegerin
OVX Ovariectomized rats
OxPhos Oxidative phosphorylation
PINP Procollagen I amino-terminal propeptide
PREDIMED PREvención con DIeta MEDiterránea
R-QUICKI Revised quantitative insulin sensitivity check index
RANK Receptor activator of nuclear factor kappa-B
RANKL Receptor activator of nuclear factor kappa-B ligand
RWAT Retroperitoneal white adipose tissue
STRAW Stages of reproductive aging workshop
SWAN Study of women's health across the nation
T2DM Type 2 diabetes mellitus
TC Total cholesterol
TG Triglycerides
TGF-β Transforming growth factor-beta
TNF-α Tumor necrosis factor-alpha
VMS Vasomotor symptoms
VLDL-c Very-low-density lipoprotein cholesterol.
VTE Venous thromboembolism
WAT White adipose tissue
WHI Women's Health Initiative trial

UNIVERSITAT ROVIRA I VIRGILI
NUTRITIONAL STRATEGIES BASED ON THE COMBINED SUPPLEMENTATION OF BIOACTIVE COMPOUNDS TO AMELIORATE OBESITY AND METABOLIC ALTERATIONS OCCURRING AT KEY STAGES OF FEMALE REPRODUCTIVE AGING
Julio Carlos Baudin Luque

I. INTRODUCTION

1. Menopausal Transition and Postmenopause

1.1. Physiology

Beyond natural chronological senescence, the physiological changes of female reproductive aging begin to manifest during the menopausal transition, known as perimenopause (1–4). This phase is characterized by the progressive depletion of ovarian and oocyte function through normal atresia and ovulation, which in turn leads to a decline in oestrogen and progesterone production (4–7). These changes ultimately mark the end of the woman's reproductive years, culminating in the postmenopausal state (1–8). This phase typically occurs between 45 and 55 years of age, occurring at the onset of perimenopause, on average, at the age of 47.5 (9), and can trigger various changes in the body, affecting multiple systems and leading to distinct physiological symptoms and health risks (7–10).

During the reproductive years, the menstrual cycle is regulated by a complex interplay of hormones that govern the processes of folliculogenesis and ovulation. As women enter the menopausal transition, these processes become irregular and finally cease, as the ovaries exhaust their follicular reserves, leading to the end of menstrual cycles and fertility (6,7).

Interestingly, the changes that emerge during menopausal transition, emphasize the concept of gender dimorphism (11,12). This is based on observed differences in metabolic responses between women and men, particularly in fat distribution and accumulation, as well as the risk of developing certain diseases (12). During the menopausal transition, gender dimorphism becomes apparent in metabolic responses, with premenopausal women generally experiencing a lower prevalence of cardiovascular diseases (CVDs), metabolic syndrome (MetS), and osteoporosis compared to men of the same age. This

pattern can change during perimenopause and menopause due to the gradual decline in oestrogen levels, which can be translated to higher rates of these alterations in women (13–17).

1.1.1. Menstrual cycle dynamics: Hypothalamus-Pituitary-Gonadal (HPG) axis, folliculogenesis and ovulation

In a normal ovulatory menstrual cycle, which typically lasts between 25 to 35 days, with an average duration of 28 days in the absence of pregnancy, there is a complex intricate feedback system among the hypothalamus, pituitary gland, and ovaries, known as the Hypothalamus-Pituitary-Gonadal (HPG) axis. This process results in the neuro-endocrine secretion of various steroidal and non-steroidal hormones, including cyclical changes in four main reproductive hormones: luteinizing hormone (LH), follicle-stimulating hormone (FSH), oestrogen, and progesterone, forming a critical feedback communication system essential for maintaining the menstrual cycle **(Figure 1)** (18,19).

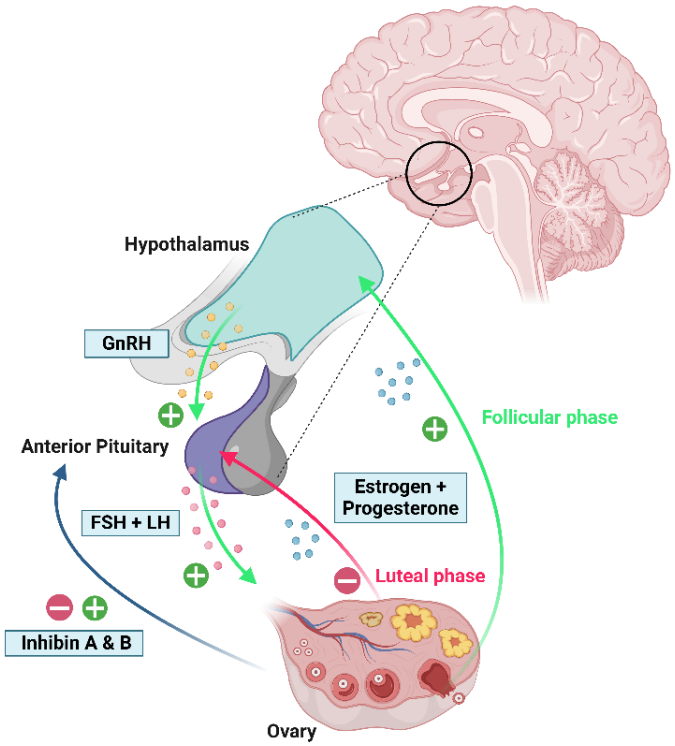


Figure 1. Diagrammatic representation of the Hypothalamus-Pituitary-Ovarian axis. GnRH: gonadotrophin-releasing hormone; LH: luteinizing hormone; FSH: follicle-stimulating hormone. Created with biorender.com.

INTRODUCTION

From puberty onward, the pulsatile release of gonadotropin-releasing hormone (GnRH) from the hypothalamus acts on the anterior pituitary gland, prompting the synthesis and secretion of the gonadotropins, FSH and LH, into the bloodstream, thus regulating ovarian function (1–3). At the beginning of the menstrual cycle, all four vital reproductive hormones (FSH, LH, oestradiol, and progesterone) are at their lowest levels. During the follicular phase, GnRH stimulates the release of FSH, which promotes the growth of antral follicles and increases the secretion of oestradiol and inhibin B. This sequence supports the development and maturation of ovarian follicles until ovulation. As levels of oestradiol and inhibin B rise, they inhibit further production of FSH and trigger a surge in LH. This surge in LH is pivotal in inducing ovulation by releasing the oocyte from the follicle (1–3). Whether fertilization does not occur, during the luteal phase, the corpus luteum forms from the ruptured follicle and becomes the primary source of progesterone, along with oestradiol and inhibin A. Approximately seven days after ovulation, the corpus luteum undergoes degeneration, causing a decline in oestrogen and progesterone levels, which initiates menstruation. This cyclic hormonal interplay ensures regular opportunities for fertilization (**Figures 1** and **2**) (1–3).

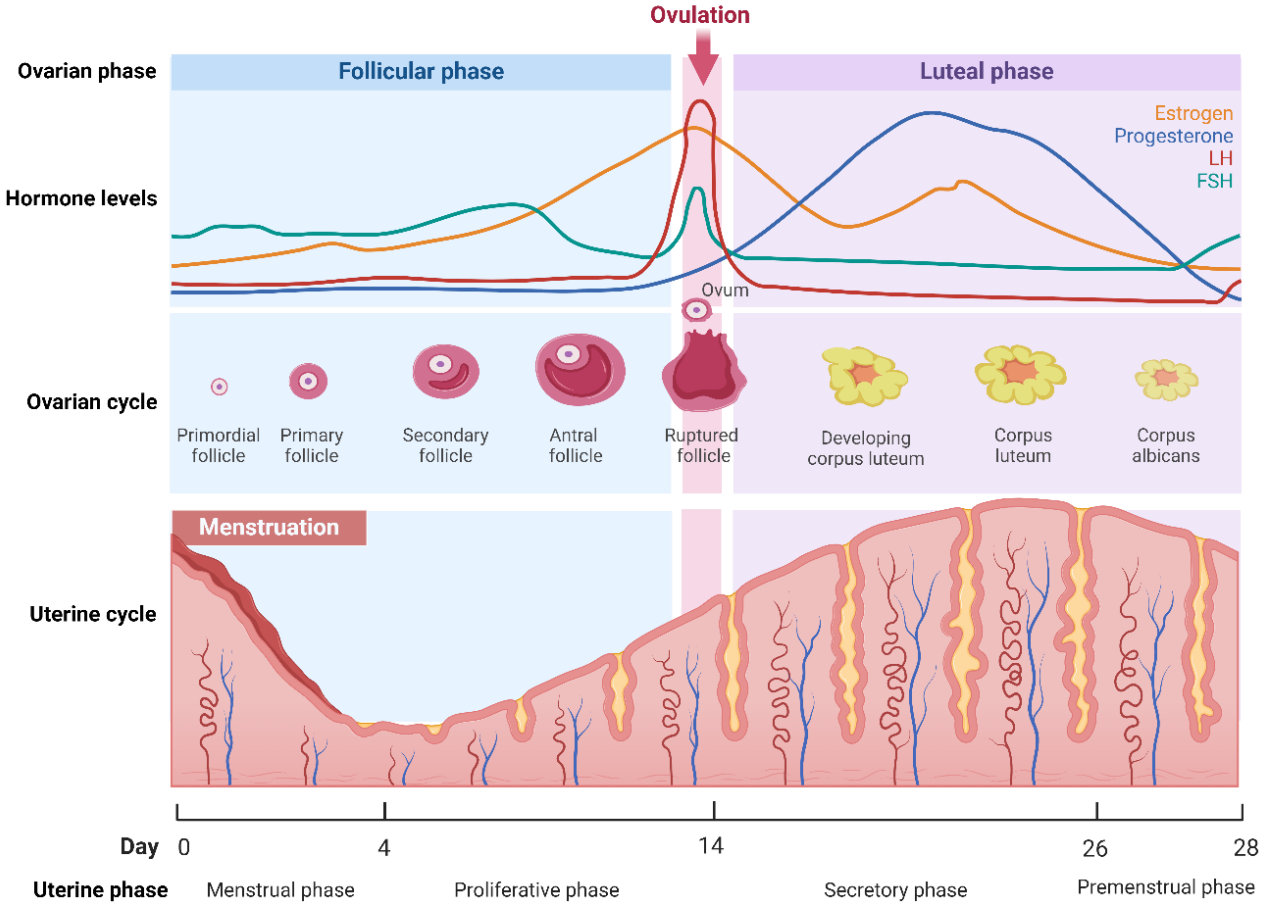


Figure 2. The human menstrual cycle has three distinct phases. The follicular phase is characterized by steadily increasing 17β-oestradiol levels. At a critical level of 17β-oestradiol, LH surges, with the trigger for ovulation occurring in the periovulatory phase. Ovulation is followed by the luteal phase, wherein progesterone levels increase, and 17β-oestradiol is present at a moderate level. Created with biorender.com.

It is well-established that women are born with a finite pool of immature ovarian follicles. Histological follicle counts and mathematical models estimate that each ovary contains around 500,000 resting follicles at birth, which decrease to approximately 200,000 per ovary by puberty. Throughout a woman's reproductive life, with the onset of the menstrual cycle and folliculogenesis, approximately 400 eggs are ovulated, while the remaining follicles undergo a continuous and natural process of cell death in the ovary known as follicular atresia (19–21). As reproductive aging progresses, this results in a nearly exhaustive depletion of follicles during the menopausal transition or perimenopause, with estimates falling below 1,000 follicles. By menopause, the number of remaining follicles is almost completely depleted, dropping below 100 (19,21–23).

This reduction in follicular reserve leads to the onset of irregular cycles in perimenopause (19,21,22,24). Anti-Müllerian hormone (AMH) and inhibin are two hormones included in the transforming growth factor-beta (TGF-β) family, produced by growing follicles and serve as markers of ovarian reserve. They play key roles in inhibiting the transition from primordial to primary follicles and in regulating FSH secretion, respectively (19,24,25). As menopause approaches and the follicular pool becomes depleted, AMH and inhibin levels decline significantly, leading to increased irregularity in the menstrual cycle and elevated FSH levels, while oestradiol and progesterone levels gradually decline over time (19,21,22,24). This diminished follicle reserve and the hormonal imbalance in the HPG axis are likely responsible for the initial changes in menstrual cycle regularity with the onset of the perimenopausal transition and exacerbated in the menopausal state (19,21,22,24). On the other hand, whether the initiation of the menopausal transition, it is stemming from reduced follicular reserves or from the dysregulation of the HPG axis in the brain, remains a topic of debate (19,21,22,24). What is evident, however, is that both the transition itself and the subsequent phase of post-reproductive life bring about physiological, behavioral, and neurological changes that can significantly impact the quality of life (26).

1.1.2. Stages of Reproductive Aging Workshop (STRAW): underlying endocrine changes during menopausal transition and menopause

Identifying the precise beginning of perimenopause using hormonal changes as diagnostic markers is extremely challenging. However, the Stages of Reproductive Aging Workshop (STRAW+10) staging system (1) categorized the menopausal transition into specific phases, helping to a better understanding and management of the changes occurring during this period.

The STRAW staging system, introduced in 2001 and updated a decade later as STRAW+10, categorizes the stages of transition to menopause primarily by analyzing changes in menstrual duration and pattern. These menstrual changes serve as the principal criteria, while known ovarian and endocrine markers of reproductive aging are considered supportive criteria. The last update included biomarkers such as FSH, AMH, Inhibin B, antral follicle count (AFC) and also vasomotor symptoms (VMS), which show considerable promise. However, the lack of standardized assays and the scarce available data obtained from non-infertility populations remain significant limitations to their incorporation into the STRAW staging system and their utility as clinical tools for staging reproductive aging (1).

STRAW+10 describes and divides the adult female life into three broad phases: reproductive, menopausal transition, and postmenopause. These three phases include a total of seven sub-stages centred on the Final Menstrual Period (FMP, Stage 0). Stages -5 to -3 include the Reproductive period; -2 to -1 the Menopausal transition; and +1 to +2 the Postmenopause (Table 1). The time including both early and late stages of menopausal transition, along with the year following the FMP, is commonly referred to as perimenopause (**Table 1)** (1).

Table 1. The Stages of Reproductive Aging Workshop + 10 staging system for reproductive aging in women. (STRAW +10)

	MENARCHE ↓						FMP (Stage 0) ↓			
Stage	**-5**	**-4**	**-3b**	**-3a**	**-2**	**-1**	**+1a**	**+1b**	**+1c**	**+2**
Terminology	**REPRODUCTIVE**				**MENOPAUSAL TRANSITION**		**POSTMENOPAUSE**			
	Early	**Peak**	**Late**		**Early**	**Late**	**Early**			**Late**
					PERIMENOPAUSE					
Duration	*variable*				*variable*	1-3 years	2 years (1+1)	3-6 years		*Remaining lifespan*
PRINCIPAL CRITERIA										
Menstrual Cycle	Variable to regular (Puberty)	Regular	Regular	Subtle changes in flow or length	*Variable Length* Persistent ≥ 7-day difference in length of consecutive cycles	≥ 2 skipped cycles and an interval of amenorrhea of ≥ 60 days	Amenorrhea for 12 months			
SUPPORTIVE CRITERIA										
FSH **AMH** **Inhibin B**			Low Low	Variable* Low Low	↑Variable Low Low	↑ > 25 IU/L** Low Low	↑ Variable* Low Low	Stabilizes Very Low Very Low		
AFC			Low	Low	Low	Low	Very Low	Very Low		
DESCRIPTIVE CHARACTERISTICS										
Symptoms						Vasomotor Symptoms *Likely*	Vasomotor symptoms *Most likely*			*Increasing* symptoms of urogenital atrophy

* Blood draw on cycle days 2-5 ↑ = elevated

**Approximate expected level based on assays using current international pituitary standard

FMP: final menstrual period; FSH: follicle-stimulating hormone; AMH: anti-müllerian hormone; AFC: antral follicle count. Adopted from Harlow *et al*. (2012).

In the late reproductive stage -3a many women often experience subtle changes in menstrual cycle length and flow, which are specifically manifested with shorter cycles (25–26 days) due to a shorter follicular phase (1,19). During the early follicular phase (cycle days 2-5), there is a slightly rise in FSH levels, which become more variable. This subtle rise in FSH has been attributed to a decrease in small antral follicle production of inhibin B and AMH, both of which fail to inhibit the anterior pituitary's FSH secretion. These decreases in inhibin B and AMH, along with low AFC, become evident with advancing reproductive age and are already apparent in stage -3b (1,19).

1.1.2.1. Menopausal transition: perimenopause

Perimenopause is the transition period from the reproductive to the nonreproductive stage of life, including the last reproductive years through the first twelve consecutive months of amenorrhea (1). It is characterized by irregular menstrual cycles (with more frequent occurrence of anovulatory or delayed ovulatory cycles) and by fluctuating hormone levels, which can lead to bothersome symptoms and increased health risk factors. These changes in hormone levels (elevated early follicular phase FSH, and decreased oestradiol, AMH and inhibin B) mark the progression through the menopausal transition, which typically lasts about 4-5 years (24). However, the duration of the transition and symptoms can vary significantly depending on when the menopausal transition begins. On average, it starts between 44 and 48 years old, with some women experiencing symptoms as early as 31 years old and others as late as 54 years old (5,6). The age at the FMP is usually between 51-52 years, ranging from 35 to 58 years (5,6). Studies such as the Study of Women's Health Across the Nation (SWAN) with multiethnic cohorts have revealed that women experiencing earlier onset of perimenopausal symptoms tend to have a more

extended median transition period (8.6 years), compared to those with later onset symptoms who may undergo a shorter median transition (4.3 years) (25).

During perimenopause, the decline in follicle numbers, which correlates directly with decreased AMH levels, reaches a critical point when concentrations of inhibin B in the follicular phase start to decrease and FSH levels rise (1,27–31). This increase in FSH secretion is also associated with a decline in inhibin B (32). Furthermore, it has been reported a significant and inverse correlation between these two hormones (**Figure 3)** (33). These changes are recognized as potential early markers of the perimenopausal transition; however, their predictive value varies considerably.

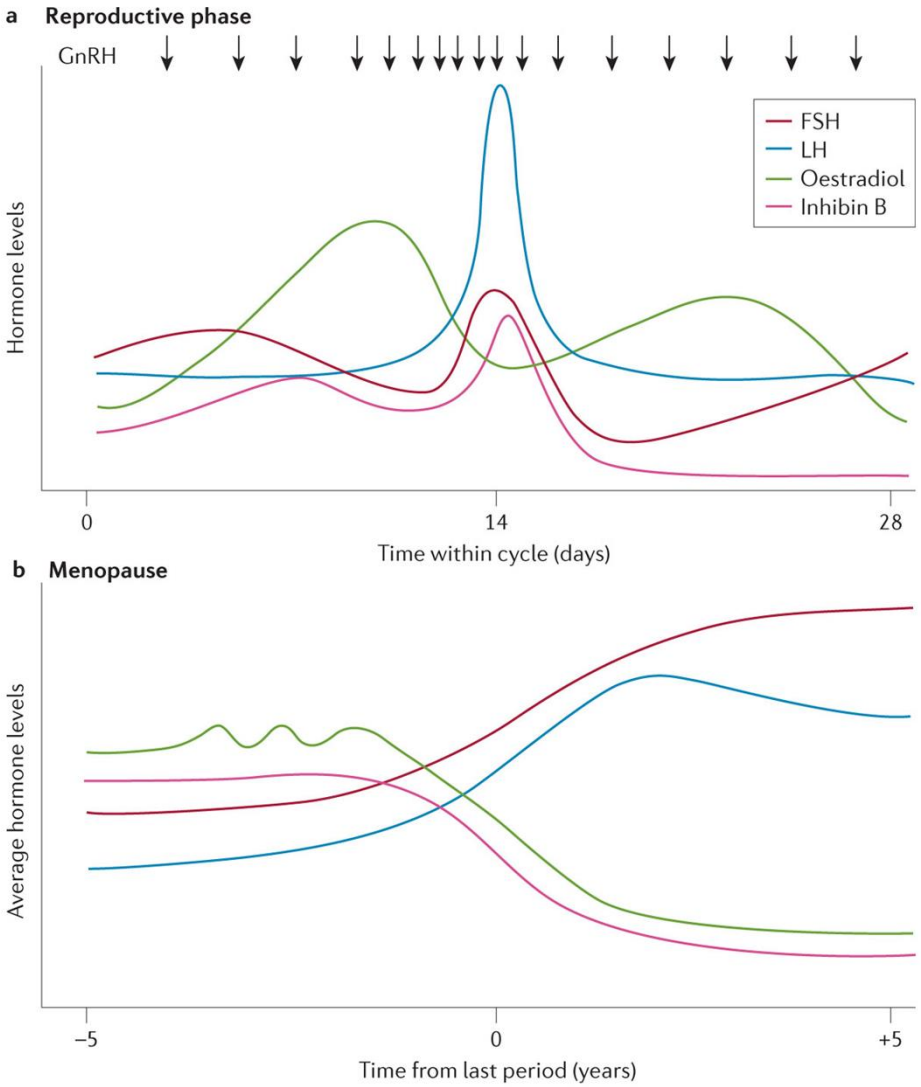


Figure 3. Sex hormone levels during the human menstrual cycle and menopausal transition. Image obtained from Davis SR *et al.* (2015).

Some researchers attribute the initial endocrine changes in perimenopause primarily to declining AFC and subsequent alterations in feedback mechanisms that regulate the HPG axis (34). Others emphasize that a decrease in inhibin could be the earliest detectable event (35). Recent analyses from population-based cohort studies indicate that an AMH level of at least 200 pg/ml in late reproductive-age women reliably predicts that menopause will not occur within the next 5 years (36). AMH has shown greater accuracy in predicting the time to the FMP compared to FSH, oestradiol, or inhibin, and is less influenced by factors such as body mass index (BMI), race, or ethnicity (37). However, despite its potential as a marker of ovarian follicular reserve, AMH is not currently recommended as a routine diagnostic test for perimenopause.

Furthermore, the role of FSH remains complex; it is often elevated prior to the onset of menstrual cycle irregularities, sometimes even up to 10 years before the menopausal transition begins (25). This variability underscores the challenge of using hormonal markers, including those in the STRAW criteria, beyond cycle length alone. The lack of consensus on what triggers these hormonal alterations complicates their utility as reliable biomarkers for perimenopause, it is essential to consider that the menopausal transition is a dynamic and continuous process with substantial interpersonal variations in the frequency, intensity and age of onset of symptoms.

In terms of STRAW+10 stages related to menopausal transition, they consist of two phases and an extra phase for the perimenopausal state, the latter corresponding to the first year after the last menstrual period. This third stage is the temporal point of consensus to consider that the woman has reached menopause and, therefore, it is the starting point of the stage known as postmenopause (1).

During **early menopausal transition Stage -2**, women typically experience heightened variability in menstrual cycle length, characterized by increased variability in menstrual cycle length, defined as a persistent difference by more than 7 days in the length of two consecutive cycles, counting the last 10 cycles since the first variable cycle in terms of length appears. This phase could be marked by menstrual cycles ranging approximately from 14 to 50 days (19). In this stage, women also exhibit consistently low levels of AMH and Inhibin B, alongside reduced AFC. Despite these hormonal changes, residual ovarian follicles in early perimenopause continue to support mostly ovulatory cycles (1). Elevated FSH levels contribute to the variability in cycle length, which encompasses both normal-length ovulatory cycles and variable-length anovulatory cycles.

Late menopausal transition Stage -1 is characterized by the occurrence of at least two skipped menstrual cycles and a minimum of one period of amenorrhea exceeding 60 days (1). During this stage, menstrual cycles become highly variable in length, accompanied by significant fluctuations in hormonal levels and an increased incidence of anovulation.

FSH levels may rise into the menopausal range, with levels exceeding 25 IU/L in random blood draws serving as a characteristic marker of late transition (1). Studies, including those from the SWAN cohort, have identified distinct patterns of FSH and oestradiol changes leading up to and following the FMP. Approximately 10 years prior to the FMP, FSH levels begin to rise steadily, accelerating markedly around 2 years before the FMP, decelerating shortly before, and stabilizing approximately 2 years post-FMP (24,38). Conversely, oestradiol levels remain stable until approximately 2 years before the FMP, after which they decline rapidly, reaching their lowest point at the time of the FMP, and then stabilizing again by 2 years post-FMP (24,38). These patterns were consistent across different age groups at FMP and among various racial and ethnic groups, though obesity has been noted to attenuate the rise in FSH and delay its initial increase (38).

The VMS, particularly hot flashes, are common during this stage, although their prevalence tends to peak after the FMP. Thus, while the presence of VMS can indicate the late menopausal transition, bleeding patterns and an FSH level of 25 IU/L or higher are more reliable indicators (1). It is important to note that individual women may not always fit neatly into these staging categories; some may skip the early menopausal transition entirely, especially those transitioning later in life, while others may spend many years in the early stage, particularly those transitioning at younger ages (25).

1.1.2.2. Postmenopause

Menopause is the natural biological phase in a woman's life associated with reproductive aging characterized by the permanent cessation of menstrual cycles, marking the end of the reproductive stage (1,25,39,40). It is defined as the absence of menstrual periods for twelve consecutive months after the FMP, typically occurring at the age of 51-52 (9,24). Natural menopause usually occurs between 45 and 55 years of age and menopause occurring around the age of 45 is often classified as early (9,24).

While **early postmenopause Stage +1a** marks the end of the 12-month period of amenorrhea required to define that the FMP has occurred, **early postmenopause Stage +1b** encompasses the rest of the period characterized by rapid changes in mean FSH and oestradiol levels. Recent data indicate that FSH continues to rise, and oestradiol levels continue to fall until approximately 2 years after the FMP (Stage +1a and +1b) (38). Symptoms, especially VMS, are most likely to occur during Stages +1a and +1b. On the other hand, **early postmenopause Stage +1c** represents the period of hormonal stabilization, characterized by high FSH levels and low oestradiol values, lasting approximately 3 to 6 years. Therefore, the entire early postmenopause could last approximately 5 to 8 years (1,38). Finally, **late postmenopause Stage +2** represents the

period in which further changes in reproductive endocrine function are minimal, and somatic aging processes become more prominent. Symptoms such as vaginal dryness and urogenital atrophy become increasingly common during this stage.

1.2. Symptoms and health risks of menopause

Menopause is associated with a range of symptoms and health risks, which are influenced by factors such as ethnicity, individual clinical history, and current health status, especially obesity, which can affect the prevalence of certain symptoms and exacerbate both the intensity of the VMS and the risk to suffer metabolic related alterations (26). An early onset of menopausal transition predicts a longer duration with earlier and more severe symptoms, which could last more than 10 years (41). For instance, African American women have been observed to have a longer duration of the menopausal transition compared to White women (41). Additionally, White, Chinese, and Japanese women generally have a lower probability of experiencing irregular menstrual cycles compared to African American and Hispanic women (7).

During the early menopausal transition, certain menopausal symptoms, such as VMS, begin to appear, with their prevalence significantly increasing in the first 1-2 years after the FMP during the late transition. This phase is marked by the manifestation of incipient ovarian failure, leading to the onset of anovulatory cycles and a decline in oestrogen levels, thereby contributing to a broader spectrum of severe symptoms (1,42).

Although, several studies indicate that risk factors for postmenopausal diseases start to emerge during perimenopause, within the 5- to 10-year period preceding the onset of menopause (19,43). Currently, the only clinically accepted sign of the menopausal transition is cycle length according to STRAW+10 (1). Therefore, further research is

needed to explore additional biomarkers to shed light on the underlying mechanisms across different stages.

Indeed, the number of postmenopausal women is increasing as global life expectancy rises, with women now spending approximately one-third of their lives in the postmenopausal stage (1,44). Beyond chronological aging, physiological changes during the menopausal transition contribute to an elevated risk of developing non-communicable diseases evident in the postmenopausal state, such as osteoporosis, atherosclerosis, CVDs, stroke, type 2 diabetes mellitus (T2DM), and MetS (45–49). Understanding these symptoms and health-related risks is essential for developing effective prevention and management strategies to improve the quality of life for women during perimenopause and after menopause (**Figure 4**).

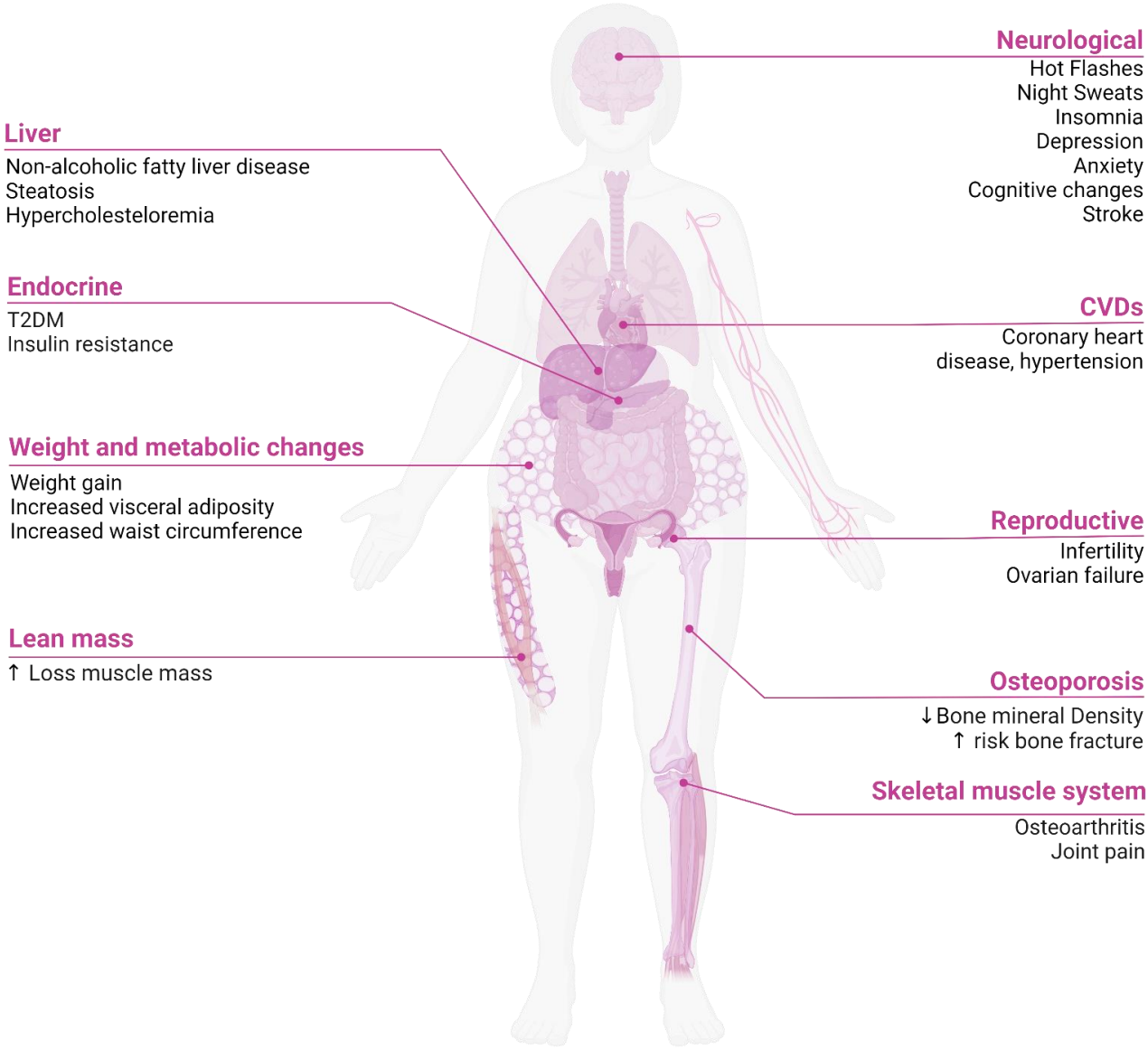


Figure 4. Symptoms and health-related complications of menopausal transition include central nervous system-related disorders, bodily alterations related to cardio-metabolic changes and musculoskeletal alterations. Created with biorender.com.

1.2.1. Vasomotor symptoms (VMS)

Central nervous system-related symptoms, including VMS, sleep issues, anxiety, depression, as well as mood and cognitive changes, result from neurobiochemical alterations that occur during menopausal transition. Among these, VMS—characterized by hot flashes and night sweats, often followed by trembling and chills—are particularly significant, manifesting in up to 75-80% of women during the menopausal transition and postmenopause. These distressing symptoms are the hallmark of menopause, substantially impacting the quality of life for many women (26).

VMS typically emerge as oestrogen levels begin to decline, starting as early as two years before the FMP. These symptoms peak one year after the FMP during the late menopausal transition and continue for approximately four years after the FMP in about 50% of women, with duration varying depending on ethnicity. While some women may experience VMS for only six months, they can last for over ten years in a minority of women (19,50,51). The multi-ethnic SWAN study reported that African American and Hispanic women had the highest rates, longest duration, and greatest severity of VMS, whereas females of Asian descent had the lowest VMS rates (26,42,51). These ethnicity-related differences are potentially influenced by the higher prevalence of obesity among African American women compared to other ethnicities (26).

Hot flashes are among the most frequent VMS experienced by menopausal women, marked by their abrupt and seemingly unpredictable onset throughout the day and night. Each episode can last several minutes, beginning with a flushing sensation that spreads across the upper body, often accompanied by profuse sweating (26,51). Hot flashes are thought to arise from dysregulation in the HPG axis, involving fluctuations in oestrogen, LH and FSH levels (51). However, their occurrence does not consistently correlate with

fluctuations of these hormones; instead, they are more directly associated with the abrupt deprivation of oestrogen (18,42,51). Menopausal women receiving oestrogen-based hormone replacement therapy (HRT) have shown higher core temperature sweating thresholds and reduced frequency of hot flashes compared to those receiving placebo (42).

The exact mechanism underlying VMS remains poorly understood but is hypothesized to involve disruptions in the hypothalamic temperature-regulation system. It is proposed that even small increases in core body temperature, acting within a narrowed thermoneutral zone, may trigger sudden bursts of warmth in the peripheral vasculature (18).

Although VMS are commonly perceived as benign, severe and persistent VMS are linked to heightened cardiovascular risk profiles (42,51,52). For instance, the SWAN study reported a 77% higher risk of CVDs among women experiencing frequent VMS compared to those with infrequent or no symptoms (53). This elevated risk is partly attributed to the decline in endothelial function that coincides with menopause, likely exacerbated by reduced oestrogen levels (42). In contrast, a longitudinal study involving 8,881 participants aged 45-50 in the Australian Longitudinal Study on Women's Health (ALSWH) over a 20-year period found no consistent evidence linking VMS with increased clinical outcomes of CVDs (54). Despite previous studies suggesting associations between VMS and cardiovascular risk factors, this comprehensive investigation did not substantiate these claims. Therefore, further research is needed to fully elucidate the implications of VMS on cardiovascular health.

1.2.2. Sleep disorders

Sleep disturbances are a significant concern for women undergoing menopause. During perimenopause, women often experience a decline in sleep quality, characterized by difficulties in falling or staying asleep and early awakening (18). A survey conducted

among over 12,000 women in the SWAN study revealed that nearly 37% of women aged 40 to 55 reported sleep difficulties correlated with the timing of menopausal transition, with higher rates observed in Caucasian and Hispanic women (55). Research indicates that sleep disturbances typically begin in the early stages of menopause and peak during the late transition, after which symptoms tend to stabilize as women progress into postmenopause (18,55,56).

The prevalence of sleep disturbances increases during the menopausal transition, with nighttime awakenings being the most frequently reported issue. Women experiencing more severe VMS are more likely to report insomnia. However, it's important to note that VMS alone does not account for all changes in sleep patterns during this transition period (18).

1.2.3. Mood changes and related disorders

The menopausal transition is recognized as a pivotal period for the onset of mood disorders, notably depression and anxiety. The prevalence of these symptoms peaks during late perimenopause and early postmenopause (18,26,42,57). The research underscores the pivotal role of fluctuating steroid hormone levels, especially oestrogen, in mood regulation (18). Women exhibit a lifetime prevalence of major depressive disorder exceeding 20%, which is twice that of men, underscoring the profound impact of hormonal fluctuations on women's mental health (26). During menopause, the decline and variability in oestrogen levels are strongly associated with heightened risks of depressive and anxiety symptoms. Three well-established longitudinal and cohort studies consistently demonstrate that women are at an increased risk of developing major depressive disorder during the menopausal transition, even in the absence of prior psychological disorders (58–60).

1.2.4. Cognitive changes and related disorders

Cognitive-related alterations are a significant concern for perimenopausal women, who often report experiencing a decline in memory and concentration (26,42). This cognitive decline can be distressing and can have clinical relevance (61). Longitudinal data obtained from the SWAN cohort over a four-year period demonstrated a reduction in cognitive performance, particularly in learning abilities, primarily during the perimenopausal stage (62). Given the hormonal fluctuations throughout the entire female lifespan, and considering the role played by sex hormones in the central nervous system, it is not surprising to observe the onset of mood or neurodegenerative disorders over time. Anatomical studies have shown that the hippocampus and prefrontal cortex, which are critical for episodic and working memory, express high levels of oestrogen receptors (ERs). In these brain regions, oestradiol-dependent activation of ERs can modulate the synthesis, release, and metabolism of neurotransmitters like serotonin, dopamine, and acetylcholine, as well as neurosteroids such as dehydroepiandrosterone (DHEA) (63). Progesterone, on the other hand, has shown opposite effects in inhibiting glutamate transmission and exciting Gamma-aminobutyric acid (GABA) transmission (64). However, the link between circulating sex hormone levels and cognitive impairment is not well-established (26,64). One study evaluated this issue in early postmenopausal women who were prescribed an HRT for four years, reporting no appreciable differences in cognition between these women and those receiving a placebo, indicating that HRT neither harms nor improves cognitive function in early postmenopausal women (65).

In summary, while perimenopausal women often experience cognitive changes, the role of oestradiol, other sexual hormones, or HRT in mitigating these changes remains unclear. Further research is needed to better understand the mechanisms underlying

cognitive disorders during the menopausal transition and to develop effective interventions.

1.2.5. Body weight gain and obesity

In women, body weight gain and the prevalence of obesity can increase during midlife. Both ovarian aging and chronological aging may contribute to significant changes in body composition, including increased fat mass, decreased skeletal muscle mass, and greater waist circumference (66). Obesity has been associated with a longer menopausal transition duration (26) and it is well established that oestrogen, regardless of sex, has a key role as regulator of adipose tissue health and as mediator of adipose tissue distribution, promoting visceral fat storage (67,68). An increasing body of evidence obtained from longitudinal studies suggests that, during the menopausal transition, there is a noticeable shift in body fat distribution from a gynoid to an android pattern, contributing to increased visceral fat accumulation and a subsequent increase in waist circumference, which may contribute to increased cardiovascular risk and metabolic conditions, such insulin resistance (IR), in postmenopausal women (26,66,69–75)

However, it remains unclear whether body weight gain *per se* is primarily attributed to the menopausal transition, to aging, or to both factors. Thus, various longitudinal studies demonstrated an increase in body weight during the menopausal transition, with an average gain of approximately 0.5 Kg per year (66,71–75), and the SWAN study reported an absolute cumulative increase in waist circumference of about 5.7 cm over six years (66). Nevertheless, in some studies, no weight gain was observed (76), which could be related to the loss of lean body mass. Oestrogen deficiency after menopause leads to an increase in total body fat, but could also cause a concomitant decrease in lean body mass (67,69,75), resulting in a little net change in overall weight (77). Furthermore, oestrogen

has been shown to enhance fatty acid utilization and oxidation in skeletal muscle (13), which helps to explain why the oestrogen decline during menopause contributes to reduced fatty acid oxidation, decreased muscle mass, and lower energy expenditure (69).

On the other hand, increasing evidence from human and rodent studies indicates that oestrogen promotes the growth of metabolically healthier subcutaneous fat over visceral fat (68,78). Consequently, the decline in oestrogen levels during menopause leads to a decrease in subcutaneous fat and an increase in visceral fat (26,68,79). Furthermore, research utilizing techniques such as dual-energy X-ray absorptiometry (DEXA), microcomputed tomography (μCT), and Magnetic Resonance Imaging (MRI) have confirmed that postmenopausal women tend to accumulate more abdominal and visceral adipose tissue compared to premenopausal women (80–83). Various longitudinal studies with follow-up periods have consistently shown that the shift in body fat content toward increased visceral fat mass significantly correlates with increased circulating levels of FSH and decreased oestradiol blood concentrations (66,69). Postmenopausal women under an oestrogen-based HRT prescription displayed higher weight loss and lower waist-to-hip ratio and less visceral adipose tissue than women who did not undergo an oestrogen therapy (84,85).

Oestrogen has also been shown to increase lipolysis in adipose depots and to boost adipogenesis (hyperplasia) in healthy subcutaneous adipose tissue, while oestrogen deficiency trigger hypertrophy in unhealthy visceral adipose tissue (68). This mechanism appears to be ERα-mediated, whereas ERβ may have opposing effects. The presence of both ERα and ERβ in human subcutaneous and visceral adipose tissue depots is well established. ERα drives most oestrogen-related functions in white adipose tissue (WAT) (68,86). In overweight and obese women, differences in ER expression in abdominal adipose tissues have been reported, displaying premenopausal women a higher Erα-to-

ERβ ratio than postmenopausal women (68). Furthermore, postmenopausal women under HRT prescription showed an increased Erα-to-ERβ ratio, which was accompanied by enhanced insulin sensitivity (87). In animal studies, 17β-oestradiol administered to ovariectomized (OVX) mice —a widely recognized postmenopausal preclinical model with oestrogen deficiency— improved glucose tolerance and insulin sensitivity in wild-type but not in ERα-null mice, suggesting that the beneficial effects of oestradiol on glucose and insulin homeostasis are mediated via Erα (88,89). The protective effects of oestrogens against T2DM observed in OVX mice fed a high-fat diet would support the idea that targeting ERα could mitigate the alterations of glucose and insulin homeostasis occurring in the postmenopausal state (89).

Additionally, oestrogen has been suggested to regulate lipoprotein lipase (LPL), an enzyme responsible for catalyzing the hydrolysis of triglycerides (TG) present in TG-rich lipoproteins into free fatty acids, allowing their uptake into non-hepatic tissues for the storage of lipid droplets (68,90). The promoter region of LPL contains oestrogen response elements that interact with oestrogen receptors, inhibiting its mRNA expression in 3T3 adipocyte cells (91). Ferrara et al. (92) observed that in obese peri- and postmenopausal women matched for whole-body composition, abdominal LPL activity was higher and lipolysis was lower in postmenopausal compared to perimenopausal women. Another study demonstrated that the visceral to subcutaneous LPL activity ratio and visceral adipocyte basal lipolysis were significantly higher in ovarian hormone-deficient women, indicating a shift towards visceral fat storage (79). In addition, in this study, significant positive correlations between visceral fat area and visceral LPL activity and adipocyte cell size were found, supporting the notion of fat redistribution towards the visceral compartment in ovarian hormone-deficient women, an effect that could be mediated, at

least in part, through the interplay between oestrogen and LPL (79), although correlations do not imply causality.

WAT acts as an endocrine organ, producing adipokines such as leptin and adiponectin, which are crucial indicators of metabolic health (93). Leptin, circulates in proportion to body energy stores, decreases food intake by interacting with its receptor in the hypothalamus and avoids the ectopic accumulation of fat in tissues other than WAT, such as the liver and muscle. It has been described that obesity is associated with increased circulating levels of leptin and IR (94,95). Conversely, adiponectin acts as an insulin sensitizer and is inversely associated with obesity, T2DM, and MetS (96). In this regard, Juppi *et al.* (2022) observed that during the menopausal transition, android adipose tissue was positively associated with both adiponectin and leptin circulating levels (75). This increase in adiponectin levels was confirmed by other authors as well (70), although it appears counterintuitive since lower adiponectin levels are typically linked to increased visceral adipose tissue (97). A growing body of scientific evidence indicates that the ratios between insulin and leptin, namely adiponectin to leptin ratio (ALR) and leptin to adiponectin ratio (LAR), can correlate better with IR and insulin sensitivity than adiponectin, leptin and the surrogate markers of insulin resistance and sensitivity, the homeostatic model assessment for insulin resistance (HOMA-IR) and the revised quantitative insulin sensitivity check index (R-QUICKI), respectively (98–102). Thus, LAR has been described as a good predictor of T2DM and MetS (98) and, similarly, ALR would be a biomarker of insulin resistance and adipose tissue inflammation and dysfunction in humans and has been shown to be clinically useful to identify subjects susceptible to cardiometabolic diseases (99–102). In this sense, an ALR $\geq$ 1.0 is considered normal, while an ALR between $\geq$0.5 and <1.0 suggests moderate-to-medium

increased risk, and an ALR <0.5 indicates a severe risk of suffering from cardiometabolic diseases (99).

1.2.6. Cardiovascular diseases (CVDs)

The menopausal transition and the decline in oestrogen levels are linked to alterations in the peripheral vasculature and lipid profiles as well as to increased visceral fat accretion, which leads to the elevated risk of suffering MetS and CVDs in postmenopausal women (86,103–106). The early menopausal transition stage is consistently associated with a higher risk of coronary heart disease, stroke and mortality in later life in the postmenopausal state (107–109). Furthermore, longitudinal studies have highlighted the FMP as a crucial marker for understanding the timing of metabolic changes related to menopause (4,17,110). During the 10-year follow-up carried out in the SWAN study, it was observed that blood lipid profiles became more atherogenic in women within the year interval before and after the FMP, with significant increases in total cholesterol (TC), low-density lipoprotein cholesterol (LDL-c) and apolipoprotein B, regardless of age, ethnicity, or weight (4). High-density lipoprotein cholesterol (HDL-c) levels increased regularly until the FMP occurred, peaking at this point and then declining, leading to a small overall decrease in HDL-c across the menopausal transition (4). Consequently, the protective anti-atherogenic effect of HDL-c appears to be diminished from perimenopause (3,4,106,111). These findings suggest that the increased prevalence of CVDs and MetS in postmenopausal women is more likely due to changes occurring during the menopausal transition rather than during the postmenopausal state. Monitoring lipid profiles in perimenopausal women could improve the primary prevention of CVDs. Additionally, women who experience premature menopause display a greater risk of developing obesity, which, in turn, is associated with a higher incidence of CVDs and MetS (112).

Normal levels of endogenous oestrogen exert several cardioprotective effects, improving endothelial function, decreasing vascular resistance, blood pressure and cardiac hypertrophy, attenuating proinflammatory pathways, and inhibiting atherogenic oxidation of LDL (51,113–116). The significant reduction in oestrogen levels during menopause can adversely affect endothelial cell growth and diminish the inhibitory impact of female sex hormones on the growth and proliferation of vascular smooth muscle cells (104). Oestrogen deficiency after menopause may activate the renin-angiotensin system, upregulate vasoconstrictor endothelin, and impair nitric oxide-mediated vasodilation (117–119). In addition, ectopic fat accumulation in visceral tissues, such as the heart, has been observed in postmenopausal women (111). El Khoudary *et al.* (2020) reported that perimenopausal women at the latter stage and postmenopausal women had higher volumes of pericardial fat than premenopausal women regardless of age, race, obesity or other covariates (111). Thus, all these changes might collectively contribute to faster atherogenesis and a higher susceptibility to CVDs in postmenopausal women.

A meta-analysis study conducted by Pu *et al.* (2017) concluded that oestrogen deficiency is a crucial factor in the development of MetS in postmenopausal women (106). In this study, it was estimated that the prevalence of MetS in postmenopausal women was between 31–55% (106). The metanalysis highlighted that nearly all components associated with MetS (BMI, waist circumference, LDL-c, TG, blood pressure, fasting glucose, and insulin) showed adverse changes after menopause, except for HDL-c. For instance, TG levels increased by an average of 20.44 mg/dL, and LDL-c by 20.77 mg/dL in postmenopausal women. Additionally, fasting glucose and insulin levels were significantly higher in postmenopausal women by 4.64 mg/dl and 20.88 mmol/l, respectively, compared to premenopausal women (106). In line with increased obesity, BMI and waist circumference were higher by 0.94 kg/m² and 4.12 cm, respectively, in

postmenopausal women compared to premenopausal women (106). This meta-analysis also reported increases in both systolic (6.11 mmHg) and diastolic (3.54 mmHg) blood pressures in postmenopausal women (106).

In line with these findings, another study concluded that abdominal obesity, a major risk factor for CVDs and MetS, was observed nearly three to five times more frequently in postmenopausal women compared to their premenopausal counterparts (120). Furthermore, oestrogen deficiency in nearly half of the postmenopausal women resulted in the development of MetS, affecting 41.5% of these women, and led to hypertriglyceridemia in 56.9% of the cases (17,121). On the other hand, a 6-year follow-up study carried out with premenopausal and early perimenopausal women reported an absolute cumulative increase of approximately 5.7 cm in waist circumference, which positively correlated with FSH levels, even after adjusting for baseline waist circumference (66). In addition, a waist circumference > 88 cm was the most prevalent factor in menopausal women with MetS across various countries (14,15,122).

In conclusion, the menopausal transition and the associated decline in oestrogen levels lead to significant metabolic and vascular changes that increase the risk of suffering CVDs and MetS in postmenopausal women. Understanding these changes and their implications is crucial for developing effective strategies to mitigate these risks and improve cardiovascular health in this population.

1.2.7. Osteoporosis

Osteoporosis is a degenerative bone disorder characterized by low bone mass and altered bone structure, leading to reduced bone mineral density (BMD) and increased susceptibility to fractures, particularly in the spine, hip, and wrist in postmenopausal women (26), with around 40% of women over 50 years old experiencing osteoporotic

fractures (123,124). Although BMD is not considered a direct health threat, the decrease in this parameter is often associated with bone fragility and increased susceptibility to fractures, which are significant clinical events (125). While, there are minimal changes in BMD during premenopausal or the early menopausal transition stage, BMD sharply declines during the late perimenopause stage (126). Prospective examinations of BMD across the menopausal transition reveal that bone loss increases dramatically starting a year before the FMP and continues for the first two years after FMP. In the SWAN study and in another study, bone loss was found to accelerate from early to late perimenopause and postmenopause, with annual losses after the FMP of 2.4% in the lumbar spine, 1.4% in the hip, and 1.7% in the femoral neck (19,126).

Bone mass and strength are significantly determined during perimenopause, a critical window for modulating bone health and preventing osteoporosis in later life (49,127). Metabolic factors such as inflammation as well as micronutrient deficiencies during this period are linked to lower bone strength and mass (127). Notably, the highest rates of osteoporotic fractures in Europe are observed in northern countries, likely due to differences in sun exposure and vitamin D production, essential for calcium absorption and bone mineralization (128). Furthermore, a study carried out in postmenopausal Japanese women found that vitamin D, K, and B deficiencies significantly increased fracture risk, with the lowest incidence in those without deficiencies (129).

It is well-established that oestrogen plays a crucial role in bone remodeling by regulating the activities of osteoblasts and osteoclasts (130). In osteoblasts, oestrogen promotes differentiation and maturation through the production of insulin-like growth factors (IGF-1) and the activation of ERα and ERβ receptors (131). These receptors mediate both genomic and non-genomic actions, enhancing osteoblast proliferation and function. Additionally, oestrogen exhibits anti-apoptotic and apoptotic effects on osteoblasts and

osteoclasts, respectively, particularly in the presence of oestradiol, thereby prolonging their lifespan and activity (132,133). Bone turnover markers in blood, such as serum C-terminal telopeptide of type I collagen (CTX-1) for bone resorption, and serum procollagen type I N propeptide (PINP) and osteocalcin (OC) for bone formation, are utilized to assess bone metabolism (131). These markers indicate a disrupted balance between bone resorption and formation, which is crucial in the pathogenesis of osteoporosis. Following menopause, the marker of bone resorption, CTX-1, is significantly elevated in women with osteoporosis, increasing by 79-97%. Markers of bone formation, such as OC, were elevated by 37-52%, whereas the increase in PINP was not significant and may even be reduced in postmenopausal women (77,78). During the menopausal transition, particularly in the late stage, the decline in oestrogen levels leads to a significant increase in bone resorption. This is primarily due to the elevated production of pro-inflammatory cytokines and the increased expression of receptor activator of nuclear factor kappa-B ligand (RANKL) by osteoblast-lineage cells (131,133). RANKL binds to its receptor activator of nuclear factor kappa-B (RANK) on pre-osteoclasts and mature osteoclasts, promoting osteoclastogenesis and bone resorption (134). Concurrently, the production of osteoprotegerin (OPG), a natural inhibitor of RANKL, decreases, further exacerbating bone loss (135,136). Studies in OVX rodent models have shown that macrophages and monocytes from these animals exhibit increased osteoclastogenic potential, even in the absence of macrophage colony-stimulating factor (M-CSF) and RANKL (13,137). Similarly, peripheral blood mononuclear cells (PBMCs) from postmenopausal women demonstrate heightened osteoclast activity compared to age-matched controls, indicating that oestrogen deficiency directly enhances osteoclast formation and activity (137). These findings underscore the critical role of oestrogen in maintaining bone density and highlight the

mechanisms by which its deficiency accelerates bone resorption, leading to increased susceptibility to osteoporosis and fractures in postmenopausal women.

In addition to osteoporosis, changes in body composition during midlife in women lead to a decrease in lean muscle mass, which is more pronounced after menopause (138). Although sarcopenia cannot be currently attributed to menopause, this degenerative process is more evident in aging women than in aging men and seems to occur more rapidly after menopause and could be related to the increased prevalence of osteoarthritis after the FMP. Common symptoms of osteoarthritis include pain in the distal interphalangeal joints and thumb base. This hand osteoarthritis usually subsides within 2–3 years but often predicts future joint disease in the knee and spine. Most women report knee osteoarthritis symptoms during perimenopause or within five years post-menopause, likely due to oestrogen deficiency affecting joint tissues (26).

2. Hormone Replacement Therapy (HRT): benefits & risks

HRT is widely prescribed to postmenopausal women to alleviate vasomotor symptoms and to prevent and ameliorate osteoporosis and metabolic-related alterations associated with the postmenopausal state. It is currently recognized as the most effective treatment for acute climacteric syndrome, effectively alleviating vasomotor symptoms, and for reducing the risk of osteoporosis and T2DM. Nevertheless, there is less evidence concerning the benefits of HRT against CVDs, showing the treatment neutral or beneficial effects depending on the patient's medical history (139–141).

The prescription of HRT has undergone changes over time in relation to its modalities (types, routes, and formulations) and clinical decision making based on the risk-benefit balance (139). HRT typically involves the administration of oestrogen and progesterone

(progestogen). Oestrogen therapy alone is suitable for post-menopausal women who have undergone hysterectomy, whereas combined oestrogen-progestogen therapy is recommended for those women with an intact uterus to prevent endometrial cancer. Administration methods include oral, transdermal or vaginal routes, each of them having different potential risks. For instance, oral oestrogen therapy, although is widely used, is associated with a higher risk of venous thromboembolism (VTE) and stroke. In contrast, transdermal and vaginal therapies generally pose lower systemic risks, including a reduced risk of VTE and stroke, due to their avoidance of first-pass metabolism in the liver, which minimizes their impact on coagulation factors and TG (139). The dynamic nature of ovarian endocrine function, characterized by hormonal fluctuations throughout the menstrual cycle and fertile years, makes it challenging to replicate these natural patterns through HRT prescription during menopause (140). Consequently, the complexity of mimicking the hormonal rhythms experienced naturally throughout the postmenopausal period would imply a long-term prescription of HRT, which can potentially lead to unintended side effects (**Figure 5**).

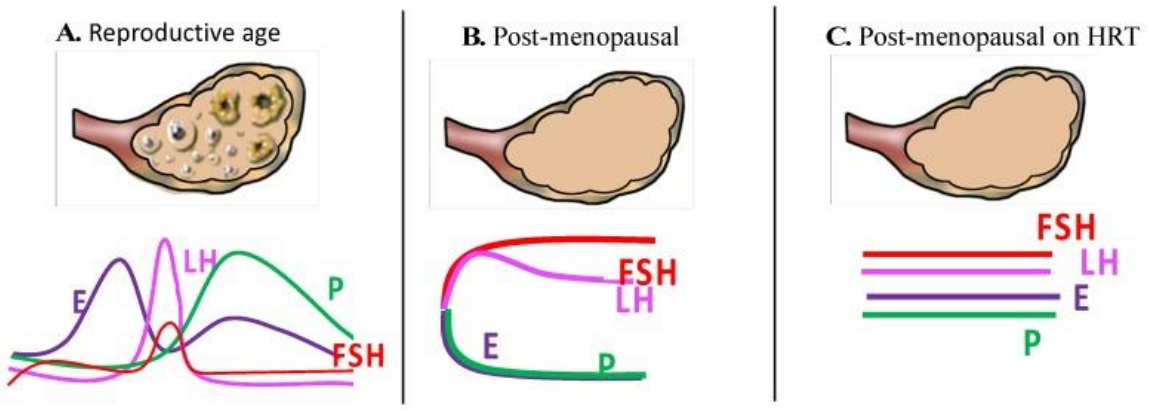


Figure 5. Schematic representation of the level of various ovarian hormones in reproductive age, post-menopausal and in women on HRT. Image obtained from Agarwal *et al.* (2018).

In the early 1980s, combining progestogen with oestrogen therapy was found to reduce the risk of endometrial cancer associated with treatment based only on oestrogen. This discovery led to a substantial increase in HRT use, widely prescribed over the next two decades for its perceived benefits in reducing coronary heart disease risk. By the late 1990s, annual HRT prescriptions in the U.S. peaked at around 90 million, benefiting approximately 15 million women. However, in 2002, the release of the Women's Health Initiative trial (WHI) trial results, including post-intervention analysis and cumulative 18-year follow-up, highlighted increased risks of breast cancer, coronary heart disease, and stroke associated with HRT, which led to a sharp decline in its use (**Figure 6)**.

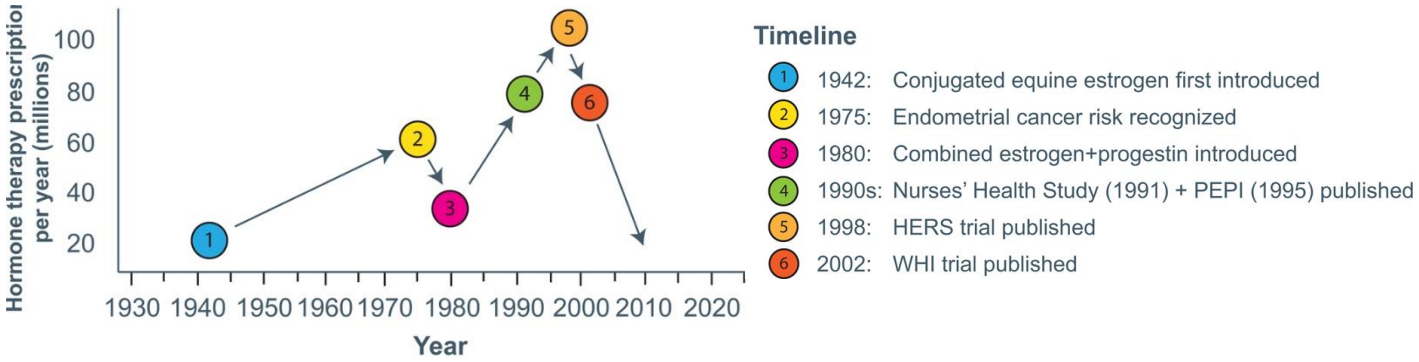


Figure 6. Timeline of HT use in US. HT hormone therapy; HERS Heart and Oestrogen/progestin Replacement Study; PEPI Postmenopausal Oestrogen/Progestins Interventions; WHI Women's Health Initiative. Image adapted from Cho *et al.* (2023).

The WHI findings underscored the importance of evaluating the risks and benefits of HRT on an individual basis, particularly concerning the age and health status of the women receiving it (141). Since the WHI trial findings, it became clear that the safety and beneficial effects of HRT are most pronounced when it is initiated under the age of 60 or within the first 10 years of amenorrhea (139–141). However, these effects also vary depending on the type of treatment, route of administration, and duration of use, which is generally recommended to be in the short term. Typically, HRT is recommended for up to 5 years, with a reduction in dosage if continued beyond this period (141). Therefore,

nowadays, the convenience of HRT prescription is carefully evaluated by physicians for each woman (139). In this sense, if HRT is prescribed out of the aforementioned periods, its potential risks may outweigh the benefits, underscoring the need for personalized evaluation based on each patient's medical history, symptoms, and risk factors (**Table 2**) (139–141).

Table 2. Risk-benefit balance of menopausal hormone replacement therapy (HRT).

Outcome/Symptom	Formulation	Benefit	Risk	Probable Benefit or Risk
Vasomotor Symptoms	E or E+P	✓		
Osteoporosis and fractures				
Type 2 Diabetes Mellitus				
Coronary Heart Disease	E	✓*	✓**	*Decreased risk in women <60 within 10 years of menopause **Increased risk in women many years past menopause
	E+P	↔	↔	
Stroke	E or E+P		✓	
Venous Thromboembolism				
All-Cause Mortality	E or E+P	↔		Trend toward decreased risk when started early in menopause and neutral or increased risk when started later in menopause.
Breast Cancer	E	✓		
	E+P		✓	
Endometrial Cancer	E		✓	
	E+P	✓		

E: oestrogen; P: Progestogen. Adapted from Mehta *et al.* (2021).

Due to controversy about the risks associated with HRT and the decline in its prescription, it is imperative to explore alternative therapeutic approaches through nutritional interventions. These strategies have the potential to provide sustained benefits over extended periods of consumption, offering a promising avenue for effectively managing postmenopausal symptoms and metabolic changes.

3. Nutritional strategies to ameliorate symptoms and metabolic disturbances related to menopause

HRT prescription is still considered the first line of treatment to manage symptoms or metabolic disturbances occurring in postmenopausal women (139). Nevertheless, the controversy about the risks associated with HRT derived from the unexpected findings of the WHI study in 2002, has led many women to look for alternative therapies, such as healthy diets, functional foods, supplements, natural extracts or bioactive compounds (142,143), to tackle obesity and the associated metabolic disorders that can occur in menopause due to the cessation of oestrogen production. These therapies offer alternative treatments for women who cannot undergo HRT for clinical reasons or for those who prefer not to be prescribed with HRT.

Increasing evidence supports that changes in dietary habits are crucial to prevent and manage obesity, even to reduce cardiovascular risk. A high adherence to the Mediterranean diet (MD), which is characterized by high consumption of unsaturated fat from vegetable sources (virgin olive oil and nuts) and of minimally processed plant foods (vegetables, fruits, nuts, whole grains and legumes), low consumption of sweets and red and processed meat and moderate consumption of fish and dairy products (mainly yogurt and cheese) (144), has been shown to significantly reduce cardiovascular risk and, especially if the diet is energy-restricted, can also reduce body weight and adiposity (145). Thus, The PREvención con DIeta MEDiterránea (PREDIMED) study, which was carried out on more than 7,000 middle-aged and elderly subjects from Spain, clearly demonstrated that an MD supplemented with extra-virgin olive oil or nuts was associated with a reduced risk of CVDs and death compared with a low-fat control diet (146). Furthermore, results from the PREDIMED-PLUS study indicated that a 12-month nutritional intervention

based on an energy-restricted MD with a reduction of about 30% of the daily caloric intake decreased adiposity and improved different factors for CVDs in overweight and obese middle-aged and elderly subjects with MetS (147). In line with these findings, recent evidence indicates that high adherence to this diet provides a cardioprotective effect in both perimenopausal and menopausal women (148,149), reducing the risk of weight gain, improving cardiometabolic risk factors, and alleviating menopausal symptoms during menopause (149).

Dietary and nutraceutical supplements are composed of natural compounds extracted from foods, such as phytoestrogens (e.g., genistein, daidzein), polyphenols (e.g., curcumin, hesperidin), phytosterols, and amino acids (e.g., carnosine, histidine, cysteine, serine), which provide health benefits, including the prevention and/or treatment of diseases at their onset, helping to protect the human body against harmful metabolic changes.

Isoflavones derived from soy, also known as phytoestrogens, are among the most studied natural bioactive compounds against menopause-related alterations due to their oestrogenic properties (150). However, the outcomes on the health of genistein and daidzein, the most abundant isoflavones in soy, on menopausal symptoms have shown mixed findings. Several studies indicate that genistein can modestly reduce the frequency of hot flashes, and similarly, both genistein and daidzein improved bone health markers in postmenopausal women, suggesting potential benefits (150). Nonetheless, other research has not discovered significant advantages derived from the intake of these phytoestrogens, leading to inconclusive results about its overall impact (150–152). The discrepancies concerning the effectiveness of genistein and daidzein in reducing menopause symptoms can be related to differences in their biological activity among individuals due to inter-individual effects on the specific intestinal bacteria and the

hepatic enzymes needed to produce equol, a higher bioactive and absorbable oestrogenic metabolite (150–152). In Western populations, only about 25-30% of adults are equol-producers, whereas in Asian countries such as Japan, Korea, and China, the prevalence is significantly higher, ranging from 50-60% (151). This disparity may be attributed to dietary habits, as Asian diets typically include a higher intake of fermented soy foods containing more bioavailable isoflavone aglycons. These aglycones are more easily converted to equol by gut microbiota than the glycoside forms prevalent in Western soy food (150–152).

Several lines of research suggest that the intake of combined supplementation with different bioactive compounds (multi-ingredients -MI-), including some studies performed by our research group, have shown that a combined intake of various bioactive compounds acting against complementary targets is an effective strategy to ameliorate obesity and to improve the cardiometabolic health (153–157). To name a few, our group demonstrated that the supplementation of combined metabolic activators (CMA), including nicotinamide riboside (NAD+ precursor), the potent glutathione precursors betaine and N-acetyl-l-cysteine, and L-carnitine tartrate decreased hepatic steatosis in hamsters (156) and ameliorated obesity and insulin resistance in mice (153). In this line, menopause, which is characterized by multifactorial alterations commonly related to cardiometabolic risks and osteoporosis, could also be effectively managed with MI, including a blend of bioactive compounds acting against different biological targets involved in key processes that can be altered during menopausal transition and menopause, in agreement with the idea that better outcomes can be obtained when treatments are performed under a multifaceted approach.

3.1. Polyphenols and phytosterols

Many studies have shown the role of dietary polyphenols and phytosterols in the prevention of obesity and related chronic health conditions (158–160), exerting many beneficial effects related to the prevention or amelioration of CVDs and different features of MetS (158,159). The polyphenols curcumin and hesperidin, as well as phytosterols, are natural bioactive compounds that show promising effects against metabolic disturbances associated with menopause. Various studies carried out in both humans and animals have reported the protective effects of the polyphenols curcumin (161,162) and hesperidin (163,164) as well as phytosterols (159) against obesity and related diseases.

Curcumin is a polyphenol that displays well-known antioxidant and anti-inflammatory properties. It is obtained from *Curcuma longa*, the principal source of curcuminoids of the spice turmeric, which is used as curry powder in curry dishes (165). Different studies carried out in both animals and humans have shown the beneficial effects of curcumin on obesity, MetS, T2DM, bone, and female reproductive health (158,160,166–173). With regard to obesity in menopause, Morrone *et al.* (2016) conducted a study in OVX rats demonstrating that the oral supplementation with curcumin for 30 days decreased intestinal adiposity accretion, which was accompanied by decreases in the circulating levels of interleukin-6 (IL-6) and TG (161). Other studies carried out in male obese, diabetic rodents observed a reduction in total fat mass (171,172,174), decreased WAT depots as retroperitoneal WAT (RWAT) (171) and lower macrophage infiltration in perigonadal WAT (172) after the intake of curcumin. Furthermore, increased lean mass (172), increased adiponectin and reduced leptin levels (171), improved insulin sensitivity (172,174), and reduced fasting glucose levels (172), even in animals challenged with a high-fat (172) and/or high-sugar high-fat diet (174) were reported. Interestingly, curcumin's impact on food intake was negligible, indicating that its observed benefits

were not mediated by decreased caloric consumption (174). Three mechanisms that can explain the anti-obesity effects of curcumin are the activation of thermogenesis, the enhancement of energy expenditure (EE) and the regulation of lipid metabolism. In this regard, curcumin was also able to enhance EE and stimulate thermogenesis efficiently by enhancing the activity of AMP-activated protein kinase (AMPK) and increasing ATP production, causing browning of subcutaneous WAT and RWAT in mice (158,160), while the browning effects of curcumin *in vitro* have also been confirmed stimulated gene expression of thermogenic genes (*Ucp1*, *Pgc-1α*, *Ppar-γ*, and *Prdm16*) in both 3T3-L1 and primary adipocytes derived from subcutaneous WAT (175). Curcumin inhibits differentiation and reduces fat accumulation in a dose-dependent manner (10–20 μM) in 3T3-L1 cells. Concurrently, curcumin decreased the mRNA levels of CD36, a fatty acid transporter located on the adipocyte membrane and also reduced the expression of *fasn* (176), a key enzyme in the *de novo* long-chain fatty acid synthesis pathway, and glycerol-3-phosphate acyltransferase-1 (GPAT-1) (177).

In humans, long-term curcumin treatments have shown significant benefits in subjects with T2DM. In a 9-month study after curcumin supplementation, 16.4% of participants in the placebo group were diagnosed with T2DM, whereas none of the subjects included in the curcumin-treated group were diagnosed with T2DM. The authors found elevated adiponectin levels and reduced HOMA-IR and fasting glucose levels, improving the response to the oral glucose tolerance test (OGTT) in the curcumin-treated group (173). In another 6-month study by the same research group, the authors reported increased adiponectin and decreased leptin levels, along with improved IR, reduced circulating TG and visceral and total fat accumulation in diabetic patients (170). Additionally, a meta-analysis confirmed that the significant decrease in plasma leptin concentrations is

associated with curcumin supplementation, highlighting its potential metabolic benefits (169).

Recent studies have evaluated the impact of curcumin and turmeric on female reproductive processes and aging as well as on symptoms related to the menopausal status. Interestingly, curcumin influences various physiological processes in the female reproductive system, including reproductive aging, ovarian folliculogenesis, and oogenesis. Its antioxidant, anti-inflammatory, and anti-apoptotic properties have been shown to mitigate the effects of ovarian failure (166,167). In rodent models, curcumin promotes ovarian growth and maturation through enhanced proliferation and anti-apoptotic mechanisms (178–182), stimulates folliculogenesis and shows higher follicle reserve (178,180,181,183–185), decreases the concentration of the gonadotropins FSH and LH and increases the levels of oestradiol and AMH (180,186). Interestingly, in line with the idea that the combined supplementation of bioactive compounds can be a suitable strategy to tackle reproductive status and menopause, an MI based on curcumin and hesperidin significantly increased oestradiol levels and markedly reduced FSH levels in ovarian tissues, demonstrating greater efficacy compared to the individual treatments (187).

Concerning bone health, a study performed in C57BL/6J OVX mice demonstrated that curcumin supplementation for 8 weeks ameliorated progressive bone loss and osteoporosis. It increased the BMD of the femurs and reduced CTX-1 levels, suggesting decreased osteoclast activity. Additionally, curcumin inhibited osteoclastogenesis by enhancing the activity and expression of the antioxidant enzyme glutathione peroxidase-1 (Gpx-1), thereby reducing oxidative stress and impairing RANKL signaling pathways critical for osteoclast differentiation (188). Another study confirmed that curcumin significantly reversed the bone deterioration caused by ovariectomy in rats over a 60-day

treatment period, mitigating bone resorption and promoting bone formation (189). Furthermore, two studies demonstrated that curcuminoids intake for 4 weeks reduced pain and improved physical function in osteoarthritis patients (190,191), showing an efficacy comparable to ibuprofen (190). Nevertheless, further clinical trials are needed to confirm the potential of curcumin to improve bone health and to ameliorate osteoporosis in humans.

Hesperidin is a flavanone mainly present in citrus fruits (oranges, tangerines, lemons, limes, and grapefruits) and in their juices. Recently, hesperidin has emerged as a new potential therapeutic agent, showing this bioactive compound's beneficial effects against CVDs risk factors, T2DM, obesity and MetS in both animals and humans. (163,164,192–198).

Regarding glucose metabolism, increasing evidence demonstrates that hesperidin can exert glucose-lowering properties and can improve IR-related parameters both in rodents (199–203) and humans (204–206). In humans, the daily intake of a hesperidin supplement (500 mg for 12 weeks in MetS patients (205) or the consumption of 300 mL of orange juice/day for 60 days in healthy women (204) decreased fasting glucose and insulin levels, as well as the HOMA-IR index. In this line, Ribeiro *et al.* (2017) also observed reduced insulin levels and HOMA-IR index after 12 weeks of daily consumption of 500 mL of orange juice in obese individuals (206). These effects of hesperidin on glucose metabolism may be partially attributed to the modulation of key regulatory enzymes, such as the upregulation of glucokinase, which is involved in glycolysis, and the downregulation of the gluconeogenic enzyme glucose-6-phosphatase (199–201,207,208). On the other hand, Mosqueda-Solís *et al.* (2018) showed that the administration of hesperidin (100 mg/kg/day) for 8 weeks decreased the gene expression levels of *Isnr* in

RWAT and the mRNA levels of *Isnr* and *Lepr* in the liver of male Wistar rats fed a hypercaloric western diet (209).

Hesperidin has also proven to be effective in ameliorating lipid-related alterations in both animal models and humans, exhibiting lipid-lowering properties, helping to modulate dyslipidemia associated with MetS, which is a significant risk factor for atherosclerosis (164,206,209–215). One study carried out by Sun *et al.* (2017) showed that hesperidin intake in an LDL receptor-deficient ($LDLr^{-/-}$) model mice fed with a high-fat diet reduced the hyperlipidemia and the atherosclerotic plaque area, inhibiting the macrophage foam cell formation (210). Furthermore, Mosqueda-Solís *et al*. found reduced circulating TG levels and lower gene expression levels of *Lpl* and *Fasn* in RWAT in Wistar rats supplemented with this bioactive compound. Although no significant changes were observed in body weight or fat mass in these rats, the authors reported smaller adipocyte size. Furthermore, the antihypertensive effects of hesperidin were explored, demonstrating a significant reduction in both systolic and diastolic blood pressure (209). On the other hand, findings from a systematic review and meta-analysis evaluating the efficacy of hesperidin supplementation on blood pressure concluded that hesperidin intake is not consistently associated with significant changes in humans (216).

The biological properties of hesperidin on bone tissue have also been reported in several studies, suggesting this bioactive compound as a potential treatment for managing bone diseases like osteoporosis and osteoarthritis (217). Different studies demonstrated that dietary intake of hesperidin significantly prevents bone loss in rodent models of osteoporosis induced by ovariectomy and these effects were accompanied by an improved lipid profile (218–220). According to these authors, hesperidin consumption enhanced BMD in the femurs (218–220) and improved femoral strength, preventing trabecula bone resorption by reducing the number of osteoclasts (218,219). Furthermore, Lim *et al.*

(2014) also observed in OVX rats a reduction in blood markers of bone resorption (CTX-1) and formation (OC) following 8 weeks of hesperidin supplementation (220). Overall, hesperidin intake was accompanied by a lipid-lowering effect, reducing the circulating levels of TG, TC (218–220), and LDL-c (220). Thus, these results suggest that hesperidin protects may be useful in the prevention and control against ovariectomy-induced bone loss and disrupted lipid metabolism. Hesperidin has also shown beneficial effects on arthritis conditions. In this regard, Umar *et al.* (2013) revealed that hesperidin mitigated the detrimental effects on bones and joints associated with rheumatoid arthritis, thereby suppressing the progression of the disease (221).

Although these results obtained at the preclinical level are promising, human clinical trials have generally obtained inconclusive findings (192,222). For instance, the uncertain outcomes regarding blood pressure after hesperidin intake in humans may be attributed to the limited absorption and bioavailability of hesperidin. Our research team has recently shown that the supplementation with a micronized form of hesperidin extract, primarily containing the 2S isomer (M2SH), significantly improves the bioavailability of this flavanone (222). This exciting discovery opens up opportunities for further investigations to determine if this heightened bioavailability results in amplified cardioprotective and bone-related benefits.

Phytosterols are phytosteroids with a similar structure to cholesterol that are naturally present in large levels in seeds such as pumpkin and sesame; nuts such as pistachios, walnuts, peanuts and almonds; and vegetable oils derived from rapeseed, sunflower, wheat germ, corn, soybean and avocado; and legumes, whereas, grains, fruits, and vegetables contain smaller amounts (223). The body acquires cholesterol through two main pathways: consumption of cholesterol-containing foods and endogenous production by the liver. Unlike cholesterol, humans are not able to endogenously synthesize

phytosterols and just can be obtained from the diet. Because of their comparable structure, ingested phytosterols cause a competitive exclusion of cholesterol from bile acid micelles in the digestive tract, reducing intestinal cholesterol absorption (159,224–227). However, once absorbed and metabolized, phytosterols just are maintained in plasma levels at approximately 0.5% of TC concentrations. It has been demonstrated that a moderate and consistent dose of sterols administered over an extended period can lead to increased levels and enhanced effects of these compounds (228). Generally, the intake of phytosterols is related to lower TC and LDL-c concentrations (159,224–227). Indeed, the European Food Safety Authority (EFSA) supports phytosterol supplementation, concluding that consuming 1.5 to 2.4 g/day of phytosterols may lower blood cholesterol levels and reduce the risk of coronary heart disease (229). On the other hand, in line with menopausal status, Xia *et al*. (2019) revealed that the consumption of 2 g/day of phytosterols significantly lowered blood TC and LDL-c in postmenopausal women with a BMI higher than 25 Kg/m², while the supplementation did not show significant effects on TG and HDL-C levels (224). Furthermore, an increasing number of clinical trials further support the anti-obesity effects of these phytosterols in patients with obesity. A cross-sectional Chinese study carried out by Li *et al*. (2018) demonstrated that a high dietary intake of phytosterols was associated with lower BMI and waist circumference, and was effective in preventing obesity and overweight conditions (230). In 2019, highlights obtained from randomized controlled trials evidenced that 1-2 g/day of phytosterol intake over 16 weeks significantly reduced BMI and body weight in individuals with a baseline BMI > 25 kg/m² (231).

On the other hand, some lines of research suggest that phytosterols may have significant effects on glucose metabolism. Studies have shown that phytosterols enhance the expression of the glucose transporter 4 (GLUT4) in key tissues such as skeletal muscle,

liver, and white adipose tissue, contributing to reduced glucose levels and improved insulin sensitivity (232,233). The activation of the AMPK pathway promotes GLUT4 translocation and elevates adiponectin levels, thereby supporting glucose homeostasis and potentially providing benefits against obesity, T2DM, and MetS (159,227). However, additional clinical trials would be of great value in shedding more light on the anti-hyperglycaemic and anti-diabetic effects of phytosterols.

3.2. Amino acid-related compounds

Amino acids (AAs) are organic substances with multifaceted functions that are crucial to maintaining whole-body homeostasis, such as cell signaling, redox balance, energy regulation, immunity, reproduction, and biosynthetic processes. As an example, AAs play a vital role in maintaining mucosal integrity and barrier function in the intestinal tract. They serve as essential precursors for the synthesis of metabolic active proteins, glutathione (GSH), and other molecules utilized by small intestinal mucosal cells (234). Given that not all AAs can be synthesized by mammals, an optimal balance of AAs in the diet and circulation is crucial for whole-body homeostasis (235). While the role of dietary lipids and carbohydrates has been comprehensively studied, there is limited information on the significance of dietary AAs in mitigating health risk factors. Different health risk factors or diseases associated with menopausal status have been shown to be accompanied by diminished circulating levels of some AAs. Thus, negative correlations have been found between the circulating levels of glycine, and histidine with obesity and metabolic alterations such as IR (236,237), and between cysteine and BMD in postmenopausal women with osteoporosis (238). Regarding obesity, higher dietary intake of certain AAs, including histidine, cysteine and serine, have been shown to be inversely associated with obesity risk (239). These three AAs are intricately connected in the histidine metabolism

and are essential for the synthesis of GSH (240,241).

Although there is limited information about the effects derived from the intake of different AAs, in the context of a nutraceutical supplementation, in mitigating health risk factors, increasing accumulative evidence, primarily obtained in rodents, but also in humans, have shown that intake of AAs such as histidine (5,8,10,15–17), carnosine (9,11), serine (7,12), and cysteine (13,14) can reduce obesity, improve glycaemic control, and alleviate IR, inflammation, and oxidative stress.

L-histidine is a crucial essential AA for mammals and other species, which cannot be synthesized *de novo* in humans and must be obtained through dietary sources (242,243). Although it is particularly abundant in red meat and fish, supplementation may be necessary in various populations. Some studies linked lower circulating levels of histidine to pathological conditions, such as non-alcoholic fatty liver disease (NAFLD), chronic obstructive pulmonary disease and chronic kidney disease, in addition to obesity (157,239,243). Remarkably, multiple investigations in humans have demonstrated associations between the histidine intake and improved conditions related to MetS, including overweight and obesity (242–248), especially in women (244,246–248). Thus, dietary intake of histidine or the supplementation with this AA restored the circulating levels of histidine, which were inversely associated with fat mass (244,248), BMI (244,248), waist circumference (244), HOMA-IR (244,248) acute inflammation biomarker C-reactive protein (CRP) (244,246) and some pro-inflammatory cytokines such as IL-6 and tumor necrosis factor-alpha (TNF-α) (244,246,248). Furthermore, increasing evidence in rodents suggests that histidine supplementation exerts an inhibitory effect against obesity by suppressing food intake, possibly due to activation of histamine neurons in the hypothalamus, where histidine is converted into histamine by

histidine decarboxylase (HDC) (242,249–251). On the other hand, some preclinical studies have shown that increased levels of histamine in the brain observed after the oral supplementation with histidine or via injections of this AAs ameliorated cognitive decline, improving learning and memory (252,253), and reducing anxiety-like behavior in HDC knock out mice (254,255).

L-carnosine, a dipeptide synthesized through ATP hydrolysis of β-alanine and histidine, is naturally abundant in skeletal muscle and the brain and is found in smaller amounts in other tissues such as the heart, liver and adipose tissue (256). It is present in dietary sources such as red meat and fish (256). It has been reported that carnosine supplementation has potential preventative and therapeutic benefits against CVDs, obesity, MetS and T2DM (256–261). Its beneficial effects can be partly attributed to the fact that carnosine acts as a nonenzymatic free-radical scavenger and a natural antioxidant. It plays a vital role in inhibiting the formation of advanced glycation end products (AGEs), such as glycated hemoglobin (HbA1c), and advanced lipoxidation end products (ALEs), such as malondialdehyde (MDA) and 4-hydroxynonenal (HNE), through its ability to prevent non-enzymatic glycation and the formation of reactive carbonyl species (RCS) generated by lipid and sugar oxidation, which are common mechanisms in the pathogenesis of CVDs, diabetes and Alzheimer disease (257,260). These inhibitory actions can contribute to improve glucose metabolism and to reduce IR, as was evidenced by the decreased HOMA-IR observed in different studies (257,260,262,263). Thus, in a double-blind randomized pilot trial, the intake of 2g/day of carnosine for 12 weeks reduced fasting insulin circulating levels and HOMA-IR, and significantly improved the pre-existing impaired glucose tolerance in individuals with overweight or obesity (263). Furthermore, L-carnosine can ameliorate atherosclerosis by facilitating the removal of aldehydes from atherosclerotic lesions (258). Concerning the

effects of this AA on lipid metabolism, Al-Sawalha *et al*. (2019) observed that a 16-week L-carnosine intervention countered the increases in RWAT weight, TC, and LDL-c induced by the intake of a high-fat, high-carbohydrate diet in rats (264). Furthermore, Mong *et al.* (2011) reported that histidine and carnosine intake, separately, for 8 weeks significantly reduced body weight, epididymal fat, and hepatic TG and TC levels, counteracting the lipogenic effects of a high-fat diet in mice by suppressing the activity and mRNA expression of key lipogenic enzymes (Glucose-6-phosphate dehydrogenase, malic enzyme, fatty acid synthase, and HMG-CoA reductase) and sterol regulatory element-binding proteins (SREBP-1a, -1c, and -2), thereby reducing lipid accumulation in the liver and adipose tissue (265). Furthermore, carnosine supplementation improved cognitive decline in animal models of Alzheimer's disease, aged people, and people with mild cognitive decline (257). On the other hand, carnosine intake showed positive effects on anxiety, stress, and depression-like behaviors in rodents (266,267) and humans (268).

L-cysteine is considered a semi-essential AA because human beings have the capacity to synthesize it from the AA methionine (269) and its circulating levels are regulated by its precursors, essentially serine (270). Altered cysteine homeostasis and reduced blood levels of this AA have been reported in diabetic human subjects (271,272) and in diabetic animal models, such as streptozotocin-treated rats (273) and Zucker diabetic fatty rats (274–276). It has been reported that circulating and tissue GSH levels decrease with age and diabetes (277). GSH is synthesized de novo from glycine, cysteine, and glutamate, being L-cysteine the rate-limiting AA for this reaction (240,277). Several preclinical studies showed that cysteine supplementation restored the hepatic GSH levels (271,274) and Jain, Sushil K *et al.* (2009) also observed a reduction in inflammatory markers (MCP-1 and CRP) and decreased HOMA-IR (275) in Zucker diabetic rats. Furthermore, L-cysteine is well-described as an inhibitor of the hepatic enzyme histidine ammonia lyase

(HAL), leading to higher histidine levels through the suppression of its catabolic activity (278). This makes it an ideal candidate for regulating histidine levels, particularly in the liver. On the other hand, two studies identified a robust association between lower circulating levels of cysteine and low BMD (238,279). Baine *et al.* (2007) reported these associations in 110 postmenopausal women with osteoporosis including an increase in the bone turnover marker CTX-1 (279). Elshorbagy *et al.* (2009) found similar associations in both men and women over age 40, with the correlations being stronger in the 3,009 women included in the study (238). Furthermore, cysteine supplementation for 8 weeks had similar effects to 17β-oestradiol injections in counteracting the loss in BMD in OVX mice (280), suggesting an important role for this semi-essential AA in bone metabolism.

L-serine is traditionally considered a non-essential AA because it is synthesized in mammals from 3-phosphoglycerate. Serine has a crucial role in central metabolism, participating in the synthesis of proteins, nucleic acids, and lipids (281) and therefore, it is involved in metabolic homeostasis (241,282). Lower circulating levels of serine in humans have been linked to obesity as well as to T2DM (246,282) and have been found in patients with NAFLD (283). Serine serves as a precursor for the synthesis of the AAs glycine and cysteine (270). Furthermore, serine plays a crucial role in maintaining redox balance by facilitating the synthesis of GSH and folate-dependent NADPH in the liver. In response to oxidative stress conditions, serine-dependent one-carbon metabolism switches from methylation to trans-sulphuration, which results in the condensation of serine with homocysteine to generate cysteine, thereby increasing GSH synthesis (241). A combined supplementation of serine and cysteine contributed to elevate the hepatic levels of GSH (284) and the intake of serine improved hepatic tissue in injured liver mice models by increasing GSH and lowering TG levels, lipid accretion, and reactive oxidative OS levels (283).

In another study carried out with C57BL/6J mice, serine supplementation increased total GSH, GSH/GSSG ratio and superoxide dismutase (SOD), and diminished the circulating levels of leptin, MDA, interleukin-1 beta (IL-1β) and homocysteine (285). Additionally, serine intake ameliorated glucose homeostasis reducing body weight, HOMA-IR and glucose levels in a non-obese diabetic mouse model (286).

NAFLD is a metabolic disorder that frequently accompanies obesity and MetS, and that can also appear with menopause (287–289). In a very recent study carried out by members of our group it was reported a significant decrease in the circulating levels of histidine in patients with morbid obesity as the severity of NAFLD increases (157). Interestingly, in the same work, the authors demonstrated that the combined supplementation with histidine, serine, cysteine and carnosine decreased hepatic steatosis in both diet-induced and genetic leptin-deficient ob/ob mouse models and in OVX rats as well as ameliorated liver inflammation, IR and hypercholesterolemia in the mice models (157). The authors stated that this MI could be an effective therapy for ameliorating NAFLD because (i) histidine is an essential AA that needs to be obtained from the diet; (ii) carnosine is a histidine-containing dipeptide and, therefore, can increase histidine levels; (iii) cysteine is an inhibitor of the histidine catabolizing HAL; (iv) serine is a precursor of cysteine; and (v) one of the main hallmarks of NAFLD is oxidative stress, and serine and cysteine may increase the cellular levels of glutathione, the most abundant endogenous antioxidant (284).

4. Biomarkers: essential indicators of the health status and their role in nutrition studies

According to the National Institutes of Health (NIH), a biomarker is defined as "a characteristic that is objectively measured and evaluated as an indicator of normal biological processes, pathogenic processes, or pharmacologic responses to a therapeutic intervention." (290) Therefore, a biomarker refers to any feature that can be objectively quantified or measured through various biochemical samples, assessing an organism's exposure to normal or pathological processes, or their response to dietary or pharmacological interventions, such as nutraceutical supplements or HRT.

A key focus in modern biomedical research is to decode the intricate relationships between health, disease states, nutrition, and medications (290,291). In this context, the discovery of biomarkers serves as invaluable tools for personalized identification of the boundaries between health and disease, as well as monitoring their progression in response to dietary interventions. In this context, three main classes of biomarkers can be identified: **(1) the diagnostic biomarkers**, detect or confirm the presence of a disease or an abnormal condition; **(2) prognostic biomarkers** are employed to assess the probability of a clinical event, the recurrence of a disease, or the progression of a disease in patients with a particular medical condition; and **(3) predictive biomarkers**, which can indicate the likelihood of an individual or group effectively responding to a specific treatment due to their inherent characteristics (290,292).

Currently, there are few biomarkers applicable to nutrition, since most are end-point biomarkers, used in the clinic and which indicate an advanced pathophysiological state, at which point nutritional interventions as a strategy to prevent diseases or reverse their onset it is in most cases not useful. For this reason, there is a need to identify biomarkers

of homeostatic robustness that allow the scientific community to; a) detect early alterations that can be influenced through a nutritional intervention; b) identify the metabolic and physiological processes on which foods and nutritional supplements can act. These biomarkers can, therefore, make it possible to support health claims made on food, in accordance with European legislation. Thus, it is essential to identify biomarkers that indicate a predisposition to a pathological state to explore the effects of nutraceutical/food supplementations on our metabolism (293). Understanding how nutritional strategies can influence and potentially mitigate this predisposition is crucial for preventing the progression to more serious health conditions. By detecting early changes, there is potential to reverse this propensity before it develops into a more severe condition, such as menopause-related diseases (e.g. obesity, CVDs and osteoporosis). Given that early changes induced by nutraceutical supplementation are typically subtle compared to those brought about by pharmacological treatments, new approaches using sensitive and advanced techniques are necessary for the detection of these small changes as biomarkers. These approaches should require the collection of non-invasive or minimally invasive biological material, such as body fluids like blood (the most used), urine, saliva, and even tears, allowing for their application in clinical studies and the subsequent identification of biological profiles (gene expression, proteins, and/or metabolites) associated with a higher risk of developing pathologies (290,292). In this sense, advancements in omics sciences, including genomics, metabolomics, transcriptomics, and proteomics, have expanded opportunities for identifying novel biomarkers of different types due to their high sensitivity (294,295). These approaches have been extensively researched in the context of various pathophysiological disorders, utilizing advanced tools to investigate alterations in nucleic acids, proteins, peptides and metabolites (294–296).

The boundary between good health and illness is not clearly defined and can vary significantly among individuals (297). This variability is particularly evident in the context of female reproductive aging, which is influenced by a multitude of factors. These factors include changes in cycle length, hormonal alterations within the HPG axis, the age at which the FMP occurs, and the resulting pathophysiological conditions. Furthermore, genetic individuality and environmental interactions play critical roles in this process, among other variables (298).

On the other hand, the relationship between a healthy, balanced eating pattern and health promotion, particularly in nutritional aspects, is relatively well-defined (157,192,225,299). However, the intricate composition of food supplements and dietary patterns means they can exert both beneficial and detrimental effects on health. Therefore, robust evaluation systems are necessary to assess the impacts of alternative therapies to HRT, such as nutraceutical supplements, on health and disease states in peri- and post-menopausal women (300).

Currently, health promotion strategies that rely on food supplements are often hindered by the absence of **early** and measurable **biomarkers**, specifically predictive biomarkers. These types of biomarkers are particularly valuable for identifying individuals at risk or detecting the onset of a disease even before symptoms appear. Furthermore, they could also anticipate the long-term effects of adopting specific dietary patterns (301,302). Therefore, it is of paramount importance to identify and validate **early biomarkers** that can provide insights into the health impacts of nutraceutical supplements before functional and physiological alterations manifest during the menopausal transition and subsequently in menopause.

In this scenario, although a biomarker can simply be the level of a certain molecule, the concept of multivariate biomarkers becomes crucial. Multivariate biomarkers combine variables of different natures, providing precise information about an individual's health status. To obtain these biomarkers, it is essential to integrate all the data generated by omics techniques through systems biology. In this context, metabolomics emerges as a highly valuable tool for assessing evolutionary and multifactorial changes from the onset of female reproductive aging to menopause (3). These physiological processes rely on a complex network of mechanisms governed by biochemical reactions mediated by enzymes and regulatory proteins. The culmination of these interactions manifests in the metabolome of an organism, which encompasses the complete set of metabolites present in a cell, tissue, or entire organism. Metabolism functions to counteract these challenges in order to maintain homeostasis. Over time, disruptions to homeostasis can lead to alterations in the organism's metabolomic profile. Metabolomic analyses using multiple platforms [(Nuclear Magnetic Resonance (NMR), Liquid chromatography-mass spectrometry (LC-MS), Gas chromatography-mass spectrometry (GC-MS)] and carried out in plasma/serum to detect both polar and hydrophobic metabolites and in urine (polar metabolites) serve as a critical tool for identifying these disturbances, potentially yielding new biomarkers for early detection and diagnosis. These approaches can be of great value to elucidate how menopause impacts on regulatory systems affected by changes in hormones and metabolites (303). Consistent cross-sectional and longitudinal studies have revealed correlations between menopause and a wide array of metabolic biomarkers, suggesting that the transition to menopause triggers various metabolic changes independent of chronological aging (3). Nonetheless, despite these findings, there remains a limited understanding of the underlying mechanisms associated with the menopausal transition. For instance,

hypoestrogenism associated with menopause has been linked to adverse effects on the gut microbiome (113), biochemical pathways involving carbohydrates and lipids (2), AA metabolism (2), and hormone regulation (25). Moreover, metabolomics opens avenues for developing novel strategies, both pharmacological and nutritional, to reprogram metabolism and restore homeostatic balance (304). In shedding more light on the elucidation of the mechanisms of different diseases of metabolic origin, such as obesity, osteoporosis, CVDs, IR, T2DM, and dyslipidemias (4,143,305–309).

4.1. Peripheral Blood Mononuclear Cells (PBMCs) as a source of omics-based biomarkers

Blood is composed of two phases:

(1) **Solid phase**, also referred to as the cellular component, which includes erythrocytes (red blood cells) and platelets without nuclei; and leukocytes, divided into mononuclear types such as lymphocytes (T cells, B cells, Natural Killer cells) and monocytes (macrophages and dendritic cells), which present a single round nuclei, as well as granulocytes (neutrophils, basophils, and eosinophils), having a multi-lobed nuclei (**Figure 7**) (310,311).

(2) **Liquid phase**, known as serum or plasma component, which acts as the medium for transporting all molecules carried by the blood (310,311).

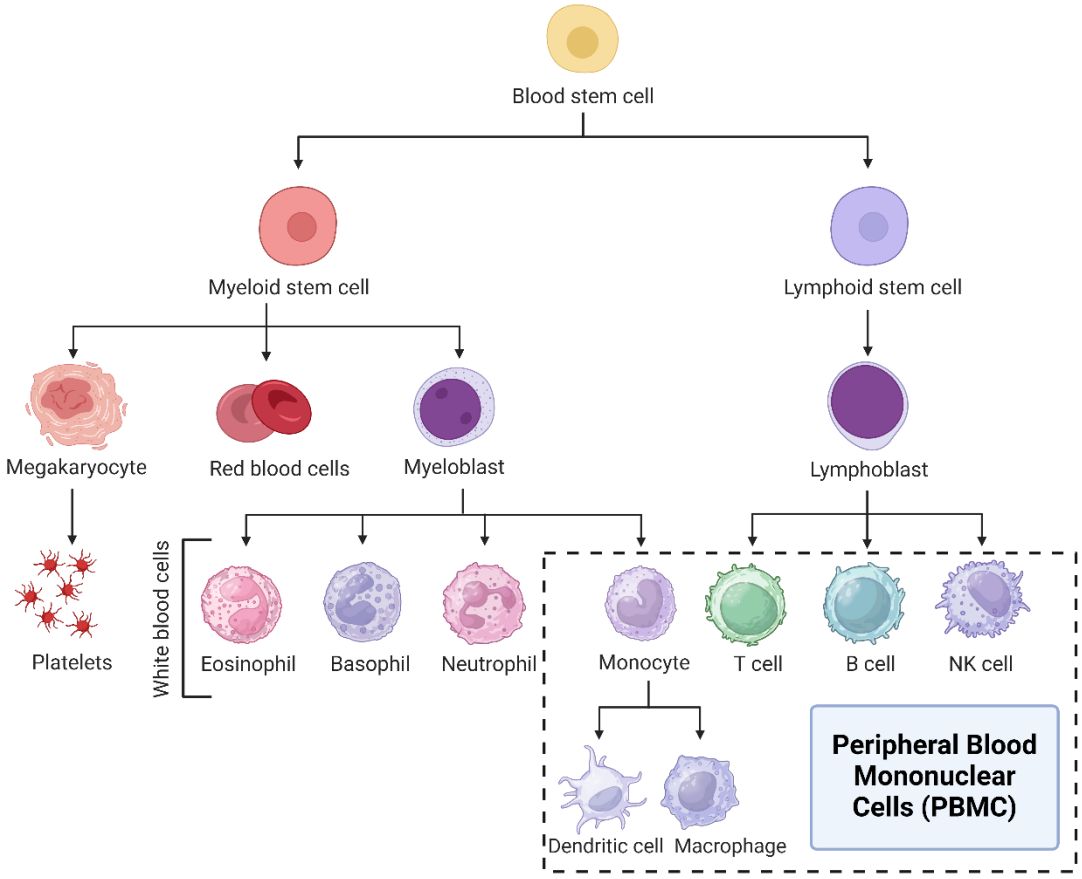


Figure 7. Lineage diagram of blood cell types in circulation. Created with biorender.com.

Although erythrocytes are the most abundant type of blood cells and are responsible for transporting oxygen and carbon dioxide throughout the tissues and the entire body, leukocytes, while less abundant, play a crucial role in the body's defense against infections and diseases (310,311).

PBMCs are a subgroup of mononuclear white blood cells composed of approximately 80-85% of lymphocytes (including Natural Killer cells, B cells, and T cells), with the remaining 15-20% represented by monocytes, particularly macrophages, whereas dendritic cells constitute only 1-2% of all PBMCs (312). PBMCs have been widely recognized as a valuable biological material for studying diseases related to the immune system, such as autoimmunity-related disorders, and to predict immune-related responses to specific interventions (313–317). Furthermore, the use of PBMCs in clinical research

has been extended to other disorders such as T2DM, obesity, cancer, and Alzheimer's disease, as the immune system is closely linked to these pathologies (318–329).

Recent studies have demonstrated that transcriptomic biomarkers derived from PBMCs offer valuable insights into disrupted global gene expression patterns observed in various pathologies. PBMCs express about 80% of the genes encoded in the human genome and reflect the pathophysiological profiles of other internal organs, making them crucial in toxicological, nutritional, and clinical studies (330–336). This is why they are used as surrogate tissues that are harder to access directly (337).

Furthermore, these cells offer several advantages. Thus, PBMCs are an easily obtainable biological material, collected from humans using minimally invasive blood extraction and easily obtained using isolation techniques (330,334). The sampling requires very basic means, and this subset of blood cells can be repeatedly collected over the course of a study differently from what occurs with other tissues such as white adipose depots, muscle, and liver, allowing for great repeatability. The utilization of PBMCs as a model that can capture the molecular changes that occur in response to different interventions in key internal tissues streamlines the extrapolation of findings from animal models to humans, mitigating the need for invasive procedures such as biopsies and the related significant discomfort that people may suffer (338–340).

Their utility is underscored by their role as sentinel cells, traversing the body and actively interacting with various tissues to gather information on changes in response to different stimuli. They respond to internal signals like sex hormones and external factors such as dietary or bioactive compounds intake (333,341). These interactions can profoundly influence their gene expression profiles (333) making these changes valuable biomarkers for diagnosing or predicting the progression of various diseases (342,343).

Given their potential, research into the gene expression profile of PBMCs has surged, establishing these cells as valuable tools for identifying diagnostic markers for conditions such as obesity, cancer, and CVDs (320,342,344–349). Typically, these studies imply the analysis of the entire gene expression profile of PBMCs from both healthy subjects and from individuals with different degrees of illness, using microarray analysis to detect even the smallest variations that may significantly impact on disease progression (347,349). In the nutrigenomics framework, PBMCs have been extensively utilized as a tissue model in both human and animal studies related to dietary interventions and nutraceutical supplementation. Remarkably, PBMCs have demonstrated the ability to reflect the transcriptomic profile of key organs like the liver, adipose tissue, muscle, and hypothalamus in response to different feeding conditions (299,330,350) and diverse dietary patterns (320,330,342–344,350–358).

Recent studies have emphasized the usefulness of examining the effects of bioactive compounds, such as isoflavones, on PBMCs in postmenopausal women and OVX rats, especially concerning CVDs and cancer (357–359). Isoflavones, discussed earlier in section 3, are phytoestrogens that mimic oestrogenic activity and have been shown to potentially have a generally positive impact on menopausal women. However, in the framework of PBMCs, the translational potential of the isoflavones-related findings from OVX rats to humans remains unclear. Research indicates that, in this subset of blood cells, the gene expression response to isoflavones is significantly more pronounced in rodent models compared to humans (357). This discrepancy underscores the necessity for studying other bioactive compounds in preclinical postmenopausal preclinical models, such as OVX rats, to gain more knowledge about the translational potential of PBMCs to reflect at molecular level the effects produced by these therapeutic interventions to mitigate the adverse effects of menopause on women's health.

Moreover, the ability of PBMCs to capture changes in bone-related metabolism has been evidenced in several studies showing that these cells can reflect changes in bone remodeling dynamics, making them a valuable tool for investigating osteoporosis (360,361). Notably, a recent study carried out by Li Gao *et al*. (2021) demonstrated that the expression levels of *tgfb3* were significantly downregulated in PBMCs and *tgfb3* mRNA levels in these cells were positively correlated with multiple parameters that indicated an altered bone microstructure in OVX rats. Furthermore, under the stimulus of moderate-intensity treadmill exercise, the expression of *tgfb3* in PBMCs increased, which was associated with improvements in trabecular bone parameters. These findings suggest that the TGF-β signaling pathway plays a crucial role in bone health and its dysregulation may contribute to osteoporosis in postmenopausal women, and that, remarkably, PBMCs reflect at gene expression level the alterations of this pathway occurring during the postmenopausal state, being also sensitive to interventions addressed to improve bone health, such as exercise (361). Therefore, these results reinforce the ability of PBMCs to exhibit early changes in response to various stimuli, making these cells a sensitive tool for monitoring the effects of different interventions on menopausal health.

Both the menopausal transition and the postmenopausal state represent significant periods in a woman's life, characterized by profound hormonal changes that can influence long-term health and well-being. There is a clear imperative for substantial advancement in research in this field, particularly in the identification of biomarkers associated with the menopausal transition. These biomarkers not only can contribute to a better understanding of the responsiveness to diverse nutritional interventions but also facilitate the characterization of mechanisms of action of bioactive ingredients that may offer health benefits during peri- and postmenopause. Therefore, transcriptomics-based approaches in PBMCs cannot only help to obtain a deeper knowledge at the molecular level of the

metabolic and hormonal changes associated with menopause but also lay the groundwork for personalized and effective management strategies to enhance the quality of life of women during this life stage.

II. HYPOTHESIS AND OBJECTIVES

Menopause is a natural phase in a woman's life associated with reproductive aging. It is characterized by a decline in ovarian function and by a reduction in oestrogen production that already occurs with the appearance of irregular menstrual cycles during the menopausal transition, known as perimenopause, and is exacerbated during the postmenopausal state. This can lead to vasomotor symptoms and osteoporosis, which are frequent health-related complications associated with menopause, but also to obesity and metabolic-related disturbances such as hypertension, dyslipidemia, insulin resistance, and metabolic syndrome, which, in turn, can increase the risk of suffering from cardiovascular diseases. Given the notable rise in women's life expectancy, women may spend at least a third of their lives in a postmenopausal state, and therefore, there is worldwide interest in slowing down and ameliorating menopause-related alterations to improve their being and quality of life.

Some cross-sectional and longitudinal studies have revealed associations between menopause and alterations in a wide array of metabolic biomarkers that were independent of the women’s chronological age, suggesting that this biological stage *per se* triggers various metabolic changes. Nevertheless, so far, very few studies have identified circulating signatures characteristic of perimenopause and there is still a limited understanding about the underlying mechanisms associated with menopause transition. Filling this gap can provide valuable scientific knowledge concerning the molecular changes occurring at very early stages of perimenopause to pave the way for developing novel treatments and lifestyle interventions aimed at preserving the endocrine and metabolic functions of perimenopausal women and alleviating at later stages postmenopausal-related alterations.

In recent years, the controversy about some potential risks associated with the prescription of hormone replacement therapy (HRT), which usually consists of the

administration of oestradiol and progestin, alone or in combination, has prompted many women to look for alternative therapies to address menopause. Although HRT remains the most effective solution for vasomotor symptoms, osteoporosis and metabolic disturbances related to the postmenopausal state, its prescription is not recommended for women over 60 years old, nor after more than 10 years since their last menstrual cycle or during prolonged treatment periods. This caution comes from the controversy over HRT benefits and risks derived from the unexpected findings of the Women's Health Initiative (WHI), pointing towards a higher risk of suffering cardiovascular diseases, and endometrial and breast cancers in response to certain HRT treatments. Hence, the decision to prescribe HRT should be thoroughly evaluated and personalized according to each patient's medical history, symptoms, and risk factors.

In this framework, alternative therapies have emerged to ameliorate the metabolic alterations associated with menopause. Several lines of research, including some carried out by our research group, suggest that the combined supplementation of various bioactive compounds, natural extracts or amino acid-related compounds, targeting complementary pathways is an effective strategy to ameliorate multifactorial diseases, such as fatty liver, and cardiometabolic risk factors. These compounds can positively influence cellular mechanisms and biochemical pathways disrupted by the metabolic disorders that can be associated with menopause, providing benefits from the early onset of these conditions during the menopausal transition through their progression into the postmenopausal state.

Over recent years, our research has combined the use of classical biochemical and molecular techniques with the application of omics sciences, as well as system biology approaches, to deeply characterize the effects of these bioactive compounds, to shed light on their underlying mechanisms and to identify novel biomarkers reflecting at the

molecular level the effects of these compounds. Nutrigenetics studies have identified genetic variants that condition a woman's metabolism during the transition to menopause, as well as the response to certain nutrients, predicting individual responses to nutritional interventions. Detecting specific biomarkers using other omics sciences, such as metabolomics and transcriptomics, can help to monitor and measure these responses, providing a clearer understanding of the effectiveness of these bioactive compounds and their mechanism of action. Our research has shown that, by interacting with molecular-level mechanisms, the intake of these natural extracts, bioactive compounds and nutraceuticals can promote health benefits by reducing systemic resistance. This experience forms the basis from which we pose the challenge of developing precision nutrition strategies for one of the least explored woman's life stages from this perspective: the transition to menopause (perimenopause) and postmenopause, aiming to maintain a healthier and more sustained state over time.

In this present PhD thesis focused on this line of research, **we hypothesized that the consumption of two different multi-ingredients (MI), including each of them a blend of bioactive compounds that act against complementary targets can serve as an alternative therapy, designed under a multifaceted approach, to ameliorate obesity and to improve the cardiometabolic risk associated with the menopausal status through the regulation of key biochemical and molecular pathways involved in the appearance and progression of these menopausal-related complications**. In summary, the intake of these two MI-based supplements could induce significant physiological and metabolic changes, providing benefits during perimenopause and through their progression into the postmenopausal state.

For this purpose, we selected two distinct blends: the first comprising three bioactive compounds of natural origin (curcumin, hesperidin, and phytosterols) and the second

consisting of four amino acid-related compounds (histidine, serine, cysteine, and carnosine). While most of these compounds have been shown to reduce fat mass and to mitigate menopausal-related metabolic changes when administered individually, mainly in animal models, to the best of our knowledge, the combined supplementation of the three natural bioactive compounds and the four amino acid-related compounds has not been yet evaluated. This multifaceted approach could provide better outcomes against various health risk factors that manifest during the postmenopausal period.

In addition, the precise characterization of the menopausal transition (perimenopause) and the postmenopausal state using preclinical models to reproduce the early and advanced alterations occurring during menopause can enable us to elucidate the molecular mechanisms underlying the metabolic adaptations occurring in response to these predictable changes, which are crucial for understanding exacerbated effects in postmenopausal women. This approach may provide insights into identifying their metabolic signatures in response to nutritional interventions.

The main objective of this PhD thesis was **to assess the potential benefits of consuming two different multi-ingredients (MI) — one containing curcumin, hesperidin, and phytosterols, and another comprising amino acid-related compounds such as histidine, serine, cysteine, and carnosine — on the physiology and metabolism of ovariectomized Sprague-Dawley rats**, a postmenopausal model with oestrogen deficiency, evaluating a wide range of cardiometabolic risk factors associated with the postmenopausal status and gaining knowledge on their underlying mechanisms. Additionally, the thesis aimed to **identify biomarkers of these metabolic risks at the early stages of natural reproductive aging using an ovarian-intact middle-aged model of rats resembling the characteristics of human perimenopause.**

To fulfill this purpose, the following objectives were set:

1. To accurately characterize menopausal transition in an ovarian-intact middle-aged model of Sprague-Dawley rats and to identify circulating signatures across perimenopause using metabolomics and lipidomics approaches (**Manuscript 1**).
2. To precisely characterize a preclinical model of postmenopausal state, namely ovariectomized Sprague-Dawley rats, assessing biometric, metabolic and biochemical parameters related to obesity, metabolic alterations and osteoporosis, as well as to evaluate whether these parameters are affected by age (**Manuscript 2**).
3. To elucidate whether PBMCs can reflect molecular changes associated with oestrogen deficiency in the postmenopausal stage induced by ovariectomy in Sprague-Dawley rats using a transcriptomics approach (**Manuscript 2**).
4. To investigate whether an oral supplementation with a multi-ingredient (MI) including hesperidin, phytosterols, and curcumin exerts beneficial effects against fat mass accretion and metabolic alterations associated with menopause in ovariectomized Sprague-Dawley rats (**Manuscript 3**).
5. To assess whether an oral supplementation with a multi-ingredient (MI) of amino acid-related compounds, including L-histidine, L-Carnosine, L-Serine and L-Cysteine exerts beneficial effects against fat mass accretion and cardiometabolic risk factors related to the postmenopausal state in an ovariectomized Sprague-Dawley rat model (**Manuscript 4**).
6. To explore the underlying mechanisms involved in the beneficial effects against fat mass accretion observed after the supplementation with the amino acid-related MI, using a transcriptomic approach carried out in the retroperitoneal white adipose tissue of ovariectomized Sprague-Dawley rats (**Manuscript 4**).

III. RESULTS

MANUSCRIPT 1

Impact of the Natural Female Reproductive Aging on the Rat Serum Lipidome

Julio Baudin,[a,b] Salvador Fernández-Arroyo[c], Antoni Del Pino[c], Francesc Puiggròs,[d] Lluís Arola,[b] Antoni Caimari [d]

[a] Eurecat, Centre Tecnològic de Catalunya, Technological Unit of Nutrition and Health, 43204 Reus, Spain

[b] Nutrigenomics Research Group, Department of Biochemistry and Biotechnology, Universitat Rovira i Virgili, 43007 Tarragona, Spain

[c] Eurecat, Centre Tecnològic de Catalunya, Centre for Omic Sciences, Joint Unit Eurecat-Universitat Rovira i Virgili, Unique Scientific and Technical Infrastructure (ICTS), Reus, Spain.

[d] Eurecat, Centre Tecnològic de Catalunya, Biotechnology Area, 43204 Reus, Spain.

Manuscript in preparation

ABSTRACT

Perimenopause is a transitional phase leading to female reproductive senescence, which can cause vasomotor symptoms and increase the risk of osteoporosis, obesity, and metabolic-related disturbances in middle-aged and elderly women. Nevertheless, little is known regarding the underlying mechanisms linked to menopausal transition, which could be of great value in designing new treatments and lifestyle-based interventions addressed to preserve the endocrine and metabolic functions of perimenopausal women and to ameliorate the postmenopausal-related alterations. In this study, we used an ovarian-intact middle-aged model of rats resembling the characteristics of human perimenopause and applied liquid and gas chromatography quadrupole time-of-flight mass spectrometry approaches for the determination of polar and lipid-related metabolites to identify characteristic circulating signatures across perimenopause. The gradual loss of regularity in the oestrous cycle occurring during the natural transition to reproductive senescence was associated with altered circulating levels of oestradiol, progesterone and luteinizing hormone and, in rats that were in an acyclic state, with histomorphological changes in the ovaries, including atrophy and a lack of stromal luteinization and corpus luteum. These results were accompanied by progressive significant changes in the lipidomic profile detected in serum as the oestrous cycles were losing regularity. Furthermore, we identified a set of lipid-related metabolites that already changed with the transition from a regular to an irregular oestrous cycle, including 9 phosphatidylcholines, 4 lysophosphatidylcholines, 2 phosphatidylethanolamines, cholesterol ester (18:2), 5a-androstan-3,17-diol and 17,18-Dihydroxyarachidonic acid, which could be used as a potential multivariate biomarker of early perimenopause. The translational applicability of these findings deserves further research.

Keywords: Lipidomics, perimenopause, immunometabolic health, osteoporosis, molecular biomarkers

INTRODUCTION

Perimenopause is a transitional phase leading to menopause, which can extend over several years with varying onset, duration and completion times (1,2). During this transition, women experience a variety of physical and psychological symptoms that could be directly or indirectly linked to changes in sex hormone secretion due to a dysregulation of the hypothalamic-pituitary–gonadal/ovarian (HPG) axis, longer periods between consecutive menstrual cycles, gradual decline in ovarian follicular function and others physiological changes (2–4). The appearance of the first symptoms related to the menopausal transition are usually vasomotor such as hot flushes, night sweats, sleep alterations, migraines, and affective disorders. However, the duration and intensity of these symptoms can vary greatly among women, ethnicity and age of first experience (5,6). In contrast, postmenopausal symptoms tend to be more detectable due to increased health risk factors associated with complete oestrogen depletion/deficiency, including osteoporosis, cardiovascular disease, stroke, insulin resistance, diabetes, metabolic syndrome (MetS), and ovarian cancer (7–10). Thus, the variability in the vasomotor symptoms and the lack of longitudinal studies tracking women through the perimenopausal transition, makes difficult to establish a clear understanding of perimenopausal symptoms and their underlying mechanisms linked to menopausal transition.

Preclinical studies with rodents have demonstrated that rats provide a well-established model for natural reproductive aging. The examination of vaginal smears (cytology) and vaginal histology are commonly used methods for the identification of the different stages of the oestrous cycle and assessing the ovarian function during the reproductive senescence (11–14). The oestrous cycle characterization is crucial, as oocytes have no regenerative ability and any abnormalities in the ovaries may be directly linked to

impairment in female reproductive aging. Ovulation in rats occurs at a regular interval of 4 or 5 days in young-mature adult female rats (sexual maturity at around 8 weeks of age) (15,16). At middle age, when rats are approximately 7-8 months-old (15,17,18), female rats proceed through sequential reproductive stages, experimenting with a transition from regular oestrous cycles to irregular cycles and becoming later acyclic (persistent oestrous). After the cessation of ovulation and entry into persistent oestrous, there is still some maturation of follicles, followed by atresia without ovulation, culminating in complete follicular depletion, arriving when the rats are about 20 month-old to the final stage of reproductive senescence in old rats, which is named persistent anoestrous (11,15,19). This progression in rat female reproductive aging mirrors the transitions seen in women from premenopausal, perimenopausal, and postmenopausal stages (17,20,21).

Despite these similarities in reproductive aging between female rats and women, there has been limited exploration of rodents' natural transition to acyclicity to gain insight into adjacent mechanisms of reproductive senescence progression. This is partly due to the more common use of ovariectomized models, which are useful in replicating rapid hormone depletion and evaluating the postmenopausal stage but may miss underlying mechanism changes that initiate and perpetuate the dysregulation of reproductive physiology in middle-age (21,22).

Different studies have identified molecular neuroendocrine changes in the hypothalamus during the natural progression from regular reproductive cycles to acyclicity in middle-aged female rats, comparable with the perimenopausal progression in women (21). These changes were associated with altered genes related to sex hormone feedback in HPG functions and the DNA methylation of genes required for hormone signaling, as well as melatonin and circadian pathways during the different stages of natural reproductive aging in female Sprague-Dawley rats (18,23). From a translational perspective, it would

be of great value to use biological samples obtained in an easy and minimally invasive way to detect changes across perimenopause to settle the bases for designing and implementing strategies and interventions at the early stages of natural reproductive senescence aimed at preserving the endocrine and metabolic function in women. Recent studies in women have revealed an association between reproductive senescence in the postmenopausal stage and alterations in the circulating lipidome. Post-menopausal women tended to exhibit accelerated patterns of lipidome aging compared to their pre-menopausal counterparts of the same biological age (24,25). However, the cause-effect relationship between lipidomic changes and reproductive senescence remains unclear and, to the best of our knowledge, there are no studies based on metabolomic and lipidomic approaches to identify circulating signatures characteristic of perimenopause. We hypothesized here that changes in circulating metabolite patterns already occur during the menopausal transition and, consequently, appear before reaching an advanced stage of menopause.

The objectives of this study were **(1)** to identify novel circulating metabolites influenced by natural reproductive senescence in female rats, **(2)** to elucidate further changes across perimenopause in the metabolome and lipidome to gain insight into the mechanisms underlying natural reproductive aging, **(3)** to identify potential non-invasive early biomarkers of perimenopause during the transition from regular oestrous cycles to irregular cycles. For this purpose, we deeply characterized a rat model resembling the characteristics of human perimenopause and used both liquid and gas chromatography quadrupole time-of-flight mass spectrometry methods for the determination of polar and lipid-related metabolites to identify characteristic circulating signatures across perimenopause. We reported changes in lipid-related metabolites with the appearance of irregular oestrous cycles, which could pave the way to design and implement potential

therapies in a very early stage of female reproductive aging to slow down or ameliorate the health risk factors that can appear with menopause.

MATERIALS & METHODS

Animal care

All procedures related to animal experimentation were approved by the Animal Ethics Committee of the Technological Unit of Nutrition and Health of Eurecat (Reus, Spain) and the Generalitat de Catalunya (protocol code 11223). The study complied with the ARRIVE guidelines, followed the 'Principles of Laboratory Animal Care' and was carried out in accordance with the EU Directive 2010/63/EU for animal experiments. Twelve young (3.5 months-old, sexually naïve) and sixty middle-aged (8 months-old), female Sprague Dawley rats (INOTIV, Horst, Netherlands) were used at the beginning of the study. At their arrival at the animal facility of Eurecat and during the whole study, rats were housed in pairs at 22 °C under a 12 h light/dark cycle (lights on at 9:00 am) and had *ad libitum* access to food and water.

A daily assessment of oestrous cycling of female rats was conducted using the procedure described by McLean *et al.* (2012) (26). To ensure the rats were less stressed or more accustomed to handling, one week prior to the study's commencement, rats were handled for 5 minutes per day before monitoring oestrous cyclicity through daily vaginal lavage with ultrapure distilled water. The ovarian function/cycle status was evaluated daily via cytology of uterine cells obtained from vaginal lavage at 11 am. Vaginal smears were morphologically characterized based on the four stages of the cycle: estrus (E), metestrus (M), diestrus (D), and proestrus (P) (16,26). Animals were categorized as regular, irregular, or acyclic based on the last two weeks (14 days) of their smears. To ensure a more accurate interpretation of vaginal cytology and oestrous cycle stages, consecutive

daily samples were collected and analyzed collectively after one week. Cycle regularity was assessed based on the last two weeks (14 days) of their smears. This approach aimed to minimize differences in cell morphology among rats and reduce the likelihood of capturing transition stages in the oestrous cycle during sample collection. Regular animals exhibited three consecutive 4- to 5-day cycles, irregular animals showed two consecutive cycles that were 6 days or longer, and acyclic animals displayed 14 continuous days in persistent oestrous. Rats that exhibited persistent oestrous during the initial 14 days were excluded from the study. This decision was made to focus on evaluating biomarkers or early changes in the menopausal transition, and such as, the duration of acyclicity in these rats prior to the study was unknown. Based on age and oestrous cycle status, rats were assigned to one of the following four categories: young rats with regular cycling (Reg-Yng; n=10), middle-aged rats with regular cycling (Reg-Ma; n=7), middle-aged rats with irregular cycling (Irreg-Ma; n=8), and middle-aged rats with persistent oestrous (Acyc-Ma; n=8). All groups were fed a standard chow diet (Teklad Global 14% Protein Rodent Diet 2014, Harlan, Barcelona, Spain). The caloric breakdown of the diet (2.9 kcal/g) was 20% protein, 13% fat, and 67% carbohydrates. Body weight was recorded once each week, food was renewed daily, and the food intake was documented every 7 days. Rats at designated age and cycling status were euthanized at proestrus (regular and irregular groups) or persistent proestrus/estrus (acyclic group) after 4 h of diurnal fasting. Rats that did not meet the cytological criteria for each group were excluded from analyses for this study. Blood was collected by beheading and serum was obtained by centrifugation and stored at -80 °C until analysis. The liver, caecum, kidneys, left ovary, gastrocnemius and soleus muscle, and right femur, and the white adipose tissue depots (mesenteric -MWAT- and periovarian -POWAT- white adipose tissue depots) were rapidly removed, weighed, frozen in liquid nitrogen and stored at -70 °C until further analysis. The right ovary was

removed from attached tissues such as perigonadal white adipose tissue and uterine horns, weighted and fixed in 4 vol% neutral buffered formalin until ovarian cytology and histologic analyses. The left femur was also collected, immersed in 70% ethanol and stored at room temperature until to carry out a three-dimensional microcomputed tomography (microCT) analysis.

HOMA-IR and R-QUICKI analyses

The homeostasis model assessment-estimated insulin resistance (HOMA-IR) was calculated using the following formula: (Fasting Glucose level –mmol/L- × Fasting Insulin level-µU/mL-)/22.5 (27). Insulin sensitivity was evaluated by the revised quantitative insulin sensitivity check index (R-QUICKI) using the following formula: 1/[log insulin (µU/mL) + log glucose (mg/dL) + log FFA (mmol/l)] (28).

Serum analysis

Enzymatic colorimetric kits were used to determine serum total cholesterol (TC) (995280/QCA, Barcelona, Spain), triglycerides (TG) (992330/QCA, Barcelona, Spain), glucose (992330/QCA, Barcelona, Spain) and non-esterified free fatty acids (NEFAs) (WAKO, Neuss, Germany). Circulating insulin levels were measured using a rat/mouse ELISA kit (10-1250-01/MERCODIA, Uppsala, Sweden), and C-reactive protein (CRP) was quantified using the ERCRP ELISA kit (INVITROGEN, Massachusetts, USA). Serum leptin levels were determined with a rat ELISA kit (EZRL-83K/Millipore, Barcelona, Spain), and serum adiponectin levels were quantified by a Rat Total Adiponectin/Acrp30 Quantikine ELISA Kit (RRP300/R&D systems, Minnesota, USA). To quantify the levels of circulating female sex hormones of oestradiol (17β-E2), progesterone (P), luteinizing hormone (LH) and follicle-stimulating hormone (FSH) at the endpoint, the ELISA E2 kit (CSB-E05110r/CUSABIO, Houston, USA), ELISA

progesterone kit (CSB-E07282r/CUSABIO Houston, USA), ELISA LH kit (CSB-E12654r /CUSABIO, Houston, USA) and ELISA FSH kit (CEA830Ra/Cloud-Clone Corp., Houston, USA) were used, respectively.

Cytological and Histological Analyses

The excised right ovary from each rat was immediately preserved in buffered formalin (4% formaldehyde, 4 gr/L NaH2PO4, 6.5 gr/L Na2HPO4; pH 6.8), sectioned at a thickness of 5 µm, and subsequently stained with hematoxylin & eosin (H & E). Ovarian images (magnification 15×) were captured using a microscope (SMZ745T; Nikon, Tokyo, Japan) coupled with a digital sight camera (DS-Ri1, Nikon). Ovarian examinations were performed according to the criteria of previous reports (12,13,15,29). In order to avoid any bias in the analysis, the study employed a double-blind design, preventing the researchers from viewing any data from the rats during the histopathological analysis. A detailed microscopic examination of the prepared ovarian and the criteria for assessment was established through a double correlation by professional histopathologists (Eldine Patologia SLP, Tarragona, Spain). The ovarian histopathological examination included an evaluation of follicular development (changes in the number of primordial, primary, secondary, and antral follicles development, presence/absence of corpus luteum, changes in development, regression in the number of corpus luteum) as previously described (19,29,30) in addition to any abnormalities/ lesions, such as the presence/absence of ovarian atrophy. Features of the ovaries throughout the reproductive aging period are described in detail in the Results section.

Microcomputed tomography analyses

Bone composition of the left femur was determined post-mortem in fixed samples by three-dimensional MicroCT analysis, as was previously described (31). The bone mineral

content (BMC) and bone mineral density (BMD) values were quantified from MicroCT scans using the GE MicroView software v2.2.

Metabolomics and lipidomics analyses of serum

Sample preparation for metabolomic analysis

Metabolites were extracted from serum using a hydroalcoholic solution. 100 µL of serum sample were added to 400 µL of a solution of 80% methanol containing the internal standards, succinic-D4 acid, myristic acid-D27, glucose-13C6 and L-Methionine-(carboxy-13C, methyl-D3) (Sigma-Aldrich, St. Louis, MO) and labeled amino acid mix standards (Cambridge Isotope Laboratories, Massachusetts, USA). Samples were vortexed and centrifuged for 5 minutes at 15000 rpm and 4 ºC. Supernatants (450 µL) were transferred to a new tube and evaporated in a SpeedVac at 45 ºC to dryness. Afterward, samples were reconstituted with 30 µL of methoxyamine (40 mg/mL) in pyridine and incubated for 90 min at 37 ºC. Finally, samples were sylilated with 45 µL of MSTFA + 1 % TMCS at room temperature for 60 min.

GC-EI-qTOF-MS analyses for the determination of polar compounds

A semi-targeted analysis of the serum polar metabolites was performed using a Gas Chromatography-Quadrupole Time-Of-Flight (GC-qTOF) 7200 equipped with an electron impact (EI) source (Agilent Technologies, Palo Alto, California, USA). The chromatographic separation was performed with helium (purity >99.999%) as carrier gas at a constant flow of 1.1 mL/min. The ramp temperature to perform the separation of derivatized polar compounds was as follows: initial GC oven temperature was 60 °C; 1 min after injection, the GC oven temperature was increased by 10 °C/min to 320 °C and held for 10 min. In the inlet, 1 µL of samples were injected with split mode 1:20 at 250 ºC. Detection was achieved using mass spectrometry (MS) in electron impact (70 eV)

mode and full-scan monitoring mode (*m/z* 50–600) with an acquisition rate of 5 spectra/s. The ion source and quadrupole temperatures were set at 250 °C and 200 °C, respectively (Table 5). Identification of metabolites was performed using commercial internal standards and by matching their EI mass spectrum and retention time to the metabolomic Fiehn library (from Agilent Technologies, Palo Alto, California, USA), which contains more than 1.400 metabolites. The internal standards used were Succinic-D4 acid, myristic acid-D27, glucose-13C6 and L-Methionine-(carboxy-13C, methyl-D3) (Sigma Aldrich) and labeled amino acid mix standards (Cambridge Isotope Laboratories). After putative identification of metabolites, these were semi-quantified in terms of internal standard response ratio.

Sample preparation for lipidomics analyses

For the semi-targeted analysis of the serum lipids, electrospray ionization (ESI- and ESI+) was employed to cover all ranges of metabolites. For methanol extraction (ESI-), serum samples were thawed at 4ºC. 50 µL of serum was mixed with 200 µL of 100% methanol and a set of labelled internal standards: cholic acid, chenodeoxycholic acid, deoxycholic acid, hyodeoxycholic acid, lithocholic acid, ursodeoxycholic acid, taurocholic acid, taurochenodeoxycholic acid, taurodeoxycholic acid, taurolithocholic acid, glycocholic acid, glycochenodeoxycholic acid, glycodeoxycholic acid, tauroursodeoxycholic acid, decanoic acid c10:0, dodecanoic acid c12:0, palmitic acid c16:0, stearic acid c18:0, oleic acid c18:1, linoleic acid c18:2, linolenic acid c18:3, arachidic acid c20:0, arachidonic acid c20:4, t4, dehydroisoandrosterone 3-sulfate (DHEAS), oestrone sulfate, corticosterone, myristic-d27, cortisol-d4, 4-hydroxy-3-methoxymandelic acid-d3, 3-hydroxytetradecanoic acid-2,2,3,4,4-d5, cholic acid-d4, all of them were purchased to Sigma Aldrich (St. Louis, MO); LPE 18:1, LPC 20:0, LPC 16:0, LPC 18:0, LPC 18:1, LPE 16:0, LPC 18:1 -d7, all of them were purchased to Avanti Polar Lipids

(Alabaster,USA); 12(13)-DiHOME, 9(10)-DiHOME, 9(s)-HODE, 13(s)-HODE, 12(13)-EpOME, 9(10)-EpOME, thromboxane B2, 15(s)-HETE, 12(s)-HETE, AA-d8, oxy deuterated linoleic acid oxylipins, deuterated primary COX and LOX, all of them were purchased to Cayman Chemical (Michigan, USA); and 3-(3-hydroxy-4-methoxyphenyl)propionic acid d3, Taurocholic Acid-d5, both were purchased to Toronto Research Chemicals, Toronto, Canada. The mixture was vortexed and centrifuged for 10 min at 15000 rpm at 4ºC. The supernatant was evaporated to dryness using a SpeedVac concentrator, reconstituted with 50 µL of methanol, and analyzed by an Ultra-High-Performance Liquid Chromatography analysis, UHPLC-(-ESI)-qTOF-MS. For the extraction of hydrophobic lipids (ESI+), a liquid-liquid extraction with chloroform:methanol (2:1) based on the Folch procedure was performed. Briefly, 20 µL of serum was mixed with 20 µL of 0.8% NaCl and vortexed. Then, 200 µL of chloroform:methanol (2:1) was added, and samples were vortexed and centrifuged at 15000 rpm at 4 ºC for 10 minutes. The lower phase was recovered, evaporated to dryness, reconstituted with 100 µL of methanol:methyl-tert-butyl ether (9:1), and analyzed by UHPLC-(+ESI)-qTOF-MS using a set of labeled lipid internal standards (SPLASH, purchased to Avanti Polar Lipids (Alabaster, USA): LPC 18:1-d7, PC 33:1-d7, SM 36:2-d9, DG 33:1-d7, TG 48:1-d7 and ChoE 18:1-d7.

UHPLC-ESI-qTOF-MS analyses for the detection of the hydrophobic compounds

For the semi-targeted analysis of the serum lipids by methanol extraction (ESI-) and Folch extraction (ESI+), both methods utilized an Ultra-High-Performance Liquid Chromatograph (UHPLC) 1290 Infinity II Series coupled with a Q-TOF tunnel 6550 mass spectrometer (Agilent Technologies, Palo Alto, California, USA). Chromatographic separation employed different analytical columns: a CORTECS C18 Column (1.6 µm, 2.1 x 150 mm) from Waters for the methanol extraction method (ESI-) and a Kinetex 2.6

μm EVO-C18 column (100 Å, 100 x 2.1 mm) from Phenomenex for the Folch extraction method (ESI+). For the ESI- methodology, chromatographic separation was performed with a mobile phase of 100% water with 0.05% acetic acid for phase A and 100% acetonitrile for phase B. The column temperature was maintained at 40 ºC, and the injection volume was 2 μL. For the ESI+ methodology, the chromatographic method involved elution with a ternary mobile phase containing water, methanol, and 2-propanol with 10mM ammonium formate and 0.1% formic acid at a 0.6 mL/min flow rate. The stationary phase was a Kinetex EVO C18 column (2.6 μm, 2.1 mm X 100 mm), thermostated at 60 ºC, enabling the sequential elution of hydrophobic lipids such as lysophospholipids, sphingomyelins, phospholipids, diglycerides, triglycerides, and cholesteryl esters, among others. The chromatographic separation for ESI+ and ESI- was conducted using the gradients specified in Table 1 and the source parameters outlined in Table 2. Identification of metabolites was performed using commercial standards and by matching their EI mass spectrum and retention time to metabolomic Fiehn library (from Agilent) which contains more than 1.400 metabolites. After putative identification of lipid-related metabolites, these were semi-quantified in terms of internal standard response ratio.

Table 1. UHPLC gradient

ESI (-)			ESI (+)		
Time (min)	**%B**	**Flow (mL/min)**	**Time (min)**	**%B**	**%C**
0	2	0.4	**0**	10.0	45.0
1.5	2	0.4	**0.5**	9.5	45.0
2.25	7.5	0.4	**1.5**	7.5	47.7
8.0	30	0.4	**1.6**	7.0	58.5
11.0	50	0.4	**5.0**	4.0	61.2
25.0	85	0.4	**5.1**	3.5	77.4
26.0	95	0.4	**7.5**	3.5	80.1
30.0	95	0.4	**9.0**	0.0	80.1
30.1	2	0.4	**9.5**	0.0	100.0
31.0	2	0.4	**11.5**	10.0	100.0
34.0	2	0.4	**11.6**	10.0	45.0
			14.0	10.0	45.0

Table 2. Source parameters

Parameter	ESI (+ & -)
Gas Temp. (ºC)	225
Gas Flow (L/min)	11
Sheath Gas Temp. (ºC)	300
Sheath Gas Flow (L/min)	12
Nebulizer (psi)	35
Capillary Voltage (V)	3500
Nozzle Voltage (V)	500

Multivariate and univariate statistical analyses in metabolomics and lipidomics datasets

Statistical multivariate analyses were conducted using both serum metabolomic and lipidomic data obtained from middle-aged rat groups (Reg-Ma, Irreg-Ma, and Acyc-Ma) to assess the impact of the transition in female reproductive aging on the circulating metabolome. These analyses were carried out using RStudio v.2024.04.1 for data visualization. Principal component analysis (PCA) was performed to identify grouping trends and outliers. Partial least-squares discriminant analysis (PLS-DA) was subsequently carried out to assess global metabolic changes across the menopausal transition groups. The supervised PLS-DA model was validated using permutation tests with 999 iterations and a 5-fold cross-validation method. The top 40 discriminant metabolites lipids with variable importance in projection (VIP) values greater than 1 were selected as early biomarkers for diagnosing menopausal transition. To evaluate the utility of the supervised PLS-DA model and the top 40 lipids identified from the VIP scores as potential early biomarkers, we performed area under the ROC curve (AUC) analyses for all lipids and the top 40 selected metabolites to examine their utility in predicting transition of reproductive senescence. A value of AUC greater than 0.7 among groups were considered indicative of a good discriminative capacity of the model.

Analysis of variance (ANOVA) was employed to identify significant differences in the normalized abundances of the filtered features. To account for multiple comparisons and

control false discovery rates (FDR), significance was determined using the Benjamini-Hochberg correction with an adjusted p-value (p adj) < 0.05. Fold change values between groups for the significant lipids were calculated within RStudio. All results deemed statistically significant at FDR < 0.05 were utilized for further analyses. Statistical multivariate analyses were conducted using hierarchical clustering analysis (HCA or heatmap), Bonferroni-adjusted Pearson correlation matrix (p adj. < 0.05), boxplots, as well as PCA. For PCAs and boxplots among middle-aged rat groups, we utilized the R/Bioconductor package ggplot2 v3.4.4 (32). For PLS-DA, VIP score values, and AUC curves, we used the R/Bioconductor package mixOmics v.6.26.0. The Bonferroni-adjusted Pearson correlation matrix was generated using the R/Bioconductor package corrplot v.092. The heatmaps were generated using the R/Bioconductor package ComplexHeatmap v2.16.0 (33), with the Euclidean distance metric selected. The study utilized various biological databases such as HMDB, PubChem, and LIPID MAPS, along with scientific literature included in PubMed, to gain insight into the biological function of the metabolites that were identified as statistically significant among groups and with the top 40 discriminant lipids detected. The lipids were referenced according to the HMDB nomenclature recommendations.

Statistical analyses

Statistical analyses to detect differences among the four groups in biometric, histological and biochemical parameters were performed with IBM SPSS Statistics 28.0 (SPSS, IBM Corp. Armonk, New York, USA). Grubbs' test was used to detect outliers, which were discarded for further analysis. The assumption of normality was determined using the Kolmogorov-Smirnov test, and the homoscedasticity among groups was evaluated using Levene's test. When one or both of these conditions were not accomplished, data were transformed to base-10 logarithms to obtain a normal distribution and/or similar variances

before statistical testing. One-way ANOVA followed by Duncan's *post hoc* test (p value ≤0.05) was used to assess differences among the four groups in most of the variables analyzed in the present study. Welch's test followed by Games–Howell's *post hoc* test was used when homoscedasticity was not assumed. The Kruskal–Wallis test followed by the Mann–Whitney U *post hoc* test was used as the nonparametric version of one-way ANOVA when the data did not follow a normal distribution. Differences in ovarian atrophy and stromal luteinization were detected using the Chi-squared test. Linear relationships between key variables were tested using Pearson's correlation coefficients. Student's t-test was also used for some single statistical comparisons to detect residual differences. Data are presented as the means ± SEM (n = 7-10). The level of statistical significance was set at bilateral 5%.

RESULTS

Monitorization and characterization of the different stages of natural reproductive senescence in female rats

The cycling status of 3.5-and 8-month-old female Sprague-Dawley rats was assessed longitudinally for a total period of about 2 months in which the rats were stratified into groups according to the stage of ovarian senescence following the classification of the human perimenopause-menopause transition as per Stages of Reproductive Aging Workshop (STRAW). At the end of this process, all the rats included in the Reg-Yng group (n=10), which were included to distinguish chronological aging, displayed regular cycling (showing cycles of 4–5 days), whereas 23 middle-aged rats were selected to be included in the Reg-Ma group (n=7, displaying cycles of 4–5 days), in the Irreg-Ma group (n= 8, showing two consecutive cycles that were 6 days or longer) and in the Acyc-Ma group (n=8, displaying 14 continuous days in persistent oestrous) (Table 3). At the end of

the study, Reg-Yng animals were about 5 months-old whereas middle-aged rats were about 10 months-old and no significant differences among the three middle-aged groups were found concerning age (Table 3).

Table 3. Biometric parameters, and serum parameters in female rats during natural reproductive aging

	Reg-Yng (n = 10)	**Reg-Ma (n = 7)**	**Irreg-Ma (n =8)**	**Acyc-Ma (n = 8)**
Initial Age (days ≈ months)	106 ≈ 3.5	247 ≈ 8	247 ≈ 8	247 ≈ 8
Final Age (days ≈ months)	157 ≈ 5	295 ≈ 10	294 ≈ 10	293 ≈ 10
Cycling Status	Regular	Regular	Irregular	Acyclic
Biometric parameters				
Initial Body Weight (g)	238 ± 3^{a}	273 ± 7^{b}	281 ± 11^{b}	263 ± 4^{b}
Final Body Weight (g)	268 ± 6^{ab}	282 ± 6^{a}	288 ± 11^{a}	257 ± 5^{b}
Tissue weights (%)				
Uterine horns (%)	0.166 ± 0.020^{a}	0.160 ± 0.018^{a}	0.143 ± 0.013^{a}	0.232 ± 0.014^{b}
POWAT (%)	1.59 ± 0.19^{ab}	2.13 ± 0.23^{a}	2.17 ± 0.28^{a}	1.48 ± 0.15^{b}
Liver (%)	2.67 ± 0.09^{a}	2.26 ± 0.04^{b}	2.48 ± 0.09^{a}	2.53 ± 0.05^{a}
Caecum (%)	1.26 ± 0.12	1.11 ± 0.06	1.38 ± 0.13	1.15 ± 0.09
MWAT (%)	0.94 ± 0.11	1.20 ± 0.09	1.13 ± 0.16	0.93 ± 0.10
Gastrocnemius (%)	0.714 ± 0.013	0.660 ± 0.037	0.678 ± 0.021	0.698 ± 0.024
Soleus (%)	0.044 ± 0.001	0.043 ± 0.004	0.039 ± 0.003	0.045 ± 0.003
Serum parameters				
Glucose (*mmol/L*)	6.28 ± 0.22	6.22 ± 0.20	6.00 ± 0.22	6.35 ± 0.14
Insulin (*pmol/L*)	19.6 ± 1.5	20.6 ± 0.9	23.3 ± 2.4	27.8 ± 3.6
NEFAs (*mmol/L*)	0.88 ± 0.04	1.04 ± 0.06	0.93 ± 0.05	0.95 ± 0.07
R-QUICKI	0.039 ± 0.002	0.036 ± 0.001	0.034 ± 0.002	0.030 ± 0.002
HOMA-IR	5.53 ± 0.57	5.73 ± 0.33	5.58 ± 0.49	7.95 ± 1.21
TG *(mmol/L)*	0.96 ± 0.06	0.90 ± 0.10	1.10 ± 0.10	1.21 ± 0.13
TC *(mmol/L)*	4.02 ± 0.21^{ab}	3.45 ± 0.22^{a}	4.00 ± 0.22^{ab}	4.45 ± 0.22^{b}
Adiponectin (*µg/mL*)	15.5 ± 1.7^{ab}	17.2 ± 1.3^{a}	15.9 ± 1.5^{ab}	11.2 ± 0.5^{b}
Leptin (*ng/mL*)	3.60 ± 0.68^{a}	8.71 ± 1.62^{b}	6.45 ± 1.18^{b}	4.77 ± 0.61^{ab}
Adiponectin/Leptin Ratio	5.08 ± 0.69^{a}	2.65 ± 0.63^{b}	2.81 ± 0.36^{b}	2.55 ± 0.30^{b}
Leptin/Adiponectin Ratio	0.23 ± 0.03^{a}	0.54 ± 0.13^{b}	0.35 ± 0.05^{b}	0.43 ± 0.05^{b}
CRP (*µg/mL*)	613 ± 99	452 ± 62	605 ± 76	742 ± 100

Data are given as the mean ± SEM (n = 7-10). Relative tissue weights (%) were calculated according to the formula (100 * tissue weight/body weight) and were expressed as a percentage of body weight. The concentrations of serum parameters were determined at the end of the experiment. Leptin-to-adiponectin ratio was calculated as the circulating levels of leptin divided by circulating levels of adiponectin. Adiponectin-to-leptin ratio was calculated as the circulating levels of adiponectin divided by circulating levels of leptin. Different superscript lowercase letters (a, b) indicate significant different mean values (one-way ANOVA and Duncan's *post hoc* test or Welch test and Games–Howell *post hoc* test, $p < 0.05$). Reg-Yng: regular young rats; Reg-Ma: regular middle-aged rats; Irreg-Ma: irregular middle-aged rats; Acyc-Ma: acyclic middle-aged rats. CRP: C-reactive protein; HOMA-IR: homeostasis model assessment-estimated insulin resistance; MWAT: mesenteric white adipose tissue; NEFAs: nonesterified fatty acids; POWAT: periovarian white adipose tissue; R-QUICKI: revised quantitative insulin sensitivity check index; TG: triglycerides; TC: total cholesterol.

Natural reproductive senescence produced slight changes in biometric parameters and in classical glucose, lipid and inflammation-related biomarkers

As expected, at baseline, middle-aged rats displayed higher body weight than young rats (Table 3). At the end of the study, both the Reg-Ma and the Irreg-Ma rats showed higher body weight than the Acyc-Ma animals, whereas Reg-Ma displayed decreased relative liver weight than their Irreg-Ma and Acyc-Ma counterparts (Table 3). This latter effect could be attributed, at least in part, to the slight differences in body weight reported among the three middle-aged groups of rats because the visual examination of the livers did not reveal apparent lipid accumulation in any of the groups. The Acyc-Ma group displayed a significant increase in the serum total cholesterol when compared to their Reg-Ma counterparts (Table 3). No significant changes were found among the four groups either in the circulating levels of TG or in the parameters related to glucose and insulin homeostasis, although Acyc-Ma animals displayed numerically higher values of insulin, TG and HOMA-IR than their counterparts (Table 3). Similarly, no significant differences among groups were found in the circulating levels of the acute inflammation marker CRP (Table 3).

The Reg-Ma group exhibited higher adiponectin serum levels than the Acyc-Ma group, while no significant differences were found among the other groups (Table 3). Regarding leptin levels, although no significant differences were observed within the middle-aged animals, both Reg-Ma and Irreg-Ma rats exhibited higher levels compared to the Reg-Yng group (Table 3). Despite these slight effects observed among groups in the circulating levels of these two key adipocytokines, all middle-aged groups exhibited a lower adiponectin/leptin ratio and a higher leptin/adiponectin ratio than the young animals, which would suggest an increased cardiometabolic risk with aging regardless the ovarian function/oestrous cycle status of middle-aged rats (Table 3).

Natural female reproductive aging altered the circulating levels of sexual hormones

17β-E2 circulating levels were similar between Reg-Yng and Reg-Ma animals and significatively decreased as mature female rats progressed to irregular cycles and to reproductive senescence, showing both Irreg-Ma and Acyc-Ma animals similar values of this hormone (Figure 1A). As was previously described (12,14,15), progesterone serum concentrations were significantly decreased in the acyclic females (Figure 1B), an effect that could be attributed, at least in part, to a lack of ovulation and corpus luteum production, effects that were observed in the Acyc-Ma group according to both the cytological analyses and the ovarian histological determinations carried out in these middle-aged animals (Figures 2 and 3). In addition, Acyc-Ma rats displayed a significant increase in the 17β-oestradiol/progesterone ratio (Figure 1C), as was previously described (12,14) in animals presenting a persistent oestrous state with an absence of corpus luteum. In this regard, a negative correlation was found between 17β-oestradiol/progesterone ratio and the total number of corpus luteum ($r = -0.440$, 95% CI = -0.114 to -0.681, $p = 0.010$).

No significant changes among groups were observed in the circulating levels of LH and FSH levels ($p= 0.099$ and $p = 0.969$ respectively, one-way ANOVA) (Figure 1D and 1E, respectively). However, subsequent pairwise comparisons revealed that serum LH concentrations residually decreased in acyclic rats when were compared to their young and middle-aged regular counterparts (45.1% lower and 49.4%; $p=0.029$ and $p=0.013$, respectively, Student's t test), and a similar pattern of decrease were observed in acyclic versus irregular animals (43.9% lower, $p=0.066$, Student's t test) (Figure 1D).

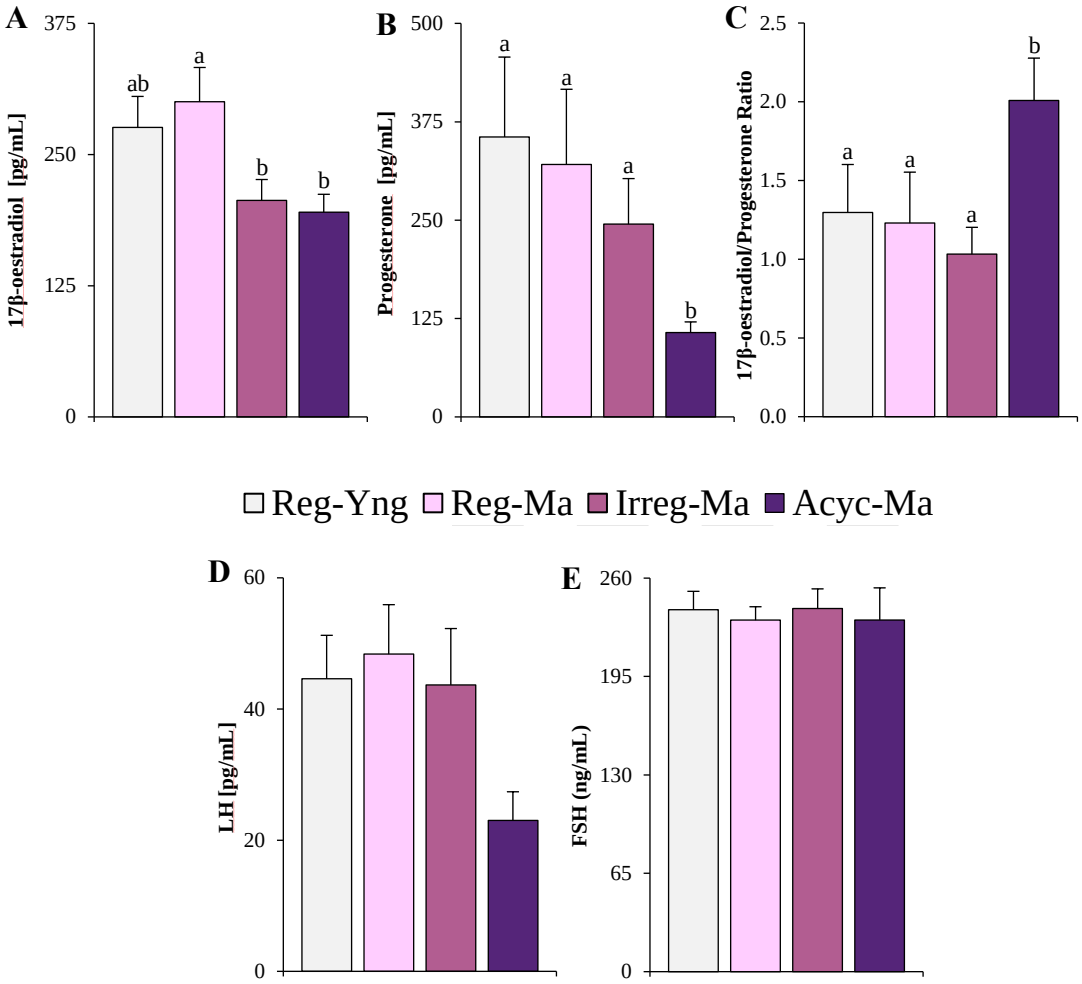


Figure 1. Circulating sex hormone levels during natural female reproductive ageing in Sprague-Dawley rats. Data are given as the mean ± SEM (n = 7-10). Serum 17β-oestradiol (A), progesterone (B), 17β-oestradiol/progesterone ratio (C), luteinizing hormone (D) and follicle stimulating hormone (E) in ovarian-intact Sprague Dawley females at 5- and 10-month-old. 17β-oestradiol/progesterone ratio was calculated as the circulating levels of 17β-oestradiol divided by circulating levels of progesterone. Different superscript lowercase letters (a, b) indicate significant different mean values (one-way ANOVA and Duncan's *post hoc* test or Welch test and Games–Howell *post hoc* test, $p < 0.05$). Reg-Yng: regular young rats; Reg-Ma: regular middle-aged rats; Irreg-Ma: irregular middle-aged rats; Acyc-Ma: acyclic middle-aged rats. LH: luteinizing hormone; FSH: follicle stimulating hormone.

Gonadal-related parameters were altered across perimenopause

The Acyc-Ma animals displayed significant lower relative weight of the ovaries than the other groups (Figure 2A), suggesting ovary atrophy, which was confirmed with the histological analyses, in which was observed that 60% of the acyclic rats showed this alteration (Figure 2B). A very similar pattern was reported in the three groups of middle-aged rats regarding the POWAT/weight (%), displaying the Acyc-Ma animals decreased relative weight of the WAT surrounding the ovaries compared to their Reg-Ma and Irreg-

Ma counterparts (Table 3). In contrast, the Acyc-Ma group showed higher uterine horns/weight (%) than the other groups (Table 3), which would suggest differences in uterine morphology associated with acyclic reproductive patterns.

The ovarian histological analyses revealed that acyclic rats did not present either stromal luteinization or corpus luteum (Figures 2C and 2D), differently to what was observed in the other three groups of animals, which showed similar stromal luteinization (Figure 2C), and stages of development of the corpus luteum (Figure 2D), indicating that in the Reg-Yng, Reg-Ma and Irreg-Ma groups there were a progression of follicular luteinization towards the formation and development of normal corpus luteum during the oestrous cycle. The lack of corpus luteus reported in the Acy-Ma rats is illustrated in the representative ovarian section depicted in the Figure 2I, which showed the characteristic pattern of changes occurring in persistent oestrous, including the presence of numerous follicular cysts (FC) and the absence of corpus luteum (12,19). By contrast, the young cyclic rats (Figure 2F) and both the middle-aged cyclic and irregular animals (Figures 2G and 2H) exhibited the presence of follicles and corpus luteum in the ovary.

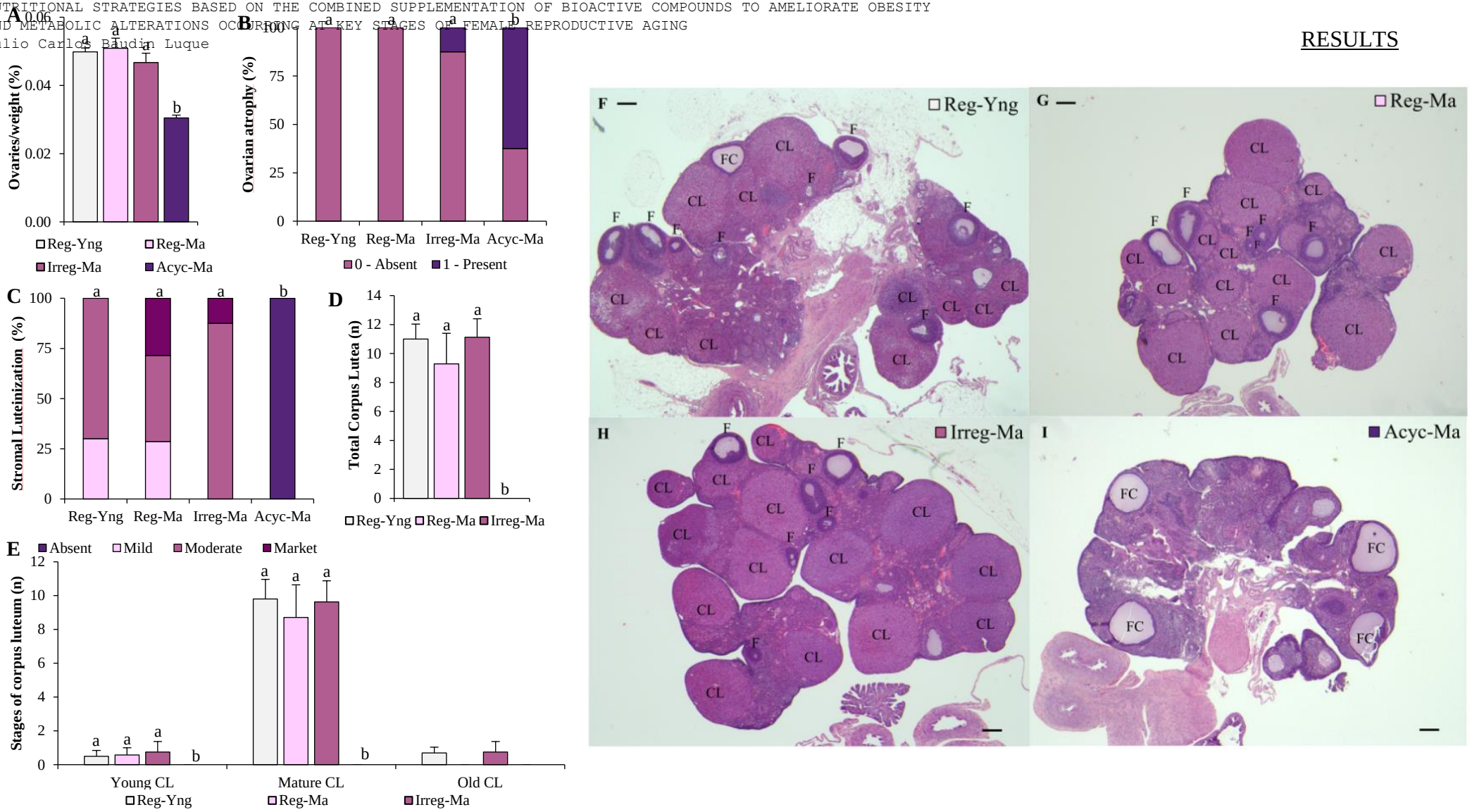


Figure 2. Ovaries/weight (%) and ovarian histological analyses. Ovaries/weight(%) (A), ovarian atrophy (%) (B) Stromal luteinization (%) (C), total number of Corpus luteum (CL) (D) and stages of Corpus Lutea (CL) (n) (E) in ovarian-intact Sprague Dawley females at 5- and 10-month-old. The figures 2B and 2C present qualitative observations and different superscript lowercase letters (a, b) indicate significantly different mean values among groups (Pearson's chi-square test, $p < 0.05$). The figures 2A and, 2D the data are given as the mean ± SEM (n = 7-10) and different superscript lowercase letters (a, b) indicate significantly different mean values among groups (Kruskal–Wallis test and Mann–Whitney U *post hoc* test, $p < 0.05$). The figures 2E-2H represent the photomicrographs of hematoxylin–eosin-stained ovarian sections (Bar = 100 µm) in ovarian-intact Sprague Dawley females at 5- and 10-month-old. CL: corpus luteum; POWAT: periovarian white adipose tissue. FC = follicles cysts; CL: corpus luteum; F: secondaries, preantral and antral follicles. Reg-Yng: regular young rats; Reg-Ma: regular middle-aged rats; Irreg-Ma: irregular middle-aged rats; Acyc-Ma: acyclic middle-aged rats. CL: corpus luteum; POWAT: periovarian white adipose tissue.

Identification of lipidomic-based signatures across perimenopause

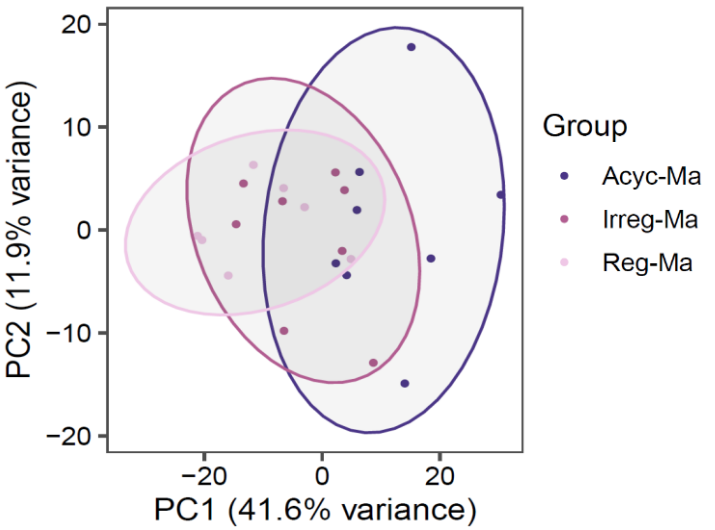
To identify changes in circulating metabolites occurring along natural reproductive senescence, semi-targeted metabolomic and lipidomic analyses were carried out in the serum of the Reg-Ma, Irreg-Ma and Acyc-Ma groups. The initial unsupervised PCA performed on the polar metabolomics did not reveal separation trends among the groups of interest. Furthermore, after adjusting p-values for FDR, no significant changes were found in the circulating levels of polar metabolites among the Reg-Ma, Irreg-Ma, and Acyc-Ma groups (padj > 0.05, one-way ANOVA) (Supplementary data S1).

Regarding the semi-targeted serum lipidomic analyses, the initial unsupervised PCA performed with the 403 hydrophobic metabolites revealed slight separation trends among the three groups that were at different stages of natural reproductive senescence (Figure 3A). Afterwards, a PLS-DA was performed to further explore the lipidomic differences among groups. Both the PLS-DA plot (Figure 3B) and its three-dimensional representation with three components (Figure 3C), showed a clear separation and discriminations among Reg-Ma, Irreg-Ma, and Acyc-Ma groups. Following the successful establishment of this PLS-DA model, VIP scores were calculated to identify the lipid-related metabolites that contributed more to discriminate the three groups. Based on VIP values with thresholds of 1, we selected the top 40 metabolites out of 186 lipids with VIP values higher than 1, including 14 phosphatidylcholines (PC), 6 Lysophosphatidylcholines (LysoPC), 5 TGs, 4 fatty acids (FA), 3 lysophosphatidylethanolamines (LysoPE), 2 cholesterol ester (ChoE), the phosphatidylethanolamine PE(34:2), the diacylglyceride DG(38:7), the androgen 5a-androstan-3,17-diol-monosulfate-iso3 (5-α-androstan-diol), the muricholic acid (MCA-iso3), 13-hydroxydocosahexaenoic acid (13-HDHA) and 17,18-Dihydroxyarachidonic acid (17,18-DiHETE) (Figure 3D). In addition, ROC curves based on all lipids and the

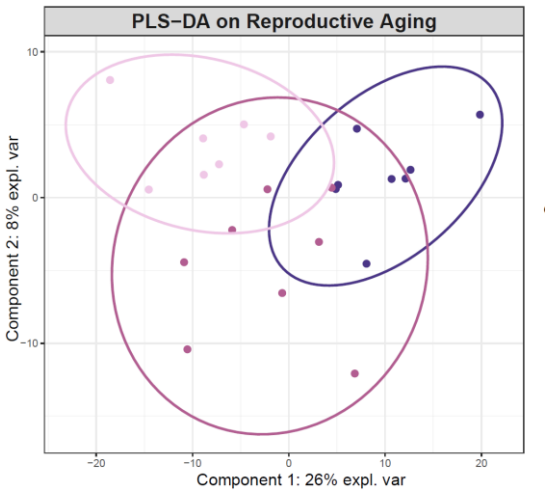
top 40 metabolites with VIP scores higher than 1 were performed (Figure 3D and 3F, respectively). Both ROC curves showed an AUC higher than 0.7 in all comparisons among groups, demonstrating the utility of these lipid-related metabolites for discriminating the rats according to their regularity of the oestrous cycle. Interestingly, the results revealed that the accuracy of the model was maximal when the top 40 metabolites with VIP scores higher than 1 were used, presenting a ROC AUC of 1 in all comparisons, suggesting that these 40 lipid-related metabolites could be a reliable multivariate biomarker to precisely distinguish rats at different stages of perimenopause (Figure 3F).

RESULTS

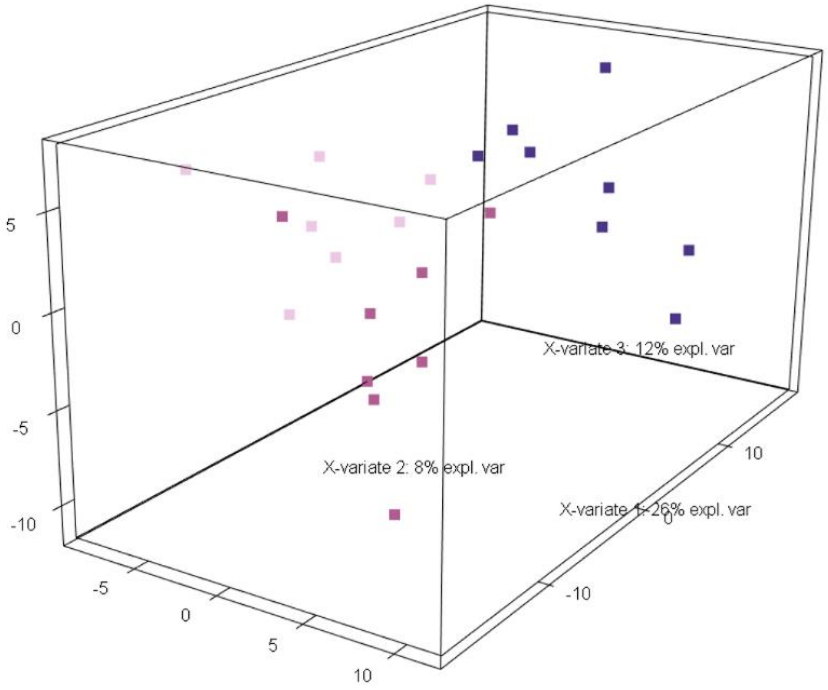
A



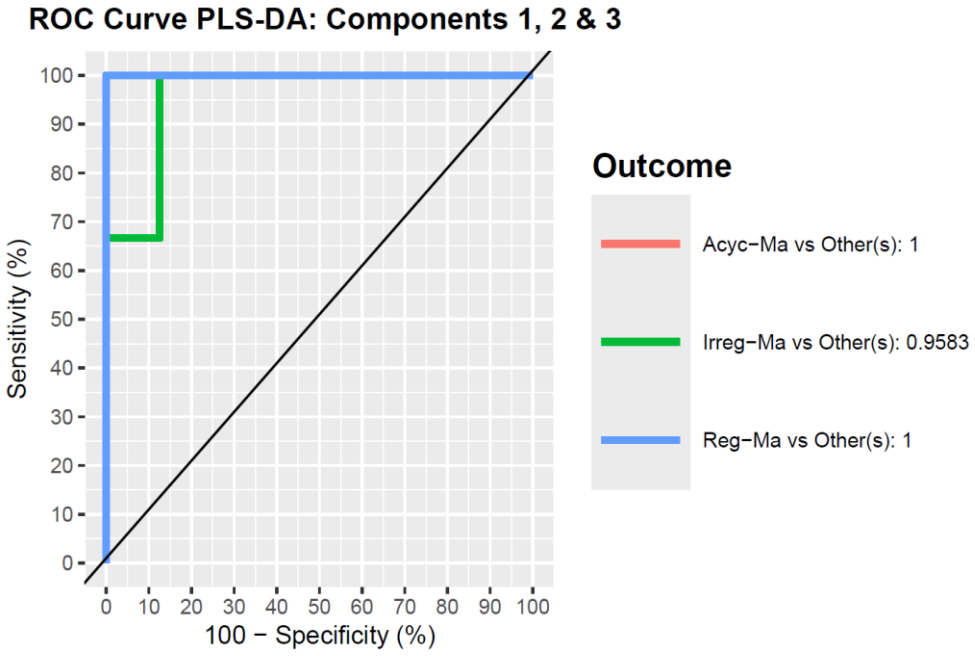
B



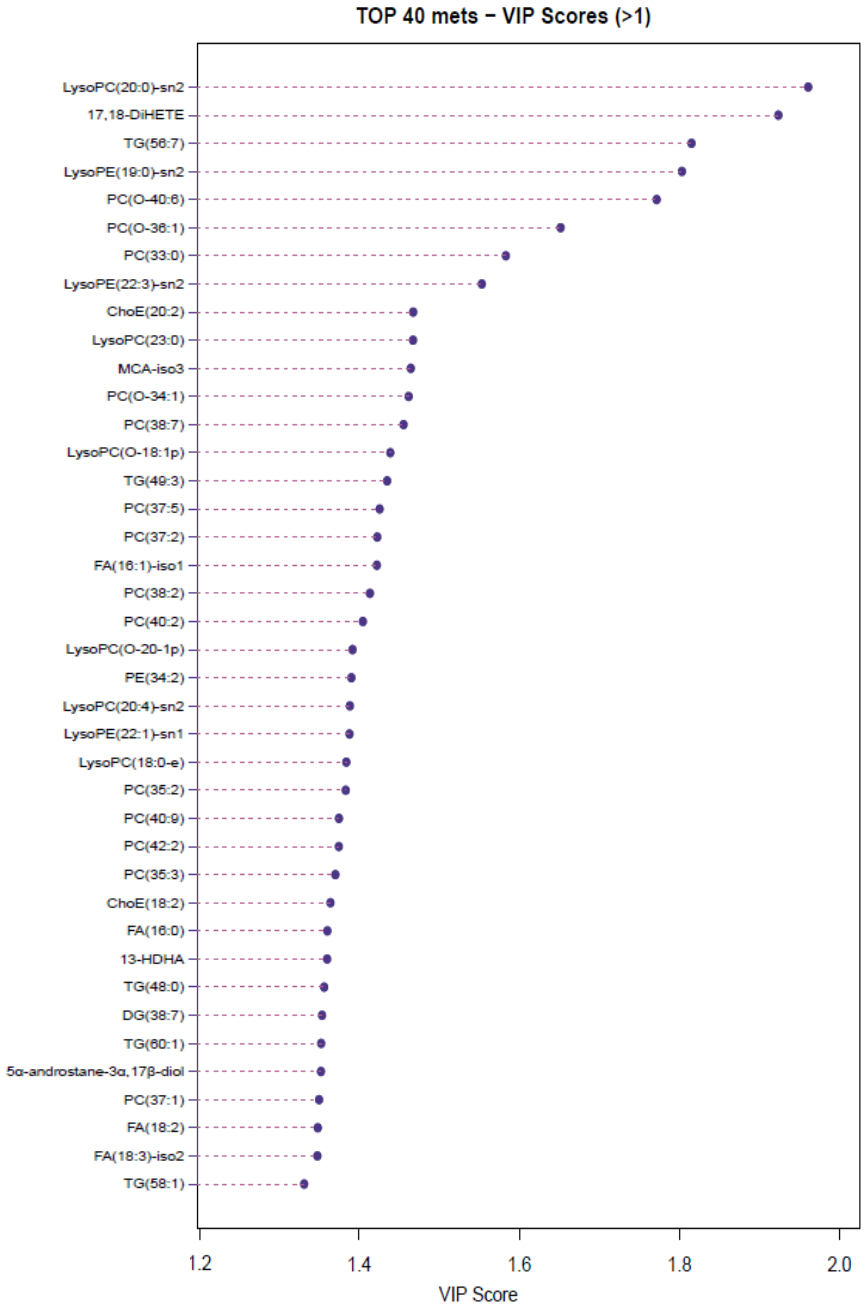
C



D



E



F

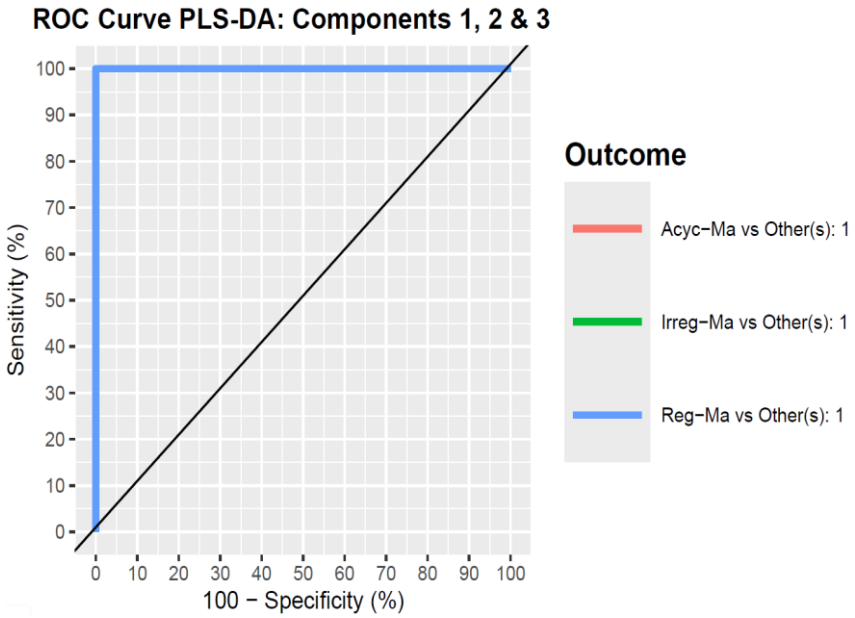


Figure 3. Effects of natural reproductive senescence on serum lipidomic of middle-aged female Sprague-Dawley rats. (A) Principal components analysis (PCA) plot of the 403 lipid metabolites. (B) 403 measured parameters were used to set up a PLS-DA-predictive model with components 1 & 2. (C) 3D PLS-DA-predictive model, 3 components. (D) ROC curve PLS-DA 3 components of the 403 lipid metabolites. (E) The distributions of lipid species with the top 40 VIP scores (>1) in 3 components. (F) ROC curve 3 components of top 40 discriminant lipids. Reg-Yng: regular young rats; Reg-Ma: regular middle-aged rats; Irreg-Ma: irregular middle-aged rats; Acyc-Ma: acyclic middle-aged rats. PC: Principal component; PCA: Principal components analysis; PLS-DA: partial least square discriminant analysis; ROC curve: receiver operating characteristic curve. 13-HDHA: 13-hydroxydocosahexaenoic acid; 17,18-DiHETE: 17,18-Dihydroxyarachidonic acid; ChoE: cholesterol ester; FA: fatty acids; LysoPC: Lysophosphatidylcholines; LysoPE: lysophosphatidylethanolamines; MCA-iso3: muricholic acid-iso3; PC: phosphatidylcholines; PE: phosphatidylethanolamines; TG: triglycerides.

On the other hand, the univariate statistical analyses revealed that 144 out of 403 hydrophobic metabolites identified were significantly different among Reg-Ma, Irreg-Ma and Acyc-Ma groups (padj < 0.05, one-way ANOVA) (Supplementary data S2). Specifically, changes in the circulating levels of 68/76 PCs, 30/80 LysoPCs, 16/65 TGs, 12/45 LysoPEs, 6/7 phosphatidylethanolamines (PE), 4/16 ChoEs, 4/23 sphingomyelins (SM), 2/13 diacylglycerides (DG), 5-α-androstan-diol, thyroxine hormone (T4) and 17,18-DiHETE were found. Notably, the families of lysophospholipids showed the highest saturation levels, being saturated 40% of LysoPCs and 33% of LysoPEs. In contrast, the families showing the lowest saturation levels were PCs (9%) and TGs (6%). The PCA performed with the 144 lipids that were significantly changed revealed that the clustering according to the group's regularity was notable, showing a progressive discrimination among groups as the regularity of the cycles diminished (Figure 4A). Furthermore, to better illustrate the changes observed in the PCA, we constructed a heatmap of the 144 lipids clustered by groups. This visualization method provides a clearer depiction of the variations in lipid-related metabolites according to the regularity of the cycles (Figure 4B).

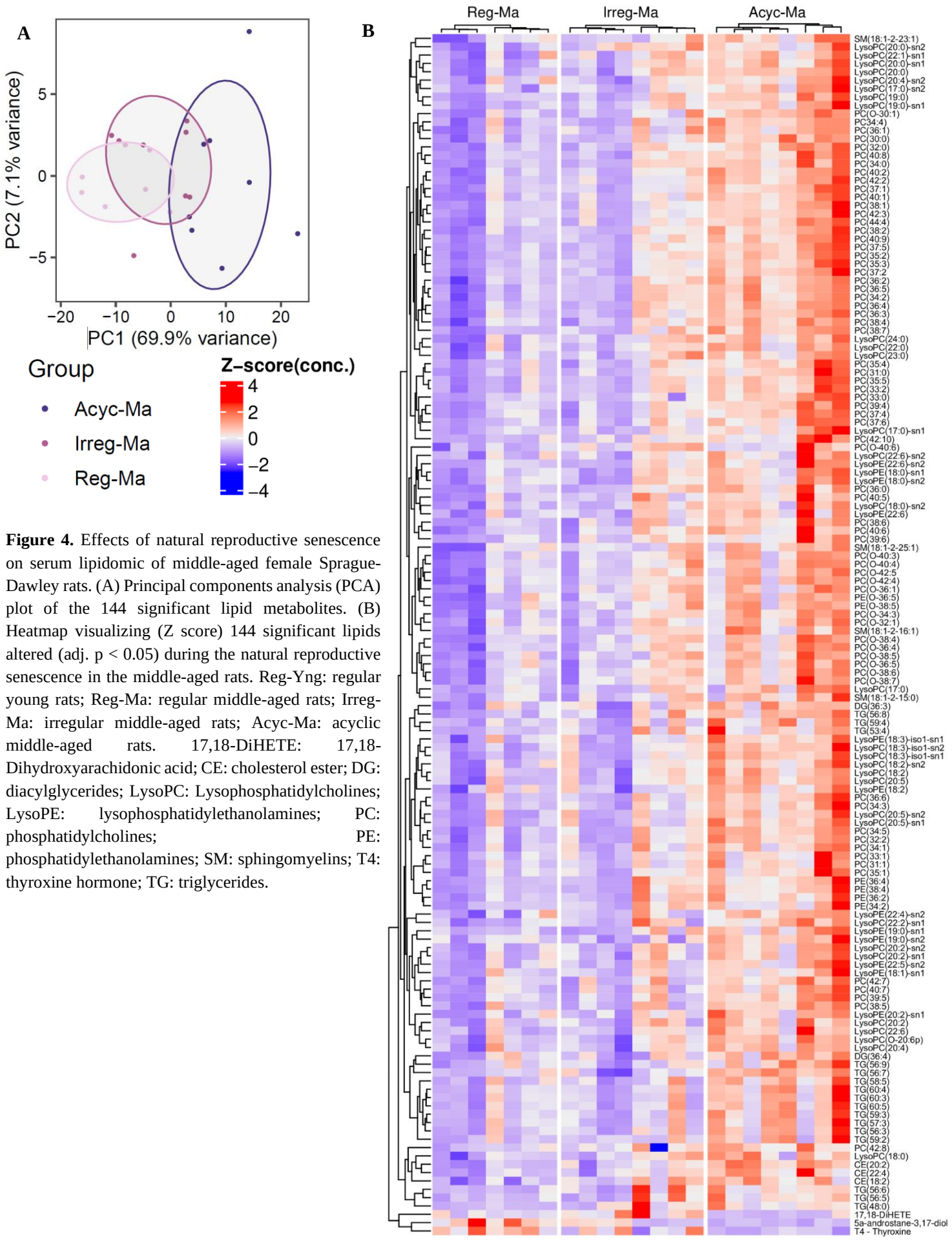


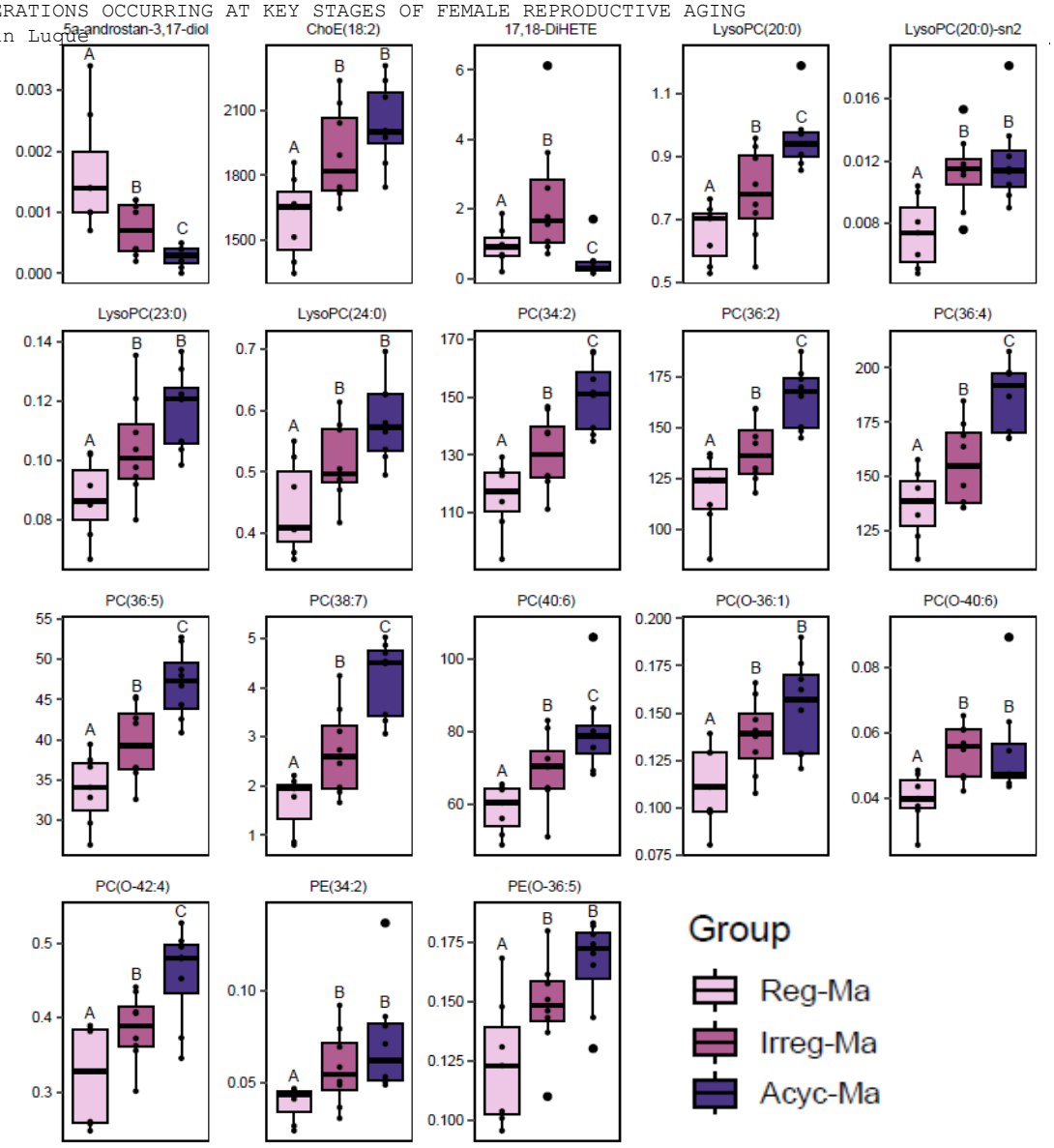
Figure 4. Effects of natural reproductive senescence on serum lipidomic of middle-aged female Sprague-Dawley rats. (A) Principal components analysis (PCA) plot of the 144 significant lipid metabolites. (B) Heatmap visualizing (Z score) 144 significant lipids altered (adj. $p < 0.05$) during the natural reproductive senescence in the middle-aged rats. Reg-Yng: regular young rats; Reg-Ma: regular middle-aged rats; Irreg-Ma: irregular middle-aged rats; Acyc-Ma: acyclic middle-aged rats. 17,18-DiHETE: 17,18-Dihydroxyarachidonic acid; CE: cholesterol ester; DG: diacylglycerides; LysoPC: Lysophosphatidylcholines; LysoPE: lysophosphatidylethanolamines; PC: phosphatidylcholines; PE: phosphatidylethanolamines; SM: sphingomyelins; T4: thyroxine hormone; TG: triglycerides.

Interestingly, both the multivariate analysis of the top 40 metabolites with VIP scores higher than 1 and the univariate analysis showing that 144 lipids that were significantly different under the one-way ANOVA, revealed a higher proportion of PC and LysoPC families the abundance of which clearly differed among Reg-Ma, Irreg-Ma and Acyc-Ma groups. Thus, in addition to cholesterol ester ChoE(18:2), the androgen 5-α-androstan-diol, (a derivative of dehydroepiandrosterone sulfate -DHEA-S- and dihydrotestosterone -DHT-), and 17,18-DiHETE (a metabolite derived from arachidonic acid), metabolites included in these families were consistently identified after carrying out both analyses: PC(38:7), PC(O-36:1), PC(O-40:6), LysoPC(20:0)-sn2, LysoPC(23:0), LysoPC(24:0) and PE(34:2).

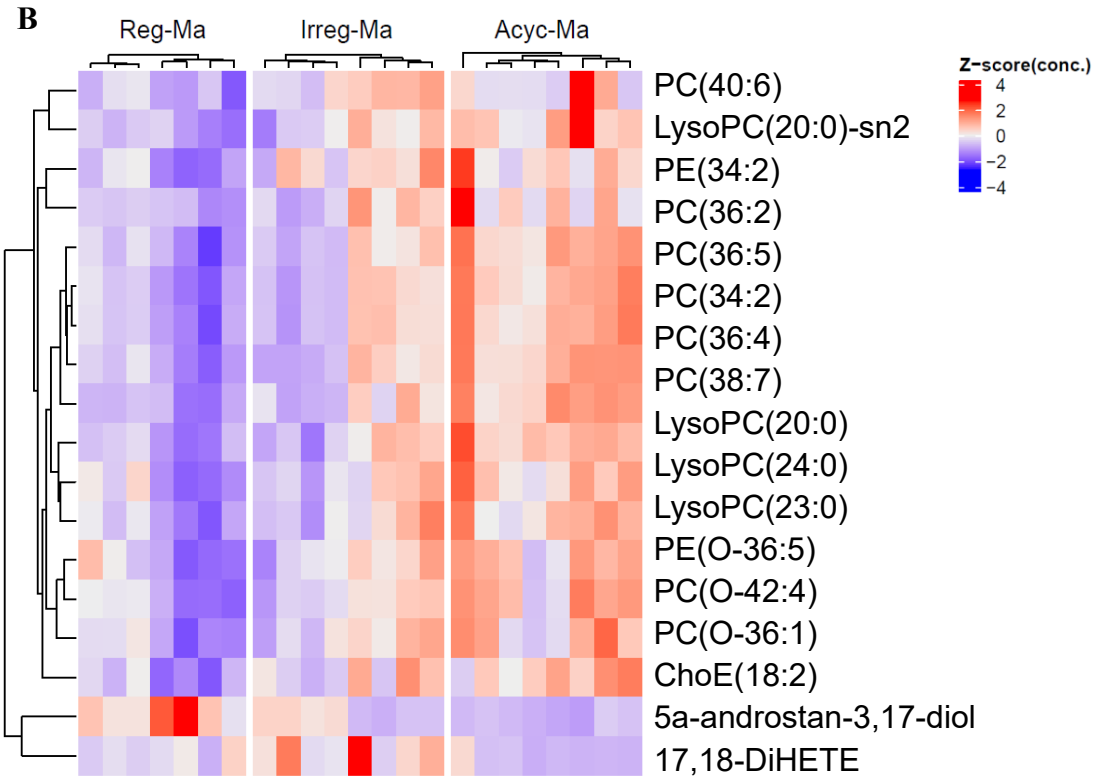
To detect putative early biomarkers of natural female reproductive aging, we selected, among the 144 metabolites that were significantly different among the three groups using the one-way ANOVA, those lipid-related metabolites that were significantly different between Reg-Ma and Irreg-Ma rats, according to the Duncan *post hoc* test. In total, we identified 18 parameters that already changed with the transition from the regular oestrous cycle characteristic of the Reg-Ma animals to the irregular cycling observed in the Irreg-Ma rats, suggesting that these metabolites could be potential early biomarkers of perimenopause. Specifically, we found changes in the circulating levels of 9 PCs, 4 LysoPCs, 2 PEs, ChoE(18:2), 5-α-androstan-diol and 17,18-DiHETE. A boxplot including these 18 metabolites and their relative quantification in the three middle-aged groups was depicted in Figure 5A. A consistent trend of increasing values was observed as the cyclicality diminished for most of these parameters, with the exception of 5-α-androstan-diol, which displayed an inverse behavior. Finally, we generated a new heatmap specifically focusing on these 18 metabolites, clearly illustrating their discriminatory pattern between the Ma-Reg and the Irreg-Ma groups (Figure 5B). A

Bonferroni-adjusted Pearson correlation matrix plot was generated to visualize the relationships between these 18 metabolites and the circulating levels of the main sex hormones, triglycerides and total cholesterol, as well as the surrogate markers of insulin resistance and sensitivity, HOMA-IR and R-QUICKI, respectively (Figure 5C). Surprisingly, although no correlations were found with the analyzed sex hormones, the androgen derivative of DHT, 5-α-androstan-diol, showed strong negative correlations with the phosphatidylcholines PC(34:2), PC(36:4), PC(36:5), and LysoPC(20:0). Furthermore, as expected, these mentioned PC species exhibited very strong positive correlations among themselves, as well as with the other PC species and with LysoPCs. This observation may be attributed to their metabolic interconversion, which supports a strong and positive correlation. Interestingly, total serum cholesterol positively correlated with most PC and LysoPC species, while serum triglycerides surprisingly showed a strongly positive correlation with PE(34:2).

A


5a-androstan-3,17-diol
ChoE(18:2)
17,18-DiHETE
LysoPC(20:0)
LysoPC(20:0)-sn2
LysoPC(23:0)
LysoPC(24:0)
PC(34:2)
PC(36:2)
PC(36:4)
PC(36:5)
PC(38:7)
PC(40:6)
PC(O-36:1)
PC(O-40:6)
PC(O-42:4)
PE(34:2)
PE(O-36:5)
Group
Reg-Ma
Irreg-Ma
Acyc-Ma

B


Reg-Ma
Irreg-Ma
Acyc-Ma
Z-score(conc.)
PC(40:6)
LysoPC(20:0)-sn2
PE(34:2)
PC(36:2)
PC(36:5)
PC(34:2)
PC(36:4)
PC(38:7)
LysoPC(20:0)
LysoPC(24:0)
LysoPC(23:0)
PE(O-36:5)
PC(O-42:4)
PC(O-36:1)
ChoE(18:2)
5a-androstan-3,17-diol
17,18-DiHETE

C

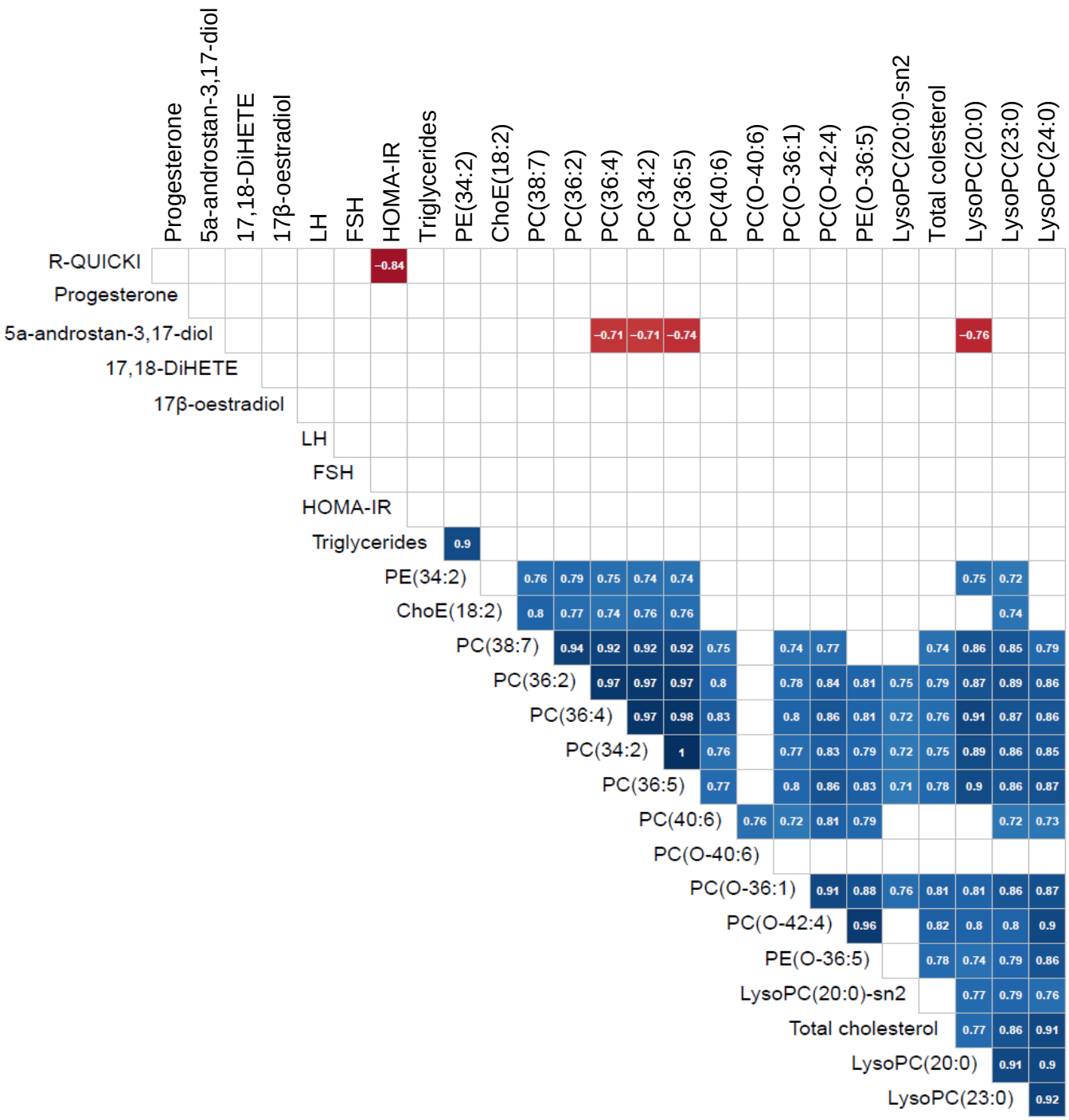


Figure 5. Effects of natural reproductive senescence on serum lipidomic of middle-aged female Sprague-Dawley rats. (A) Boxplots showing the 18 significant early lipid biomarkers selected by $p < 0.05$ in post hoc test applied between regular and irregular middle-aged rats. Different superscript lowercase letters (A, B, C) indicate significant different mean values (one-way ANOVA and Duncan's post hoc test or Welch test and Games–Howell post hoc test, $p < 0.05$). (B) Heatmap visualizing (Z score) top 18F significant lipids altered (adj. $p < 0.05$) between regular and irregular middle-aged rats. (C) Bonferroni-adjusted Pearson correlation matrix of significant circulating hormone and metabolic levels and 18 significant metabolites. Only correlations adjusted with $P<0.05$ are plotted. Reg-Yng: regular young rats; Reg-Ma: regular middle-aged rats; Irreg-Ma: irregular middle-aged rats; Acyc-Ma: acyclic middle-aged rats. 17,18-DiHETE: 17,18-Dihydroxyarachidonic acid; ChoE: cholesterol ester; FSH: follicle stimulating hormone; HOMA-IR: homeostasis model assessment-estimated insulin resistance; LH: luteinizing hormone; LysoPC: Lysophosphatidylcholines; PC: phosphatidylcholines; PE: phosphatidylethanolamines

Bone-related parameters did not change during natural female reproductive aging

No significant changes were found among groups in bone-related parameters, including the weight and length of femurs, as well as the femur bone mineral content (BMC) and bone mineral density (BMD) analyzed by μCT (Table 4).

Table 4: Bone-related parameters in female rats during reproductive aging

	Reg-Yng	**Reg-Ma**	**Irreg-Ma**	**Acyc-Ma**
Biometric parameters				
Femurs (g)	1.75 ± 0.03	1.85 ± 0.06	1.82 ± 0.03	1.79 ± 0.03
Femurs (cm)	3.55 ± 0.02	3.62 ± 0.03	3.64 ± 0.02	3.61 ± 0.02
Microcomputed tomography analyses				
BMD (mg/cc)	750 ± 10	709 ± 17	732 ± 17	749 ± 15
BMC (mg)	522 ± 12	547 ± 17	563 ± 5	557 ± 9

Data are given as the mean ± SEM (n = 7-10). Microcomputed tomography analyses in femur were quantified from MicroCT scans using GE MicroView software v2.2. Reg-Yng: Regular young rats; Reg-Ma: Regular middle-aged rats; Irreg-Ma: Irregular middle-aged rats; Acyc-Ma: Acyclic middle-aged rats. BMD: bone mineral density; BMC: bone mineral content.

DISCUSSION

Reproductive senescence, resulting from hypothalamic and ovarian aging, manifests oestrous cycle irregularities in rats and mice, marking the decline of their reproductive lifespan. Vaginal smears (cytology) and histology are common methods to identify rodent cycle stage, interpret potential cycle perturbations, and assess the functional status of the HPG axis and reproductive system (12,13,15,34,35). While other indices are more useful in humans to determine the reproductive system's functional status (for example, menses, basal body temperature, alterations in vaginal pH and cervical mucous viscosity) (16), assessments of rodent oestrous cyclicity can offer mechanism insights into potential adverse effects occurring during the early menopausal transition, given the similarities in the regulatory mechanisms of the female reproductive axis across species.

Two studies have reported molecular neuroendocrine alterations in the hypothalamus affecting HPG functions, leading to reproductive cycle irregularity and acyclicity in middle-aged female Sprague-Dawley rats similar to menopausal transition in women (18,23). In one of these studies, Kermath *et al.* (2014) examined the circulating levels of sex hormones and found no significant differences in oestradiol (23). However, our study revealed lower levels of this hormone associated with the onset of cycle irregularity and acyclicity, which would resemble the situation occurring in women. In this regard, the SWAN study, which followed 3302 women aged 42-52 over 8 years, found that the circulating levels of oestradiol remained stable until a rapid decline during the last two years of the late phase in the perimenopausal woman, with levels settled at low values two years after the final menstrual period (FMP) (36). Furthermore, in women, the late menopausal transition is also characterized by an increase in the circulating levels of FSH (23,36,37) and, in agreement with this behavior, Kermath *et al.* (2014) reported a surge in FSH levels coinciding with the onset of irregularity and acyclicity in middle-aged rats. By contrast, we did not observe such differences, which could be attributed at first glance to the fact that rats were not sacrificed during the estrus phase of the cycle, when the FSH secretion peak occurs (30). Additionally, in our study, the decreased LH levels observed in the acyclic animals, when compared to their middle-aged regular and irregular counterparts, would indicate altered gonadotropin secretion patterns during reproductive aging (38–40), a pattern that was also observed in Kermath *et al*., although the differences were not statistically significant (23). While a regular vaginal cycle does not always indicate ovulation, stromal luteinization, which confirms ovulation, transforms follicles into corpora lutea (16). As previously described in numerous studies, persistent oestrous is characterized by low levels of progesterone and an increased 17 beta-oestradiol/progesterone ratio, which is attributed to a lack of ovulation and corpus luteum

production, and is also accompanied by the presence of numerous follicular cysts and age-related ovarian atrophy (12,13,15,19,29,41). In our study, all these hallmarks were reported in the acyclic group, reinforcing the translational applicability of this natural female reproductive aging rat model, characterized by a decline in ovarian function during reproductive senescence caused by hormonal imbalances and changes in the HPG axis, leading to ovulation failure and the end of the oestrous cycle.

The hormonal and histological alterations detailed above can have profound implications beyond the reproductive system. Given that lipid compounds, such as glycerolipids, glycerophospholipids and sterols play critical roles in cellular structure, energy storage and signaling, changes in the circulating lipidome can reflect and potentially drive changes in metabolic and physiological states linked with endocrine function (42). Lipidomics, the large-scale study of pathways and networks of cellular lipids in biological systems, provides a comprehensive understanding of the diverse lipid species and their roles in health and diseases such as cardiovascular disease (CVD), MetS, neurodegenerative diseases and different types of cancer (42). In our study, we identified circulating signatures of perimenopause using a semi-targeted lipidomics approach that allows the identification of more than 400 metabolites, reporting that the progressive transition of oestrous cycles encompassing regular, irregular and acyclic stages that characterized the natural reproductive senescence was associated with marked changes in serum lipid-related metabolites, with an independent effect of age. Specifically, PCs were the most represented family, and as a general trend, most of the identified lipid families (PCs, LysoPCs, PEs, LysoPEs, ChoEs, and TGs) increased as the reproductive aging was more evident, while the steroid metabolite 5-α-androstan-diol exhibited the opposite pattern.

To date, only two studies reported changes in circulating lipid-related metabolites between premenopausal and postmenopausal women using lipidomics approaches. However, none of these studies directly examined these biomarkers in the early stages of perimenopause or longitudinally during the menopausal transition (24,25). Nogueira *et al.* showed significant increases in PCs in the postmenopausal state, with strong positive correlations between total cholesterol and low-density lipoprotein cholesterol (LDL-c) and PC(38:1) and PC(38:2) (24). The significant increase observed in our study in the circulating levels of these PCs among Reg-Ma, Irreg-Ma and Acyc-Ma groups are in line with these findings and the fact that, in our study, PC(38:2) was one of the top 40 metabolites that contributed more to discriminate the three groups would suggest that this lipid specie is already altered in an early stage of female reproductive aging, as occurred with PC(34:2), PC(36:2), and PC(36:4), which in the present research were significantly higher in irregular than in regular rats and displayed strong positive correlations with the circulating levels of cholesterol. Recent studies showed that plasma levels of PC(34:2) and PC(36:2) increased in patients with type 2 diabetes (43,44). In our study, these PCs changes cannot be linked to impaired glucose and insulin metabolism because no significant changes among middle-aged groups were found in the surrogate markers of insulin resistance and sensitivity, HOMA-IR and R-QUICKI, respectively, and no correlations were found between these both parameters and the circulating levels of PC(34:2) and PC(36:2). Remarkably, the increase in the circulating levels of LysoPE(22:6), LysoPE(22:5), and LysoPC(17:0) and the decrease in the plasma 5-α-androstan-diol sulfate concentrations found in our study during the natural transition to reproductive senescence are in line with the results obtained by Ke *et al.*, which reported that these lipid species followed the same behavior in postmenopausal women compared

to climacteric women (25). These findings would reinforce our idea that changes in lipid-related metabolites are already occurring in the early stages of perimenopause.

The higher levels of PCs, PEs, LysoPCs and LPEs species observed in postmenopausal women in the aforementioned studies may reflect hormonal changes during menopause impacting liver lipoprotein metabolism (45) and could be involved in the appearance of metabolic-related alterations. Thus, fasting blood phospholipid composition primarily reflects hepatic phospholipid synthesis (46) and it was shown that saturated phospholipids were positively associated with CVD risk (47). Furthermore, LPCs, the most abundant lysophospholipid species found in human blood, have been suggested to promote atherosclerosis by eliciting an inflammatory response when they contain saturated acyl chains (48,49). Additionally, Steinberg *et al.* (49) demonstrated that lysoPCs were presented in higher concentrations in oxidized LDLs. In our study, 40% of the LysoPCs that significantly changed among the three middle-aged rat groups contained a saturated acyl chain, including the LysoPC(20:0), LysoPC(20:0)-sn2, LysoPC(23:0) and LysoPC(24:0) species, which were 4 out of 18 lipids that were already altered coinciding with the onset of irregular cycles, exhibiting significant increases compared to the regular cycle group. Remarkably, LysoPC(20:0)-sn2, emerged as the most discriminative parameter according to the VIP score analysis. The combination of fatty acids bound at the sn-1 and sn-2 positions largely determines the biophysical properties of cell membranes, which influence the activities of integral membrane proteins (50,51) and provide substrates for signaling processes (52,53). Therefore, factors that ensure membrane phospholipid homeostasis are crucial for maintaining cell function with liver also playing a relevant role, being involved in extracellular lysophospholipid levels regulation by modifying the expression of several enzymes (54). Related to this, lecithin cholesterol acyltransferase (LCAT) cleaves fatty acids from the sn-2 position of PC,

resulting in lysoPC primarily containing saturated fatty acids (55). Therefore, it is plausible to speculate that an increased plasma LCAT activity may be one of the factors causing the increase in the serum levels of saturated species of lysoPC observed in this study. Other studies have reported that elevated LPCs levels can be produced by increased phospholipase A2 (PLA2) activity, which hydrolyzes PC, influencing cell proliferation, invasion, and migration in various cancers (55–59) and is overexpressed in breast and ovarian cancer patients (59–63). In the present study, the circulating levels of TC progressively increased as there was a loss of cyclicity in the middle-aged rats and, interestingly, in the Irreg-Ma group, the increase reported in the LysoPC(20:0), LysoPC(20:0)-sn2, LysoPC(23:0) and LysoPC(24:0) plasma levels preceded the rise in TC, which was only significantly reported in rats displaying acyclicity. These results would suggest these four LPCs as potential early biomarkers of hypercholesterolemia and would be in agreement with the potential harmful effect on the cardiometabolic health of the LPCs containing a saturated fatty acyl chain. Further studies, such as those carried out with rats challenged with a hyperlipidemic and atherogenic diet and analyzing additional related parameters, such us PLA2 and LCAT activities, at different time points, would be of interest to provide more insights into the pathophysiological significance of the increased LysoPC(20:0), LysoPC(20:0)-sn2, LysoPC(23:0) and LysoPC(24:0) circulating levels concerning CVD and cancer risks in the framework of menopausal transition and postmenopause.

Circulating lipidomes exhibit significant sex-related differences that tend to narrow or reverse with age due to the distinct effects of aging on males and females (47,64–69). Thus, glycerophospholipid levels are lower in young women than men, but increase more rapidly with age in women, resulting in higher levels in older women compared to older men (70), which can partly be explained by a drop in oestrogen levels after menopause

(71). To name some examples, females displayed greater age-related increases in both TGs and glycerophospholipid species (PC, LPC, SM, ChoE, and PE), while in males these glycerophospholipids decreased (64,67,68,70,72–76). Furthermore, higher levels and abundance of most PCs have been observed in women compared to men in many studies (65,67,74,77–79), including species such as PC(40:6), PC(36:5), PC(36:2) and PC(34:2) (78,80,81). In women, many studies reported that, regardless of the menstrual cycle or reproductive status, glycerophospholipid species concentrations are generally lowest and stable during the late 30s to mid-40s, slightly increasing during the mid-40s and showing a higher increase in the late 40s and early 50s. Thus, higher concentrations of PC, PE and TAG were found in postmenopausal women compared with premenopausal women (47), PCs being the species showing the greatest tendency to increase (47,64,65). In our study, the increased circulating levels of PC(40:6), PC(36:5), PC(36:2) and PC(34:2) observed in rats in response to the progressive loss of oestrous cycle regularity are in line with these previous findings observed in women. Furthermore, it was reported that the proportion of PE(O-36:5) was significantly greater in women than men (78), and this metabolite was detected in our study as an early biomarker of the transition between regular and irregular cycles. It is well known that men display a higher risk for CVD early in life, while women have a higher risk later in life (82,83) and both the sex and age-related differences in CVD risk have been linked to changes in glycerophospholipid metabolism (67). It is well known that circulating lipoproteins are affected by female sex steroids, and that primary changes are observed during the altered fluctuations in sex hormone levels during the menopausal transition (84–86). Whether the differences in the circulating glycerophospholipid composition reported in this rat model of natural female reproductive senescence could impact on patterns of health and disease during

perimenopause and could contribute to sexual dimorphism in CVD risk at middle age deserves further research.

The progressive significant decrease reported in the circulating levels of 5-α-androstandiol, a metabolite of DHEA-S and DHT linked to androgenic activity, as the loss of regularity occurred, would also contribute to reinforce the reliability and the translational applicability of our findings because it was observed that the circulating levels of DHT decreased along with the oestradiol and testosterone concentrations in postmenopausal women compared to premenopausal women (87). In the same line, it was described a pronounced decline in DHEA and its sulfate form, DHEA-S, in aged women (88). Interestingly, higher levels of PCs were linked to lower androgenic steroid levels in postmenopausal women (25,72) and, in line with this results, in our study, strong negative correlations between these metabolite and the phosphatidylcholines PC(34:2), PC(36:4), and PC(36:5) were found. These findings suggest a link between androgenic hormones and PCs in reproductive senescence, although additional research would be needed to gain knowledge on this issue.

DiHETE family is associated with type II diabetes and inflammatory diseases (89,90). The transitory increase reported in rats displaying irregular cycles concerning the circulating levels of 17,18-dihydroxyeicosatrienoic acid (17,18-DiHETE), a metabolite derived of the omega-6 fatty acid arachidonic acid, and, to a lesser extent, in the plasma concentrations of 13-HDHA, a metabolite derived from the omega-3 fatty acid docosahexaenoic acid (DHA) that was identified as one of the 40 metabolites that contributed more to discriminate the three groups of middle-aged rats, was, at first glance, an unexpected result. Intriguingly, the levels of these metabolites declined in the acyclic group of rats, showing these animals even lower levels than those reported in the middle-aged rats showing regular cycles. PC species stand as a primary reservoir of

polyunsaturated fatty acids, such as arachidonic and linoleic acids. These fatty acids serve as precursors for eicosanoids, which exhibit diverse biological activities (91–93). Interestingly, all the PCs that differed statistically between rats with regular and irregular cycles were polyunsaturated, except for PC(0-36:1). It is well-established that PUFA metabolites, including those originating from arachidonic acid, along with eicosapentaenoic acid (EPA) and DHA, play a key role in the regulation of the inflammatory response (94). Oestrogens stimulate DHA production in rats, suggesting that post-menopause oestrogen changes may affect DHA metabolism (95). However, because the circulating levels of this hormone decreased at similar levels in both irregular and acyclic groups, it seems unlikely that oestradiol could be responsible, at least in part, for transitory effects observed in the circulating levels 17,18-DiHETE and 13-HDHA. Further studies would be needed to clarify this issue.

Given that the average menopausal age for European women is 51 (96), the significant increases observed around age 50 in the above-commented lipid-related metabolites likely would correspond to changes in the reproductive status (84). However, many studies overlook the fact that menopause is preceded by the menopausal transition, a period marked by menstrual cycle irregularity starting typically in the mid-40s (64), which could account for early changes in metabolites that could be useful as potential early biomarkers of perimenopause. In this regard, to the best of our knowledge, there are only two studies that reported changes in classical lipid-related metabolites within the 1-year interval before and after the final menstrual period (FMP), or during a follow-up carried out after 2.5 years during menopausal transition, including increased concentrations of VLDLs, LDLs, total cholesterol, and LDL-cholesterol, apolipoprotein B, and reduced LDL particle size. These changes were independent of the women’s chronological age and may underlie women's increased cardiometabolic risk in their post-

menopausal years (84,85). These studies highlight the importance of identifying biomarkers for early diagnosis of perimenopause to minimize the risk of suffering from CVDs. Our findings give additional insights into this issue, identifying, using a semi-targeted lipidomic approach, up to 18 lipid-related metabolites that already changed with the appearance of the irregular cycles, and before that, a significant increase in the circulating levels of TC was reported. Therefore, it is tempting to speculate that these lipid-related compounds, including 9 PCs, 4 LysoPCs, 2 PEs, ChoE(18:2), 5-α-androstan-diol and 17,18-DiHETE, could be used as a potential multivariate biomarker to monitor, at molecular level, the response to new treatments and lifestyle-based interventions carried out at very early stages of natural reproductive senescence to preserve the endocrine and metabolic functions of perimenopausal women.

The present study has some limitations. First, the metabolites detected in this work were semi-quantified in terms of internal standard response ratio and an absolute quantification by correlating signal intensities of the lipid-related metabolites with a calibration curve would be needed to validate the lipidomic changes reported during perimenopausal transition. In addition, further advances in lipidomics platforms might help capture more comprehensive and complete lipidome profiles, including the position and saturation and/or unsaturation of fatty acyl chains in different lipid species, which can impact on the functionality of lipid-related metabolites. Finally, our results were obtained at preclinical level and with a relatively small sample size and further clinical trials carried out with perimenopausal women would be needed to validate our findings. A thorough assessment of premenopause, perimenopause, and menopause would require highly detailed targeting of the final menstrual period and the appearance of preceding menopause-related symptoms, including longitudinal hormone and risk factor measures before, during, and

after the menopausal transition. Incorporating lipidomic analysis into this assessment can provide deeper insights into the molecular changes occurring during these stages.

CONCLUSIONS

In the present study, we showed that, in an ovarian-intact middle-aged model of rats, the gradual loss of regularity in the oestrous cycle occurring during the natural transition to reproductive senescence was associated with altered circulating levels of different HPG-related sex hormones (oestradiol, progesterone and LH) and, in rats that were in persistent oestrous, with histomorphological changes in the ovaries, including atrophy and a lack of stromal luteinization and corpus luteum. These results were accompanied by progressive significant changes in the lipidomic profile detected in serum as the oestrous cycles were losing regularity. Although circulating lipidomic changes are well-documented in postmenopausal women, as far as we know, this is the first work reporting that lipidomic-related shifts in serum are already detected at very early stages of female reproductive senescence in a rat model that resembles the early menopausal transition occurring in women. These findings are in line with our hypothesis and allowed us to identify a set of metabolites that already changed with the transition from a regular to an irregular oestrous cycle, including 9 PCs, 4 LysoPCs, 2 PEs, ChoE(18:2), 5-α-androstan-diol and 17,18-DiHETE, which could be used as a potential multivariate biomarker of early perimenopause. Further clinical trials performed with this target population would be of great value to reinforce our findings. A detailed understanding of the molecular changes that occur during the menopausal transition can pave the way to design new treatments and lifestyle-based interventions addressed to preserve the endocrine and metabolic functions of perimenopausal women and to ameliorate in later stages the vasomotor symptoms, osteoporosis and metabolic-related diseases that can appear in postmenopausal women.

ABBREVIATIONS

17β-E2, 17β-oestradiol; 5-α-androstan-diol, 5a-androstan-3,17-diol-monosulfate-iso3; Acyc-Ma, acyclic middle-aged rats, ANOVA, analysis of variance; AUC, area under ROC curve; BMC, bone mineral content; BMD, bone mineral density; CRP, C-reactive protein; CVDs, cardiovascular diseases; ESI, electrospray ionization, FDR, false discovery rate; FSH, follicle-stimulating hormone; GC, gas chromatography; HOMA-IR, homeostasis model assessment-estimated insulin resistance; HPG, hypothalamic–pituitary–gonadal/ovarian; Irreg-Ma, irregular cycling middle-aged rats; LDL, low-density lipoprotein; LH, luteinizing hormone; MetS, metabolic syndrome; MWAT, mesenteric white adipose tissue; R-QUICKI, revised quantitative insulin sensitivity check index; POWAT, periovarian white adipose tissue; PCA, principal components analysis; PLS-DA, partial least-squares discriminant analysis; QTOF, quadrupole time-of-flight; Reg-Ma, regular cycling middle-aged rats; Reg-Yng, regular cycling young rats; T2DM, Type 2 Diabetes Mellitus; TC, total cholesterol; TG, triglycerides, UHPLC, ultra-high-performance liquid chromatography; VIP, variable importance in projection; VLDL, very low-density lipoprotein.

REFERENCES

1. Harlow SD, Gass M, Hall JE, Lobo R, Maki P, Rebar RW, et al. Executive Summary of the Stages of Reproductive Aging Workshop + 10: Addressing the Unfinished Agenda of Staging Reproductive Aging. J Clin Endocrinol Metab. 2012, 97, 1159–68.
2. Delamater L, Santoro N. Management of the Perimenopause. Clin Obstet Gynecol. 2018, 61, 419–32.
3. Santoro N, Randolph JF. Reproductive Hormones and the Menopause Transition. Obstet Gynecol Clin North Am. 2011, 38, 455–66.
4. Santoro N, Crawford SL, El Khoudary SR, Allshouse AA, Burnett-Bowie SA, Finkelstein J, et al. Menstrual cycle hormone changes in women traversing menopause: Study of women's health across the nation. J Clin Endocrinol Metab. 2017, 2218–29.
5. Gold EB, Colvin A, Avis N, Bromberger J, Greendale GA, Powell L, et al. Longitudinal Analysis of the Association Between Vasomotor Symptoms and Race/Ethnicity Across the Menopausal Transition: Study of Women's Health Across the Nation. Am J Public Health. 2006, 96, 1226–35.
6. Avis NE, Crawford SL, Greendale G, Bromberger JT, Everson-Rose SA, Gold EB, et al. Duration of Menopausal Vasomotor Symptoms Over the Menopause Transition. JAMA Intern Med. 2015, 175, 531.
7. Thapa S, Nandy A, Rendina-Ruedy E. Endocrinal metabolic regulation on the skeletal system in post-menopausal women. Front Physiol. 2022, 13, 1052429.
8. McNeil MA, Merriam SB. Menopause. Ann Intern Med. 2021, 174, ITC97-ITC112.
9. Kaaja RJ. Metabolic syndrome and the menopause. Menopause Int. 2008, 14, 21–5.
10. Fenton A, Smart C, Goldschmidt L, Price V, Scott J. Fat mass, weight and body shape changes at menopause – causes and consequences: a narrative review. Climacteric. 2023, 26, 381–7.
11. Lefevre J, Mcclintock MK. Reproductive Senescence in Female Rats: A Longitudinal Study of Individual Differences in Estrous Cycles and Behavior. Biol Reprod. 1988, 38, 780–9.
12. Westwood FR. The Female Rat Reproductive Cycle: A Practical Histological Guide to Staging. Toxicol Pathol. 2008, 36, 375–84.
13. Dixon D, Alison R, Bach U, Colman K, Foley GL, Harleman JH, et al. Nonproliferative and proliferative lesions of the rat and mouse female reproductive system. J Toxicol Pathol. 2014, 27, 1S-107S.
14. Sato J, Hashimoto S, Doi T, Yamada N, Tsuchitani M. Histological characteristics of the regression of corpora lutea in Wistar Hannover rats: The comparisons with Sprague-Dawley rats. J Toxicol Pathol. 2014, 27, 107–13.
15. Shirai N, Houle C, Mirsky ML. Using histopathologic evidence to differentiate reproductive senescence from xenobiotic effects in middle-aged female sprague-dawley rats. Toxicol Pathol. 2015, 43, 1158–61.

16. Goldman JM, Murr AS, Cooper RL. The rodent estrous cycle: characterization of vaginal cytology and its utility in toxicological studies. Birth Defects Res Part B Dev Reprod Toxicol. 2007, 80, 84–97.
17. Yin F, Yao J, Sancheti H, Feng T, Melcangi RC, Morgan TE, et al. The perimenopausal aging transition in the female rat brain: Decline in bioenergetic systems and synaptic plasticity. Neurobiol Aging. 2015, 36, 2282–95.
18. Bacon ER, Mishra A, Wang Y, Desai MK, Yin F, Brinton RD. Neuroendocrine aging precedes perimenopause and is regulated by DNA methylation. Neurobiol Aging. 2019, 74, 213–24.
19. Vidal JD. The Impact of Age on the Female Reproductive System. Toxicol Pathol. 2017, 45, 206–15.
20. Finch CE. The menopause and aging, a comparative perspective. J Steroid Biochem Mol Biol. 2014, 142, 132–41.
21. Kermath BA, Gore AC. Neuroendocrine Control of the Transition to Reproductive Senescence: Lessons Learned from the Female Rodent Model. Neuroendocrinology. 2012, 96, 1–12.
22. Brinton RD. Minireview: Translational animal models of human menopause: Challenges and emerging opportunities. Endocrinology. 2012, 153, 3571–8.
23. Kermath BA, Riha PD, Woller MJ, Wolfe A, Gore AC. Hypothalamic Molecular Changes Underlying Natural Reproductive Senescence in the Female Rat. Endocrinology. 2014, 155, 3597–609.
24. Nogueira IAL, da Cruz ÉJSN, Fontenele AMM, Figueiredo Neto JA de. Alterations in postmenopausal plasmatic lipidome. Monleon D, editor. PLoS One. 2018, 13, e0203027.
25. Ke C, Hou Y, Zhang H, Yang K, Wang J, Guo B, et al. Plasma Metabolic Profiles in Women are Menopause Dependent. Kim KH, editor. PLoS One. 2015, 10, e0141743.
26. McLean AC, Valenzuela N, Fai S, Bennett SAL. Performing Vaginal Lavage, Crystal Violet Staining, and Vaginal Cytological Evaluation for Mouse Estrous Cycle Staging Identification. J Vis Exp. 2012, 15, 4–9.
27. Matthews DR, Hosker JR, Rudenski AS, Naylor BA, Treacher DF, Turner RC. Homeostasis model assessment: insulin resistance and fl-cell function from fasting plasma glucose and insulin concentrations in man. Diabetologia. 1985, 28, 412-9.
28. Perseghin G, Caumo A, Caloni M, Testolin G, Luzi L. Incorporation of the Fasting Plasma FFA Concentration into QUICKI Improves Its Association with Insulin Sensitivity in Nonobese Individuals. J Clin Endocrinol Metab. 2001, 86, 4776–81.
29. Yoshida M, Sanbuissyo A, Hisada S, Takahashi M, Ohno Y, Nishikawa A. Morphological characterization of the ovary under normal cycling in rats and its viewpoints of ovarian toxicity detection. J Toxicol Sci. 2009, 34, 189–97.
30. Sato J, Nasu M, Tsuchitani M. Comparative histopathology of the estrous or menstrual cycle in laboratory animals. J Toxicol Pathol. 2016, 29, 155–62.

31. Baudin J, Hernandez-Baixauli J, Quesada-Vázquez S, Mulero F, Puiggròs F, Arola L, et al. Combined supplementation with hesperidin, phytosterols and curcumin decreases adiposity and improves metabolic health in ovariectomized rats. Food Funct. 2024,15, 4905–24.
32. Wickham H. ggplot2: Elegant Graphics for Data Analysis. Springer-Verlag New York. 2016, 35, 211.
33. Gu Z, Eils R, Schlesner M. Complex heatmaps reveal patterns and correlations in multidimensional genomic data. Bioinformatics. 2016, 32, 2847–9.
34. Cora MC, Kooistra L, Travlos G. Vaginal Cytology of the Laboratory Rat and Mouse:Review and Criteria for the Staging of the Estrous Cycle Using Stained Vaginal Smears. Toxicol Pathol. 2015, 43, 776–93.
35. Sano K, Matsuda S, Tohyama S, Komura D, Shimizu E, Sutoh C. Deep learning-based classification of the mouse estrous cycle stages. Sci Rep. 2020, 10, 1–8.
36. Randolph JF, Zheng H, Sowers MR, Crandall C, Crawford S, Gold EB, et al. Change in Follicle-Stimulating Hormone and Estradiol Across the Menopausal Transition: Effect of Age at the Final Menstrual Period. J Clin Endocrinol Metab. 2011, 96, 746–54.
37. Burger H, Woods NF, Dennerstein L, Alexander JL, Kotz K, Richardson G. Nomenclature and endocrinology of menopause and perimenopause. Expert Rev Neurother. 2007, 7, S35–43.
38. SCARBROUGH K, WISE PM. Age-Related Changes in Pulsatile Luteinizing Hormone Release Precede the Transition to Estrous Acyclicity and Depend upon Estrous Cycle History. Endocrinology. 1990, 126, 884–90.
39. Wise PM. Alterations in Proestrous LH, FSH, and Prolactin Surges in Middle-Aged Rats. Exp Biol Med. 1982, 169, 348–54.
40. Cooper RL, Michael Conn P, Walker RF. Characterization of the LH Surge in Middle-Aged Female Rats1. Biol Reprod. 1980, 23, 611–5.
41. Cruz G, Fernandois D, Paredes AH. Ovarian function and reproductive senescence in the rat: role of ovarian sympathetic innervation. Reproduction. 2017, 153, R59–68.
42. Gross RW, Han X. Lipidomics at the Interface of Structure and Function in Systems Biology. Chem Biol. 2011, 18, 284–91.
43. Rhee EP, Cheng S, Larson MG, Walford GA, Lewis GD, McCabe E, et al. Lipid profiling identifies a triacylglycerol signature of insulin resistance and improves diabetes prediction in humans. J Clin Invest. 2011. 121, 1402–11.
44. Celis-Morales C, Livingstone KM, Marsaux CFM, Macready AL, Fallaize R, O'Donovan CB, et al. Effect of personalized nutrition on health-related behaviour change: Evidence from the Food4Me European randomized controlled trial. Int J Epidemiol. 2017, 46, 578–88.
45. Hodson L, Banerjee R, Rial B, Arlt W, Adiels M, Boren J, et al. Menopausal Status and Abdominal Obesity Are Significant Determinants of Hepatic Lipid Metabolism in Women. J Am Heart Assoc. 2015, 4, 1–14.
46. Pynn CJ, Henderson NG, Clark H, Koster G, Bernhard W, Postle AD. Specificity and rate of human and mouse liver and plasma phosphatidylcholine synthesis

analyzed in vivo. J Lipid Res. 2011, 52, 399–407.
47. Beyene HB, Olshansky G, T. Smith AA, Giles C, Huynh K, Cinel M, et al. High-coverage plasma lipidomics reveals novel sex-specific lipidomic fingerprints of age and BMI: Evidence from two large population cohort studies. Locasale JW, editor. PLOS Biol. 2020, 18, e3000870.
48. Knuplez E, Marsche G. An Updated Review of Pro- and Anti-Inflammatory Properties of Plasma Lysophosphatidylcholines in the Vascular System. Int J Mol Sci. 2020, 21, 4501.
49. Epstein FH, Steinberg D, Parthasarathy S, Carew TE, Khoo JC, Witztum JL. Beyond Cholesterol. Modifications of low-density lipoprotein that increase its atherogenicity. N Engl J Med. 1989, 320, 915–24.
50. Ces O, Mulet X. Physical coupling between lipids and proteins: a paradigm for cellular control. Signal Transduct. 2006, 6, 112–32.
51. Dymond MK, Hague C V., Postle AD, Attard GS. An in vivo ratio control mechanism for phospholipid homeostasis: evidence from lipidomic studies. J R Soc Interface. 2013, 10, 20120854.
52. Heung YMM, Postle AD. The molecular selectivity of phospholipase D in HL60 granulocytes. FEBS Lett. 1995, 364, 250–4.
53. Heung YMM, Postle AD. Substrate selectivity of phospholipase D in HL60 granulocytes: Effects of fatty acid supplementation. Biochem Soc Trans. 1995, 23, 1991.
54. Suárez-García S, Caimari A, del Bas JM, Suárez M, Arola L. Serum lysophospholipid levels are altered in dyslipidemic hamsters. Sci Rep. 2017, 7, 10431.
55. Okita M, Gaudette DC, Mills GB, Holub BJ. Elevated levels and altered fatty acid composition of plasma lysophosphatidylcholine(lysoPC) in ovarian cancer patients. Int J Cancer. 1997, 71, 31–4.
56. Giallourou N, Urbaniak C, Puebla-Barragan S, Vorkas PA, Swann JR, Reid G. Characterizing the breast cancer lipidome and its interaction with the tissue microbiota. Commun Biol. 2021, 4, 1229.
57. Xu Y. Lysophospholipid Signaling in the Epithelial Ovarian Cancer Tumor Microenvironment. Cancers (Basel). 2018, 10, 227.
58. Pyragius C, Fuller M, Ricciardelli C, Oehler M. Aberrant Lipid Metabolism: An Emerging Diagnostic and Therapeutic Target in Ovarian Cancer. Int J Mol Sci. 2013, 14, 7742–56.
59. Dong Q, Patel M, Scott KF, Graham GG, Russell PJ, Sved P. Oncogenic action of phospholipase A2 in prostate cancer. Cancer Lett. 2006, 240, 9–16.
60. Laye JP, Gill JH. Phospholipase A2 expression in tumours: a target for therapeutic intervention? Drug Discov Today. 2003, 8, 710–6.
61. Yamashita SI, Yamashita JI, Sakamoto K, Inada K, Nakashima Y, Murata K, et al. Increased expression of membrane-associated phospholipase A2 shows malignant potential of human breast cancer cells. Cancer. 1993, 71, 3058–64.
62. Ke C, Hou Y, Zhang H, Fan L, Ge T, Guo B, et al. Large-scale profiling of metabolic dysregulation in ovarian cancer. Int J Cancer. 2015, 136, 516–26.

63. Zhang Y, Liu Y, Li L, Wei J, Xiong S, Zhao Z. High resolution mass spectrometry coupled with multivariate data analysis revealing plasma lipidomic alteration in ovarian cancer in Asian women. Talanta. 2016, 150, 88–96.
64. Auro K, Joensuu A, Fischer K, Kettunen J, Salo P, Mattsson H, et al. A metabolic view on menopause and aging. Nat Commun. 2014, 5, 4708.
65. Tabassum R, Ruotsalainen S, Ottensmann L, Gerl MJ, Klose C, Tukiainen T, et al. Lipidome- and Genome-Wide Study to Understand Sex Differences in Circulatory Lipids. J Am Heart Assoc. 2022, 11, e027103.
66. Wong MWK, Braidy N, Pickford R, Vafaee F, Crawford J, Muenchhoff J, et al. Plasma lipidome variation during the second half of the human lifespan is associated with age and sex but minimally with BMI. Ginsberg SD, editor. PLoS One. 2019, 14, e0214141.
67. Tabassum R, Widén E, Ripatti S. Effect of biological sex on human circulating lipidome: An overview of the literature. Atherosclerosis. 2023, 384, 117274.
68. Mohammadzadeh Honarvar N, Zarezadeh M, Molsberry SA, Ascherio A. Changes in plasma phospholipids and sphingomyelins with aging in men and women: A comprehensive systematic review of longitudinal cohort studies. Aging Res Rev. 2021, 68, 101340.
69. Slade E, Irvin MR, Xie K, Arnett DK, Claas SA, Kind T, et al. Age and sex are associated with the plasma lipidome: findings from the GOLDN study. Lipids Health Dis. 2021, 20, 30.
70. Muilwijk M, Callender N, Goorden S, Vaz FM, van Valkengoed IGM. Sex differences in the association of sphingolipids with age in Dutch and South-Asian Surinamese living in Amsterdam, the Netherlands. Biol Sex Differ. 2021, 12, 13.
71. Colleluori G, Chen R, Napoli N, Aguirre LE, Qualls C, Villareal DT, et al. Fat mass follows a U-shaped distribution based on estradiol levels in postmenopausal women. Front Endocrinol (Lausanne). 2018, 9, 1–6.
72. Darst BF, Koscik RL, Hogan KJ, Johnson SC, Engelman CD. Longitudinal plasma metabolomics of aging and sex. Aging. 2019, 11, 1262–82.
73. Chak C, Lacruz M, Adam J, Brandmaier S, Covic M, Huang J, et al. Aging Investigation Using Two-Time-Point Metabolomics Data from KORA and CARLA Studies. Metabolites. 2019, 9, 44.
74. Mittelstrass K, Ried JS, Yu Z, Krumsiek J, Gieger C, Prehn C, et al. Discovery of Sexual Dimorphisms in Metabolic and Genetic Biomarkers. McCarthy MI, editor. PLoS Genet. 2011, 7, e1002215.
75. Rist MJ, Roth A, Frommherz L, Weinert CH, Krüger R, Merz B, et al. Metabolite patterns predicting sex and age in participants of the Karlsruhe Metabolomics and Nutrition (KarMeN) study. PLoS One. 2017, 12, e0183228.
76. Gonzalez-Covarrubias V, Beekman M, Uh H, Dane A, Troost J, Paliukhovich I, et al. Lipidomics of familial longevity. Aging Cell. 2013, 12, 426–34.

77. Weir JM, Wong G, Barlow CK, Greeve MA, Kowalczyk A, Almasy L, et al. Plasma lipid profiling in a large population-based cohort. J Lipid Res. 2013, 54, 2898–908.
78. West AL, Michaelson L V., Miles EA, Haslam RP, Lillycrop KA, Georgescu R, et al. Lipidomic Analysis of Plasma from Healthy Men and Women Shows Phospholipid Class and Molecular Species Differences between Sexes. Lipids. 2021, 56, 229–42.
79. Lizardo DY, Parisi LR, Li N, Atilla-Gokcumen GE. Noncanonical Roles of Lipids in Different Cellular Fates. Biochemistry. 2018, 57, 22–9.
80. Kawanishi N, Kato Y, Yokozeki K, Sawada S, Sakurai R, Fujiwara Y, et al. Effects of aging on serum levels of lipid molecular species as determined by lipidomics analysis in Japanese men and women. Lipids Health Dis. 2018, 17, 135.
81. Quehenberger O, Armando AM, Brown AH, Milne SB, Myers DS, Merrill AH, et al. Lipidomics reveals a remarkable diversity of lipids in human plasma. J Lipid Res. 2010, 51, 3299–305.
82. Finegold JA, Asaria P, Francis DP. Mortality from ischaemic heart disease by country, region, and age: Statistics from World Health Organisation and United Nations. Int J Cardiol. 2013, 168, 934–45.
83. The Emerging Risk Factors Collaboration. Diabetes mellitus, fasting blood glucose concentration, and risk of vascular disease: a collaborative meta-analysis of 102 prospective studies. Lancet. 2010, 375, 2215-22.
84. Wang Q, Ferreira DLS, Nelson SM, Sattar N, Ala-Korpela M, Lawlor DA. Metabolic characterization of menopause: cross-sectional and longitudinal evidence. BMC Med. 2018, 16, 17.
85. Matthews KA, Crawford SL, Chae CU, Everson-Rose SA, Sowers MF, Sternfeld B, et al. Are Changes in Cardiovascular Disease Risk Factors in Midlife Women Due to Chronological Aging or to the Menopausal Transition? J Am Coll Cardiol. 2009, 54, 2366–73.
86. Knopp RH, Zhu X, Bonet B. Effects of estrogens on lipoprotein metabolism and cardiovascular disease in women. Atherosclerosis. 1994, 110, S83–91.
87. Rothman MS, Carlson NE, Xu M, Wang C, Swerdloff R, Lee P, et al. Reexamination of testosterone, dihydrotestosterone, estradiol and estrone levels across the menstrual cycle and in postmenopausal women measured by liquid chromatography–tandem mass spectrometry. Steroids. 2011, 76, 177–82.
88. Davison SL, Bell R, Donath S, Montalto JG, Davis SR. Androgen Levels in Adult Females: Changes with Age, Menopause, and Oophorectomy. J Clin Endocrinol Metab. 2005, 90, 3847–53.
89. Giera M, Ioan-Facsinay A, Toes R, Gao F, Dalli J, Deelder AM, et al. Lipid and lipid mediator profiling of human synovial fluid in rheumatoid arthritis patients by means of LC-MS/MS. Biochim Biophys Acta - Mol Cell Biol Lipids. 2012, 1821, 1415–24.
90. Heemskerk M, Giera M, Bouazzaoui F, Lips M, Pijl H, van Dijk K, et al. Increased PUFA Content and 5-Lipoxygenase Pathway Expression Are Associated with Subcutaneous Adipose Tissue Inflammation in Obese Women with Type 2

Diabetes. Nutrients. 2015, 7, 7676–90.

91. Yin M zhu, Tan S, Li X, Hou Y, Cao G, Li K, et al. Identification of phosphatidylcholine and lysophosphatidylcholine as novel biomarkers for cervical cancers in a prospective cohort study. Tumor Biol. 2016, 37, 5485–92.
92. Asaoka Y, Yoshida K, Sasaki Y, Nishizuka Y. Potential role of phospholipase A2 in HL-60 cell differentiation to macrophages induced by protein kinase C activation. Proc Natl Acad Sci. 1993, 90, 4917–21.
93. Yoshida K, Asaoka Y, Nishizuka Y. Platelet activation by simultaneous actions of diacylglycerol and unsaturated fatty acids. Proc Natl Acad Sci. 1992, 89, 6443–6.
94. Serhan CN, Chiang N, Van Dyke TE. Resolving inflammation: dual anti-inflammatory and pro-resolution lipid mediators. Nat Rev Immunol. 2008, 8, 349–61.
95. Alessandri JM, Extier A, Al-Gubory KH, Harbeby E, Lallemand MS, Linard A, et al. Influence of gender on DHA synthesis: the response of rat liver to low dietary α-linolenic acid evidences higher ω3 Δ4-desaturation index in females. Eur J Nutr. 2012, 51, 199–209.
96. Schoenaker DAJM, Jackson CA, Rowlands J V., Mishra GD. Socioeconomic position, lifestyle factors and age at natural menopause: a systematic review and meta-analyses of studies across six continents. Int J Epidemiol. 2014, 43, 1542–62.

MANUSCRIPT 2

Peripheral blood mononuclear cells capture alterations in bone and inmunometabolic-related metabolisms in ovariectomized rats, a postmenopausal model with oestrogen deficiency

Julio Baudin[a,b], Dorota Komar[c], Hong Yang[d], Francesc Puiggròs[e], Adil Mardinoglu[d,f], Lluís Arola[b], Antoni Caimari[e]

[a] Eurecat, Centre Tecnològic de Catalunya, Technological Unit of Nutrition and Health, 43204 Reus, Spain

[b] Nutrigenomics Research Group, Department of Biochemistry and Biotechnology, Universitat Rovira i Virgili, 43007 Tarragona, Spain

[c] Eurecat, Centre Tecnològic de Catalunya, Centre for Omic Sciences, Joint Unit Eurecat-Universitat Rovira i Virgili, Unique Scientific and Technical Infrastructure (ICTS), Reus, Spain.

[d] Science for Life Laboratory, KTH Royal Institute of Technology, SE-17165 Stockholm, Sweden.

[e] Eurecat, Centre Tecnològic de Catalunya, Biotechnology Area, 43204 Reus, Spain.

[f] Centre for Host-Microbiome Interactions, Faculty of Dentistry, Oral & Craniofacial Sciences, King's College London, London, United Kingdom.

Manuscript in preparation

ABSTRACT

Peripheral blood mononuclear cells (PBMCs) represent an accessible tissue that can reflect at the gene expression level the metabolic adaptations that occur in different tissues and distinguish a disease state from a healthy state. We evaluated whether the alterations occurring in ovariectomized rats, a postmenopausal oestrogen deficiency model, were affected by the age at which the ovariectomy were performed and, using a transcriptomic approach, we aimed to elucidate whether PBMCs reflected the molecular changes associated with the postmenopausal state. Rats who underwent a sham operation were used as control groups. Our results showed that ovariectomized rats recapitulated most of the alterations that can occur during the postmenopausal state in women, including obesity, adipocyte hypertrophy and increased osteoporosis and cardiometabolic risks, being these effects slightly more evident in rats induced to ovariectomy at a more advanced age. Our transcriptomic analysis carried out in PBMCs revealed that this subset of blood cells captured the molecular changes associated with oestrogen deficiency occurring in the postmenopausal state, which were evidenced by changes at mRNA level of genes mainly related to immune function, response to stress, lipid metabolism, and bone homeostasis, providing valuable insights into the pathophysiology of postmenopausal-related alterations, such as osteoporosis and inmunometabolic diseases. These findings can pave the way for investigating whether the molecular mechanisms underlying oestrogen deficiency identified in PBMCs can be modulated by different therapeutic interventions to monitor and predict the potential effects on the health of these interventions carried out in the postmenopausal state using cells that can be easily and repeatedly collected.

Keywords: PBMCs, transcriptomics, menopause, immunometabolic health, osteoporosis, molecular biomarkers

INTRODUCTION

Menopause is an aging-related biological stage in women, marked by the permanent cessation of the menstrual cycle due to the loss of ovarian function. This leads to a gradual decline in oestrogen production, which is exacerbated during the postmenopausal phase, triggering various health concerns (1). The decline in ovarian function and the hypoestrogenic levels occurring in the postmenopausal stage result in vasomotor symptoms, such as sleep disturbances, night sweats and hot flashes (2–4), as well as increased risk of osteoporosis (5), decreased muscle mass (5–7) and body weight gain accompanied by increased abdominal fat accretion, shifting from a gynoid to an android fat distribution pattern (5–9). This fat accumulation may contribute to oxidative stress and low-grade inflammation, potentially leading to the development of metabolic disorders hallmarking metabolic syndrome (MetS) such as hypertension, dyslipidemia and insulin resistance (IR), thereby increasing cardiovascular diseases (CVD) risk (10–15). Notably, both osteoporosis and CVD risk rise with age, with CVD being a leading cause of death worldwide, accounting for 47% of deaths among women (16) and around 40% of women over 50 years old experience osteoporotic fractures (17). Furthermore, it is well known that men have a higher risk for MetS and CVD early in life, while women's risk increases in the post-menopausal stage, indicating oestrogen's fundamental role in developing risk factors associated with menopause independent of aging (18–23).

Oestrogens are crucial for cardiovascular and metabolic health, regulating body fat distribution, preventing visceral fat accumulation, and maintaining metabolic health through mechanisms such as reducing food intake, enhancing energy expenditure, and improving fatty acid and glucose catabolism as well as insulin and leptin sensitivity (24–28). Oestrogens also act as anti-inflammatory and antioxidant agents, preventing endothelial dysfunction and atherosclerosis (29–33). Conversely, low oestrogen levels in

postmenopausal women can lead to rapid bone loss due to increased osteoclast activity and are associated with high levels of biomarkers for both bone resorption and formation (34–37). Considering these positive effects, low oestrogen levels in postmenopausal women likely contribute to the development of risk factors and diseases common during this stage, which can affect women for a third or more of their lifetime.

The scientific community has developed advanced rodent models that effectively mimic human menopause, providing valuable tools for studying the aging female reproductive system. These models enable the generation of preclinical data that can be potentially translated to human health, predicting outcomes and addressing menopausal health questions. Ovariectomized (OVX) rodents are the gold-standard animal models for studying the effects of reproductive aging in menopause. This surgical procedure removes the ovaries, mimicking the oestrogen deficiency that occurs during menopause leading to osteoporosis and metabolic disorders (38–42), such as visceral obesity, IR, oxidative stress, inflammation, atherogenic dyslipidemia, hepatic steatosis, hypertension, low bone mineral density (BMD) and trabecular bone remodeling (39,41–43). OVX rodents are a good model for studying hormone deprivation effects; however, the age at which OVX is performed in rodents may affect the results (41,44). For instance, rats ovariectomized between 6-9 months old, exhibited lower bone growth rate and BMD, and more pronounced changes in trabecular bone remodeling compared to younger OVX rats (41).

Peripheral blood mononuclear cells (PBMCs) represent a subset of white blood cells comprising lymphocytes and monocytes/macrophages. They traverse the body and can mirror gene expression alterations occurring in various tissues in response to internal or external stimuli (45). Their accessibility in humans, facilitated by blood isolation techniques (46,47), makes that PBMCs can be used to assess biological responses as their gene expression profile may reflect the physiological and the pathological states of the

organism (46–50). Furthermore, PBMCs have proven valuable in nutritional studies, highlighting specific effects of diets or nutrients (51–59) and their responses to fasting (46,57,58). Thus, these cells are known to reflect how nutrients and diets affect different tissues, playing a crucial role in the regulation of energy metabolism (51,57,58,60). Notably, PBMCs express molecules implicated in energy homeostasis, such as leptin and resistin, which are known to be dysregulated in obesity (51,61–68). Furthermore, PBMCs can serve as reliable indicators of gene expression responses to physiological changes in tissues that are harder to access directly, such as muscle, white adipose tissue (WAT) and liver (58,69–71). Consequently, PBMCs are regarded as sentinels and can be utilized as a surrogate tissue for gene expression analyses (45), although some studies showed discordant results between PBMCs and other tissues (70,71), especially concerning the expression of nuclear receptors (71,72).

In this study, we aimed to evaluate whether the alterations occurring in OVX rats related to osteoporosis and obesity and its associated metabolic disturbances are affected by the age at which the ovariectomy is performed by precisely characterizing this postmenopausal animal model. Furthermore, we used a transcriptomics approach to analyze PBMCs gene expression in these OVX animals to elucidate whether these cells can reflect molecular changes associated with oestrogen deficiency occurring in the postmenopausal state. This research can pave the way for investigating, in further studies, whether the molecular mechanisms underlying oestrogen deficiency identified in PBMCs can be modulated by different nutritional strategies to monitor and predict the potential effects on the health of these interventions carried out in the postmenopausal state using cells that can be easily and repeatedly collected.

MATERIALS & METHODS

Animal care

All procedures related to animal experimentation (two independent studies: 25-week-old and 35-week-old studies) were approved by the Animal Ethics Committee of the Technological Unit of Nutrition and Health of Eurecat (Reus, Spain) and the Generalitat de Catalunya (protocol code 11223). The studies complied with the ARRIVE guidelines, followed the 'Principles of Laboratory Animal Care' and were carried out in accordance with the EU Directive 2010/63/EU for animal experiments. Female Sprague-Dawley rats of different ages (12 weeks and 24 weeks, purchased to ENVIGO, Indianapolis, USA and JANVIER LABS, Saint-Berthevin, France, respectively) were used. At each age of study, 10 rats were bilaterally ovariectomized (OVX) and 10 rats were sham-operated (SHAM) at the facilities of the suppliers. The animals were fed a maintenance rat chow diet to stabilize them after ovariectomy, before shipment at 15 and 25 weeks of age, respectively. During the whole study, rats were housed in pairs at 22 °C under a 12 h light/dark cycle (lights on at 9:00 am) and had *ad libitum* access to food and water. Both OVX and SHAM animals were fed a standard chow diet (Teklad Global 14% Protein Rodent Diet 2014, Harlan, Barcelona, Spain). The caloric breakdown of the diet (2.9 kcal/g) was 20% protein, 13% fat, and 67% carbohydrates. Body weight was recorded once each week, food was renewed daily, and the food intake was documented every 7 days. Ten weeks after the arrival of the rats at the animal facility of Eurecat, rats were sacrificed under anaesthesia (pentobarbital sodium, 60 mg/kg body weight) after 6 h of diurnal fasting. Blood was collected by cardiac puncture, and serum and plasma were obtained by centrifugation and stored at -80 °C until analysis. The liver, caecum, kidneys, spleen, gastrocnemius and soleus muscle, the femur of the left leg, the tibia of the left leg (only in the 35-week-old study) and the white adipose tissue depots (retroperitoneal -RWAT-,

mesenteric –MWAT- and inguinal IWAT- white adipose tissue depots) were rapidly removed, weighed, frozen in liquid nitrogen and stored at -70 °C until further analysis. The right femur (in both studies) and the right tibia (only in the 35-week-old study) were also collected, immersed in 70% ethanol and stored at room temperature until to carry out a three-dimensional microcomputed tomography analysis.

Blood analysis

Enzymatic colorimetric kits were used to determine the circulating levels of triglycerides (992330/QCA, Barcelona, Spain), glucose (992330/QCA, Barcelona, Spain), nonesterified free fatty acids (NEFAs) (WAKO, Neuss, Germany), total cholesterol (TC) (995280/QCA, Barcelona, Spain) and HDL-cholesterol (HDL-c) (EHDL-100/Bioassay Systems, California, USA). The non-high-density lipoprotein cholesterol (non-HDL-c) level was calculated by subtracting the HDL cholesterol concentration from the TC concentration. Circulating insulin levels were measured using a rat/mouse ELISA kit (10-1250-01/MERCODIA, Upssala, Sweden). Circulating leptin and adiponectin levels were determined with a rat ELISA kit (EZRL-83K/Millipore, Barcelona, Spain) and a Rat Total Adiponectin/Acrp30 Quantikine ELISA Kit (RRP300/R&Dsystems, Minnesota, USA), respectively. The levels of the inflammatory marker monocyte chemoattractant protein-1 (MCP-1) were quantified using the BMS631INST (INVITROGEN, Massachusetts, USA). To quantify the circulating levels of the biomarkers of bone turnover Procollagen I amino-terminal propeptide (PINP), osteocalcin (OC) and carboxy-terminal telopeptide of type I collagen (CTX), the PINP ELISA kit (AC-33F1, IDS, UK), the osteocalcin ELISA Kit (AC-12F1, IDS, UK) and the CTX (AC-06F1, IDS, UK) were used, respectively.

Body composition analyses

Lean and fat mass measurements (in grams) were performed without anaesthesia at the beginning and at the end of the study using an EchoMRI-700™ device (Echo Medical Systems, L.L.C., Houston, USA). The measurements were performed in triplicate under *ad libitum* conditions and at 8:00 am, and the results were expressed as a percentage of body weight.

Adiposity index

The adiposity index was calculated as the sum of the weights of the IWAT, MWAT and RWAT depot weights (in grams) for each rat and was expressed as a percentage of body weight.

HOMA-IR and R-QUICKI analyses

The homeostasis model assessment-estimated insulin resistance (HOMA-IR) was calculated using the following formula: (Fasting Glucose level –mmol/L- × Fasting Insulin level-μU/mL-)/22.5 (73). Insulin sensitivity was evaluated by the revised quantitative insulin sensitivity check index (R-QUICKI) using the following formula: 1/[log insulin (μU/mL) + log glucose (mg/dL) + log FFA (mmol/l)] (74).

Microcomputed tomography analyses

Bone composition of the right femur (in both 25- and 35-week-old rats) and right tibia (only in 35-week-old rats) were determined post-mortem in fixed samples by three-dimensional microcomputed tomography (μCT or microCT) analysis, as was previously described (75). The bone mineral content (BMC) and BMD values were quantified from MicroCT scans using GE MicroView software v2.2.

Indirect calorimetry

The Oxylet Pro^{TM} System (PANLAB, Cornellà, Spain) was used to carry out indirect calorimetry analyses of the different groups at week 5, throughout 22 h (from 11:00 am to 09:00 am), under *ad libitum* conditions and with free access to water. At 09:00 am, the animals received the corresponding treatment and were transferred from their cages to an acrylic box (Oxylet LE 1305 Physiocage, PANLAB). After an initial acclimatisation period of 2 h, the respiratory quotient (RQ), the fat and carbohydrate oxidation (CH) rates and the energy expenditure (EE) were calculated as previously described (76).

Analysis of total, oxidized and reduced glutathione in liver (GSH/GSSG)

Liver samples were used to quantify the levels of total glutathione (GSH), reduced GSH, and oxidized GSH (GSSG) using the Glutathione Colorimetric Detection Kit from EIAGSHC/INVITROGEN (Massachusetts, USA). The results were expressed in µmol per g of hepatic protein, which was calculated using the BCA assay method.

Histological Analysis

Fixed portions of MWAT (25-week-old rats) or RWAT (35-week-old rats) (n = 8 per group) were preserved in buffered formalin (4% formaldehyde, 4 gr/L NaH2PO4, 6.5 gr/L Na2HPO4; pH 6.8) were cut at a thickness of 5 µm and stained with hematoxylin & eosin (H & E). MWAT and RWAT images (magnification 100×) were taken with a microscope (ECLIPSE Ti; Nikon, Tokyo, Japan) and coupled to a digital sight camera (DS-Ri1, Nikon). Image analyses were performed using the ImageJ NDPI software (National Institutes of Health, Bethesda, MD, USA; https://imagej.nih.gov/ij, accessed on 22 March 2024, version 1.54g). Adipocyte area quantification in the MWAT and RWAT sections of both groups was analysed using the Adiposoft plugin.

PBMCs isolation

PBMCs were isolated from blood obtained in 35-weeks-old rats. Briefly, blood samples (2.5-3.0 mL) were diluted (1:1) with balanced salt solution (BSS), which was prepared by mixing two stock solutions (1/10); solution A (5.5mM anhydrous D-glucose, 5mM $CaCl_2$ $2H_20$, 0.98mM $MgCl_2$ $6H_20$, 5.4mM KCl, 145mM Tris, pH: 7.4) and solution B (140mM NaCl). PBMCs were isolated by Ficoll gradient separation, according to the instructions indicated by the manufacturer (GE Healthcare Bio Sciences, Barcelona, Spain). The pellet was carefully resuspended with 1.5 mL of erythrocyte lysis buffer (155 mM NH_4Cl, 10 mM $KHCO_3$, and 100 µM EDTA, pH 7.4) and incubated at room temperature for 5 minutes. Afterwards, 5 ml of BSS were added to the tube, which was gently inverted 5 times and centrifuged at 400 g for 10 minutes. Finally, the supernatant was aspirated and the PBMCs pellet was stored at -70°C until RNA extraction.

Transcriptomic and gene set enrichment analyses

The transcriptomic analysis was performed on RNA samples from the PBMCs of 35-weeks-old rats in the OVX and SHAM groups (n = 6 per group). Total RNA was extracted using β-mercaptoethanol and purified with the NucleoSpin® TriPrep Column (Macherey-Nagel, Düren, Germany) according to the manufacturer's instructions, and RNA integrity was measured on an Agilent Bioanalyzer (Agilent Technologies, South Queensferry, UK). All samples had optimal quality parameters (RIN > 7) and were used for the construction of next-generation sequencing (NGS) libraries. The subsequent NGS libraries were converted to FASTQ format using Illumina NovaSeq 6000 in S4 flow cell mode (Illumina Way, California, USA). Gene abundance of all RNA-seq data (in both raw counts and transcripts per million) was processed using the Kallisto pipeline (77) based on *rattus norvergicus* genome from Ensembl release version 107. The differential gene expression (DGE) analysis was performed using the R/Bioconductor package

DESeq2 v1.40.2 (77), and the Benjamini–Hochberg false discovery rate (FDR) test was performed to manage false-positive outcomes. Only the genes exhibiting an FDR derived q-value less than 0.1 (*adj.* p value < 0.1) were recognized as DGEs. The resulting gene lists were annotated and filtered for significantly differentially up- and down-regulated genes (*adj*. $p < 0.1$ and log2(fold change) > |0| or < |-0|, respectively). The log2 fold changes for each gene calculated using the R Package Piano v2.16.0 (gene set statistic=reporter) (78). Fold change values of the significant genes were calculated in Microsoft Excel from the log2 (fold changes). The fold change equals the OVX/SHAM ratio when the ratio increases or equals -1/ratio when the ratio decreases. KEGG pathway analysis was performed separately for distinctly upregulated, mixed-direction upregulated, mixed-direction downregulated and distinctly downregulated genes based on an *adj.* p value < 0.05 that indicated the enrichment of pathways according to the R package Piano v2.16.0 (nperm=1000) (78). For the Gene Ontology analysis using g:Profiler, only the "biological process" category (g:GOst, https://biit.cs.ut.ee/gprofiler/gost, accessed on 17 March 2024, version e110_eg57_p18_4b54a898) was applied to test functional enrichment analysis of significantly differentially expressed genes in biological process pathways (79). Because the results of the whole genome array revealed that not all the significantly differentially expressed genes were identified by the KEGG pathway and g:Profiler programs, we supplemented the significantly enriched biological processes with nonannotated genes from the selected gene set using the scientific literature from biological databases (NCBI, PubMed and Human Protein Atlas, https://www.proteinatlas.org/, accessed 4 April 2024). As processes overlapped, we consolidated them and assigned new names to better reflect their combined nature. The R package ggplot2 v3.4.4. (80) was used to create a volcano plot with the DGEs to visualize changes in gene expression between groups.

R/Bioconductor package ComplexHeatmap v2.16.0. (81) was used to create a heatmap to visualize significantly regulated KEGG pathways (*adj.* $p < 0.05$) in OVX animals compared with their SHAM counterparts.

Statistical analyses

The data are presented as the means ± SEM (n = 10). Statistical analyses were performed with IBM SPSS Statistics 28.0 (SPSS, IBM Corp. Armonk, New York, USA). Grubbs' test was used to detect outliers, which were discarded from further analysis. All the variables of both studies were analyzed by Student's t-test to assess differences between SHAM and OVX animals at 25 and 35 weeks, respectively. The level of statistical significance was set at bilateral 5%.

RESULTS

Ovariectomy increased body weight, adiposity, fat accretion and food intake and decreased energy expenditure and lean mass content

As was previously described, ovariectomized rats exhibited significant increases in initial and final body weight as well as in body weight gain compared to SHAM animals in both 25- and 35-week-old rats (Student's t-test) (Table 1). Furthermore, these effects were accompanied by higher adiposity index, relative fat mass and fat mass gain in the OVX animals than in SHAM rats regardless of the age of the study (Figures 1D-F). The dissection of the specific WAT depots revealed that 25-weeks-old OVX rats only displayed a significant increase in IWAT relative weight whereas 35-weeks-old OVX animals showed higher relative weight of RWAT, MWAT and IWAT than their SHAM counterparts (Figures 1A-1C). These results reported in both studies concerning body weight and adiposity could be attributed, at least in part, to the increased daily food intake (Table 1) and the decreased EE (Figure 2B) observed in OVX rats in comparison with

their SHAM counterparts of their respective ages. Specifically, ovariectomy-induced a reduction in EE during the 21-hour and dark phase at 35 weeks of age and the light phase at 25 weeks of age compared to SHAM rats (Fig. 2B). This decreased EE observed in OVX animals was not accompanied by shifts in the use of fat and carbohydrates as energy sources because no changes were observed between groups at both ages in RQ, lipid and CH oxidation (Fig. 2A, 2C and 2D, respectively).

Furthermore, the impact of ovariectomy also led to decreased lean mass content (Fig. 1G) and increased loss of muscle mass (Fig. 1H) in both 25 and 35-week-old rats compared to their respective SHAM counterparts at the end of both studies. These changes in fat mass accretion and loss of muscle content observed in ovariectomized rats of both ages were reflected in a decreased lean-to-fat ratio, indicating a less healthy body composition profile resulting from ovariectomy (Fig. 1I).

Concerning the weight of other tissues analyzed, regardless of the age of the study, ovariectomy resulted in significantly lower relative weight of brown adipose tissue (BAT), liver and kidneys than their respective SHAM groups. These effects could be attributed to the higher body weight reported in OVX rats than in SHAM animals because no differences in these parameters were found when they were expressed in absolute weight (data not shown). No significant decreases were found in the weight of spleen and soleus muscle expressed as a percentage of body weight in OVX animals when compared to SHAM rats at the age of 25 weeks, differently to what was observed in 35-week-old SHAM and OVX groups (Table 1). The removal of the ovaries in the OVX groups did not change the relative caecum weight at any age of study (Table 1).

Table 1: food intake, biometric and blood parameters in sham-operated (SHAM) and ovariectomized (OVX) rats at 25 and 35 weeks

	25 weeks			35 weeks		
	SHAM	**OVX**	**t-test**	**SHAM**	**OVX**	**t-test**
Food Intake (g/d)	13.6 ± 0.2	15.5 ± 0.5	**	8.5 ± 0.1	10.5 ± 0.3	***
Biometric parameters						
Initial body weight (g)	236 ± 3	276 ± 5	***	338 ± 8	412 ± 4	***
Final body weight (g)	264 ± 4	329 ± 8	***	358 ± 7	472 ± 12	***
Δ Body weight (g)	18.5 ± 3.5	35.1 ± 3.5	**	20.1 ± 5.1	59.3 ± 7.9	***
BAT (%)	0.116 ± 0.009	0.088 ± 0.004	*	0.113 ± 0.005	0.088 ± 0.006	**
Liver (%)	2.66 ± 0.05	2.30 ± 0.03	***	2.70 ± 0.05	2.20 ± 0.03	***
Caecum (%)	1.08 ± 0.11	0.99 ± 0.05	NS	1.42 ± 0.03	1.31 ± 0.10	NS
Kidneys (%)	0.537 ± 0.010	0.454 ± 0.009	***	0.597 ± 0.014	0.424 ± 0.008	***
Spleen (%)	0.224 ± 0.008	0.211 ± 0.005	NS	0.238 ± 0.007	0.209 ± 0.007	**
Gastrocnemius (%)	0.744 ± 0.011	0.704 ± 0.011	*	0.623 ± 0.022	0.556 ± 0.012	*
Soleus (%)	0.044 ± 0.001	0.043 ± 0.001	NS	0.054 ± 0.002	0.042 ± 0.002	***
Blood parameters						
TG (mmol/L)	0.482 ± 0.060	0.408 ± 0.056	NS	1.371 ± 0.110	1.030 ± 0.030	*
TC (mmol/L)	2.50 ± 0.15	3.01 ± 0.13	*	3.73 ± 0.30	4.05 ± 0.12	NS
HDL-c (mmol/L)	1.74 ± 0.10	1.98 ± 0.07	NS	2.79 ± 0.24	3.07 ± 0.16	NS
Non-HDL-c (mmol/L)	0.881 ± 0.070	0.907 ± 0.028	NS	0.940 ± 0.071	0.976 ± 0.124	NS
MCP-1 (ng/mL)	6403 ± 328	9373 ± 844	**	4328 ± 682	5803 ± 503	NS
Hepatic parameters						
Total GSH (µmol/g protein)	46.2 ± 9.9	22.9 ± 3.7	*	58.7 ± 3.3	67.7 ± 2.7	*
Reduced GSH (µmol/g protein)	39.1 ± 9.9	17.5 ± 2.9	NS	48.9 ± 3.1	56.1 ± 2.5	NS
Oxidized GSH (µmol/g protein)	7.08 ± 0.74	8.09 ± 0.95	NS	9.78 ± 0.21	11.65 ± 0.35	***
GSH/GSSG Ratio	6.27 ± 1.96	2.03 ± 0.40	*	4.77 ± 0.18	4.81 ± 0.16	NS

Data are given as the mean ± SEM (n = 10). Δ body weight was calculated as the difference between the final body weight and the initial body weight. Relative tissue weights (%) were calculated according to the formula (100* tissue weight/body weight) and were expressed as a percentage of body weight. The concentrations of blood parameters were determined at the end of the experiment. The GSSG/GSH ratio was calculated as the oxidized GSH divided by reduced GSH. Differences between SHAM and OVX groups at 25- and 35-week-old were determined by Student's t-test (*$p < 0.05$, **$p < 0.01$, ***$p < 0.001$). NS: non-significant difference. SH: sham-operated rats; OVX: ovariectomized rats. BAT: brown adipose tissue; GSH: glutathione; GSSG: oxidized glutathione; HDL-c: high-density lipoprotein cholesterol; MCP-1: monocyte chemoattractant protein-1; non-HDL-c: non-high-density lipoprotein cholesterol; TC: total cholesterol; TG: triglycerides.

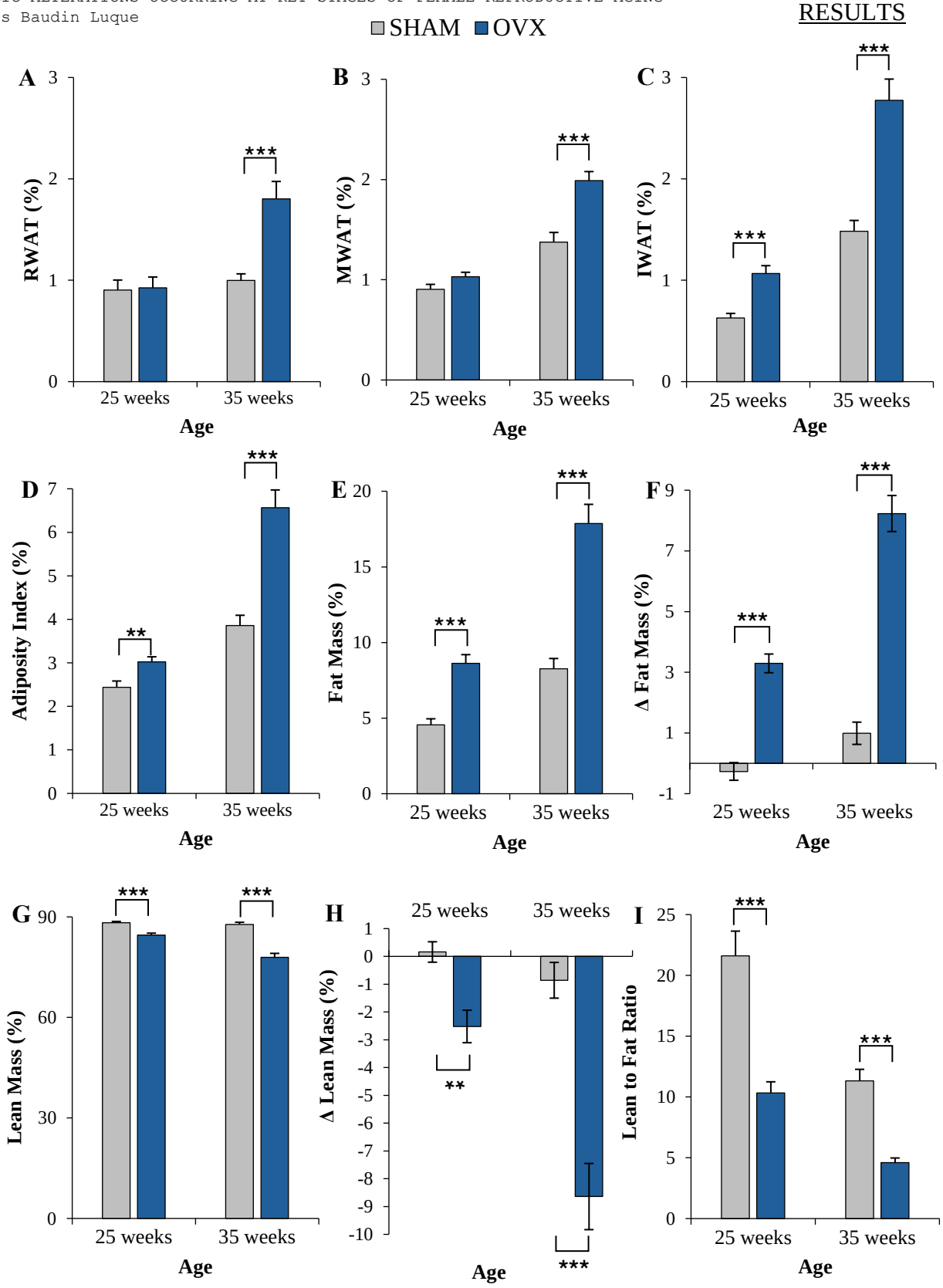


Figure 1 Effects of ovariectomy on RWAT (A), MWAT (B), and IWAT (C) depot weights, adiposity index (D), fat mass (E) Δ fat mass (F), lean mass (G), Δ lean mas (H) and lean/fat ratio (I) in sham-operated (SHAM) and ovariectomized (OVX) rats at 25- and 35-week-old. Data are given as the mean ± SEM (n = 10). Relative RWAT, MWAT and IWAT weights (%) were calculated according to the formula (100* tissue weight/body weight) and were expressed as a percentage of body weight. The adiposity index was computed as the sum of the RWAT, MWAT and IWAT depot weights (in grams) and is expressed as a percentage of body weight. Fat mass and lean mass weights (%) were calculated according to the formula (100* fat or Lean/body weight) and were expressed as a percentage of body weight. Lean/fat mass ratio was calculated as the lean mass divided by fat mass. Changes in body weight, fat mass and lean mass were calculated as the differences between the final and the initial values of these parameters and are depicted in the figures as Δ values. Differences between SHAM and OVX groups at 25- and 35-week-old were determined by Student's t-test **p < 0.01, ***p < 0.001). NS: non-significant difference. SHAM: sham-operated rats; OVX: ovariectomized rats. IWAT: inguinal white adipose tissue; MWAT: mesenteric white adipose tissue; RWAT: retroperitoneal white adipose tissue.

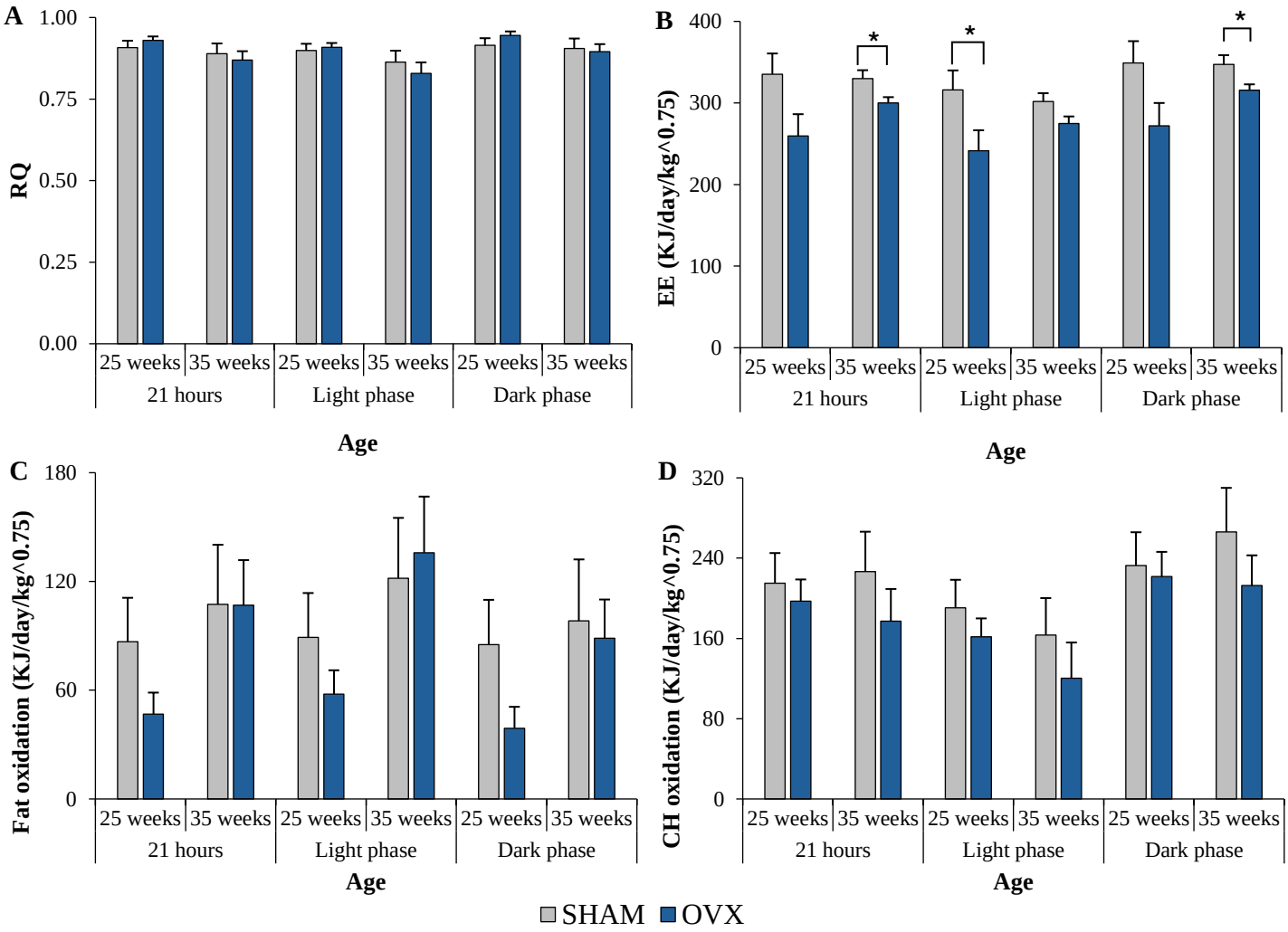


Figure 2. Effects of ovariectomy on respiratory quotient (A), EE (B), fat oxidation (C) and carbohydrate oxidation (D) in sham-operated (SHAM) and ovariectomized (OVX) rats at 25- and 35-week-old. Data are given as the mean ± SEM (n = 10). Indirect calorimetric measurements were performed between Days 37 and 42 at 25 weeks and beweeen Day 29 and 33 under ad libitum conditions and over 22 h (from 11:00 am to 09:00 am) after the beginning of the studies . The data obtained during the first hour were discarded for final analyses. All rats were fed a standard chow diet during the measurements. Data are given as the mean ± SEM (n = 9–10). Differences between SHAM and OVX groups at 25- and 35-week-old were determined by Student's t-test (*p < 0.05). NS: non-significant difference. SHAM: Sham-operated rats; OVX: Ovariectomized rats. RQ: respiratory quotient; EE: energy expenditure.

Ovariectomized rats displayed increased adipocyte hypertrophy and decreased adipocyte number

The histological analysis carried out in the MWAT of 25-weeks-old rats (Fig. 3A-3E) and in the RWAT of 35-weeks-old animals (Fig. 3F-3J) revealed a significant increase in the average adipocyte area (Fig. 3A and 3F, respectively) and a lower adipocyte number (Fig. 3B & 3G, respectively) in OVX rats compared to their SHAM counterparts. Regarding the adipocyte size distribution quantified at both 25 and 35 weeks (Fig. 3C & 3H, respectively), there was a significantly higher proportion of larger adipocytes in both RWAT and MWAT depots of OVX rats compared to SHAM rats, indicating adipocyte hypertrophy at both ages as a consequence of the removal of the ovaries. In agreement with these results, representative MWAT and RWAT histological images (H & E staining) illustrated larger adipocytes and a lower number of these cells in the OVX animals than in SHAM rats (Fig. 3D-3E for 25-weeks-old rats and Fig. 3I-3J for 35-weeks-old animals).

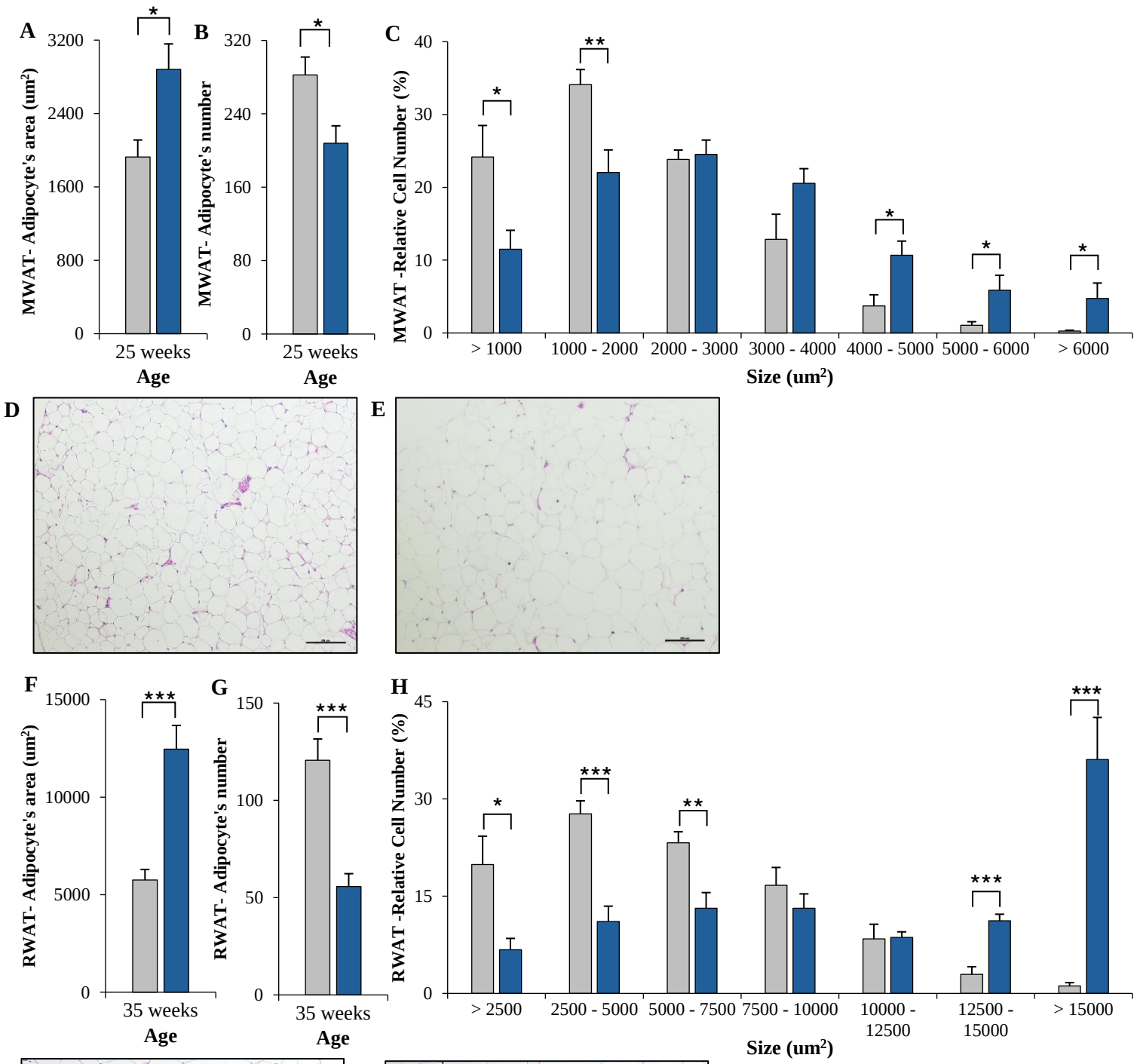


Figure 3. Effects of ovariectomy on adipocyte's area (A), adipocyte's number (B), adipocyte's size distribution (C) and representative micrographs of hematoxylin–eosin stained MWAT sections (bar = 100 µm) from sham-operated (SHAM) and ovariectomized (OVX) groups (D and E, respectively) in SHAM and OVX rats at 25-week-old. Effects of ovariectomy on adipocyte's area (F), adipocyte's number (G), adipocyte's size distribution (H) and representative micrographs of hematoxylin–eosin stained RWAT sections (bar = 100 µm) from SHAM and OVX groups (I and J, respectively) in SHAM and OVX rats at 35-week-old. Data are given as the mean ± SEM (n = 10). Differences between SHAM and OVX groups at 25- and 35-week-old were determined by Student's t-test (*p < 0.05, **p < 0.01, ***p < 0.001). NS: non-significant difference. SHAM: sham-operated rats; OVX: ovariectomized rats. MWAT: mesenteric white adipose tissue; RWAT: retroperitoneal white adipose tissue.

Age-dependent effects of ovariectomy on parameters related to lipid metabolism, oxidative stress, inflammation and glucose and insulin homeostasis

Circulating triglyceride levels were significantly decreased in the OVX animals compared to their SHAM counterparts only at 35 weeks while circulating TC levels significantly increased by the ovariectomy at the age of 25 weeks (Table 1). In addition, the circulating levels of the inflammatory marker MCP1-1 were significantly higher in ovariectomized 25-week-old rats than in the SHAM group of the same age (Table 1).

In terms of hepatic parameters related to glutathione metabolism clear age-dependent effects were observed. Thus, at 25 weeks, OVX rats showed lower levels of total GSH than their SHAM counterparts, whereas an inverse pattern was reported in 35-weeks-old animals (Table 1). Although a similar behaviour to what was observed for total GSH was reported for reduced GSH, no significant changes between OVX and SHAM groups were found in this parameter at any age, whereas 35-weeks-old rats displayed increased levels of oxidized GSH than their sham-operated counterparts (Table 1). The removal of the ovaries in the OVX group significantly decreased the GSH/GSSG ratio only in 25-weeks-old animals (Table 1).

No significant changes were observed in blood glucose levels between OVX and SHAM groups at any age (Fig. 4A). However, ovariectomy specifically produced a significant increase in the circulating levels of insulin in 35-weeks-old rats (Fig. 4B), which resulted in significant higher values of the surrogate marker of insulin resistance, HOMA-IR, in this ovariectomized animals (Fig. 4D). Despite the decreased blood concentrations of NEFAs reported in 35-weeks-old OVX rats (Fig. 4D), these animals also displayed lower values of the surrogate marker of insulin sensitivity, R-QUICKI, than their sham-operated counterparts (Fig. 4E). Concerning 25-weeks-old rats, the removal of the ovaries in the

OVX group only produced a slight, but significant decrease in R-QUICKI when compared to the SHAM animals (Fig. 4E).

According to the increased adiposity found in both 25 and 35-weeks-old OVX rats, these animals displayed a sharp increase in the circulating leptin levels compared to their respective SHAM counterparts (Fig. 4F). Concerning adiponectin blood concentrations, higher levels of this adipokine were observed in OVX rats only at 35 weeks (Fig. 4G). When this parameter was corrected by the total weight of white adipose tissue, which gives an estimation of the effective production of adiponectin by white adipocytes, a significant decrease in the adiponectin/g WAT ratio was observed in OVX rats only at 25 weeks of age (Fig. 4H). Possibly due to the higher levels of leptin observed in OVX rats at both ages, ovariectomy caused a significant decrease in the adiponectin-to-leptin ratio, a biomarker of adipose tissue inflammation and IR (75), and a significant increase in the leptin-to-adiponectin ratio, a reliable marker of diabetes risk and MetS (27,82), compared to their respective SHAM counterparts (Fig. 4I & 4J).

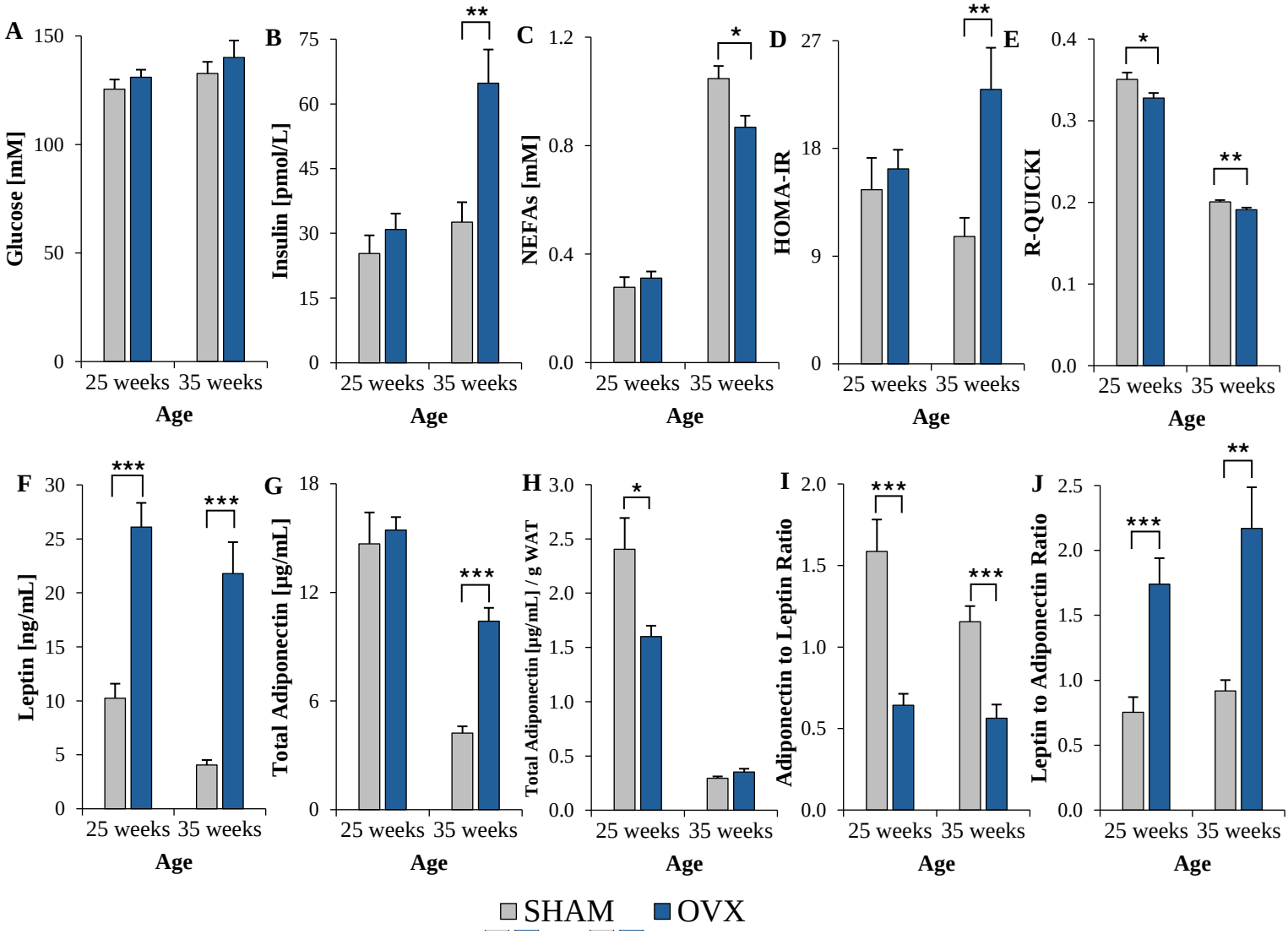


Figure 4 Effects of ovariectomy on RWAT (A), MWAT (B), and IWAT (C) depot weights, adiposity index (D), fat mass (E) Δ fat mass (F), lean mass (G), Δ lean mas (H) and lean/fat ratio (I) in sham-operated (SHAM) and ovariectomized (OVX) rats at 25- and 35-week-old. Data are given as the mean ± SEM (n = 10). The concentrations of serum/plasma parameters were determined at the end of the experiment. The ratio of total adiponectin/g WAT was computed as the quotient between the circulating levels of total adiponectin and the grams of fat mass. Leptin/adiponectin ratio was calculated as the circulating levels of leptin divided by the circulating levels of adiponectin. Adiponectin/leptin ratio was calculated as the circulating levels of adiponectin divided by the circulating levels of leptin. Differences between SHAM and OVX groups at 25- and 35-week were determined by Student's t-test (*p < 0.05, **p < 0.01, ***p < 0.001). NS: non-significant difference. SHAM: sham-operated rats; OVX: ovariectomized rats. HOMA-IR: homeostasis model assessment-estimated insulin resistance; NEFAs: nonesterified fatty acids; R-QUICKI: revised quantitative insulin sensitivity check index; WAT: white adipose tissue.

Ovariectomy increased the biochemical markers of bone turnover and produced slight changes in bone composition

The analysis of bone-related parameters revealed that the relative weight of the collected femur at both ages and the tibia collected at 35 weeks were lower in rats undergoing ovariectomy (Table 2). Concerning the circulating levels of bone turnover biomarkers,

the removal of the ovaries in the OVX group induced significantly increased levels of the bone formation biomarker OC and the bone resorption biomarker CTX-1, as was previously described, suggesting an unbalanced bone formation and resorption activity. According to the μCT analyses conducted in the right femur, no significant changes between OVX and SHAM groups were observed in BMD and BMC at any age. Meanwhile, the μCT determinations performed in the right tibia revealed that ovariectomy reduced BMD at 35 weeks (Table 2).

Table 2: Bone-related parameters in sham-operated (SHAM) and ovariectomized (OVX) rats at 25 and 35 weeks

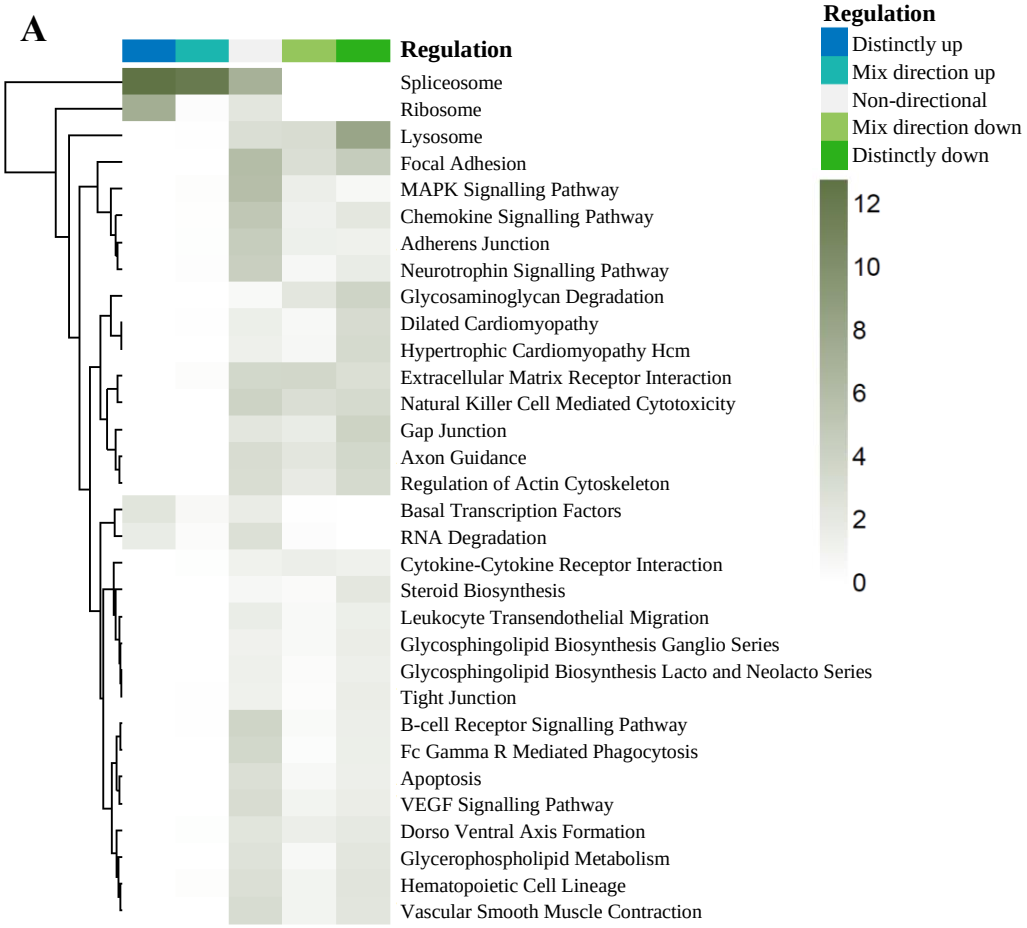
	25 weeks			35 weeks		
	SHAM	**OVX**	**t-test**	**SHAM**	**OVX**	**t - test**
Biometric parameters						
Femurs (%)	0.756 ± 0.015	0.656 ± 0.012	***	0.643 ± 0.011	0.515 ± 0.009	***
Tibias (%)	-	-	-	0.519 ± 0.007	0.417 ± 0.008	***
Blood or Serum/Plasma parameters						
OC (ng/mL)	292 ± 11	377 ± 16	***	114 ± 10	209 ± 24	**
CTX-1 (ng/mL)	14.9 ± 1.4	20.7 ± 1.2	**	14.4 ± 1.4	22.0 ± 1.1	***
PINP (ng/mL)	5.85 ± 0.27	6.38 ± 0.40	NS	7.94 ± 0.66	11.10 ± 1.51	NS
Microcomputed tomography analyses (μCT)						
Femur (μCT)						
BMD (mg/cc)	634 ± 16	618 ± 21	NS	356 ± 14	328 ± 14	NS
BMC (mg)	569 ± 5	591 ± 16	NS	142 ± 6	140 ± 3	NS
Tibia (μCT)						
BMD (mg/cc)	-	-	-	271 ± 15	224 ± 8	*
BMC (mg)	-	-	-	140 ± 5	134 ± 3	NS

Data are given as the mean ± SEM (n = 10). Relative Femurs and tibias weights (%) were calculated according to the formula (100* tissue weight/body weight) and were expressed as a percentage of body weight. The circulating levels of the biomarkers of bone turnover in plasma/serum were determined at the end of the experiment. Microcomputed tomography analyses in the femur were quantified from MicroCT scans using GE MicroView software v2.2. Differences between SHAM and OVX groups at 25- and 35-week-old were determined by Student's t-test (*$p < 0.05$, **$p < 0.01$, ***$p < 0.001$). NS: non-significant difference. SHAM: sham-operated rats; OVX: ovariectomized rats. OC: osteocalcin; CTX-1: carboxy-terminal telopeptide of type I collagen; PINP: procollagen I amino-terminal propeptide; BMD: bone mineral density; BMC: bone mineral content.

Transcriptional changes in PBMCs after ovariectomy

To shed light on the mechanisms underlying the effects of ovariectomy reported, we carried out a transcriptomic analysis in PBMCs samples of OVX and SHAM animals. KEGG pathway analysis of all the gene expression data revealed that the most significantly affected (downregulated) pathways encompassed a comprehensive range of immune, inflammation and defence processes, including cytokine–cytokine receptor interactions, chemokine signalling pathways, natural killer cell-mediated cytotoxicity and B-cell receptor signalling pathways, among others (Fig 5A). Other frequently classified processes included cytoskeleton and cellular networks, such as focal adhesion, adherens junction, gap junction, extracellular matrix (ECM) receptor interaction and regulation of actin cytoskeleton, as well as pathways related to the degradation of cellular components, such as the lysosome (Fig. 5A). Furthermore, glycoconjugate and glycerophospholipid metabolism, as well as pathways related to glucose homeostasis, were also affected (Fig. 5A). Interestingly, most of the pathways related to RNA processing and degradation processing and degradation a lesser extent, RNA degradation (Fig. 5A). DGE analysis identified 230 genes that were differentially regulated between OVX and SHAM animals, being many of them (60%, 138 genes) downregulated in OVX rats (Fig. 5B). Furthermore, the hierarchical clustering analysis based on the significantly regulated genes also revealed distinct clustering patterns between OVX and SHAM rats (Fig. 5C). Of these 230 genes, 43 were unknown, and could not be grouped into any pathway. The 187 remaining known genes were distributed into different biological processes, according to the information obtained via KEGG pathway analysis, enrichment analyses using the g:Profiler program, and information obtained from the scientific literature and various biological databases (NCBI, PubMed and Human Protein Atlas) (Fig. 5D). The most

representative biological processes were cell proliferation, differentiation and death, cytoskeleton and cellular network, and immunity, inflammation and response to stress, RNA processing, signalling and lipid metabolism (Fig. 5D). Other biological processes that were also affected included energy homeostasis, carbohydrate and lipid metabolism, transport of small molecules (ions, amino acids and vitamins) and protein processing and ubiquitination (Fig. 5D). The pathways related to these biological processes, and the most representative genes belonging to these pathways, are included in Table 3. The patterns of expression of many of these genes are analysed in the Discussion section.



RESULTS

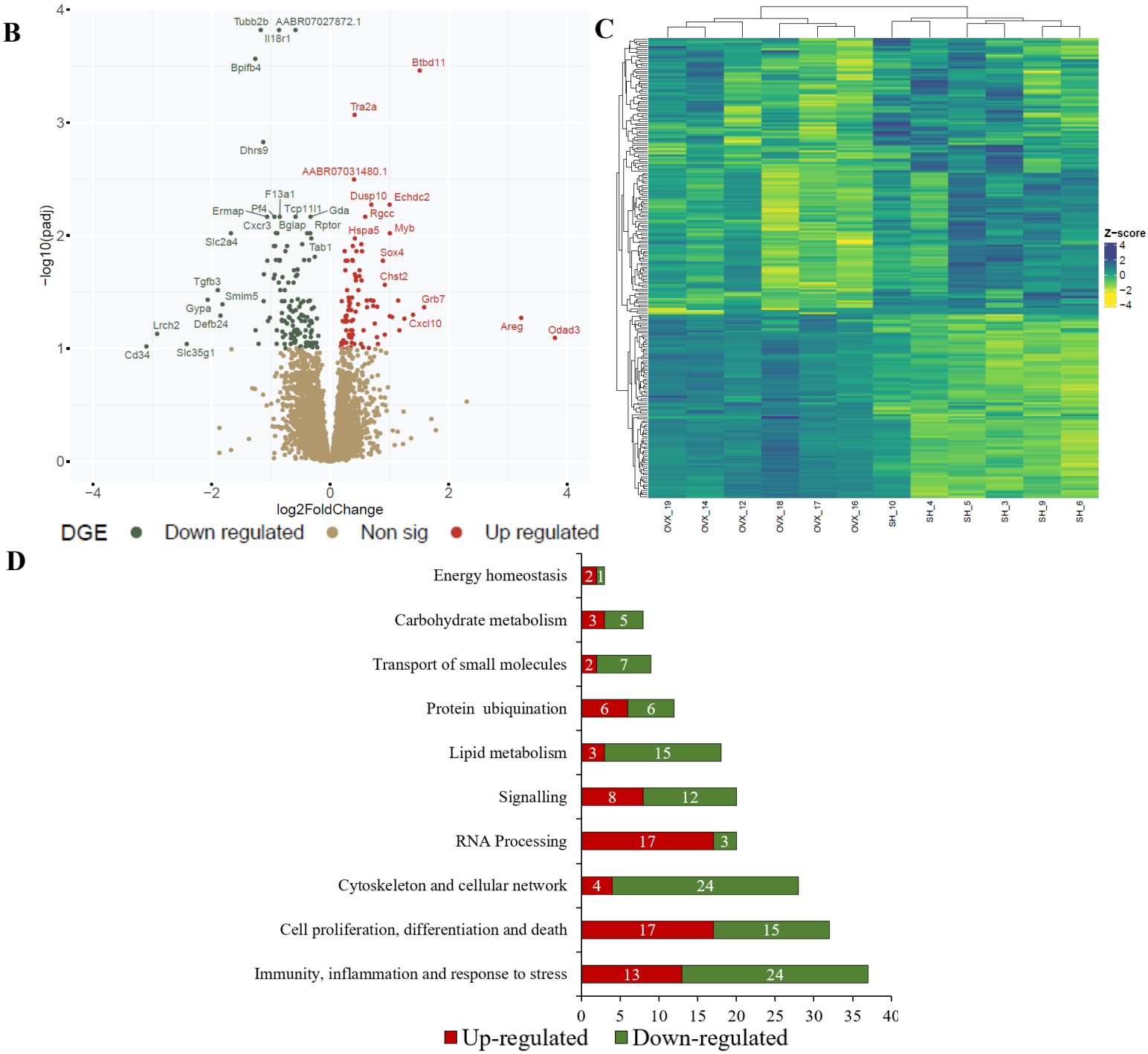


Figure 5 Transcriptional changes in PBMCs of OVX and SHAM rats (n =6 per group) at 35-week-old. Figure 5A, Heatmap visualizing significantly regulated KEGG pathways (adj. $p < 0.05$) in OVX group in comparison with SHAM group. The colour scale represents negative log10 scale adjusted p values of classes with different directions of regulation. The nondirectionally adjusted p values were computed from the gene statistics, disregarding the direction of expression. Mix-direction down- and mix-direction up adjusted p values were computed by considering the segment of the statistics for genes that were downregulated and upregulated, respectively. Dynamically adjusted p values were calculated using the expression direction and gene statistics. The distinct direction up adjusted p values were exclusively influenced by the upregulation of genes. In contrast, distinct direction down adjusted p values were influenced by the downregulation of genes and not influenced by genes with upregulation and downregulation together. Figure 5B, volcano plot visualizing gene expression changes in PBMCs of OVX rats *versus* SHAM animals. Significant down and up genes regulated were highlighted with an *adj.* $p < 0.1$ and a log2 (Fold-Change) ≤ -1 or ≥ 1 in green and red colour, respectively. Statistical significance was tested using DESeq2. Figure 5C, heatmap visualizing expression pattern of the 230 significant genes with an *adj.* $p < 0.1$ represented by Z score transformed log2 counts per million. Figure 5D, Classification of the biological processes of the genes affected by ovariectomy. All known genes (230) that were differentially expressed (adj. $p < 0.1$) between the OVX-MI and OVX animals were classified using g:Profiler, KEGG, biological databases (NCBI, human protein atlas) and the scientific literature. OVX: Ovariectomized rats; SHAM: sham operated rats. KEGG: Kyoto Encyclopaedia of Genes and Genomes; PBMCs: peripheral blood mononuclear cells.

Table 3: Functional categorization of differentially expressed genes in thePBMCs of OVX rats

Biological process	***Main-related pathway***	***Gene name***	**Gene symbol**	**Gene ID**	**FC**	**Adj. p value**
Immunity, inflammation and response to stress	Cytokine mediated inflammation	*Interleukin 18 receptor 1*	*Il18r1*	301365	-1.82	0.000
		Interleukin 18 receptor accessory protein	*Il18rap*	373540	-1.49	0.023
		Interleukin 16	*Il16*	116996	-1.27	0.057
		Interleukin 12 receptor subunit beta 1	*Il12rb1*	171333	-1.39	0.012
		Prostaglandin-endoperoxide synthase 2	*Ptgs2*	29527	2.38	0.054
		Suppressor of cytokine signaling 3	*Socs3*	89829	1.66	0.042
	Chemokine mediated inflammation	*BPI fold containing family B, member 4*	*Bpifb4*	499925	-2.40	0.000
		C-X-C motif chemokine receptor 3	*Cxcr3*	84475	-1.88	0.010
		Platelet factor 4	*Pf4*	360918	-1.92	0.007
	NK cell-mediated citotoxicity	*SH3-domain binding protein 2*	*Sh3bp2*	305450	-1.31	0.010
	Response to stress	*DnaJ heat shock protein family (Hsp40) member B4*	*Dnajb4*	295549	1.25	0.038
		DnaJ heat shock protein family (Hsp40) member B6	*Dnajb6*	362293	1.15	0.091
		Oxidative stress responsive serine rich 1	*Oser1*	296346	1.23	0.017
		DnaJ heat shock protein family (Hsp40) member B9	*Dnajb9*	24908	1.39	0.041
		Heat shock protein 90 alpha family class A member 1	*Hsp90aa1*	299331	1.21	0.058
		Heat shock protein family A (Hsp70) member 5	*Hspa5*	25617	1.34	0.011
Lipid metabolism	Fatty acid metabolism	*Androgen induced 1*	*Aig1*	292486	-1.40	0.057
		3-hydroxyacyl-CoA dehydratase 4	*Hacd4*	362540	-1.76	0.038
		Enoyl CoA hydratase domain containing 2	*Echdc2*	298381	2.01	0.005
	Sterol metabolism	*STAR related lipid transfer domain containing 5*	*Stard5*	502348	-1.50	0.085
		ATP binding cassette subfamily A member 1	*Abca1*	313210	-1.58	0.046
		SREBF pathway regulator in golgi 1	*Spring1*	498188	-1.41	0.040
		Phospholipase A2 group IID	*Pla2g2d*	298579	-1.46	0.020
		Phospholipid transfer protein	*Pltp*	296371	-1.79	0.030
	Sex steroid hormone-related	*HEXIM P-TEFb complex subunit 1*	*Hexim1*	498008	1.30	0.017
Carbohydrate metabolism	Glucose and insulin homeostasis	*Solute carrier family 2 member 4*	*Slc2a4*	25139	-3.19	0.010
		Regulatory associated protein of MTOR complex 1	*Rptor*	287871	-1.26	0.010
		Growth factor receptor bound protein 7	*Grb7*	84427	3.00	0.043
Cell proliferation, differentiation and death	Cell differentiation	*Inhibitor of DNA binding 3*	*Id3*	25585	-1.82	0.017
		KLF transcription factor 6	*Klf6*	58954	1.41	0.023
	Cell proliferation	*BTG anti-proliferation factor 2*	*Btg2*	29619	1.35	0.025
		MYB proto-oncogene, transcription factor	*Myb*	498982	2.01	0.010
		PBX homeobox 1	*Pbx1*	304947	1.54	0.043
		Jun proto-oncogene, AP-1 transcription factor subunit	*Jun*	24516	1.69	0.060
	Cell death - *Apoptosis*	*Proliferation and apoptosis adaptor protein 15*	*Pea15*	364052	-1.28	0.063
		Activating transcription factor 5	*Atf5*	282840	-1.82	0.026
		SRY-box transcription factor 4	*Sox4*	364712	1.85	0.017
		MCL1 apoptosis regulator, BCL2 family member	*Mcl1*	60430	1.19	0.014
Cytoskeleton and cellular network	Extracellular matrix (ECM) organization	*Bone gamma-carboxyglutamate protein*	*Bglap*	25295	-1.85	0.010
		Biglycan	*Bgn*	25181	-1.66	0.060
	Regulation of actin cytoskeleton	*FYVE, RhoGEF and PH domain containing 4*	*Fgd4*	246174	-1.49	0.046
		CD84 molecule	*Cd84*	501872	-1.42	0.073
		CD28 molecule	*Cd28*	25660	1.26	0.040
	Cytoskeletal filaments	*Tubulin beta 2B class Iib*	*Tubb2b*	291081	-2.25	0.000
		Outer dynein arm docking complex subunit 3	*Odad3*	315465	13.86	0.081
RNA processing	Splicing	*Serine and arginine rich splicing factor 3*	*Srsf3*	361814	1.14	0.089
		Serine and arginine rich splicing factor 5	*Srsf5*	29667	1.22	0.030
Signaling	MAPK signaling pathway	*Mitogen-activated protein kinase 1*	*Mapk1*	116590	-1.36	0.052
		Dual specificity phosphatase 10	*Dusp10*	63995	1.62	0.005
	TGF-beta signaling pathway	*TGF-beta activated kinase 1 binding protein 1*	*Tab1*	315139	-1.25	0.011
		Transforming growth factor, beta 2	*Tgfb2*	81809	-1.52	0.069
		Transforming growth factor, beta 3	*Tgfb3*	25717	-3.72	0.030

Abbreviations: PBMCs, peripheral blood mononuclear cells, NK, natural killer; OVX, ovariectomized rats. FC: fold changes in OVX vs. SHAM animals. The + symbol indicates upregulation, and the - symbol indicates downregulation in the OVX animals. Genes with*adj. p* value < 0.1 from the microarray data analysis are shown.

DISCUSSION

In this study, we explored the impact on health of ovariectomy performed at 15 weeks and 25 weeks on female Sprague-Dawley rats over a 10-week period. Our findings are in line with those previously described in this animal model (42), showing that ovariectomy

exacerbated various health concerns associated with obesity and immunocardiometabolic alterations regardless of the age at which ovariectomy was performed. The worsened body composition, characterized by increased fat mass accumulation and muscle loss, resulting in a decreased lean-to-fat mass ratio, as well as enlarged adipocyte size and a shift towards a greater number of larger adipocytes, indicating hypertrophy in RWAT and MWAT depots, observed in both OVX groups, can be attributed, at least in part, to the increased food intake and the decreased energy expenditure reported in these oestrogen deficient rats compared to their respective SHAM counterparts (83–85). In addition, the elevated leptin-to-adiponectin and decreased adiponectin-to-leptin ratios displayed by OVX animals suggested an increased cardiometabolic risk and adipose tissue inflammation (27,82,86,87), which would be consistent with previous research showing that WAT hypertrophy is associated with IR and inflammation (88). Furthermore, the enhanced secretion of bone formation and resorption biomarkers, which was evidenced by the higher circulating levels of osteocalcin and CTX-1, respectively, would account for an increased risk of osteoporosis, as was previously reported in both postmenopausal women and OVX rodents (5,41,89).

However, we observed, at the end of the study, a pronounced response in the circulating levels of TC and the inflammatory marker MCP-1 in the rats that were ovariectomized at 15 weeks of age, which displayed significantly higher values than their SHAM counterparts, an effect that was not observed when the removal of the ovaries was carried out at 25 weeks of age. Very similarly, the hepatic values of the antioxidant marker GSH/GSSG ratio significantly decreased only in the younger OVX animals. At first glance, these results were unexpected, and it is tempting to speculate that these different responses can be attributed to age-related adaptive mechanisms, which might be more evident in the older 35-week-old animals, helping to mitigate the severity of these metabolic, inflammatory, and oxidative stress-related alterations occurring in response to

ovariectomy. On the other hand, the significantly increased values of the surrogate marker of insulin resistance, HOMA-IR, observed only in the older OVX rats when compared to their age-matched SHAM counterparts, would agree with the results previously described in other animal models, showing an increase in this parameter with age (90). In the same line, the decreased BMD observed specifically in the tibia of the older OVX animals would be in line with previous research demonstrating that rats that underwent ovariectomy at 6-9 months of age exhibited the most osteoporotic response due to have a lower skeletal bone growth and trabecular connectivity compared to rats in which ovariectomy was induced before 6 months of age (41).

Overall, our results indicated that ovariectomy-induced at both ages triggered health-related complications, most of them being similar in both 25 and 35-week-old animals, although the disturbances concerning IR and osteoporosis were higher in the older model, and the cholesterol, inflammation, and oxidative stress-related alterations were more exacerbated in the younger animals. Considering that osteoporosis is one of the most common hallmarks of menopause and that there is a clear relationship between insulin resistance and increased CVD risk (91), and keeping in mind that the rat is not the most appropriate animal model for diseases related to cholesterol alterations (92–94), we considered that the rats in which ovariectomy was induced at 25 weeks (i.e. 35-week-old animals) may offer a more accurate reflection of the postmenopausal condition. Therefore, we assessed gene expression profiles in PBMCs of 35-week-old rats to understand the potential underlying mechanisms associated with the postmenopausal state.

The downregulation of most of the immune-related pathways observed at gene expression level in PBMCs of the oestrogen deficient OVX rats would be in line with previous research showing that the loss of ovarian steroid production occurring in postmenopausal

women declines the immune function, an alteration that is also associated with aging and is known as immunosenescence (95,96). Thus, several reports showed that the changes in sex steroid hormone levels characterizing the menopausal state lead to a dysregulation of the immune function, which can trigger relevant health problems, including obesity, osteoporosis, autoimmune diseases, and immunodeficiency (95–98). Steroid hormones exert a profound influence on the immune response by modulating gene expression in cells possessing hormone receptors (95–98). During these stages of a woman's life, there is an increase in pro-inflammatory serum markers such as MCP-1, IL1, IL6, and TNF-alpha, accompanied by a decrease in T and B lymphocytes, along with a clear diminished cytotoxic activity of NK cells (95–98), being reversed most of these dysregulations in response to hormone replacement therapy (HRT) prescription (96). The decreased mRNA levels of *sh3bp2*, a gene specifically associated with a positive regulation of Natural Killer Cell Mediated Cytotoxicity pathway (99), observed in the PBMCs of OVX rats, would support the idea towards a lower NK cell-mediated cytotoxicity occurring in the postmenopausal state. Several studies reported that IL-18, in synergy with IL-12, activates NK cells to produce IFN-γ and enhances their cytotoxicity against tumor cells (100–103). Additionally, IL-18 and IL-12 can also activate T cells and B cells to produce IFN-γ (104–106). A deficiency in IL-18 results in defective NK cell activity (101), demonstrating the critical role of these cytokines in maintaining effective immune responses. The downregulation of *il18r1, il18rap,* and *il12rb1*, observed in our study in the PBMCs of the OVX animals are in agreement with these findings and would reinforce the hypothesis that there is an impairment of NK-related immune function in the postmenopausal state. Human patients with obesity displayed *SOCS3* overexpression in PBMCs and it was demonstrated that both SOCS-3 and leptin play a very important role in inhibiting the type I interferon (IFN-1) response in these cells during obesity (107),

which could lead to the suppression of the immune response to viral infections, considering the key role of IFN-1 in antiviral defense. The higher mRNA levels of *socs3* observed in PBMCs of our OVX rats would be in line with the aforementioned impaired immune response. Our findings are also supported by a previous study carried out in OVX rats that showed increased *socs3* mRNA expression in ventricular tissue, which was associated with an inflammatory response (108). Interestingly, increased *socs3* mRNA levels were counteracted by oestrogen replacement treatment, although this effect was not observed at the protein level, suggesting posttranscriptional regulation mechanisms that maintain SOCS3 protein at similar levels regardless of the oestrogen levels (108).

SOCS3 binds to the insulin receptor and inhibits the activation of insulin receptor substrate 1 (IRS1) and insulin signaling pathways, enhancing insulin resistance (109,110), an effect that is induced, at least in part, by leptin through the upregulation of SOCS3. The higher mRNA levels of *socs3* observed in PBMCs of our OVX rats would be in line with the sharp increase of the surrogate marker of insulin resistance, HOMA-IR, observed in our study in the postmenopausal model with oestrogen deficiency. Numerous studies have reported that ovariectomy in rats leads to significant metabolic disturbances, including elevated fasting blood glucose and insulin levels, and increased HOMA-IR, indicating IR and glucose intolerance (111–113). These systemic effects can also be partly explained by the reduced expression of slc2a4, also known as glut4, in the liver, pancreas, and skeletal muscle of these animals (111–113). Furthermore, phosphorylated levels of P38 MAPK and AKT are significantly reduced in OVX rats, linking the inactivation of the P38 MAPK/GLUT4 signaling pathway to decreased GLUT4 expression and impaired glucose metabolism (112). In addition, GRB7 is an adaptor protein involved in intracellular signaling pathways, impacting insulin sensitivity, among other processes (114–117). Different studies showed that female *grb7*-null mice

exhibit improved glycaemic control and enhanced insulin signalling in the liver, evidenced by increased insulin-stimulated phosphorylation of the insulin receptor and Akt, indicating that GRB7 negatively regulates insulin sensitivity (114). Therefore, the lower *glut4* mRNA levels and the higher *grb7* and *socs3* gene expression levels found in our study in the PBMCs of OVX rats would support the utility of PBMCs to reflect metabolic alterations related to glucose and insulin homeostasis that are produced in response to oestrogen deficiency induced by ovariectomy.

BPIFB4 is a protein linked to longevity that is found at high levels in Long-Living Individuals, correlating with a tendency for monocyte-derived macrophages to adopt an anti-inflammatory M2 phenotype, which is understood as a protective mechanism against age-related cardiovascular diseases and inflammation (118,119). It is tempting to hypothesize that the sharp downregulation of *bpifb4* expression observed in the present study might impair immune response modulation and fail to reduce cellular senescence in postmenopausal rats with oestrogen deficiency. Whether the lower *bpifb4* mRNA levels observed in PBMCs of OVX animals could contribute to accelerated aging and to the onset of age-related diseases in the postmenopausal stage, potentially increasing the risk of atherosclerosis and diabetic cardiomyopathy (118,119) would deserve further research. Related also to aging, the decreased expression of *mapk1* reported in the present research is consistent with the findings obtained in a study in which inhibition of MAPK1 was found in both OVX and natural aging-induced ovarian senescence oestrogen deficient mice models, suggesting increased apoptotic pathway activation and cytoskeletal disturbances in muscle tissue (120), which could be linked to the increased muscle mass loss observed in our OVX rats, highlighting the role of oestrogen deficiency and aging in promoting muscle atrophy.

Dnajb4, *dnajb6*, *dnajb9*, *hspa5* and *hsp90aa1* genes encode for heat shock proteins (HSPs) that are molecular chaperones activated in response to stress and that play critical roles in protein folding and cellular homeostasis, being their overexpression linked to drug resistance and cancer progression, promoting malignant behaviors and poor prognosis, including ovarian, endometrial, cervical, bladder, pancreatic and breast cancers in women (121–126). In this sense, the higher mRNA levels of these genes and the gene encoding the protein OSER1 (oxidative stress-responsive serine-rich 1) reported in our OVX rats compared to their SHAM counterparts would suggest an increased stress response occurring in this postmenopausal model that is reflected at gene expression levels in PBMCs. *Hexim1* encodes the HEXIM P-TEFb complex subunit 1, which is a protein that inhibits the activity of ligand-bound oestrogen receptor alpha (ERα), leading to the suppression of ERα-dependent gene expression of these receptors (127–129). The complex interplay between progesterone receptors (PR) and ER receptors plays a crucial role in the activation and regulation of progesterone and oestrogen signaling pathways (130). It has been described that the maturation and stabilization of the PR can occur through the Hsp90 chaperone pathway, involving a collaborative mechanism with Hsp40 and Hsp70 (121). In our study the lower *hexim1* mRNA levels in the PBCMs of OVX animals accompanied by the overexpression of genes encoding various HSPs of the HSP40 family, such as DNAJB4, DNAJB6 and DNAJB9, HSPA5 (an HSP70 molecular chaperone also known as binding immunoglobulin protein -BIP-), and HSP90α, would be in line with the aforementioned mechanism concerning the chaperoning of PR by HSPs, which has been described in different tissues, such as endometrium (131), vascular smooth muscle cells (132), and lung (131,132), and would also be reflected in PBMCs. Another study demonstrated that the impact of exogenous HRT treatment including oestradiol and progesterone on mammary gland cells in OVX mice was effectively

counteracted by progesterone receptor antagonists, thereby suppressing the pathways induced by both oestrogen and progesterone (133). Therefore, this antagonistic effect observed after ovariectomy could modulate HSPs expression, suggesting a compensatory mechanism where the deficiency of oestrogens, as seen in OVX models, accompanied by decreased levels of progesterone (134–136), could enhance PR availability and chaperone efficiency, potentially activating or increasing the availability and activity of PR. On the other hand, *hspa5* overexpression in OVX mice negatively impacted bone health by promoting adipogenesis over osteogenesis in bone marrow stromal cells and a treatment with the HSPA5 inhibitor HA15 ameliorated bone loss in OVX mice (137). Therefore, the increased hspa5 mRNA levels observed in PBMCS of OVX rats would suggest that these blood cells capture to some degree the osteoporosis occurring in our postmenopausal model, which, considering the important role of progesterone against bone loss (136), could be related, at least in part, to the decreased of both oestrogen and progesterone levels reported in the postmenopausal state. This differential regulation of HSPs and hormone receptors underscores the importance of understanding the distinct and combined roles of oestrogen and progesterone in both normal and cancerous tissues, offering insights into potential therapeutic targets for hormone-related cancers and conditions such as osteoporosis that could be potentially monitored at the molecular level using PBMCs, although further research would be need to shed light on this issue.

17β-oestradiol (17β-E2) significantly enhances macrophage cholesterol efflux, a key process in preventing atherosclerosis, by upregulating *abca1* via ERα. *In vivo* experiments with OVX mice treated with 17β-E2 showed increased *abca1* expression and cholesterol efflux in macrophages, corroborating the results obtained in cell line studies (138). Furthermore, a 3-month HRT study consisting of oral oestrogen and progestin supplementation to non-obese, normolipidemic post-menopausal women revealed an

increase in the HDL cholesterol and apoA-I blood levels, a decrease in the circulating levels of low-density lipoprotein (LDL) cholesterol and apoB as well as elevated leukocyte *ABCA1* mRNA expression (139). The positive correlation observed between increased HDL levels and *abca1* expression would suggest that HRT protect against atherosclerosis by promoting ABCA1-mediated cholesterol efflux to HDL particles (139). Another gene playing an important role in cholesterol homeostasis is *stard5,* the deletion of which led to decreased plasma membrane cholesterol content and diminished intracellular cholesterol levels in macrophages, primarily by reducing cholesterol efflux through the ABCA1 pathway (140), highlighting the interconnected roles of *stard5* and *abca1* in maintaining lipid homeostasis. Other studies demonstrated that mice lacking for *stard5* displayed increased hepatic levels of cholesterol and triglycerides (140,141), showing also a dysregulation in the fatty acid synthesis pathway, leading to intracellular vacuolization in hepatocytes, elevated IR (HOMA-IR), and accelerated liver fibrosis and steatosis as previously reported by members of our research group in OVX rats (43). Therefore, it is tempting to speculate that, in the present study, the decreased *abca1* and *stard5* mRNA levels observed in the PBMCs of OVX rats could be potential early molecular biomarkers of lipid metabolic-related diseases, such as atherosclerosis, in 35-week-old OVX animals, although these animals did not display changes in either the circulating levels of TC or the non-HDL and HDL plasma concentrations at sacrifice. Recent studies have also elucidated the crucial role in lipid homeostasis metabolism of *spring*, also known as C12orf49 (142–145). SPRING exhibits ubiquitous expression, with slightly higher levels observed in the liver (143), functioning as a crucial regulator in the processing of SREBPs transcription factors, the master regulators of lipid homeostasis, particularly in cholesterol and fatty acid synthesis (146). Loss of SPRING function leads to decreased levels of precursor and mature SREBPs, impairing the cell's

ability to respond to sterol depletion and affecting lipid homeostasis (143). Additionally, SPRING depletion disrupts SREBP signaling, impairing SREBP-driven de novo lipogenesis and resulting in reduced surface LDLR protein levels and diminished LDL uptake, underscoring the role of *spring* in lipid metabolism (142,143). The lower *spring* expression levels observed in the PBMCs of OVX rats, together with the observed downregulation of *abca1* and *stard5* would reinforce the idea that these blood cells can be used as an easily obtainable biological source to characterize potential aspects of both cholesterol and lipid metabolism in physiological or pathological conditions, as was previously described by members of our group (57,58,69).

Postmenopausal osteoporosis is characterized by low BMD (17,147) and induces relatively rapid bone loss due to increased osteoclast activity (34,35). Related to this, Gao *et al.* observed significantly lower BMD and severe trabecular bone damage in OVX rats when compared to their SHAM counterparts and reported a positive correlation between the expression of *Tgfb3* and multiple parameters involved in bone microstructure, suggesting the members of the TGF-β family as potential biomarkers for postmenopausal osteoporosis in OVX rats, due to the key role of these genes in bone homeostasis and bone repair, osteogenic differentiation, osteoclast formation, maintaining an optimal osteoblast/osteoclast balance (148–150). Very interestingly, peripheral blood monocytes have been described as an important source of osteoclast precursors, making these cells a suitable model for studying bone metabolism (151). In our study, the downregulation of the genes encoding TAB1, TGFB2 and TGFB3 reported in the PBMCs of OVX rats fully supports this idea, giving extra evidence of the usefulness of these blood cells to reflect alterations occurring in internal tissues. Notably, our findings regarding the decreased expression of *bglap*, the gene encoding for osteocalcin, found in OVX animals reinforces our hypothesis. Despite increased circulating levels of osteocalcin observed in

postmenopausal women (152–154) and in OVX animals, as occurs in our study, several studies have shown that the expression of the *bglap* gene is significantly downregulated in OVX rats in bone marrow mesenchymal cells, alveolar bone osteoblastic cells, and femoral tissues (155–157). Overall, our results concerning the downregulation of *bglap*, *tab1, tgfb2* and *tgfb3* observed in PBMCs would be in agreement with the idea pointing toward the lower capability of bone mineralization and reduced BMD during the postmenopausal state (148–150,155–157). Furthermore, the *bgn* gene and its protein biglycan are crucial for bone and cartilage health. Studies on biglycan-deficient mice have demonstrated a reduced capacity to generate bone marrow stromal cells (BMSCs), being this deficiency worsening with age (158). Normally, high levels of biglycan in BMSCs help control cell proliferation and apoptosis, ensuring a proper population of mature osteoblasts. In addition, these cells exhibit a diminished response to TGF-β, decreased collagen synthesis, and increased apoptosis compared to normal cells (158). In our study, the downregulation of *bgn* observed in the PBMCs of OVX rats is consistent with the link between its under expression and bone metabolism-related disorders, and confirms that the interplay between *bgn*, TGF-β-related genes and *bglap* reported in previous studies (148–150,155–158) is also reflected in PBMCs. Additionally, two studies reported that ovariectomy led to a significant increase in both mRNA and protein levels of PTGS2, also known as COX-2, in trabecular tibias (159,160), which is fully aligned with our findings observed at gene expression level in PBMCs. These studies indicated that *cox-2* overexpression might aggravate OVX-induced bone loss by deteriorating trabecular bone mass and architecture through reduced bone remodeling and decreased resorptive activity. Therefore, inhibitors of COX-2 could serve as therapeutic agents by correcting these adverse effects, potentially preserving bone mass and improving bone architecture in the context of oestrogen deficiency (160). Overall, considering our results obtained at

gene expression level in PBMCs concerning genes related to bone metabolism, it is tempting to hypothesize this subset of cells could provide a source of molecular biomarkers to monitor the response to nutritional and pharmacological treatments against osteoporosis, although further research would be needed to gain knowledge on this issue.

CONCLUSION

We reported here that ovariectomized rats recapitulated most of the alterations that can occur during the postmenopausal state in women, including obesity, adipocyte hypertrophy and increased osteoporosis and cardiometabolic risks, being these effects slightly more evident in rats induced to ovariectomy at a more advanced age. Our transcriptomic approach carried out in PBMCs revealed that this subset of blood cells reflected molecular changes associated with oestrogen deficiency occurring in the postmenopausal state in these rats, which were evidenced by changes at the mRNA level of genes mainly related to immune function, response to stress, lipid metabolism, and bone homeostasis, providing valuable insights into the pathophysiology of postmenopausal-related alterations, such as osteoporosis and inmunometabolic diseases. Understanding these molecular mechanisms can pave the way for the design of targeted therapeutic interventions to mitigate the adverse effects of menopause on women's health, which could be monitored at the gene expression level using PBMCs, a biological material that can be easily and repeatedly collected.

REFERENCES

1. Santoro N, Randolph JF. Reproductive Hormones and the Menopause Transition. Obstet Gynecol Clin North Am. 2011, 38, 455–66.
2. McNeil MA, Merriam SB. Menopause. Ann Intern Med. 2021, 174, ITC97-ITC112.
3. Thurston RC, Johnson BD, Shufelt CL, Braunstein GD, Berga SL, Stanczyk FZ, et al. Menopausal symptoms and cardiovascular disease mortality in the Women's Ischemia Syndrome Evaluation (WISE). Menopause. 2017, 24, 126–32.
4. Harlow SD, Gass M, Hall JE, Lobo R, Maki P, Rebar RW, et al. Executive Summary of

the Stages of Reproductive Aging Workshop + 10: Addressing the Unfinished Agenda of Staging Reproductive Aging. J Clin Endocrinol Metab. 2012, 97, 1159–68.
5. Thapa S, Nandy A, Rendina-Ruedy E. Endocrinal metabolic regulation on the skeletal system in post-menopausal women. Front Physiol. 2022, 13, 1052429.
6. Juppi H, Sipilä S, Fachada V, Hyvärinen M, Cronin N, Aukee P, et al. Total and regional body adiposity increases during menopause—evidence from a follow-up study. Aging Cell. 2022, 21, e13621.
7. Sowers M, Zheng H, Tomey K, Karvonen-Gutierrez C, Jannausch M, Li X, et al. Changes in Body Composition in Women over Six Years at Midlife: Ovarian and Chronological Aging. J Clin Endocrinol Metab. 2007, 92, 895–901.
8. Fenton A, Smart C, Goldschmidt L, Price V, Scott J. Fat mass, weight and body shape changes at menopause – causes and consequences: a narrative review. Climacteric. 2023, 26, 381–7.
9. Kapoor E, Collazo-Clavell ML, Faubion SS. Weight Gain in Women at Midlife: A Concise Review of the Pathophysiology and Strategies for Management. Mayo Clin Proc. 2017, 92, 1552–8.
10. Barrea L, Pugliese G, Laudisio D, Colao A, Savastano S, Muscogiuri G. Mediterranean diet as medical prescription in menopausal women with obesity: a practical guide for nutritionists. Crit Rev Food Sci Nutr. 2021, 61, 1201–11.
11. Ko SH, Kim HS. Menopause-Associated Lipid Metabolic Disorders and Foods Beneficial for Postmenopausal Women. Nutrients. 2020, 12, 202.
12. Taleb-Belkadi O, Chaib H, Zemour L, Fatah A, Chafi B, Mekki K. Lipid profile, inflammation, and oxidative status in peri- and postmenopausal women. Gynecol Endocrinol. 2016, 32, 982–5.
13. Rosano GMC, Vitale C, Marazzi G, Volterrani M. Menopause and cardiovascular disease: the evidence. Climacteric. 2007, 10, 19–24.
14. Mesch VR, Boero LE, Siseles NO, Royer M, Prada M, Sayegh F, et al. Metabolic syndrome throughout the menopausal transition: influence of age and menopausal status. Climacteric. 2006, 9, 40–8.
15. Carr MC. The Emergence of the Metabolic Syndrome with Menopause. J Clin Endocrinol Metab. 2003, 88, 2404–11.
16. The European Society of Cardiology. Understanding the burden of CVD [Internet]. 2022. Available from: https://www.escardio.org/The-ESC/Advocacy/understanding-the-burden-of-cvd-facts-and-figures.
17. Sozen T, Ozisik L, Calik Basaran N. An overview and management of osteoporosis. Eur J Rheumatol. 2017, 4, 46–56.
18. Finegold JA, Asaria P, Francis DP. Mortality from ischaemic heart disease by country, region, and age: Statistics from World Health Organisation and United Nations. Int J Cardiol. 2013, 168, 934–45.
19. The Emerging Risk Factors Collaboration. Diabetes mellitus, fasting blood glucose concentration, and risk of vascular disease: a collaborative meta-analysis of 102 prospective studies. Lancet. 2010, 135, 2215-22.
20. Marchi R de, Dell'Agnolo CM, Lopes TCR, Gravena AAF, Demitto MDO, Brischiliari SCR, et al. Prevalence of metabolic syndrome in pre- and postmenopausal women. Arch Endocrinol Metab. 2017, 61, 160–6.
21. Ruan X, Jin J, Hua L, Liu Y, Wang J, Liu S. The prevalence of metabolic syndrome in Chinese postmenopausal women and the optimum body composition indices to predict it. Menopause. 2010, 17, 566–70.
22. Kim HM, Park J, Ryu SY, Kim J. The Effect of Menopause on the Metabolic Syndrome Among Korean Women. Diabetes Care. 2007, 30, 701–6.
23. Eshtiaghi R, Esteghamati A, Nakhjavani M. Menopause is an independent predictor of metabolic syndrome in Iranian women. Maturitas. 2010, 65, 262–6.
24. Palmer BF, Clegg DJ. The sexual dimorphism of obesity. Mol Cell Endocrinol. 2015, 402, 113–9.

25. Lizcano F, Guzmán G. Estrogen Deficiency and the Origin of Obesity during Menopause. Biomed Res Int. 2014, 2014, 1–11.
26. Mauvais-Jarvis F, Clegg DJ, Hevener AL. The role of estrogens in control of energy balance and glucose homeostasis. Endocrine Reviews. 2013, 34, 309–38.
27. Gupta V, Mishra S, Mishra S, Kumar S, Gupta V. Association of Leptin: Adiponectin ratio and metabolic risk markers in postmenopausal women. Immunol Lett. 2018, 196, 63–7.
28. Xu Y, López M. Central regulation of energy metabolism by estrogens. Mol Metab. 2018, 15, 104–15.
29. Trenti A, Tedesco S, Boscaro C, Trevisi L, Bolego C, Cignarella A. Estrogen, Angiogenesis, Immunity and Cell Metabolism: Solving the Puzzle. Int J Mol Sci. 2018, 19, 859.
30. Chakrabarti S, Lekontseva O, Davidge ST. Estrogen is a modulator of vascular inflammation. IUBMB Life. 2008, 60, 376–82.
31. Strehlow K, Rotter S, Wassmann S, Adam O, Grohé C, Laufs K, et al. Modulation of Antioxidant Enzyme Expression and Function by Estrogen. Circ Res. 2003, 93,170–7.
32. Sheng-Huang C, Chieh-Hsin C, Mu-Chun Y, Wen-Tung H, Chia-Ying H, Ya-Ting H, et al. Effects of estrogen on glutathione and catalase levels in human erythrocyte during menstrual cycle. Biomed Reports. 2015, 3, 266–8.
33. Straub RH. The Complex Role of Estrogens in Inflammation. Endocr Rev. 2007, 28, 521–74.
34. Duque G, Troen BR. Understanding the Mechanisms of Senile Osteoporosis: New Facts for a Major Geriatric Syndrome. J Am Geriatr Soc. 2008, 56, 935–41.
35. Riggs BL, Melton LJ. Involutional Osteoporosis. N Engl J Med. 1986, 314, 1676–86.
36. Garnero P, Sornay-Rendu E, Chapuy MC, Delmas PD. Increased bone turnover in late postmenopausal women is a major determinant of osteoporosis. J Bone Miner Res. 1996, 11, 337–49.
37. Charatcharoenwitthaya N, Khosla S, Atkinson EJ, McCready LK, Riggs BL. Effect of Blockade of TNF-α and Interleukin-1 Action on Bone Resorption in Early Postmenopausal Women. J Bone Miner Res. 2007, 22, 724–9.
38. Sophocleous A, Idris AI. Ovariectomy/orchiectomy in rodents. Methods in Molecular Biology. 2019, 1914, 261–7.
39. Koebele S V., Bimonte-Nelson HA. Modeling menopause: The utility of rodents in translational behavioral endocrinology research. Maturitas. 2016, 87, 5–17.
40. Brinton RD. Minireview: Translational animal models of human menopause: Challenges and emerging opportunities. Endocrinology. 2012, 153, 3571–8.
41. Yousefzadeh N, Kashfi K, Jeddi S, Ghasemi A. Ovariectomized rat model of osteoporosis: A practical guide. EXCLI Journal. 2020, 19, 89–107.
42. Medina-Contreras J, Villalobos-Molina R, Zarain-Herzberg A, Balderas-Villalobos J. Ovariectomized rodents as a menopausal metabolic syndrome model. A minireview. Molecular and Cellular Biochemistry. 2020, 475, 261–76.
43. Quesada-Vázquez S, Castells-Nobau A, Latorre J, Oliveras-Cañellas N, Puig-Parnau I, Tejera N, et al. Potential therapeutic implications of histidine catabolism by the gut microbiota in NAFLD patients with morbid obesity. Cell Reports Med. 2023, 4, 101341.
44. Diz-Chaves Y, Kwiatkowska-Naqvi A, Von Hülst H, Pernía O, Carrero P, Garcia-Segura LM. Behavioral effects of estradiol therapy in ovariectomized rats depend on the age when the treatment is initiated. Exp Gerontol. 2012, 47, 93–9.
45. Liew CC, Ma J, Tang HC, Zheng R, Dempsey AA. The peripheral blood transcriptome dynamically reflects system wide biology: a potential diagnostic tool. J Lab Clin Med. 2006, 147, 126–32.
46. Bouwens M, Afman LA, Müller M. Fasting induces changes in peripheral blood

mononuclear cell gene expression profiles related to increases in fatty acid β-oxidation: functional role of peroxisome proliferator–activated receptor α in human peripheral blood mononuclear cells. Am J Clin Nutr. 2007, 86,1515–23.

47. Bouwens M, Afman LA, Müller M. Activation of peroxisome proliferator-activated receptor alpha in human peripheral blood mononuclear cells reveals an individual gene expression profile response. BMC Genomics. 2008, 9, 262.
48. Maas K, Chan S, Parker J, Slater A, Moore J, Olsen N, et al. Cutting Edge: Molecular Portrait of Human Autoimmune Disease. J Immunol. 2002, 169, 5–9.
49. Burczynski ME, Dorner AJ. Transcriptional Profiling of Peripheral Blood Cells in Clinical Pharmacogenomic Studies. Pharmacogenomics. 2006, 7, 187–202.
50. Visvikis-Siest S, Marteau JB, Samara A, Berrahmoune H, Marie B, Pfister M. Peripheral blood mononuclear cells (PBMCs): a possible model for studying cardiovascular biology systems. Clin Chem Lab Med. 2007, 45, 1154–68.
51. Caimari A, Oliver P, Rodenburg W, Keijer J, Palou A. Slc27a2 expression in peripheral blood mononuclear cells as a molecular marker for overweight development. Int J Obes. 2010, 34, 831–9.
52. Aljada A, Mohanty P, Ghanim H, Abdo T, Tripathy D, Chaudhuri A, et al. Increase in intranuclear nuclear factor κB and decrease in inhibitor κB in mononuclear cells after a mixed meal: evidence for a proinflammatory effect. Am J Clin Nutr. 2004, 79, 682–90.
53. Bouwens M, van de Rest O, Dellschaft N, Bromhaar MG, de Groot LC, Geleijnse JM, et al. Fish-oil supplementation induces antiinflammatory gene expression profiles in human blood mononuclear cells. Am J Clin Nutr. 2009, 90, 415–24.
54. Mohanty P, Ghanim H, Hamouda W, Aljada A, Garg R, Dandona P. Both lipid and protein intakes stimulate increased generation of reactive oxygen species by polymorphonuclear leukocytes and mononuclear cells. Am J Clin Nutr. 2002, 75, 767–72.
55. Radler U, Stangl H, Lechner S, Lienbacher G, Krepp R, Zeller E, et al. A Combination of (ω–3) Polyunsaturated Fatty Acids, Polyphenols and *L*-Carnitine Reduces the Plasma Lipid Levels and Increases the Expression of Genes Involved in Fatty Acid Oxidation in Human Peripheral Blood Mononuclear Cells and HepG2 Cells. Ann Nutr Metab. 2011, 58, 133–40.
56. van Erk MJ, Blom WAM, van Ommen B, Hendriks HFJ. High-protein and high-carbohydrate breakfasts differentially change the transcriptome of human blood cells. Am J Clin Nutr. 2006, 84, 1233–41.
57. Caimari A, Oliver P, Rodenburg W, Keijer J, Palou A. Feeding conditions control the expression of genes involved in sterol metabolism in peripheral blood mononuclear cells of normoweight and diet-induced (cafeteria) obese rats. J Nutr Biochem. 2010, 21, 1127–33.
58. Caimari A, Oliver P, Keijer J, Palou A. Peripheral Blood Mononuclear Cells as a Model to Study the Response of Energy Homeostasis-Related Genes to Acute Changes in Feeding Conditions. Omi A J Integr Biol. 2010, 14, 129–41.
59. de Mello VDF, Kolehmanien M, Schwab U, Pulkkinen L, Uusitupa M. Gene expression of peripheral blood mononuclear cells as a tool in dietary intervention studies: What do we know so far? Mol Nutr Food Res. 2012, 56, 1160–72.
60. van Dijk SJ, Mensink M, Esser D, Feskens EJM, Müller M, Afman LA. Responses to High-Fat Challenges Varying in Fat Type in Subjects with Different Metabolic Risk Phenotypes: A Randomized Trial. Tomé D, editor. PLoS One. 2012, 7, e41388.
61. Bokarewa M, Nagaev I, Dahlberg L, Smith U, Tarkowski A. Resistin, an Adipokine with Potent Proinflammatory Properties. J Immunol. 2005, 174, 5789–95.
62. de Mello VDF, Kolehmainen M, Schwab U, Mager U, Laaksonen DE, Pulkkinen L, et al. Effect of weight loss on cytokine messenger RNA expression in peripheral blood mononuclear cells of obese subjects with the metabolic syndrome. Metabolism. 2008, 57, 192–9.
63. Ghanim H, Aljada A, Hofmeyer D, Syed T, Mohanty P, Dandona P. Circulating Mononuclear Cells in the Obese Are in a Proinflammatory State. Circulation. 2004, 110, 1564–71.

64. Goyenechea E, Parra D, Crujeiras AB, Abete I, Martínez JA. A Nutrigenomic Inflammation-Related PBMC-Based Approach to Predict the Weight-Loss Regain in Obese Subjects. Ann Nutr Metab. 2009, 54, 43–51.
65. Napoleone E, Di Santo A, Amore C, Baccante G, Di Febbo C, Porreca E, et al. Leptin induces tissue factor expression in human peripheral blood mononuclear cells: a possible link between obesity and cardiovascular risk? J Thromb Haemost. 2007, 5, 1462–8.
66. O'Rourke RW, Kay T, Lyle EA, Traxler SA, Deveney CW, Jobe BA, et al. Alterations in peripheral blood lymphocyte cytokine expression in obesity. Clin Exp Immunol. 2006, 146, 39–46.
67. Patel L, Buckels AC, Kinghorn IJ, Murdock PR, Holbrook JD, Plumpton C, et al. Resistin is expressed in human macrophages and directly regulated by PPARγ activators. Biochem Biophys Res Commun. 2003, 300, 472–6.
68. Samara A, Marie B, Pfister M, Visvikis-Siest S. Leptin expression in Peripheral Blood Mononuclear Cells (PBMCs) is related with blood pressure variability. Clin Chim Acta. 2008, 395, 47–50.
69. Caimari A, Crescenti A, Puiggròs F, Boqué N, Arola L, del Bas JM. The intake of a high-fat diet and grape seed procyanidins induces gene expression changes in peripheral blood mononuclear cells of hamsters: capturing alterations in lipid and cholesterol metabolisms. Genes Nutr. 2015, 10, 438.
70. Rudkowska I, Raymond C, Ponton A, Jacques H, Lavigne C, Holub BJ, et al. Validation of the Use of Peripheral Blood Mononuclear Cells as Surrogate Model for Skeletal Muscle Tissue in Nutrigenomic Studies. Omi A J Integr Biol. 2011, 15, 1–7.
71. O'Grada CM, Morine MJ, Morris C, Ryan M, Dillon ET, Walsh M, et al. PBMCs reflect the immune component of the WAT transcriptome—Implications as biomarkers of metabolic health in the postprandial state. Mol Nutr Food Res. 2014, 58, 808–20.
72. van der Velpen V, Geelen A, Schouten EG, Hollman PC, Afman LA, van 't Veer P. Estrogen Receptor–Mediated Effects of Isoflavone Supplementation Were Not Observed in Whole-Genome Gene Expression Profiles of Peripheral Blood Mononuclear Cells in Postmenopausal, Equol-Producing Women. J Nutr. 2013, 143, 774–80.
73. Matthews DR, Hosker JR, Rudenski AS, Naylor BA, Treacher DF, Turner RC. Homeostasis model assessment: insulin resistance and fl-cell function from fasting plasma glucose and insulin concentrations in man. Diabetologia. 1985, 28, 412–9.
74. Perseghin G, Caumo A, Caloni M, Testolin G, Luzi L. Incorporation of the Fasting Plasma FFA Concentration into QUICKI Improves Its Association with Insulin Sensitivity in Nonobese Individuals. J Clin Endocrinol Metab. 2001, 86, 4776–81.
75. Baudin J, Hernandez-Baixauli J, Quesada-Vázquez S, Mulero F, Puiggròs F, Arola L, et al. Combined supplementation with hesperidin, phytosterols and curcumin decreases adiposity and improves metabolic health in ovariectomized rats. Food Funct. 2024, 15, 4905–24.
76. Crescenti A, del Bas JM, Arola-Arnal A, Oms-Oliu G, Arola L, Caimari A. Grape seed procyanidins administered at physiological doses to rats during pregnancy and lactation promote lipid oxidation and up-regulate AMPK in the muscle of male offspring in adulthood. J Nutr Biochem. 2015, 26, 912–20.
77. Love MI, Huber W, Anders S. Moderated estimation of fold change and dispersion for RNA-seq data with DESeq2. Genome Biol. 2014, 15, 550.
78. Väremo L, Nielsen J, Nookaew I. Enriching the gene set analysis of genome-wide data by incorporating directionality of gene expression and combining statistical hypotheses and methods. Nucleic Acids Res. 2013, 41, 4378–91.
79. Kolberg L, Raudvere U, Kuzmin I, Adler P, Vilo J, Peterson H. g:Profiler—interoperable web service for functional enrichment analysis and gene identifier mapping (2023 update). Nucleic Acids Res. 2023, 51, W207–12.
80. Wickham H. ggplot2: Elegant Graphics for Data Analysis. Springer-Verlag New York. 2016, 35, 21.

81. Gu Z, Eils R, Schlesner M. Complex heatmaps reveal patterns and correlations in multidimensional genomic data. Bioinformatics. 2016, 32, 2847–9.
82. Finucane FM, Luan J, Wareham NJ, Sharp SJ, O'Rahilly S, Balkau B, et al. Correlation of the leptin:adiponectin ratio with measures of insulin resistance in non-diabetic individuals. Diabetologia. 2009, 52, 2345–9.
83. Gavin KM, Kohrt WM, Klemm DJ, Melanson EL. Modulation of Energy Expenditure by Estrogens and Exercise in Women. Exerc Sport Sci Rev. 2018, 46, 232–9.
84. Lovejoy JC, Champagne CM, de Jonge L, Xie H, Smith SR. Increased visceral fat and decreased energy expenditure during the menopausal transition. Int J Obes. 2008, 32, 949–58.
85. Day DS, Gozansky WS, Van Pelt RE, Schwartz RS, Kohrt WM. Sex Hormone Suppression Reduces Resting Energy Expenditure and β-Adrenergic Support of Resting Energy Expenditure. J Clin Endocrinol Metab. 2005, 90, 3312–7.
86. Frühbeck G, Catalán V, Rodríguez A, Ramírez B, Becerril S, Salvador J, et al. Adiponectin-leptin Ratio is a Functional Biomarker of Adipose Tissue Inflammation. Nutrients. 2019, 11, 454.
87. Frühbeck G, Catalán V, Rodríguez A, Gómez-Ambrosi J. Adiponectin-leptin ratio: A promising index to estimate adipose tissue dysfunction. Relation with obesity-associated cardiometabolic risk. Adipocyte. 2018, 7, 57–62.
88. Hepler C, Bass J. Circadian mechanisms in adipose tissue bioenergetics and plasticity. Genes Dev. 2023, 37, 454–73.
89. Shetty S, Kapoor N, Bondu J, Thomas N, Paul T. Bone turnover markers: Emerging tool in the management of osteoporosis. Indian Journal of Endocrinology and Metabolism. 2016, 20, 846–52.
90. Caimari A, Oliver P, Palou A. Impairment of nutritional regulation of adipose triglyceride lipase expression with age. Int J Obes. 2008, 32, 1193–200.
91. Tanaka A, Node K. Associations of metabolic disorders with hypertension and cardiovascular disease: recent findings and therapeutic perspectives. Hypertens Res. 2024, May 29.
92. Dillard A, Matthan NR, Lichtenstein AH. Use of hamster as a model to study diet-induced atherosclerosis. Nutr Metab (Lond). 2010, 7, 89.
93. Zhang Z, Wang H, Jiao R, Peng C, Wong YM, Yeung VSY, et al. Choosing hamsters but not rats as a model for studying plasma cholesterol-lowering activity of functional foods. Mol Nutr Food Res. 2009, 53, 921–30.
94. Bravo E, Cantafora A, Calcabrinil A, Ortu G. Why prefer the golden Syrian hamster (Mesocricetus auratus) to the Wistar rat in experimental studies on plasma lipoprotein metabolism? Comp. Biochem. Physiol. 1994, 107B, 347–355.
95. Horváthová M, Ilavská S, Štefíková K, Szabová M, Krivošíková Z, Jahnová E, et al. The Cell Surface Markers Expression in Postmenopausal Women and Relation to Obesity and Bone Status. Int J Environ Res Public Health. 2017, 14, 751.
96. Ghosh M, Rodriguez-Garcia M, Wira CR. The immune system in menopause: Pros and cons of hormone therapy. J Steroid Biochem Mol Biol. 2014, 142, 171–5.
97. Cutolo M, Capellino S, Sulli A, Serioli B, Secchi ME, Villaggio B, et al. Estrogens and Autoimmune Diseases. Ann N Y Acad Sci. 2006, 1089, 538–47.
98. Olsen NJ. Gonadal steroids and immunity. Endocr Rev. 1996, 17, 369–84.
99. Saborit-Villarroya I, Del Valle JM, Romero X, Esplugues E, Lauzurica P, Engel P, et al. The Adaptor Protein 3BP2 Binds Human CD244 and Links this Receptor to Vav Signaling, ERK Activation, and NK Cell Killing. J Immunol. 2005, 175, 4226–35.
100. Okamura H, Kashiwamura S ichiro, Tsutsui H, Yoshimoto T, Nakanishi K. Regulation of interferon-γ production by IL-12 and IL-18. Curr Opin Immunol. 1998, 10, 259–64.

101. Hyodo Y, Matsui K, Hayashi N, Tsutsui H, Kashiwamura S ichiro, Yamauchi H, et al. IL-18 Up-Regulates Perforin-Mediated NK Activity Without Increasing Perforin Messenger RNA Expression by Binding to Constitutively Expressed IL-18 Receptor. J Immunol. 1999, 162, 1662–8.
102. Yasuda K, Nakanishi K, Tsutsui H. Interleukin-18 in Health and Disease. Int J Mol Sci. 2019, 20, 649.
103. Kaplanski G. Interleukin-18: Biological properties and role in disease pathogenesis. Immunol Rev. 2018, 281, 138–53.
104. Yoshimoto T, Takeda K, Tanaka T, Ohkusu K, Kashiwamura S ichiro, Okamura H, et al. IL-12 Up-Regulates IL-18 Receptor Expression on T Cells, Th1 Cells, and B Cells: Synergism with IL-18 for IFN-γ Production. J Immunol. 1998, 161, 3400–7.
105. Nakanishi K, Yishimoto T, Tsutsui H, Okamura H. Interleukin-18 is a unique cytokine that stimulates both Th1 and Th2 responses depending on its cytokine milieu. Cytokine Growth Factor Rev. 2001, 12, 53–72.
106. Tsutsui H, Matsui K, Okamura H, Nakanishi K. Pathophysiological roles of interleukin-18 in inflammatory liver diseases. Immunol Rev. 2000, 174, 192–209.
107. Terán-Cabanillas E, Hernández J. Role of Leptin and SOCS3 in Inhibiting the Type I Interferon Response During Obesity. Inflammation. 2017, 40, 58–67.
108. Hamilton KL, Lin L, Wang Y, Knowlton AA. Effect of ovariectomy on cardiac gene expression: inflammation and changes in SOCS gene expression. Physiol Genomics. 2008, 32, 254–63.
109. Wang R, Yu C, Tang Z, Sun J, Wang Y, Zhao Z, et al. Leptin induces altered differentiation of keratinocytes by inducing insulin resistance: implications for metabolic syndrome-induced resistance of psoriatic therapy. J Dermatolog Treat. 2024, 35, 2309305.
110. Emanuelli B, Peraldi P, Filloux C, Chavey C, Freidinger K, Hilton DJ, et al. SOCS-3 Inhibits Insulin Signaling and Is Up-regulated in Response to Tumor Necrosis Factor-α in the Adipose Tissue of Obese Mice. J Biol Chem. 2001, 276, 47944–9.
111. Dharmani M, Kamarulzaman K, Giribabu N, Choy KW, Zuhaida MZ, Aladdin NA, et al. Effect of Marantodes pumilum Blume (Kuntze) var.alata on β-cell function and insulin signaling in ovariectomised diabetic rats. Phytomedicine. 2019, 65, 153101.
112. Min W, Fang P, Huang G, Shi M, Zhang Z. The decline of whole-body glucose metabolism in ovariectomized rats. Exp Gerontol. 2018, 113, 106–12.
113. Sankar P, Zachariah B, Vickneshwaran V, Jacob SE, Sridhar MG. Amelioration of oxidative stress and insulin resistance by soy isoflavones (from Glycine max) in ovariectomized Wistar rats fed with high fat diet: The molecular mechanisms. Exp Gerontol. 2015, 63, 67–75.
114. Vermehren-Schmaedick A, Joshi S, Wagoner W, Norgard MA, Packwood W, Diba P, et al. Grb7 Ablation in Mice Improved Glycemic Control, Enhanced Insulin Signaling, and Increased Abdominal fat Mass in Females. Endocrinology. 2024, 29, 165, 1–15.
115. Kasus-Jacobi A, Béréziat V, Perdereau D, Girard J, Burnol AF. Evidence for an interaction between the insulin receptor and Grb7. A role for two of its binding domains, PIR and SH2. Oncogene. 2000, 19, 2052–9.
116. Shen TL. Grb7 in intracellular signaling and its role in cell regulation. Front Biosci. 2004, 9, 192.
117. Han DC, Shen TL, Guan JL. The Grb7 family proteins: structure, interactions with other signaling molecules and potential cellular functions. Oncogene. 2001, 20, 6315–21.
118. Ciaglia E, Montella F, Lopardo V, Scala P, Ferrario A, Cattaneo M, et al. Circulating BPIFB4 Levels Associate With and Influence the Abundance of Reparative Monocytes and Macrophages in Long Living Individuals. Front Immunol. 2020, 11, 1–8.
119. Montella F, Lopardo V, Cattaneo M, Carrizzo A, Vecchione C, Ciaglia E, et al. Role of BPIFB4 in Immune System and Cardiovascular Disease: the Lesson from Centenarians. Transl Med @ UniSa. 2022, 24, 1–12.

120. Peyton MP, Yang TY, Higgins L, Markowski TW, Murray K, Vue C, et al. Natural aging and ovariectomy induces parallel phosphoproteomic alterations in skeletal muscle of female mice. Aging. 2023, 15, 7362–80.
121. Cintron NS, Toft D. Defining the Requirements for Hsp40 and Hsp70 in the Hsp90 Chaperone Pathway. J Biol Chem. 2006, 281, 26235–44.
122. Kim HY, Hong S. Multi-Faceted Roles of DNAJB Protein in Cancer Metastasis and Clinical Implications. Int J Mol Sci. 2022, 23, 14970.
123. Somu P, Mohanty S, Basavegowda N, Yadav AK, Paul S, Baek KH. The Interplay between Heat Shock Proteins and Cancer Pathogenesis: A Novel Strategy for Cancer Therapeutics. Cancers (Basel). 2024, 16, 638.
124. Tausif YM, Thekkekkara D, Sai TE, Jahagirdar V, Arjun HR, Meheronnisha SK, et al. Heat shock protein paradigms in cancer progression: future therapeutic perspectives. 3 Biotech. 2024, 14, 96.
125. Wang J, Lee J, Liem D, Ping P. HSPA5 Gene encoding Hsp70 chaperone BiP in the endoplasmic reticulum. Gene. 2017, 618, 14–23.
126. Zuehlke AD, Beebe K, Neckers L, Prince T. Regulation and function of the human HSP90AA1 gene. Gene. 2015, 570, 8–16.
127. Mozar F, Sharma V, Gorityala S, Albert JM, Xu Y, Montano MM. Downregulation of Dihydrotestosterone and Estradiol Levels by HEXIM1. Endocrinology. 2022, 163, 1–13.
128. Wittmann BM, Wang N, Montano MM. Identification of a novel inhibitor of breast cell growth that is down-regulated by estrogens and decreased in breast tumors. Cancer Res. 2003, 63, 5151–8.
129. Ogba N, Chaplin LJ, Doughman YQ, Fujinaga K, Montano MM. HEXIM1 Regulates 17β-Estradiol/Estrogen Receptor-α–Mediated Expression of Cyclin D1 in Mammary Cells via Modulation of P-TEFb. Cancer Res. 2008, 68, 7015–24.
130. Thomas C, Gustafsson JÅ. Progesterone receptor-estrogen receptor crosstalk: a novel insight. Trends Endocrinol Metab. 2015, 26, 453–4.
131. Tang PZ, Gannon MJ, Andrew A, Miller D. Evidence for oestrogenic regulation of heat shock protein expression in human endometrium and steroid-responsive cell lines. Eur J Endocrinol. 1995, 133, 598–605.
132. Tofovic PS, Zhang X, Petrusevska G. Progesterone inhibits vascular remodeling and attenuates monocrotaline-induced pulmonary hypertension in estrogen-deficient rats. Prilozi. 2009, 30, 25–44.
133. Ranjan M, Lee O, Cottone G, Mirzaei Mehrabad E, Spike BT, Zeng Z, et al. Progesterone receptor antagonists reverse stem cell expansion and the paracrine effectors of progesterone action in the mouse mammary gland. Breast Cancer Res. 2021, 23, 78.
134. Brännström M, Janson PO. Progesterone is a Mediator in the Ovulatory Process of the in Vitro-Perfused Rat Ovary1. Biol Reprod. 1989, 40, 1170–8.
135. Meijs Roelofs HMA, De Greef WJ, Uilenbroek Th. JJ. Plasma progesterone and its relationship to serum gonadotrophins in immature female rats. J Endocrinol. 1975, 64, 329–36.
136. Barengolts EI, Gajardo HF, Rosol TJ, D'Anza JJ, Pena M, Botsis J, et al. Effects of progesterone on postovariectomy bone loss in aged rats. J Bone Miner Res. 1990, 5, 1143–7.
137. Han C, Xie K, Yang C, Zhang F, Liang Q, Lan C, et al. HA15 alleviates bone loss in ovariectomy-induced osteoporosis by targeting HSPA5. Exp Cell Res. 2021, 406, 112781.
138. Bao Z, Liu ZQ, He PY, Adali J, Yang YC, Wulasihan M. 17B-Estradiol Regulates Adenosine Triphosphate-Binding Cassette Transporters a1 Expression Via Estrogen Receptor A To Increase Macrophage Cholesterol Efflux. J Physiol Pharmacol. 2023, 74, 527–36.
139. Darabi M, Rabbani M, Ani M, Zarean E, Panjehpour M, Movahedian A. Increased

leukocyte ABCA1 gene expression in post-menopausal women on hormone replacement therapy. Gynecol Endocrinol. 2011, 27, 701–5.
140. Rodriguez-Agudo D, Malacrida L, Kakiyama G, Sparrer T, Fortes C, Maceyka M, et al. StarD5: an ER stress protein regulates plasma membrane and intracellular cholesterol homeostasis. J Lipid Res. 2019, 60, 1087–98.
141. Kakiyama G, Minoiwa K, Bai-Kamara N, Hashiguchi T, Pandak WM, Rodriguez-Agudo D. StarD5 levels of expression correlate with onset and progression of steatosis and liver fibrosis. Am J Physiol Liver Physiol. 2024, 326, G747–61.
142. Hendrix S, Zelcer N. A new SPRING in lipid metabolism. Curr Opin Lipidol. 2023, 34, 201–7.
143. Loregger A, Raaben M, Nieuwenhuis J, Tan JME, Jae LT, van den Hengel LG, et al. Haploid genetic screens identify SPRING/C12ORF49 as a determinant of SREBP signaling and cholesterol metabolism. Nat Commun. 2020, 11, 1128.
144. Aregger M, Lawson KA, Billmann M, Costanzo M, Tong AHY, Chan K, et al. Systematic mapping of genetic interactions for de novo fatty acid synthesis identifies C12orf49 as a regulator of lipid metabolism. Nat Metab. 2020, 2, 499–513.
145. Bayraktar EC, La K, Karpman K, Unlu G, Ozerdem C, Ritter DJ, et al. Metabolic coessentiality mapping identifies C12orf49 as a regulator of SREBP processing and cholesterol metabolism. Nat Metab. 2020, 2, 487–98.
146. Horton JD, Goldstein JL, Brown MS. SREBPs: activators of the complete program of cholesterol and fatty acid synthesis in the liver. J Clin Invest. 2002, 109, 1125–31.
147. Alswat KA. Gender Disparities in Osteoporosis. J Clin Med Res. 2017, 9, 382–7.
148. MacFarlane EG, Haupt J, Dietz HC, Shore EM. TGF-β Family Signaling in Connective Tissue and Skeletal Diseases. Cold Spring Harb Perspect Biol. 2017, 9, a022269.
149. Jann J, Gascon S, Roux S, Faucheux N. Influence of the TGF-β Superfamily on Osteoclasts/Osteoblasts Balance in Physiological and Pathological Bone Conditions. Int J Mol Sci. 2020, 21, 7597.
150. Gao L, Li Y, Yang YJ, Zhang DY. The Effect of Moderate-Intensity Treadmill Exercise on Bone Mass and the Transcription of Peripheral Blood Mononuclear Cells in Ovariectomized Rats. Front Physiol. 2021, 12, 1–11.
151. Zhou Y, Deng HW, Shen H. Circulating monocytes: an appropriate model for bone-related study. Osteoporos Int. 2015, 26, 2561–72.
152. Pacifici R, Brown C, Puscheck E, Friedrich E, Slatopolsky E, Maggio D, et al. Effect of surgical menopause and estrogen replacement on cytokine release from human blood mononuclear cells. Proc Natl Acad Sci. 1991, 88, 5134–8.
153. Del Pino J, Martin-Gomez E, Martin-Rodriguez M, Lopez-Sosa C, Cordero M, Lanchares JL, et al. Influence of sex, age, and menopause in serum osteocalcin (BGP) levels. Maturitas. 1992, 15, 160–1.
154. Shinkov AD, Borissova AMI, Kovatcheva RD, Atanassova lliana B, Vlahov JD, Dakovska LN. Age and Menopausal Status Affect Osteoprotegerin and Osteocalcin Levels in Women Differently, Irrespective of Thyroid Function. Clin Med Insights Endocrinol Diabetes. 2014, 7, CMED.S15466.
155. Semeghini MS, Scalize PH, Coelho MC, Fernandes RR, Pitol DL, Tavares MS, et al. Lycopene prevents bone loss in ovariectomized rats and increases the number of osteocytes and osteoblasts. J Anat. 2022, 241, 729–40.
156. Ren L, Zhu X, Tan J, Lv X, Wang J, Hua F. MiR-210 promotes bone formation in ovariectomized rats by regulating osteogenic/adipogenic differentiation of bone marrow mesenchymal stem cells through downregulation of EPHA2. J Orthop Surg Res. 2023, 18, 811.
157. Vargas-Sanchez PK, Fernandes RR, Furlaneto FAC, Sousa LG De, Siéssere S, Bombonato-Prado KF. Osteoporosis Affects Functional Activity and Gene Expression of Osteoblastic Cells Derived from Rat Alveolar Bone. Braz Dent J. 2020, 31, 617–22.
158. Young MF, Bi Y, Ameye L, Chen XD. Biglycan knockout mice: New models for musculoskeletal diseases. Glycoconj J. 2002, 19, 257–62.

159. Li L, Chen X, Lv S, Dong M, Zhang L, Tu J, et al. Influence of Exercise on Bone Remodeling-Related Hormones and Cytokines in Ovariectomized Rats: A Model of Postmenopausal Osteoporosis. PLoS One. 2014, 9, e112845.
160. Gregory LS, Kelly WL, Reid RC, Fairlie DP, Forwood MR. Inhibitors of cyclo-oxygenase-2 and secretory phospholipase A2 preserve bone architecture following ovariectomy in adult rats. Bone. 2006, 39, 134–42.

Abbreviations

17β-E2, 17β-oestradiol; ANOVA, analysis of variance; BMC, bone mineral content; BMD, bone mineral density; CRP, C-reactive protein; CTX-1, carboxy-terminal telopeptide of type I collagen; CVD, cardiovascular diseases; DGE, differential gene expression; EE, energy expenditure; ER, oestrogen receptor; FDR, false discovery rate; GSH, glutathione; GSSG, oxidized glutathione; HDL-c, high-density lipoprotein cholesterol; HOMA-IR, homeostasis model assessment-estimated insulin resistance; HSPs, heat shock proteins; HRT, hormone replacement therapy; IWAT, inguinal white adipose tissue; IR, insulin resistance; KEGG, Kyoto Encyclopaedia of Genes and Genomes; LDL, low-density lipoprotein; MetS, metabolic syndrome; microCT/ μCT, three-dimensional microcomputed tomography; MWAT, mesenteric white adipose tissue; NEFAs, nonesterified fatty acids; NGS, next-generation sequencing; non-HDL-c, non-high-density lipoprotein cholesterol; OC, osteocalcin; OVX, ovariectomized rats; PBMCs, peripheral blood mononuclear cells; PINP, procollagen I amino-terminal propeptide; PR, progesterone receptor; R-QUICKI, revised quantitative insulin sensitivity check index; RIN, RNA integrity number; RQ, respiratory quotient; RWAT, retroperitoneal white adipose tissue; SHAM, sham-operated rats; TC, total cholesterol; TG, triglycerides; WAT, white adipose tissue.

MANUSCRIPT 3

Combined supplementation with hesperidin, phytosterols and curcumin decreases adiposity and improves metabolic health in ovariectomized rats

Julio Baudin,[a,b] Julia Hernandez-Baixauli,[a#] Sergio Quesada-Vázquez,[a$] Francisca Mulero,[c] Francesc Puiggròs,[d] Lluís Arola,[b] Antoni Caimari [d]

[a] Eurecat, Centre Tecnològic de Catalunya, Technological Unit of Nutrition and Health, 43204 Reus, Spain

[b] Nutrigenomics Research Group, Department of Biochemistry and Biotechnology, Universitat Rovira i Virgili, 43007 Tarragona, Spain

[c] Molecular Imaging Unit, Spanish National Cancer Research Centre (CNIO), Madrid, Spain

[d] Eurecat, Centre Tecnològic de Catalunya, Biotechnology Area, 43204 Reus, Spain.

[#] Present address: Laboratory of Metabolism and Obesity, Vall d'Hebron-Institut de Recerca, Universitat Autònoma de Barcelona, Barcelona, Spain

[$] Present address: Liver Vascular Biology Research Group, IDIBAPS Biomedical Research Institute, CIBEREHD, University of Barcelona, Spain

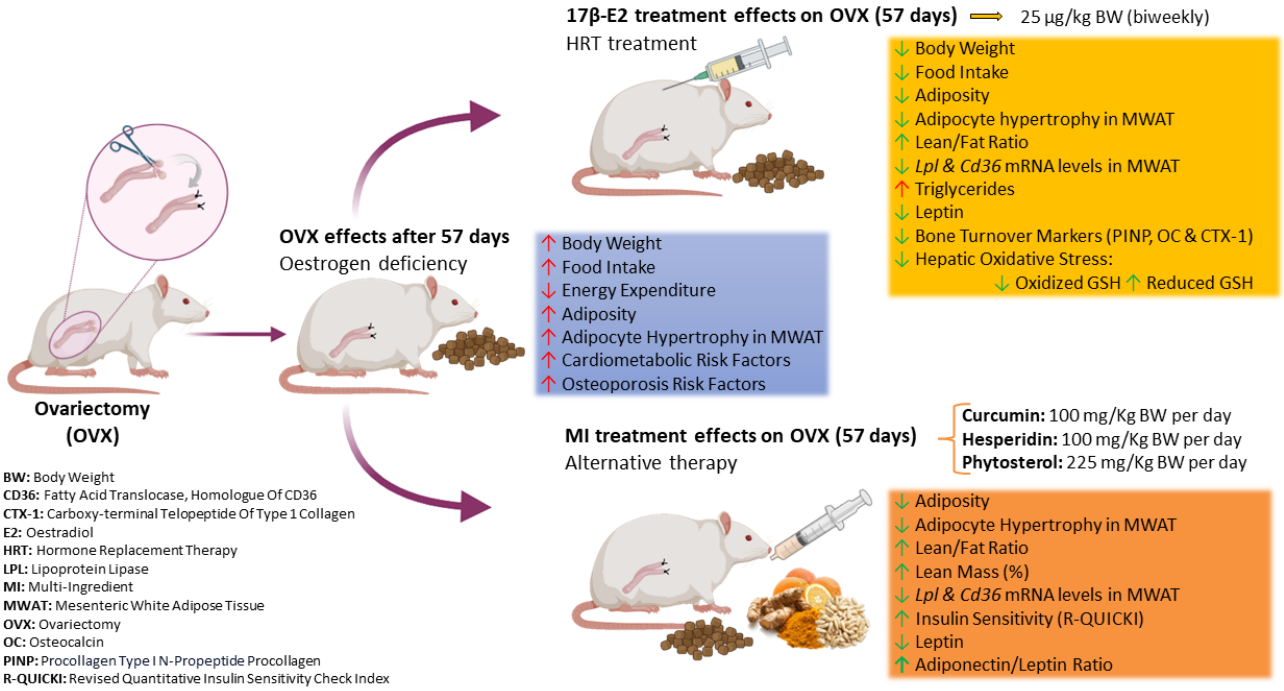
Published, *FOOD AND FUNCTIONS 2024, DOI: 10.1039/D3FO05122F*

ABSTRACT

In recent years many women have looked for alternative therapies to address menopause. Hesperidin, phytosterols and curcumin are bioactive compounds that can ameliorate some cardiovascular risk factors associated with menopause, although there are no data concerning the effects of their combined supplementation. We used ovariectomized (OVX) rats, a postmenopausal model with oestrogen deficiency, to evaluate whether supplementation with a multi-ingredient (MI) including hesperidin, phytosterols and curcumin for 57 days would display beneficial effects against fat mass accretion and metabolic disturbances associated with menopause. Twenty OVX rats were orally supplemented with either MI (OVX-MI) or vehicle (OVX). Furthermore, 10 OVX rats orally received the vehicle along with subcutaneous injections of 17β-oestradiol biweekly (OVX-E2), whereas 10 rats were sham operated and received oral and injected vehicles (control group; SH). MI supplementation partly counteracted the fat mass accretion observed in OVX animals, which was evidenced by decreased total fat mass, adiposity index, the weight of retroperitoneal, inguinal and mesenteric white adipose tissue (MWAT) depots and MWAT adipocyte hypertrophy. These effects were accompanied by a significant decrease in the circulating levels of leptin and the mRNA levels of the fatty acid uptake-related genes *Lpl* and *Cd36* in MWAT. These results were very similar to those observed in OVX-E2 animals. OVX-MI rats also displayed a higher lean body mass, lean/fat mass ratio, adiponectin-to-leptin ratio and insulin sensitivity than their OVX counterparts. Our findings can pave the way for using this MI formulation as an alternative therapy to manage obesity and to improve the cardiometabolic health of menopausal women.

Key words: Hesperidin, phytosterols, curcumin, nutraceuticals, menopause, obesity, cardiometabolic health, complementary and alternative therapies

[1] **Running title.** Multi-ingredient supplementation and menopause-related alterations.



Graphical abstract

INTRODUCTION

Menopause is a biological stage in a woman's life that is defined as the permanent cessation of menstrual cycles by reproductive aging. The decline and gradual cessation of oestrogen production by loss of ovarian follicular activity and function[1] occurring during the menopausal transition and menopause can cause a variety of vasomotor symptoms, such as hot flushes, sleep disturbances and night sweats.[2–4] In addition, this aging process may be associated with osteoporosis,[5] increased body weight and a change in body fat distribution from a gynoid to an android pattern, contributing to increased abdominal fat accretion.[6–8] This excess of adiposity can exacerbate the appearance of metabolic alterations such as hypercholesterolemia, hypertension and insulin resistance, increasing the risk of suffering cardiovascular diseases (CVDs),[6–10] which become more evident with age and are one of the leading causes of death worldwide, accounting for 47% of deaths in women.[11]

Hormone replacement therapy (HRT) prescription remains the most effective solution for symptoms or metabolic disturbances related to the postmenopausal state. Nevertheless, HRT prescription was challenged by the controversy over its benefits and risks derived from the unexpected findings of Women's Health Initiative (WHI) study in 2002, pointing towards a higher risk of suffering CVDs and endometrial and breast cancers for some of the HRT treatments.[12] Currently, the safety and main side effects depend on the type of HRT, the duration of the treatment and the woman's age at which the HRT starts after the final menstrual period occurs. Thus, it was described that the benefits are higher than the risks when HRT is prescribed to healthy women under 60 or within the first ten years of menopause.[12] HRT effectively reduces vasomotor symptoms and osteoporosis.[12] However, HRT has been shown to be less effective (favourable or neutral effects) in ameliorating body weight gain and reducing the risk of CVDs (coronary heart disease, thromboembolism, blood clots and stroke) and affective disorders such as dementia or Alzheimer's disease, and it is not advised for women with a medical history of breast or endometrial cancers.[12]

In recent years, due to controversy about the risks associated with HRT, many women have looked for alternative therapies to address menopause. Some supplements, such as natural extracts, bioactive compounds and nutraceuticals, have been used as alternative therapies to manage vasomotor symptoms and metabolic disturbances related to menopausal state. One of the best-known natural bioactive compounds with scientific evidence-based effects is the isoflavones obtained from soy, also called phytoestrogens, with genistein being the most abundant of them, accounting for 60% of the total isoflavones found in soy.[13] Phytoestrogens are chemically similar to 17β-oestradiol (17β-E2), and they have been extensively studied due to their ability to bind to oestrogen receptors, producing oestrogenic effects in target organs. Genistein has twenty times more

selectivity for oestrogen receptor (ER) β than for α, which is a favourable property because most of the side effects are produced through binding to ER-α.[13,14] Nevertheless, there are many types of phytoestrogens, and their activity in humans seems to vary between subjects because specific intestinal bacteria and/or individual-based hepatic modifications are needed to convert a precursor into a more active compound. As an example, only 30% of the population is able to convert daidzein, a well-studied phytoestrogen of soy, to the most bioactive and absorbable isoform, called equol diadzein.[15]

Curcumin, hesperidin and phytosterols are other bioactive compounds from natural origin with promising effects against metabolic-related disturbances associated with menopause, although the body of scientific evidence about their effects is lower when compared to what is reported for phytoestrogens. Curcumin is a polyphenol obtained from *Curcuma longa* (turmeric) powdered roots commonly used as part of curry powder in curry dishes and displays well-known antioxidant and anti-inflammatory properties.[16] In humans, curcumin also improves metabolic health by decreasing the surrogated marker of insulin resistance homeostasis model assessment-estimated insulin resistance (HOMA-IR).[17] Additionally, in ovariectomized (OVX) rats, a well-established preclinical model to study menopause in which the ovaries are surgically removed to mimic the deficiency of circulating oestrogen levels occurring in menopause and the associated osteoporosis and metabolic disorders,[18–21] curcumin supplementation ameliorated progressive bone loss and osteoporosis.[22] Furthermore, Morrone et al. demonstrated that this bioactive compound displayed an anti-hypercholesterolaemic effect and reduced oxidative stress and visceral adiposity in this animal model.[23]

Hesperidin is a flavonoid mainly present in citrus fruits (oranges, tangerines, lemons, limes, and grapefruits), in the juices obtained from these fruits. This bioactive compound

has shown protective effects in humans on the cardiovascular system because, despite its low bioavailability, it is able to modulate and reduce several biomarkers of risk factors for CVDs, such as triglycerides (TG), total cholesterol (TC), LDL-cholesterol, TNF-α, systolic blood pressure and insulin.[24–26] Furthermore, mounting evidence suggests that hesperidin supplementation exerts an inhibitory effect against obesity, modulating lipid metabolism,[27] and beneficial effects on bone metabolism[28] were also reported in OVX rats, improving their bone mineral density (BMD).[29,30] Recently, members of our group demonstrated, in humans, that supplementation with a hesperidin extract mainly rich in the 2S isomer and presented in a micronized form (M2SH) increased the bioavailability of this flavanone,[31] paving the way for carrying out additional studies to evaluate whether this boosted bioavailability is translated into enhanced cardioprotective effects.

Phytosterols are phytosteroids that present a similar structure to cholesterol and that are naturally present in considerable amounts in pistachios and in oils obtained from rapeseed, wheat germ and corn, whilst legumes, cereals, fruits, and vegetables contain lower quantities. The mechanism of action of ingested phytosterols, due to their similar structure, produces a competitive exclusion of cholesterol from bile acid micelles in the intestinal tract, which reduces intestinal cholesterol reabsorption. Phytosterol supplementation is supported by the European Food Safety Authority (EFSA), which concluded that the consumption of approximately 1.5 to 2.4 g per day of phytosterols and/or stanols may reduce circulating cholesterol levels in the blood and decrease the risk of coronary heart disease.[32] Xia et al. 2022 demonstrated that in postmenopausal women, consuming 2 g per day phytosterols reduced serum TC and LDL-cholesterol.[33]

Although supplementation with curcumin, hesperidin and phytosterol separately exert potential beneficial effects against fat mass accretion and/or menopausal-related metabolic alterations, mainly in animal models, to the best of our knowledge, the effects

of combined supplementation with these three bioactive compounds have not yet been evaluated. Different studies, including some carried out by our research group,[34–37] have shown that the combined administration of different bioactive compounds acting against complementary targets is a suitable strategy to tackle fatty liver and cardiometabolic risk factors. In line with the idea that better outcomes can be obtained when treatments are performed under a multifaceted approach,[38] we hypothesized that a multi-ingredient (MI) supplement based on the combined supplementation of curcumin, hesperidin and pine-tree phytosterols could be an effective approach to ameliorate the multifactorial alterations related to the postmenopausal state. The aim of this study was to evaluate, in an OVX rat model, whether oral supplementation for 8 weeks with an MI supplement including hesperidin (M2SH), phytosterols and curcumin would exert beneficial effects against fat mass accretion, metabolic alterations and osteoporosis associated with menopause. The effects of this MI were compared to those produced by the administration of 17β-E2, an agent that resembles HRT, in the treatment of menopause symptoms and associated diseases.

MATERIALS AND METHODS

Ingredients

Lipophytol®-P (PHY; ref no.: LI0056) was kindly supplied by Lipotec S.A.U. (Gavà, Spain). This PHY is a dispersible form of microencapsulated pine tree phytosterols that facilitates their incorporation in food matrices. According to the supplier, the product contains 88% phytosterols and 10% maltodextrin.

Curcumin (CUR; ref no.: EXT-887) is a lipophilic polyphenol [7-bis(4-hydroxy-3-methoxyphenyl)hepta-1,6-diene-3,5-dione] that was provided by NUTRIFOODS S.L.U.

(Barcelona, Spain). According to the supplier, the total curcuminoid content of the dry extract was ≥95%.

Micronized 2S-hesperidin (M2SH; Cardiose®; ref no.: 1306615) was obtained from sweet orange extract (*Citrus sinensis*) and was kindly provided by HealthTech BioActives –HTBA– (Murcia, Spain). According to the supplier, the S-isomer content of this flavanone was 93%.

Animals, diet and treatments

All procedures related to animal experimentation were approved by the Animal Ethics Committee of the Technological Unit of Nutrition and Health of Eurecat (Reus, Spain) and the Generalitat de Catalunya (protocol code 11223). The study complied with the ARRIVE guidelines, followed the 'Principles of Laboratory Animal Care' and was carried out in accordance with the EU Directive 2010/63/EU for animal experiments.

The animals used in this study were forty 12-week-old female Sprague-Dawley rats (ENVIGO, Indianapolis, USA). Thirty rats were bilaterally ovariectomized (OVX), and 10 rats were sham-operated (SH) at the ENVIGO facilities. The animals were fed a maintenance rat chow diet for 3 weeks to stabilize them after ovariectomy, before shipment at 15 weeks of age. At their arrival at the animal facility of Eurecat and during the whole study, rats were housed in pairs at 22 °C under a 12 h light/dark cycle (lights on at 9:00 am) and had *ad libitum* access to food and water. After an adaptation period of 1 week, the 30 OVX rats were distributed into three experimental groups depending on the treatment received for 8 weeks (OVX; OVX-E2; OVX-MI; n = 10 per group), and the 10 sham-operated (SH; n = 10) rats were assigned as the control group. OVX-MI was supplemented daily for 8 weeks with MI, which included three products at the following doses per body weight: PHY at 225 mg kg−1; CUR at 100 mg kg−1; and M2SH at 100

mg kg−1. The three bioactive compounds were dissolved together in low-fat condensed milk diluted 1 : 3 with water. Taking into account the content of each bioactive compound present in each ingredient, the doses of PHY, CUR and M2SH used were equivalent to the daily consumption of 1926 mg of phytosterols, 924 mg of curcumin and 905 mg of hesperidin for a 60 kg human.[39] These dosages are considered acceptable and safe in the context of multi-ingredient supplementation.[26,32,40,41] The SH, OVX and OVX-E2 groups were also supplemented daily with low-fat condensed milk, which was diluted 1 : 3 with water (vehicle), for 8 weeks. Both treatments (in a volume of 0.5–0.6 mL) were administered orally by a 1 mL syringe at the same time each day (between 09:00 and 10:00 am). Five days before the beginning of the treatments, the rats were trained to lick diluted low-fat condensed milk (0.3 mL) to ensure voluntary consumption. Each rat fully ingested the daily dose of the corresponding treatment. OVX-E2 rats also received biweekly subcutaneous injections of 25 μg kg−1 17β-E2 (Sigma-Aldrich, St Louis, MO) via a carrier solution of corn oil, whereas the remaining groups received the same dose of a vehicle (corn oil).

All groups were fed a standard chow diet (Teklad Global 14% Protein Rodent Diet 2014, Harlan, Barcelona, Spain). The caloric breakdown of the diet (2.9 kcal g^{-1}) was 20% protein, 13% fat, and 67% carbohydrates. Body weight was recorded once each week, food was renewed daily, and the food intake was documented every 7 days.

On day 57, rats were sacrificed under anaesthesia (pentobarbital sodium, 60 mg per kg body weight) after 6 h of diurnal fasting. Blood was collected by cardiac puncture, and serum was obtained by centrifugation and stored at −80 °C until analysis. The liver, caecum, kidneys, gastrocnemius and soleus muscle, the femur of the left leg and the white adipose tissue depots (retroperitoneal – RWAT–, mesenteric – MWAT– and inguinal – IWAT – white adipose tissue depots) were rapidly removed, weighed, frozen in liquid

nitrogen and stored at −70 °C until further analysis. The femur of the right leg was also collected and immersed in physiological serum and frozen at −20 °C until three-dimensional microcomputed tomography analysis.

Body composition analyses

Lean and fat mass measurements (in grams) were performed without anaesthesia at the beginning and at the end of the study using an EchoMRI-700™ device (Echo Medical Systems, L.L.C., Houston, USA). The measurements were performed in triplicate under *ad libitum* conditions and at 8:00 am, and the results were expressed as a percentage of body weight.

Adiposity index

The adiposity index was calculated as the sum of the weights of the IWAT, MWAT and RWAT depot weights (in grams) and was expressed as a percentage of body weight.

HOMA-IR and R-QUICKI analyses

The HOMA-IR was calculated using the following formula: (fasting glucose level – mmol L^{-1} × fasting insulin level – μU mL^{-1})/22.5.[42] Insulin sensitivity was evaluated by the revised quantitative insulin sensitivity check index (R-QUICKI) using the following formula: 1/[log insulin (μU mL^{-1}) + log glucose (mg dL^{-1}) + log FFA (mmol l^{-1})].[43]

Serum analysis

Enzymatic colorimetric kits were used to determine serum TC (995280/QCA, Barcelona, Spain), HDL-cholesterol (HDL-c) and VLDL-cholesterol + LDL-cholesterol (VLDL-c + LDL-c) (EHDL-100/Bioassay Systems, California, USA), triglycerides (992330/QCA, Barcelona, Spain), glucose (992330/QCA, Barcelona, Spain) and nonesterified free fatty acids (NEFAs) (WAKO, Neuss, Germany). To analyse the levels of 17β-E2 at baseline

and progesterone at the end point, the ELISA E2 kit (CSB-E05110r/CUSABIO, Houston, USA) and the ELISA progesterone kit (CSB-E07282r/CUSABIO Houston, USA) were used, respectively. Circulating insulin levels were measured using a rat/mouse ELISA kit (10-1250-01/MERCODIA, Upssala, Sweden). Serum leptin levels were determined with a rat ELISA kit (EZRL-83K/Millipore, Barcelona, Spain), and serum adiponectin levels were quantified by a Rat Total Adiponectin/Acrp30 Quantikine ELISA kit (RRP300/R&D systems, Minnesota, USA). To quantify the circulating levels of the biomarkers of bone turnover procollagen I amino-terminal propeptide (PINP), osteocalcin (OC) and carboxy-terminal telopeptide of type I collagen (CTX-1), the PINP ELISA kit (AC-33F1, IDS, UK), the osteocalcin ELISA kit (AC-12F1, IDS, UK) and the CTX-1 (AC-06F1, IDS, UK) were used, respectively.

Oral glucose tolerance test (OGTT)

On day 43, rats were submitted to 6 h of diurnal fasting (from 08:00 am to 02:00 pm). Afterwards, blood was collected from the saphenous vein (baseline point; time 0), and immediately after, the rats were challenged with 2 g per kg body weight of glucose loaded by oral gavage. Blood samples were also collected at 15, 30, 60 and 120 minutes after the glucose load. Glucose and insulin levels at all time-points were analysed using the same kits included in the previous section.

Microcomputed tomography analyses

The bone composition of the right femur was determined postmortem by three-dimensional microcomputed tomography (μCT or microCT) analysis. For this purpose, the samples were immersed in physiological serum and frozen at −20 °C. Afterwards, femur samples were fixed in 10% neutral buffered formalin. Comparable regions of interest (ROIs) consisting of the superior epiphysis, the diaphysis and the inferior

epiphysis from each rat were selected for analysis. Imaging by three-dimensional microcomputed tomography was performed with a CompaCT scanner (SEDECAL, Madrid, Spain). Data were acquired with 720 projections per 360-degree scan, an integration time of 100 ms with three frames, a photon energy of 50 keV, and a current of 100 μA. The duration of the imaging time was 20 min per scan. Three-dimensional rendered images of femur samples were generated through original volumetric reconstructed images by MicroView software (GE Healthcare). The tissue mineral content (TMC), bone mineral content (BMC), tissue mineral density (TMD) and BMD values were quantified from MicroCT scans using GE MicroView software v2.2. These bone composition results were calculated as the sum of the three ROIs selected for each right femur in nine rats per group.

Indirect calorimetry and activity measurements

These analyses were performed between days 37 and 42 after the beginning of the treatments using the Oxylet Pro™ System (PANLAB, Cornellà, Spain), under ad libitum conditions and with free access to water, over a period of 22 h (from 11.00 am to 09.00 am). At 09:00 am, the rats received the corresponding treatment at 09:00 am and were transferred from their cages to an acrylic box (Oxylet LE 1305 Physiocage, PANLAB). After an initial acclimatization period of 2 h, the energy expenditure (EE), respiratory quotient (RQ), fat and carbohydrate oxidation rates, locomotor activity, and number of rearings were calculated as previously described.[44]

Analysis of total, oxidized and reduced glutathione in liver (GSH/GSSG)

Total glutathione (GSH), reduced GSH and oxidized GSH (GSSG) were analysed in the liver samples with the commercial glutathione colorimetric detection kit

(EIAGSHC/INVITROGEN; Massachusetts, USA). The results are expressed as µmol g^{-1} of hepatic protein, which was calculated using the BCA assay method.

Histological analysis

Fixed portions of MWAT (n = 8 per group) were preserved in buffered formalin (4% formaldehyde, 4 g L^{-1} NaH_2PO_4, 6.5 g L^{-1} Na_2HPO_4; pH 6.8) were cut at a thickness of 5 µm and stained with haematoxylin & eosin (H & E). MWAT images (magnification 100×) were taken with a microscope (ECLIPSE Ti; Nikon, Tokyo, Japan) and coupled to a digital sight camera (DS-Ri1, Nikon). Image analyses were performed using the ImageJ NDPI software (National Institutes of Health, Bethesda, MD, USA; https://imagej.nih.gov/ij, accessed on 22 February 2024, version 1.54 g). Adipocyte area quantification in the MWAT sections of the different groups was analysed using the Adiposoft plugin.

Gene expression analysis

RNA extraction, cDNA synthesis, and gene expression analyses using real-time quantitative PCR from MWAT were performed as previously described,[44] using primers for the different genes obtained from Biomers.net (Ulm, Germany) and included in ESI Table 1.† Each PCR was performed at least in duplicate, and hypoxanthine guanine phosphoribosyl transferase (*Hprt*) and peptidylprolyl isomerase A (*Ppia*) were used as reference genes.

Statistical analyses

Statistical analyses were performed with IBM SPSS Statistics 28.0 (SPSS, IBM Corp. Armonk, New York, USA). Grubbs' test was used to detect outliers, which were discarded for further analysis. The assumption of normality was determined using the

Kolmogorov–Smirnov test, and the homoscedasticity among groups was evaluated using Levene's test. When one or both of these conditions were not accomplished, data were transformed to base-10 logarithm to obtain a normal distribution and/or similar variances before statistical testing. One-way ANOVA followed by Duncan's *post hoc* test (p value ≤ 0.05) was used to assess differences among the four groups in most of the variables analysed in the present study. Welch's test followed by Games–Howell's *post hoc* test was used when homoscedasticity was not assumed. The Kruskal–Wallis test followed by the Mann–Whitney U *post hoc* test was used as the nonparametric version of one-way ANOVA when the data did not follow a normal distribution. Linear relationships between key variables were tested using Pearson's correlation coefficients. Differences among groups in the circulating levels of glucose and insulin during the OGTT were analysed by repeated measures (RM-) ANOVA with time as a within-subject factor and intervention as a between-subject factor. Overall differences among groups in the area under the curve (AUC) analysis, which was calculated for the circulating levels of glucose and insulin at all study time points with the trapezoid rule using GraphPad Prism software (GraphPad Software, Inc., La Joya, CA, USA), were assessed using one-way ANOVA and Duncan's *post hoc* tests. The Mann–Whitney U *post hoc t* test was used for single statistical comparisons of oestrogen levels at baseline between the SH group (n = 10) and OVX rats (n = 30). Student's t test was also used for some single statistical comparisons to detect residual differences. Data are presented as the means ± SEM (n = 9–10). The level of statistical significance was set at bilateral 5%.

RESULTS

Ovariectomy induced oestrogen deficiency, fat mass accretion and metabolic alterations related to the postmenopausal state

After 3 weeks of recovery from surgery, before the beginning of the treatments, the efficacy of ovariectomy was evaluated by analysing the circulating levels of 17β-E2. As expected, the OVX rats displayed significantly lower levels of this hormone than their sham-operated counterparts (467 ± 124 pg mL^{-1} *vs.* 183 ± 49 pg mL^{-1}; 60.8% lower, p = 0.005, Mann–Whitney U *post hoc t* test).[45]

Compared to the sham operation performed in SH rats, the removal of the ovaries in the OVX group increased food intake (Table 1) and decreased EE (Fig. 1), which accounted for the higher body weight, weight gain, fat mass percentage, MWAT and IWAT weight, adiposity index and adipocyte hypertrophy in MWAT in comparison with their SH counterparts (Table 1 and Fig. 2). Furthermore, OVX animals also showed higher cholesterol and monocyte chemoattractant protein-1 (MCP-1) circulating levels (Table 1) and a lower hepatic GSH/GSSG ratio than SH animals (Table 2). Altogether, these results indicate that OVX rats developed hallmarks of cardiometabolic alterations that can occur in the postmenopausal state, as was previously reported.[46] In addition, compared with SH rats, the OVX animals showed increased circulating levels of the bone biomarkers OC and CTX-1 (for formation and resorption activity, respectively) analysed in serum (Table 3), which accounted for an increased risk of osteoporosis.[47]

Table 1: Biometric parameters, cumulative food intake, serum parameters in sham-operated (SH) and ovariectomized (OVX) rats after 8 weeks of intervention

	SHAM	**OVX**	**OVX-E2**	**OVX-MI**	**Intervention effect (*p* value)**
Cumulative food intake (g)	94.9 ± 1.2^{a}	108.4 ± 3.3^{b}	92.9 ± 2.9^{a}	106.4 ± 1.6^{b}	*I* (<0.001)
Biometric parameters					
Initial body weight (g)	245 ± 3^{a}	297 ± 5^{b}	289 ± 6^{b}	292 ± 3^{b}	*I* (<0.001)
Final body weight (g)	264 ± 4^{a}	329 ± 8^{b}	285 ± 5^{c}	323 ± 6^{b}	*I* (<0.001)
Body weight gain (g)	18.5 ± 3.5^{a}	35.1 ± 3.5^{b}	-4.8 ± 3.2^{c}	30.6 ± 4.7^{b}	*I* (<0.001)
Final fat mass (%)	4.55 ± 0.40^{a}	8.63 ± 0.57^{b}	6.09 ± 0.70^{a}	6.02 ± 0.32^{a}	*I* (<0.001)
Fat mass gain (g)	0.2 ± 0.9^{a}	12.5 ± 1.1^{b}	2.7 ± 0.6^{a}	8.6 ± 0.6^{c}	*I* (<0.001)
Final lean mass (%)	88.3 ± 0.4^{a}	84.6 ± 0.6^{b}	85.9 ± 0.8^{ab}	87.0 ± 0.3^{a}	*I* (<0.001)
Lean/fat mass ratio	21.6 ± 2.0^{a}	10.3 ± 0.9^{b}	15.8 ± 1.7^{c}	14.7 ± 0.8^{c}	*I* (<0.001)
Final total body water (%)	73.1 ± 0.3^{a}	70.2 ± 0.5^{b}	71.2 ± 0.7^{b}	72.5 ± 0.5^{ab}	*I* (<0.001)
Liver (g)	6.91 ± 0.19	7.59 ± 0.29	7.72 ± 0.32	7.52 ± 0.16	NS (0.109)
Caecum (g)	2.80 ± 0.29	3.18 ± 0.13	3.51 ± 0.25	3.43 ± 0.15	NS (0.122)
Kidneys (g)	1.39 ± 0.03	1.47 ± 0.04	1.50 ± 0.04	1.42 ± 0.03	NS (0.175)
Gastrocnemius (g)	1.88 ± 0.06^{a}	2.29 ± 0.06^{b}	2.07 ± 0.11^{ab}	2.18 ± 0.06^{b}	*I* (0.007)
Soleus (g)	0.11 ± 0.00^{a}	0.14 ± 0.01^{b}	0.13 ± 0.01^{b}	0.14 ± 0.01^{b}	*I* (0.006)
Serum parameters					
TG (mmol L^{-1})	0.48 ± 0.06^{a}	0.41 ± 0.06^{a}	0.89 ± 0.12^{b}	0.46 ± 0.02^{a}	*I* (<0.001)
MCP-1 (ng mL^{-1})	6403 ± 328^{a}	9373 ± 844^{b}	9119 ± 1274^{ab}	9969 ± 850^{b}	*I* (0.040)
TC (mmol L^{-1})	2.38 ± 0.09^{a}	2.90 ± 0.07^{bc}	2.62 ± 0.10^{ab}	3.06 ± 0.16^{c}	*I* (<0.001)
HDL-c (mmol L^{-1})	1.64 ± 0.09^{a}	1.98 ± 0.08^{b}	1.56 ± 0.06^{a}	2.16 ± 0.12^{b}	*I* (<0.001)
VLDL-c+LDL-c (mmol L^{-1})	0.81 ± 0.05	0.91 ± 0.03	0.91 ± 0.06	0.81 ± 0.03	NS (0.193)
Progesterone (pg mL^{-1})	159 ± 18	101 ± 8	116 ± 30	109 ± 10	NS (0.144)

Data are given as the mean ± SEM (n = 9–10). Body weight gain was calculated as the difference between the final body weight and the initial body weight. Fat mass gain was calculated as the difference between fat mass at the end of the experiment and the baseline point. Fat mass and lean mass weights (%) were calculated according to the formula (100 × fat or lean/body weight) and were expressed as a percentage of body weight. The lean/fat mass ratio was calculated as the lean mass divided by fat mass. The concentrations of serum parameters were determined at the end of the experiment. Different superscript lowercase letters (a, b, c) indicate significant different mean values (one-way ANOVA and Duncan's *post hoc* test. Welch test and Games-Howell *post hoc* test or Kruskal–Wallis test and Mann–Whitney U *post hoc* test, $p < 0.05$). *I*: the effect of intervention. NS: non-significant differences. SH: sham-operated rats; OVX: ovariectomized rats; OVX-E2: OVX rats treated with 17β-oestradiol; OVX-MI: OVX rats supplemented with the multi-ingredient; TG: triglycerides; MCP-1: monocyte chemoattractant protein-1; TC: total cholesterol; HDL-c: high-density lipoprotein cholesterol; VLDL-c: very-low-density lipoprotein cholesterol; LDL-c: low-density lipoprotein cholesterol.

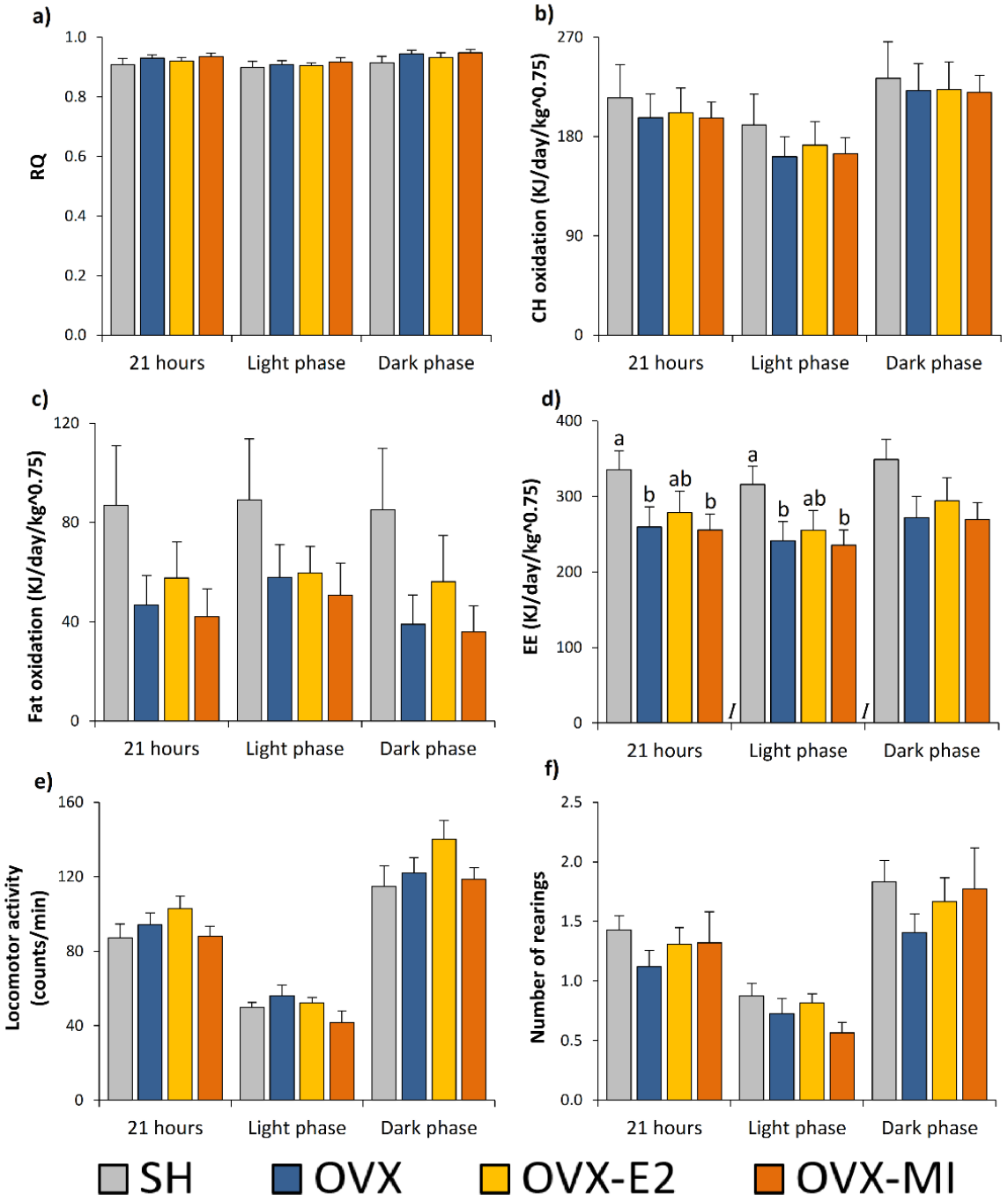


Fig. 1 Effects of ovariectomy, 17β-E2 injections and MI treatment on respiratory quotient (a), carbohydrate oxidation (b), fat oxidation (c), EE (d), spontaneous locomotor activity (e) and number of rearings (f) in sham-operated (SH) and ovariectomized (OVX) rats between days 37 and 42 after the beginning of the treatments. Indirect calorimetric measurements were performed between days 37 and 42 under *ad libitum* conditions and over 22 h (from 11:00 am to 09:00 am). The data obtained during the first hour were discarded for final analyses. All rats were fed a standard chow diet during the measurements. Data are given as the mean ± SEM (n = 9–10). In Fig. 1d, different superscript lowercase letters (a, b) indicate significantly different mean values among groups (Kruskal–Wallis test and Mann–Whitney U *post hoc* test, $p < 0.05$). *I*: effect of intervention. SH: sham-operated rats, OVX: ovariectomized rats, OVX-E2: OVX rats treated with 17β-oestradiol, OVX-MI: OVX rats supplemented with the multi-ingredient. RQ: respiratory quotient; EE: energy expenditure.

MI and 17β-E2 treatments decreased adiposity and adipocyte hypertrophy and promoted a healthier body composition

As expected, 17β-E2 administration significantly reduced the final body weight compared to the OVX animals and fully counteracted the increase in body weight gain observed in the OVX group (Table 1).[48] These results could be attributed, at least in part, to the lower cumulative food intake observed in the OVX-E2 animals in comparison with their OVX counterparts (Table 1).[45] MI supplementation did not attenuate the increase in body weight and body weight gain observed in OVX animals (Table 1). This lack of effect could be partly related to the similar food intake observed in the OVX-MI rats compared to the OVX group (Table 1). Remarkably, the rats that received the MI supplement or 17β-E2 showed, at the end point, a significant decrease in fat mass compared to the OVX group (Table 1). These results agree with the significant decrease in the weight of all the white adipose tissues analysed (MWAT, RWAT and IWAT, Fig. 2a–c) as well as with the lower adiposity index observed in both the OVX-MI and OVX-E2 groups in comparison with their OVX counterparts (Fig. 2d). Consequently, both the OVX-MI and OVX-E2 groups displayed a significantly lower total fat mass gain than the OVX animals (Table 1). This effect was more evident in the OVX-E2 group, which showed similar levels of fat accretion to those observed in the SH animals (Table 1). Both MI supplementation and 17β-E2 injections fully counteracted the increased MWAT average adipocyte area observed in the OVX group, showing very similar values to those observed in SH rats (Fig. 2e). An inverse pattern was reported for the number of adipocytes, which were significantly lower in the OVX group compared to the other three groups (Fig. 2f). In agreement with these results, representative MWAT histological images (H & E staining) illustrated larger adipocytes and a lower number of these cells in the OVX group (Fig. 2h) than in their SH (Fig. 2g), OVX-E2 (Fig. 2i) and OVX-MI (Fig. 2j) counterparts.

Furthermore, a decrease in the percentage of larger adipocytes and an increase of smaller adipocytes were found in the MWAT of both OVX-MI and OVX-E2 animals when compared to the OVX group, showing both groups of treated rats a very similar pattern to those observed in control SH animals (Fig. 2k). Remarkably, OVX-MI rats showed a higher lean mass than OVX animals (Table 1). In line with this result, the OVX-MI group also displayed an increased lean/fat mass ratio in comparison with their OVX counterparts. Although no significant changes were found in the lean mass at the end point in the animals that received 17β-E2 (Table 1), they also displayed a significant increase in the lean/fat mass ratio when compared to the OVX group, similar to what was observed in response to MI administration (Table 1). In addition, both the OVX and OVX-E2 groups showed a significant reduction in the final total body water when compared to the SH animals, while no significant changes were found between the OVX-MI group and their SH counterparts (Table 1).

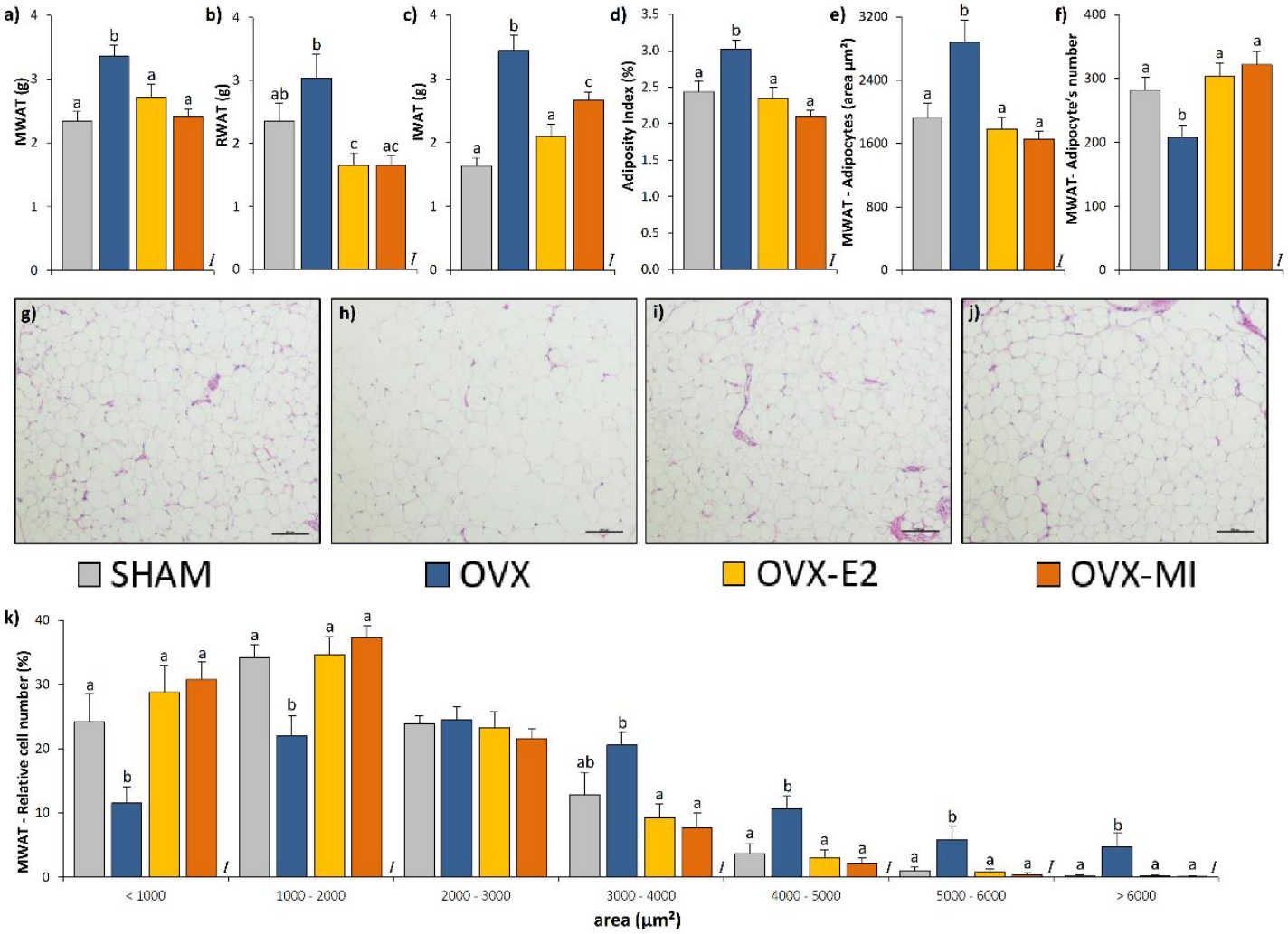


Fig. 2 Effects of ovariectomy, 17β-E2 injections and MI treatment on MWAT (a), RWAT (b), and IWAT (c) depot weights, adiposity index (d), adipocyte's area (e), adipocyte's number (f), representative micrographs of hematoxylin–eosin stained MWAT sections (bar = 100 µm) from SHAM, OVX, OVX-E2 and OVX-MI groups (g–j, respectively) and adipocyte's size distribution (k) in sham-operated (SH) and ovariectomized (OVX) rats after 8 weeks of intervention. Data are given as the mean ± SEM (n = 9–10). The adiposity index was computed as the sum of the IWAT, MWAT and RWAT depot weights (in grams) and is expressed as a percentage of body weight. In each figure, different superscript lowercase letters (a, b, c) indicate significantly different mean values among groups (one-way ANOVA and Duncan's *post hoc* test or Kruskal–Wallis test and Mann–Whitney *U post hoc* test, $p < 0.05$). *I*: effect of intervention. SH: sham-operated rats, OVX: ovariectomized rats, OVX-E2: OVX rats treated with 17β-oestradiol, OVX-MI: OVX rats supplemented with the multi-ingredient. MWAT: mesenteric white adipose tissue; RWAT: retroperitoneal white adipose tissue; IWAT: inguinal white adipose tissue.

MI supplementation decreased the circulating levels of leptin and increased the circulating levels of adiponectin corrected by the WAT weight and adiponectin-to-leptin ratio

In agreement with the lower final fat accretion and adiposity index shown in both groups in comparison with their OVX counterparts (Table 1 and Fig. 2d), both the OVX-E2 and

OVX-MI groups showed a significant decrease in the circulating levels of leptin (Fig. 3a). Although no significant changes among groups were found in the circulating levels of adiponectin (Fig. 3b), the animals supplemented with the MI displayed a significant increase in the circulating adiponectin per g WAT ratio (Fig. 3c) as well as a higher adiponectin-to-leptin (AL) ratio than their OVX counterparts (Fig. 3d). These significant effects were not observed in response to 17β-E2 treatment (Fig. 3c and d).

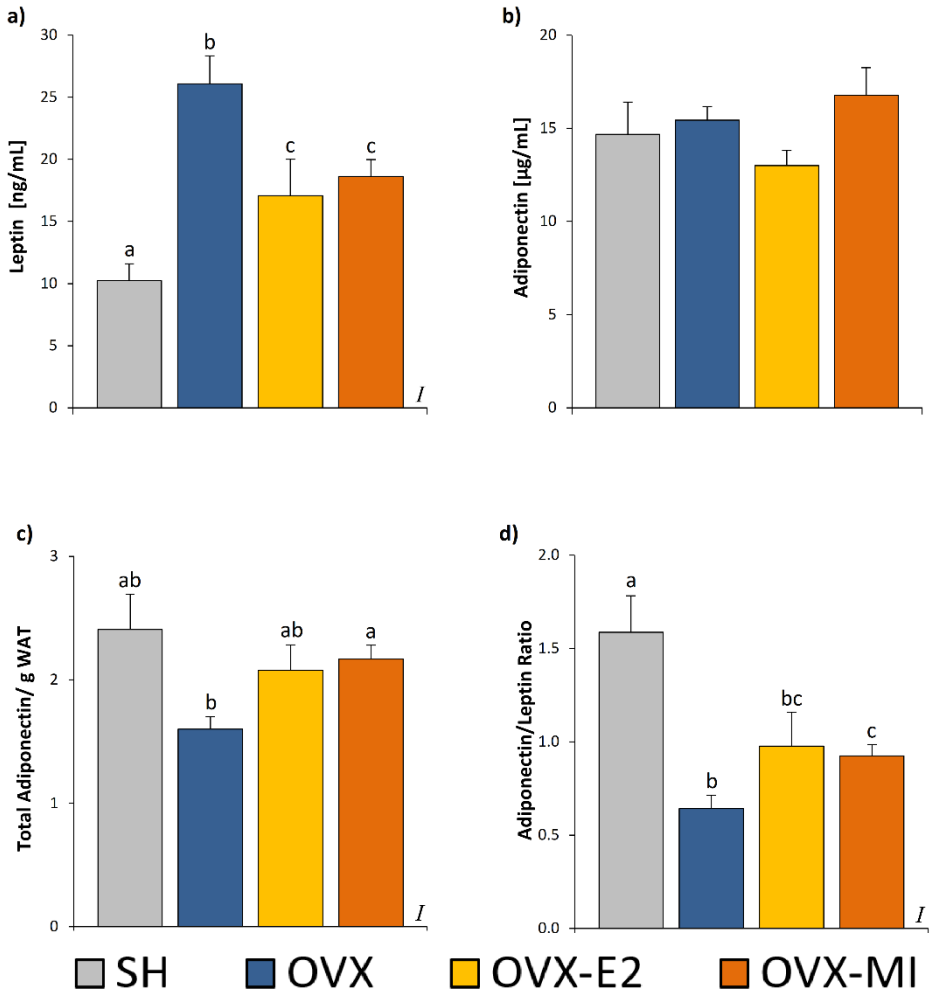


Fig. 3 Circulating levels of leptin (a), adiponectin (b), total adiponectin per g WAT (c) and adiponectin/leptin ratio (d) in sham-operated (SH) and ovariectomized (OVX) rats after 8 weeks of intervention. Data are given as the mean ± SEM (n = 9–10). The ratio of total adiponectin per g WAT was computed as the quotient between the circulating levels of total adiponectin and the sum of the IWAT, MWAT and RWAT depot weights. In the figures, different superscript lowercase letters (a, b, c) indicate significantly different mean values among groups (one-way ANOVA and Duncan's *post hoc* test, Welch test and Games-Howell *post hoc* test or Kruskal–Wallis test and Mann–Whitney *U post hoc* test, $p < 0.05$). *I*: effect of intervention. SH: sham-operated rats, OVX: ovariectomized rats, OVX-E2: OVX rats treated with 17β-oestradiol, OVX-MI: OVX rats supplemented with the multi-ingredient. MWAT: mesenteric white adipose tissue; RWAT: retroperitoneal white adipose tissue; IWAT: inguinal white adipose tissue.

MI intake improved the surrogate marker of insulin sensitivity R-QUICKI

OVX rats displayed similar serum levels of glucose and insulin at baseline and after the glucose load in comparison with their SH counterparts (Fig. 4a and b, respectively). The OGTT performed on day 43 also revealed that neither 17β-E2 injections nor MI supplementation produced significant changes in the circulating levels of glucose and insulin when compared to those in the OVX group (Fig. 4a and b, respectively). No changes among groups were found in the circulating levels of glucose and NEFAs at the endpoint of the study, 57 days after the beginning of the different treatments (Fig. 4c and e, respectively). However, 17β-E2 injections significantly increased the insulin levels and the surrogate marker of insulin resistance HOMA-IR in comparison with their SH and OVX-MI counterparts at the end point (Fig. 4d and f, respectively). Although no significant changes were found either in insulin levels or HOMA-IR among the SH, OVX and OVX-MI groups under one-way ANOVA, MI intervention for 57 days residually decreased HOMA-IR (26.3% lower, $p = 0.043$ *versus* OVX rats, Student's *t* test) and circulating insulin levels (27.5% lower, $p = 0.084$ *versus* OVX rats, Student's *t* test) and produced a significant increase in the R-QUICKI value compared to that in the OVX and OVX-E2 animals, which suggests an improvement in insulin sensitivity (Fig. 4g). In contrast, the OVX-E2 group displayed a significant decrease in R-QUICKI in comparison with the SH and OVX-MI animals (Fig. 4g).

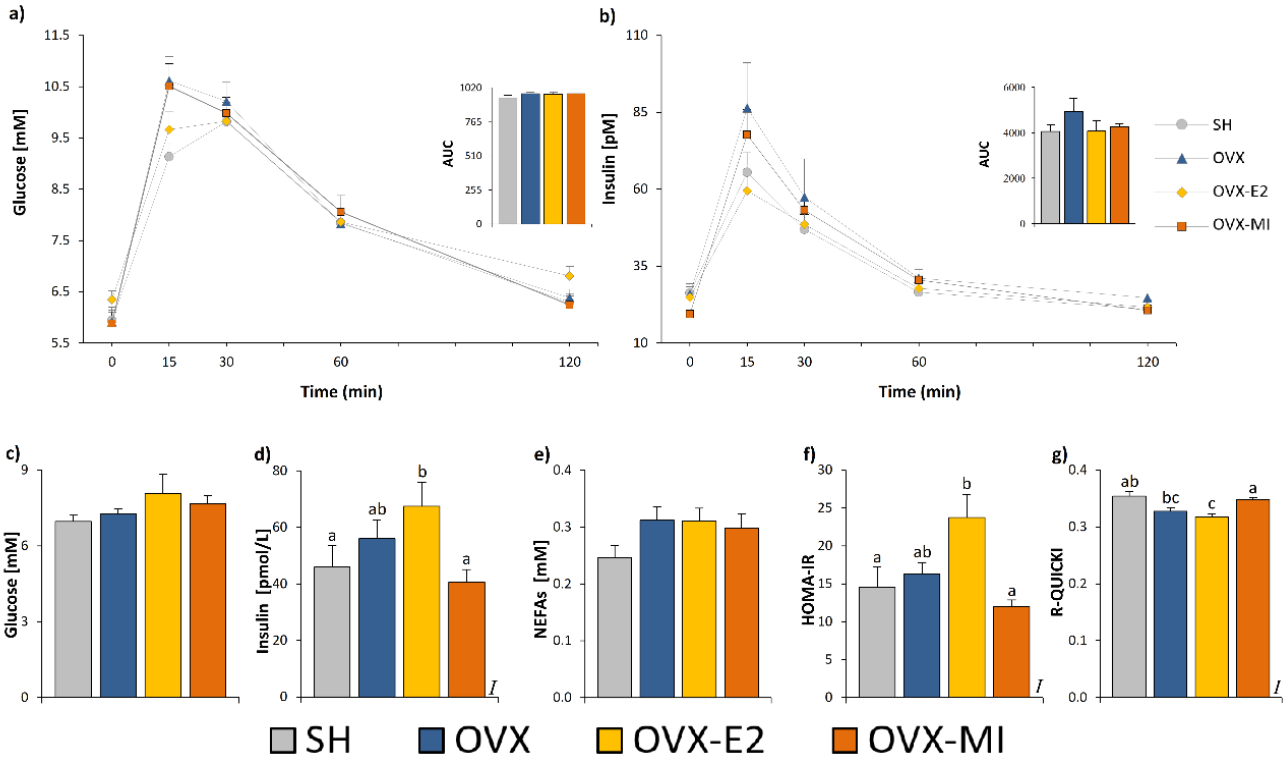


Fig. 4 Serum levels of glucose (a) and insulin (b) performed on day 43 after an OGTT (2 g kg^{-1} of body weight) and glucose (c), insulin (d), NEFAs (e), HOMA-IR (f), and R-QUICKI (g) at the end of the study in sham-operated (SH) and ovariectomized (OVX) rats after 8 weeks of intervention. The integrated area under the curve (AUC) was determined for glucose and insulin circulating levels using GraphPad Prism software (GraphPad Software, Inc., La Joya, CA, USA). Glucose (c), insulin (d), NEFAs (e), HOMA-IR (f) and R-QUICKI (g) at the end of the study are also shown. Data are given as the mean ± SEM (n = 9–10). In Fig. 4a and b, the statistical comparisons among groups were conducted using RM-ANOVA or two-way ANOVA, $p < 0.05$. In Fig. 4c–g, different superscript lowercase letters (a, b, c) indicate significantly different mean values among groups (one-way ANOVA and Duncan's *post hoc* test, Welch test and Games-Howell *post hoc* test or Kruskal–Wallis test and Mann–Whitney *U post hoc* test, $p < 0.05$). *I*: effect of intervention. SH: sham-operated rats, OVX: ovariectomized rats, OVX-E2: OVX rats treated with 17β-oestradiol, OVX-MI: OVX rats supplemented with the multi-ingredient. HOMA-IR: homeostasis model assessment-estimated insulin resistance; NEFAs: nonesterified fatty acids; R-QUICKI: revised quantitative insulin sensitivity check index.

MI and 17β-E2 treatments did not enhance energy expenditure, substrate oxidation or locomotor activity

No significant changes were found in RQ among the groups (Fig. 1a). Consequently, no changes in carbohydrate and fat oxidation were reported (Fig. 1b and c, respectively). Both the OVX and OVX-MI groups showed a significant decrease in EE when compared to their SH counterparts, considering both the whole period of 21 hours and the light phase (Fig. 1d). A similar pattern was observed for the animals that received 17β-E2, although the differences were not statistically significant when compared to the SH

animals (Fig. 1d). There was a strong positive correlation between EE and fat oxidation ($r = 0.659$, $p < 0.001$), which was not found between EE and the oxidation of carbohydrates. This result suggests that the decreased EE found in the OVX groups compared to their SH counterparts was mainly due to their lower fat oxidation. The decreased EE observed in the OVX and OVX-MI animals cannot be attributed to lower locomotor activity since no changes were found either in this parameter (Fig. 1e) or in the number of rearings (Fig. 1f).

MI supplementation did not produce the deleterious effects on HDL-c and TG observed in response to 17β-E2 treatment

17β-E2 injections residually decreased the circulating levels of TC ($p = 0.043$ *versus* OVX rats, Student's *t* test), although the differences between these two groups were not statistically significant according to one-way ANOVA (Table 1). This result was mainly explained by the significant decrease in HDL-c serum levels observed in OVX-E2 animals compared to their OVX counterparts (Table 1). MI intake fully counteracted the decrease in HDL-c reported in OVX-E2 rats (Table 1). Furthermore, MI supplementation slightly decreased the VLDL-c + LDL-c serum cholesterol levels in comparison with OVX rats, although the differences were not statistically significant (11% decrease; $p = 0.055$ *versus* OVX animals, Student's *t* test) (Table 1). In addition, the circulating TG levels in serum were significantly higher in OVX-E2 rats than in their OVX-MI counterparts (Table 1).

17β-E2 treatment increased hepatic GSH levels

Significantly higher hepatic levels of total and reduced GSH were observed in OVX-E2 rats than in OVX and OVX-MI rats, attaining numerically higher levels in OVX-E2 animals than in their SH counterparts (Table 2). Although no changes among groups were

found in oxidized GSH (Table 2), the animals treated with oestrogens also displayed a significant increase in the GSH/GSSG ratio, showing similar levels of this parameter as the SH rats (Table 2).

Table 2: Hepatic GSH levels in sham-operated (SH) and ovariectomized (OVX) rats after 8 weeks of intervention

	SHAM	OVX	OVX-E2	OVX-MI	Intervention effect (p value)
Hepatic parameters					
Total GSH (µmol g protein^{-1})	46.2 ± 9.9^{ab}	22.9 ± 3.7^{a}	65.6 ± 9.7^{b}	25.7 ± 4.9^{a}	*I* (0.010)
Reduced GSH (µmol g protein^{-1})	39.1 ± 9.9^{ab}	17.5 ± 2.9^{a}	57.4 ± 9.8^{b}	15.0 ± 1.4^{a}	*I* (0.001)
Oxidized GSH (µmol g protein^{-1})	7.08 ± 0.74	8.09 ± 0.95	8.21 ± 0.74	8.85 ± 0.53	NS (0.456)
GSH/GSSG Ratio	6.27 ± 1.96^{a}	2.03 ± 0.40^{b}	7.88 ± 1.62^{a}	1.74 ± 0.20^{b}	*I* (0.004)

Data are given as the mean ± SEM (n = 9-10). GSSG/GSH ratio was calculated as the oxidized GSH divided by reduced GSH. Different superscript lowercase letters (a, b) indicate significant different mean values (one-way ANOVA and Duncan's *post hoc* test, Welch test and Games–Howell *post hoc* test or Kruskal–Wallis test and Mann–Whitney U *post hoc* test, $p < 0.05$). *I:* effect of intervention. NS: non-significant differences. SH: Sham-operated rats; OVX: Ovariectomized rats; OVX-E2: OVX rats treated with 17β-oestradiol; OVX-MI: OVX rats supplemented with the Multi-Ingredient. GSH: glutathione; GSSG: oxidized glutathione.

17β-E2 injections fully counteracted the increase in biochemical markers of bone turnover induced by ovariectomy

The OVX and OVX-MI groups showed an increase in femur weight (Table 3) compared to that in SH and OVX-E2 animals. No significant changes were found in femur length, BMD, BMC or TMC among the groups (Table 3). Nevertheless, the OVX-E2 group displayed a significant increase in TMD when compared to their OVX counterparts (Table 3). 17β-E2 administration counteracted the increase observed in the OVX animals concerning the circulating levels of the biomarkers of bone formation and resorption activity, OC and CTX-1, an effect that was not observed after MI supplementation (Table 3). In addition, OVX-E2 animals showed a significant decrease in the circulating levels of PINP, a biomarker of bone formation, in comparison with both the SH and OVX groups (Table 3).

Table 3: Bone-related parameters in sham-operated (SH) and ovariectomized (OVX) rats after 8 weeks of intervention

	SHAM	OVX	OVX-E2	OVX-MI	Intervention effect (p value)
Biometric parameters					
Femurs (g)	1.95 ± 0.02^{a}	2.13 ± 0.06^{b}	1.93 ± 0.06^{a}	2.16 ± 0.06^{b}	*I* (0.004)
Femurs (cm)	3.73 ± 0.04	3.81 ± 0.03	3.66 ± 0.05	3.78 ± 0.04	NS (0.068)
Serum parameters					
OC (ng mL^{-1})	292 ± 11^{a}	377 ± 16^{b}	255 ± 13^{a}	410± 27^{b}	*I* (<0.001)
CTX-1 (ng mL^{-1})	14.9 ± 1.4^{a}	20.7 ± 1.2^{b}	12.7 ± 0.9^{a}	18.2 ± 2.3^{ab}	*I* (0.004)
PINP (ng mL^{-1})	5.85 ± 0.27^{a}	6.38 ± 0.40^{a}	4.45 ± 0.45^{b}	6.16 ± 0.86^{ab}	*I* (0.039)
Microcomputed tomography analyses					
BMD (mg cc^{-1})	634 ± 16	618 ± 21	666 ± 19	623 ± 11	NS (0.209)
TMD (µg cc^{-1})	19.3 ± 0.5^{ab}	18.3 ± 1.0^{a}	21.2 ± 0.9^{b}	19.1 ± 0.5^{ab}	*I* (0.044)
BMC (mg)	569 ± 5	591 ± 16	547 ± 12	570 ± 9	NS (0.065)
TMC (µg)	11.96 ± 0.06	11.94 ± 0.05	12.14 ± 0.05	11.95 ± 0.09	NS (0.099)

Data are given as the mean ± SEM (n = 9-10). The circulating levels of the biomarkers of bone turnover in serum were determined at the end of the experiment. Microcomputed tomography analyses in femur were quantified from MicroCT scans using GE MicroView software v2.2. Different superscript lowercase letters (a, b) indicate significant different mean values (one-way ANOVA and Duncan's *post hoc* test, Welch test and Games–Howell *post hoc* test or Kruskal–Wallis test and Mann–Whitney U *post hoc* test, $p < 0.05$). *I:* effect of intervention. NS: non-significant differences. SH: Sham-operated rats; OVX: Ovariectomized rats; OVX-E2: OVX rats treated with 17β-oestradiol; OVX-MI: OVX rats supplemented with the Multi- Ingredient; OC: osteocalcin; CTX-1: carboxy-terminal telopeptide of type I collagen; PINP: procollagen I amino-terminal propeptide; BMD: bone mineral density; TMD: tissue mineral density; BMC: bone mineral content; TMC: tissue mineral content.

Both MI and 17β-E2 treatments led to a downregulation of genes associated with fatty acid uptake in MWAT

The mRNA levels of the key genes involved in lipid uptake, *Lpl* and *Cd36*, were significantly upregulated in the MWAT of the OVX group compared to their control SH counterparts (Fig. 5a). Supplementation with MI and treatment with oestradiol fully counteracted this increase (Fig. 5a). Furthermore, regarding the expression levels of *Acc1*, a gene involved in fatty acid synthesis, the 17β-E2 group exhibited higher mRNA levels of *Acc1* compared to their OVX counterparts and displayed similar expression levels of this gene to what was observed in the SH group (Fig. 5a). Compared to their OVX counterparts, the OVX-MI and OVX-E2 groups showed no changes in the expression levels of the key genes related to lipogenesis (*Fas*), lipolysis (*Atgl* and *Hsl*), β-oxidation (*Cpt1b* and *Had*) and insulin signalling (*Insr* and *Irs1*) (Fig. 5a). The mRNA levels

of *Cd36* and *Lpl* showed a strong positive correlation (r = 0.722, 95% CI = 0.523–0.846, $p < 0.0001$) (Fig. 5b). Furthermore, MWAT weight was also positively correlated with *Lpl* gene expression values in this tissue (r = 0.494, 95% CI = 0.207–0.703, p = 0.002) (Fig. 5c). Although no significant changes were found among the four groups in the mRNA levels of the master regulator of adipogenesis and adipose tissue function,[49] *Cebpa*, 17β-E2 injections residually decreased the expression levels of this gene in comparison with the OVX animals (27.1% decrease; p = 0.026, Student's t test) (Fig. 5a). Furthermore, a very similar pattern of expression was observed for the pro-inflammatory gene *Emr1*, which encodes the F4/80 antigen, a marker of M1 classical activated macrophages,[50] in both OVX-E2 (22.6% lower; p = 0.038 *versus* OVX animals, Student's t test) and OVX-MI (32.0% lower; p = 0.027 *versus* OVX animals, Student's t test), suggesting a slight anti-inflammatory effect of both treatments in MWAT (Fig. 5a).

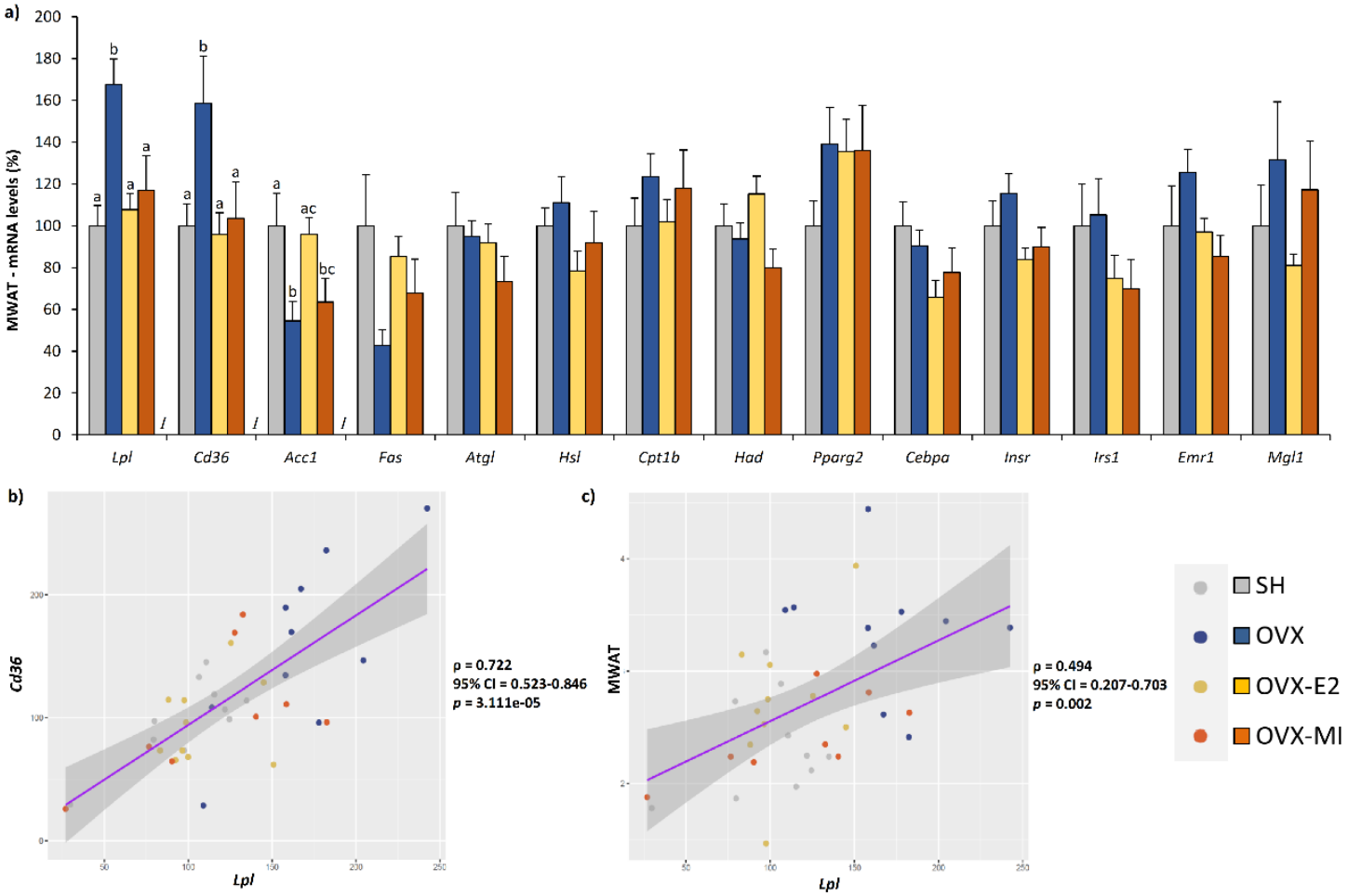


Fig. 5 The mRNA expression levels of genes related to lipid metabolism in sham-operated (SH) and ovariectomized (OVX) rats after 8 weeks of intervention (a). Data are given as the mean ± SEM (n = 9–10). In each figure, different superscript lowercase letters (a, b, c) indicate significantly different mean values among groups (one-way ANOVA and Duncan's *post hoc* test, $p < 0.05$). *I*: effect of intervention. Correlation between *Lpl* and *Cd36* expression levels of genes (b) or MWAT weight (c) in sham-operated (SH) and ovariectomized (OVX) rats after 8 weeks of intervention. The continuous line represents the least-squares regression fit, and the shaded area shows the confidence intervals. The Pearson correlation coefficient (ρ) and its confidence intervals are presented together with the p value of the correlation analysis. *Acc1*: acetyl CoA carboxylase 1; *Atgl*: adipose triglyceride lipase; *Cd36*: fatty acid translocase: homologue of CD36; *Cebpa*: CCAAT/enhancer binding protein alpha; *Cpt1b*: carnitine palmitoyltransferase 1 beta; *Emr1*: EGF-like module containing, mucin-like, hormone receptor-like 1; *Fas*: fatty acid synthase; *Had*: hydroxyacyl-CoA dehydrogenase; *Hprt*: hypoxanthine guanine phosphoribosyl transferase; *Hsl*: hormone-sensitive lipase; *Insr*: insulin receptor; *Irs1*: insulin receptor substrate 1; Lpl: lipoprotein lipase; *Mgl1*: C-type lectin domain family 10, member A; *Pparg2*: peroxisome proliferator-activated receptor gamma 2; *Ppia*: peptidylprolyl isomerase A.

DISCUSSION

Recently, there has been increasing interest in finding therapies that are alternative or complementary to HRT in order to address undesired menopausal symptoms and associated metabolic disorders. In this regard, several lines of research suggest that the intake of hesperidin, phytosterols and curcumin may be beneficial for the management of these complications. Nevertheless, no studies thus far have elucidated whether, in

agreement with our hypothesis that more healthy effects can be obtained using ingredients acting against complementary targets, the combined supplementation of these three bioactive compounds can be a potential alternative therapy to address menopause. In this research, we found oral treatment with a MI supplement, including curcuminoids, phytosterols and hesperidin, for 57 days was able to exert beneficial effects against obesity, and metabolic alterations were observed in a preclinical model of a postmenopausal state with oestrogen deficiency, namely, OVX rats, including (1) decreased fat mass accretion, (2) diminished adipocyte size and promoted a shift towards decreased number of large adipocytes and increased number of small adipocytes in MWAT, (3) downregulated mRNA levels of key genes involved in fatty acid uptake from the bloodstream (*Lpl* and *Cd36*) in MWAT, (4) enhanced lean body mass and lean/fat mass ratio, (5) increased the AL ratio and (6) an improved R-QUICKI value, the surrogate marker for insulin sensitivity. These results confirmed our hypothesis, and interestingly, most of them were very similar or even superior to what we reported in response to 17β-E2 administration.

Many women at menopause experience changes in body composition and body fat redistribution, particularly fat accretion in the abdominal region, which could lead to the appearance of metabolic disturbances, increasing the risk of metabolic syndrome (MetS) and CVDs.[6,7] These effects are more pronounced in women who are overweight or obese prior to reaching the postmenopausal state.[6] The lower adiposity observed in OVX-MI rats that were supplemented with the MI when compared to their OVX counterparts demonstrated herein could be attributed, at first glance, to the protective effect against obesity that has been previously reported for different polyphenols, including curcumin and hesperidin, and, to a lesser extent, for phytosterols, in both animal models and humans.[23,24,27,51,52] Nevertheless, to the best of our knowledge, there are few data

available concerning the anti-obesity effects of these 3 bioactive compounds administered alone or in combination in OVX rodent models. In this regard, only one study has demonstrated that the oral supplementation of curcumin for 30 days significantly decreases intestinal adiposity accumulation in OVX rats.[23] The protective effects of hesperidin and phytosterols orally administered to OVX rodents against fat accretion have not previously been reported. Several studies have demonstrated that the significant body weight gain and progressive fat accretion in different body areas occurring in menopausal and postmenopausal women can be related to a decreased EE.[53–55] This effect and a significant increase in food intake were observed in the present study in OVX rats, one of the best characterized and described animal models to resemble postmenopausal women, when compared to their SH counterparts. In the present study, it was plausible to speculate that supplementation with MI could partly counteract fat mass gain through the enhancement of EE and the inhibition of food intake, two very well-reported mechanisms by which different bioactive compounds can exert this beneficial effect.[54] In this regard, Receno *et al.* showed that the prolonged intake of curcumin in aged male F344Xbn rats decreased food intake.[56] Curcumin was also able to enhance EE and to stimulate thermogenesis efficiently by enhancing the activity of AMP-activated protein kinase (AMPK) and increasing ATP production.[57,58] Nevertheless, the lack of effects on EE and food intake observed after treatment with this MI supplement would rule out these two mechanisms to explain the anti-obesity effects reported in OVX-MI rats.

Another potential mechanism involved in the antiobesity effects of bioactives is the regulation of lipid metabolism. The lower adiposity found in the OVX-MI group could be related to the fact that MI supplementation fully counteracted the overexpression of the *Lpl* and *Cd36* genes in MWAT caused by ovariectomy. *Cd36* encodes a cell surface receptor known as fatty acid translocase (FAT), which is responsible for long-chain fatty

acid uptake from the bloodstream.[59] On the other hand, although the main function of LPL is to hydrolyse the TG core of circulating TG-rich lipoproteins, tissue-specific regulation of *Lpl* provides a mechanism for localized control of the uptake of lipoprotein lipids that results in a physiologically appropriate distribution of lipids among tissues.[59] In WAT, *Lpl* is a marker for adipocyte differentiation, and *Lpl* expression increases in parallel with cellular TG accumulation as preadipocytes differentiate, thus contributing to the growth and expansion of adipose tissue.[60,61] Therefore, our results suggest that a lower fatty acid uptake and storage in white adipose tissue, evidenced by decreased MWAT gene expression levels of *Cd36* and *Lpl*, could be one of the mechanisms to explain the lower fat mass observed in OVX-MI rats compared to their OVX counterparts. The diminished adipocyte area reported in the MWAT in response to MI supplementation, which indicated decreased adipocyte hypertrophy, would be in agreement with this idea. In agreement with the results reported here, Mosqueda-Solís *et al.* showed that the administration of hesperidin (100 mg per kg per day) for 8 weeks decreased the gene expression levels of *Lpl* in RWAT in male Wistar rats fed a hypercaloric western diet, which resulted in a nonsignificant reduction in this adipose tissue depot.[62] In addition, three different studies demonstrated that curcumin supplementation attenuated the overexpression of the hepatic mRNA levels of *Cd36* in a high-fat-diet-fed C57BL/6J mouse model, which was accompanied by an inhibitory effect of curcumin on hepatic lipid accumulation.[63–65]

The antiadiposity effect observed in the rats treated with the MI supplement was very similar to what we reported in response to 17β-E2 injections. Interestingly, both nutritional and pharmacologic treatments seemed to share a common antiadiposity mechanism, namely, decreased expression of the *Lpl* and *Cd36* genes. The strong positive correlation found between the mRNA levels of both genes found in the present

study suggests a potential coregulation mechanism, emphasizing the coordinated role of Cd36 and LPL in fatty acid uptake and storage. Furthermore, the positive correlation between *Lpl* mRNA levels and MWAT weight would also be in agreement with the key role of this gene in the growth and expansion of WAT. Therefore, although correlations do not imply causality, these results contribute to supporting our hypothesis.

The decreased food intake observed in OVX-E2 animals, which was previously reported,[66,67] is another mechanism that helps explain the lower fat mass accretion triggered by oestradiol administration, which also produced a clear decrease in body weight, different from what was observed in response to supplementation with MI. The increased lean mass found in OVX-MI rats when compared to their OVX counterparts could explain, at least in part, why the decreased adiposity observed after MI supplementation was not accompanied by lower body weight gain. Lean mass, which was calculated by quantitative magnetic resonance, provides an accurate measurement of muscle mass.[68] Therefore, the higher lean body mass observed in MI animals might also be the result of muscle mass accretion and would also contribute to the higher lean/fat mass ratio found in these rats and in OVX-E2 animals, suggesting a healthier body composition in both groups.[69,70]

As was previously reported, the lower adiposity found in OVX-MI and OVX-E2 rats was translated into significantly lower circulating levels of leptin, which are highly and positively related to body fat mass, in both individuals with normoweight and obesity.[71–73] Although the anti-obesity effects produced by both the nutraceutical and drug treatments were not translated to increased levels of the anti-inflammatory and insulin sensitivity-related adipokine adiponectin in the bloodstream,[72,73] remarkably, only MI supplementation significantly increased adiponectin plasma levels corrected by WAT weight, a surrogate marker of effective adiponectin production.[74,76] Curcumin

administration has been shown *in vitro* and in animal models of obesity and type 2 diabetes mellitus (T2DM), as well as in humans with obesity, MetS, and/or T2DM to significantly ameliorate diabetes, to increase adiponectin production by adipose tissue and to decrease the serum levels of leptin.[17,76–80] Several publications have described the AL ratio as a biomarker of adipose tissue dysfunction and insulin resistance.[81–83] The AL ratio has been better correlated with insulin resistance and insulin sensitivity than adiponectin, leptin, HOMA-IR and R-QUICKI and is clinically useful to identify subjects susceptible to cardiometabolic diseases.[81–84] An AL ratio ≥1.0 is considered normal, while a ratio between ≥0.5 and <1.0 suggests moderate-to-medium increased risk, and a ratio <0.5 indicates a severe risk of suffering from cardiometabolic diseases.[81,82] Remarkably, in this report, the OVX group exhibited an AL ratio close to 0.5, indicating a medium to high cardiometabolic risk, and this ratio was increased to 1 in response to MI supplementation.[81,82] These findings strongly suggest that the combined intake of hesperidin, phytosterols and curcumin improved metabolic health in the OVX-MI group. The 27.5% and 26.3% decrease in the circulating levels of insulin and HOMA-IR, respectively, and the significant increase in the surrogate marker of insulin sensitivity R-QUICKI found in OVX-MI rats when compared to their OVX counterparts would reinforce this idea. The inclusion of curcumin in the MI supplement may explain, at least in part, the aforementioned effects observed in OVX-MI. In this regard, in humans, it was shown that after 9 months of curcumin treatment, none of the subjects were diagnosed with T2DM, and they exhibited significantly lower HOMA-IR levels,[17] indicating improved insulin resistance. Additionally, hesperidin could have contributed to the insulin-sensitivity effects reported in OVX-MI rats since two studies showed significant reductions in insulin and HOMA-IR levels after the consumption of orange juice rich in hesperidin.[85,86] However, these insulin-related effects were not observed in response to

oestradiol injections,[87] as occurred in our study in OVX-E2 animals. Altogether, our results underscore the potential of MI supplementation as a natural therapy to improve insulin sensitivity in postmenopausal women, although further randomized controlled trials are needed to shed more light on this issue.

In the present study, MI supplementation exerted slight beneficial effects on cholesterol metabolism, which were evidenced by significantly counteracting the decrease in HDL-c serum cholesterol concentrations observed in OVX-E2 animals. Different studies have reported that rats are not the most appropriate animal model for diseases related to cholesterol alterations[88–90] since they efficiently eliminate excess cholesterol through bile acid synthesis, imparting a high resistance to cholesterol accumulation in the body, unlike what happens with other animal models such as Golden Syrian hamsters.[88–90] This consideration (and the fact that, in this study, rats were not fed a high-fat-high-cholesterol diet) could help to explain the aforementioned results and the lower beneficial effects observed in this study compared to the one carried out by our group with Golden Syrian hamsters fed a hyperlipidic diet, in which phytosterols significantly decreased both TC and VLDL-c + LDL-c.[91] Further studies carried out with OVX rats fed a high-fat-high-cholesterol diet would be useful to gain insight into the potential anti-hypercholesterolaemic effect of MI.

Many studies carried out in both OVX rodents and postmenopausal women have demonstrated that oestrogen deficiency induces bone loss and osteoporosis, which is mainly characterized by decreased BMD[5,47] and a significant increase in bone turnover (both formation and resorption) markers.[30,47,92] These bone-related alterations are normally counteracted or ameliorated after HRT treatment.[12,93] In the present study, 17β-E2 administration counteracted the increase in the circulating levels of both bone resorption (CTX-1) and bone formation (PINP and OC) turnover markers displayed by

OVX animals, an effect that was not observed in rats receiving MI supplementation. However, no significant changes in femur BMD among groups were reported, which could be attributed to the young age of the rats and to the fact that, in rats, in the short term, the femur is more resistant to bone loss and BMD-related alterations than the tibia. Therefore, further studies in which the proximal tibia is collected and analysed with rats aged between 6–9 months at the time of surgery, which have a lower bone growth rate and a significantly more pronounced alteration in trabecular bone remodelling compared to younger rats,[47] would be very useful to gain more knowledge on this issue.

In agreement with what was previously described for sex steroids, such as oestrogen, which has a well-known antioxidant activity reducing the production of reactive oxygen species,[94,95] in our study, 17β-E2 treatment fully counteracted the decrease in total and reduced GSH as well as in the GSSG/GSH ratio levels observed in OVX animals. The anti-inflammatory and antioxidant properties of the polyphenols curcumin and hesperidin have been well reported.[17,27,96] However, in this study, we observed that MI supplementation was not able to prevent the increase in the inflammation marker MCP-1 and counteract the well-described GSH redox impairment associated with ovariectomy surgery.[94,97–99] This lack of effects could be tentatively attributed, at least in part, to the lower bioavailability of curcumin, since it has been described that the intestinal absorption of curcumin is poor and there is a high rate of metabolism and rapid systemic degradation of this bioactive compound in the body.[100–102] To enhance the absorption and health effects of curcumin, several studies focused on loading curcumin into capsules[17,103,104] and therefore, microencapsulation would be a potential next step to take into account in further studies.

The present study has some limitations. In this regard, it would have been interesting to compare the effects of the supplementation of the three bioactive compounds included in

the MI (hesperidin, phytosterols and curcumin) separately to elucidate whether the combination of these ingredients exerted a synergic or an additive effect. In addition, our molecular analyses were limited to gene expression data in MWAT, which were useful to shed light on some of the potential mechanisms by which the MI exerted the reporting effects, but they do not always match protein levels. Therefore, additional research focused on protein levels and/or activity of key players involved in lipolysis (ATGL and HSL) and/or β-oxidation (CPT1B and HAD) in MWAT would have been useful to elucidate whether the effects of the MI against fat accretion and adipocyte hypertrophy were mediated, at least in part, by the activation of these lipid catabolic pathways. Finally, immunohistochemical staining to evaluate macrophage infiltration in MWAT and molecular analyses in other tissues that play a key role in lipid and glucose metabolism, such as liver, would have been of great value to gain more insight into the beneficial effects produced by MI supplementation.

CONCLUSIONS

We demonstrated here that combined supplementation with hesperidin, phytosterols and curcumin reduced fat accretion and adipocyte hypertrophy, and improved the body composition in OVX rats. The lower mRNA levels of fatty acid uptake-related genes (*Lpl* and *Cd36*) in the visceral MWAT may have accounted for the beneficial antiadiposity effects of MI supplementation. These effects were accompanied by a significant decrease in the circulating levels of leptin, an increase in the AL ratio and an improvement in insulin sensitivity, suggesting an enhancement of the metabolic health of the MI-supplemented rats. As far as we know, this is the first study evidencing that the combination of hesperidin, phytosterols and curcumin exerted such effects and that these effects were very similar or in some cases even better to what was observed in response to oestradiol administration, a treatment that resembles one of the HRTs given to

menopausal women. These results pave the way to promote the use of this MI supplement to tackle obesity and to improve the metabolic health of menopausal women. Further randomized controlled clinical trials carried out with this target population supplemented with this MI formulation would be of great value to shed more light on this issue.

ABBREVIATIONS

17β-E2 17β-oestradiol
Acc1 Acetyl-CoA carboxylase 1
AL ratio Adiponectin/leptin ratio
ANOVA Analysis of variance
Atgl Adipose triacylglycerol lipase
AUC Area under the curve
BMC Bone mineral content
BMD Bone mineral density
Cd36 Fatty acid translocase, homologue of CD36
Cebpa CCAAT/enhancer binding protein alpha
Cpt1b Carnitine palmitoyltransferase 1 beta
CTX-1 Carboxy-terminal telopeptide of type I collagen
CUR Curcumin
CVDs Cardiovascular diseases
EE Energy expenditure
Fas Fatty acid synthase
Emr1 EGF-like module containing, mucin-like, hormone receptor-like 1
ER Oestrogen receptor
GSH Glutathione
GSSG Oxidized glutathione
Had Hydroxyacyl-CoA dehydrogenase
HDL-c High-density lipoprotein cholesterol
HOMA-IR Homeostasis model assessment-estimated insulin resistance
Hprt Hypoxanthine guanine phosphoribosyl transferase
HRT Hormone replacement therapy
Hsl Hormone-sensitive lipase

Insr Insulin receptor

IR Insulin resistance

Irs1 Insulin receptor substrate 1

IWAT Inguinal white adipose tissue

LDL-c Low-density lipoprotein cholesterol

Lpl Lipoprotein lipase

MCP-1 Monocyte chemoattractant protein-1

Mgl1 C-type lectin domain family 10, member A

MI Multi-ingredient

MWAT Mesenteric white adipose tissue

M2SH Micronized 2-S-hesperidin

NEFAs Nonesterified fatty acids

OC Osteocalcin

OGTT Oral glucose tolerance test

OVX Ovariectomized rats

PHY Phytosterol

PINP Procollagen I amino-terminal propeptide

Pparg2 Peroxisome proliferator-activated receptor gamma 2

Ppia Peptidylprolyl isomerase A

ROI Regions of interest

RQ Respiratory quotient

R-QUICKI Revised quantitative insulin sensitivity check index

RWAT Retroperitoneal white adipose tissue

SH Sham-operated rats

T2DM Type 2 diabetes mellitus

TC Total cholesterol

TG Triglycerides

TMC Tissue mineral content

TMD tissue mineral density

VLDL-c Very-low-density lipoprotein cholesterol.

AUTHOR CONTRIBUTIONS

Julio Baudin (JB), Francesc Puiggròs (FP), Lluís Arola (LA) and Antoni Caimari (AC) designed the research; JB, Julia Hernandez-Baixauli (JHB), Sergio Quesada-Vázquez (SQV), Francisca Mulero (FM) and AC conducted the research and analysed the data; JB and AC wrote the manuscript. Funding acquisition was conducted by FM, FP, LA and AC. All the authors read, reviewed and approved the final manuscript.

CONFLICTS OF INTEREST

The authors declare that they have no conflicts of interest.

ACKNOWLEDGEMENTS

The research described here was financially supported by the Agency for Business Competitiveness of the Government of Catalonia (ACCIÓ/TECCT11-1-0012) and by Comunidad de Madrid (S2022/BMD-7403 RENIM-CM).

Julio Baudin, Julia Hernandez-Baixauli and Sergio Quesada were supported by the Vicente López fellowship granted by Eurecat.

We gratefully acknowledge the help given by Dr Juan Maria Alcaide-Hidalgo and Dr Xavier Escoté, researchers at the Nutrition and Health Unit (Eurecat, Reus, Spain) to carry out the study at the animal facility and to perform the histological analyses in MWAT, respectively. We also appreciate the assistance provided by Yaiza Tobajas, Iris Triguero, Anna Antolin, Cristina Egea and Gertruda Chomiciute, laboratory technicians at the Nutrition and Health Unit (Eurecat, Reus, Spain). Moreover, we would like to thank the PhD Students Irene Bravo and David Sabador at the National Cancer Research Center (CNIO) for their support in the microcomputed tomography analyses.

We thank the companies Lipotec S.A.U. and HealthTech BioActives – HTBA – for kindly providing Lipophytol®-P (PHY; ref no.: LI0056) and Micronized 2S-Hesperidin (M2SH; Cardiose®; ref no.: 1306615), respectively.

REFERENCES

1. N. Santoro and J. F. Randolph , Reproductive Hormones and the Menopause Transition, *Obstet. Gynecol. Clin. North Am.*, 2011, **38** , 455 —466.
2. M. A. McNeil and S. B. Merriam , Menopause, *Ann. Intern. Med.*, 2021, **174** , ITC97 —IT112.
3. R. C. Thurston , B. D. Johnson , C. L. Shufelt , G. D. Braunstein , S. L. Berga and F. Z. Stanczyk , *et al.*, Menopausal symptoms and cardiovascular disease mortality in the Women's Ischemia Syndrome Evaluation (WISE), *Menopause*, 2017, **24** , 126 — 132.
4. S. D. Harlow , M. Gass , J. E. Hall , R. Lobo , P. Maki and R. W. Rebar , *et al.*, Executive Summary of the Stages of Reproductive Aging Workshop + 10: Addressing the Unfinished Agenda of Staging Reproductive Aging, *J. Clin. Endocrinol. Metab.*, 2012, **97** , 1159 —1168.
5. S. Thapa , A. Nandy and E. Rendina-Ruedy , Endocrinal metabolic regulation on the skeletal system in post-menopausal women, *Front. Physiol.*, 2022, **13** , 1 —10.
6. A. Fenton , C. Smart , L. Goldschmidt , V. Price and J. Scott , Fat mass, weight and body shape changes at menopause – causes and consequences: a narrative review, *Climacteric*, 2023, **26** , 381 —387.
7. H. Juppi , S. Sipilä , V. Fachada , M. Hyvärinen , N. Cronin and P. Aukee , *et al.*, Total and regional body adiposity increases during menopause—evidence from a follow–up study, *Aging Cell*, 2022, **21** , 1 —17.
8. G. M. C. Rosano , C. Vitale , G. Marazzi and M. Volterrani , Menopause and cardiovascular disease: the evidence, *Climacteric*, 2007, **10** , 19 —24.
9. E. Kapoor , M. L. Collazo-Clavell and S. S. Faubion , Weight Gain in Women at Midlife: A Concise Review of the Pathophysiology and Strategies for Management, *Mayo Clin. Proc.*, 2017, **92** , 1552 —1558.
10. V. R. Mesch , L. E. Boero , N. O. Siseles , M. Royer , M. Prada and F. Sayegh , *et al.*, Metabolic syndrome throughout the menopausal transition: influence of age and menopausal status, *Climacteric*, 2006, **9** , 40 —48.
11. The European Society of Cardiology. Understanding the burden of CVD. 2023. https://www.escardio.org/The-ESC/Advocacy/understanding-the-burden-of-cvd-facts-and-figures (accessed September 2023). (accessed September 2023)
12. J. Mehta , J. M. Kling and J. E. Manson , Risks, Benefits, and Treatment Modalities of Menopausal Hormone Therapy: Current Concepts, *Front. Endocrinol.*, 2021, **12** , 1 —14.

13. P. Thangavel , A. Puga-Olguín , J. F. Rodríguez-Landa and R. C. Zepeda , Genistein as Potential Therapeutic Candidate for Menopausal Symptoms and Other Related Diseases, *Molecules*, 2019, **24** , 3892.
14. J. Sharifi-Rad , C. Quispe , M. Imran , A. Rauf , M. Nadeem and T. A. Gondal , *et al.*, Genistein: An Integrative Overview of Its Mode of Action, Pharmacological Properties, and Health Benefits, *Oxid. Med. Cell. Longevity*, 2021, **2021** , 3268136.
15. A. M. P. Romani The controversy on the beneficial effect of phytoestrogens in diabetic treatment in postmenopausal women, *Biochem. Pharmacol.*, 2021, **190** , 114619.
16. A. B. Kunnumakkara , D. Bordoloi , G. Padmavathi , J. Monisha , N. K. Roy and S. Prasad , *et al.*, Curcumin, the golden nutraceutical: multitargeting for multiple chronic diseases, *Br. J. Pharmacol.*, 2017, **174** , 1325 —1348.
17. S. Chuengsamarn , S. Rattanamongkolgul , R. Luechapudiporn , C. Phisalaphong and S. Jirawatnotai , Curcumin Extract for Prevention of Type 2 Diabetes, *Diabetes Care*, 2012, **35** , 2121 —2127.
18. A. Sophocleous and A. I. Idris , Ovariectomy/Orchiectomy in Rodents, *Methods in molecular biology* , A. I. IdrisSpringer, New York, 2019, vol. 1914, 261–267.
19. V. R. Shouza , E. Mendes , M. Casaro , A. T. F. B. Antiorio , F. A. Oliveira and C. M. Ferreira , Description of Ovariectomy Protcol in Mice, *Methods in molecular biology* , P. C. GuestSpringer, New York, 1916, vol. 29, 303–309.
20. S. V. Koebele and H. A. Bimonte-Nelson , Modeling menopause: The utility of rodents in translational behavioral endocrinology research, *Maturitas*, 2016, **87** , 5 — 17.
21. R. Diaz Brinton Minireview: Translational Animal Models of Human Menopause: Challenges and Emerging Opportunities, *Endocrinology*, 2012, **153** , 3571 —3578.
22. W. K. Kim , K. Ke , O. J. Sul , H. J. Kim , S. H. Kim and M. H. Lee , *et al.*, Curcumin protects against ovariectomy–induced bone loss and decreases osteoclastogenesis, *J. Cell. Biochem.*, 2011, **112** , 3159 —3166.
23. M. D. S. Morrone , C. E. Schnorr , G. A. Behr , J. Gasparotto , R. C. Bortolin and K. da Boit Martinello , *et al.*, Curcumin Supplementation Decreases Intestinal Adiposity Accumulation, Serum Cholesterol Alterations, and Oxidative Stress in Ovariectomized Rats, *Oxid. Med. Cell. Longevity*, 2016, **2016** , 1 —12.
24. A. S. Khorasanian , S. T. Fateh , F. Gholami , N. Rasaei , H. Gerami and S. S. Khayyatzadeh , *et al.*, The effects of hesperidin supplementation on cardiovascular risk factors in adults: a systematic review and dose–response meta-analysis, *Front. Nutr.*, 2023, **10** , 1177708.
25. R. M. Valls , A. Pedret , L. Calderón-Pérez , E. Llauradó , L. Pla-Pagà and J. Companys , *et al.*, Effects of hesperidin in orange juice on blood and pulse pressures in mildly hypertensive individuals: a randomized controlled trial (Citrus study), *Eur. J. Nutr.*, 2021, **60** , 1277 —1288.
26. A. Mas-Capdevila , J. Teichenne , C. Domenech-Coca , A. Caimari , J. M. Del Bas and X. Escoté , *et al.*, Effect of Hesperidin on Cardiovascular Disease Risk Factors: The Role of Intestinal Microbiota on Hesperidin Bioavailability, *Nutrients*, 2020, **12** , 1488.

27. H. Xiong , J. Wang , Q. Ran , G. Lou , C. Peng and Q. Gan , *et al.*, Hesperidin: A Therapeutic Agent For Obesity, *Drug Des., Dev. Ther.*, 2019, **13** , 3855 —3866.
28. A. d. C. Ortiz , S. O. M. Fideles , C. H. B. Reis , M. Z. Bellini , E. d. S. Pereira and J. P. G. Pilon , *et al.*, Therapeutic Effects of Citrus Flavonoids Neohesperidin, Hesperidin and Its Aglycone, Hesperetin on Bone Health, *Biomolecules*, 2022, **12** , 626.
29. D. Lim , Y. Lee and Y. Kim , Preventive Effects of Citrus unshiu Peel Extracts on Bone and Lipid Metabolism in OVX Rats, *Molecules*, 2014, **19** , 783 —794.
30. M. N. Horcajada , V. Habauzit , A. Trzeciakiewicz , C. Morand , A. Gil-Izquierdo and J. Mardon , *et al.*, Hesperidin inhibits ovariectomized-induced osteopenia and shows differential effects on bone mass and strength in young and adult intact rats, *J. Appl. Physiol.*, 2008, **104** , 648 —654.
31. A. Crescenti , A. Caimari , J. M. Alcaide-Hidalgo , R. Mariné-Casadó , R. M. Valls and J. Companys , *et al.*, Hesperidin Bioavailability Is Increased by the Presence of 2S-Diastereoisomer and Micronization—A Randomized, Crossover and Double-Blind Clinical Trial, *Nutrients*, 2022, **14** , 2481.
32. S. Opinion Scientific Opinion on the substantiation of a health claim related to 3 g/day plant sterols/stanols and lowering blood LDL-cholesterol and reduced risk of (coronary) heart disease pursuant to Article 19 of Regulation (EC) No 1924/2006, *EFSA J.*, 2012, **10** , 2693.
33. W. Xia , S. Xiang , M. Gaman , P. Jamilian , K. Prabahar and G. Du , *et al.*, The effects of phytosterol and phytostanol supplementation on the lipid profile in postmenopausal women: A systematic review and meta–analysis of randomized controlled trials, *Phyther. Res.*, 2022, **36** , 4398 —4408.
34. S. Quesada-Vázquez , A. Antolín , M. Colom-Pellicer , G. Aragonès , L. Herrero and J. M. Del Bas , *et al.*, Reduction of Obesity and Insulin Resistance through Dual Targeting of VAT and BAT by a Novel Combination of Metabolic Cofactors, *Int. J. Mol. Sci.*, 2022, **23** , 14923.
35. J. Companys , L. Calderón-Pérez , L. Pla-Pagà , E. Llauradó , B. A. Sandoval-Ramirez and M. J. Gosalbes , *et al.*, Effects of enriched seafood sticks (heat-inactivated B. animalis subsp. lactis CECT 8145, inulin, omega-3) on cardiometabolic risk factors and gut microbiota in abdominally obese subjects: randomized controlled trial, *Eur. J. Nutr.*, 2022, **61** , 3597 —3611.
36. S. Quesada-Vázquez , M. Colom-Pellicer , È. Navarro-Masip , G. Aragonès , J. M. Del Bas and A. Caimari , *et al.*, Supplementation with a Specific Combination of Metabolic Cofactors Ameliorates Non-Alcoholic Fatty Liver Disease, Hepatic Fibrosis, and Insulin Resistance in Mice, *Nutrients*, 2021, **13** , 3532.
37. H. Yang , J. Mayneris-Perxachs , N. Boqué , J. M. del Bas , L. Arola and M. Yuan , *et al.*, Combined Metabolic Activators Decrease Liver Steatosis by Activating Mitochondrial Metabolism in Hamsters Fed with a High-Fat Diet, *Biomedicines*, 2021, **9** , 1440.
38. M. Suárez , N. Boqué , J. del Bas , J. Mayneris-Perxachs , L. Arola and A. Caimari , Mediterranean Diet and Multi-Ingredient-Based Interventions for the Management of Non-Alcoholic Fatty Liver Disease, *Nutrients*, 2017, **9** , 1052.

39. S. Reagan–Shaw , M. Nihal and N. Ahmad , Dose translation from animal to human studies revisited, *FASEB J.*, 2008, **22** , 659 —661.
40. Y. Li , A. D. Kandhare , A. A. Mukherjee and S. L. Bodhankar , Acute and sub-chronic oral toxicity studies of hesperidin isolated from orange peel extract in Sprague Dawley rats, *Regul. Toxicol. Pharmacol.*, 2019, **105** , 77 —85.
41. V. Soleimani , A. Sahebkar and H. Hosseinzadeh , Turmeric (Curcuma longa) and its major constituent (curcumin) as nontoxic and safe substances: Review, *Phyther. Res.*, 2018, **32** , 985 —995.
42. D. R. Matthews , J. P. Hosker , A. S. Rudenski , B. A. Naylor , D. F. Treacher and R. C. Turner , Homeostasis model assessment: insulin resistance and beta-cell function from fasting plasma glucose and insulin concentrations in man, *Diabetologia*, 1985, **28** , 412 —419.
43. G. Perseghin , A. Caumo , M. Caloni , G. Testolin and L. Luzi , Incorporation of the Fasting Plasma FFA Concentration into QUICKI Improves Its Association with Insulin Sensitivity in Nonobese Individuals, *J. Clin. Endocrinol. Metab.*, 2001, **86** , 4776 —4781.
44. A. Crescenti , J. M. del Bas , A. Arola-Arnal , G. Oms-Oliu , L. Arola and A. Caimari , Grape seed procyanidins administered at physiological doses to rats during pregnancy and lactation promote lipid oxidation and up-regulate AMPK in the muscle of male offspring in adulthood, *J. Nutr. Biochem.*, 2015, **26** , 912 —920.
45. M. M. Witte , D. Resuehr , A. R. Chandler , A. K. Mehle and J. M. Overton , Female mice and rats exhibit species-specific metabolic and behavioral responses to ovariectomy, *Gen. Comp. Endocrinol.*, 2010, **166** , 520 —528.
46. J. Medina-Contreras , R. Villalobos-Molina , A. Zarain-Herzberg and J. Balderas-Villalobos , Ovariectomized rodents as a menopausal metabolic syndrome model. A minireview, *Mol. Cell. Biochem.*, 2020, **475** , 261 —276.
47. N. Yousefzadeh , K. Kashfi , S. Jeddi and A. Ghasemi , Ovariectomized rat model of osteoporosis: A practical guide, *EXCLI J.*, 2020, **19** , 89 —107.
48. L. Mosquera , L. Shepherd and A. I. Torrado , Comparison of Two Methods of Estradiol Replacement: their Physiological and Behavioral Outcomes, *J. Vet. Sci. Technol.*, 2015, **6** , 276.
49. D. Moseti , A. Regassa and W. K. Kim , Molecular Regulation of Adipogenesis and Potential Anti-Adipogenic Bioactive Molecules, *Int. J. Mol. Sci.*, 2016, **17** , 124.
50. L. A. Waddell , L. Lefevre , S. J. Bush , A. Raper , R. Young and Z. M. Lisowski , *et al.*, ADGRE1 (EMR1, F4/80) Is a Rapidly-Evolving Gene Expressed in Mammalian Monocyte-Macrophages, *Front. Immunol.*, 2018, **9** , 1 —14.
51. T. M. Panknin , C. L. Howe , M. Hauer , B. Bucchireddigari , A. M. Rossi and J. L. Funk , Curcumin Supplementation and Human Disease: A Scoping Review of Clinical Trials, *Int. J. Mol. Sci.*, 2023, **24** , 4476.
52. T. Vezza , F. Canet , A. M. de Marañón , C. Bañuls , M. Rocha and V. M. Víctor , Phytosterols: Nutritional Health Players in the Management of Obesity and Its Related Disorders, *Antioxidants*, 2020, **9** , 1266.

53. K. M. Gavin , W. M. Kohrt , D. J. Klemm and E. L. Melanson , Modulation of Energy Expenditure by Estrogens and Exercise in Women, *Exerc. Sport Sci. Rev.*, 2018, **46** , 232 —239.
54. J. C. Lovejoy , C. M. Champagne , L. de Jonge , H. Xie and S. R. Smith , Increased visceral fat and decreased energy expenditure during the menopausal transition, *Int. J. Obes.*, 2008, **32** , 949 —958.
55. D. S. Day , W. S. Gozansky , R. E. Van Pelt , R. S. Schwartz and W. M. Kohrt , Sex Hormone Suppression Reduces Resting Energy Expenditure and β-Adrenergic Support of Resting Energy Expenditure, *J. Clin. Endocrinol. Metab.*, 2005, **90** , 3312 —3317.
56. C. Receno , C. Liang , D. Korol , M. Atalay , K. Heffernan and T. Brutsaert , *et al.*, Effects of Prolonged Dietary Curcumin Exposure on Skeletal Muscle Biochemical and Functional Responses of Aged Male Rats, *Int. J. Mol. Sci.*, 2019, **20** , 1178.
57. L. Mele , G. Bidault , P. Mena , A. Crozier , F. Brighenti and A. Vidal-Puig , *et al.*, Dietary (poly)phenols, brown adipose tissue activation, and energy expenditure: A narrative review, *Adv. Nutr.*, 2017, **8** , 694 —704.
58. S. Wang , N. Moustaid-Moussa , L. Chen , H. Mo , A. Shastri and R. Su , *et al.*, Novel insights of dietary polyphenols and obesity, *J. Nutr. Biochem.*, 2014, **25** , 1 —18.
59. H. Wang and R. H. Eckel , Lipoprotein lipase: from gene to obesity, *Am. J. Physiol.: Endocrinol. Metab.*, 2009, **297** , E271 —E288.
60. P. Björntorp , M. Karlsson , H. Pertoft , P. Pettersson , L. Sjöström and U. Smith , Isolation and characterization of cells from rat adipose tissue developing into adipocytes, *J. Lipid Res.*, 1978, **19** , 316 —324.
61. P. Bjorntorp Hormonal control of regional fat distribution, *Hum Reprod.*, 1997, **12** , 21 —25.
62. A. Mosqueda-Solís , J. Sánchez , B. Reynés , M. Palou , M. P. Portillo and A. Palou , *et al.*, Hesperidin and capsaicin, but not the combination, prevent hepatic steatosis and other metabolic syndrome-related alterations in western diet-fed rats, *Sci. Rep.*, 2018, **8** , 15100.
63. Y. Liu , F. Cheng , Y. Luo , Z. Zhan , P. Hu and H. Ren , *et al.*, PEGylated Curcumin Derivative Attenuates Hepatic Steatosis via CREB/PPAR- γ /CD36 Pathway, *BioMed. Res. Int.*, 2017, **2017** , 8234507.
64. M. Y. Um , K. H. Hwang , J. Ahn and T. Y. Ha , Curcumin Attenuates Diet–Induced Hepatic Steatosis by Activating AMP–Activated Protein Kinase, *Basic Clin. Pharmacol. Toxicol.*, 2013, **113** , 152 —157.
65. J. Mun , S. Kim , H. G. Yoon , Y. You , O. K. Kim and K. C. Choi , *et al.*, Water Extract of Curcuma longa L. Ameliorates Non-Alcoholic Fatty Liver Disease, *Nutrients*, 2019, **11** , 2536.
66. F. Mauvais-Jarvis , D. J. Clegg and A. L. Hevener , The Role of Estrogens in Control of Energy Balance and Glucose Homeostasis, *Endocr. Rev.*, 2013, **34** , 309 —338.
67. Y. Q. Liang , M. Akishita , S. Kim , J. Ako , M. Hashimoto and K. Iijima , *et al.*, Estrogen receptor β is involved in the anorectic action of estrogen, *Int. J. Obes.*, 2002, **26** , 1103 —1109.

68. G. Z. Taicher , F. C. Tinsley , A. Reiderman and M. L. Heiman , Quantitative magnetic resonance (QMR) method for bone and whole-body-composition analysis, *Anal. Bioanal. Chem.*, 2003, **377** , 990 —1002.
69. N. López , J. Sánchez , C. Picó , A. Palou and F. Serra , Dietary l-leucine supplementation of lactating rats results in a tendency to increase lean/fat ratio associated to lower orexigenic neuropeptide expression in hypothalamus, *Peptides*, 2010, **31** , 1361 —1367.
70. A. Caimari , J. M. del Bas , N. Boqué , A. Crescenti , F. Puiggròs and E. Chenoll , *et al.*, Heat-killed Bifidobacterium animalis subsp. Lactis CECT 8145 increases lean mass and ameliorates metabolic syndrome in cafeteria-fed obese rats, *J. Funct. Foods*, 2017, **38** , 251 —263.
71. J. Gómez-Ambrosi , J. Salvador , C. Silva , C. Pastor , F. Rotellar and M. Gil , *et al.*, Increased cardiovascular risk markers in obesity are associated with body adiposity: Role of leptin, *Thromb. Haemostasis*, 2006, **95** , 991 —996.
72. L. Recinella , G. Orlando , C. Ferrante , A. Chiavaroli , L. Brunetti and S. Leone , Adipokines: New Potential Therapeutic Target for Obesity and Metabolic, Rheumatic, and Cardiovascular Diseases, *Front. Physiol.*, 2020, **11** , 578966.
73. S. Zhao , C. M. Kusminski and P. E. Scherer , Adiponectin, Leptin and Cardiovascular Disorders, *Circ. Res.*, 2021, **128** , 136 —149.
74. R. Mariné-Casadó , C. Domenech-Coca , A. Crescenti , M. Á. Rodríguez Gómez , J. M. Del Bas and L. Arola , *et al.*, Maternal Supplementation with a Cocoa Extract during Lactation Deeply Modulates Dams' Metabolism, Increases Adiponectin Circulating Levels and Improves the Inflammatory Profile in Obese Rat Offspring, *Nutrients*, 2022, **14** , 5134.
75. A. Caimari , R. Mariné-Casadó , N. Boqué , A. Crescenti , L. Arola and J. M. del Bas , Maternal intake of grape seed procyanidins during lactation induces insulin resistance and an adiponectin resistance-like phenotype in rat offspring, *Sci. Rep.*, 2017, **7** , 12573.
76. Y. Panahi , M. S. Hosseini , N. Khalili , E. Naimi , S. S. Soflaei and M. Majeed , *et al.*, Effects of supplementation with curcumin on serum adipokine concentrations: A randomized controlled trial, *Nutrition*, 2016, **32** , 1116 —1122.
77. S. L. Atkin , N. Katsiki , G. Derosa , P. Maffioli and A. Sahebkar , Curcuminoids Lower Plasma Leptin Concentrations: A Meta-analysis, *Phyther. Res.*, 2017, **31** , 1836 —1841.
78. S. Chuengsamarn , S. Rattanamongkolgul , B. Phonrat , R. Tungtrongchitr and S. Jirawatnotai , Reduction of atherogenic risk in patients with type 2 diabetes by curcuminoid extract: a randomized controlled trial, *J. Nutr. Biochem.*, 2014, **25** , 144 —150.
79. M. Kubota , M. Shimizu , H. Sakai , Y. Yasuda , D. Terakura and A. Baba , *et al.*, Preventive Effects of Curcumin on the Development of Azoxymethane-Induced Colonic Preneoplastic Lesions in Male C57BL/KsJ- db/db Obese Mice, *Nutr. Cancer.*, 2012, **64** , 72 —79.

80. S. P. Weisberg , R. Leibel and D. V. Tortoriello , Dietary Curcumin Significantly Improves Obesity-Associated Inflammation and Diabetes in Mouse Models of Diabesity, *Endocrinology*, 2008, **149** , 3549 —3558.
81. G. Frühbeck , V. Catalán , A. Rodríguez , B. Ramírez , S. Becerril and J. Salvador , *et al.*, Adiponectin-leptin Ratio is a Functional Biomarker of Adipose Tissue Inflammation, *Nutrients*, 2019, **11** , 454.
82. G. Frühbeck , V. Catalán , A. Rodríguez and J. Gómez-Ambrosi , Adiponectin-leptin ratio: A promising index to estimate adipose tissue dysfunction. Relation with obesity-associated cardiometabolic risk, *Adipocyte*, 2018, **7** , 57 —62.
83. M. Inoue , M. Yano , M. Yamakado , E. Maehata and S. Suzuki , Relationship between the adiponectin-leptin ratio and parameters of insulin resistance in subjects without hyperglycemia, *Metabolism*, 2006, **55** , 1248 —1254.
84. G. Frühbeck , V. Catalán , A. Rodríguez , B. Ramírez , S. Becerril and J. Salvador , *et al.*, Involvement of the leptin-adiponectin axis in inflammation and oxidative stress in the metabolic syndrome, *Sci. Rep.*, 2017, **7** , 6619.
85. C. Ribeiro , G. Dourado and T. Cesar , Orange juice allied to a reduced-calorie diet results in weight loss and ameliorates obesity-related biomarkers: A randomized controlled trial, *Nutrition*, 2017, **38** , 13 —19.
86. A. C. D. Lima , C. Cecatti , M. P. Fidélix , M. A. T. Adorno , I. K. Sakamoto and T. B. Cesar , *et al.*, Effect of Daily Consumption of Orange Juice on the Levels of Blood Glucose, Lipids, and Gut Microbiota Metabolites: Controlled Clinical Trials, *J. Med. Food*, 2019, **22** , 202 —210.
87. P. Babaei , R. Mehdizadeh , M. M. Ansar and A. Damirchi , Effects of Ovariectomy and Estrogen Replacement Therapy on Visceral Adipose Tissue and Serum Adiponectin Levels in Rats, *Menopause Int.*, 2010, **16** , 100 —104.
88. A. Dillard , N. R. Matthan and A. H. Lichtenstein , Use of hamster as a model to study diet-induced atherosclerosis, *Nutr. Metab.*, 2010, **7** , 89.
89. Z. Zhang , H. Wang , R. Jiao , C. Peng , Y. M. Wong and V. S. Y. Yeung , *et al.*, Choosing hamsters but not rats as a model for studying plasma cholesterol-lowering activity of functional foods, *Mol. Nutr. Food Res.*, 2009, **53** , 921 —930.
90. E. Bravo , A. Cantafora , A. Calcabrini and G. Ortu , Why prefer the golden Syrian hamster (Mesocricetus auratus) to the Wistar rat in experimental studies on plasma lipoprotein metabolism?, *Comp. Biochem. Physiol.*, 1994, **107B** , 347 —355.
91. S. Laos , A. Caimari , A. Crescenti , J. Lakkis , F. Puiggròs and L. Arola , *et al.*, Long-term intake of soyabean phytosterols lowers serum TAG and NEFA concentrations, increases bile acid synthesis and protects against fatty liver development in dyslipidaemic hamsters, *Br. J. Nutr.*, 2014, **112** , 663 —673.
92. S. Shetty , N. Kapoor , J. Bondu , N. Thomas and T. Paul , Bone turnover markers: Emerging tool in the management of osteoporosis, *Indian J. Endocrinol. Metab.*, 2016, **20** , 846 —852.
93. J. V. Pinkerton , F. S. Aguirre , J. Blake , F. Cosman , H. Hodis and S. Hoffstetter , *et al.*, The 2017 hormone therapy position statement of The North American Menopause Society, *Menopause*, 2017, **24** , 728 —753.

94. M. Ulas and M. Cay , 17β-Estradiol and Vitamin E Modulates Oxidative Stress-Induced Kidney Toxicity in Diabetic Ovariectomized Rat, *Biol. Trace Elem. Res.*, 2011, **144** , 821 —831.
95. P. J. Devine , S. D. Perreault and U. Luderer , Roles of Reactive Oxygen Species and Antioxidants in Ovarian Toxicity1, *Biol. Reprod.*, 2012, **86** , 1 —10.
96. K. Yang , J. Chen , T. Zhang , X. Yuan , A. Ge and S. Wang , *et al.*, Efficacy and safety of dietary polyphenol supplementation in the treatment of non-alcoholic fatty liver disease: A systematic review and meta-analysis, *Front. Immunol.*, 2022, **13** , 949746.
97. J. F. Machi , D. da Silva Dias , S. Freitas , O. Albuquerque de Moraes , M. Barbosa da Silva and P. L. Cruz , *et al.*, Impact of aging on cardiac function in a female rat model of menopause: role of autonomic control, inflammation, and oxidative stress, *Clin. Interventions Aging*, 2016, **11** , 341.
98. Y. Y. Kim , S. H. Kim , S. Oh , O. J. Sul , H. Y. Lee and H. J. Kim , *et al.*, Increased fat due to estrogen deficiency induces bone loss by elevating monocyte chemoattractant protein-1 (MCP-1) production, *Mol. Cells*, 2010, **29** , 277 —282.
99. M. Delgobo , J. P. Agnes , R. M. Gonçalves , V. W. dos Santos , E. B. Parisotto and A. Zamoner , *et al.*, N-acetylcysteine and alpha-lipoic acid improve antioxidant defenses and decrease oxidative stress, inflammation and serum lipid levels in ovariectomized rats via estrogen-independent mechanisms, *J. Nutr. Biochem.*, 2019, **67** , 190 —200.
100. L. Z. Racz , C. P. Racz , L. C. Pop , G. Tomoaia , A. Mocanu and I. Barbu , *et al.*, Strategies for Improving Bioavailability, Bioactivity, and Physical-Chemical Behavior of Curcumin, *Molecules*, 2022, **27** , 6854.
101. M. Funamoto , K. Shimizu , Y. Sunagawa , Y. Katanasaka , Y. Miyazaki and H. Kakeya , *et al.*, Effects of Highly Absorbable Curcumin in Patients with Impaired Glucose Tolerance and Non-Insulin-Dependent Diabetes Mellitus, *J. Diabetes Res.*, 2019, **2019** , 8208237.
102. X. Y. Xu , X. Meng , S. Li , R. Y. Gan , Y. Li and H. B. Li , Bioactivity, Health Benefits, and Related Molecular Mechanisms of Curcumin: Current Progress, Challenges, and Perspectives, *Nutrients*, 2018, **10** , 1553.
103. K. Priyadarsini The Chemistry of Curcumin: From Extraction to Therapeutic Agent, *Molecules*, 2014, **19** , 20091 —20112.
104. P. Neerati , R. Devde and A. K. Gangi , Evaluation of the Effect of Curcumin Capsules on Glyburide Therapy in Patients with Type–2 Diabetes Mellitus, *Phyther. Res.*, 2014, **28** , 1796 —1800.

FOOTNOTES

1. † Electronic supplementary information (ESI) available. See DOI: https://doi.org/10.1039/d3fo05122f
2. ‡ Present address: Laboratory of Metabolism and Obesity, Vall d'Hebron-Institut de Recerca, Universitat Autònoma de Barcelona, Barcelona, Spain.
3. § Present address: Liver Vascular Biology Research Group, IDIBAPS Biomedical Research Institute, CIBEREHD, University of Barcelona, Spain.

Supplementary table 1: Nucleotide sequences of primers used for real time quantitative PCR in sham-operated (SH) and ovariectomized (OVX) rats after 8 weeks of intervention

Gene	Forward primer (5' to 3')	Reverse primer (5' to 3')
Acc1	TGCAGGTATCCCCACTCTTC	TTCTGATTCCCTTCCCTCCT
Atgl	CACTTTAGCTCCAAGGATGA	TGGTTCAGTAGGCCATTCCT
Cd36	GTCCTGGCTGTGTTTGGA	GCTCAAAGATGGCTCCATTG
Cepba	AGCCGAGATAAAGCCAAACA	CCTTGACCAAGGAGCTCTCA
Cpt1β	GCAAACTGGACCGAGAAGAG	CCTTGAAGAAGCGACCTTTG
Emr1	GATGTGGAGGATGGGAGATG	GCACGAAACAACAGGAAGGT
Fas	CGGCGAGTCTATGCCACTAT	ACACAGGGACCGAGTAATGC
Had	ATCGTGAACCGTCTCTTGGT	AGGACTGGGCTGAAATAAGG
Hprt	TCCCAGCGTCGTGATTAGTGA	CCTTCATGACATCTCGAGCAAG
Hsl	TCACGCTACATAAAGGCTGCT	CCACCCGTAAAGAGGGAACT
Insr	AACGACATTGCCCTGAAGAC	CATCCTGCCCATCAAACTCT
Irs1	CTACACCCGAGACGAACACT	TAACCTGCCAGACCTCCTTG
Lpl	TATGGCACAGTGGCTGAAAG	CTGACCAGCGGAAGTAGGAG
Mgl1	CTCCAACACCAAGGCTGAAC	GGTCTTCAAGTCCTTCCCCA
Pparg2	CTGGACCTCTGCTGGTGAT	CCGTGGTAAAGGGTTTGATG
Ppia	CCAAACACAAATGGTTCCCAGT	ATTCCTGGACCCAAAACGCT

The table shows the nucleotide sequences of primers used for PCR amplification. Primer pairs for PCR were designed using Primer3 software and the sequence information were obtained from Genbank. *Acc1*: acetyl CoA carboxylase 1; *Atgl*: adipose triglyceride lipase; *Cd36*: fatty acid translocase: homologue of CD36; *Cebpa*: CCAAT/enhancer binding protein alpha; *Cpt1b*: carnitine palmitoyltransferase 1 beta; *Emr1*: EGF-like module containing, mucin-like, hormone receptor-like 1; *Fas*: fatty acid synthase; *Had*: hydroxyacyl-CoA dehydrogenase; *Hprt*: hypoxanthine guanine phosphoribosyl transferase; *Hsl*: hormone-sensitive lipase; *Insr*: insulin receptor; *Irs1*: insulin receptor substrate 1; Lpl: lipoprotein lipase; *Mgl1*: C-type lectin domain family 10, member A; *Pparg2*: peroxisome proliferator-activated receptor gamma 2; *Ppia*: peptidylprolyl isomerase A.

MANUSCRIPT 4

Combined histidine, carnosine, cysteine and serine consumption reduces adiposity and improves metabolic health and adipose tissue immunometabolic function in ovariectomized rats

Julio Baudin [a,b], Julia Hernandez-Baixauli [a,1], Jordi Romero-Giménez [a], Hong Yang [c], Francisca Mulero [d], Francesc Puiggròs [e], Adil Mardinoglu [c,f], Lluís Arola [b*], and Antoni Caimari[e*]

[a] Eurecat, Centre Tecnològic de Catalunya, Technological Unit of Nutrition and Health, 43204 Reus, Spain.

[b] Nutrigenomics Research Group, Department of Biochemistry and Biotechnology, Universitat Rovira i Virgili, 43007 Tarragona, Spain.

[c] Science for Life Laboratory, KTH Royal Institute of Technology, SE-17165 Stockholm, Sweden.

[d] Molecular Imaging Unit, Spanish National Cancer Research Centre (CNIO), Madrid, Spain.

[e] Eurecat, Centre Tecnològic de Catalunya, Biotechnology Area, 43204 Reus, Spain.

[f] Centre for Host-Microbiome Interactions, Faculty of Dentistry, Oral & Craniofacial Sciences, King's College London, London, United Kingdom.

*Correspondence: lluis.arola@urv.cat (L.A.); antoni.caimari@eurecat.org (A.C.).

[1] Present address: Laboratory of Metabolism and Obesity, Vall d'Hebron-Institut de Recerca, Universitat Autònoma de Barcelona, Barcelona, Spain.

Under supervision, Biomedicine and Pharmacotherapy 2024

ABSTRACT

Many women have sought alternative therapies to address menopause. Recently, a multi-ingredient (MI) containing L-histidine, L-carnosine, L-serine, and L-cysteine has been shown to be effective at ameliorating hepatic steatosis (HS) in ovariectomized (OVX) rats, a postmenopausal oestrogen deficiency model. Considering that HS frequently accompanies obesity, which often occurs during menopause, we aimed to investigate the effects of supplementation with this MI for 8 weeks in OVX rats. Twenty OVX rats were orally supplemented with either MI (OVX-MI) or vehicle (OVX). Ten OVX rats received vehicle orally along with subcutaneous injections of 17β-oestradiol (OVX-E2), whereas 10 rats underwent a sham operation and received oral and injected vehicles (control group). MI consumption partly counteracted the fat mass accretion observed in OVX animals, leading to decreased total fat mass, adiposity index and retroperitoneal white adipose tissue (RWAT) adipocyte hypertrophy. OVX-MI rats also displayed increased lean mass and lean/fat ratio, suggesting a healthier body composition, similar to the results reported for OVX-E2 animals. MI consumption decreased the circulating levels of the proinflammatory marker CRP, the total cholesterol-to-HDL-cholesterol ratio and the leptin-to-adiponectin ratio, a biomarker of diabetes risk and metabolic syndrome. RWAT transcriptomics indicated that MI supplementation favourably regulated genes involved in adipocyte structure and morphology, cell fate determination and differentiation, glucose/insulin homeostasis, inflammation, response to stress and oxidative phosphorylation, which may be mechanisms underlying the beneficial effects described for OVX-MI rats. Our results pave the way for using this MI formulation to improve the body composition and immunometabolic health of menopausal women.

Keywords: histidine, serine, carnosine, cysteine, menopause, obesity, immunometabolic health, nutraceuticals, complementary and alternative therapies

[1] **Running title**: Multi-ingredient consumption and menopause-related alterations

INTRODUCTION

Menopause is an aging-related biological stage in a woman's life that is characterized by the permanent cessation of menstrual cycles due to the loss of ovarian function, which leads to a gradual decline in oestrogen production that already appears during the menopausal transition and is exacerbated during the postmenopausal state [1]. This reproductive aging process can boost the appearance of different vasomotor symptoms, including sleep disturbances, night sweats and hot flashes [2–4], in addition to osteoporosis [5], decreased muscle mass content [5–7] and body weight gain accompanied by a shift in body fat distribution from a gynoid to an android pattern, contributing to increased abdominal fat accumulation [5–9]. Fat accretion may increase oxidative stress and low-grade inflammation and may trigger the development of metabolic disorders, such as hypertension, dyslipidaemia and insulin resistance (IR), thereby increasing the risk of cardiovascular disease (CVD) [10–14]. Notably, both the risks of osteoporosis and CVD increase with age, and CVD is one of the most prominent causes of death worldwide, accounting for 47% of deaths among women [15].

Hormone replacement therapy (HRT) is a widely prescribed solution for alleviating symptoms and ameliorating metabolic alterations associated with the postmenopausal state. However, the benefits and risks of HRT have been a matter of debate due to the unexpected findings obtained in 2002 in the Women's Health Initiative (WHI) study, which reported increased risks of suffering from CVDs and endometrial and breast cancers for certain HRT treatments [16]. Currently, the safety and main side effects of this treatment depend on variables such as the type of HRT, treatment duration, and age at which the HRT begins after the final menstrual cycle. Remarkably, the safety and benefits of HRT appear to surpass the risks when it is prescribed to healthy women under 60 years of age or within the first ten years of amenorrhea [16]. While HRT effectively reduces

vasomotor symptoms and osteoporosis, this treatment is less effective at reducing body weight gain and the risk of CVDs (blood clots, stroke, thromboembolism and coronary heart disease) and at ameliorating affective disorders such as Alzheimer's disease and dementia. Moreover, HRT is not advised for women with a medical history of endometrial or breast cancer [16].

In recent years, the controversy about the risks associated with HRT has prompted many women to look for alternative therapies to address menopause, promoting the emergence of alternative approaches such as natural extracts, bioactive compounds and nutraceuticals to ameliorate vasomotor symptoms and metabolic disturbances related to menopause. Among them, isoflavones derived from soy, commonly known as phytoestrogens, are well-researched natural bioactive compounds with beneficial effects on menopause-related alterations. Genistein, the most abundant isoflavone in soy, accounts for 60% of total isoflavones and exhibits twenty-fold greater selectivity for oestrogen receptor (ER) β than for ERα. This selectivity is advantageous because most side effects are associated with binding to ERα [17,18]. However, the biological activity of phytoestrogens varies among individuals because their activity depends on the metabolism of these precursors into more active compounds, which requires the activity of specific intestinal bacteria and hepatic enzymes, and both processes involve well-described interindividual variations. For instance, only the isoflavonoid daidzein is converted into its most bioactive and absorbable isoform, equol daidzein, by approximately 30% of the population [19].

In a very recent study, members of this current team showed that, in ovariectomized (OVX) rats, a postmenopausal model with oestrogen deficiency, the combined consumption of the bioactive compounds hesperidin, phytosterols and curcumin effectively reduced obesity and improved metabolism-related alterations to a very similar

extent to those observed in response to subcutaneous injections of 17β-oestradiol (17β-E2), a treatment that resembles one of the HRTs administered to menopausal women [20]. Specifically, supplementation with this multi-ingredient (MI) significantly decreased the total fat mass content; the weights of mesenteric (MWAT), retroperitoneal (RWAT) and inguinal (IWAT) white adipose tissue depots; and the adiposity index in addition to increasing the total lean mass content and the lean/fat mass ratio, clearly indicating an improvement in body composition. In addition, MI consumption decreased the circulating leptin levels and increased the level of the surrogate marker of insulin sensitivity, R-QUICKI, as well as the adiponectin-to-leptin ratio, which has been described in humans as a predictive and reliable biomarker for adipose tissue inflammation and the cardiometabolic risk associated with obesity [21,22]. These findings paved the way to promote the use of this MI supplement as an alternative therapy to ameliorate obesity and to improve the cardiometabolic health of menopausal women and were consistent with our idea that combined supplementation with different bioactive compounds that act against complementary targets is a suitable strategy to ameliorate cardiometabolic risk factors, as was previously documented in different studies, including some performed by the authors of the present work [23–27]. Similarly, members of our group have consistently reported a significant decrease in the circulating level of histidine in patients with morbid obesity as the severity of nonalcoholic fatty liver disease (NAFLD) increases [27] and based on these findings, we hypothesized that the consumption of a blend of amino acid-related compounds, including histidine, serine, cysteine and carnosine (β-alanyl-L-histidine dipeptide), could be an effective therapy for ameliorating NAFLD because (i) histidine is an essential amino acid that needs to be obtained from the diet; (ii) carnosine is a histidine-containing dipeptide and, therefore, can increase histidine levels; (iii) cysteine is an inhibitor of the histidine catabolizing enzyme ammonia lyase (HAL); (iv)

serine is a precursor of cysteine; and (v) one of the main hallmarks of NAFLD is oxidative stress, and serine and cysteine may increase the cellular levels of glutathione, the most abundant endogenous antioxidant [28]. This hypothesis was validated in both diet-induced and genetic leptin-deficient *ob*/*ob* mouse models and in OVX rats, which displayed decreased hepatic steatosis after the consumption of this amino acid-related MI [27]. Considering our previous results concerning the reported beneficial effects on hepatic steatosis in OVX rats, that NAFLD is a metabolic disorder that frequently accompanies obesity and metabolic syndrome (MetS) [29], that different studies performed mainly in rodents but also in humans have shown that supplementation with carnosine [30,31], serine [32,33], cysteine [34,35] and especially histidine [36–40] can ameliorate obesity, promote glycaemic control, and ameliorate IR, inflammation or oxidative stress, in the present study, we hypothesized that this amino acid-related MI would also be an effective approach for ameliorating obesity and metabolism-related alterations that can occur during the postmenopausal period.

Menopausal women can present increased risks of suffering cognitive impairment, anxiety and depression [41]. Some preclinical studies have shown that histidine intake increases the levels of histamine in the brain, improving learning and memory impairments [42,43] and reducing anxiety-like behaviours [44,45]. Furthermore, different preclinical and clinical studies have shown that carnosine supplementation ameliorates cognitive decline in animal models of Alzheimer's disease, in elderly individuals and in subjects with mild cognitive decline [30]. In addition, some studies performed with rodents [46,47] and one clinical study [48] suggested that carnosine has beneficial effects on anxiety, stress and depression-like behaviours. On the other hand, significant associations between lower levels of cysteine and a lower bone mineral density (BMD) [49] and higher levels of the bone turnover marker carboxy-terminal telopeptide of type I collagen (CTX-1) were

found in postmenopausal women [50], suggesting an important role for this semiessential amino acid in bone metabolism. This idea was reinforced by the fact that cysteine supplementation for 8 weeks counteracted the loss of BMD in OVX mice, showing effects similar to those observed after 17β-E2 injections [51].

The main aim of the present study was to evaluate whether oral intake of an MI supplement including L-histidine, L-carnosine, L-serine and L-cysteine for 8 weeks would exert beneficial effects on fat mass accretion and cardiometabolic risk factors related to the postmenopausal state in an OVX rat model and to explore the underlying mechanisms involved. In this work, we also aimed to investigate the effects of the chronic administration of the MI on bone and behavioural-related parameters to provide insights into the potential of this amino acid-related MI to ameliorate the multifactorial alterations that can occur during menopause. The effects of this MI were compared to those of subcutaneous injections of 17β-E2, an agent that resembles HRT.

MATERIALS & METHODS

Ingredients

L-Histidine base (HIS; Ref.: AMI-019) and L-Cysteine (CYS; Ref.: AMI-011) were purchased from NUTRIFOODS S.L.U. (Barcelona, Spain). According to the supplier, the products were 99.6% and 99.7% pure, respectively. L- Carnosine 98% (CAR; 208170250) was purchased from Thermo Fischer Scientific (Massachusetts, USA). L-Serine (SER; Ref.: S4500) was purchased from Merck KGaA (Frankfurt, Germany).

Animals, diet and treatments

The Animal Ethics Committee of the Technological Unit of Nutrition and Health of EURECAT (Reus, Spain) and the Generalitat de Catalunya approved all procedures (protocol code 11223). The study followed the ‘Principles of Laboratory Animal Care’,

complied with the ARRIVE guidelines and was conducted in compliance with the EU Directive 2010/63/EU for animal experiments. The rodents used in this research consisted of forty 24-week-old female Sprague–Dawley rats (JANVIER LABS, Saint-Berthevin, France). Thirty rats were bilaterally ovariectomized (OVX), and 10 rats underwent a sham operation (SHAM) at the JANVIER facility. Before they arrived at the animal facility of Eurecat, the 40 animals were fed a maintenance rodent chow diet for 1 week to stabilize them because of ovariectomy surgery before shipment at the age of 25 weeks. Throughout the study, all rats were housed in pairs at 22 °C on a 12 h light/dark cycle with lights on at 9:00 am, and they had ad libitum access to food and water. After an acclimatization period of 1 week, the 30 OVX rats were divided into three experimental groups based on the treatment they received for 8 weeks (OVX, OVX-E2, and OVX-MI; n=10 rats per group), and the 10 sham-operated (SHAM; n=10) rats were assigned to the control group. OVX-MI was supplemented daily for 8 weeks with an MI that included four amino acid-related compounds at the following doses per body weight: L-histidine, carnosine and L-serine at 105 mg/kg and L-cysteine at 245 mg/kg. The dosages were obtained by extrapolating the doses used by our group for mice in a previous study [27]. Considering the Reagan–Shaw formula, the doses of histidine, carnosine, and serine used were equivalent to the daily consumption of 1022 mg of these compounds for a 60-kg human [52]. For cysteine, the extrapolated daily intake using the same formula was 2384 mg. For each compound, these dosages are considered acceptable, well tolerated and safe in the context of nutraceutical supplementation [28,36,53,54]. The amino acid-related compounds were dissolved in peach juice enriched with 45.71 mg/mL fructose along with an acid taste masker (AROMA ACTI'MASK PRO, [E414 or gum Arabic]; Metarom Ibérica S.A., Barcelona, Spain) at 10 mg/mL to ensure voluntary consumption and minimize the stress of the animals. The SHAM, OVX and OVX-E2 groups were supplemented daily

with peach juice + fructose at 45.71 mg/mL (vehicle) for 8 weeks. Half of the daily treatment was administered orally via a syringe of 1 mL in a volume of 0.3-0.4 mL between 09:00 and 10:00 am, and the other half was administered via the same protocol between 12:00 and 1:00 pm to guarantee the full voluntary consumption of the treatments. Four days before the beginning of the treatments, the rats were trained to lick peach juice (0.3 mL) to ensure voluntary consumption. OVX-E2 rats also received biweekly subcutaneous injections of 25 μg/kg body weight 17β-oestradiol (Sigma–Aldrich, St. Louis, MO) in a carrier solution of corn oil, whereas the remaining groups received the same dose of the vehicle (corn oil). All groups were fed a standard chow diet (Teklad Global 14% Protein Rodent Diet 2014, Harlan, Barcelona, Spain). The caloric breakdown of the diet (2.9 kcal/g) was 20% protein, 13% fat, and 67% carbohydrates. Body weight was recorded once each week, food was renewed daily, and food intake was documented every 7 days. On Day 57, the rats were sacrificed by decapitation after 6 h of diurnal fasting and without receiving any treatment. Blood samples were collected in heparinized tubes, and plasma was obtained by centrifugation and stored at -70 °C until further analysis. The liver, caecum, kidneys, gastrocnemius and soleus muscles, the left femur and tibia, and the RWAT, MWAT and IWAT depots were rapidly removed, weighed, frozen in liquid nitrogen and stored at -70 °C until further analysis. The right femur and tibia were also collected, immersed in 70% ethanol and stored at room temperature until the three-dimensional microcomputed tomography analysis.

Body composition analyses

An EchoMRI-700™ device (Echo Medical Systems, L.L.C., Houston, TX, USA) was used to evaluate the relative lean and fat mass contents of the rats without anaesthesia on Days 1, 30 and 57. The analyses were performed in triplicate at 8:00 am under ad libitum conditions, and the results are presented as a percentage of body weight.

Adiposity index

The adiposity index was calculated as the sum of the weights of the IWAT, MWAT and RWAT depots (in grams) for each rat and was reported as a percentage of body weight.

HOMA-IR analysis

The homeostasis model assessment-estimated insulin resistance (HOMA-IR) was calculated with the following formula: (fasting glucose level –mmol/L- × fasting insulin level-µU/mL-)/22.5 [55].

Plasma analysis

An enzymatic colorimetric kit was used to determine plasma glucose levels (992330/QCA, Barcelona, Spain). The circulating levels of total cholesterol and high-density lipoprotein cholesterol (HDL-c) were measured using reflectance spectrophotometry with the Vitros® 5600 Integrated System (QuidelOrtho Corporation, San Diego, CA, USA). The non-high-density lipoprotein cholesterol (non-HDL-c) level was calculated by subtracting the HDL cholesterol concentration from the total cholesterol concentration. Circulating insulin levels were measured using a rat/mouse ELISA kit (10-1250-01/MERCODIA, Upssala, Sweden). Plasma leptin levels were determined with a rat ELISA kit (EZRL-83K/Millipore, Barcelona, Spain), and the circulating levels of adiponectin were quantified using a rat total adiponectin/Acrp30 Quantikine ELISA Kit (RRP300/R&D systems, Minnesota, USA). The levels of the inflammatory markers monocyte chemoattractant protein-1 (MCP-1) and C-reactive protein (CRP) were quantified in plasma using the BMS631INST and the ERCRP ELISA kits, respectively (INVITROGEN, Massachusetts, USA). The circulating levels of the biomarkers of bone turnover, procollagen I amino-terminal propeptide (PINP), osteocalcin (OC) and carboxy-terminal telopeptide of type I collagen (CTX-1), were

measured using PINP ELISA kit (AC-33F1, IDS, UK), osteocalcin ELISA kit (AC-12F1, IDS, UK) and CTX ELISA kit (AC-06F1, IDS, UK).

Urine analysis

A commercial ELISA kit was used to quantify the levels of 8-hydroxy-2'-deoxyguanosine (8-OHdG) (STA-320/CELL BIOLABS INC. Chicago, USA) in urine. The levels of this metabolite were normalized to the creatinine levels, which were analysed using the Creatinine Urinary Detection Kit (EIACUN/Thermo Fischer Scientific, Massachusetts, USA).

Analysis of total, oxidized and reduced glutathione levels in the liver (GSH/GSSG ratio)

Liver samples were used to quantify the levels of total glutathione (GSH), reduced GSH, and oxidized GSH (GSSG) using the Glutathione Colorimetric Detection Kit from EIAGSHC/INVITROGEN (Massachusetts, USA). The results are presented in µmol per g of hepatic protein, which was calculated using the BCA assay method.

Histological analysis

Buffered formalin (4% formaldehyde, 4 g/L NaH_2PO_4, 6.5 g/L Na_2HPO_4; pH 6.8) was used to preserve fixed portions of RWAT (n = 8 per group), which were cut at a thickness of 5 µm and stained with haematoxylin & eosin (H&E). An ECLIPSE microscope (ECLIPSE Ti; Nikon, Tokyo, Japan) coupled to a digital sight camera (DS-Ri1, Nikon) was used to obtain the RWAT images (magnification 100×). Image analyses were performed using ImageJ NDPI software (National Institutes of Health, Bethesda, MD, USA; https://imagej.nih.gov/ij, accessed on 22 March 2024, version 1.54g). The

AdipoSoft plugin was used to quantify the adipocyte area in the RWAT sections from the different groups.

Microcomputed tomography analyses

The bone composition of the right tibia and femur was determined postmortem in fixed samples by performing three-dimensional microcomputed tomography (μCT or microCT) analysis, as previously described [20]. The tissue mineral content (TMC), bone mineral content (BMC), tissue mineral density (TMD) and BMD values were quantified from MicroCT scans using GE MicroView software v2.2.

Indirect calorimetry

The Oxylet Pro™ System (PANLAB, Cornellà, Spain) was used to perform indirect calorimetry analyses of the different groups between Days 29 and 33 after the beginning of the treatments, throughout 22 h (from 11:00 am to 09:00 am), under ad libitum conditions and with free access to water. At 09:00 am, the animals received the corresponding treatment and were transferred from their cages to an acrylic box (Oxylet LE 1305 Physiocage, PANLAB). After an initial acclimatization period of 2 h, the respiratory quotient (RQ), the fat and carbohydrate oxidation rates and the energy expenditure (EE) were calculated as previously described [56].

Behavioural evaluation

Elevated plus maze (EPM)—anxiety-like behaviour

The animals were tested in the EPM [57,58] on Day 36 to evaluate anxiety-like behaviour. The EPM test apparatus consisted of four arms, two open arms (45 cm long × 10 cm wide) and two enclosed arms with walls (45 cm long × 10 cm wide × 35 cm height), which were positioned alternatively and extended from a 10 cm square, common central platform

positioned 90° from each other to form the shape of a plus sign. The apparatus was elevated 50 cm above the floor. The rat was placed in the centre of the maze (always facing the same closed arm), and videos of the EPM test were recorded for five minutes (300 s) using a tracking system (ANY-Maze, version 4.82, SD Instruments, US) and analysed to score the distance travelled, time spent and the number of entries into each arm. The apparatus was wiped clean with 70% ethanol before each animal was tested. Behavioural measures were defined according to previous studies [59] and included the following: the frequency of open and enclosed arm entries (OAEs and EAEs), defined as all four paws placed inside an arm; total arm entries; and total time spent in the open (OAT) and enclosed arms (EAT) and in the central area (CT). These data were used to calculate the percentage of OAEs [% OAEs; (open entries/open + enclosed entries) × 100], the percentage of EAEs [% EAEs; (enclosed entries/open + enclosed entries) × 100], the percentage of OAT [%OAT; (time in open arms/300) × 100], the percentage of EAT [%EAT; (time in enclosed arms/300) × 100] and the percentage of CT [%CT; (time in central zone/300) × 100].

Y-maze test—spatial reference memory

The rodents were subjected to the Y-Maze [60] test on Day 40 to assess spatial reference memory. This equipment is composed of three identical arms (45 cm long × 10 cm wide × 25 cm (walls) tall) that are symmetrically placed at an angle of 120° to each other to form a Y shape. This assessment consisted of a habituation phase and a test phase. In the habituation phase, the rats were placed at the end of one of the arms (“start arm”) facing the wall. The rats were allowed to explore two arms of the Y-maze for five minutes (300 s), while entry into the third arm was blocked. The blocked arm was arranged alternately to mitigate potential bias. After the habituation phase, the rats were returned to their home cage for a 1 h intertrial interval. During the test phase, the rats were allowed to explore

all 3 arms of the maze (including the novel third arm, which was previously blocked) for 5 minutes (300 s). The apparatus was wiped clean with 70% ethanol before the habituation and test phases of each animal. The time and number of entries into the novel arm were analysed using a tracking system (ANY-Maze, version 4.82), and the number of alternations was calculated as the number of entries into three different arms in succession. These data were used to calculate the percentage of entries in the novel arm (number of entries in the novel arm/total number of entries × 100), the novel arm preference index (%) using the formula [(time in novel arm/300) × 100] and the spontaneous alternation (%) with the following formula: {[number of alternations/(total number of arm entries - 2)] × 100} [43].

Transcriptomic and gene set enrichment analyses

The transcriptomic analysis was performed on RNA samples from the RWAT of rats in the OVX and OVX-MI groups (n = 7 rats per group). Total RNA was extracted using Tripure Reagent (Roche Diagnostic, Barcelona, Spain) and purified with Qiagen RNeasy Mini Kit spin columns (Izasa, Barcelona, Spain) according to the manufacturer's instructions, and RNA integrity was measured on an Agilent Bioanalyzer (Agilent Technologies, South Queensferry, UK). All samples had optimal quality parameters (RIN > 5) and were used for the construction of next-generation sequencing (NGS) libraries. The subsequent NGS libraries were converted to FASTQ format using Illumina NovaSeq 6000 in S4 flow cell mode (Illumina Way, California, USA). Gene abundance in all RNA-seq data (in both raw counts and transcripts per million) was processed using the Kallisto pipeline [61] based on the *Rattus norvegicus* genome from Ensembl release version 107. The differential gene expression (DGE) analysis was performed using the R/Bioconductor package DESeq2 v1.40.2 [61], and the Benjamini–Hochberg false discovery rate (FDR) test was performed to manage false-positive outcomes. Only the

genes exhibiting an FDR-derived q-value less than 0.1 (*adj.* p value < 0.1) were recognized as DEGs. The resulting gene lists were annotated and filtered for significantly differentially up- and downregulated genes (*adj*. $p < 0.1$ and log2(fold change) > |0| or < |-0|, respectively). The log2(fold changes) for each gene were calculated using the R package Piano v2.16.0 (gene set statistic=reporter) [62]. Fold change values of the significant genes were calculated in Microsoft Excel from the log2(fold changes). The fold change equals the OVX-MI/OVX ratio when the ratio increases or equals -1/ratio when the ratio decreases. KEGG pathway analysis was performed separately for distinctly upregulated, mixed-direction upregulated, mixed-direction downregulated and distinctly downregulated genes based on an *adj.* p value < 0.05 that indicated the enrichment of pathways according to the R package Piano v2.16.0 (nperm=1000) [62]. For the Gene Ontology analysis using g:Profiler, only the "biological process" category (g:GOst, https://biit.cs.ut.ee/gprofiler/gost, accessed on 17 February 2024, version e110_eg57_p18_4b54a898) was applied to test functional enrichment analysis of significantly differentially expressed genes in biological process pathways [63]. Because the results of the whole genome array revealed that not all the significantly differentially expressed genes were identified by the KEGG pathway and g:Profiler programs, we supplemented the significantly enriched biological processes with nonannotated genes from the selected gene set using the scientific literature from biological databases (NCBI, PubMed and Human Protein Atlas, https://www.proteinatlas.org/, accessed on 4 March 2024). As processes overlapped, we consolidated them and assigned new names to better reflect their combined nature. The R package ggplot2 v3.4.4 [64] was used to create a volcano plot with the DGEs to visualize changes in gene expression between groups. R/Bioconductor package ComplexHeatmap v2.16.0 [65] was used to create a heatmap to

visualize significantly regulated KEGG pathways (*adj.* $p < 0.05$) in OVX-MI animals compared with their OVX counterparts.

Statistical analyses

Statistical analyses were performed with IBM SPSS Statistics 28.0 (SPSS, IBM Corp. Armonk, New York, USA). Grubbs' test was used to detect outliers, which were discarded from further analysis. The assumption of normality was determined using the Kolmogorov–Smirnov test, and the homoscedasticity among groups was evaluated using Levene's test. When one or both of these conditions were not met, the data were transformed to the base-10 logarithm to obtain a normal distribution and/or similar variances before statistical testing. One-way ANOVA followed by Duncan's *post hoc* test (p value ≤ 0.05) were used to assess differences among the four groups in the variables analysed at one time point in the present study. The Welch test followed by the Games–Howell *post hoc* test were used when homoscedasticity was not assumed. The Kruskal–Wallis test followed by the Mann–Whitney U *post hoc* test were used as the nonparametric version of one-way ANOVA when the data did not follow a normal distribution. Differences among groups in the evolution of body weight (g), fat (%) and lean mass (%) on Days 1, 30 and 57 were analysed with repeated measures (RM-) ANOVA with time as a within-subject factor and intervention as a between-subject factor. When a significant interaction was found between both factors, one-way ANOVA followed by Duncan's *post hoc* test were used to determine intervention-related differences at each time point among groups. The data are presented as the means ± SEMs (n = 9-10). The level of statistical significance was set at bilateral 5%.

RESULTS

Ovariectomy increased body weight gain and fat accretion and triggered metabolic alterations related to the postmenopausal state

At the beginning of the study, two weeks after surgery, the removal of the ovaries led to a greater baseline body weight in the OVX animals than in their SHAM counterparts (Table 1). As expected [20], at the end of the study, the OVX group displayed increased food intake (Table 1) and decreased EE (Supplementary Table 1) compared to the SHAM group. This finding could explain, at least in part, the greater body weight, body weight gain, fat mass percentage and fat mass gain observed at the end of the study in the OVX group than in the SHAM group (Table 1 and Figures 1A-D). Consistent with the increased fat mass percentage observed in OVX rats, a significant increase in RWAT, MWAT and IWAT depots, as well as an increase in the adiposity index, were reported in these animals (Figures 2A-D). Concurrently, the OVX group exhibited a lower final lean mass percentage, a greater loss of lean mass and a lower lean-to-fat ratio (Figures 1E-G) than the SHAM group. Furthermore, untreated OVX animals displayed elevated circulating levels of leptin, adiponectin and insulin (Figures 2E-G) in addition to an increased HOMA-IR, a surrogate marker of IR [55], and leptin-to-adiponectin ratio (LAR), a good predictor of type 2 diabetes and MetS [66] (Figures 2H and 2I, respectively). In addition, according to the histological analyses of the RWAT, the removal of the ovaries also triggered adipocyte hypertrophy, increased the percentage of larger adipocytes and decreased the number of these cells in the OVX group (Figure 3). OVX rats also displayed higher hepatic levels of oxidized glutathione (GSSG) (Figure 4F) than did their SHAM counterparts. Aside from the metabolic changes observed, OVX rats had a lower TMD in the right femur and a lower BMD and TMB in the right tibia than SHAM animals (Table 2). These results were accompanied by elevated circulating levels of the bone biomarkers

of formation and resorption, OC and CTX-1, respectively (Table 2). Taken together, these results clearly indicate that OVX rats exhibit different hallmarks that can appear in the postmenopausal state, such as body weight gain, fat mass accretion, adipocyte hypertrophy, IR and greater risks of CVD and osteoporosis, as was previously reported [20,67,68].

Table 1: Cumulative food intake and biometric and plasma parameters in sham-operated (SHAM) and ovariectomized (OVX) rats after 8 weeks of intervention

	SHAM	OVX	OVX-E2	OVX-MI	Intervention effect (p value)
Cumulative Food Intake (g)	59.7 ± 0.4^{a}	73.4 ± 1.9^{b}	63.5 ± 2.7^{ac}	67.7 ± 1.7^{bc}	*I* (<0.001)
Biometric parameters					
Initial body weight (g)	338 ± 8^{a}	412 ± 4^{b}	407 ± 9^{b}	414 ± 6^{b}	*I* (<0.001)
Final body weight (g)	358 ± 7^{a}	472 ± 12^{b}	407 ± 15^{c}	455 ± 12^{b}	*I* (<0.001)
Liver (g)	9.8 ± 0.4	10.2 ± 0.3	10.0 ± 0.6	10.0 ± 0.2	NS (0.943)
Caecum (g)	5.15 ± 0.15	6.05 ± 0.45	5.26 ± 0.19	5.45 ± 0.37	NS (0.206)
Kidneys (g)	2.10 ± 0.07	1.96 ± 0.05	2.11 ± 0.10	1.98 ± 0.05	NS (0.348)
Gastrocnemius (g)	2.19 ± 0.09^{a}	2.57 ± 0.09^{b}	2.43 ± 0.10^{b}	2.65 ± 0.05^{b}	*I* (0.002)
Soleus (g)	0.190 ± 0.007	0.202 ± 0.011	0.210 ± 0.011	0.202 ± 0.009	NS (0.562)
Plasma parameters					
Glucose (mmol/L)	7.36 ± 0.30	7.77 ± 0.44	7.92 ± 0.15	7.83 ± 0.15	NS (0.343)
TC (mmol/L)	3.73 ± 0.30	4.05 ± 0.12	3.52 ± 0.14	4.07± 0.15	NS (0.153)
HDL-c (mmol/L)	2.79 ± 0.24	3.07 ± 0.16	2.96 ± 0.20	3.35± 0.11	NS (0.235)
Non-HDL-c (mmol/L)	0.94 ± 0.07^{a}	0.98 ± 0.12^{ab}	0.57 ± 0.10^{c}	0.73 ± 0.06^{bc}	*I* (0.009)
TC/HDL-c Ratio	1.35 ± 0.02^{a}	1.34 ± 0.06^{ab}	1.21 ± 0.04^{bc}	1.22 ± 0.01^{c}	*I* (0.001)

Data are presented as the means ± SEMs (n = 9-10). The serum concentrations of various parameters were determined at the end of the experiment. The TC/HDL-c ratio was calculated as the total cholesterol level divided by the HDL-c level. Different superscript lowercase letters (a, b, c) indicate significantly different mean values (one-way ANOVA and Duncan's *post hoc* test or Welch's test and Games–Howell *post hoc* test or Kruskal–Wallis test and Mann–Whitney U *post hoc* test, $p < 0.05$). *I*: the effect of the intervention. NS: nonsignificant differences. SHAM: sham-operated rats; OVX: ovariectomized rats; OVX-E2: OVX rats treated with 17β-oestradiol; OVX-MI: OVX rats supplemented with the multi-ingredient; TC: total cholesterol; HDL-c: high-density lipoprotein cholesterol; Non-HDL-c: non-high-density lipoprotein cholesterol.

MI and 17β-E2 interventions decreased the body fat content and adipocyte hypertrophy and improved the body composition

As expected, 17β-E2 administration significantly reduced the increase in body weight observed in the OVX group from Day 30 of intervention onwards (Figure 1A) and fully counteracted the body weight gain at the end of the experimental period (Figure 1B) [69]. These findings could be related, at least in part, to the lower food intake observed in the OVX-E2 group than in the OVX group (Table 1) [70]. OVX-MI animals displayed slight decreases in body weight and body weight gain, although the differences compared with

those in the OVX group were not statistically significant (Figures 1A and 1B). This lack of significant effects of MI consumption could be partly explained by the similar cumulative food intake observed between OVX-MI rats and their OVX counterparts (Table 1). Compared with OVX animals, both the MI group and the 17β-E2 injection group showed a significant progressive decrease in fat mass accretion, an effect that was statistically significant from Day 30 of intervention onwards (Figure 1C). This result indicated a significant decrease in fat mass accumulation in both OVX-MI and OVX-E2 rats (30% and 69% lower, respectively) (Figure 1D). These findings are consistent with the significant decreases in RWAT weight (Figure 2A) and adiposity index (26% and 14% lower in OVX-E2 and OVX-MI rats, respectively) (Figure 2D) observed in both groups of animals. Nevertheless, these antiadipogenic effects were more evident in the animals that received the 17β-E2 injections, which also displayed lower MWAT and IWAT weights than their OVX counterparts (Figures 2B & 2C, respectively).

Remarkably, both MI supplementation and 17β-E2 injection effectively ameliorated the adipocyte hypertrophy observed in the RWAT of the OVX group to a similar extent (Figure 3A). An inverse pattern was reported for the number of adipocytes, which was significantly lower in the OVX group than in the OVX-MI and OVX-E2 groups (Figure 3B). Consistent with these findings, representative RWAT histological images (H&E staining) revealed larger adipocytes and fewer adipocytes in the OVX group (Figure 3D) than in the OVX-E2 (Figure 3E) and OVX-MI (Figure 3F) groups. Furthermore, the adipocyte size distribution revealed a decrease in the percentage of larger adipocytes and an increase in the percentage of smaller adipocytes in the RWAT of both OVX-MI and OVX-E2 animals compared to those in the OVX rats, exhibiting a similar pattern to that observed in SHAM rats (Figure 3G). In this study, we also investigated the impacts of the interventions on the lean mass content and body composition. Both OVX-MI and OVX-

E2 animals showed a greater lean mass content than their OVX counterparts from Day 30 onwards (Figure 1E). Consequently, both groups exhibited less lean mass loss than did the OVX group (Figure 1F). In agreement with these findings, MI supplementation and 17β-E2 treatment resulted in an increased lean/fat mass ratio compared to that of their OVX counterparts from Day 30 onwards (Figure 1G).

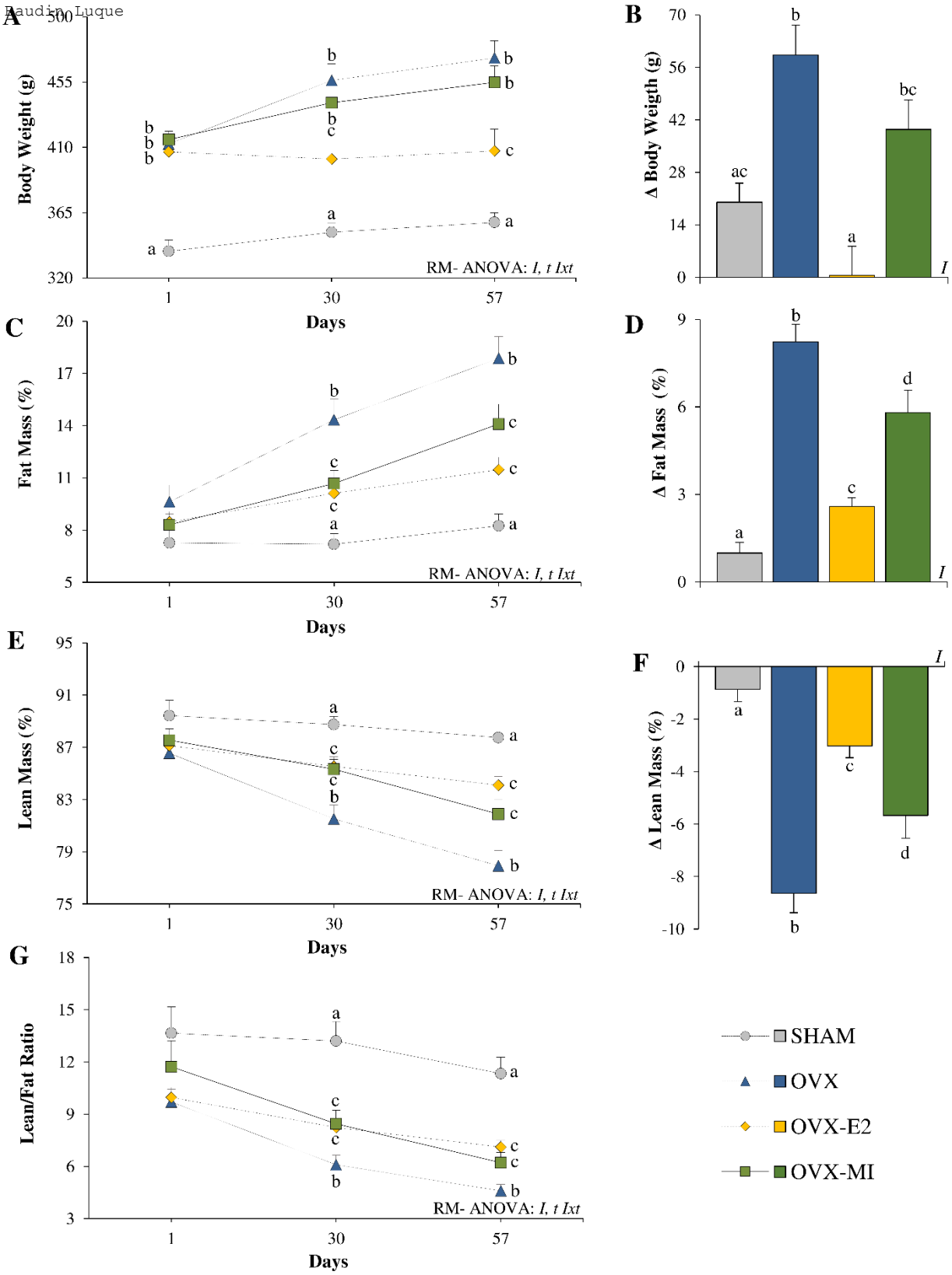


Figure 1 Body weight (A), Δ body weight (B), fat mass (C), Δ fat mass (D), lean mass (E), Δ lean mass (F) and lean/fat ratio (G) in sham-operated (SHAM) and ovariectomized (OVX) rats after 8 weeks of intervention. The data are presented as the means ± SEMs (n = 10). Fat mass and lean mass weights (%) were calculated according to the formula (100* fat or lean/body weight) and are presented as a percentage of body weight. The lean/fat mass ratio was calculated as the lean mass divided by the fat mass. Changes in body weight, fat mass and lean mass were calculated as the differences between the final and initial values of these parameters and are depicted in the figures as Δ values. In Figures 1A, 1C, 1F and 1D, in which the evolution of the variables was analysed over time, the statistical comparisons among groups were conducted using RM-ANOVA. *I*: the effect of intervention, *t*: the effect of time, *Ixt*: the interaction between intervention and time (RM-ANOVA, $p<0.05$). When a significant interaction was observed between both factors, one-way ANOVA followed by Duncan's *post hoc* test or the Kruskal–Wallis test and Mann–Whitney U *post hoc* test ($p < 0.05$) were used to determine intervention-related differences at each time point among groups. In Figures 1B, 1D and 1F, in which the variables were only analysed at the end of the intervention period, one-way ANOVA followed by Duncan's *post hoc* test or the Kruskal–Wallis test and Mann–Whitney U *post hoc* test ($p < 0.05$) were used to assess the effects of the intervention among the four groups. *I*: the effect of the intervention. In all the figures, different superscript lowercase letters (a, b, c, d) indicate significantly different mean values among the groups. SHAM: sham-operated rats, OVX: ovariectomized rats, OVX-E2: OVX rats treated with 17β-oestradiol, OVX-MI: OVX rats supplemented with the multi-ingredient.

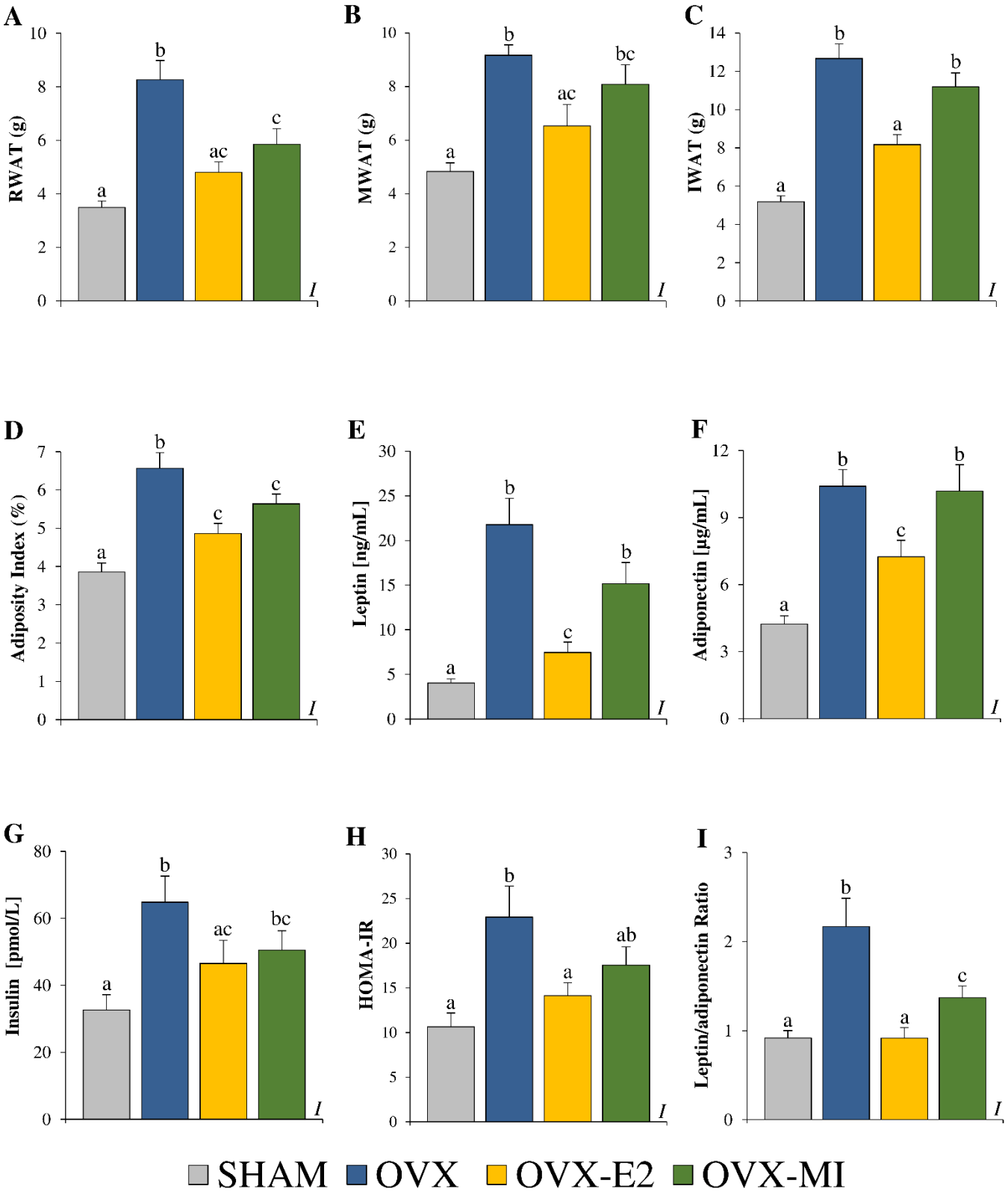


Figure 2 Effects of ovariectomy, 17β-E2 injections and MI treatment on MWAT (A), RWAT (B), and IWAT (C) depot weights; the adiposity index (D); the circulating levels of leptin (E), adiponectin (F) and insulin (G); HOMA-IR (H); and the leptin/adiponectin ratio (I) in sham-operated (SHAM) and ovariectomized (OVX) rats after 8 weeks of intervention. The data are presented as the means ± SEMs (n = 9-10). The adiposity index was computed as the sum of the IWAT, MWAT and RWAT depot weights (in grams) and is reported as a percentage of body weight. The leptin/adiponectin ratio was calculated as the circulating levels of leptin divided by the circulating levels of adiponectin. In each figure, different superscript lowercase letters (a, b, c) indicate significantly different mean values among groups (one-way ANOVA and Duncan's *post hoc* test, $p < 0.05$). *I:* effect of the intervention. SHAM: sham-operated rats, OVX: ovariectomized rats, OVX-E2: OVX rats treated with 17β-oestradiol, OVX-MI: OVX rats supplemented with the multi-ingredient. HOMA-IR: homeostasis model assessment-estimated insulin resistance; IWAT: inguinal white adipose tissue; MWAT: mesenteric white adipose tissue; RWAT: retroperitoneal white adipose tissue.

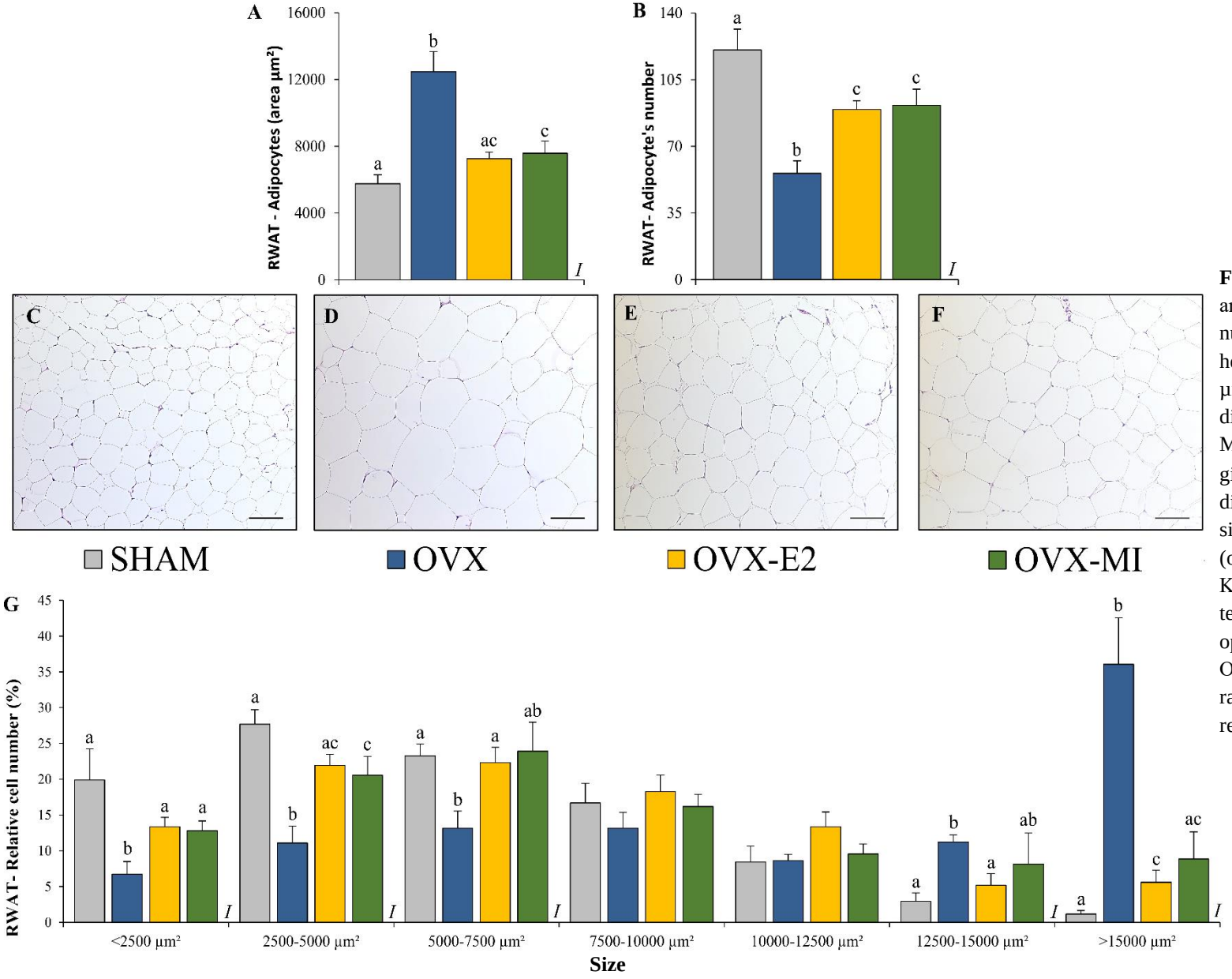


Figure 3 Effects of ovariectomy, 17β-E2 injections and MI treatment on adipocyte's area (A), adipocyte's number (B), representative micrographs of hematoxylin–eosin stained RWAT sections (bar = 100 µm) (C-F, respectively) and adipocyte's size distribution (G) of SHAM, OVX, OVX-E2 and OVX-MI groups after 8 weeks of intervention. Data are given as the mean ± SEM (n = 8). In each figure, different superscript lowercase letters (a, b, c) indicate significantly different mean values among groups (one-way ANOVA and Duncan's post hoc test or Kruskal–Wallis test and Mann–Whitney U post hoc test, $p < 0.05$). *I*: effect of intervention. SHAM: Sham-operated rats, OVX: ovariectomized rats, OVX-E2: OVX rats treated with 17β-oestradiol, OVX-MI: OVX rats supplemented with the multi-ingredient. RWAT: retroperitoneal white adipose tissue.

MI intake improved the total cholesterol to HDL-c ratio, and 17β-E2 intervention decreased circulating non-HDL-c levels

Although no significant differences were observed in the circulating levels of total cholesterol (TC) and HDL-c among groups (Table 1), MI supplementation resulted in a lower atherogenic TC/HDL-c ratio [71] in the OVX-MI group than in their OVX counterparts, and a similar result was found in the OVX-E2 group, although the differences were not statistically significant (Table 1). The OVX-E2 group exhibited significantly lower circulating levels of non-HDL-c than the OVX group (Table 1).

Both MI and 17β-E2 treatments decreased the leptin-to-adiponectin ratio, and 17β-E2 injections improved the surrogate marker of insulin resistance HOMA-IR

In agreement with the decreased adiposity found in OVX-E2 rats and according to the well-known association between circulating levels of leptin and fat mass accretion [72], 17β-E2 treatment resulted in a significant decrease in plasma leptin levels, an effect that was nuanced in the OVX-MI rats in which numerically lower values of this hormone were detected, although no significant differences were reported (Figure 2E). OVX-E2 animals also displayed decreased circulating levels of adiponectin, whereas no significant differences were observed between OVX and OVX-MI rats (Figure 2F). No significant changes were found in plasma glucose levels among the groups (Table 1). Remarkably, 17β-E2 injections significantly counteracted the increases in the circulating levels of insulin (Figure 2G) and in the surrogate marker of IR, HOMA-IR, observed in OVX rats (Figure 2H) (28% and 38% lower, respectively, than those in the OVX group). MI intake produced decreases in both parameters (22% and 24% lower for plasma insulin levels and HOMA-IR, respectively, than in the OVX group), although the differences were not statistically significant (Figure 2G and 2H). Interestingly, both OVX-MI and OVX-2 rats

showed a significantly lower LAR than their OVX counterparts (Figure 2I). A correlation analysis between HOMA-IR and the LAR revealed a strong positive correlation (r = 0.585, 95% CI = 0.330 to 0.760, p < 0.0005). This result suggested that an increased LAR could be associated with IR, as was previously reported [73,74]. Notably, our analysis also revealed significant correlations between the area and number of adipocytes and these metabolic parameters. Thus, strong positive correlations were observed between the adipocyte area and HOMA-IR (r = 0.672, 95% CI = 0.422 to 0.827, p < 0.0005) and between the adipocyte area and the LAR (r = 0.734, 95% CI = 0.517 to 0.862, p < 0.0005). Conversely, strong inverse correlations were found between the number of adipocytes and the HOMA-IR score (r = -0.583, 95% CI = -0.774 to -0.294, p < 0.0005) and between the number of adipocytes and the LAR (r = -0.596, 95% CI = -0.782 to -0.312, p < 0.0005).

MI supplementation reduced the plasma levels of the inflammatory marker CRP, and 17β-E2 injections increased the urinary levels of the marker of oxidative damage of DNA 8-OHdG

Concerning the levels of proinflammatory biomarkers analysed in plasma, no significant changes were observed in the circulating levels of the chemokine MCP-1 among the groups (p= 0.238, one-way ANOVA). Subsequent pairwise comparisons revealed that plasma MCP-1 concentrations tended to increase in OVX rats compared to those in their SHAM counterparts (34.1% higher; p=0.099, Student's t test), and both the E2 and MI treatments counteracted this increase, although the differences were not statistically significant with respect to their OVX counterparts (22.2% and 18.5% lower, p=0.118 and p=0.102, respectively, Student's t test) (Figure 4A). In addition, an inverse correlation was observed between the adipocyte number and MCP1 levels (r = -0.395, 95% CI = -0.653 to -0.053, p < 0.0005). Although the circulating levels of the acute proinflammatory

marker CRP did not increase in OVX rats compared with SHAM rats, the animals that received the MI displayed lower circulating levels of this protein than their OVX counterparts (Figure 4B). Intriguingly, OVX-E2 rats showed a sharp increase (146% higher compared with OVX animals) in the urinary levels of the marker of oxidative damage of DNA 8-OHdG [75] (Figure 4C), an effect that was not observed in response to MI supplementation. Although no changes in total GSH levels, reduced GSH levels or the GSH/GSSG ratio were detected among the groups (Figure 4D, 4E & 4G, respectively), all three ovariectomized groups exhibited significantly higher hepatic levels of oxidized GSH than their SHAM counterparts, and any treatment could counteract this increase caused by ovariectomy (Figure 4F).

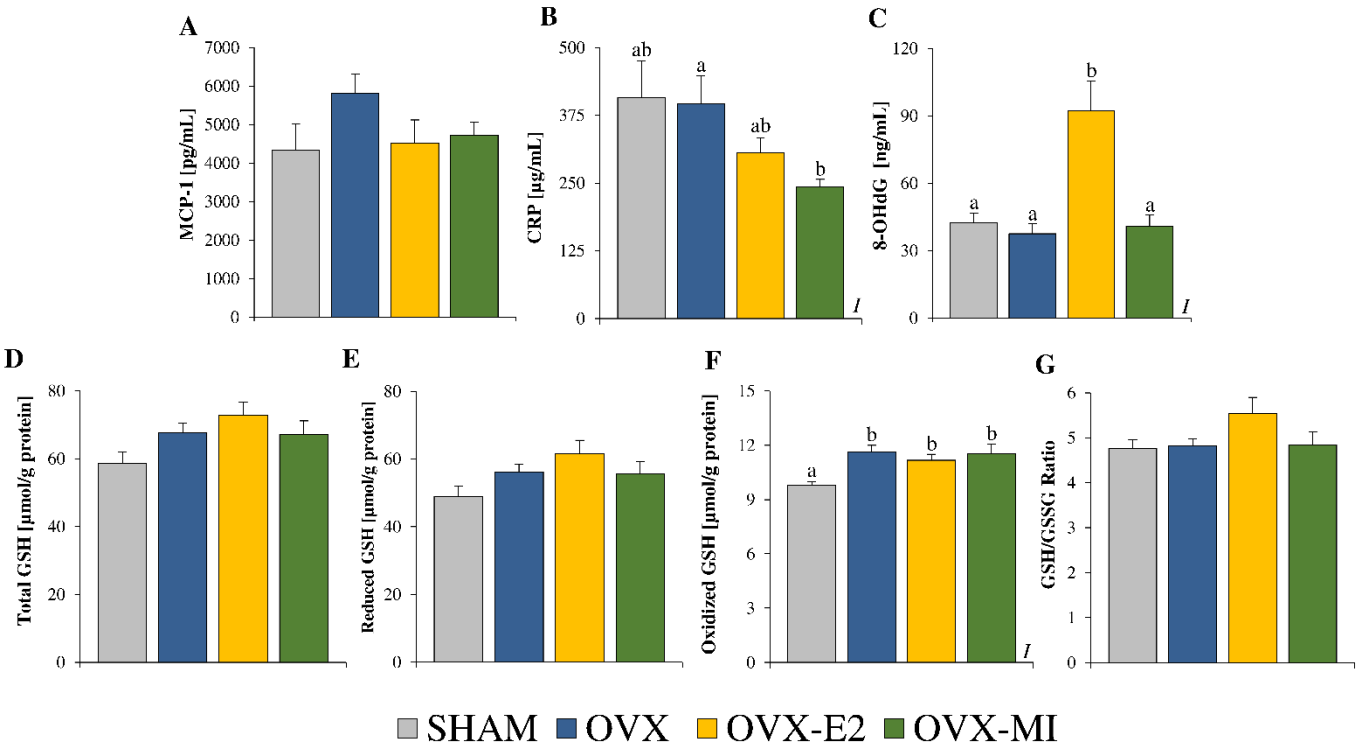


Figure 4 Effects of ovariectomy, 17β-E2 injections and MI treatment on the circulating levels of MCP-1 (A) and CRP (B); urinary 8-OHdG concentrations (C); total GSH (D), reduced GSH (E) and oxidized GSH levels in the liver (F); and the hepatic GSH/GSSG ratio (G) in sham-operated (SHAM) and ovariectomized (OVX) rats after 8 weeks of intervention. The GSSG/GSH ratio was calculated as the oxidized GSH level divided by the reduced GSH level. The data are presented as the means ± SEMs (n = 9-10). In the figures, different superscript lowercase letters (a, b) indicate significantly different mean values among groups (one-way ANOVA and Duncan's *post hoc* test or Kruskal–Wallis test and Mann–Whitney U *post hoc* test, $p < 0.05$). *I:* effect of the intervention. SHAM: sham-operated rats, OVX: ovariectomized rats, OVX-E2: OVX rats treated with 17β-oestradiol, OVX-MI: OVX rats supplemented with the multi-ingredient. MCP-1: monocyte chemoattractant protein-1; CRP: C-reactive protein; 8-OHdG: 8-hydroxy-2'-deoxyguanosine; GSH: glutathione; GSSG: oxidized glutathione.

17β-E2 injections increased the bone mineral content in the tibia and counteracted the increase in the level of the biochemical marker of bone turnover osteocalcin induced by ovariectomy

No significant changes in the weight or length of either femurs or tibias were found among the groups (Table 2). According to the μCT analyses performed on the right femur, no significant changes in BMD, BMC or TMC were observed among the groups (Table 2). However, 17β-E2 treatment resulted in an increased TMD in the femur, consistent with the effects of ovariectomy on the OVX group (Table 2). Moreover, μCT analyses of the right tibia revealed that 17β-E2 administration increased the BMC and TMC compared to those in the OVX group (Table 2). Concerning the circulating levels of the biomarkers of bone turnover, 17β-E2 injections counteracted the increase observed in the level of the biomarker of bone formation OC in the OVX animals and decreased the circulating levels of the bone resorption biomarker CTX-1, but the latter effect was not statistically significant (12.6% lower, p=0.188 compared with OVX rats, Student's t test) (Table 2). Conversely, MI consumption did not improve μCT-related parameters in either the femur or tibia and did not change the circulating levels of bone turnover biomarkers (Table 2).

Table 2: Bone-related parameters in sham-operated (SH) and ovariectomized (OVX) rats after 8 weeks of intervention

	SHAM	OVX	OVX-E2	OVX-MI	Intervention effect
Biometric parameters					
Femurs (g)	2.26 ± 0.04	2.38 ± 0.06	2.28 ± 0.05	2.31 ± 0.04	NS (0.350)
Femurs (cm)	3.80 ± 0.03	3.88 ± 0.03	3.83 ± 0.03	3.91 ± 0.03	NS 0.058)
Tibias (g)	1.82 ± 0.03	1.93 ± 0.05	1.89 ± 0.04	1.91 ± 0.04	NS (0.282)
Tibias (cm)	1.21 ± 0.04	0.93 ± 0.04	1.09 ± 0.02	0.97 ± 0.02	NS (0.304)
Microcomputed tomography analyses (μCT)					
BMD (mg/cc)	356 ± 14	328 ± 14	343 ± 9	312 ± 10	NS (0.074)
TMD (mg/cc)	1020 ± 14^{a}	936 ± 10^{b}	977 ± 19^{c}	920 ± 12^{b}	*I* (<0.001)
BMC (mg)	142 ± 6	140 ± 3	145 ± 4	138 ± 3	NS (0.717)
TMC (mg)	137 ± 6	135 ± 3	139 ± 4	132 ± 2	NS (0.790)
Right tibia (μCT)					
BMD (mg/cc)	271 ± 15^{a}	224 ± 8^{b}	228 ± 11^{b}	201 ± 7^{b}	*I* (0.003)
TMD (mg/cc)	900 ± 24^{a}	793 ± 9^{bc}	838 ± 21^{b}	779 ± 11^{c}	*I* (<0.001)
BMC (mg)	140 ± 5^{ab}	134 ± 3^{b}	153 ± 7^{a}	134 ± 4^{b}	*I* (<0.001)
TMC (mg)	135 ± 5^{ab}	128 ± 2^{b}	147 ± 6^{a}	127 ± 4^{b}	*I* (0.015)
Plasma parameters					
OC (ng/mL)	114 ± 10^{a}	209 ± 24^{b}	137 ± 4^{a}	245 ± 14^{b}	*I* (<0.001)
CTX-1 (ng/mL)	14.4 ± 1.3^{a}	22.0 ± 1.1^{bc}	19.2 ± 1.7^{b}	23.5 ± 1.5^{c}	*I* (<0.001)
PINP (ng/mL)	7.94 ± 0.66	11.10 ± 1.51	8.22 ± 0.36	8.29 ± 0.50	NS (0.463)

Data are presented as the means ± SEMs (n = 9-10). The circulating levels of the biomarkers of bone turnover in serum were determined at the end of the experiment. Microcomputed tomography analyses of the right femur and tibia were quantified from MicroCT scans using GE MicroView software v2.2. Different superscript lowercase letters (a, b, c) indicate significantly different mean values (one-way ANOVA and Duncan's *post hoc* test, $p < 0.05$). *I*: effect of the intervention. NS: nonsignificant differences. SHAM: sham-operated rats; OVX: ovariectomized rats; OVX-E2: OVX rats treated with 17β-oestradiol; OVX-MI: OVX rats supplemented with the multi-ingredient; OC: osteocalcin; CTX-1: carboxy-terminal telopeptide of type I collagen; PINP: procollagen I amino-terminal propeptide; BMD: bone mineral density; TMD: tissue mineral density; BMC: bone mineral content; TMC: tissue mineral content.

Transcriptional changes in the RWAT of ovariectomized rats after MI supplementation

We performed a transcriptomic analysis of RWAT samples from OVX and OVX-MI animals to provide insights into the mechanisms underlying the antiadiposity effects on OVX-MI rats. KEGG pathway analysis of all the gene expression data revealed that the most significantly affected (downregulated) pathways encompassed a comprehensive range of immune, inflammation and defence processes, including the T-cell and B-cell receptor signalling pathways, cytokine–cytokine receptor interactions and chemokine signalling pathways, among others (Figure 5A). Other frequently classified processes included cytoskeleton and cellular networks, such as focal adhesion and extracellular matrix (ECM) receptor interaction, as well as pathways related to the degradation of cellular components, such as the proteasome, endocytosis and lysosome (Figure 5A). Furthermore, glycoconjugate and lipid metabolism, as well as pathways related to glucose

homeostasis, were also affected (Figure 5A). The differential gene expression (DGE) analysis revealed 188 genes that were differentially regulated between OVX and OVX-MI animals, many of which (62.8%, 118 genes) were downregulated (Figure 5B). Furthermore, hierarchical clustering analysis based on the significantly differentially expressed genes revealed distinct clustering patterns between the OVX and OVX-MI groups (Figure 5C). Of these 188 genes, 14 were unknown and therefore could not be grouped into any pathway. The 174 remaining known genes were distributed into different biological processes according to the information obtained via KEGG pathway analysis, enrichment analyses using the g:Profiler program, and information obtained from the scientific literature and various biological databases (NCBI, PubMed and Human Protein Atlas) (Figure 5D). The most representative biological processes were cell proliferation, differentiation and death, cytoskeleton and cellular network, and immunity, inflammation and response to stress (Figure 5D). Other biological processes that were also affected included energy homeostasis, carbohydrate and lipid metabolism, transport of small molecules (ions, amino acids and vitamins) and protein processing and ubiquitination (Figure 5D). The pathways related to these biological processes, as well as the most representative genes belonging to these pathways, are included in Table 3. The patterns of expression of many of these genes are analysed in the Discussion section.

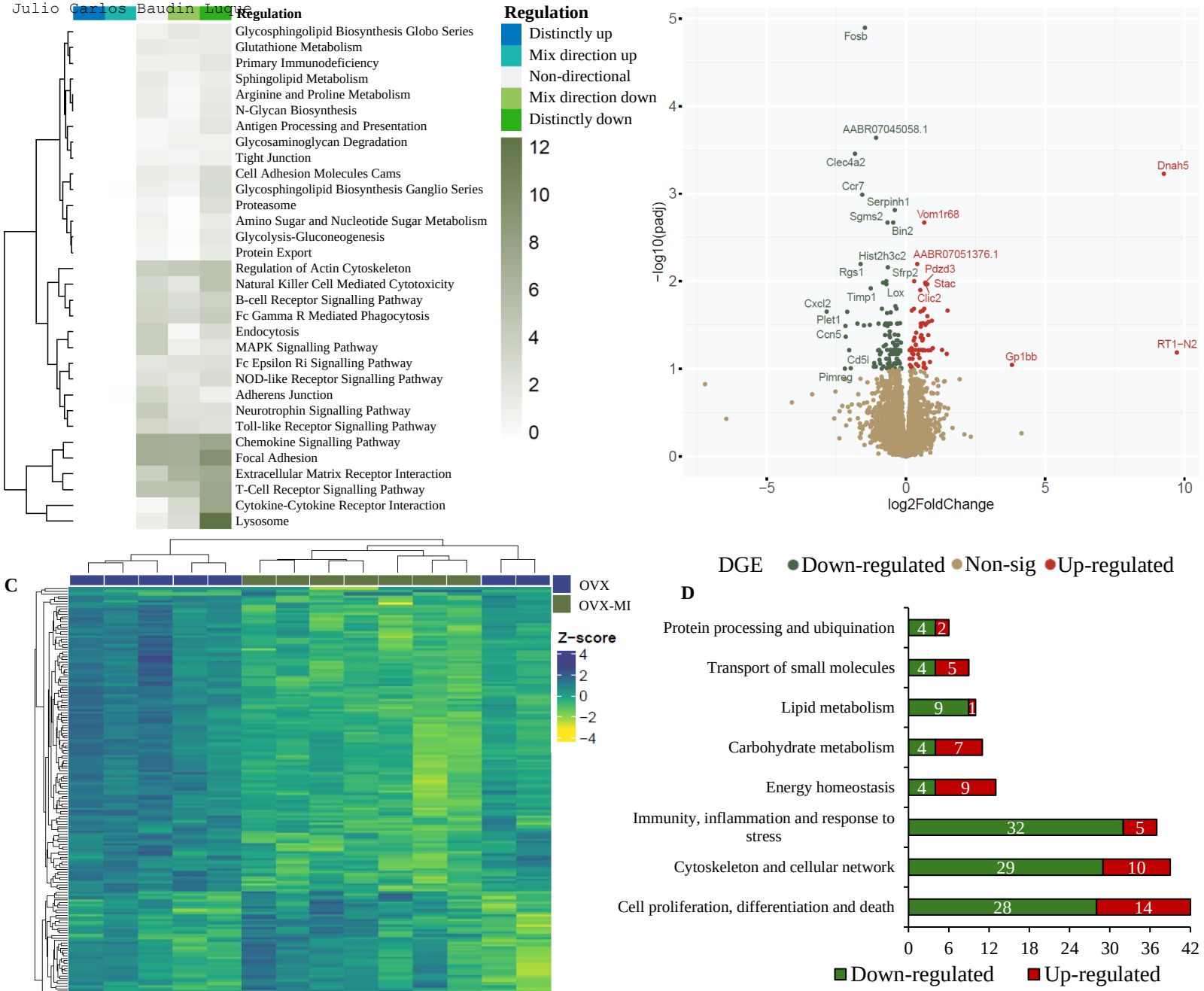


Figure 5 Transcriptional changes in RWAT of OVX and OVX-MI rats (n =7 per group) after 8 weeks of intervention. Figure 4A, heatmap visualizing significantly regulated KEGG pathways (*adj.* p < 0.05) in OVX-MI group in comparison with OVX group. The colour scale represents negative log10 scaled adjusted p values of different directionality regulation classes. The non-directional adjusted p values were computed from the gene statistics disregarding the direction of expression. Mix-direction down and mix-direction up adjusted p values were computed by considering the segment of the gene statistics that are downregulated and upregulated, respectively. Distinct-directional adjusted p values were calculated using expression direction along with gene statistics. The distinct-direction up adjusted p values were exclusively influenced by the upregulation of genes. By contrast, distinct-direction down adjusted p values were influenced by downregulation of genes and not influenced by upregulation and downregulation together. Figure 4B, volcano plot visualizing gene expression changes in RWAT of OVX-MI rats *versus* OVX animals. Significant down and up genes regulated were highlighted with an *adj.* p < 0.1 and a log2 (Fold-Change) ≤ -1 or ≥ 1 in green and red colour, respectively. Statistical significance was tested using DESeq2. Figure 4C, heatmap visualizing expression pattern of the 188 significant genes with an *adj.* p < 0.1 represented by Z score transformed log2 counts per million. Column annotation represents intervention groups OVX and OVX-MI. Figure 4D, classification into biological processes of the genes affected by MI consumption. All known genes (188) differentially expressed (*adj.* p < 0.1) between the OVX-MI and OVX animals were classified using the g:Profiler, KEGG, biological databases (NCBI, human protein atlas) and the scientific literature. OVX: Ovariectomized rats; OVX-MI: OVX rats supplemented with the Multi-Ingredient; KEGG: Kyoto Encyclopaedia of Genes and Genomes; RWAT: retroperitoneal white adipose tissue.

Table 3: Functional categorization of differentially expressed genes in the RWAT of OVX-MI rats

Biological process	*Main-related pathway*	*Gene name*	*Gene symbol*	*Gene ID*	*FC*	*Adj. p value*
Immunity, inflammation and response to stress	Cytokine mediated inflammation	*Interleukin 1 beta*	*Il1b*	24494	-2.11	0.095
		Fas ligand	*Faslg*	25385	-1.63	0.077
		Prostaglandin-endoperoxide synthase 2	*Ptgs2*	25526	-1.90	0.087
	Chemokine mediated inflammation	*C-X-C motif chemokine ligand 2*	*Cxcl2*	114105	-7.19	0.022
		C-C motif chemokine receptor 7	*Ccr7*	287673	-2.97	0.001
	Immune cell-cell communication	*Cd5 molecule-like*	*Cd5l*	310693	-3.95	0.099
		Cd28 molecule	*Cd28*	25660	-1.67	0.030
		C-type lectin domain family 4, member A2	*Clec4a2*	297584	-3.56	0.000
	Signalling	*Fc gamma receptor 1A*	*Fcgr1a*	295279	-1.58	0.032
		Spi-B transcription factor	*Spib*	499146	-2.84	0.032
		Bruton tyrosine kinase	*Btk*	367901	-1.46	0.093
Lipid metabolism	Fatty acid metabolism	*Fatty acid binding protein 3*	*Fabp3*	79131	-2.20	0.086
		Acyl-coa thioesterase 4	*Acot4*	681337	1.56	0.088
	Sterol metabolism	*Cytochrome P450, family 11, subfamily a, polypeptide 1*	*Cyp11a1*	29680	-1.65	0.053
		Oxidized low density lipoprotein receptor 1	*Olr1*	140914	-3.35	0.030
		Vacuole membrane protein 1	*Vmp1*	192129	-1.30	0.059
	Phospholipid metabolism	*Sphingomyelin synthase 2*	*Sgms2*	310849	-1.58	0.002
		Sphingomyelin phosphodiesterase 3	*Smpd3*	94338	-1.68	0.041
Carbohydrate metabolism	Glucose and insulin homeostasis	*Growth factor receptor bound protein 14*	*Grb14*	58844	-1.51	0.030
		Gamma-aminobutyric acid type A receptor subunit gamma 3	*Gabrg3*	79211	1.82	0.084
		Zinc finger protein 407	*Zfp407*	307213	1.23	0.010
		Glucagon receptor	*Gcgr*	24953	2.82	0.022
Cell proliferation, differentiation and death	Cell fate determination and differentiation	*Fosb proto-oncogene, AP-1 transcription factor subunit*	*Fosb*	100360880	-2.78	0.000
		Fos proto-oncogene, AP-1 transcription factor subunit	*Fos*	314322	-2.46	0.032
		Cellular communication network factor 5	*Ccn5*	29576	-4.51	0.032
		Mesenteric estrogen-dependent adipogenesis	*Medag*	360757	-1.40	0.062
		GLI pathogenesis-related 1	*Glipr1*	299783	-1.62	0.030
		Growth differentiation factor 10	*Gdf10*	79216	-1.83	0.099
		Activating transcription factor 5	*Atf5*	282840	-1.46	0.023
		Secreted frizzled-related protein 2	*Sfrp2*	310552	-1.63	0.010
		Bone morphogenetic protein 2	*Bmp2*	29373	-1.30	0.019
		Snail family transcriptional repressor 1	*Snai1*	1164903	-1.43	0.100
		Early growth response 2	*Egr2*	114090	-1.91	0.068
		V-set immunoregulatory receptor	*Vsir*	690899	-1.30	0.068
		Tax1 binding protein 3	*Tax1bp3*	360564	-1.28	0.088
		Activating transcription factor 3	*Atf3*	25389	-1.51	0.092
		Early growth response 1	*Egr1*	24330	-1.50	0.037
	Cell proliferation	*Marker of proliferation Ki-67*	*Mki67*	291234	-1.46	0.030
	Cell death - *Apoptosis*	*Niban apoptosis regulator 2*	*Niban2*	362115	-1.19	0.061
		BCL2-related protein A1	*Bcl2a1*	170929	-1.73	0.055
Cytoskeleton and cellular network	Extracellular matrix (ECM) organization	*Thrombospondin 2*	*Thbs2*	292406	-1.69	0.032
		Secreted protein acidic and cysteine rich	*Sparc*	24791	-1.32	0.041
		Lysyl oxidase	*Lox*	24914	-1.63	0.011
		Htra serine peptidase 1	*Htra1*	65164	-1.15	0.063
		Camp responsive element binding protein 3-like 1	*Creb3l1*	362165	-1.35	0.087
		Biglycan	*Bgn*	25181	-1.51	0.084
		TIMP metallopeptidase inhibitor 1	*Timp1*	116510	-2.40	0.012
		Collagen type I alpha 2 chain	*Col1a2*	84352	-1.47	0.096
		Collagen type V alpha 1 chain	*Col5a1*	85490	-1.23	0.066
		Collagen type V alpha 2 chain	*Col5a2*	85250	-1.21	0.041
		Serpinh1 serpin family H member 1	*Serpinh1*	29345	-1.32	0.002
	Regulation of actin cytoskeleton	*Lymphocyte cytosolic protein 1*	*Lcp1*	306071	-1.52	0.092
		Profilin 1	*Pfn1*	64303	-1.25	0.068
	Cell adhesion	*FERM domain containing kindlin 3*	*Fermt3*	309186	-1.52	0.099
		Cadherin 11	*Cdh11*	84407	-1.87	0.065
	Cytoskeletal filaments	*Actin, beta*	*Actb*	81822	-1.23	0.048
Energy homeostasis	Mitochondrial ATP system/oxidative phosphorylation	*Uncoupling protein 2*	*Ucp2*	54315	-1.24	0.054
		Cytochrome c oxidase II, mitochondrial	*Mt-co2*	26198	1.44	0.022
		NADH dehydrogenase 5, mitochondrial	*Mt-nd5*	26202	1.40	0.075
		NADH dehydrogenase 6, mitochondrial	*Mt-nd6*	26203	1.43	0.013
		NUBP iron-sulfur cluster assembly factor like	*Nubpl*	299008	1.37	0.061
	Cellular energy sensing	*Nicotinamide nucleotide adenylyltransferase 2*	*Nmnat2*	289095	1.66	0.030

Abbreviations: RWAT, retroperitoneal white adipose tissue; FDR, false discovery rate; MI, multi-ingredient; OVX, ovariectomized rats. FC: fold changes in OVX-MI vs. OVX animals. The + symbol indicates upregulation, and the - symbol indicates downregulation in the OVX-MI animals. Genes with FDR-derived *adj. p* value < 0.1 from the microarray data analysis are shown.

MI and 17β-E2 treatments did not increase energy expenditure or substrate oxidation

No significant variations were identified either in the RQ or in fat and carbohydrate oxidation among the groups (Supplementary Table 1). A lower EE was observed in both OVX and OVX-MI animals than in their SHAM counterparts, after considering the whole 21-hour period and both the light and dark phases separately (Supplementary Table 1). A comparable pattern was observed in the animals that received the 17β-E2 injections, although the differences were not statistically significant compared to the SHAM animals across the entire 21-hour period and the dark phase (Supplementary Table 1).

MI and 17β-E2 treatments did not affect anxiety-like behaviours or short-term memory

Rats were subjected to the EPM test to evaluate their anxiety-like behaviours and the effects of MI and 17β-E2 treatments/intervention. Behaviour in the open arms is indicative of anxiety in the animal, with a large amount of time and entries into the open arms indicating low anxiety [58], while the distance travelled in the enclosed arms is considered a measure of locomotion [76]. No significant differences in any anxiety-like behaviour-related parameters were detected in the percentage of entries (in the open and enclosed arms, OAE % and EAE %, respectively) or in the time spent (in the central zone, open arm and enclosed arm, CT %, OAT % and EAT %, respectively) among the groups (Supplementary Figures 1A and 1B). Animals were also challenged with the Y-maze to evaluate their short-term spatial reference memory and the effects of MI and 17β-E2 treatments. This test is based on the natural drive due to the innate curiosity of rodents to explore novel environments, and a rat with no preference for any of the arms during the testing session is classified as having poor spatial memory [60]. No differences were detected among the experimental groups in terms of the percentage of entries and time spent in the novel arm (novel arm preference index (%)) or spontaneous alternation (%) (Supplementary Figures 1C-E). These data indicate that ovariectomy did not produce

alterations in behaviour-related parameters, unlike what was previously described [77,78], and this result could partially explain the lack of beneficial effects of MI consumption or 17β-E2 injections on anxiety-related behaviours and short-term memory.

DISCUSSION

In this study, we examined the effects of 8 weeks of supplementation with the MI containing histidine, carnosine, cysteine and serine on menopause-related complications in OVX rats, a well-established preclinical model of postmenopausal oestrogen deficiency. We found that this treatment exerted beneficial effects on obesity and immunometabolic-related alterations, including (1) decreased adiposity and RWAT adipocyte hypertrophy, (2) improved body composition, as evidenced by the increased lean body mass and lean/fat mass ratio, (3) reduced leptin-to-adiponectin and cholesterol to HDL-cholesterol ratios, (4) decreased circulating levels of the proinflammatory marker CRP, and (5) improved RWAT gene expression profile towards better adipocyte structure, morphology and immunometabolic function. Overall, these findings confirmed our hypothesis and highlighted the potential of the consumption of this amino acid-related MI as an alternative therapy for managing obesity and improving immunometabolic health in menopausal women.

Many postmenopausal women experience changes in body composition and a redistribution of body fat towards increased fat accumulation in the abdominal region. These changes may lead to the appearance of metabolic disturbances, increasing the risks of MetS and CVDs [6,8]. The reduced adiposity observed in OVX rats supplemented with the MI compared to their OVX counterparts shown herein could be attributed, at first glance, to the protective effect on obesity that has been previously reported for different amino acids, including histidine and carnosine, and, to a much lesser extent, for serine

and cysteine, in both animal models and humans [30,36,37]. Nevertheless, to the best of our knowledge, very limited data are available regarding the antiobesity effects of these four bioactive compounds administered alone or in combination on OVX rodent models. To the best of our knowledge, only one study has focused on the effects of a 5-day treatment with histidine between nonovariectomized and OVX rats in the context of obesity, reporting a lower suppressive effect on food intake in OVX animals than in their counterparts and suggesting the activation of histamine neurons as a possible potential mechanism to explain the described effects [79]. The decreased EE reported in OVX rats compared to their SHAM counterparts was consistent with numerous studies showing that the body weight gain accompanied by progressive fat accretion occurring in menopausal and postmenopausal women can be associated with a decreased EE [80–82]. In the present study, a reasonable speculation was that supplementation with the MI could mitigate fat mass gain through the enhancement of EE and the inhibition of food intake, two well-established mechanisms by which different bioactive compounds could exert their beneficial effects [81]. In this context, two studies showed that the intake of histidine decreased food intake, which was accompanied by decreased RWAT weight in aged male Wistar rats [83,84]. Furthermore, López-Gonzales et al. showed that serine supplementation increased EE by activating brown fat thermogenesis in high-fat diet-fed C57BL/6N-Rj male mice [85], and long-term L-serine administration for 6 months to aged C57BL/6J mice significantly reduced food intake and body weight gain [33]. In our study, the lack of effects on food intake and EE observed in OVX-MI *versus* OVX rats indicated that the modulation of these processes was not the mechanism underlying the antiobesity effects observed in response to MI consumption.

The effect on fat mass accretion reported in the OVX-MI animals, although significant, was weaker than we observed in response to 17β-E2 injections. This superior effect

observed on OVX-E2 animals could be attributed to their decreased EE and food intake, two effects that were previously described [20,86,87] and that also contributed to explaining the clear decrease in body weight and body weight gain observed in response to this pharmacological treatment, which was not significantly reported after MI consumption. Remarkably, both groups of treated rats displayed a lower loss of lean mass (expressed as a percentage of body weight) than their OVX counterparts over time, which is indicative of greater muscle mass accretion [88] and explains, at least in part, why the decreased adiposity reported after MI consumption was not accompanied by significantly lower body weight in OVX-MI rats. The increased lean/fat mass ratio found in both OVX-MI and OVX-E2 animals reinforces the idea that both 17β-E2 injections and MI consumption promoted a shift towards a healthier body composition in ovariectomized rats [89,90], which was previously described by our group in response to other bioactive compounds [20].

The hypertrophy observed in the RWAT of OVX animals compared to that in their SHAM counterparts, which was accompanied by increased circulating levels of insulin, HOMA-IR and LAR, a reliable biomarker of MetS and diabetes risk, is consistent with scientific evidence indicating that WAT hypertrophy is associated with IR and inflammation [91]. Thus, the lower RWAT hypertrophy observed in both OVX-E2 and OVX-MI animals compared to OVX rats could explain, at least in part, the improved metabolic health observed in both groups of animals, as evidenced by the significant decrease in the LAR and by the lower circulating levels of insulin (28.2% and 22.1% in OVX-E2 and OVX-MI rats, respectively) and HOMA-IR (38.4% and 23.6% in OVX-E2 and OVX-MI rats, respectively), although the differences in these two latter parameters were statistically significant only for the rats that received the E2 injections. Although these correlations do not imply causality, the strong positive correlations found between HOMA-IR/LAR

and the adipocyte area of the RWAT in all the animals included in the study, as well as the decreased circulating CRP levels reported in OVX-MI rats, also suggest an improvement in the immunometabolic health of the rats supplemented with the MI.

Our transcriptomic analysis of the RWAT of both OVX and OVX-MI animals reinforced our hypothesis that decreased hypertrophy in response to MI supplementation is associated with an immunometabolic benefit. Thus, the increased mRNA levels of the gene encoding ZFP407, which stimulates insulin-mediated glucose uptake in adipocytes and protects against adipocyte hypertrophy and IR in mice [92], as well as the overexpression of the gene encoding GABRG3, a γ-aminobutyric acid (GABA) receptor that mediates the antiadipogenic, antidiabetic and anti-inflammatory effects of GABA [93,94], which is found in the RWAT of OVX-MI animals, are consistent with this idea. We also detected marked overexpression of *Gcgr*, a gene that encodes the glucagon receptor, which is expressed (at low levels) in WAT and mediates both lipolysis and glucose uptake induced by glucagon in adipocytes. Remarkably, in humans, *GCGR* expression was positively associated with a reduction in both the visceral and subcutaneous WAT volume and with improved insulin sensitivity, and in rodents, GCGR activation protected against obesity [95,96]. The decreased expression of *grb14*, a negative regulator of the insulin receptor signalling pathway that is overexpressed in the WAT of obese animals and humans and/or in individuals with type 2 diabetes [97–99], in the RWAT of OVX-MI animals supports our hypothesis.

Obesity is characterized by increased collagen production in WAT, which can be interpreted as an adaptative response to fat mass accretion, requiring the remodelling of the ECM to support adipocyte growth [100–102]. Thus, the downregulation of the genes encoding the collagens COL1A2, COL5A1, and COL5A2 observed in the RWAT of OVX-MI rats, the levels of which were increased in the epididymal WAT of obese and

type II diabetic *db/db* mice [100], is consistent with the protective effect on hypertrophy observed in response to the consumption of this blend of amino acid-related compounds. The lower *creb3l1*, *bmp2, lox*, *timp1, sparc, bgn* and *htra1* expression levels reported in our study reinforce this idea. Thus, CREB3L1 is a transcription factor that can be activated by BMP2, which induces the expression of *col1a1*, *col5a1* and possibly *col1a2* [103]. LOX is a protein that enhances collagen crosslinking in the ECM and enhances adipocyte tissue stiffness, and its activity and mRNA and protein levels are increased in adipocytes and adipose tissue macrophages (ATMs) of both mice and humans with obesity [104,105]. Bariatric surgery decreased *LOX* expression in both subcutaneous WAT and peripheral blood mononuclear cells, and macrophage depletion ameliorated obesity-induced LOX and WAT stiffening [104], which is in agreement with the beneficial effect associated with *LOX* downregulation. The levels of the tissue inhibitor of matrix metalloproteinase 1 (TIMP1), which suppresses the transformation of the ECM, were increased in both the WAT [106,107] and serum [106] of obese mice. In addition, *timp1* mRNA levels are positively correlated with gonadal fat weight [107], and diet-induced obese mice lacking TIMP1 displayed smaller adipocyte diameters than their wild-type counterparts [108]. Similarly, the expression of the gene encoding SPARC, an ECM-related protein involved in adipose tissue remodelling and fibrosis due to its role in collagen assembly, was increased in animal models and humans with obesity [109–111], and SPARC mRNA and circulating protein levels were positively correlated with BMI in humans [110,111] and with waist circumference and total adipose tissue area in women [111]. Furthermore, the mRNA levels of the gene encoding biglycan (BGN), which interacts with collagens and elastins in the ECM, were higher in both subcutaneous and visceral adipose tissues from obese women than in those from normal-weight women and were positively correlated with BMI, adipocyte size and total adipose tissue area [112]. OVX-MI rats also displayed

significantly decreased RWAT expression of the gene encoding a serine protease present in WAT, HTRA1, which plays a key role in ECM turnover in WAT [113]. Treatment of mesenchymal stem cells (MSCs) undergoing adipogenesis with exogenous HTRA1 impaired their development into lipid-laden adipocytes and provoked a loss of important ECM components [113]. Overall, the downregulation of these ECM-related genes could be interpreted as a favourable adaptative response to the adipocyte hypertrophy observed in response to MI supplementation. The decreased mRNA levels of *serpinh1*, which encodes the collagen-specific molecular chaperone HSP47 that protects PPARγ from proteasomal degradation, are also consistent with this idea. Thus, *HSP47* expression increases with obesity and in response to insulin and is positively correlated with BMI, fat mass, and waist and hip circumferences in humans, and pharmacological inhibition of HSP47 and knockout of *serpinh1* in mice results in decreased adiposity [114]. Interestingly, both SPARC mRNA and circulating protein levels positively correlated with fasting insulin levels and HOMA-IR [109,110], and *sparc* gene expression with CRP [109] in humans with obesity, and TIMP1-injected mice displayed IR [106]. Furthermore, increased levels of the proinflammatory proteins TNF-α, IL-6 and MCP-1 and decreased IL-10 concentrations were reported in 3T3-L1 adipocytes overexpressing SPARC [109]. In addition, biglycan mRNA levels are positively correlated with the expression of inflammation-related genes such as *TNFα* and *CD68*, mainly in VAT, and with the circulating levels of CRP, insulin, HOMA-IR and leptin in women [112]. These results suggest that the decreased *sparc*, *timp1*, and *bgn* expression observed in the RWAT of OVX-MI rats could partly account for the improvements in adipocyte structure, morphology and immunometabolic function observed in the present study in response to MI supplementation. Furthermore, the decreased expression of genes involved in cytoskeletal organization (*actb, lcp1,* and *pfn1*) [115] and cell adhesion (*fermt3* and *cdh11*), the mRNA and/or protein levels of which

increase with obesity [115,116], are positively correlated with adipocyte size [117] and negatively associated with WAT inflammation and glucose and insulin homeostasis [115,116,118], supporting our hypothesis.

The sharp downregulation of the mRNA levels of genes mainly expressed in hypertrophied WAT by ATMs and encoding proteins involved in cytokine (IL1B, FASLG, and PTGS2)- and chemokine (CXCL2, CCR7)-mediated inflammation, whose levels were increased in WAT in the obese state [119–123] and correlated with macrophage infiltration and adipocyte size in visceral WAT [120], strongly suggested that MI consumption ameliorated the low-grade inflammation in WAT that occurred as a consequence of the fat accretion produced in OVX rats after ovariectomy. The decreased *cd5l, fcgr1a, spib* and *btk* expression levels found in the RWAT of OVX-MI animals reinforce this idea. Notably, *cd5l* encodes the apoptosis inhibitor of macrophages (AIM)/CD5L, which plays an important role in the crosstalk between adipocytes and macrophages, activating the TLR-4 pathway in individuals with obesity and, therefore, triggering the secretion of proinflammatory chemokines, such as MCP-1, to induce the recruitment of proinflammatory M1 macrophages to WAT [124]. Interestingly, human macrophages stimulated with PC:CRP, which is formed by the binding of CRP to phosphocholine—PC—moieties, exhibited increased secretion of proinflammatory cytokines (TNF, IL-1β, and IL-23) in combination with TLRs, identifying Fcγr1a as one of the main receptors that triggers PC:CRP-induced inflammation [125]. Relatedly, gene regulatory network analyses performed using gene expression data obtained from periaortic adipose tissue (PAT) samples from patients with abdominal aortic aneurysm (AAA) identified SPIB as one of the main transcription factors regulating key genes involved in the TLR and Fcγ receptor signalling pathways [126]. Based on these results, the modulation of SPIB to downregulates Fc receptor signalling was proposed as a

potential therapeutic strategy to ameliorate inflammation induced by the AAA PAT [126]. The downregulation of the gene encoding BTK, a kinase that enhances the proinflammatory response in macrophages through NF-κB and NLRP3 inflammasome activity and is overexpressed in diet-induced obese mice [127] and patients with obesity and diabetes [128], provides additional scientific evidence supporting our hypothesis. Thus, the inhibition of BKT signalling promoted an anti-inflammatory M2-like phenotype in macrophages through the activation of oxidative phosphorylation (OxPhos) via the upregulation of different genes related to the mitochondrial electron transport chain, including *mt-co2* [128], which was also overexpressed in the present study. The significantly higher expression of three additional genes related to mitochondrial respiratory chain complex I (*mt-nd5*, *mt-nd6* and *nubpl*) in OVX-MI animals than in their OVX counterparts suggests, at first glance, an immune-related benefit of the MI in RWAT by enhancing the M2-like phenotype in macrophages through the activation of OxPhos, although additional research is needed to shed more light on this issue. In addition to ATMs, adaptative immune cells, such as T cells, can also play an important role in early inflammatory responses in WAT during obesity [129]. Relatedly, the downregulation of the gene encoding CD28, which is the strongest T-cell costimulatory molecule in naïve T cells, would be consistent with a protective anti-inflammatory effect produced in response to MI supplementation since diet-induced obese CD28 knockout mice displayed reduced levels of proinflammatory cytokines in the EWAT [129].

Another interesting result of this study is the decreased expression of the gene encoding the ECM-related protein TSP2 (also known as THBS2), which has been shown to have an inhibitory effect on adipogenesis [130], as was also described for SPARC [131]. Furthermore, both SPARC [131] and TIMP1 [132] negatively regulate adipogenesis through the Wnt signalling pathway, an effect that has also been reported for the gene encoding

WISP2 (*ccn5*), a member of the Wnt1 inducible signalling pathway [133]. Therefore, a reasonable speculation is that, at first glance, MI supplementation would activate adipogenesis in the RWAT of OVX-MI rats at least in part due to the inhibition of this pathway, which would be evidenced by the decreased mRNA levels of *sparc*, *timp1* and *ccn5*. The observed downregulation of the genes encoding the transcription factors ATF3 [134] and EGR1 [135] and the proteins SNAIL1 [136] and GDF10, also known as BMP3B [137], which inhibit adipocyte differentiation, would also be, at first glance, consistent with an enhancement of the adipogenic program in the RWAT in response to MI supplementation. These results are reinforced by the increased number of adipocytes found in the RWAT of both OVX-E2 and OVX-MI animals compared to OVX rats according to histological analyses, and the strong inverse correlation pattern observed between the adipocyte number and HOMA-IR/LAR is in agreement with the idea that adipocyte hyperplasia protects against metabolic dysfunctions and preserves adequate WAT expansion [91]. Conversely, our findings also revealed decreased mRNA levels of genes encoding important transcription factors (*fos* [138], *fosb* [138], *atf5* [139], and egr2 [135]) and proteins (*medag* [140], *glipr1* [141], *sfrp2* [142], *bmp2* [143] and *vsir* [144]) involved in the activation of adipogenesis, which would not support the increased formation of adipocytes. Remarkably, we did not observe significant increases in the expression of the adipogenesis gatekeeper preadipocyte factor 1 [145] (*pref-1*, also known as *dk1,* which was sharply decreased in our study, FC: -11.7; p adj.=0.21) or in the mRNA levels of the genes encoding the master regulators of adipogenesis, PPARγ and C/EBPα [91,145]. Overall, our findings did not support increased adipogenesis in the RWAT of OVX-MI animals, although additional research focused on the protein levels of key factors involved in the adipogenic program and/or on the quantification of RWAT DNA content would be useful for shedding more light on this issue. Notably, many of the genes involved in cell fate

determination and differentiation that were downregulated in the RWAT of OVX-MI rats are increased with obesity (e.g., *egr1* [146], *egr2* [147], *ccn5* [133], *medag* [140], *gdf10* [137], *atf3* [148], *atf5* [139], *sfrp2* [142], and *bmp2* [143]), and some of these genes are involved in obesity-related metabolic alterations, such as IR/type 2 diabetes (*egr1* [146], *ccn5* [133], *atf3* [148], *sfrp2* [142], and *bmp2* [143]), low-grade chronic inflammation (*egr1* [146], *egr2* [147], and *fos* [149]) and the cellular stress response (*egr1*, *egr2*, *fos*, *fosb* and *atf3*) [150]. Interestingly, fat or weight loss was associated with the downregulation of *fos* [151] and *sfrp2* [152] expression in human WAT. Overall, these results indicate that the modulation of these genes, which play important roles in adipose tissue function and stress response, is a favourable adaptive response to the decreased fat accretion and hypertrophy observed in the RWAT of OVX-MI rats, which reinforces our hypothesis that an improved immunometabolic profile occurs in response to MI supplementation. The impairment of the sirtuin (SIRT)/NAD pathway can lead to obesity and WAT dysfunction, considering the essential role of this system as a cellular energy sensor [153]. The upregulation of the NAD+ biosynthesis-related gene *nmnat2* found in the RWAT of OVX-MI animals is an additional result that reinforces our findings since, in WAT from monozygotic twins whose body weights were discordant, *nmnat2* mRNA levels were increased in leaner cotwins and negatively correlated with inflammation [153].

MI consumption also altered the mRNA levels of genes related to cholesterol homeostasis (*cyp11a1*, *olr1*, and *vmp1*) and fatty acid (*fabp3* and *acot4*) and sphingolipid (*sgms2* and *smpd3*) metabolism. Takanabe-Mori et al. [154] reported that the expression of the gene encoding LOX-1 (also named OLR1), a receptor for oxidized LDL, increased in diet-induced obese mice and that this protein enhanced the expression of proinflammatory cytokines in WAT. Furthermore, increased circulating LOX-1 levels were found in menopausal women with obesity, and the plasma levels of this protein positively

correlated with BMI and body fat [155]. Interestingly, genetic inhibition of *sgms2* boosted glucose clearance in part through the enhancement of insulin signalling in WAT [156], and in humans, *SMPD3* mRNA levels were higher in the WAT of obese women with an increased liver fat content, who displayed an inflammatory profile, than in that of obese women with a normal hepatic fat content [157]. Thus, the downregulation of *olr1*, *sgms2* and *smpd3* observed in the present study would also favour a healthier immunometabolic profile in the RWAT of OVX-MI rats. Two mechanisms involved in the effects of bioactive compounds against fat accretion are the activation of lipid catabolism-related pathways (lipolysis and β-oxidation) and the inhibition of lipogenesis. At first glance, the increased mRNA levels of the gene encoding peroxisomal ACOT4 could suggest the activation of β-oxidation, since the acyl-CoA esters are transported into the peroxisome via ABCD transporters and undergo β-oxidation, and the resulting products succinyl-CoA and glutaryl-CoA can be hydrolysed by this auxiliary enzyme to obtain succinate and glutarate, which are subsequently transported to mitochondria [158]. Nevertheless, we did not observe changes in the mRNA levels of key genes involved in lipolysis (*hsl* and *atgl*), β-oxidation (*cpt1b* and *had*) or lipogenesis (*acc1*, *fas, gpat*, and *dgat2*); therefore, the reported antiobesity effect of MI is not due to the modulation of these key lipid-related pathways in the RWAT, at least at the gene expression level.

Supplementation with MI also produced slight beneficial effects on cholesterol metabolism, significantly decreasing the TC/HDL-c ratio compared to that in their OVX counterparts. This atherogenic ratio, called the Castelli risk index 1 [71], constitutes a risk indicator for CVDs with greater predictive value than each variable separately since an increase in the TC concentration is a marker of atherogenic lipoproteins, while a decrease in the HDL-C concentration is correlated with numerous risk factors, including the components of MetS. At first glance, this result could be partly attributed to the

antihypercholesterolaemic and antiatherosclerotic effects of carnosine, which can facilitate the removal of aldehydes from atherosclerotic lesions [159] and counteract the increased circulating levels of TC and LDL-c in rats fed a high-fat high-carbohydrate diet [160]. Nevertheless, in the present study, OVX rats did not show significant changes in either TC levels or the TC/HDL-c ratio compared to SHAM animals. Therefore, additional studies in which OVX rats are challenged with a hyperlipidic and atherogenic diet to induce hypercholesterolemia would be valuable to provide more insights into the physiological significance of this effect.

Surprisingly, we did not observe increased hepatic GSH levels in response to MI consumption, contrary to what would be expected in response to the consumption of the potent glutathione precursors serine and cysteine, which, in combination with L-carnitine and nicotinamide riboside, have been proposed as treatments for NAFLD in humans [161]. Remarkably, the increased urinary levels of 8-OHdG observed in OVX-E2 animals, an effect that was not observed after MI consumption, could be interpreted as a side effect of the 7β-E2 treatment because the 8-OHdG levels increased in response to oestrogen-induced oxidative stress in a rat model of breast cancer [162], and a nested case–control study concluded that the long-term use of an oestrogen-based HRT was associated with an increased risk of suffering from breast cancer in postmenopausal women [163].

CONCLUSIONS

We reported here that the consumption of a blend of histidine, carnosine, cysteine and serine by a postmenopausal model with oestrogen deficiency, namely, OVX rats, decreased adiposity and RWAT adipocyte hypertrophy and improved body composition, as also evidenced by the increased lean body mass and lean/fat mass ratio. The decreases in the leptin-to-adiponectin and TC/HDL-c ratios and in the CRP plasma levels, as well

as the favourable expression profile of key genes involved in the regulation of the cytoskeleton and ECM reorganization, glucose and insulin homeostasis, oxidative phosphorylation, cell fate determination and differentiation, inflammation and stress response found in the RWAT in response to MI supplementation strongly suggest an improvement in immunometabolic health in OVX-MI rats in response to MI supplementation. To the best of our knowledge, this study is the first to report that the combination of these amino acid-related compounds exerted such effects. Our findings pave the way for promoting the use of this MI formulation to ameliorate obesity and to improve the immunometabolic health of menopausal women. Further randomized controlled clinical trials performed with this target population treated with this MI supplement are warranted.

ABBREVIATIONS

μCT, three-dimensional microcomputed tomography; 17β-E2, 17β-oestradiol; 8-OHdG, 8-hydroxy-2'-deoxyguanosine; ANOVA, analysis of variance; ATMs, adipose tissue macrophages; BMC, bone mineral content; BMD, bone mineral density; CRP, C-reactive protein; CT, central zone time spent; CTX-1, carboxy-terminal telopeptide of type I collagen; CVDs, cardiovascular diseases; DGE, differential gene expression; EAE, enclosed arms entries; EAT, enclosed arms time spent; ECM, extracellular matrix; EE, energy expenditure; EPM, elevated plus maze; ER, oestrogen receptor; FDR, false discovery rate; GSH, glutathione; GSSG, oxidized glutathione; HAL, histidine ammonia lyase; HDL-c, high-density lipoprotein cholesterol; HOMA-IR, homeostasis model assessment-estimated insulin resistance; HRT, hormone replacement therapy; IR, insulin resistance; IWAT, inguinal white adipose tissue; KEGG, Kyoto Encyclopaedia of Genes and Genomes; LAR, leptin-to-adiponectin ratio; MCP-1, monocyte chemoattractant protein-1; MetS, metabolic syndrome; MI, multi-ingredient; MWAT, mesenteric white

adipose tissue; NAFLD, non-alcoholic fatty liver disease; NGS, next-generation sequencing; non-HDL-c, high-density lipoprotein cholesterol; OAE, open arm entries; OAT, time spent in open arms; OC, osteocalcin; OVX, ovariectomized rats; PINP, procollagen I amino-terminal propeptide; RIN, RNA integrity number; RQ, respiratory quotient; R-QUICKI, revised quantitative insulin sensitivity check index; RWAT, retroperitoneal white adipose tissue; SHAM, sham-operated rats; T2DM, type 2 diabetes mellitus; TC, total cholesterol; TC/HDL-c, total cholesterol-to-high-density lipoprotein cholesterol ratio; TMC, tissue mineral content; TMD, tissue mineral density.

FUNDING SOURCES

This research was financially supported by the Agency for Business Competitiveness of the Government of Catalonia (ACCIÓ/TECCT11-1-0012) and by Comunidad de Madrid (S2022/BMD-7403 RENIM-CM).

AUTHOR CONTRIBUTIONS

Julio Baudin: conceptualization, methodology, software, validation, formal analysis, investigation, resources, data curation, writing - original draft, writing - review & editing, visualization. **Julia Hernandez-Baixauli:** methodology, investigation, resources. **Jordi Romero-Giménez:** investigation, resources. **Hong Yang:** methodology, software, validation, formal analysis, investigation, resources, data curation. **Francisca Mulero:** investigation, resources, funding acquisition. **Francesc Puiggròs:** conceptualization, validation, resources, funding acquisition. **Adil Mardinoglu**: conceptualization, validation, resources. **Lluís Arola:** conceptualization, validation, resources, writing - review & editing, supervision, funding acquisition. **Antoni Caimari:** conceptualization, methodology, validation, resources, writing - review & editing, supervision; funding acquisition. All the authors have read and agreed to the final version of the manuscript.

DATA AVAILABILITY STATEMENT

All raw RNA-sequencing data generated from this study can be accessed through accession number GSEXXXXXX.

CONFLICTS OF INTEREST

The authors declare that they have no conflicts of interest.

ACKNOWLEDGEMENTS

Julio Baudin and Julia Hernandez-Baixauli were supported by a Vicente López fellowship (Eurecat).

We gratefully acknowledge the help from Dr. Juan Maria Alcaide-Hidalgo and Dr. Xavier Escoté, researchers at the Nutrition and Health Unit (Eurecat, Reus, Spain), who performed the study at the animal facility and performed the histological analyses in the RWAT, respectively. We also appreciate the assistance provided by Yaiza Tobajas, Anna Antolin, Cristina Egea and Gertruda Chomiciute, laboratory technicians at the Nutrition and Health Unit (Eurecat, Reus, Spain). The authors would like to thank the students Irene Bravo and David Sabador at the National Cancer Research Center (CNIO) for their support in the microcomputed tomography analyses.

REFERENCES

[1] Santoro N, Randolph JF. Reproductive Hormones and the Menopause Transition. *Obstet Gynecol Clin North Am*. 2011, **38**, 455–66. https://doi.org/10.1016/j.ogc.2011.05.004.
[2] McNeil MA, Merriam SB. Menopause. *Ann Intern Med*. 2021, **174**, ITC97–112. https://doi.org/10.7326/AITC202107200.
[3] Thurston RC, Johnson BD, Shufelt CL, Braunstein GD, Berga SL, Stanczyk FZ, et al. Menopausal symptoms and cardiovascular disease mortality in the Women's Ischemia Syndrome Evaluation (WISE). *Menopause*. 2017, **24**, 126–32. https://doi.org/10.1097/GME.0000000000000731.
[4] Harlow SD, Gass M, Hall JE, Lobo R, Maki P, Rebar RW, et al. Executive Summary of the Stages of Reproductive Aging Workshop + 10: Addressing the

Unfinished Agenda of Staging Reproductive Aging. *J Clin Endocrinol Metab*. 2012, **97**, 1159–68. https://doi.org/10.1210/jc.2011-3362.

[5] Thapa S, Nandy A, Rendina-Ruedy E. Endocrinal metabolic regulation on the skeletal system in post-menopausal women. *Front Physiol*. 2022, **13**, 1–10. https://doi.org/10.3389/fphys.2022.1052429.

[6] Juppi H, Sipilä S, Fachada V, Hyvärinen M, Cronin N, Aukee P, et al. Total and regional body adiposity increases during menopause—evidence from a follow-up study. *Aging Cell*. 2022, **21**, 1–17. https://doi.org/10.1111/acel.13621.

[7] Sowers M, Zheng H, Tomey K, Karvonen-Gutierrez C, Jannausch M, Li X, et al. Changes in Body Composition in Women over Six Years at Midlife: Ovarian and Chronological Aging. *J Clin Endocrinol Metab*. 2007, **92**(3), 895–901. https://doi.org/10.1210/jc.2006-1393.

[8] Fenton A, Smart C, Goldschmidt L, Price V, Scott J. Fat mass, weight and body shape changes at menopause – causes and consequences: a narrative review. *Climacteric*. 2023, **26**, 381–7. https://doi.org/10.1080/13697137.2023.2178892.

[9] Kapoor E, Collazo-Clavell ML, Faubion SS. Weight Gain in Women at Midlife: A Concise Review of the Pathophysiology and Strategies for Management. *Mayo Clin Proc*. 2017, **92**, 1552–8. https://doi.org/10.1016/j.mayocp.2017.08.004.

[10] Barrea L, Pugliese G, Laudisio D, Colao A, Savastano S, Muscogiuri G. Mediterranean diet as medical prescription in menopausal women with obesity: a practical guide for nutritionists. *Crit Rev Food Sci Nutr*. 2021, **61**(7), 1201–11. https://doi.org/10.1080/10408398.2020.1755220.

[11] Ko SH, Kim HS. Menopause-Associated Lipid Metabolic Disorders and Foods Beneficial for Postmenopausal Women. *Nutrients*. 2020, **12**(1), 202. https://doi.org/10.3390/nu12010202.

[12] Taleb-Belkadi O, Chaib H, Zemour L, Fatah A, Chafi B, Mekki K. Lipid profile, inflammation, and oxidative status in peri- and postmenopausal women. *Gynecol Endocrinol*. 2016, **32**(12), 982–5. https://doi.org/10.1080/09513590.2016.1214257.

[13] Rosano GMC, Vitale C, Marazzi G, Volterrani M. Menopause and cardiovascular disease: the evidence. *Climacteric*. 2007, **10**, 19–24. https://doi.org/10.1080/13697130601114917.

[14] Mesch VR, Boero LE, Siseles NO, Royer M, Prada M, Sayegh F, et al. Metabolic syndrome throughout the menopausal transition: influence of age and menopausal status. *Climacteric*. 2006, **9**, 40–8. https://doi.org/10.1080/13697130500487331.

[15] The European Society of Cardiology. Understanding the burden of CVD. 2023. https://www.escardio.org/The-ESC/Advocacy/understanding-the-burden-of-cvd-facts-and-figures (accessed September 2023).

[16] Mehta J, Kling JM, Manson JE. Risks, Benefits, and Treatment Modalities of Menopausal Hormone Therapy: Current Concepts. *Front Endocrinol*. 2021, **26**, 1–14. https://doi.org/10.3389/fendo.2021.564781.

[17] Thangavel P, Puga-Olguín A, Rodríguez-Landa JF, Zepeda RC. Genistein as Potential Therapeutic Candidate for Menopausal Symptoms and Other Related Diseases. *Molecules*. 2019, **24**, 3892. https://doi.org/10.3390/molecules24213892.

[18] Sharifi-Rad J, Quispe C, Imran M, Rauf A, Nadeem M, Gondal TA, et al. Genistein: An Integrative Overview of Its Mode of Action, Pharmacological Properties, and Health Benefits. *Oxid Med Cell Longev*. 2021, **2021**, 3268136. https://doi.org/10.1155/2021/3268136.

[19] Romani AMP. The controversy on the beneficial effect of phytoestrogens in diabetic treatment in postmenopausal women. *Biochem Pharmacol*. 2021, **190**, 114619. https://doi.org/10.1016/j.bcp.2021.114619.

[20] Baudin J, Hernandez-Baixauli J, Quesada-Vázquez S, Mulero F, Puiggròs F, Arola L, et al. Combined supplementation with hesperidin, phytosterols and curcumin decreases adiposity and improves metabolic health in ovariectomized rats. *Food Funct*. 2024, **15**, 4905-4924. https://doi.org/10.1039/d3fo05122f.

[21] Frühbeck G, Catalán V, Rodríguez A, Ramírez B, Becerril S, Salvador J, et al. Adiponectin-leptin Ratio is a Functional Biomarker of Adipose Tissue Inflammation. *Nutrients*. 2019, **11**, 454. https://doi.org/10.3390/nu11020454.

[22] Frühbeck G, Catalán V, Rodríguez A, Ramírez B, Becerril S, Salvador J, et al. Involvement of the leptin-adiponectin axis in inflammation and oxidative stress in the metabolic syndrome. *Sci Rep*. 2017, **7**, 6619. https://doi.org/10.1038/s41598-017-06997-0.

[23] Quesada-Vázquez S, Antolín A, Colom-Pellicer M, Aragonès G, Herrero L, Del Bas JM, et al. Reduction of Obesity and Insulin Resistance through Dual Targeting of VAT and BAT by a Novel Combination of Metabolic Cofactors. *Int J Mol Sci*. 2022, **23**, 14923. https://doi.org/10.3390/ijms232314923.

[24] Companys J, Calderón-Pérez L, Pla-Pagà L, Llauradó E, Sandoval-Ramirez BA, Gosalbes MJ, et al. Effects of enriched seafood sticks (heat-inactivated B. animalis subsp. lactis CECT 8145, inulin, omega-3) on cardiometabolic risk factors and gut microbiota in abdominally obese subjects: randomized controlled trial. *Eur J Nutr*. 2022, **61**, 3597–611. https://doi.org/10.1007/s00394-022-02904-0.

[25] Quesada-Vázquez S, Colom-Pellicer M, Navarro-Masip È, Aragonès G, Del Bas JM, Caimari A, et al. Supplementation with a Specific Combination of Metabolic Cofactors Ameliorates Non-Alcoholic Fatty Liver Disease, Hepatic Fibrosis, and Insulin Resistance in Mice. *Nutrients*. 2021, **13**, 3532. https://doi.org/10.3390/nu13103532.

[26] Yang H, Mayneris-Perxachs J, Boqué N, del Bas JM, Arola L, Yuan M, et al. Combined Metabolic Activators Decrease Liver Steatosis by Activating Mitochondrial Metabolism in Hamsters Fed with a High-Fat Diet. *Biomedicines*. 2021, **9**, 1440. https://doi.org/10.3390/biomedicines9101440.

[27] Quesada-Vázquez S, Castells-Nobau A, Latorre J, Oliveras-Cañellas N, Puig-Parnau I, Tejera N, et al. Potential therapeutic implications of histidine catabolism by the gut microbiota in NAFLD patients with morbid obesity. *Cell Reports Med*. 2023, **4**(12),101341. https://doi.org/10.1016/j.xcrm.2023.101341.

[28] Mardinoglu A, Ural D, Zeybel M, Yuksel HH, Uhlén M, Borén J. The Potential Use of Metabolic Cofactors in Treatment of NAFLD. *Nutrients*. 2019, **11**, 1578. https://doi.org/10.3390/nu11071578.

[29] Suárez M, Boqué N, del Bas J, Mayneris-Perxachs J, Arola L, Caimari A. Mediterranean Diet and Multi-Ingredient-Based Interventions for the Management of Non-Alcoholic Fatty Liver Disease. *Nutrients*. 2017, **9**, 1052. https://doi.org/10.3390/nu9101052.

[30] Caruso G, Di Pietro L, Cardaci V, Maugeri S, Caraci F. The therapeutic potential of carnosine: Focus on cellular and molecular mechanisms. *Curr Res Pharmacol Drug Discov.* 2023, **4**, 100153. https://doi.org/10.1016/j.crphar.2023.100153.

[31] Matthews JJ, Dolan E, Swinton PA, Santos L, Artioli GG, Turner MD, et al. Effect of Carnosine or β-Alanine Supplementation on Markers of Glycemic

Control and Insulin Resistance in Humans and Animals: A Systematic Review and Meta-analysis. *Adv Nutr*. 2021, **12**, 2216–31. https://doi.org/10.1093/advances/nmab087.

[32] He L, Ding Y, Zhou X, Li T, Yin Y. Serine signaling governs metabolic homeostasis and health. *Trends Endocrinol Metab*. 2023, **34**, 361–72. https://doi.org/10.1016/j.tem.2023.03.001.

[33] Zhou X, Zhang H, He L, Wu X, Yin Y. Long-Term l-Serine Administration Reduces Food Intake and Improves Oxidative Stress and Sirt1/NFκB Signaling in the Hypothalamus of Aging Mice. *Front Endocrinol*. 2018, **9**, 476. https://doi.org/10.3389/fendo.2018.00476.

[34] Jain SK, Kanikarla-Marie P, Warden C, Micinski D. L-cysteine supplementation upregulates glutathione (GSH) and vitamin D binding protein (VDBP) in hepatocytes cultured in high glucose and in vivo in liver, and increases blood levels of GSH, VDBP, and 25-hydroxy-vitamin D in Zucker diabetic fatty rats. *Mol Nutr Food Res*. 2016, **60**, 1090–8. https://doi.org/10.1002/mnfr.201500667.

[35] Jain SK, Velusamy T, Croad JL, Rains JL, Bull R. l-Cysteine supplementation lowers blood glucose, glycated hemoglobin, CRP, MCP-1, and oxidative stress and inhibits NF-κB activation in the livers of Zucker diabetic rats. *Free Radic Biol Med*. 2009, **46**, 1633–8. https://doi.org/10.1016/j.freeradbiomed.2009.03.014.

[36] Thalacker-Mercer AE, Gheller ME. Benefits and Adverse Effects of Histidine Supplementation. *J Nutr*. 2020. **150**, 2588S-2592S. https://doi.org/10.1093/jn/nxaa229.

[37] Moro J, Tomé D, Schmidely P, Demersay T chalvon, Azzout-Marniche D. Histidine: A Systematic Review on Metabolism and Physiological Effects in Human and Different Animal Species. *Nutrients*. 2020, **12**, 1414. https://doi.org/10.3390/nu12051414.

[38] Li YC, Li CL, Qi JY, Huang LN, Shi D, Du SS, et al. Relationships of Dietary Histidine and Obesity in Northern Chinese Adults, an Internet-Based Cross-Sectional Study. *Nutrients*. 2016, **8**, 420. https://doi.org/10.3390/nu8070420.

[39] Sun X, Feng R, Li Y, Lin S, Zhang W, Li Y, et al. Histidine supplementation alleviates inflammation in the adipose tissue of high-fat diet-induced obese rats via the NF-κB- and PPARγ-involved pathways. *Br J Nutr*. 2014, **112**, 477–85. https://doi.org/10.1017/S0007114514001056.

[40] Feng RN, Niu YC, Sun XW, Li Q, Zhao C, Wang C, et al. Histidine supplementation improves insulin resistance through suppressed inflammation in obese women with the metabolic syndrome: a randomised controlled trial. *Diabetologia*. 2013, **56**, 985–94. https://doi.org/10.1007/s00125-013-2839-7.

[41] Decandia D, Landolfo E, Sacchetti S, Gelfo F, Petrosini L, Cutuli D. n-3 PUFA Improve Emotion and Cognition during Menopause: A Systematic Review. *Nutrients*. 2022, **14**, 1982. https://doi.org/10.3390/nu14091982.

[42] Nakamura T, Naganuma F, Kudomi U, Roh S, Yanai K, Yoshikawa T. Oral histidine intake improves working memory through the activation of histaminergic nervous system in mice. *Biochem Biophys Res Commun*. 2022, **609**, 141–8. https://doi.org/10.1016/j.bbrc.2022.04.016.

[43] Nozawa Y, Mimura M, Yamada K, Sugita M, Shibakusa T, Koyama N. Dried bonito broth improves cognitive function via the histaminergic system in mice. *Biomed Res*. 2014, **35**, 311–9. https://doi.org/10.2220/biomedres.35.311.

[44] Acevedo SF, Pfankuch T, Ohtsu H, Raber J. Anxiety and cognition in female histidine decarboxylase knockout (Hdc -/-) mice. *Behav Brain Res*. 2006, **168**, 92–9. https://doi.org/10.1016/j.bbr.2005.10.016.

[45] Acevedo SF, Ohtsu H, Benice TS, Rizk-Jackson A, Raber J. Age-dependent measures of anxiety and cognition in male histidine decarboxylase knockout (Hdc-/-) mice. *Brain Res*. 2006, **1071**, 113–23. https://doi.org/10.1016/j.brainres.2005.11.067.

[46] Tomonaga S, Yamane H, Onitsuka E, Yamada S, Sato M, Takahata Y, et al. Carnosine-induced antidepressant-like activity in rats. *Pharmacol Biochem Behav*. 2008, **89**, 627–32. https://doi.org/10.1016/j.pbb.2008.02.021.

[47] Li YF, He RR, Tsoi B, Li XD, Li WX, Abe K, et al. Anti-Stress Effects of Carnosine on Restraint-Evoked Immunocompromise in Mice through Spleen Lymphocyte Number Maintenance. Frasch MG, editor. *PLoS One*. 2012, **7**, e33190. https://doi.org/10.1371/journal.pone.0033190.

[48] Araminia B, Shalbafan M, Mortezaei A, Shirazi E, Ghaffari S, Sahebolzamani E, et al. L-Carnosine combination therapy for major depressive disorder: A randomized, double-blind, placebo-controlled trial. *J Affect Disord*. 2020, **267**, 131–6. https://doi.org/10.1016/j.jad.2020.02.020.

[49] Elshorbagy AK, Gjesdal CG, Nurk E, Tell GS, Ueland PM, Nygård O, et al. Cysteine, homocysteine and bone mineral density: A role for body composition? *Bone*. 2009, **44**, 954–8. https://doi.org/10.1016/j.bone.2008.12.018.

[50] Baines M, Kredan MB, Davison A, Higgins G, West C, Fraser WD, et al. The Association Between Cysteine, Bone Turnover, and Low Bone Mass. *Calcif Tissue Int*. 2007, **81**, 450–4. https://doi.org/10.1007/s00223-007-9089-y.

[51] Han NR, Kim NR, Kim HM, Jeong HJ. Cysteine Prevents Menopausal Syndromes in Ovariectomized Mouse. *Reprod Sci*. 2016, **23**, 670–9. https://doi.org/10.1177/1933719115612133.

[52] Reagan-Shaw S, Nihal M, Ahmad N. Dose translation from animal to human studies revisited. *FASEB J*. 2008, **22**, 659–61. https://doi.org/10.1096/fj.07-9574LSF.

[53] Holeček M. Side Effects of Amino Acid Supplements. *Physiol Res.* 2022, **71**, 29–45. https://doi.org/10.33549/physiolres.934790.

[54] Dröge W. Oxidative stress and aging: is aging a cysteine deficiency syndrome? *Philos Trans R Soc B Biol Sci*. 2005, **360**, 2355–72. https://doi.org/10.1098/rstb.2005.1770.

[55] Matthews DR, Hosker JP, Rudenski AS, Naylor BA, Treacher DF, Turner RC. Homeostasis model assessment: insulin resistance and beta-cell function from fasting plasma glucose and insulin concentrations in man. *Diabetologia*. 1985, **28**, 412–9. https://doi.org/10.1007/BF00280883.

[56] Crescenti A, del Bas JM, Arola-Arnal A, Oms-Oliu G, Arola L, Caimari A. Grape seed procyanidins administered at physiological doses to rats during pregnancy and lactation promote lipid oxidation and up-regulate AMPK in the muscle of male offspring in adulthood. *J Nutr Biochem*. 2015, **26**, 912–20. https://doi.org/10.1016/j.jnutbio.2015.03.003.

[57] Kraeuter AK, Guest PC, Sarnyai Z. "The Elevated Plus Maze Test for Measuring Anxiety-Like Behavior in Rodents" *in Methods in molecular biology*, ed. Guest PC, Springer, New York, 2019, 2nd edit. vol. 1916, 4, 69-74. https://doi.org/10.1007/978-1-4939-8994-2_4.

[58] Pellow S, Chopin P, File SE, Briley M. Validation of open : closed arm entries in an elevated plus-maze as a measure of anxiety in the rat. *J Neurosci Methods*. 1985, **14**, 149–67. https://doi.org/10.1016/0165-0270(85)90031-7.

[59] Rodgers RJ, Johnson NJT. Factor analysis of spatiotemporal and ethological measures in the murine elevated plus-maze test of anxiety. *Pharmacol Biochem Behav*. 1995, **52**, 297–303. https://doi.org/10.1016/0091-3057(95)00138-m.

[60] Kraeuter AK, Guest PC, Sarnyai Z. "The Y-Maze for Assessment of Spatial Working and Reference Memory in Mice" in *Methods in molecular biology*, ed. Guest PC, Springer, New York, 2019, 2nd edit. vol. 1916, 10, 105-111. https://doi.org/10.1007/978-1-4939-8994-2_10.

[61] Love MI, Huber W, Anders S. Moderated estimation of fold change and dispersion for RNA-seq data with DESeq2. *Genome Biol*. 2014, **15**, 550. https://doi.org/10.1186/s13059-014-0550-8.

[62] Väremo L, Nielsen J, Nookaew I. Enriching the gene set analysis of genome-wide data by incorporating directionality of gene expression and combining statistical hypotheses and methods. *Nucleic Acids Res*. 2013, **41**, 4378–91. https://doi.org/10.1093/nar/gkt111.

[63] Kolberg L, Raudvere U, Kuzmin I, Adler P, Vilo J, Peterson H. g:Profiler—interoperable web service for functional enrichment analysis and gene identifier mapping (2023 update). *Nucleic Acids Res*. 2023, **51**, W207–12. https://doi.org/10.1093/nar/gkad347.

[64] Wickham H. "Ggplot2: Elegant Graphics for Data Analysis" in *Use R!*, ed. Gentleman R, Hornik K, Parmigian G, Springer, Switzerland, 2016, 2nd edit. https://doi.org/10.1007/978-3-319-24277-4

[65] Gu Z, Eils R, Schlesner M. Complex heatmaps reveal patterns and correlations in multidimensional genomic data. *Bioinformatics*. 2016, **32**, 2847–9. https://doi.org/10.1093/bioinformatics/btw313.

[66] López-Jaramillo P, Gómez-Arbeláez D, López-López J, López-López C, Martínez-Ortega J, Gómez-Rodríguez A, et al. The role of leptin/adiponectin ratio in metabolic syndrome and diabetes. *Horm Mol Biol Clin Investig*. 2014, **18**, 37–45. https://doi.org/10.1515/hmbci-2013-0053.

[67] Medina-Contreras J, Villalobos-Molina R, Zarain-Herzberg A, Balderas-Villalobos J. Ovariectomized rodents as a menopausal metabolic syndrome model. A minireview. *Mol Cell Biochem*. 2020, **475**, 261–76. https://doi.org/10.1007/s11010-020-03879-4.

[68] Yousefzadeh N, Kashfi K, Jeddi S, Ghasemi A. Ovariectomized rat model of osteoporosis: A practical guide. *EXCLI J*. 2020, **19**, 89–107. https://doi.org/10.17179/excli2019-1990.

[69] Mosquera L, Shepherd L, Torrado AI. Comparison of Two Methods of Estradiol Replacement: their Physiological and Behavioral Outcomes. *J Vet Sci Technol*. 2015, **6**, 276. https://doi.org/10.4172/2157-7579.1000276.

[70] Witte MM, Resuehr D, Chandler AR, Mehle AK, Overton JM. Female mice and rats exhibit species-specific metabolic and behavioral responses to ovariectomy. *Gen Comp Endocrinol*. 2010, **166**, 520–8. https://doi.org/10.1016/j.ygcen.2010.01.006.

[71] Gaggini M, Gorini F, Vassalle C. Lipids in Atherosclerosis: Pathophysiology and the Role of Calculated Lipid Indices in Assessing Cardiovascular Risk in Patients with Hyperlipidemia. *Int J Mol Sci*. 2022, **24**, 75. https://doi.org/10.3390/ijms24010075.

[72] Obradovic M, Sudar-Milovanovic E, Soskic S, Essack M, Arya S, Stewart AJ, et al. Leptin and Obesity: Role and Clinical Implication. *Front Endocrinol*. 2021, **12**, 1–14. https://doi.org/10.3389/fendo.2021.585887.

[73] Gupta V, Mishra S, Mishra S, Kumar S, Gupta V. Association of Leptin: Adiponectin ratio and metabolic risk markers in postmenopausal women. *Immunol Lett*. 2018, **196**, 63–7. https://doi.org/10.1016/j.imlet.2018.01.008.

[74] Finucane FM, Luan J, Wareham NJ, Sharp SJ, O'Rahilly S, Balkau B, et al. Correlation of the leptin:adiponectin ratio with measures of insulin resistance in non-diabetic individuals. *Diabetologia*. 2009, **52**, 2345–9. https://doi.org/10.1007/s00125-009-1508-3.

[75] Valavanidis A, Vlachogianni T, Fiotakis C. 8-hydroxy-2′ -deoxyguanosine (8-OHdG): A Critical Biomarker of Oxidative Stress and Carcinogenesis. *J Environ Sci Heal Part C*. 2009, **27**, 120–39. https://doi.org/10.1074/jbc.M110.103713.

[76] Dawson GR, Tricklebank MD. Use of the elevated plus maze in the search for novel anxiolytic agents. *Trends Pharmacol Sci*. 1995, **16**, 33–6. https://doi.org/10.1016/s0165-6147(00)88973-7.

[77] Dornellas APS, Boldarine VT, Pedroso AP, Carvalho LOT, de Andrade IS, Vulcani-Freitas TM, et al. High-Fat Feeding Improves Anxiety-Type Behavior Induced by Ovariectomy in Rats. *Front Neurosci*. 2018, **12**, 1–13. https://doi.org/10.3389/fnins.2018.00557.

[78] Da Rocha RVO, Martins MIM, Antunes FTT, Martins MG, Klein AB, Corrêa DS, et al. Behavioral, Oxidative, and Biochemical Effects of Omega-3 on an Ovariectomized Rat Model of Menopause. *J Menopausal Med*. 2021, **27**, 132. https://doi.org/10.6118/jmm.21016.

[79] Kasaoka S, Kawahara Y, Inoue S, Tsuji M, Kato H, Tsuchiya T, et al. Gender effects in dietary histidine-induced anorexia. *Nutrition*. 2005, **21**, 855–8. https://doi.org/10.1016/j.nut.2004.12.009.

[80] Gavin KM, Kohrt WM, Klemm DJ, Melanson EL. Modulation of Energy Expenditure by Estrogens and Exercise in Women. *Exerc Sport Sci Rev*. 2018, **46**, 232–9. https://doi.org/10.1249/JES.0000000000000160.

[81] Lovejoy JC, Champagne CM, de Jonge L, Xie H, Smith SR. Increased visceral fat and decreased energy expenditure during the menopausal transition. *Int J Obes*. 2008, **32**, 949–58. https://doi.org/10.1038/ijo.2008.25.

[82] Day DS, Gozansky WS, Van Pelt RE, Schwartz RS, Kohrt WM. Sex Hormone Suppression Reduces Resting Energy Expenditure and β-Adrenergic Support of Resting Energy Expenditure. *J Clin Endocrinol Metab*. 2005, **90**, 3312–7. https://doi.org/10.1210/jc.2004-1344.

[83] Kasaoka S, Tsuboyama-Kasaoka N, Kawahara Y, Inoue S, Tsuji M, Ezaki O, et al. Histidine supplementation suppresses food intake and fat accumulation in rats. *Nutrition*. 2004, **20**, 991–6. https://doi.org/10.1016/j.nut.2004.08.006.

[84] Asahi R, Tanaka K, Fujimi TJ, Kanzawa N, Nakajima S. Proline Decreases the Suppressive Effect of Histidine on Food Intake and Fat Accumulation. *J Nutr Sci Vitaminol*. 2016, **62**, 277–80. https://doi.org/10.3177/jnsv.62.277.

[85] López-Gonzales E, Lehmann L, Ruiz-Ojeda FJ, Hernández-Bautista R, Altun I, Onogi Y, et al. L-Serine Supplementation Blunts Fasting-Induced Weight Regain by Increasing Brown Fat Thermogenesis. *Nutrients*. 2022, **14**, 1922. https://doi.org/10.3390/nu14091922.

[86] Mauvais-Jarvis F, Clegg DJ, Hevener AL. The Role of Estrogens in Control of Energy Balance and Glucose Homeostasis. *Endocr Rev*. 2013, 34, 309–38. https://doi.org/10.1210/er.2012-1055.

[87] Liang YQ, Akishita M, Kim S, Ako J, Hashimoto M, Iijima K, et al. Estrogen receptor β is involved in the anorectic action of estrogen. *Int J Obes*. 2002, **26**, 1103–9. https://doi.org/

[88] Taicher GZ, Tinsley FC, Reiderman A, Heiman ML. Quantitative magnetic resonance (QMR) method for bone and whole-body-composition analysis. *Anal Bioanal Chem*. 2003, **377**, 990–1002. https://doi.org/10.1007/s00216-003-2224-3.

[89] López N, Sánchez J, Picó C, Palou A, Serra F. Dietary l-leucine supplementation of lactating rats results in a tendency to increase lean/fat ratio associated to lower orexigenic neuropeptide expression in hypothalamus. *Peptides*. 2010, **31**, 1361–7. https://doi.org/10.1016/j.peptides.2010.03.028.

[90] Caimari A, del Bas JM, Boqué N, Crescenti A, Puiggròs F, Chenoll E, et al. Heat-killed Bifidobacterium animalis subsp. Lactis CECT 8145 increases lean mass and ameliorates metabolic syndrome in cafeteria-fed obese rats. *J Funct Foods*. 2017, **38**, 51–63. https://doi.org/10.1016/j.jff.2017.09.029.

[91] Hepler C, Bass J. Circadian mechanisms in adipose tissue bioenergetics and plasticity. *Genes Dev*. 2023, **37**, 454–73. https://doi.org/10.1101/gad.350759.123.

[92] Charrier A, Xu X, Guan BJ, Ngo J, Wynshaw-Boris A, Hatzoglou M, et al. Adipocyte-specific deletion of zinc finger protein 407 results in lipodystrophy and insulin resistance in mice. *Mol Cell Endocrinol*. 2021, **521**, 111109. https://doi.org/10.1016/j.mce.2020.111109.

[93] Tian J, Dang HN, Yong J, Chui WS, Dizon MPG, Yaw CKY, et al. Oral Treatment with γ-Aminobutyric Acid Improves Glucose Tolerance and Insulin Sensitivity by Inhibiting Inflammation in High Fat Diet-Fed Mice. *PLoS One*. 2011, **6**, 25338. https://doi.org/10.1371/journal.pone.0025338.

[94] Heli Z, Hongyu C, Dapeng B, Yee Shin T, Yejun Z, Xi Z, et al. Recent advances of γ-aminobutyric acid: Physiological and immunity function, enrichment, and metabolic pathway. *Front Nutr*. 2022, **9**, 1–16. https://doi.org/10.3389/fnut.2022.1076223.

[95] Conceição-Furber E, Coskun T, Sloop KW, Samms RJ. Is Glucagon Receptor Activation the Thermogenic Solution for Treating Obesity? *Front Endocrinol.* 2022, **13**, 1–9. https://doi.org/10.3389/fendo.2022.868037.

[96] Pereira MJ, Thombare K, Sarsenbayeva A, Kamble PG, Almby K, Lundqvist M, et al. Direct effects of glucagon on glucose uptake and lipolysis in human adipocytes. *Mol Cell Endocrinol*. 2020, **503**, 110696. https://doi.org/10.1016/j.mce.2019.110696.

[97] Schleinitz D, Klöting N, Lindgren CM, Breitfeld J, Dietrich A, Schön MR, et al. Fat depot-specific mRNA expression of novel loci associated with waist–hip ratio. *Int J Obes*. 2014, **38**, 120–5. https://doi.org/10.1038/ijo.2013.56.

[98] Cariou B, Capitaine N, Le Marcis V, Vega N, Béréziat V, Kergoat M, et al. Increased adipose tissue expression of Grb14 in several models of insulin resistance. *FASEB J*. 2004, **18**, 965–7. https://doi.org/10.1096/fj.03-0824fje.

[99] Sun C, Förster F, Gutsmann B, Moulla Y, Stroh C, Dietrich A, et al. Metabolic Effects of the Waist-To-Hip Ratio Associated Locus GRB14/COBLL1 Are Related to GRB14 Expression in Adipose Tissue. *Int J Mol Sci*. 2022, **23**, 8558. https://doi.org/10.3390/ijms23158558.

[100] Khan T, Muise ES, Iyengar P, Wang Z V., Chandalia M, Abate N, et al. Metabolic Dysregulation and Adipose Tissue Fibrosis: Role of Collagen VI. *Mol Cell Biol*. 2009, **29**, 1575–91. https://doi.org/10.1128/MCB.01300-08.

[101] Munoz A, Abate N, Chandalia M. Adipose Tissue Collagen and Inflammation in Nonobese Asian Indian Men. *J Clin Endocrinol Metab*. 2013, **98**, E1360–3. https://doi.org/10.1210/jc.2012-3841.

[102] Chun TH. Peri-adipocyte ECM remodeling in obesity and adipose tissue fibrosis. *Adipocyte*. 2012, **1**, 89–95. https://doi.org/10.4161/adip.19752.

[103] Zhao Y, Yu Z, Song Y, Fan L, Lei T, He Y, et al. The Regulatory Network of CREB3L1 and Its Roles in Physiological and Pathological Conditions. *Int J Med Sci*. 2024, **21**, 123–36. https://doi.org/10.7150/ijms.90189.

[104] Huang A, Lin Y, Kao L, Chiou Y, Lee G, Lin H, et al. Inflammation-induced macrophage lysyl oxidase in adipose stiffening and dysfunction in obesity. *Clin Transl Med*. 2021, **11**, 2–8. https://doi.org/10.1002/ctm2.543.

[105] Soták M, Rajan MR, Clark M, Biörserud C, Wallenius V, Hagberg CE, et al. Healthy Subcutaneous and Omental Adipose Tissue Is Associated with High Expression of Extracellular Matrix Components. *Int J Mol Sci*. 2022, **23**, 520. https://doi.org/10.3390/ijms23010520.

[106] Meissburger B, Stachorski L, Röder E, Rudofsky G, Wolfrum C. Tissue inhibitor of matrix metalloproteinase 1 (TIMP1) controls adipogenesis in obesity in mice and in humans. *Diabetologia*. 2011, **54**, 1468–79. https://doi.org/10.1007/s00125-011-2093-9.

[107] Maquoi E, Munaut C, Colige A, Collen D, Lijnen HR. Modulation of Adipose Tissue Expression of Murine Matrix Metalloproteinases and Their Tissue Inhibitors With Obesity. *Diabetes*. 2002, **51**, 1093–101. https://doi.org/10.2337/diabetes.51.4.1093.

[108] Roger Lijnen H, Demeulemeester D, Van Hoef B, Collen D, Maquoi E. Deficiency of tissue inhibitor of matrix metalloproteinase-1 (TIMP-1) impairs nutritionally induced obesity in mice. *Thromb Haemost*. 2003, **89**, 249–55. https://doi.org/10.1055/s-0037-1613439.

[109] Ren Y, Zhao H, Yin C, Lan X, Wu L, Du X, et al. Adipokines, Hepatokines and Myokines: Focus on Their Role and Molecular Mechanisms in Adipose Tissue Inflammation. *Front Endocrinol*. 2022, **13**, 1–26. https://doi.org/10.3389/fendo.2022.873699.

[110] Takahashi M, Nagaretani H, Funahashi T, Nishizawa H, Maeda N, Kishida K, et al. The Expression of SPARC in Adipose Tissue and Its Increased Plasma Concentration in Patients with Coronary Artery Disease. *Obes Res*. 2001, **9**, 388–93. https://doi.org/10.1038/oby.2001.50.

[111] Lee SH, Lee JA, Park HS, Song YS, Jang YJ, Kim JH, et al. Associations among SPARC mRNA expression in adipose tissue, serum SPARC concentration and metabolic parameters in Korean women. *Obesity*. 2013, **21**, 2296–302. https://doi.org/10.1002/oby.20183.

[112] Kim J, Lee SK, Shin J min, Jeoun U woo, Jang YJ, Park HS, et al. Enhanced biglycan gene expression in the adipose tissues of obese women and its association with obesity-related genes and metabolic parameters. *Sci Rep*. 2016, **6**, 30609. https://doi.org/10.1038/srep30609.

[113] Tiaden AN, Bahrenberg G, Mirsaidi A, Glanz S, Blüher M, Richards PJ. Novel Function of Serine Protease HTRA1 in Inhibiting Adipogenic Differentiation of Human Mesenchymal Stem Cells via MAP Kinase-Mediated MMP Upregulation. *Stem Cells*. 2016, **34**, 1601–14.

https://doi.org/10.1002/stem.2297.

[114] Shin J, Toyoda S, Okuno Y, Hayashi R, Nishitani S, Onodera T, et al. HSP47 levels determine the degree of body adiposity. *Nat Commun*. 2023, **14**, 7319. https://doi.org/10.1038/s41467-023-43080-x.

[115] Pae M, Romeo GR. The multifaceted role of profilin-1 in adipose tissue inflammation and glucose homeostasis. *Adipocyte*. 2014, **3**, 69–74. https://doi.org/10.4161/adip.26965.

[116] Sharma NK, Comeau ME, Montoya D, Pellegrini M, Howard TD, Langefeld CD, et al. Integrative analysis of glucometabolic traits, adipose tissue dna methylation, and gene expression identifies epigenetic regulatory mechanisms of insulin resistance and obesity in African Americans. *Diabetes*. 2020, **69**, 2779–93. https://doi.org/10.2337/db20-0117.

[117] Vogel MAA, Wang P, Bouwman FG, Hoebers N, Blaak EE, Renes J, et al. A comparison between the abdominal and femoral adipose tissue proteome of overweight and obese women. *Sci Rep*. 2019, **9**, 4202. https://doi.org/10.1038/s41598-019-40992-x.

[118] Chang SK, Kohlgruber AC, Mizoguchi F, Michelet X, Wolf BJ, Wei K, et al. Stromal cell cadherin-11 regulates adipose tissue inflammation and diabetes. *J Clin Invest*. 2017, **127**, 3300–12. https://doi.org/10.1172/JCI86881.

[119] Ballak DB, Stienstra R, Tack CJ, Dinarello CA, van Diepen JA. IL-1 family members in the pathogenesis and treatment of metabolic disease: Focus on adipose tissue inflammation and insulin resistance. *Cytokine*. 2015, **75**, 280–90. https://doi.org/10.1016/j.cyto.2015.05.005.

[120] Blüher M, Klöting N, Wueest S, Schoenle EJ, Schön MR, Dietrich A, et al. Fas and FasL Expression in Human Adipose Tissue Is Related to Obesity, Insulin Resistance, and Type 2 Diabetes. *J Clin Endocrinol Metab*. 2014, **99**, E36–44. https://doi.org/10.1210/jc.2013-2488.

[121] Rouault C, Pellegrinelli V, Schilch R, Cotillard A, Poitou C, Tordjman J, et al. Roles of chemokine ligand-2 (CXCL2) and neutrophils in influencing endothelial cell function and inflammation of human adipose tissue. *Endocrinology*. 2013, **154**, 1069–79. https://doi.org/10.1210/en.2012-1415.

[122] Hellmann J, Sansbury BE, Holden CR, Tang Y, Wong B, Wysoczynski M, et al. CCR7 Maintains Nonresolving Lymph Node and Adipose Inflammation in Obesity. *Diabetes*. 2016, **65**, 2268–81. https://doi.org/10.2337/db15-1689.

[123] Pan Y, Cao S, Tang J, Arroyo JP, Terker AS, Wang Y, et al. Cyclooxygenase-2 in adipose tissue macrophages limits adipose tissue dysfunction in obese mice. *J Clin Invest*. 2022, **132**, e152391. https://doi.org/10.1172/JCI1523912.

[124] Wang L, Wang Y, Zhang C, Li J, Meng Y, Dou M, et al. Inhibiting Glycogen Synthase Kinase 3 Reverses Obesity-Induced White Adipose Tissue Inflammation by Regulating Apoptosis Inhibitor of Macrophage/CD5L-Mediated Macrophage Migration. *Arterioscler Thromb Vasc Biol*. 2018, **38**, 2103–16. https://doi.org/10.1161/ATVBAHA.118.311363.

[125] Newling M, Sritharan L, van der Ham AJ, Hoepel W, Fiechter RH, de Boer L, et al. C-Reactive Protein Promotes Inflammation through FcγR-Induced Glycolytic Reprogramming of Human Macrophages. *J Immunol*. 2019, **203**, 225–35. https://doi.org/10.4049/jimmunol.1900172.

[126] Piacentini L, Chiesa M, Colombo GI. Gene Regulatory Network Analysis of Perivascular Adipose Tissue of Abdominal Aortic Aneurysm Identifies Master

Regulators of Key Pathogenetic Pathways. *Biomedicines*. 2020. **8**, 288. https://doi.org/10.4049/jimmunol.1900172.

[127] Purvis GSD, Collino M, Aranda-Tavio H, Chiazza F, O'Riordan CE, Zeboudj L, et al. Inhibition of Bruton's TK regulates macrophage NF-κB and NLRP3 inflammasome activation in metabolic inflammation. *Br J Pharmacol*. 2020, **177**, 4416–32. https://doi.org/10.1111/bph.15182.

[128] Purvis GSD, Collino M, van Dam AD, Einaudi G, Ng Y, Shanmuganathan M, et al. OxPhos in adipose tissue macrophages regulated by BTK enhances their M2-like phenotype and confers a systemic immunometabolic benefit in obesity. *Diabetes*. 2024, 1–50. https://doi.org/10.2337/db22-0275.

[129] Morin SO, Poggi M, Alessi MC, Landrier JF, Nunès JA. Modulation of T Cell Activation in Obesity. *Antioxid Redox Signal*. 2017, **26**, 489–500. https://doi.org/10.1089/ars.2016.6746.

[130] Shitaye HS, Terkhorn SP, Combs JA, Hankenson KD. Thrombospondin-2 is an endogenous adipocyte inhibitor. *Matrix Biol*. 2010, **29**, 549–56. https://doi.org/10.1016/j.matbio.2010.05.006.

[131] Nie J, Sage EH. SPARC Inhibits Adipogenesis by Its Enhancement of β-Catenin Signaling. *J Biol Chem.* 2009, **284**, 1279–90. https://doi.org/10.1074/jbc.M808285200.

[132] Wang L, Zhang C guang, Jia Y lin, Hu L. Tissue Inhibitor of Metalloprotease-1 (TIMP-1) Regulates Adipogenesis of Adipose-derived Stem Cells (ASCs) via the Wnt Signaling Pathway in an MMP-independent Manner. *Curr Med Sci*. 2020, **40**, 989–96. https://doi.org/10.1007/s11596-020-2265-2.

[133] Hammarstedt A, Hedjazifar S, Jenndahl L, Gogg S, Grünberg J, Gustafson B, et al. WISP2 regulates preadipocyte commitment and PPARγ activation by BMP4. *Proc Natl Acad Sci*. 2013, **110**, 2563–8. https://doi.org/10.1073/pnas.1211255110.

[134] Jang MK, Kim CH, Seong JK, Jung MH. ATF3 inhibits adipocyte differentiation of 3T3-L1 cells. *Biochem Biophys Res Commun*. 2012, **421**, 38–43. https://doi.org/10.1016/j.bbrc.2012.03.104.

[135] Boyle KB, Hadaschik D, Virtue S, Cawthorn WP, Ridley SH, O'Rahilly S, et al. The transcription factors Egr1 and Egr2 have opposing influences on adipocyte differentiation. *Cell Death Differ*. 2009, **16**, 782–9. https://doi.org/10.1016/j.bbrc.2012.03.104.

[136] Park YM, Lee Y ho, Kim SH, Lee EY, Kim KS, Williams DR, et al. Snail, a transcriptional regulator, represses adiponectin expression by directly binding to an E-box motif in the promoter. *Metabolism*. 2012, **61**, 1622–32. https://doi.org/10.1016/j.metabol.2012.04.014.

[137] Hino J, Miyazawa T, Miyazato M, Kangawa K. Bone morphogenetic protein-3b (BMP-3b) is expressed in adipocytes and inhibits adipogenesis as a unique complex. *Int J Obes*. 2012, **36**, 725–34. https://doi.org/10.1038/ijo.2011.124.

[138] Butterwith SC. Molecular events in adipocyte development. *Pharmacol Ther*. 1994, **61**, 399–411. https://doi.org/10.1016/0163-7258(94)90018-3.

[139] Zhao Y, Zhang YD, Zhang YY, Qian SW, Zhang ZC, Li SF, et al. p300-Dependent Acetylation of Activating Transcription Factor 5 Enhances C/EBPβ Transactivation of C/EBPα during 3T3-L1 Differentiation. *Mol Cell Biol*. 2014, **34**, 315–24. https://doi.org/10.1128/MCB.00956-13.

[140] Zhang H, Chen X, Sairam MR. Novel Genes of Visceral Adiposity: Identification of Mouse and Human Mesenteric Estrogen-Dependent Adipose

(MEDA)-4 Gene and Its Adipogenic Function. *Endocrinology*. 2012, **153**, 2665–76. https://doi.org/10.1210/en.2011-2008.

[141] Liu X, Li H, Zhang L, Wang L, Wang L. Expression and Genetic Effects of GLI Pathogenesis-Related 1 Gene on Backfat Thickness in Pigs. *Genes*. 2022, **13**, 1448. https://doi.org/0.3390/genes13081448.

[142] Ehrlund A, Mejhert N, Lorente-Cebrián S, Åström G, Dahlman I, Laurencikiene J, et al. Characterization of the Wnt Inhibitors Secreted Frizzled-Related Proteins (SFRPs) in Human Adipose Tissue. *J Clin Endocrinol Metab*. 2013, **98**, E503–8. https://doi.org/10.1210/jc.2012-3416.

[143] Guiu-Jurado E, Unthan M, Böhler N, Kern M, Landgraf K, Dietrich A, et al. Bone morphogenetic protein 2 (BMP2) may contribute to partition of energy storage into visceral and subcutaneous fat depots. *Obesity*. 2016, **24**, 2092–100. https://doi.org/10.1002/oby.21571.

[144] Ren G, Beech C, Smas CM. The Immunoglobulin Superfamily Protein Differentiation of Embryonic Stem Cells 1 (Dies1) Has a Regulatory Role in Preadipocyte to Adipocyte Conversion. Vinciguerra M, editor. *PLoS One*. 2013, **8**, e65531. https://doi.org/10.1371/journal.pone.0065531.

[145] Hudak CS, Sul HS. Pref-1, a Gatekeeper of Adipogenesis. *Front Endocrinol*. 2013, **4**, 1–6. https://doi.org/10.3389/fendo.2013.00079.

[146] Yu X, Shen N, Zhang ML, Pan FY, Wang C, Jia WP, et al. Egr-1 decreases adipocyte insulin sensitivity by tilting PI3K/Akt and MAPK signal balance in mice. *EMBO J*. 2011, **30**, 3754–65. https://doi.org/10.1038/emboj.2011.277.

[147] Hua Y, Xie D, Zhang Y, Wang M, Wen W, Sun J. Identification and analysis of key genes in adipose tissue for human obesity based on bioinformatics. *Gene*. 2023, **888**, 147755. https://doi.org/10.1016/j.gene.2023.147755.

[148] Favre D, Le Gouill E, Fahmi D, Verdumo C, Chinetti-Gbaguidi G, Staels B, et al. Impaired Expression of the Inducible cAMP Early Repressor Accounts for Sustained Adipose CREB Activity in Obesity. *Diabetes*. 2011, **60**, 3169–74. https://doi.org/10.2337/db10-1743.

[149] Zhang X, Liu Z, Li W, Kang Y, Xu Z, Li X, et al. MAPKs/AP-1, not NF-κB, is responsible for MCP-1 production in TNF-α-activated adipocytes. *Adipocyte*. 2022, **11**, 477–86. https://doi.org/10.1080/21623945.2022.2107786.

[150] Bahrami S, Drabløs F. Gene regulation in the immediate-early response process. *Adv Biol Regul*. 2016, **62**, 37–49. https://doi.org/10.1016/j.jbior.2016.05.001.

[151] Dankel SN, Fadnes DJ, Stavrum AK, Stansberg C, Holdhus R, Hoang T, et al. Switch from Stress Response to Homeobox Transcription Factors in Adipose Tissue After Profound Fat Loss. Sorensen TIA, editor. *PLoS One*. 2010, **5**, e11033. https://doi.org/10.1371/journal.pone.0011033.

[152] Schübel R, Sookthai D, Greimel J, Johnson T, Grafetstätter M, Kirsten R, et al. Key Genes of Lipid Metabolism and WNT-Signaling Are Downregulated in Subcutaneous Adipose Tissue with Moderate Weight Loss. *Nutrients*. 2019, **11**, 639. https://doi.org/10.3390/nu11030639.

[153] Jukarainen S, Heinonen S, Rämö JT, Rinnankoski-Tuikka R, Rappou E, Tummers M, et al. Obesity Is Associated With Low NAD + /SIRT Pathway Expression in Adipose Tissue of BMI-Discordant Monozygotic Twins. *J Clin Endocrinol Metab*. 2016, **101**, 275–83. https://doi.org/10.1210/jc.2015-3095.

[154] Takanabe-Mori R, Ono K, Sowa N, Wada H, Takaya T, Horie T, et al. Lectin-like oxidized low-density lipoprotein receptor-1 is required for the adipose tissue expression of proinflammatory cytokines in high-fat diet-induced obese

mice. *Biochem Biophys Res Commun*. 2010, **398**, 576–80. https://doi.org/10.1016/j.bbrc.2010.06.123.

[155] Brinkley TE, Kume N, Mitsuoka H, Phares DA, Hagberg JM. Elevated Soluble Lectin-like Oxidized LDL Receptor-1 (sLOX-1) Levels in Obese Postmenopausal Women. *Obesity*. 2008, **16**, 1454–6. https://doi.org/10.1038/oby.2008.213.

[156] Sugimoto M, Shimizu Y, Zhao S, Ukon N, Nishijima K ichi, Wakabayashi M, et al. Characterization of the role of sphingomyelin synthase 2 in glucose metabolism in whole-body and peripheral tissues in mice. *Biochim Biophys Acta - Mol Cell Biol Lipids*. 2016, **1861**, 688–702. https://doi.org/10.1016/j.bbalip.2016.04.019.

[157] Kolak M, Westerbacka J, Velagapudi VR, Wågsäter D, Yetukuri L, Makkonen J, et al. Adipose Tissue Inflammation and Increased Ceramide Content Characterize Subjects With High Liver Fat Content Independent of Obesity. *Diabetes*. 2007, **56**, 1960–8. https://doi.org/10.2337/db07-0111.

[158] Hunt MC, Siponen MI, Alexson SEH. The emerging role of acyl-CoA thioesterases and acyltransferases in regulating peroxisomal lipid metabolism. *Biochim Biophys Acta - Mol Basis Dis*. 2012, **1822**, 1397–410. https://doi.org/10.1016/j.bbadis.2012.03.009.

[159] Feehan J, Hariharan R, Buckenham T, Handley C, Bhatnagar A, Baba SP, et al. Carnosine as a potential therapeutic for the management of peripheral vascular disease. *Nutr Metab Cardiovasc Dis*. 2022, **32**, 2289–96. https://doi.org/10.1016/j.numecd.2022.07.006.

[160] Al-Sawalha NA, Alshogran OY, Awawdeh MS, Almomani BA. The effects of L-Carnosine on development of metabolic syndrome in rats. *Life Sci*. 2019, **237**. https://doi.org/10.1016/j.lfs.2019.116905.

[161] Zeybel M, Altay O, Arif M, Li X, Yang H, Fredolini C, et al. Combined metabolic activators therapy ameliorates liver fat in nonalcoholic fatty liver disease patients. *Mol Syst Biol*. 2021, **17**, 1–18. https://doi.org/10.15252/msb.202110459.

[162] Singh B, Bhat NK, Bhat HK. Induction of NAD(P)H-quinone oxidoreductase 1 by antioxidants in female ACI rats is associated with decrease in oxidative DNA damage and inhibition of estrogen-induced breast cancer. *Carcinogenesis*. 2012 Jan 1;**33**(1):156–63. https://doi.org/10.1093/carcin/bgr237

[163] Chen CL. Hormone Replacement Therapy in Relation to Breast Cancer. *JAMA*. 2002, **287**, 734–41. https://doi.org/10.1001/jama.287.6.734.

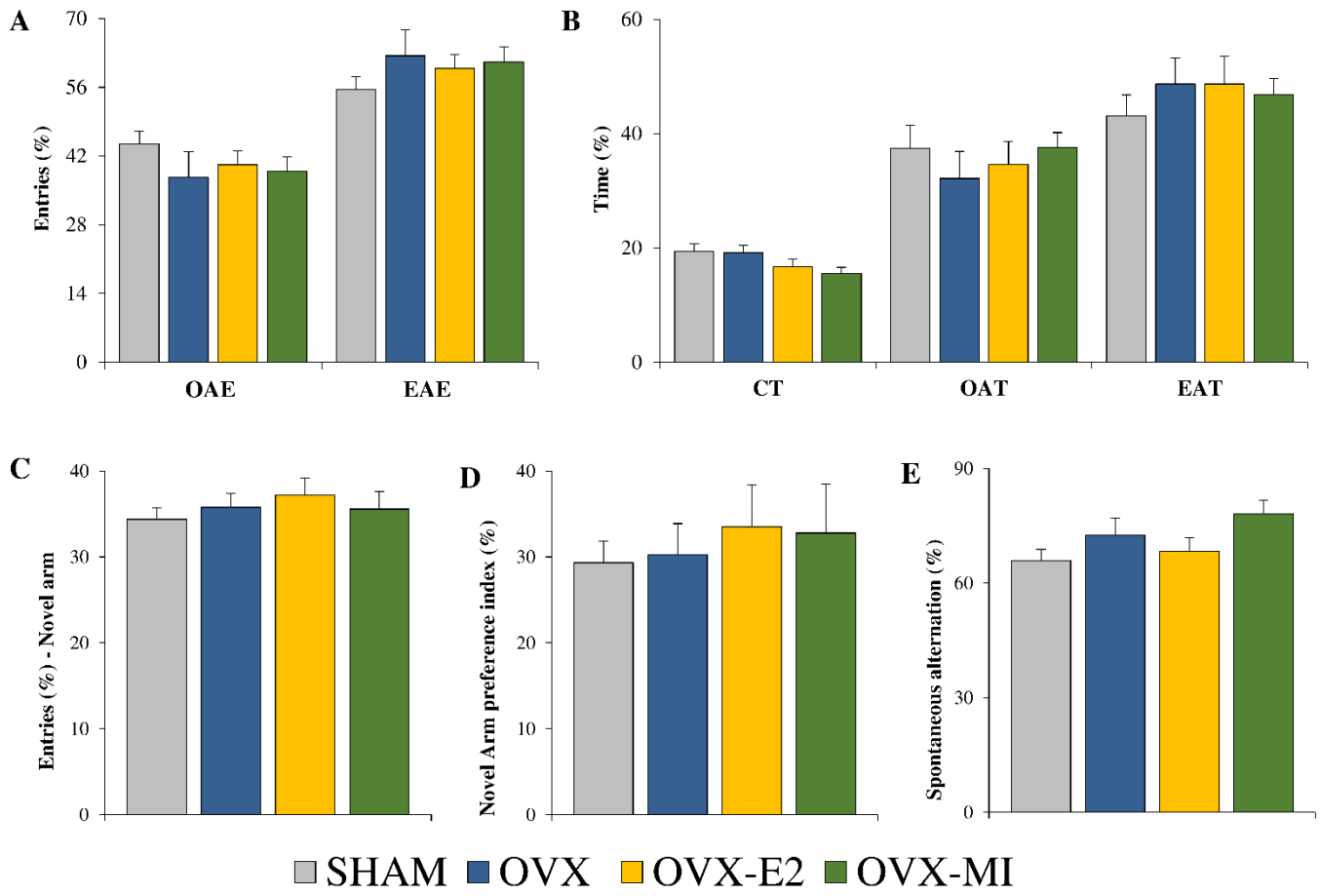
Appendix - Supplementary material

The following are available online at XXXX, Dataset S1: List of genes identified in RWAT transcriptomics and DEGs comparing OVX-MI to control OVX. Supplementary Table 1: Indirect calorimetry measurements in sham-operated (SH) and ovariectomized (OVX) rats between Days 29 and 33 after the beginning of the treatments. Supplementary Figure 1: Effects of ovariectomy, 17β-E2 injections and MI treatment on anxiety-like behaviour in the EPM (A & B) on Day 36 and on spatial reference memory in the Y-maze (C-E) on Day 40 of the study in sham-operated (SHAM) and ovariectomized (OVX) rats.

Supplementary Table 1: Indirect calorimetry measurements in sham-operated (SH) and ovariectomized (OVX) rats between Days 29 and 33 after the beginning of the treatments

	SHAM	OVX	OVX-E2	OVX-MI	Intervention effect (p value)
RQ					
21 hours	0.89 ± 0.03	0.87 ± 0.03	0.87 ± 0.02	0.85 ± 0.02	NS (0.803)
Light phase	0.86 ± 0.04	0.83 ± 0.03	0.83 ± 0.03	0.81 ± 0.03	NS (0.695)
Dark phase	0.91 ± 0.03	0.90 ± 0.02	0.90 ± 0.02	0.88 ± 0.02	NS (0.878)
Energy Expenditure (KJ/day/kg 0.75)					
21 hours	330 ± 10^{a}	300 ± 7^{b}	304 ± 11^{ab}	289 ± 8^{b}	*I* (0.027)
Light phase	302 ± 10^{a}	275 ± 9^{b}	276 ± 8^{b}	266 ± 8^{b}	*I* (0.038)
Dark phase	347 ± 11^{a}	316 ± 7^{b}	322 ± 13^{ab}	304 ± 9^{b}	*I* (0.037)
Fat oxidation (KJ/day/kg^0.75)					
21 hours	107 ± 33	107 ± 25	108 ± 22	118 ± 19	NS (0.988)
Light phase	122 ± 33	136 ± 31	134 ± 27	145 ± 22	NS (0.952)
Dark phase	98 ± 34	89 ± 21	91 ± 19	101 ± 17	NS (0.983)
Carbohydrate oxidation (KJ/day/kg^0.75)					
21 hours	227 ± 40	177 ± 32	182 ± 27	155 ± 30	NS (0.475)
Light phase	163 ± 37	120 ± 36	119 ± 26	93 ± 25	NS (0.689)
Dark phase	266 ± 44	213 ± 30	222 ± 29	194 ± 33	NS (0.505)

Indirect calorimetric measurements were performed between Days 29 and 33 under ad libitum conditions and for 22 h (from 11:00 am to 09:00 am). The data obtained during the first hour were discarded from the final analyses. All rats were fed a standard chow diet during the measurements. The data are presented as the means ± SEMs (n = 10). Different superscript lowercase letters (a, b) indicate significantly different mean values (one-way ANOVA and Duncan's *post hoc* test, $p < 0.05$). *I*: the effect of the intervention. NS: nonsignificant differences. SHAM: sham-operated rats; OVX: ovariectomized rats; OVX-E2: OVX rats treated with 17β-oestradiol; OVX-MI: OVX rats supplemented with the multi-ingredient. RQ: respiratory quotient.



Supplementary Figure 1 Effects of ovariectomy, 17β-E2 injections and MI treatment on anxiety-like behaviour in the EPM (A & B) on Day 36 and on spatial reference memory in the Y-maze (C-E) on Day 40 of the study in sham-operated (SHAM) and ovariectomized (OVX) rats. The data are presented as the means ± SEMs (n = 10). Supplementary Figure 1A, Percentages of entries into the open arms (OAE) and entries into the enclosed arms (EAE) in the EPM. Supplementary Figure 1B, Percentage of time spent exploring the central zone (CT), open arms (OATs) and enclosed arms (EATs) in the EPM. Supplementary Figure 1C, Percentage of entries into the novel arm in the Y-maze. In Supplementary Figure 1D, the percentage of time spent in the novel arm is presented as the arm preference index (%). Supplementary Figure 1E, Frequency of alternation into the novel arm as spontaneous alternation (%). SHAM: sham-operated rats, OVX: ovariectomized rats, OVX-E2: OVX rats treated with 17β-oestradiol, OVX-MI: OVX rats supplemented with the multi-ingredient. OAE: open arm entry. EAE: enclosed arm entry. CT: central zone time. OAT: open arm time. EAT: enclosed arm time.

IV. GENERAL DISCUSSION

Menopause is a natural phase in a woman's life associated with reproductive aging. It is linked to senescence in ovarian function accompanied by a decline in oestrogen production that is already evident at the onset of irregular menstrual cycles occurring during the menopausal transition, known as perimenopause, and exacerbated during the postmenopausal state (362). This reproductive aging process is often accompanied by various VMS, such as sleep disturbances, night sweats, and hot flashes (1,6,363), and can be associated with an increased risk of osteoporosis and with the appearance of CVDs risk factors (13,66,75,364,365). While VMS are more common in the early stages of the menopausal transition, other alterations become more evident in the postmenopausal state when there is a nearly complete depletion of oestrogen. Thus, the sharp decline in oestrogen production can increase fat mass accretion (especially in the abdominal region), oxidative stress and low-grade inflammation, which, in turn, can trigger the appearance of metabolic disorders, such as hypertension, dyslipidemia and IR, thereby increasing the risk of suffering MetS and CVDs (14,16,143,366,367). Considering the rise in women's life expectancy worldwide, who spend at least a third of their lives in the postmenopausal state, there is growing interest in slowing down and ameliorating menopause-related alterations to improve women's well-being and quality of life.

In recent years, the controversy about the risks associated with HRT (139) has prompted many women to look for alternative therapies to ameliorate VMS, osteoporosis and the cardiometabolic-related disturbances associated with the postmenopausal stage. In this framework, nutritional-based strategies, such as those based on the consumption of natural extracts and nutraceuticals, have been used as alternative and complementary therapies to HRT to tackle these menopausal-related alterations. Different studies, including some carried out by our research group, have shown that the combined administration of various bioactive compounds acting against complementary targets is a

suitable strategy to address cardiometabolic risk factors (153–157). However, the effects of combined supplementation with different bioactive compounds to tackle menopausal-related metabolic alterations have been scarcely evaluated. In line with the idea that better outcomes can be obtained when treatments are performed under a multifaceted approach and considering that menopause can be associated with multifactorial alterations, the supplementation with a blend of bioactive compounds that can complementarily act on cellular mechanisms and biochemical pathways that can be altered during this reproductive aging process could provide benefits during the postmenopausal state. Thus, the main aim of the present thesis was to assess the potential benefits of consuming two different (MIs)—one containing curcumin, hesperidin, and phytosterols, and another comprising amino acid-related compounds such as histidine, serine, cysteine, and carnosine—on the physiology and metabolism of OVX rats, a postmenopausal model with oestrogen deficiency, evaluating a wide range of cardiometabolic risk factors associated with the postmenopausal status and gaining knowledge on their underlying mechanisms.

Beyond the inherent and natural aging course in women, the menopausal transition, also known as perimenopause, leads to a series of physiological and cardiometabolic changes associated with female reproductive senescence (1–4). These changes are due to reduced follicular reserves and ovarian function atrophy, accompanied by dysregulation of the HPG axis as a result of declining oestrogen levels over time, which is more evident in menopausal women after the FMP (4–7,19,21,22,24). Despite this, there are very few longitudinal studies that have recognized circulating biomarkers characteristic of perimenopause, regardless of women's chronological age (3,24,362). These studies suggest that menopausal transition *per se* triggers several metabolic changes in women before reaching the postmenopausal state. However, beyond the onset of irregularity in

the menstrual cycle, changes in the circulating sex hormone levels and atherogenic lipid parameters, such as TG, TC and LDL-c (1,3,24,362), the underlying molecular mechanisms occurring at very early stages of perimenopause and its changes, remain limited and poorly understood. Gaining a deeper understanding of these mechanisms could pave the way for designing novel treatments and lifestyle-based nutritional interventions aimed at preserving the endocrine and metabolic functions in perimenopausal women and mitigating postmenopausal-related diseases that may significantly impact the quality of life throughout the remaining lifespan (26).

In this framework, it is essential to identify biomarkers that indicate a predisposition to a pathological state to explore the effects of nutraceutical supplements on our metabolism (293). Given that early changes induced by nutraceutical supplementation are often subtle, these biomarkers can be of great value for identifying at-risk individuals or detecting the onset of the disease before symptoms manifest. New approaches through sensitive and advanced techniques in omics sciences, are crucial for detecting these small changes as biomarkers. In this context, the second aim of this thesis was to identify omics-based biomarkers of metabolic risks at the early stages of natural reproductive aging using an ovarian-intact middle-aged model of rats resembling the characteristics of human perimenopause.

To accomplish the aims of the present thesis, we firstly precisely characterized a preclinical model of the natural reproductive aging based on middle-aged rats in which the ovarian function was evaluated by monitoring the regularity of their oestrous cycle and we carried out metabolic and lipidomic approaches in serum to identify circulating signatures across perimenopause (**Manuscript 1**), which was of great value to shed more light on the mechanisms involved in menopausal transition and to identify potential biomarkers at an early stage of perimenopause. Previous studies have demonstrated that

the assessment of the regularity in the oestrous cycle through cytological examination of vaginal smears, morphologically characterizing by different types of cells based on the four stages of the cycle (estrus, metestrus, diestrus, and proestrus) to detect the onset of irregularity and, in a later stage, the acyclicity in female middle-aged rats (368–370), can provide insights into mechanisms of the female reproductive axis across species, comparable to the transitions observed in women during the stages of premenopause and menopausal transition (perimenopause and early postmenopause) (22,370–372). In this regard, some studies reported neuroendocrine changes in the hypothalamus of middle-aged rats, such as the dysregulation of the expression of genes related to sex hormone feedback in the HPG axis and the DNA methylation of genes required for hormone signaling, in addition to altered circulating levels of sexual hormones, such as progesterone and FSH, similar to what is observed in women during the menopausal transition (22,371–375).

In our study, the gradual loss of regularity in the oestrous cycle occurring during the natural transition to reproductive senescence was associated with altered circulating levels of different HPG-related sex hormones (oestradiol, progesterone and LH) and, in rats that manifested acyclicity and with histomorphological changes in the ovaries, including atrophy and a lack of stromal luteinization and corpus luteum, which is in line with previous scientific evidence observed in both animal models and women (376–380). Thus, the notable decline in the circulating oestradiol levels already reported in the present study with the onset of irregularity and maintained in the acyclic rats is consistent with those observed in late perimenopause and early postmenopause in women, respectively (24,38), highlighting the usefulness of this preclinical model to resemble the menopausal transition occurring in women. Specifically, in women, the circulating levels of oestradiol are stable until approximately 2 years before the FMP. After this period,

during the late perimenopausal stage, the circulating levels decline rapidly, reaching their lowest point at the time of the FMP, and then stabilize again by 2 years post-FMP (24,38). Interestingly, in our study, these hormonal and ovarian-related changes were accompanied by altered lipid-related metabolites in serum, which were detected using lipidomic approaches. Specifically, we identified 144 metabolites that changed significantly among age-matched rats having a regular cycle (resembling premenopause), an irregular cycle (resembling perimenopause) and acyclicity (resembling early postmenopause). Through multivariate analyses, we identified the 40 metabolites that contribute most to the separation of the three stages of reproductive aging, including mainly lipids of the phosphatidylcholines, lysophosphatidylcholines, lysophosphatidylcholamines, triglycerides, fatty acids and cholesterol esters families. Remarkably, the pattern across all subclasses of glycerolipids and glycerophospholipids, specially phosphatidylcholines, displayed an accelerated increase in their circulating levels in response to the loss of regular cycles as previously described in elderly women (46,47) and postmenopausal women (381). Considering that lipid compounds, including glycerophospholipids, glycerolipids and sterols display critical roles in cellular structure, energy storage and signaling, alterations in the circulating lipidome may mirror and potentially influence changes in metabolic and physiological states associated with the endocrine function (382). To the best of our knowledge, only two studies reported previously changes in circulating lipid-related metabolites associated with reproductive aging, but these findings were found by comparing premenopausal and postmenopausal women matched by age. The authors reported a similar trend to what was observed in our study, observing an increase in the circulating levels of lipid-related metabolites in postmenopausal women (381,383). These increases in the circulating lipid-related metabolites observed in our study during menopausal transition could be explained, at

least in part, by the reported sex-related differences concerning circulating lipidomes that tend to narrow or reverse with age, increasing the circulating glycerophospholipid levels in middle-aged and elderly women, particularly in the age range of 45-66 years (60,61). In line with these findings, another study revealed that most significant age-related changes in women occurred around 48 years (64), which coincides with the average age of the onset of perimenopause stage (65). It is well known that men display a higher risk for CVD early in life, while women have a higher risk later in life (384,385) and both the sex and age-related differences in CVD risk have been linked to changes in glycerophospholipid metabolism (386). Whether the differences in the circulating glycerophospholipid composition reported in this rat model of natural female reproductive senescence could impact on patterns of health and disease during perimenopause and could contribute to sexual dimorphism in CVD risk at middle age deserves further research. To the best of our knowledge, there is a lack of studies focused on the identification of omics-based biomarkers in the early stages of perimenopause or longitudinally during the menopausal transition. In this regard, interestingly, we also identified a set of lipid-related metabolites that already changed with the transition from a regular to an irregular oestrous cycle. This combination of lipids was formed by 9 phosphatidylcholines, 4 lysophosphatidylcholines, 2 phosphatidylethanolamines, cholesterol ester (18:2), 5a-androstan-3,17-diol and 17,18-Dihydroxyarachidonic acid, and could be used as a potential multivariate biomarker of early perimenopause if these results are validated in humans. Our findings have contributed to gaining knowledge on the molecular changes that occur during the menopausal transition and can pave the way to design new nutritional-based interventions addressed to preserve the endocrine and metabolic functions of perimenopausal women and to ameliorate in later stages the

vasomotor symptoms, osteoporosis and metabolic-related diseases that can appear in postmenopausal women.

Once we characterized menopausal transition and identified circulating signatures across perimenopause, we wanted to characterize OVX rats in terms of biometric, histological, metabolic and biochemical parameters related to osteoporosis, obesity and metabolic-related alterations, to evaluate whether these parameters were affected by age and elucidate whether PBMCs could reflect molecular changes associated with oestrogen deficiency in the postmenopausal stage (**Manuscript 2**). OVX rodents are recognized as the gold standard models for studying the effects of reproductive senescence in menopause. In this preclinical model, ovaries are surgically removed, mimicking the oestrogen deficiency that occurs during menopause leading to osteoporosis and metabolic disorders (370,387–390). In our study, independently of the age at which the surgery was performed (15 or 25 weeks-old), oestrogen deficiency in OVX rats, which have been previously reported (69,390–395), led to hyperphagia and reduced EE, which would explain the higher fat mass accretion and adipocyte hypertrophy in RWAT and MWAT depots as well as the higher muscle loss and the lower lean-to-fat mass ratio when compared to their sham-operated counterparts. This shift towards an unhealthier body composition and, more specifically, the hypertrophy observed in WAT depots (396) of OVX animals could contribute to explain, at least in part, the higher cardiometabolic risk of OVX rats, which was evidenced by increased LAR, which is described as a good predictor of T2DM and MetS, and by decreased ALR, indicating levels < 1 adipose tissue dysfunction and IR (99,100,396–398). Regarding bone health, increased circulating levels of the bone turnover biomarkers OC and CTX-1 were found in both groups of OVX animals, as was previously reported in both postmenopausal women and OVX rodents (13,389,399), effects that could be attributed to the oestrogen deficiency that

characterized this preclinical postmenopausal model, considering the key role of this hormone in bone metabolism.

Some articles have shown that the age at which OVX is performed in rodents may affect some of the outcomes, especially those related to bone metabolism and osteoporosis (389,400). In line with this idea, our findings revealed that the age at which the rats underwent surgery slightly affected some of the alterations that occurred, being more evident in the deleterious effects on lipid markers (TC), oxidative stress (GSH/GSSG ratio) and inflammation (MCP-1) in rats that were ovariectomized at an earlier age (15 weeks-old). These findings were unexpected because they were not observed in the older rats, suggesting that age-related adaptive mechanisms may mitigate these metabolic disturbances in rats ovariectomized at an older age (25 weeks-old). On the other hand, in the older 35-week-old OVX animals, in which the ovariectomy was carried out at the age of 25 weeks, the oestrogen deficiency significantly increased the surrogate marker of insulin resistance, HOMA-IR, and decreased BMD in the tibia, which was consistent with previous studies showing increased HOMA-IR with age in other animal models (401) and decreased BMD in rats underwent ovariectomy between 6 and 9 months of age, which exhibited the most osteoporotic response to the surgery (389).

Given that osteoporosis is a typical hallmark of menopause and the clear link between IR and increased CVDs risk (402), and considering that the rat is not the most accurate model for studying cholesterol-related diseases (403–405), we focused on 35 weeks-old animals (ovariectomized at the age of 25 weeks) to assess the gene expression profile in PBMCs, which could offer a more precise picture of the postmenopausal condition, aiding in the understanding of the underlying mechanisms associated with this state. Our transcriptomic analysis in PBMCs revealed that this subset of blood cells reflected molecular changes linked to oestrogen deficiency that occur in the postmenopausal state,

offering insights into the pathophysiology of postmenopausal alterations, such as osteoporosis and immunometabolic diseases. Thus, the unfavorable modulation at the mRNA level of genes related to immune function, response to stress, lipid metabolism, and bone homeostasis observed in PBMCs of OVX rats would be in agreement with previous research indicating that changes in the circulating levels of sex hormones occurring during menopause can disrupt immune function, which, in turn, can trigger relevant health problems, such as obesity, osteoporosis, autoimmune diseases, and immunodeficiency (406–409). Here, we identified mRNA level changes in genes related to immune function, response to stress, lipid metabolism, and bone homeostasis, offering insights into the pathophysiology of postmenopausal alterations, such as osteoporosis and inmunometabolic diseases.

The loss of ovarian steroid production occurring in postmenopausal women causes a decline in immune function, an alteration that is also associated with aging and is known as immunosenescence (406,407). In our study, this phenomenon is reflected in the global downregulation at the gene expression level of immune-related pathways in PBMCs of the OVX animals. Specifically, the downregulation in mRNA levels of *sh3bp2*, *il18r1*, *il18rap,* and *il12rb1* observed in OVX rats would suggest a diminished NK cell-mediated cytotoxicity in the postmenopausal state, an effect that would be in line with the significant reduction in the cytotoxic activity of natural killer (NK) cells reported in postmenopausal women (406–409). Thus, the *sh3bp2* gene is associated with positive regulation of NK Mediated Cytotoxicity pathway (410), while deficiencies in interleukin-18 (IL-18) have been shown to result in impaired NK cell activity (411). Furthermore, IL-18, often in synergy with interleukin-12 (IL-12), is crucial for activating NK cells and stimulating T and B cells to produce IFN-γ, thereby enhancing their cytotoxicity against tumor cells (411–414).

The higher mRNA levels of *socs3* found in PBMCs of OVX rats would also be in line with the aforementioned impaired immune response, supported by previous findings in the same OVX model, where the increased *socs3* expression was linked to inflammation, which was partially mitigated by an HRT treatment (415). Furthermore, SOCS3 inhibits insulin signaling and enhances IR (416,417). Therefore, its overexpression in PBMCs would be in agreement with the sharp increase of HOMA-IR observed in the OVX animals of our study. The negative impact of ovariectomy on glucose and insulin homeostasis is further evidenced by the reduced expression of *slc2a4* (*glut4*) and by the increased expression of *grb7* found in the PBMCs of our OVX animals, because the reported changes of both genes were associated with the impairment of glucose and insulin signaling pathways, contributing to hyperglycemia and IR (418–421).

The lower *spring* expression levels observed in the PBMCs of OVX rats, together with the observed downregulation of *abca1* and *stard5* would suggest a pro-atherogenic profile in these oestrogen deficient animals, although they did not display changes in the circulating levels of TC, non-HDL-c and HDL-c at sacrifice. Thus, 17β-oestradiol significantly enhanced macrophage cholesterol efflux by upregulating *abca1* via ERα, a process confirmed in both *in vivo* experiments with OVX mice and their cell line studies (422). Additionally, HRT in non-obese and normolipidemic postmenopausal women increased HDL-c and reduced LDL-c levels, correlating with elevated *abca1* expression (423). On the other hand, the deletion of *stard5* resulted in reduced cholesterol efflux via the ABCA1 pathway in macrophages and increased hepatic cholesterol and TG, indicating its pivotal role in lipid homeostasis (424,425). Furthermore, loss of SPRING function impaired SREBP-driven de novo lipogenesis, and the ability to respond to sterol depletion, and diminished LDL uptake (426–430). Therefore, our findings reinforce the idea that PBMCs can be used as an easily obtainable biological source to characterize

potential aspects of both cholesterol and lipid metabolism in physiological or pathological conditions, as was previously described by members of our group (299,350,431).

Regarding bone metabolism, the clear downregulation of the TGF-β-related genes *tab1*, *tgfb2*, and *tgfb3* (361,432–436), involved in bone homeostasis, observed in PBMCs of OVX animals, align with the idea of a lower capability of bone mineralization and reduced BMD occurring during the postmenopausal state (123,437), as was observed in the tibia of our OVX animals. Gao *et al.* reported that the oestrogen deficiency significantly reduced BMD and promoted severe trabecular bone damage in OVX rats, and described a positive correlation between the expression of *Tgfb3* and multiple parameters involved in bone microstructure (361). It is well established that TGF-β family members have a key role in bone regeneration and may serve as potential biomarkers for postmenopausal osteoporosis in OVX rats, due to their key role in bone homeostasis and repair, osteogenic differentiation and osteoclast formation, maintaining an optimal osteoblast/osteoclast balance (361,435,436). In our study, the downregulation of the gene encoding biglycan (*bgn),* which is essential for bone health, ensuring a proper population of mature osteoblasts acting through the TGF-β signaling pathway, observed in the PBMCs of OVX rats, is consistent with the link between its under expression and bone metabolism-related disorders, and confirms that the interplay between *bgn* and TGF-β-related genes reported in previous studies (361,432–436,438) is also reflected in PBMCs. Our results are in line with previous findings describing that peripheral blood monocytes are an important source of osteoclast precursors, making these cells a suitable model for studying bone metabolism (439).

Overall, considering the extensive gene expression changes observed in PBMCs of OVX rats, our findings can pave the way for investigating whether the molecular mechanisms underlying oestrogen deficiency identified in PBMCs can be modulated by different

nutritional strategies to monitor and predict the potential effects on the health of these interventions carried out in the postmenopausal state using cells that can be easily and repeatedly collected and also mitigate the need for invasive procedures such as biopsies and the related significant discomfort (338–340).

Once we have described the pathophysiological and metabolic alterations during the menopausal transition and the postmenopausal state, we wanted to study, using OVX as a postmenopausal preclinical model, whether the supplementation with an MI including curcumin, hesperidin, and phytosterols could ameliorate the disturbances reported in the postmenopausal state (**Manuscript 3**). The effects of this MI were compared to those produced by the administration of 17β-oestradiol, a compound that resembles HRT, in the treatment of menopause symptoms and associated diseases. The use of these three bioactive compounds as an MI was in line with our idea that better outcomes can be obtained when treatments are performed under a multifaceted approach, using a blend of bioactive compounds that act against complementary targets. In this regard, hesperidin has shown beneficial effects against obesity and diabetes, the intake of phytosterols may be beneficial for the management of lipid metabolism-related alterations, curcumin could ameliorate inflammation and oxidative stress, and both hesperidin and curcumin have shown positive effects on bone metabolism. Although the beneficial effects of each of these compounds were previously reported, the effects of the combined supplementation with these three bioactive compounds had not yet been evaluated. The highlights of this study provide evidence that the combined supplementation of these bioactive compounds can offer significant benefits in managing obesity and menopause-related metabolic disturbances, being the observed effects very similar to those reported in response to the pharmacological treatment with 17β-oestradiol.

Firstly, the reduced fat mass accretion observed in OVX after 8 weeks of MI supplementation, which was evidenced by decreased total fat mass, adiposity index and RWAT, MWAT, and inguinal WAT (IWAT) depot weights as well as by diminished adipocyte hypertrophy in MWAT could be attributed at first glance, to the protective effect against obesity that has been previously reported for different polyphenols, including curcumin and hesperidin, to a lesser extent, for phytosterols, in both animal models and humans (159,161–164). Nevertheless, to the best of our knowledge, only one study reported beneficial effects using an OVX model, showing that a 30-day curcumin intake significantly decreased intestinal adiposity accumulation in OVX rats (161). In other studies, the prolonged intake of curcumin in aged male F344xBN rats decreased food intake (440), increased EE and stimulated thermogenesis, and ATP production (90,160). However, the lack of effects on EE and food intake observed after treatment with this MI supplement would rule out these two mechanisms for explaining the anti-obesity effects reported in OVX rats that received the MI (OVX-MI).

The gene expression analyses carried out in the MWAT depot allowed us to gain knowledge on some of the potential mechanisms by which the MI exerted its anti-adiposity effects. Thus, the full counteraction of the overexpression of the *Lpl* and *cd36* genes in MWAT caused by ovariectomy observed in OVX-MI rats and the strong positive correlation observed between both genes emphasized the coordinated role of Cd36 and LPL in fatty acid uptake and storage, suggesting that the MI exert its beneficial effects against fat accretion by down-regulation the mRNA levels of these two key lipid metabolism-related genes. The fact that CD36 is responsible for fatty acid uptake (90), while LPL, in WAT, is a marker for adipocyte differentiation, and its expression increases in parallel with cellular TG accumulation as preadipocytes differentiate, contributing to the growth and expansion of WAT (441,442), would support our idea. Our results are in

line with those reporting that hesperidin supplementation (100 mg/kg/day) for 8 weeks reduced the gene expression levels of *Lpl* in RWAT in male Wistar rats on a hypercaloric western diet (209). Furthermore, different studies showed that curcumin intake attenuated the overexpression of the hepatic mRNA levels of Cd36 in a high-fat-diet-fed C57BL/6J mouse model, which was associated with a decrease in hepatic lipid accumulation (443–445).

The lower loss in lean mass, which provides a precise measurement of muscle mass, that accompanied the decreased total mass observed in OVX-MI rats resulted in an increased lean-to-fat mass ratio in the animals that received the MI, contributing to a healthier profile of body composition (446,447). The significantly lower circulating levels of leptin, which are highly and positively related to body fat mass (93,448,449), would be in agreement with our findings.

Remarkably, although all the above-commented effects were observed in response to both MI-based and pharmacologic (17β-oestradiol) treatments, including also a common anti-adiposity mechanism by decreasing the *Lpl* and *Cd36* mRNA levels in WAT, only the MI supplementation significantly increased adiponectin plasma levels corrected by WAT weight, a surrogate marker of effective adiponectin production (168,450) and produced an increase in ALR, which has been shown to correlate better with IR than other classical indexes, such as HOMA-IR, and is clinically useful to identify subjects susceptible to suffer CVDs (99–102). The increase in the surrogate marker of insulin sensitivity, R-QUICKI, found only in OVX-MI would reinforce our results. These differential effects between the MI and 17β-oestradiol could be partly attributed to the beneficial effects on glucose and insulin homeostasis described for the polyphenols curcumin and hesperidin. Thus, concerning curcumin, different studies have shown that this bioactive compound displays anti-diabetic properties by increasing adiponectin production in WAT and

decreasing blood levels of leptin *in vitro* and in animal models of obesity, MetS, and T2DM (168–173), as well as by improving HOMA-IR in humans after 9 months of curcumin treatment (173). Furthermore, the consumption of orange juice rich in hesperidin could have contributed to the beneficial effects against IR because two studies reported significant reductions in insulin and HOMA-IR levels (204,451).

Altogether, our results underscore the potential of this MI formulation as a natural-based alternative therapy to tackle obesity and improve cardiometabolic health in postmenopausal women. Further randomized controlled clinical trials would be of great value in gaining insights into the usefulness of this MI in this target population.

Finally, also using a multifaceted approach, we investigated whether the oral supplementation with an MI including L-histidine, L-carnosine, L-serine and L-cysteine exerted beneficial effects against postmenopausal-related alterations in OVX rats (**Manuscript 4**), using the same experimental design explained in manuscript 3. This blend of amino-acid-related compounds was chosen based on the previous results obtained by members of our group, in which it was reported that the intake of this MI decreased NAFLD in both diet-induced and genetic leptin-deficient ob/ob mouse models and in OVX rats in addition to ameliorate liver inflammation, IR and hypercholesterolemia in the mice models (20). Considering that NAFLD is a metabolic disorder that frequently accompanies obesity and MetS, and that can also appear with menopause (287–289), and taking into account that previous scientific evidence carried out mainly in rodents, but also in humans, reported that supplementation with carnosine (257,260), serine (241,285), cysteine (274,275) and especially histidine (242–244,452,248) can ameliorate obesity, promote glycaemic control, and ameliorate IR, inflammation or oxidative stress, the use of this MI could be a potential therapeutic

strategy to address the metabolic alterations that can occur during the postmenopausal period.

In line with this idea and, similarly to what was reported in response to the intake of the MI including hesperidin, curcumin and phytosterols, the supplementation with the amino-acid-related MI also improved body composition, which was evidenced by decreased fat mass accretion, partially counteracting the increases in total fat mass, adiposity index and RWAT weight and hypertrophy observed in the OVX rats that received the placebo, as well as by increased lean mass and lean-to-fat ratio. These effects were slightly less evident to those observed in response to the pharmacological treatment with 17β-oestradiol, which can be related to its inhibitory effect on food intake and its enhancement of increased EE, as was previously reported (453–455). Despite the intake of histidine and serine, separately, have been shown to reduce the food intake in various animal models (242,250,251), and serine supplementation has been associated with increased EE (285). The modulation of these processes was not the mechanism underlying the beneficial effects against fat mass accretion observed in our study in response to MI consumption.

The significant amelioration of the adipocyte hypertrophy observed in the RWAT of the OVX-MI rats could contribute to explain, at least in part, their significant lower levels of LAR, which has been described as a good predictor of T2DM and MetS (98). The clear numerical decrease observed in response to the MI in the circulating levels of insulin (22.11%) and HOMA-IR (23.6%) and the strong positive correlations between HOMA-IR and LAR observed when all the animals of the study were considered would support this idea. These effects, together with the decreased circulating levels of the acute inflammatory marker CRP, an effect that was previously reported in different studies in response to the dietary intake of histidine, carnosine and cysteine (244,275,456), would

suggest that MI supplementation improved the immunometabolic health of OVX rats. These effects could be mainly attributed to histidine. On the one hand, histidine intake has been inversely associated with BMI and waist circumference in humans with obesity (244,246,248), making this relationship clearer in women (244). On the other hand, this AA has been shown to reduce IR and the circulating levels of the classical biomarkers of inflammation CRP and IL-6 (243,244,246–248) and, in obese women, the circulating levels of histidine were inversely associated with the aforementioned inflammation-related biomarkers (246). Nevertheless, the other amino-acid-related compounds were likely also responsible for the reported effects, since it has been described that carnosine intake may ameliorate CVDs diseases and T2DM, reducing atherogenic processes as well as glucose and lipid metabolism-related alterations (257,256), cysteine supplementation showed anti-diabetic and anti-inflammatory effects in Zucker diabetic rats (275), and both serine and cysteine could act against oxidative stress by elevating hepatic GSH levels (284).

The transcriptomic analyses carried out in RWAT allowed us to gain knowledge of the underlying mechanisms involved in the anti-obesity effects and the immunometabolic benefit observed in response to MI supplementation. Thus, the downregulation of a plethora of genes involved in and cytoskeletal organization (*actb*, *lcp1* and *pfn1*) (457) and extracellular matrix (ECM) remodeling, such as those related to collagen metabolism (*col1a2*, *col5a1*, *col5a2*, *sparc*, *bgn*, *lox* and *serpinh1*) (458–467) and proteolytic degradation of ECM (*timp1* and *htra1*) (468–471), would support the idea that the intake of the MI triggered a favorable adaptative response to the adipocyte hypertrophy required to support adipocyte growth in response to fat mass accretion. Interestingly, most of these genes have been shown to be upregulated with obesity and positively correlated with markers of insulin resistance and inflammation. Therefore, the decreased RWAT weight

and hypertrophy observed in OVX-MI animals were reflected at the gene expression level in improvements in the structure, morphology and immunometabolic function of their adipocytes.

WAT hypertrophy is characterized by increased expression of inflammatory-related genes in adipose tissue macrophages (ATMs). In line with the idea that MI supplementation improved the low-grade inflammation in WAT occurring as a consequence of the fat mass gain produced in OVX rats after ovariectomy, we also reported decreased mRNA levels of different pro-inflammatory genes such as those involved in cytokine (*il1b, faslg,* and *ptgs2*)- and chemokine (*cxcl2, ccr7*)-mediated inflammation (472–476) as well as in the crosstalk between adipocytes and ATMs (*cd5l, fcgr1a, spib* and *btk*) (477–481). Remarkably, it has been reported that the activation of oxidative phosphorylation (OxPhos) can promote a shift towards an anti-inflammatory M2-like phenotype in macrophages, which would be supported in our study by the overexpression of the OxPhos-related genes *mt-co2, mt-nd5, mt-nd6* and *nubpl* in the RWAT of the OVX-MI animals (481,482).

The improvement of the immunometabolic health reported in OVX rats that received the MI was also reinforced at the RWAT gene expression level by the modulation of key genes involved in glucose and insulin homeostasis. Thus, the lower mRNA levels of *grb14*, a negative regulator of the insulin receptor signaling pathway that is overexpressed in the WAT of obese animals and humans and/or in individuals with type 2 diabetes (483–485), would be in line with this idea. Similarly, the overexpression of *gabrg3*, which encodes a γ-aminobutyric acid (GABA) receptor that mediates the antiadipogenic, anti-diabetic and anti-inflammatory effects of GABA (486,487) as well as the overexpression of *zfp407,* encoding for a protein that stimulates insulin-mediated glucose uptake in adipocytes and

protects against adipocyte hypertrophy and IR in mice (488), would support our hypothesis.

Overall, the findings reported in the present study can settle the basis for promoting the consumption of a blend of histidine, carnosine, serine and cysteine to tackle obesity and to improve the immunometabolic health of menopausal women, elucidating some of the mechanisms underlying the beneficial effects of this MI, which are mainly related to the favorable modulation in RWAT of genes involved in adipocyte structure and morphology, inflammation, oxidative phosphorylation and glucose and insulin homeostasis.

V. CONCLUSIONS

CONCLUSIONS

The conclusions of the present thesis are:

1. In middle-aged rats, the natural menopausal transition, characterized by the gradual loss of regularity of the oestrous cycle, led to significant progressive changes in the serum lipidomic profile, identifying circulating signatures of this biological process, including changes in the levels of lipids of the phosphatidylcholine, lysophosphatidylcholine, phosphatidylethanolamine, lysophosphatidylethanolamine, triglycerides, fatty acids and cholesterol ester families.

2. Oestrogen deficiency induced in rats of different ages by the surgical removal of the ovaries resembled most of the alterations that can occur in women in the postmenopausal state, including obesity, adipocyte hypertrophy, and increased risks of osteoporosis and cardiovascular diseases. These effects were slightly more pronounced in ovariectomized rats who underwent ovariectomy at an older age (25 weeks).

3. The global gene expression analysis carried out in peripheral blood mononuclear cells of ovariectomized rats reflected molecular changes associated with oestrogen deficiency occurring in the postmenopausal state, which were evidenced by changes at mRNA level of genes mainly related to immune function, response to stress, lipid metabolism, and bone homeostasis, providing valuable insights into the pathophysiology of postmenopausal-related alterations, such as osteoporosis and immunometabolic alterations.

4. The combined oral supplementation with hesperidin, phytosterols and curcumin improved body composition, attenuating the loss of lean mass, the increase in body fat, and the adipocyte hypertrophy that occurs in ovariectomized rats. These effects were accompanied by an improvement in insulin sensitivity, and the adiponectin-to-leptin ratio, a marker of cardiometabolic risk, and by a decrease in the expression of fatty acid uptake-related genes (*Lpl* and *Cd36*) in the visceral mesenteric white adipose tissue.

5. The intake of a blend of amino acid-related compounds including histidine, carnosine, cysteine, and serine decreased adiposity and retroperitoneal white adipose tissue adipocyte hypertrophy and improved body composition, as evidenced by the increased lean body mass and lean-to-fat mass ratio. These effects are accompanied by decreases in the leptin-to-adiponectin ratio, a risk marker for diabetes and metabolic syndrome, and the circulating levels of the pro-inflammatory C-reactive protein.

6. The mechanisms underlying the anti-adiposity and the beneficial immunometabolic effects of the amino acid-based multi-ingredient are related to favourable changes in the expression in the retroperitoneal white adipose tissue of genes involved in inflammation, stress response, structure and morphology of adipocytes, cell proliferation and differentiation, glucose and insulin homeostasis and oxidative phosphorylation.

VI. REFERENCES

1. Harlow SD, Gass M, Hall JE, Lobo R, Maki P, Rebar RW, et al. Executive Summary of the Stages of Reproductive Aging Workshop + 10: Addressing the Unfinished Agenda of Staging Reproductive Aging. J Clin Endocrinol Metab. 2012, 97, 1159–68.
2. Auro K, Joensuu A, Fischer K, Kettunen J, Salo P, Mattsson H, et al. A metabolic view on menopause and ageing. Nat Commun. 2014, 5, 4708.
3. Wang Q, Ferreira DLS, Nelson SM, Sattar N, Ala-Korpela M, Lawlor DA. Metabolic characterization of menopause: cross-sectional and longitudinal evidence. BMC Med. 2018, 16, 17.
4. Matthews KA, Crawford SL, Chae CU, Everson-Rose SA, Sowers MF, Sternfeld B, et al. Are Changes in Cardiovascular Disease Risk Factors in Midlife Women Due to Chronological Aging or to the Menopausal Transition? J Am Coll Cardiol. 2009, 54, 2366–73.
5. Burger HG, Dudley EC, Hopper JL, Shelley JM, Green A, Smith A, et al. The endocrinology of the menopausal transition: a cross-sectional study of a population-based sample. J Clin Endocrinol Metab. 1995, 80, 3537–45.
6. McNeil MA, Merriam SB. Menopause. Ann Intern Med. 2021, 174, ITC97-ITC112.
7. Santoro N, Crawford SL, El Khoudary SR, Allshouse AA, Burnett-Bowie SA, Finkelstein J, et al. Menstrual Cycle Hormone Changes in Women Traversing Menopause: Study of Women's Health Across the Nation. J Clin Endocrinol Metab. 2017, 102, 2218–29.
8. Morabia A, Costanza MC. International Variability in Ages at Menarche, First Livebirth, and Menopause. Am J Epidemiol. 1998, 148, 1195–205.
9. Gold EB. The Timing of the Age at Which Natural Menopause Occurs. Obstet Gynecol Clin North Am. 2011, 38, 425–40.
10. Gold EB. Factors Associated with Age at Natural Menopause in a Multiethnic Sample of Midlife Women. Am J Epidemiol. 2001, 153, 865–74.
11. Mittelstrass K, Ried JS, Yu Z, Krumsiek J, Gieger C, Prehn C, et al. Discovery of Sexual Dimorphisms in Metabolic and Genetic Biomarkers. PLoS Genet. 2011, 7, e1002215.
12. Shapira N. Women's higher health risks in the obesogenic environment: a gender nutrition approach to metabolic dimorphism with predictive, preventive, and personalised medicine. EPMA J. 2013, 4, 1.
13. Thapa S, Nandy A, Rendina-Ruedy E. Endocrinal metabolic regulation on the skeletal system in post-menopausal women. Front Physiol. 2022, 13, 1052429.
14. Mesch VR, Boero LE, Siseles NO, Royer M, Prada M, Sayegh F, et al. Metabolic syndrome throughout the menopausal transition: influence of age and menopausal status. Climacteric. 2006, 9, 40–8.
15. Lejsková M, Alušík Š, Suchánek M, ŽŽecová S, Pittha J. Menopause: clustering of metabolic syndrome components and population changes in insulin resistance. Climacteric. 2011, 14, 83–91.
16. Rosano GMC, Vitale C, Marazzi G, Volterrani M. Menopause and cardiovascular disease: the evidence. Climacteric. 2007, 10, 19–24.
17. Gurka MJ, Vishnu A, Santen RJ, DeBoer MD. Progression of Metabolic Syndrome Severity During the Menopausal Transition. J Am Heart Assoc. 2016, 5, 1–20.
18. Baker FC, Driver HS. Circadian rhythms, sleep, and the menstrual cycle. Sleep

Med. 2007, 8, 613–22.

19. Hale GE, Robertson DM, Burger HG. The perimenopausal woman: Endocrinology and management. J Steroid Biochem Mol Biol. 2014, 142, 121–31.
20. Hsue AJW, Billig H, Tsafiri A. Ovarian Follicle Atresia: A Hormonally Controlled Apoptotic Process. Endocr Rev. 1994, 15, 707–24.
21. Gougeon A. Human ovarian follicular development: From activation of resting follicles to preovulatory maturation. Ann Endocrinol (Paris). 2010, 71, 132–43.
22. Finch CE. The menopause and aging, a comparative perspective. J Steroid Biochem Mol Biol. 2014, 142, 132–41.
23. Gougeon A, Chainy GBN. Morphometric studies of small follicles in ovaries of women at different ages. Reproduction. 1987, 81, 433–42.
24. Burger H, Woods NF, Dennerstein L, Alexander JL, Kotz K, Richardson G. Nomenclature and endocrinology of menopause and perimenopause. Expert Rev Neurother. 2007, 7, S35–43.
25. Delamater L, Santoro N. Management of the Perimenopause. Clin Obstet Gynecol. 2018;61:419–32.
26. Monteleone P, Mascagni G, Giannini A, Genazzani AR, Simoncini T. Symptoms of menopause — global prevalence, physiology and implications. Nat Rev Endocrinol. 2018, 14, 199–215.
27. Cui L, Qin Y, Gao X, Lu J, Geng L, Ding L, et al. Antimüllerian hormone: correlation with age and androgenic and metabolic factors in women from birth to postmenopause. Fertil Steril. 2016, 105, 481–485.e1.
28. Yeh J, Kim B, Peresie J, Liang YJ, Arroyo A. Serum and ovarian Müllerian inhibiting substance, and their decline in reproductive aging. Fertil Steril. 2007, 87, 1227–30.
29. Santoro N, Brown JR, Adel T, Skurnick JH. Characterization of reproductive hormonal dynamics in the perimenopause. J Clin Endocrinol Metab. 1996, 81, 1495–501.
30. Lee SJ, Lenton EA, Sexton L, Cooke ID. The effect of age on the cyclical patterns of plasma LH, FSH, oestradiol and progesterone in women with regular menstrual cycles. Hum Reprod. 1988, 3, 851–5.
31. Reyes FI, Winter JSD, Faiman C. Pituitary-ovarian relationships preceding the menopause. Am J Obstet Gynecol. 1977, 129, 553–6.
32. Klein NA, Houmard BS, Hansen KR, Woodruff TK, Sluss PM, Bremner WJ, et al. Age-Related Analysis of Inhibin A, Inhibin B, and Activin A Relative to the Intercycle Monotropic Follicle-Stimulating Hormone Rise in Normal Ovulatory Women. J Clin Endocrinol Metab. 2004, 89, 2977–81.
33. Lukefahr AL, Frye JB, Wright LE, Marion SL, Hoyer PB, Funk JL. Decreased Bone Mineral Density in Rats Rendered Follicle-Deplete by an Ovotoxic Chemical Correlates with Changes in Follicle-Stimulating Hormone and Inhibin A. Calcif Tissue Int. 2012, 90, 239–49.
34. Robertson DM, Hale GE, Fraser IS, Hughes CL, Burger HG. A proposed classification system for menstrual cycles in the menopause transition based on changes in serum hormone profiles. Menopause. 2008, 15, 1139–44.
35. Burger HG. Hormonal Changes in the Menopause Transition. Recent Prog Horm Res. 2002, 57, 257–75.

36. Kim C, Slaughter JC, Wang ET, Appiah D, Schreiner P, Leader B, et al. Anti-Müllerian hormone, follicle stimulating hormone, antral follicle count, and risk of menopause within 5 years. Maturitas. 2017, 102, 18–25.
37. Finkelstein JS, Lee H, Karlamangla A, Neer RM, Sluss PM, Burnett-Bowie SAM, et al. Antimullerian Hormone and Impending Menopause in Late Reproductive Age: The Study of Women's Health Across the Nation. J Clin Endocrinol Metab. 2020, 105, e1862–71.
38. Randolph JF, Zheng H, Sowers MR, Crandall C, Crawford S, Gold EB, et al. Change in Follicle-Stimulating Hormone and Estradiol Across the Menopausal Transition: Effect of Age at the Final Menstrual Period. J Clin Endocrinol Metab. 2011, 96, 746–54.
39. Santoro N, Brockwell S, Johnston J, Crawford SL, Gold EB, Harlow SD, et al. Helping midlife women predict the onset of the final menses: SWAN, the Study of Women's Health Across the Nation. Menopause. 2007, 14, 415–24.
40. World Health Organization. Research on the Menopause in the 1990s. WHO Tech Rep. 1996, 866, 1-107.
41. Paramsothy P, Harlow SD, Nan B, Greendale GA, Santoro N, Crawford SL, et al. Duration of the menopausal transition is longer in women with young age at onset: the multiethnic Study of Women's Health Across the Nation. Menopause. 2017, 24, 142–9.
42. Santoro N, Roeca C, Peters BA, Neal-Perry G. The Menopause Transition: Signs, Symptoms, and Management Options. J Clin Endocrinol Metab. 2021, 106, 1–15.
43. Matthews KA, Santoro N, Lasley B, Chang Y, Crawford S, Pasternak RC, et al. Relation of Cardiovascular Risk Factors in Women Approaching Menopause to Menstrual Cycle Characteristics and Reproductive Hormones in the Follicular and Luteal Phases. J Clin Endocrinol Metab. 2006, 91, 1789–95.
44. Canderelli R, Leccesse LA, Miller NL, Unruh Davidson J. Benefits of hormone replacement therapy in postmenopausal women. J Am Acad Nurse Pract. 2007, 19, 635–41.
45. Appt SE, Ethun KF. Reproductive aging and risk for chronic disease: Insights from studies of nonhuman primates. Maturitas. 2010, 67, 7–14.
46. Shifren JL, Gass MLS. The North American Menopause Society Recommendations for Clinical Care of Midlife Women. Menopause. 2014, 21, 1038–62.
47. Gass MLS, Manson JE, Cosman F, Grodstein F, Craig Jordan V, Karas RH, et al. The 2012 Hormone Therapy Position Statement of The North American Menopause Society. Menopause. 2012, 19, 257–71.
48. Neves-e-Castro M, Birkhauser M, Samsioe G, Lambrinoudaki I, Palacios S, Borrego RS, et al. EMAS position statement: The ten point guide to the integral management of menopausal health. Maturitas. 2015, 81, 88–92.
49. Lobo RA, Davis SR, De Villiers TJ, Gompel A, Henderson VW, Hodis HN, et al. Prevention of diseases after menopause. Climacteric. 2014, 17, 540–56.
50. Freedman RR. Menopausal hot flashes: Mechanisms, endocrinology, treatment. J Steroid Biochem Mol Biol. 2014, 142, 115–20.
51. Lee E, Anselmo M, Tahsin CT, Vanden Noven M, Stokes W, Carter JR, et al. Vasomotor symptoms of menopause, autonomic dysfunction, and cardiovascular disease. Am J Physiol Circ Physiol. 2022, 323, H1270–80.

52. Szmuilowicz ED, Manson JE, Rossouw JE, Howard B V., Margolis KL, Greep NC, et al. Vasomotor symptoms and cardiovascular events in postmenopausal women. Menopause. 2011, 18, 603–10.
53. Thurston RC, Aslanidou Vlachos HE, Derby CA, Jackson EA, Brooks MM, Matthews KA, et al. Menopausal Vasomotor Symptoms and Risk of Incident Cardiovascular Disease Events in SWAN. J Am Heart Assoc. 2021, 10, 1–17.
54. Dam V, Dobson AJ, Onland-Moret NC, van der Schouw YT, Mishra GD. Vasomotor menopausal symptoms and cardiovascular disease risk in midlife: A longitudinal study. Maturitas. 2020, 133, 32–41.
55. Kravitz HM, Joffe H. Sleep During the Perimenopause: A SWAN Story. Obstet Gynecol Clin North Am. 2011, 38, 567–86.
56. Kravitz HM, Janssen I, Bromberger JT, Matthews KA, Hall MH, Ruppert K, et al. Sleep Trajectories Before and After the Final Menstrual Period in the Study of Women's Health Across the Nation (SWAN). Curr Sleep Med Reports. 2017, 3, 235–50.
57. Maki PM, Kornstein SG, Joffe H, Bromberger JT, Freeman EW, Athappilly G, et al. Guidelines for the Evaluation and Treatment of Perimenopausal Depression: Summary and Recommendations. J Women's Heal. 2019, 28,117–34.
58. Bromberger JT, Kravitz HM. Mood and Menopause: Findings from the Study of Women's Health Across the Nation (SWAN) over 10 Years. Obstet Gynecol Clin North Am. 2011, 38, 609–25.
59. Freeman EW, Sammel MD, Lin H, Nelson DB. Associations of Hormones and Menopausal Status With Depressed Mood in Women With No History of Depression. Arch Gen Psychiatry. 2006, 63, 375.
60. Cohen LS, Soares CN, Vitonis AF, Otto MW, Harlow BL. Risk for New Onset of Depression During the Menopausal Transition. Arch Gen Psychiatry. 2006, 63, 385.
61. Weber MT, Mapstone M, Staskiewicz J, Maki PM. Reconciling subjective memory complaints with objective memory performance in the menopausal transition. Menopause. 2012, 19, 735–41.
62. Greendale GA, Huang MH, Wight RG, Seeman T, Luetters C, Avis NE, et al. Effects of the menopause transition and hormone use on cognitive performance in midlife women. Neurology. 2009, 72, 1850–7.
63. Genazzani AR, Pluchino N, Luisi S, Luisi M. Estrogen, cognition and female ageing. Hum Reprod Update. 2007, 13, 175–87.
64. Antonelli A, Giannini A, Chedraui P, Monteleone P, Caretto M, Genazzani AD, et al. Mood disorders and hormonal status across women's life: a narrative review. Gynecol Endocrinol. 2022, 38, 1019–27.
65. Espeland MA. Conjugated Equine Estrogens and Global Cognitive Function in Postmenopausal. JAMA. 2004, 291, 2959.
66. Sowers M, Zheng H, Tomey K, Karvonen-Gutierrez C, Jannausch M, Li X, et al. Changes in Body Composition in Women over Six Years at Midlife: Ovarian and Chronological Aging. J Clin Endocrinol Metab. 2007, 92, 895–901.
67. Davis SR, Castelo-Branco C, Chedraui P, Lumsden MA, Nappi RE, Shah D, et al. Understanding weight gain at menopause. Climacteric. 2012, 15,419–29.
68. Steiner BM, Berry DC. The Regulation of Adipose Tissue Health by Estrogens. Front Endocrinol (Lausanne). 2022, 13, 1–20.
69. Lovejoy JC, Champagne CM, de Jonge L, Xie H, Smith SR. Increased visceral fat

and decreased energy expenditure during the menopausal transition. Int J Obes. 2008, 32, 949–58.

70. Lee CG, Carr MC, Murdoch SJ, Mitchell E, Woods NF, Wener MH, et al. Adipokines, Inflammation, and Visceral Adiposity across the Menopausal Transition: A Prospective Study. J Clin Endocrinol Metab. 2009, 94, 1104–10.
71. Sternfeld B. Physical Activity and Changes in Weight and Waist Circumference in Midlife Women: Findings from the Study of Women's Health Across the Nation. Am J Epidemiol. 2004, 160, 912–22.
72. Guthrie JR, Dennerstein L, Dudley EC. Weight gain and the menopause: a 5-year prospective study. Climacteric. 1999, 2, 205–11.
73. Wildman RP, Tepper PG, Crawford S, Finkelstein JS, Sutton-Tyrrell K, Thurston RC, et al. Do Changes in Sex Steroid Hormones Precede or Follow Increases in Body Weight during the Menopause Transition? Results from The Study of Women's Health Across the Nation. J Clin Endocrinol Metab. 2012, 97, E1695– 704.
74. Williams LT, Collins CE, Morgan PJ, Hollis JL. Maintaining the outcomes of a successful weight gain prevention intervention in mid-age women: Two year results from the 40-somethin randomized control trial. Nutrients. 2019, 11, 1–14.
75. Juppi H, Sipilä S, Fachada V, Hyvärinen M, Cronin N, Aukee P, et al. Total and regional body adiposity increases during menopause—evidence from a follow-up study. Aging Cell. 2022, 21, e13621.
76. Michalakis K, Coppack SW. Primary ovarian insufficiency: Relation to changes in body composition and adiposity. Maturitas. 2012, 71, 320–5.
77. Greendale GA, Sternfeld B, Huang M, Han W, Karvonen-Gutierrez C, Ruppert K, et al. Changes in body composition and weight during the menopause transition. JCI Insight. 2019, 4, 1–14.
78. Leeners B, Geary N, Tobler PN, Asarian L. Ovarian hormones and obesity. Hum Reprod Update. 2017, 23, 300–21.
79. Tchernof A, Desmeules A, Richard C, Laberge P, Daris M, Mailloux J, et al. Ovarian Hormone Status and Abdominal Visceral Adipose Tissue Metabolism. J Clin Endocrinol Metab. 2004, 89, 3425–30.
80. Toth M, Tchernof A, Sites C, Poehlman E. Effect of menopausal status on body composition and abdominal fat distribution. Int J Obes. 2000, 24, 226–31.
81. Tchernof A, Poehlman ET. Effects of the Menopause Transition on Body Fatness and Body Fat Distribution. Obes Res. 1998, 6, 246–54.
82. Kanaley JA, Sames C, Swisher L, Swick AG, Ploutz-Snyder LL, Steppan CM, et al. Abdominal fat distribution in pre- and postmenopausal women: The impact of physical activity, age, and menopausal status. Metabolism. 2001, 50, 976–82.
83. Karvonen-Gutierrez C, Kim C. Association of Mid-Life Changes in Body Size, Body Composition and Obesity Status with the Menopausal Transition. Healthcare. 2016, 4, 42.
84. Espeland MA. Effect of Postmenopausal Hormone Therapy on Body Weight and Waist and Hip Girths. J Clin Endocrinol Metab. 1997, 82, 1549–56.
85. Munoz J, Derstine A, Gower BA. Fat Distribution and Insulin Sensitivity in Postmenopausal Women: Influence of Hormone Replacement. Obes Res. 2002, 10, 424–31.
86. Lizcano F, Guzmán G. Estrogen Deficiency and the Origin of Obesity during

Menopause. Biomed Res Int. 2014, 2014, 1–11.

87. Park YM, Pereira RI, Erickson CB, Swibas TA, Cox-York KA, Van Pelt RE. Estradiol-mediated improvements in adipose tissue insulin sensitivity are related to the balance of adipose tissue estrogen receptor α and β in postmenopausal women. PLoS One. 2017, 12, e0176446.
88. Naaz A, Zakroczymski M, Heine P, Taylor J, Saunders P, Lubahn D, et al. Effect of Ovariectomy on Adipose Tissue of Mice in the Absence of Estrogen Receptor Alpha (ERα): a Potential Role for Estrogen Receptor Beta (ERβ). Horm Metab Res. 2002, 34, 758–63.
89. Riant E, Waget A, Cogo H, Arnal JF, Burcelin R, Gourdy P. Estrogens Protect against High-Fat Diet-Induced Insulin Resistance and Glucose Intolerance in Mice. Endocrinology. 2009, 150, 2109–17.
90. Wang H, Eckel RH. Lipoprotein lipase: from gene to obesity. Am J Physiol Metab. 2009, 297, E271–88.
91. Homma H, Kurachi H, Nishio Y, Takeda T, Yamamoto T, Adachi K, et al. Estrogen Suppresses Transcription of Lipoprotein Lipase Gene. J Biol Chem. 2000, 275, 11404–11.
92. Ferrara CM, Lynch NA, Nicklas BJ, Ryan AS, Berman DM. Differences in Adipose Tissue Metabolism between Postmenopausal and Perimenopausal Women. J Clin Endocrinol Metab. 2002, 87, 4166–70.
93. Recinella L, Orlando G, Ferrante C, Chiavaroli A, Brunetti L, Leone S. Adipokines: New Potential Therapeutic Target for Obesity and Metabolic, Rheumatic, and Cardiovascular Diseases. Front Physiol. 2020, 11, 578966.
94. Mendoza-Herrera K, Florio AA, Moore M, Marrero A, Tamez M, Bhupathiraju SN, et al. The Leptin System and Diet: A Mini Review of the Current Evidence. Front Endocrinol. 2021, 12, 1–12.
95. Kumar R, Mal K, Razaq MK, Magsi M, Memon MK, Memon S, et al. Association of Leptin With Obesity and Insulin Resistance. Cureus. 2020, 12, 19–22.
96. Fasshauer M, Blüher M. Adipokines in health and disease. Trends Pharmacol Sci. 2015, 36, 461–70.
97. Manolopoulos KN, Karpe F, Frayn KN. Gluteofemoral body fat as a determinant of metabolic health. Int J Obes. 2010, 34, 949–59.
98. López-Jaramillo P, Gómez-Arbeláez D, López-López J, López-López C, Martínez-Ortega J, Gómez-Rodríguez A, et al. The role of leptin/adiponectin ratio in metabolic syndrome and diabetes. Horm Mol Biol Clin Investig. 2014, 18, 37–45.
99. Frühbeck G, Catalán V, Rodríguez A, Ramírez B, Becerril S, Salvador J, et al. Adiponectin-leptin Ratio is a Functional Biomarker of Adipose Tissue Inflammation. Nutrients. 2019, 11, 454.
100. Frühbeck G, Catalán V, Rodríguez A, Gómez-Ambrosi J. Adiponectin-leptin ratio: A promising index to estimate adipose tissue dysfunction. Relation with obesity-associated cardiometabolic risk. Adipocyte. 2018, 7, 57–62.
101. Inoue M, Yano M, Yamakado M, Maehata E, Suzuki S. Relationship between the adiponectin-leptin ratio and parameters of insulin resistance in subjects without hyperglycemia. Metabolism. 2006, 55, 1248–54.
102. Frühbeck G, Catalán V, Rodríguez A, Ramírez B, Becerril S, Salvador J, et al. Involvement of the leptin-adiponectin axis in inflammation and oxidative stress in

the metabolic syndrome. Sci Rep. 2017, 7, 6619.

103. Davis SR, Lambrinoudaki I, Lumsden M, Mishra GD, Pal L, Rees M, et al. Menopause. Nat Rev Dis Prim. 2015, 1, 15004.
104. Mendelsohn ME. Mechanisms of estrogen action in the cardiovascular system. J Steroid Biochem Mol Biol. 2000, 74, 337–43.
105. Naftolin F, Friedenthal J, Nachtigall R, Nachtigall L. Cardiovascular health and the menopausal woman: the role of estrogen and when to begin and end hormone treatment. F1000Research. 2019, 8, 1576.
106. Pu D, Tan R, Yu Q, Wu J. Metabolic syndrome in menopause and associated factors: a meta-analysis. Climacteric. 2017, 20, 583–91.
107. Rocca WA, Grossardt BR, Miller VM, Shuster LT, Brown RD. Premature menopause or early menopause and risk of ischemic stroke. Menopause. 2012, 19, 272–7.
108. Wellons M, Ouyang P, Schreiner PJ, Herrington DM, Vaidya D. Early menopause predicts future coronary heart disease and stroke. Menopause. 2012, 19, 1081–7.
109. De Vos M, Devroey P, Fauser BC. Primary ovarian insufficiency. Lancet. 2010, 376, 911–21.
110. Zivkovic TB, Vuksanovic M, Jelic MA, Stojanovic J, Buric B, Jojic B, et al. Obesity and metabolic syndrome during the menopause transition in Serbian women. Climacteric. 2011, 14, 643–8.
111. El Khoudary SR, Shields KJ, Janssen I, Hanley C, Budoff MJ, Barinas-Mitchell E, et al. Cardiovascular Fat, Menopause, and Sex Hormones in Women: The SWAN Cardiovascular Fat Ancillary Study. J Clin Endocrinol Metab. 2015, 100, 3304–12.
112. Muka T, Oliver-Williams C, Kunutsor S, Laven JSE, Fauser BCJM, Chowdhury R, et al. Association of Age at Onset of Menopause and Time Since Onset of Menopause With Cardiovascular Outcomes, Intermediate Vascular Traits, and All-Cause Mortality. JAMA Cardiol. 2016, 1, 767.
113. Baker JM, Al-Nakkash L, Herbst-Kralovetz MM. Estrogen–gut microbiome axis: Physiological and clinical implications. Maturitas. 2017, 103, 45–53.
114. Faulds MH, Zhao C, Dahlman-Wright K, Gustafsson JÅ. The diversity of sex steroid action: regulation of metabolism by estrogen signaling. J Endocrinol. 2012, 212, 3–12.
115. Murphy E. Estrogen Signaling and Cardiovascular Disease. Circ Res. 2011, 109, 687–96.
116. Charkoudian N, Hart ECJ, Barnes JN, Joyner MJ. Autonomic control of body temperature and blood pressure: influences of female sex hormones. Clin Auton Res. 2017, 27, 149–55.
117. Abramson BL, Melvin RG. Cardiovascular Risk in Women: Focus on Hypertension. Can J Cardiol. 2014, 30, 553–9.
118. Maric-Bilkan C, Manigrasso MB. Sex Differences in Hypertension: Contribution of the Renin–Angiotensin System. Gend Med. 2012, 9, 287–91.
119. Simoncini T, Hafezi-Moghadam A, Brazil DP, Ley K, Chin WW, Liao JK. Interaction of oestrogen receptor with the regulatory subunit of phosphatidylinositol-3-OH kinase. Nature. 2000, 407, 538–41.
120. Donato GB, Fuchs SC, Oppermann K, Bastos C, Spritzer PM. Association between menopause status and central adiposity measured at different cutoffs of waist

circumference and waist-to-hip ratio. Menopause. 2006, 13, 280–5.

121. Ben Ali S, Belfki-Benali H, Aounallah-Skhiri H, Traissac P, Maire B, Delpeuch F, et al. Menopause and Metabolic Syndrome in Tunisian Women. Biomed Res Int. 2014, 2014, 1–7.
122. Petri Nahas EA, Padoani NP, Nahas-Neto J, Orsatti FL, Tardivo AP, Dias R. Metabolic syndrome and its associated risk factors in Brazilian postmenopausal women. Climacteric. 2009, 12, 431–8.
123. Sozen T, Ozisik L, Calik Basaran N. An overview and management of osteoporosis. Eur J Rheumatol. 2017, 4, 46–56.
124. Shuhart CR, Yeap SS, Anderson PA, Jankowski LG, Lewiecki EM, Morse LR, et al. Executive Summary of the 2019 ISCD Position Development Conference on Monitoring Treatment, DXA Cross-calibration and Least Significant Change, Spinal Cord Injury, Peri-prosthetic and Orthopedic Bone Health, Transgender Medicine, and Pediatrics. J Clin Densitom. 2019, 22, 453–71.
125. Clynes MA, Harvey NC, Curtis EM, Fuggle NR, Dennison EM, Cooper C. The epidemiology of osteoporosis. Br Med Bull. 2020, 133, 105–17.
126. Finkelstein JS, Brockwell SE, Mehta V, Greendale GA, Sowers MR, Ettinger B, et al. Bone mineral density changes during the menopause transition in a multiethnic cohort of women. J Clin Endocrinol Metab. 2008, 93, 861–8.
127. Shieh A, Epeldegui M, Karlamangla AS, Greendale GA. Gut permeability, inflammation, and bone density across the menopause transition. JCI Insight. 2020, 5, e134092.
128. Johnel O, Gullberg B, Allander E, Kanis JA. The apparent incidence of hip fracture in Europe: A study of national register sources. Osteoporos Int. 1992, 2, 298–302.
129. Kuroda T, Uenishi K, Ohta H, Shiraki M. Multiple vitamin deficiencies additively increase the risk of incident fractures in Japanese postmenopausal women. Osteoporos Int. 2019, 30, 593–9.
130. Almeida M, Laurent MR, Dubois V, Claessens F, O'Brien CA, Bouillon R, et al. Estrogens and Androgens in Skeletal Physiology and Pathophysiology. Physiol Rev. 2017, 97, 135–87.
131. Eastell R, Szulc P. Use of bone turnover markers in postmenopausal osteoporosis. Lancet Diabetes Endocrinol. 2017, 5, 908–23.
132. Locatelli V, Bianchi VE. Effect of GH/IGF-1 on Bone Metabolism and Osteoporsosis. Int J Endocrinol. 2014, 2014, 1–25.
133. Marie PJ, Kassem M. Extrinsic Mechanisms Involved in Age-Related Defective Bone Formation. J Clin Endocrinol Metab. 2011, 96, 600–9.
134. Boyle WJ, Simonet WS, Lacey DL. Osteoclast differentiation and activation. Nature. 2003, 423, 337–42.
135. Tella SH, Gallagher JC. Prevention and treatment of postmenopausal osteoporosis. J Steroid Biochem Mol Biol. 2014, 142, 155–70.
136. Khosla S. Pathogenesis of Age-Related Bone Loss in Humans. Journals Gerontol Ser A Biol Sci Med Sci. 2013, 68, 1226–35.
137. Møller AMJ, Delaissé JM, Olesen JB, Madsen JS, Canto LM, Bechmann T, et al. Aging and menopause reprogram osteoclast precursors for aggressive bone resorption. Bone Res. 2020, 8, 27.

138. Douchi T, Yamamoto S, Yoshimitsu N, Andoh T, Matsuo T, Nagata Y. Relative contribution of aging and menopause to changes in lean and fat mass in segmental regions. Maturitas. 2002, 42, 301–6.
139. Mehta J, Kling JM, Manson JE. Risks, Benefits, and Treatment Modalities of Menopausal Hormone Therapy: Current Concepts. Front Endocrinol (Lausanne). 2021, 12, 564781.
140. Agarwal S, Alzahrani FA, Ahmed A. Hormone Replacement Therapy: Would it be Possible to Replicate a Functional Ovary? Int J Mol Sci. 2018, 19, 3160.
141. Cho L, Kaunitz AM, Faubion SS, Hayes SN, Lau ES, Pristera N, et al. Rethinking Menopausal Hormone Therapy: For Whom, What, When, and How Long? Circulation. 2023, 147, 597–610.
142. Geller SE, Studee L. Botanical and Dietary Supplements for Menopausal Symptoms: What Works, What Does Not. J Women's Heal. 2005, 14, 634–49.
143. Ko SH, Kim HS. Menopause-Associated Lipid Metabolic Disorders and Foods Beneficial for Postmenopausal Women. Nutrients. 2020, 12, 202.
144. Thom G, Lean M. Is There an Optimal Diet for Weight Management and Metabolic Health? Gastroenterology. 2017, 152, 1739–51.
145. Mancini JG, Filion KB, Atallah R, Eisenberg MJ. Systematic Review of the Mediterranean Diet for Long-Term Weight Loss. Am J Med. 2016, 129, 407–415.e4.
146. Estruch R, Ros E, Salas-Salvadó J, Covas MI, Corella D, Arós F, et al. Primary Prevention of Cardiovascular Disease with a Mediterranean Diet Supplemented with Extra-Virgin Olive Oil or Nuts. N Engl J Med. 2018, 378, 1–14.
147. Salas-Salvadó J, Díaz-López A, Ruiz-Canela M, Basora J, Fitó M, Corella D, et al. Effect of a Lifestyle Intervention Program With Energy-Restricted Mediterranean Diet and Exercise on Weight Loss and Cardiovascular Risk Factors: One-Year Results of the PREDIMED-Plus Trial. Diabetes Care. 2019, 42, 777–88.
148. Ruiz-Cabello P, Coll-Risco I, Acosta-Manzano P, Borges-Cosic M, Gallo-Vallejo FJ, Aranda P, et al. Influence of the degree of adherence to the Mediterranean diet on the cardiometabolic risk in peri and menopausal women. The Flamenco project. Nutr Metab Cardiovasc Dis. 2017, 27, 217–24.
149. Pugliese G, Barrea L, Laudisio D, Aprano S, Castellucci B, Framondi L, et al. Mediterranean diet as tool to manage obesity in menopause: A narrative review. Nutrition. 2020, 79–80, 110991.
150. Křížová L, Dadáková K, Kašparovská J, Kašparovský T. Isoflavones. Molecules. 2019, 24, 1076.
151. Setchell KDR, Clerici C. Equol: History, Chemistry, and Formation. J Nutr. 2010, 140, 1355S–1362S.
152. Romani AMP. The controversy on the beneficial effect of phytoestrogens in diabetic treatment in postmenopausal women. Biochemical Pharmacology. 2021, 190, 114619.
153. Quesada-Vázquez S, Antolín A, Colom-Pellicer M, Aragonès G, Herrero L, Del Bas JM, et al. Reduction of Obesity and Insulin Resistance through Dual Targeting of VAT and BAT by a Novel Combination of Metabolic Cofactors. Int J Mol Sci. 2022, 23, 14923.

154. Companys J, Calderón-Pérez L, Pla-Pagà L, Llauradó E, Sandoval-Ramirez BA, Gosalbes MJ, et al. Effects of enriched seafood sticks (heat-inactivated B. animalis subsp. lactis CECT 8145, inulin, omega-3) on cardiometabolic risk factors and gut microbiota in abdominally obese subjects: randomized controlled trial. Eur J Nutr. 2022, 61, 3597–611.
155. Quesada-Vázquez S, Colom-Pellicer M, Navarro-Masip È, Aragonès G, Del Bas JM, Caimari A, et al. Supplementation with a specific combination of metabolic cofactors ameliorates non-alcoholic fatty liver disease and, hepatic fibrosis, and insulin resistance in mice. Nutrients. 2021, 13, 3532.
156. Yang H, Mayneris-Perxachs J, Boqué N, Del Bas JM, Arola L, Yuan M, et al. Combined metabolic activators decrease liver steatosis by activating mitochondrial metabolism in hamsters fed with a high-fat diet. Biomedicines. 2021, 9, 1440.
157. Quesada-Vázquez S, Castells-Nobau A, Latorre J, Oliveras-Cañellas N, Puig-Parnau I, Tejera N, et al. Potential therapeutic implications of histidine catabolism by the gut microbiota in NAFLD patients with morbid obesity. Cell Reports Med. 2023, 4, 101341.
158. Wang S, Moustaid-Moussa N, Chen L, Mo H, Shastri A, Su R, et al. Novel insights of dietary polyphenols and obesity. J Nutr Biochem. 2014, 25, 1–18.
159. Vezza T, Canet F, de Marañón AM, Bañuls C, Rocha M, Víctor VM. Phytosterols: Nutritional health players in the management of obesity and its related disorders. Antioxidants. 2020, 9, 1266.
160. Mele L, Bidault G, Mena P, Crozier A, Brighenti F, Vidal-Puig A, et al. Dietary (poly)phenols, brown adipose tissue activation, and energy expenditure: A narrative review. Advances in Nutrition. American Society for Nutrition. 2017, 8, 694–704.
161. Morrone MDS, Schnorr CE, Behr GA, Gasparotto J, Bortolin RC, Da Boit Martinello K, et al. Curcumin Supplementation Decreases Intestinal Adiposity Accumulation, Serum Cholesterol Alterations, and Oxidative Stress in Ovariectomized Rats. Oxid Med Cell Longev. 2016, 2016, 5719291.
162. Panknin TM, Howe CL, Hauer M, Bucchireddigari B, Rossi AM, Funk JL. Curcumin Supplementation and Human Disease: A Scoping Review of Clinical Trials. Int J Mol Sci. 2023, 24, 4476.
163. Khorasanian AS, Fateh ST, Gholami F, Rasaei N, Gerami H, Khayyatzadeh SS, et al. The effects of hesperidin supplementation on cardiovascular risk factors in adults: a systematic review and dose–response meta-analysis. Frontiers in Nutrition. 2023, 10, 1177708.
164. Xiong H, Wang J, Ran Q, Lou G, Peng C, Gan Q, et al. Hesperidin: A Therapeutic Agent For Obesity. Drug Des Devel Ther. 2019, 13, 3855–66.
165. Kunnumakkara AB, Bordoloi D, Padmavathi G, Monisha J, Roy NK, Prasad S, et al. Curcumin, the golden nutraceutical: multitargeting for multiple chronic diseases. Br J Pharmacol. 2017, 174, 1325–48.
166. Kamal DAM, Salamt N, Yusuf ANM, Kashim MIAM, Mokhtar MH. Potential Health Benefits of Curcumin on Female Reproductive Disorders: A Review. Nutrients. 2021, 13, 3126.
167. Sirotkin A V. The Influence of Turmeric and Curcumin on Female Reproductive Processes. Planta Med. 2022, 88, 1020–5.

168. Panahi Y, Hosseini MS, Khalili N, Naimi E, Soflaei SS, Majeed M, et al. Effects of supplementation with curcumin on serum adipokine concentrations: A randomized controlled trial. Nutrition. 2016, 32, 1116–22.
169. Atkin SL, Katsiki N, Derosa G, Maffioli P, Sahebkar A. Curcuminoids Lower Plasma Leptin Concentrations: A Meta-analysis. Phyther Res. 2017, 31, 1836–41.
170. Chuengsamarn S, Rattanamongkolgul S, Phonrat B, Tungtrongchitr R, Jirawatnotai S. Reduction of atherogenic risk in patients with type 2 diabetes by curcuminoid extract: A randomized controlled trial. J Nutr Biochem. 2014, 25, 144–50.
171. Kubota M, Shimizu M, Sakai H, Yasuda Y, Terakura D, Baba A, et al. Preventive effects of curcumin on the development of azoxymethane-induced colonic preneoplastic lesions in male C57BL/KsJ-db/db obese mice. Nutr Cancer. 2012, 64, 72–9.
172. Weisberg SP, Leibel R, Tortoriello D V. Dietary curcumin significantly improves obesity-associated inflammation and diabetes in mouse models of diabesity. Endocrinology. 2008, 149, 3549–58.
173. Chuengsamarn S, Rattanamongkolgul S, Luechapudiporn R, Phisalaphong C, Jirawatnotai S. Curcumin extract for prevention of type 2 diabetes. Diabetes Care. 2012, 35, 2121–7.
174. Lee SJ, Chandrasekran P, Mazucanti CH, O'Connell JF, Egan JM, Kim Y. Dietary curcumin restores insulin homeostasis in diet-induced obese aged mice. Aging. 2022, 14, 225–39.
175. Lone J, Choi JH, Kim SW, Yun JW. Curcumin induces brown fat-like phenotype in 3T3-L1 and primary white adipocytes. J Nutr Biochem. 2016, 27, 193–202.
176. Zhao J, Sun XB, Ye F, Tian WX. Suppression of fatty acid synthase, differentiation and lipid accumulation in adipocytes by curcumin. Mol Cell Biochem. 2011, 351, 19–28.
177. Ejaz A, Wu D, Kwan P, Meydani M. Curcumin Inhibits Adipogenesis in 3T3-L1 Adipocytes and Angiogenesis and Obesity in C57/BL Mice. J Nutr. 2009, 139, 919–25.
178. Tiwari-Pandey R, Sairam MR. Modulation of Ovarian Structure and Abdominal Obesity in Curcumin- and Flutamide-treated Aging FSH-R Haploinsufficient Mice. Reprod Sci. 2009, 16, 539–50.
179. Destici Isgoren G, Dilbaz B, Erturk Aksakal S, Kiykac Altinbas S, Yildirim Z, Simsek G, et al. Impact of Curcumin on Ovarian Reserve After Tubal Ligation: an Experimental Study. Reprod Sci. 2021, 28, 2458–67.
180. Azami SH, Nazarian H, Abdollahifar MA, Eini F, Farsani MA, Novin MG. The antioxidant curcumin postpones ovarian aging in young and middle-aged mice. Reprod Fertil Dev. 2020, 32, 292.
181. Alekseyeva IN, Makogon N V, Bryzgina TM, Voznesenskaya TY, Sukhina VS. Effects of NF-κB Blocker Curcumin on Oogenesis and Immunocompetent Organ Cells in Immune Ovarian Injury in Mice. Bull Exp Biol Med. 2011, 151, 432–5.
182. Aktas C, Kanter M, Kocak Z. Antiapoptotic and proliferative activity of curcumin on ovarian follicles in mice exposed to whole body ionizing radiation. Toxicol Ind Health. 2012, 28, 852–63.

183. Murphy CJ, Tang H, Van Kirk EA, Shen Y, Murdoch WJ. Reproductive effects of a pegylated curcumin. Reprod Toxicol. 2012, 34, 120–4.
184. Yan Z, Dai Y, Fu H, Zheng Y, Bao D, Yin Y, et al. Curcumin exerts a protective effect against premature ovarian failure in mice. J Mol Endocrinol. 2018, 60, 261–71.
185. Fatemi Abhari SM, Khanbabaei R, Hayati Roodbari N, Parivar K, Yaghmaei P. Curcumin-loaded super-paramagnetic iron oxide nanoparticle affects on apoptotic factors expression and histological changes in a prepubertal mouse model of polycystic ovary syndrome-induced by dehydroepiandrosterone - A molecular and stereological study. Life Sci. 2020, 249, 117515.
186. Melekoglu R, Ciftci O, Eraslan S, Cetin A, Basak N. Beneficial effects of curcumin and capsaicin on cyclophosphamide-induced premature ovarian failure in a rat model. J Ovarian Res. 2018, 11, 33.
187. elnahas khaled, Aziza S, El-Senosi Y, Aggag M. Curcumin and Hesperidin alleviates oxidative stress and hormonal alterations in a rat model of cyclophosphamide-induced premature ovarian failure. Benha Vet Med J. 2020, 39, 95–100.
188. Kim WK, Ke K, Sul OJ, Kim HJ, Kim SH, Lee MH, et al. Curcumin protects against ovariectomy-induced bone loss and decreases osteoclastogenesis. J Cell Biochem. 2011, 112, 3159–66.
189. Hussan F, Ibraheem NG, Kamarudin TA, Shuid AN, Soelaiman IN, Othman F. Curcumin Protects against Ovariectomy-Induced Bone Changes in Rat Model. Evidence-Based Complement Altern Med. 2012, 2012, 1–7.
190. Kuptniratsaikul V, Dajpratham P, Taechaarpornkul W, Buntragulpoontawee M, Lukkanapichonchut P, Chootip C, et al. Efficacy and safety of Curcuma domestica extracts compared with ibuprofen in patients with knee osteoarthritis: a multicenter study. Clin Interv Aging. 2014, 9, 451.
191. Panahi Y, Rahimnia A, Sharafi M, Alishiri G, Saburi A, Sahebkar A. Curcuminoid Treatment for Knee Osteoarthritis: A Randomized Double-Blind Placebo-Controlled Trial. Phyther Res. 2014, 28, 1625–31.
192. Mas-Capdevila A, Teichenne J, Domenech-Coca C, Caimari A, Del Bas JM, Escoté X, et al. Effect of Hesperidin on Cardiovascular Disease Risk Factors: The Role of Intestinal Microbiota on Hesperidin Bioavailability. Nutrients. 2020, 12, 1488.
193. Valls RM, Pedret A, Calderón-Pérez L, Llauradó E, Pla-Pagà L, Companys J, et al. Effects of hesperidin in orange juice on blood and pulse pressures in mildly hypertensive individuals: a randomized controlled trial (Citrus study). Eur J Nutr. 2021, 60, 1277–88.
194. Dhanya R, Jayamurthy P. In vitro evaluation of antidiabetic potential of hesperidin and its aglycone hesperetin under oxidative stress in skeletal muscle cell line. Cell Biochem Funct. 2020, 38, 419–27.
195. Xuguang H, Aofei T, Tao L, Longyan Z, Weijian B, Jiao G. Hesperidin ameliorates insulin resistance by regulating the IRS1-GLUT2 pathway via TLR4 in HepG2 cells. Phyther Res. 2019, 33, 1697–705.
196. Yamamoto M, Suzuki A, Hase T. Short-Term Effects of Glucosyl Hesperidin and Hesperetin on Blood Pressure and Vascular Endothelial Function in Spontaneously Hypertensive Rats. J Nutr Sci Vitaminol (Tokyo). 2008, 54, 95–8.

197. Wang X, Hasegawa J, Kitamura Y, Wang Z, Matsuda A, Shinoda W, et al. Effects of Hesperidin on the Progression of Hypercholesterolemia and Fatty Liver Induced by High-Cholesterol Diet in Rats. J Pharmacol Sci. 2011, 117, 129–38.
198. Yamamoto M, Jokura H, Hashizume K, Ominami H, Shibuya Y, Suzuki A, et al. Hesperidin metabolite hesperetin-7-O-glucuronide, but not hesperetin-3′-O-glucuronide, exerts hypotensive, vasodilatory, and anti-inflammatory activities. Food Funct. 2013, 4, 1346.
199. Jung UJ, Choi MS, Lee MK, Jeong KS. The Hypoglycemic Effects of Hesperidin and Naringin Are Partly Mediated by Hepatic Glucose-Regulating Enzymes in C57BL/KsJ-db/db Mice. J Nutr. 2004, 134, 2499–503.
200. Jung UJ, Lee MK, Park YB, Kang MA, Choi MS. Effect of citrus flavonoids on lipid metabolism and glucose-regulating enzyme mRNA levels in type-2 diabetic mice. Int J Biochem Cell Biol. 2006, 38, 1134–45.
201. Akiyama S, Katsumata S, Suzuki K, Nakaya Y, Ishimi Y, Uehara M. Hypoglycemic and Hypolipidemic Effects of Hesperidin and Cyclodextrin-Clathrated Hesperetin in Goto-Kakizaki Rats with Type 2 Diabetes. Biosci Biotechnol Biochem. 2009, 73, 2779–82.
202. Mahmoud AM, Ashour MB, Abdel-Moneim A, Ahmed OM. Hesperidin and naringin attenuate hyperglycemia-mediated oxidative stress and proinflammatory cytokine production in high fat fed/streptozotocin-induced type 2 diabetic rats. J Diabetes Complications. 2012, 26, 483–90.
203. Jia S, Hu Y, Zhang W, Zhao X, Chen Y, Sun C, et al. Hypoglycemic and hypolipidemic effects of neohesperidin derived from Citrus aurantium L. in diabetic KK-A y mice. Food Funct. 2015, 6, 878–86.
204. Lima ACD, Cecatti C, Fidélix MP, Adorno MAT, Sakamoto IK, Cesar TB, et al. Effect of Daily Consumption of Orange Juice on the Levels of Blood Glucose, Lipids, and Gut Microbiota Metabolites: Controlled Clinical Trials. J Med Food. 2019, 22, 202–10.
205. Yari Z, Movahedian M, Imani H, Alavian SM, Hedayati M, Hekmatdoost A. The effect of hesperidin supplementation on metabolic profiles in patients with metabolic syndrome: a randomized, double-blind, placebo-controlled clinical trial. Eur J Nutr. 2020, 59, 2569–77.
206. Ribeiro C, Dourado G, Cesar T. Orange juice allied to a reduced-calorie diet results in weight loss and ameliorates obesity-related biomarkers: A randomized controlled trial. Nutrition. 2017, 38, 13–9.
207. Akiyama S, Katsumata S ichi, Suzuki K, Ishimi Y, Wu J, Uehara M. Dietary Hesperidin Exerts Hypoglycemic and Hypolipidemic Effects in Streptozotocin-Induced Marginal Type 1 Diabetic Rats. J Clin Biochem Nutr. 2009, 46, 87–92.
208. Sundaram R, Nandhakumar E, Haseena Banu H. Hesperidin, a citrus flavonoid ameliorates hyperglycemia by regulating key enzymes of carbohydrate metabolism in streptozotocin-induced diabetic rats. Toxicol Mech Methods. 2019, 29, 644–53.
209. Mosqueda-Solís A, Sánchez J, Reynés B, Palou M, Portillo MP, Palou A, et al. Hesperidin and capsaicin, but not the combination, prevent hepatic steatosis and other metabolic syndrome-related alterations in western diet-fed rats. Sci Rep. 2018, 8, 15100.

210. Sun YZ, Chen JF, Shen LM, Zhou J, Wang CF. Anti-atherosclerotic effect of hesperidin in LDLr −/− mice and its possible mechanism. Eur J Pharmacol. 2017, 815, 109–17.
211. Salden BN, Troost FJ, de Groot E, Stevens YR, Garcés-Rimón M, Possemiers S, et al. Randomized clinical trial on the efficacy of hesperidin 2S on validated cardiovascular biomarkers in healthy overweight individuals. Am J Clin Nutr. 2016, 104, 1523–33.
212. Assini JM, Mulvihill EE, Huff MW. Citrus flavonoids and lipid metabolism. Curr Opin Lipidol. 2013, 24, 34–40.
213. Simpson EJ, Mendis B, Macdonald IA. Orange juice consumption and its effect on blood lipid profile and indices of the metabolic syndrome; a randomised, controlled trial in an at-risk population. Food Funct. 2016, 7, 1884–91.
214. Aptekmann NP, Cesar TB. Orange juice improved lipid profile and blood lactate of overweight middle-aged women subjected to aerobic training. Maturitas. 2010, 67, 343–7.
215. E. Mulvihill E, W. Huff M. Citrus Flavonoids and the Prevention of Atherosclerosis. Cardiovasc Hematol Disord Targets. 2012, 12, 84–91.
216. Mohammadi M, Ramezani-Jolfaie N, Lorzadeh E, Khoshbakht Y, Salehi-Abargouei A. Hesperidin, a major flavonoid in orange juice, might not affect lipid profile and blood pressure: A systematic review and meta-analysis of randomized controlled clinical trials. Phyther Res. 2019, 33, 534–45.
217. Ortiz A de C, Fideles SOM, Reis CHB, Bellini MZ, Pereira E de SBM, Pilon JPG, et al. Therapeutic Effects of Citrus Flavonoids Neohesperidin, Hesperidin and Its Aglycone, Hesperetin on Bone Health.Biomolecules. 2022, 12, 626.
218. Horcajada MN, Habauzit V, Trzeciakiewicz A, Morand C, Gil-Izquierdo A, Mardon J, et al. Hesperidin inhibits ovariectomized-induced osteopenia and shows differential effects on bone mass and strength in young and adult intact rats. J Appl Physiol. 2008, 104, 648–54.
219. Chiba H, Uehara M, Wu J, Wang X, Masuyama R, Suzuki K, et al. Nutrient Metabolism Hesperidin, a Citrus Flavonoid, Inhibits Bone Loss and Decreases Serum and Hepatic Lipids in Ovariectomized Mice. J. Nutr. 2003, 133, 1892–7.
220. Lim DW, Lee Y, Kim YT. Preventive effects of citrus unshiu peel extracts on bone and lipid metabolism in OVX rats. Molecules. 2014, 19, 783–94.
221. Umar S, Kumar A, Sajad M, Zargan J, Ansari MM, Ahmad S, et al. Hesperidin inhibits collagen-induced arthritis possibly through suppression of free radical load and reduction in neutrophil activation and infiltration. Rheumatol Int. 2013, 33, 657–63.
222. Crescenti A, Caimari A, Alcaide-Hidalgo JM, Mariné-Casadó R, Valls RM, Companys J, et al. Hesperidin Bioavailability Is Increased by the Presence of 2S-Diastereoisomer and Micronization—A Randomized, Crossover and Double-Blind Clinical Trial. Nutrients. 2022, 14, 2481.
223. Gylling H, Simonen P. Phytosterols, Phytostanols, and Lipoprotein Metabolism. Nutrients. 2015, 7, 7965–77.
224. Xia W, Xiang S, Gaman MA, Jamilian P, Prabahar K, Du G, et al. The effects of phytosterol and phytostanol supplementation on the lipid profile in postmenopausal women: A systematic review and meta-analysis of randomized controlled trials. Phytotherapy Research. 2022, 36, 4398–408.

225. Laos S, Caimari A, Crescenti A, Lakkis J, Puiggròs F, Arola L, et al. Long-term intake of soyabean phytosterols lowers serum TAG and NEFA concentrations, increases bile acid synthesis and protects against fatty liver development in dyslipidaemic hamsters. Br J Nutr. 2014, 112, 663–73.

226. Makhmudova U, Schulze PC, Lütjohann D, Weingärtner O. Phytosterols and Cardiovascular Disease. Vol. 23, Current Atherosclerosis Reports. Springer; 2021.

227. Nattagh-Eshtivani E, Barghchi H, Pahlavani N, Barati M, Amiri Y, Fadel A, et al. Biological and pharmacological effects and nutritional impact of phytosterols: A comprehensive review. Phyther Res. 2022, 36, 299–322.

228. Amiot MJ, Knol D, Cardinault N, Nowicki M, Bott R, Antona C, et al. Phytosterol ester processing in the small intestine: impact on cholesterol availability for absorption and chylomicron cholesterol incorporation in healthy humans. J Lipid Res. 2011, 52, 1256–64.

229. Scientific Opinion on the substantiation of a health claim related to 3 g/day plant sterols/stanols and lowering blood LDL-cholesterol and reduced risk of (coronary) heart disease pursuant to Article 19 of Regulation (EC) No 1924/2006. EFSA J. 2012, 10, 2693.

230. Li YC, Li CL, Li R, Chen Y, Zhang M, Guo PP, et al. Associations of dietary phytosterols with blood lipid profiles and prevalence of obesity in Chinese adults, a cross-sectional study. Lipids Health Dis. 2018, 17, 1–9.

231. Ghaedi E, Varkaneh HK, Rahmani J, Mousavi SM, Mohammadi H, Fatahi S, et al. Possible anti-obesity effects of phytosterols and phytostanols supplementation in humans: A systematic review and dose–response meta-analysis of randomized controlled trials. Phyther Res. 2019, 33, 1246–57.

232. Xiong M, Huang Y, Liu Y, Huang M, Song G, Ming Q, et al. Antidiabetic Activity of Ergosterol from Pleurotus Ostreatus in KK-A y Mice with Spontaneous Type 2 Diabetes Mellitus. Mol Nutr Food Res. 2018, 62, 1–13.

233. Ramalingam S, Packirisamy M, Karuppiah M, Vasu G, Gopalakrishnan R, Gothandam K, et al. Effect of β-sitosterol on glucose homeostasis by sensitization of insulin resistance via enhanced protein expression of PPRγ and glucose transporter 4 in high fat diet and streptozotocin-induced diabetic rats. Cytotechnology. 2020, 72, 357–66.

234. Wu G. Intestinal Mucosal Amino Acid Catabolism. J Nutr. 1998, 128, 1249–52.

235. Wu G. Amino acids: metabolism, functions, and nutrition. Amino Acids. 2009, 37, 1–17.

236. Alves A, Bassot A, Bulteau AL, Pirola L, Morio B. Glycine Metabolism and Its Alterations in Obesity and Metabolic Diseases. Nutrients. 2019, 11, 1356.

237. Gaggini M, Carli F, Rosso C, Buzzigoli E, Marietti M, Della Latta V, et al. Altered amino acid concentrations in NAFLD: Impact of obesity and insulin resistance. Hepatology. 2018, 67, 145–58.

238. Elshorbagy AK, Gjesdal CG, Nurk E, Tell GS, Ueland PM, Nygård O, et al. Cysteine, homocysteine and bone mineral density: A role for body composition? Bone. 2009, 44, 954–8.

239. Okekunle AP, Wu X, Feng R, Li Y, Sun C. Higher intakes of energy-adjusted dietary amino acids are inversely associated with obesity risk. Amino Acids. 2019, 51, 373–82.
240. Lu SC. Regulation of glutathione synthesis. Mol Aspects Med. 2009, 30, 42–59.
241. He L, Ding Y, Zhou X, Li T, Yin Y. Serine signaling governs metabolic homeostasis and health. Trends Endocrinol Metab. 2023, 34, 361–72.
242. Moro J, Tomé D, Schmidely P, Demersay TC, Azzout-Marniche D. Histidine: A Systematic Review on Metabolism and Physiological Effects in Human and Different Animal Species. Nutrients. 2020, 12, 1414.
243. Thalacker-Mercer AE, Gheller ME. Benefits and Adverse Effects of Histidine Supplementation. J Nutr. 2020, 150, 2588S–2592S.
244. Li YC, Li CL, Qi JY, Huang LN, Shi D, Du SS, et al. Relationships of Dietary Histidine and Obesity in Northern Chinese Adults, an Internet-Based Cross-Sectional Study. Nutrients. 2016, 8, 420.
245. DiNicolantonio JJ, McCarty MF, OKeefe JH. Role of dietary histidine in the prevention of obesity and metabolic syndrome. Open Hear. 2018, 5, e000676.
246. Niu YC, Feng RN, Hou Y, Li K, Kang Z, Wang J, et al. Histidine and arginine are associated with inflammation and oxidative stress in obese women. Br J Nutr. 2012, 108, 57–61.
247. Du S, Sun S, Liu L, Zhang Q, Guo F, Li C, et al. Effects of Histidine Supplementation on Global Serum and Urine 1H NMR-based Metabolomics and Serum Amino Acid Profiles in Obese Women from a Randomized Controlled Study. J Proteome Res. 2017, 16, 2221–30.
248. Feng RN, Niu YC, Sun XW, Li Q, Zhao C, Wang C, et al. Histidine supplementation improves insulin resistance through suppressed inflammation in obese women with the metabolic syndrome: a randomised controlled trial. Diabetologia. 2013, 56, 985–94.
249. Durante W. Amino Acids in Circulatory Function and Health. Advances in Experimental Medicine and Biology. 2020, 1265, 39–56.
250. Kasaoka S, Kawahara Y, Inoue S, Tsuji M, Kato H, Tsuchiya T, et al. Gender effects in dietary histidine-induced anorexia. Nutrition. 2005, 21, 855–8.
251. Kasaoka S, Tsuboyama-Kasaoka N, Kawahara Y, Inoue S, Tsuji M, Ezaki O, et al. Histidine supplementation suppresses food intake and fat accumulation in rats. Nutrition. 2004, 20, 991–6.
252. Nakamura T, Naganuma F, Kudomi U, Roh S, Yanai K, Yoshikawa T. Oral histidine intake improves working memory through the activation of histaminergic nervous system in mice. Biochem Biophys Res Commun. 2022, 609, 141–8.
253. Nozawa Y, Mimura M, Yamada K, Sugita M, Shibakusa T, Koyama N. Dried bonito broth improves cognitive function via the histaminergic system in mice. Biomed Res. 201, 35, 311–9.
254. Acevedo SF, Ohtsu H, Benice TS, Rizk-Jackson A, Raber J. Age-dependent measures of anxiety and cognition in male histidine decarboxylase knockout (Hdc−/−) mice. Brain Res. 2006, 1071, 113–23.
255. Acevedo SF, Pfankuch T, Ohtsu H, Raber J. Anxiety and cognition in female histidine decarboxylase knockout (Hdc -/-) mice. Behav Brain Res. 2006, 168, 92–9.

256. Cesak O, Vostalova J, Vidlar A, Bastlova P, Student V. Carnosine and Beta-Alanine Supplementation in Human Medicine: Narrative Review and Critical Assessment. Nutrients. 2023, 15, 1770.

257. Caruso G, Di Pietro L, Cardaci V, Maugeri S, Caraci F. The therapeutic potential of carnosine: Focus on cellular and molecular mechanisms. Curr Res Pharmacol Drug Discov. 2023, 4, 100153.

258. Feehan J, Hariharan R, Buckenham T, Handley C, Bhatnagar A, Baba SP, et al. Carnosine as a potential therapeutic for the management of peripheral vascular disease. Nutr Metab Cardiovasc Dis. 2022, 32, 2289–96.

259. Behl T, Gupta A, Chigurupati S, Singh S, Sehgal A, Badavath VN, et al. Natural and Synthetic Agents Targeting Reactive Carbonyl Species against Metabolic Syndrome. Molecules. 2022, 27, 1583.

260. Matthews JJ, Dolan E, Swinton PA, Santos L, Artioli GG, Turner MD, et al. Effect of Carnosine or β-Alanine Supplementation on Markers of Glycemic Control and Insulin Resistance in Humans and Animals: A Systematic Review and Meta-analysis. Adv Nutr. 2021, 12, 2216–31.

261. Baye E, Ukropcova B, Ukropec J, Hipkiss A, Aldini G, de Courten B. Physiological and therapeutic effects of carnosine on cardiometabolic risk and disease. Amino Acids. 2016, 48, 1131–49.

262. Hariharan R, Cameron J, Menon K, Mesinovic J, Jansons P, Scott D, et al. Carnosine supplementation improves glucose control in adults with pre-diabetes and type 2 diabetes: A randomised controlled trial. Nutr Metab Cardiovasc Dis. 2024, 34, 485–96.

263. De Courten B, Jakubova M, De Courten MPJ, Kukurova IJ, Vallova S, Krumpolec P, et al. Effects of carnosine supplementation on glucose metabolism: Pilot clinical trial. Obesity. 2016, 24, 1027–34.

264. Al-Sawalha NA, Alshogran OY, Awawdeh MS, Almomani BA. The effects of L-Carnosine on development of metabolic syndrome in rats. Life Sci. 2019, 237, 116905.

265. Mong M chin, Chao C yi, Yin M chin. Histidine and carnosine alleviated hepatic steatosis in mice consumed high saturated fat diet. Eur J Pharmacol. 2011, 653, 82–8.

266. Tomonaga S, Yamane H, Onitsuka E, Yamada S, Sato M, Takahata Y, et al. Carnosine-induced antidepressant-like activity in rats. Pharmacol Biochem Behav. 2008, 89, 627–32.

267. Li YF, He RR, Tsoi B, Li XD, Li WX, Abe K, et al. Anti-Stress Effects of Carnosine on Restraint-Evoked Immunocompromise in Mice through Spleen Lymphocyte Number Maintenance. Frasch MG, editor. PLoS One. 2012, 7, e33190.

268. Araminia B, Shalbafan M, Mortezaei A, Shirazi E, Ghaffari S, Sahebolzamani E, et al. L-Carnosine combination therapy for major depressive disorder: A randomized, double-blind, placebo-controlled trial. J Affect Disord. 2020, 267, 131–6.

269. Elshorbagy AK, Nurk E, Gjesdal CG, Tell GS, Ueland PM, Nygård O, et al. Homocysteine, cysteine, and body composition in the Hordaland Homocysteine Study: does cysteine link amino acid and lipid metabolism? Am J Clin Nutr. 2008, 88, 738–46.

270. Metcalf JS, Dunlop RA, Powell JT, Banack SA, Cox PA. L-Serine: a Naturally-Occurring Amino Acid with Therapeutic Potential. Neurotox Res. 2018, 33, 213–21.
271. Achari AE, Jain SK. l -Cysteine supplementation increases insulin sensitivity mediated by upregulation of GSH and adiponectin in high glucose treated 3T3-L1 adipocytes. Arch Biochem Biophys. 2017, 630, 54–65.
272. Herrmann W, Schorr H, Obeid R, Makowski J, Fowler B, Kuhlmann MK. Disturbed Homocysteine and Methionine Cycle Intermediates S-Adenosylhomocysteine and S-Adenosylmethionine Are Related to Degree of Renal Insufficiency in Type 2 Diabetes. Clin Chem. 2005, 51, 891–7.
273. Gursu MF, Baydas G, Cikim G, Canatan H. Insulin Increases Homocysteine Levels in a Dose-Dependent Manner in Diabetic Rats. Arch Med Res. 2002, 33, 305–7.
274. Jain SK, Kanikarla-Marie P, Warden C, Micinski D. L-cysteine supplementation upregulates glutathione (GSH) and vitamin D binding protein (VDBP) in hepatocytes cultured in high glucose and in vivo in liver, and increases blood levels of GSH, VDBP, and 25-hydroxy-vitamin D in Zucker diabetic fatty rats. Mol Nutr Food Res. 2016, 60, 1090–8.
275. Jain SK, Velusamy T, Croad JL, Rains JL, Bull R. l-Cysteine supplementation lowers blood glucose, glycated hemoglobin, CRP, MCP-1, and oxidative stress and inhibits NF-κB activation in the livers of Zucker diabetic rats. Free Radic Biol Med. 2009, 46, 1633–8.
276. Wijekoon EP, Skinner C, Brosnan ME, Brosnan JT. Amino acid metabolism in the Zucker diabetic fatty rat: effects of insulin resistance and of type 2 diabetes. Can J Physiol Pharmacol. 2004, 82, 506–14.
277. Lu SC. Glutathione synthesis. Biochim Biophys Acta - Gen Subj. 2013, 1830, 3143–53.
278. Weber K, Rétey J. On the nature of the irreversible inhibition of histidine ammonia lyase by cysteine and dioxygen. Bioorganic Med Chem. 1996, 4, 1001–6.
279. Baines M, Kredan MB, Davison A, Higgins G, West C, Fraser WD, et al. The association between cysteine, bone turnover, and low bone mass. Calcif Tissue Int. 2007,81, 450–4.
280. Han NR, Kim NR, Kim HM, Jeong HJ. Cysteine Prevents Menopausal Syndromes in Ovariectomized Mouse. Reprod Sci. 2016, 23, 670–9.
281. Amelio I, Cutruzzolá F, Antonov A, Agostini M, Melino G. Serine and glycine metabolism in cancer. Trends Biochem Sci. 2014, 39, 191–8.
282. Holeček M. Serine Metabolism in Health and Disease and as a Conditionally Essential Amino Acid. Nutrients. 2022, 14, 1987.
283. Zhou X, He L, Zuo S, Zhang Y, Wan D, Long C, et al. Serine prevented high-fat diet-induced oxidative stress by activating AMPK and epigenetically modulating the expression of glutathione synthesis-related genes. Biochim Biophys Acta - Mol Basis Dis. 2018, 1864, 488–98.
284. Mardinoglu A, Ural D, Zeybel M, Yuksel HH, Uhlén M, Borén J. The Potential Use of Metabolic Cofactors in Treatment of NAFLD. Nutrients. 2019, 11, 1578.

285. Zhou X, Zhang H, He L, Wu X, Yin Y. Long-Term l-Serine Administration Reduces Food Intake and Improves Oxidative Stress and Sirt1/NFκB Signaling in the Hypothalamus of Aging Mice. Front Endocrinol (Lausanne). 2018, 23, 9.
286. Holm LJ, Haupt-Jorgensen M, Larsen J, Giacobini JD, Bilgin M, Buschard K. L-serine supplementation lowers diabetes incidence and improves blood glucose homeostasis in NOD mice. PLoS One. 2018, 13, e0194414.
287. Suárez M, Boqué N, del Bas JM, Mayneris-Perxachs J, Arola L, Caimari A. Mediterranean diet and multi-ingredient-based interventions for the management of non-alcoholic fatty liver disease. Nutrients. 2017, 9, 1052.
288. DiStefano JK. The Role of Choline, Soy Isoflavones, and Probiotics as Adjuvant Treatments in the Prevention and Management of NAFLD in Postmenopausal Women. Nutrients. 2023, 15, 2670.
289. Jeong HG, Park H. Metabolic Disorders in Menopause. Metabolites. 2022, 12, 954.
290. Califf RM. Biomarker definitions and their applications. Exp Biol Med. 2018, 243, 213–21.
291. Fogelholm M. Nutrition recommendations and science: next parallel steps. J Sci Food Agric. 2016, 96, 1059–63.
292. Mayeux R. Biomarkers: Potential uses and limitations. NeuroRX. 2004, 1, 182–8.
293. Gupta RC, Srivastava A, Sinha A, Lall R. Biomarkers of Foods and Nutraceuticals: Applications in Efficacy, Safety, and Toxicity. Nutraceuticals in Veterinary Medicine. 2019, 693–710.
294. Anaya Morua W. Omics analysis in nutrition science. Mex J Med Res ICSA. 2022, 10, 59–63.
295. Fowler BA. Omic Biological Markers. Molecular Biological Markers for Toxicology and Risk Assessment. 2016, 4, 63–80.
296. Ahmad A, Imran M, Ahsan H. Biomarkers as Biomedical Bioindicators: Approaches and Techniques for the Detection, Analysis, and Validation of Novel Biomarkers of Diseases. Pharmaceutics. 2023, 15, 1630.
297. Sturmberg JP, Picard M, Aron DC, Bennett JM, Bircher J, DeHaven MJ, et al. Health and Disease—Emergent States Resulting From Adaptive Social and Biological Network Interactions. Front Med. 2019, 6, 59.
298. McGrath IM, Mortlock S, Montgomery GW. Genetic Regulation of Physiological Reproductive Lifespan and Female Fertility. Int J Mol Sci. 2021, 22, 2556.
299. Caimari A, Oliver P, Keijer J, Palou A. Peripheral Blood Mononuclear Cells as a Model to Study the Response of Energy Homeostasis-Related Genes to Acute Changes in Feeding Conditions. Omi A J Integr Biol. 2010, 14, 129–41.
300. Pru JK. Persistent concerns over the use of compounded hormone therapies. Menopause. 2019, 26, 945–6.
301. van Ommen B, Keijer J, Heil SG, Kaput J. Challenging homeostasis to define biomarkers for nutrition related health. Mol Nutr Food Res. 2009, 53, 795–804.
302. Acar E, Gürdeniz G, Khakimov B, Savorani F, Korndal SK, Larsen TM, et al. Biomarkers of Individual Foods, and Separation of Diets Using Untargeted LC–MS-based Plasma Metabolomics in a Randomized Controlled Trial. Mol Nutr Food Res. 2019, 63, 1–30.

303. Cui X, Yu X, Sun G, Hu T, Likhodii S, Zhang J, et al. Differential metabolomics networks analysis of menopausal status. Onland-Moret NC, editor. PLoS One. 2019, 14, e0222353.
304. Suárez M, Caimari A, del Bas JM, Arola L. Metabolomics: An emerging tool to evaluate the impact of nutritional and physiological challenges. TrAC Trends Anal Chem. 2017, 96, 79–88.
305. Auguet T, Bertran L, Capellades J, Abelló S, Aguilar C, Sabench F, et al. LC/MS-Based Untargeted Metabolomics Analysis in Women with Morbid Obesity and Associated Type 2 Diabetes Mellitus. Int J Mol Sci. 2023, 24, 7761.
306. Zhao Z, Cai Z, Chen A, Cai M, Yang K. Application of metabolomics in osteoporosis research. Front Endocrinol (Lausanne). 2022, 13, 1–20.
307. Li Y, Gray A, Xue L, Farb MG, Ayalon N, Andersson C, et al. Metabolomic Profiles, Ideal Cardiovascular Health, and Risk of Heart Failure and Atrial Fibrillation: Insights From the Framingham Heart Study. J Am Heart Assoc. 2023, 12, e028022.
308. Gaspard U. Hyperinsulinaemia, a key factor of the metabolic syndrome in postmenopausal women. Maturitas. 2009, 62, 362–5.
309. Kalyani RR, Franco M, Dobs AS, Ouyang P, Vaidya D, Bertoni A, et al. The Association of Endogenous Sex Hormones, Adiposity, and Insulin Resistance with Incident Diabetes in Postmenopausal Women. J Clin Endocrinol Metab. 2009, 94, 4127–35.
310. Höfer T, Rodewald HR. Differentiation-based model of hematopoietic stem cell functions and lineage pathways. Blood. 2018, 132, 1106–13.
311. Seita J, Weissman IL. Hematopoietic stem cell: self-renewal versus differentiation. WIREs Syst Biol Med. 2010, 2, 640–53.
312. Verhoeckx K, Cotter P, López-Expósito I, Kleiveland C, Lea T, Mackie A, et al. The Impact of Food Bioactives on Health: In Vitro and Ex Vivo Models. 2015, 1-327.
313. Batliwalla FM, Baechler EC, Xiao X, Li W, Balasubramanian S, Khalili H, et al. Peripheral blood gene expression profiling in rheumatoid arthritis. Genes Immun. 2005, 6, 388–97.
314. Stürzebecher S, Wandinger KP, Rosenwald A, Sathyamoorthy M, Tzou A, Mattar P, et al. Expression profiling identifies responder and non-responder phenotypes to interferon-β in multiple sclerosis. Brain. 2003, 126, 1419–29.
315. Bernard-Poenaru O, Roux C, Blanque´ R, Gardner C, de Vernejoul MC, Cohen-Solal ME. Bone-Resorbing Cytokines from Peripheral Blood Mononuclear Cells after Hormone Replacement Therapy: A Longitudinal Study. Osteoporos Int. 2001, 12, 769–76.
316. Baechler EC, Batliwalla FM, Karypis G, Gaffney PM, Ortmann WA, Espe KJ, et al. Interferon-inducible gene expression signature in peripheral blood cells of patients with severe lupus. Proc Natl Acad Sci. 2003, 100, 2610–5.
317. Acosta Davila JA, Hernandez De Los Rios A. An Overview of Peripheral Blood Mononuclear Cells as a Model for Immunological Research of Toxoplasma gondii and Other Apicomplexan Parasites. Front Cell Infect Microbiol. 2019, 9, 1–10.

318. Berbudi A, Rahmadika N, Tjahjadi AI, Ruslami R. Type 2 Diabetes and its Impact on the Immune System. Curr Diabetes Rev. 2020, 16, 442–9.
319. Bokarewa M, Nagaev I, Dahlberg L, Smith U, Tarkowski A. Resistin, an Adipokine with Potent Proinflammatory Properties. J Immunol. 2005, 174, 5789–95.
320. Caimari A, Oliver P, Rodenburg W, Keijer J, Palou A. Slc27a2 expression in peripheral blood mononuclear cells as a molecular marker for overweight development. Int J Obes. 2010, 34, 831–9.
321. de Mello VDF, Kolehmainen M, Schwab U, Mager U, Laaksonen DE, Pulkkinen L, et al. Effect of weight loss on cytokine messenger RNA expression in peripheral blood mononuclear cells of obese subjects with the metabolic syndrome. Metabolism. 2008, 57, 192–9.
322. Ghanim H, Aljada A, Hofmeyer D, Syed T, Mohanty P, Dandona P. Circulating Mononuclear Cells in the Obese Are in a Proinflammatory State. Circulation. 2004, 110, 1564–71.
323. Goyenechea E, Parra D, Crujeiras AB, Abete I, Martínez JA. A Nutrigenomic Inflammation-Related PBMC-Based Approach to Predict the Weight-Loss Regain in Obese Subjects. Ann Nutr Metab. 2009, 54, 43–51.
324. Napoleone E, Di santo A, Amore C, Baccante G, Di Febbo C, Porreca E, et al. Leptin induces tissue factor expression in human peripheral blood mononuclear cells: a possible link between obesity and cardiovascular risk? J Thromb Haemost. 2007, 5, 1462–8.
325. O'Rourke RW, Kay T, Lyle EA, Traxler SA, Deveney CW, Jobe BA, et al. Alterations in peripheral blood lymphocyte cytokine expression in obesity. Clin Exp Immunol. 2006, 146, 39–46.
326. Patel L, Buckels AC, Kinghorn IJ, Murdock PR, Holbrook JD, Plumpton C, et al. Resistin is expressed in human macrophages and directly regulated by PPARγ activators. Biochem Biophys Res Commun. 2003, 300, 472–6.
327. Samara A, Marie B, Pfister M, Visvikis-Siest S. Leptin expression in Peripheral Blood Mononuclear Cells (PBMCs) is related with blood pressure variability. Clin Chim Acta. 2008, 395, 47–50.
328. Gonzalez H, Hagerling C, Werb Z. Roles of the immune system in cancer: from tumor initiation to metastatic progression. Genes Dev. 2018, 32, 1267–84.
329. Cao W, Zheng H. Peripheral immune system in aging and Alzheimer's disease. Mol Neurodegener. 2018, 13, 51.
330. Bouwens M, Afman LA, Müller M. Fasting induces changes in peripheral blood mononuclear cell gene expression profiles related to increases in fatty acid β-oxidation: functional role of peroxisome proliferator–activated receptor α in human peripheral blood mononuclear cells. Am J Clin Nutr. 2007, 86, 1515–23.
331. Burczynski ME, Dorner AJ. Transcriptional Profiling of Peripheral Blood Cells in Clinical Pharmacogenomic Studies. Pharmacogenomics. 2006, 7, 187–202.
332. Manoel-Caetano FS, Xavier DJ, Evangelista AF, Takahashi P, Collares C V, Puthier D, et al. Gene expression profiles displayed by peripheral blood

mononuclear cells from patients with type 2 diabetes mellitus focusing on biological processes implicated on the pathogenesis of the disease. Gene. 2012, 511, 151–60.

333. Liew CC, Ma J, Tang HC, Zheng R, Dempsey AA. The peripheral blood transcriptome dynamically reflects system wide biology: a potential diagnostic tool. J Lab Clin Med. 2006, 147, 126–32.
334. Bouwens M, Afman LA, Müller M. Activation of peroxisome proliferator-activated receptor alpha in human peripheral blood mononuclear cells reveals an individual gene expression profile response. BMC Genomics. 2008, 9, 262.
335. Maas K, Chan S, Parker J, Slater A, Moore J, Olsen N, et al. Cutting Edge: Molecular Portrait of Human Autoimmune Disease. J Immunol. 2002, 169, 5–9.
336. Visvikis-Siest S, Marteau JB, Samara A, Berrahmoune H, Marie B, Pfister M. Peripheral blood mononuclear cells (PBMCs): a possible model for studying cardiovascular biology systems. Clin Chem Lab Med. 2007, 45, 1154–68.
337. Ziegler-Heitbrock HWL. Definition of human blood monocytes. J Leukoc Biol. 2000, 67, 603–6.
338. Watmough S, Flynn M. A review of pain management interventions in bone marrow biopsy. J Clin Nurs. 2011, 20, 615–23.
339. Kimmelman J, Resnik DB, Peppercorn J, Ratain MJ. Burdensome Research Procedures in Trials: Why Less Is More. JNCI J Natl Cancer Inst. 2017, 109, 1–3.
340. Olson EM, Lin NU, Krop IE, Winer EP. The ethical use of mandatory research biopsies. Nat Rev Clin Oncol. 2011, 8, 620–5.
341. Rockett JC, Burczynski ME, Fornace AJ, Herrmann PC, Krawetz SA, Dix DJ. Surrogate tissue analysis: monitoring toxicant exposure and health status of inaccessible tissues through the analysis of accessible tissues and cells. Toxicol Appl Pharmacol. 2004, 194, 189–99.
342. Reynés B, Díaz-Rúa R, Cifre M, Oliver P, Palou A. Peripheral blood mononuclear cells as a potential source of biomarkers to test the efficacy of weight-loss strategies. Obesity. 2015, 23, 28–31.
343. Sánchez J, Priego T, Picó C, Ahrens W, De Henauw S, Fraterman A, et al. Blood Cells as a Source of Transcriptional Biomarkers of Childhood Obesity and Its Related Metabolic Alterations: Results of the IDEFICS Study. J Clin Endocrinol Metab. 2012, 97, E648–52.
344. Konieczna J, Sánchez J, van Schothorst EM, Torrens JM, Bunschoten A, Palou M, et al. Identification of early transcriptome-based biomarkers related to lipid metabolism in peripheral blood mononuclear cells of rats nutritionally programmed for improved metabolic health. Genes Nutr. 2014, 9, 366.
345. Oliver P, Reynés B, Caimari A, Palou A. Peripheral blood mononuclear cells: a potential source of homeostatic imbalance markers associated with obesity development. Pflügers Arch - Eur J Physiol. 2013, 465, 459–68.
346. Reynés B, Priego T, Cifre M, Oliver P, Palou A. Peripheral Blood Cells, a Transcriptomic Tool in Nutrigenomic and Obesity Studies: Current State of the Art. Compr Rev Food Sci Food Saf. 2018, 17, 1006–20.
347. Moore DF, Li H, Jeffries N, Wright V, Cooper RA, Elkahloun A, et al. Using

Peripheral Blood Mononuclear Cells to Determine a Gene Expression Profile of Acute Ischemic Stroke. Circulation. 2005, 111, 212–21.

348. Jayedi A, Soltani S, Abdolshahi A, Shab-Bidar S. Healthy and unhealthy dietary patterns and the risk of chronic disease: an umbrella review of meta-analyses of prospective cohort studies. Br J Nutr. 2020, 124, 1133–44.
349. Showe MK, Vachani A, Kossenkov A V., Yousef M, Nichols C, Nikonova E V., et al. Gene Expression Profiles in Peripheral Blood Mononuclear Cells Can Distinguish Patients with Non–Small Cell Lung Cancer from Patients with Nonmalignant Lung Disease. Cancer Res. 2009, 69, 9202–10.
350. Caimari A, Oliver P, Rodenburg W, Keijer J, Palou A. Feeding conditions control the expression of genes involved in sterol metabolism in peripheral blood mononuclear cells of normoweight and diet-induced (cafeteria) obese rats. J Nutr Biochem. 2010, 21, 1127–33.
351. Konieczna J, Sánchez J, Palou M, Picó C, Palou A. Blood cell transcriptomic-based early biomarkers of adverse programming effects of gestational calorie restriction and their reversibility by leptin supplementation. Sci Rep. 2015, 5, 9088.
352. de Mello VDF, Kolehmanien M, Schwab U, Pulkkinen L, Uusitupa M. Gene expression of peripheral blood mononuclear cells as a tool in dietary intervention studies: What do we know so far? Mol Nutr Food Res. 2012, 56, 1160–72.
353. Afman L, Milenkovic D, Roche HM. Nutritional aspects of metabolic inflammation in relation to health—insights from transcriptomic biomarkers in PBMC of fatty acids and polyphenols. Mol Nutr Food Res. 2014, 58, 1708–20.
354. Crujeiras AB, Parra D, Milagro FI, Goyenechea E, Larrarte E, Margareto J, et al. Differential Expression of Oxidative Stress and Inflammation Related Genes in Peripheral Blood Mononuclear Cells in Response to a Low-Calorie Diet: A Nutrigenomics Study. Omi A J Integr Biol. 2008, 12, 251–61.
355. Hofmann T, Klenow S, Borowicki A, Gill CIR, Pool-Zobel BL, Glei M. Gene expression profiles in human peripheral blood mononuclear cells as biomarkers for nutritional in vitro and in vivo investigations. Genes Nutr. 2010, 5, 309–19.
356. Rudkowska I, Raymond C, Ponton A, Jacques H, Lavigne C, Holub BJ, et al. Validation of the Use of Peripheral Blood Mononuclear Cells as Surrogate Model for Skeletal Muscle Tissue in Nutrigenomic Studies. Omi A J Integr Biol. 2011, 15, 1–7.
357. Islam MA, Hooiveld GJEJ, van den Berg JHJ, Boekschoten M V., van der Velpen V, Murk AJ, et al. Plasma bioavailability and changes in PBMC gene expression after treatment of ovariectomized rats with a commercial soy supplement. Toxicol Reports. 2015, 2, 308–21.
358. Islam MA, Hooiveld GJEJ, van den Berg JHJ, van der Velpen V, Murk AJ, Rietjens IMCM, et al. Soy supplementation: Impact on gene expression in different tissues of ovariectomized rats and evaluation of the rat model to predict (post)menopausal health effect. Toxicol Reports. 2018, 5, 1087–97.
359. van der Velpen V, Geelen A, Schouten EG, Hollman PC, Afman LA, van 't Veer P. Estrogen Receptor–Mediated Effects of Isoflavone Supplementation Were Not Observed in Whole-Genome Gene Expression Profiles of Peripheral Blood Mononuclear Cells in Postmenopausal, Equol-Producing Women. J Nutr. 2013, 143, 774–80.

360. Daswani B, Khatkhatay MI. 'Omics' Signatures in Peripheral Monocytes from Women with Low BMD Condition. J Osteoporos. 2018, 2018, 1–7.
361. Gao L, Li Y, Yang YJ, Zhang DY. The Effect of Moderate-Intensity Treadmill Exercise on Bone Mass and the Transcription of Peripheral Blood Mononuclear Cells in Ovariectomized Rats. Front Physiol. 2021, 12, 1–11.
362. Santoro N, Randolph JF. Reproductive Hormones and the Menopause Transition. Obstet Gynecol Clin North Am. 2011, 38, 455–66.
363. Thurston RC, Johnson BD, Shufelt CL, Braunstein GD, Berga SL, Stanczyk FZ, et al. Menopausal symptoms and cardiovascular disease mortality in the Women's Ischemia Syndrome Evaluation (WISE). Menopause. 2017, 24, 126–32.
364. Fenton A, Smart C, Goldschmidt L, Price V, Scott J. Fat mass, weight and body shape changes at menopause – causes and consequences: a narrative review. Climacteric. 2023, 26, 381–7.
365. Kapoor E, Collazo-Clavell ML, Faubion SS. Weight Gain in Women at Midlife: A Concise Review of the Pathophysiology and Strategies for Management. Mayo Clin Proc. 2017, 92, 1552–8.
366. Barrea L, Pugliese G, Laudisio D, Colao A, Savastano S, Muscogiuri G. Mediterranean diet as medical prescription in menopausal women with obesity: a practical guide for nutritionists. Crit Rev Food Sci Nutr. 2021, 61, 1201–11.
367. Taleb-Belkadi O, Chaib H, Zemour L, Fatah A, Chafi B, Mekki K. Lipid profile, inflammation, and oxidative status in peri- and postmenopausal women. Gynecol Endocrinol. 2016, 32, 982–5.
368. McLean AC, Valenzuela N, Fai S, Bennett SAL. Performing Vaginal Lavage, Crystal Violet Staining, and Vaginal Cytological Evaluation for Mouse Estrous Cycle Staging Identification. J Vis Exp. 2012, e4389.
369. Cora MC, Kooistra L, Travlos G. Vaginal Cytology of the Laboratory Rat and Mouse:Review and Criteria for the Staging of the Estrous Cycle Using Stained Vaginal Smears. Toxicol Pathol. 2015, 43, 776–93.
370. Koebele S V., Bimonte-Nelson HA. Modeling menopause: The utility of rodents in translational behavioral endocrinology research. Maturitas. 2016, 87, 5–17.
371. Yin F, Yao J, Sancheti H, Feng T, Melcangi RC, Morgan TE, et al. The perimenopausal aging transition in the female rat brain: Decline in bioenergetic systems and synaptic plasticity. Neurobiol Aging. 2015, 36, 2282–95.
372. Kermath BA, Gore AC. Neuroendocrine Control of the Transition to Reproductive Senescence: Lessons Learned from the Female Rodent Model. Neuroendocrinology. 2012, 96, 1–12.
373. Bacon ER, Mishra A, Wang Y, Desai MK, Yin F, Brinton RD. Neuroendocrine aging precedes perimenopause and is regulated by DNA methylation. Neurobiol Aging. 2019, 74, 213–24.
374. Kermath BA, Riha PD, Woller MJ, Wolfe A, Gore AC. Hypothalamic Molecular Changes Underlying Natural Reproductive Senescence in the Female Rat. Endocrinology. 2014, 155, 3597–609.
375. Levine ME, Lu AT, Chen BH, Hernandez DG, Singleton AB, Ferrucci L, et al. Menopause accelerates biological aging. Proc Natl Acad Sci U S A. 2016, 113, 9327–32.

376. Wise PM. Alterations in Proestrous LH, FSH, and Prolactin Surges in Middle-Aged Rats. Exp Biol Med. 1982, 169, 348–54.
377. Cooper RL, Michael Conn P, Walker RF. Characterization of the LH Surge in Middle-Aged Female Rats. Biol Reprod. 1980, 23, 611–5.
378. Shirai N, Houle C, Mirsky ML. Using histopathologic evidence to differentiate reproductive senescence from xenobiotic effects in middle-aged female sprague-dawley rats. Toxicol Pathol. 2015, 43, 1158–61.
379. Goldman JM, Murr AS, Cooper RL. The rodent estrous cycle: characterization of vaginal cytology and its utility in toxicological studies. Birth Defects Res Part B Dev Reprod Toxicol. 2007, 80, 84–97.
380. Vidal JD. The Impact of Age on the Female Reproductive System. Toxicol Pathol. 2017, 45, 206–15.
381. Ke C, Hou Y, Zhang H, Yang K, Wang J, Guo B, et al. Plasma Metabolic Profiles in Women are Menopause Dependent. Kim KH, editor. PLoS One. 2015, 10, e0141743.
382. Gross RW, Han X. Lipidomics at the Interface of Structure and Function in Systems Biology. Chem Biol. 2011, 18, 284–91.
383. Nogueira IAL, da Cruz ÉJSN, Fontenele AMM, Figueiredo Neto JA de. Alterations in postmenopausal plasmatic lipidome. PLoS One. 2018, 13, e0203027.
384. Finegold JA, Asaria P, Francis DP. Mortality from ischaemic heart disease by country, region, and age: Statistics from World Health Organisation and United Nations. Int J Cardiol. 2013, 168, 934–45.
385. The Emerging Risk Factors Collaboration. Diabetes mellitus, fasting blood glucose concentration, and risk of vascular disease: a collaborative meta-analysis of 102 prospective studies. Lancet. 2010, 375, 2215-2222.
386. Tabassum R, Widén E, Ripatti S. Effect of biological sex on human circulating lipidome: An overview of the literature. Atherosclerosis. 2023, 384, 117274.
387. Sophocleous A, Idris AI. Ovariectomy/orchiectomy in rodents. Methods in Molecular Biology. 2019, 1914, 261–7.
388. Brinton RD. Minireview: Translational animal models of human menopause: Challenges and emerging opportunities. Endocrinology. 2012, 153, 3571–8.
389. Yousefzadeh N, Kashfi K, Jeddi S, Ghasemi A. Ovariectomized rat model of osteoporosis: A practical guide. Vol. 19, EXCLI Journal. 2020, 19, 89–107.
390. Medina-Contreras J, Villalobos-Molina R, Zarain-Herzberg A, Balderas-Villalobos J. Ovariectomized rodents as a menopausal metabolic syndrome model. A minireview. Molecular and Cellular Biochemistry. 2020, 475, 261–76.
391. Jiang JMY, Sacco SM, Ward WE. Ovariectomy-Induced Hyperphagia Does Not Modulate Bone Mineral Density or Bone Strength in Rats. J Nutr. 2008, 138, 2106–10.
392. Chen W, Meng F, Zeng X, Cao X, Bu G, Du X, et al. Mechanic Insight into the Distinct and Common Roles of Ovariectomy Versus Adrenalectomy on Adipose Tissue Remodeling in Female Mice. Int J Mol Sci. 2023, 24, 2308.

393. Gavin KM, Kohrt WM, Klemm DJ, Melanson EL. Modulation of Energy Expenditure by Estrogens and Exercise in Women. Exerc Sport Sci Rev. 2018, 46, 232–9.
394. Day DS, Gozansky WS, Van Pelt RE, Schwartz RS, Kohrt WM. Sex Hormone Suppression Reduces Resting Energy Expenditure and β-Adrenergic Support of Resting Energy Expenditure. J Clin Endocrinol Metab. 2005, 90, 3312–7.
395. Witte MM, Resuehr D, Chandler AR, Mehle AK, Overton JM. Female mice and rats exhibit species-specific metabolic and behavioral responses to ovariectomy. Gen Comp Endocrinol. 2010, 166, 520–8.
396. Hepler C, Bass J. Circadian mechanisms in adipose tissue bioenergetics and plasticity. Genes Dev. 2023, 37, 454–73.
397. Gupta V, Mishra S, Mishra S, Kumar S, Gupta V. Association of Leptin: Adiponectin ratio and metabolic risk markers in postmenopausal women. Immunol Lett. 2018, 196, 63–7.
398. Finucane FM, Luan J, Wareham NJ, Sharp SJ, O'Rahilly S, Balkau B, et al. Correlation of the leptin:adiponectin ratio with measures of insulin resistance in non-diabetic individuals. Diabetologia. 2009, 52, 2345–9.
399. Shetty S, Kapoor N, Bondu J, Thomas N, Paul T. Bone turnover markers: Emerging tool in the management of osteoporosis. Indian Journal of Endocrinology and Metabolism. 2016, 20, 846–52.
400. Diz-Chaves Y, Kwiatkowska-Naqvi A, Von Hülst H, Pernía O, Carrero P, Garcia-Segura LM. Behavioral effects of estradiol therapy in ovariectomized rats depend on the age when the treatment is initiated. Exp Gerontol. 2012, 47, 93–9.
401. Caimari A, Oliver P, Palou A. Impairment of nutritional regulation of adipose triglyceride lipase expression with age. Int J Obes. 2008, 32, 1193–200.
402. Tanaka A, Node K. Associations of metabolic disorders with hypertension and cardiovascular disease: recent findings and therapeutic perspectives. Hypertens Res. 2024, May 29.
403. Dillard A, Matthan NR, Lichtenstein AH. Use of hamster as a model to study diet-induced atherosclerosis. Nutr Metab (Lond). 2010, 7, 89.
404. Zhang Z, Wang H, Jiao R, Peng C, Wong YM, Yeung VSY, et al. Choosing hamsters but not rats as a model for studying plasma cholesterol-lowering activity of functional foods. Mol Nutr Food Res. 2009, 53, 921–30.
405. Bravo E, Cantafora A, Calcabrinil A, Ortu G. Why prefer the golden Syrian hamster (Mesocricetus auratus) to the Wistar rat in experimental studies on plasma lipoprotein metabolism? Comp. Biochem. Physiol. 1994, 107, 347-355.
406. Horváthová M, Ilavská S, Štefíková K, Szabová M, Krivošíková Z, Jahnová E, et al. The Cell Surface Markers Expression in Postmenopausal Women and Relation to Obesity and Bone Status. Int J Environ Res Public Health. 2017, 14, 751.
407. Ghosh M, Rodriguez-Garcia M, Wira CR. The immune system in menopause: Pros and cons of hormone therapy. J Steroid Biochem Mol Biol. 2014, 142, 171–5.
408. Cutolo M, Capellino S, Sulli A, Serioli B, Secchi ME, Villaggio B, et al. Estrogens and Autoimmune Diseases. Ann N Y Acad Sci. 2006, 1089, 538–47.

409. Olsen NJ. Gonadal steroids and immunity. Endocr Rev. 1996, 17, 369–84.
410. Saborit-Villarroya I, Del Valle JM, Romero X, Esplugues E, Lauzurica P, Engel P, et al. The Adaptor Protein 3BP2 Binds Human CD244 and Links this Receptor to Vav Signaling, ERK Activation, and NK Cell Killing. J Immunol. 2005, 175, 4226–35.
411. Hyodo Y, Matsui K, Hayashi N, Tsutsui H, Kashiwamura S ichiro, Yamauchi H, et al. IL-18 Up-Regulates Perforin-Mediated NK Activity Without Increasing Perforin Messenger RNA Expression by Binding to Constitutively Expressed IL-18 Receptor. J Immunol. 1999, 162, 1662–8.
412. Okamura H, Kashiwamura S ichiro, Tsutsui H, Yoshimoto T, Nakanishi K. Regulation of interferon-γ production by IL-12 and IL-18. Curr Opin Immunol. 1998, 10, 259–64.
413. Yoshimoto T, Takeda K, Tanaka T, Ohkusu K, Kashiwamura S ichiro, Okamura H, et al. IL-12 Up-Regulates IL-18 Receptor Expression on T Cells, Th1 Cells, and B Cells: Synergism with IL-18 for IFN-γ Production. J Immunol. 1998, 161, 3400–7.
414. Nakanishi K, Yoshimoto T, Tsutsui H, Okamura H. Interleukin-18 is a unique cytokine that stimulates both Th1 and Th2 responses depending on its cytokine milieu. Cytokine Growth Factor Rev. 2001, 12, 53–72.
415. Hamilton KL, Lin L, Wang Y, Knowlton AA. Effect of ovariectomy on cardiac gene expression: inflammation and changes in SOCS gene expression. Physiol Genomics. 2008, 32, 254–63.
416. Wang R, Yu C, Tang Z, Sun J, Wang Y, Zhao Z, et al. Leptin induces altered differentiation of keratinocytes by inducing insulin resistance: implications for metabolic syndrome-induced resistance of psoriatic therapy. J Dermatolog Treat. 2024, 35, 2309305.
417. Emanuelli B, Peraldi P, Filloux C, Chavey C, Freidinger K, Hilton DJ, et al. SOCS-3 Inhibits Insulin Signaling and Is Up-regulated in Response to Tumor Necrosis Factor-α in the Adipose Tissue of Obese Mice. J Biol Chem. 2001, 276, 47944–9.
418. Dharmani M, Kamarulzaman K, Giribabu N, Choy KW, Zuhaida MZ, Aladdin NA, et al. Effect of Marantodes pumilum Blume (Kuntze) var.alata on β-cell function and insulin signaling in ovariectomised diabetic rats. Phytomedicine. 2019, 65, 153101.
419. Min W, Fang P, Huang G, Shi M, Zhang Z. The decline of whole-body glucose metabolism in ovariectomized rats. Exp Gerontol. 2018, 113, 106–12.
420. Sankar P, Zachariah B, Vickneshwaran V, Jacob SE, Sridhar MG. Amelioration of oxidative stress and insulin resistance by soy isoflavones (from Glycine max) in ovariectomized Wistar rats fed with high fat diet: The molecular mechanisms. Exp Gerontol. 2015, 63, 67–75.
421. Vermehren-Schmaedick A, Joshi S, Wagoner W, Norgard MA, Packwood W, Diba P, et al. Grb7 Ablation in Mice Improved Glycemic Control, Enhanced Insulin Signaling, and Increased Abdominal fat Mass in Females. Endocrinology. 2024, 165, 1–15.
422. Bao Z, Liu ZQ, He PY, Adali J, Yang YC, Wulasihan M. 17B-Estradiol Regulates

Adenosine Triphosphate-Binding Cassette Transporters a1 Expression Via Estrogen Receptor A To Increase Macrophage Cholesterol Efflux. J Physiol Pharmacol. 2023, 74, 527–36.

423. Darabi M, Rabbani M, Ani M, Zarean E, Panjehpour M, Movahedian A. Increased leukocyte ABCA1 gene expression in post-menopausal women on hormone replacement therapy. Gynecol Endocrinol. 2011, 27, 701–5.
424. Rodriguez-Agudo D, Malacrida L, Kakiyama G, Sparrer T, Fortes C, Maceyka M, et al. StarD5: an ER stress protein regulates plasma membrane and intracellular cholesterol homeostasis. J Lipid Res. 2019, 60, 1087–98.
425. Kakiyama G, Minoiwa K, Bai-Kamara N, Hashiguchi T, Pandak WM, Rodriguez-Agudo D. StarD5 levels of expression correlate with onset and progression of steatosis and liver fibrosis. Am J Physiol Liver Physiol. 2024, 326, G747–61.
426. Hendrix S, Zelcer N. A new SPRING in lipid metabolism. Curr Opin Lipidol. 2023, 34, 201–7.
427. Loregger A, Raaben M, Nieuwenhuis J, Tan JME, Jae LT, van den Hengel LG, et al. Haploid genetic screens identify SPRING/C12ORF49 as a determinant of SREBP signaling and cholesterol metabolism. Nat Commun. 2020, 11, 1128.
428. Aregger M, Lawson KA, Billmann M, Costanzo M, Tong AHY, Chan K, et al. Systematic mapping of genetic interactions for de novo fatty acid synthesis identifies C12orf49 as a regulator of lipid metabolism. Nat Metab. 2020, 2, 499–513.
429. Bayraktar EC, La K, Karpman K, Unlu G, Ozerdem C, Ritter DJ, et al. Metabolic coessentiality mapping identifies C12orf49 as a regulator of SREBP processing and cholesterol metabolism. Nat Metab. 2020, 2, 487–98.
430. Horton JD, Goldstein JL, Brown MS. SREBPs: activators of the complete program of cholesterol and fatty acid synthesis in the liver. J Clin Invest. 2002, 109, 1125–31.
431. Caimari A, Crescenti A, Puiggròs F, Boqué N, Arola L, del Bas JM. The intake of a high-fat diet and grape seed procyanidins induces gene expression changes in peripheral blood mononuclear cells of hamsters: capturing alterations in lipid and cholesterol metabolisms. Genes Nutr. 2015, 10, 438.
432. Semeghini MS, Scalize PH, Coelho MC, Fernandes RR, Pitol DL, Tavares MS, et al. Lycopene prevents bone loss in ovariectomized rats and increases the number of osteocytes and osteoblasts. J Anat. 2022, 241, 729–40.
433. Ren L, Zhu X, Tan J, Lv X, Wang J, Hua F. MiR-210 promotes bone formation in ovariectomized rats by regulating osteogenic/adipogenic differentiation of bone marrow mesenchymal stem cells through downregulation of EPHA2. J Orthop Surg Res. 2023, 18, 811.
434. Vargas-Sanchez PK, Fernandes RR, Furlaneto FAC, Sousa LG De, Siéssere S, Bombonato-Prado KF. Osteoporosis Affects Functional Activity and Gene Expression of Osteoblastic Cells Derived from Rat Alveolar Bone. Braz Dent J. 2020, 31, 617–22.
435. MacFarlane EG, Haupt J, Dietz HC, Shore EM. TGF-β Family Signaling in Connective Tissue and Skeletal Diseases. Cold Spring Harb Perspect Biol. 2017, 9, a022269.

436. Jann J, Gascon S, Roux S, Faucheux N. Influence of the TGF-β Superfamily on Osteoclasts/Osteoblasts Balance in Physiological and Pathological Bone Conditions. Int J Mol Sci. 2020, 21, 7597.
437. Alswat KA. Gender Disparities in Osteoporosis. J Clin Med Res. 2017, 9, 382–7.
438. Young MF, Bi Y, Ameye L, Chen XD. Biglycan knockout mice: New models for musculoskeletal diseases. Glycoconj J. 2002, 19, 257–62.
439. Zhou Y, Deng HW, Shen H. Circulating monocytes: an appropriate model for bone-related study. Osteoporos Int. 2015, 26, 2561–72.
440. Receno CN, Liang C, Korol DL, Atalay M, Heffernan KS, Brutsaert TD, et al. Effects of prolonged dietary curcumin exposure on skeletal muscle biochemical and functional responses of aged male rats. Int J Mol Sci. 2019, 20, 1178.
441. Björntorp P, Karlsson M, Pertoft H, Pettersson P, Sjöström L, Smith U. Isolation and characterization of cells from rat adipose tissue developing into adipocytes. J Lipid Res. 1978, 19, 316–24.
442. Bjorntorp P. Hormonal control of regional fat distribution. Hum Reprod. 1997, 12, 21–5.
443. Liu Y, Cheng F, Luo Y, Zhan Z, Hu P, Ren H, et al. PEGylated Curcumin Derivative Attenuates Hepatic Steatosis via CREB/PPAR-γ/CD36 Pathway. Biomed Res Int. 2017, 2017, 8234507.
444. Mun J, Kim S, Yoon HG, You Y, Kim OK, Choi KC, et al. Water extract of Curcuma longa l. Ameliorates non-alcoholic fatty liver disease. Nutrients. 2019, 11, 2536.
445. Um MY, Hwang KH, Ahn J, Ha TY. Curcumin Attenuates Diet-Induced Hepatic Steatosis by Activating AMP-Activated Protein Kinase. Basic Clin Pharmacol Toxicol. 2013, 113, 152–7.
446. López N, Sánchez J, Picó C, Palou A, Serra F. Dietary l-leucine supplementation of lactating rats results in a tendency to increase lean/fat ratio associated to lower orexigenic neuropeptide expression in hypothalamus. Peptides. 2010, 31, 1361–7.
447. Caimari A, del Bas JM, Boqué N, Crescenti A, Puiggròs F, Chenoll E, et al. Heat-killed Bifidobacterium animalis subsp. Lactis CECT 8145 increases lean mass and ameliorates metabolic syndrome in cafeteria-fed obese rats. J Funct Foods. 2017, 38, 251–63.
448. Gómez-Ambrosi J, Salvador J, Silva C, Pastor C, Rotellar F, Gil M, et al. Increased cardiovascular risk markers in obesity are associated with body adiposity: Role of leptin. Thromb Haemost. 2006, 95, 991–6.
449. Zhao S, Kusminski CM, Scherer PE. Adiponectin, Leptin and Cardiovascular Disorders. Circ Res. 2021, 128, 136–49.
450. Mariné-Casadó R, Domenech-Coca C, Crescenti A, Rodríguez Gómez MÁ, Del Bas JM, Arola L, et al. Maternal Supplementation with a Cocoa Extract during Lactation Deeply Modulates Dams' Metabolism, Increases Adiponectin Circulating Levels and Improves the Inflammatory Profile in Obese Rat Offspring. Nutrients. 2022, 14, 5134.
451. Ribeiro C, Dourado G, Cesar T. Orange juice allied to a reduced-calorie diet results in weight loss and ameliorates obesity-related biomarkers: A randomized controlled trial. Nutrition. 2017, 38, 13–9.

452. Sun X, Feng R, Li Y, Lin S, Zhang W, Li Y, et al. Histidine supplementation alleviates inflammation in the adipose tissue of high-fat diet-induced obese rats via the NF-κB- and PPARγ-involved pathways. Br J Nutr. 2014, 112, 477–85.
453. Baudin J, Hernandez-Baixauli J, Quesada-Vázquez S, Mulero F, Puiggròs F, Arola L, et al. Combined supplementation with hesperidin, phytosterols and curcumin decreases adiposity and improves metabolic health in ovariectomized rats. Food Funct. 2024, 15, 4905–24.
454. Mauvais-Jarvis F, Clegg DJ, Hevener AL. The role of estrogens in control of energy balance and glucose homeostasis. Endocrine Reviews. 2013, 34, 309–38.
455. Liang YQ, Akishita M, Kim S, Ako J, Hashimoto M, Iijima K, et al. Estrogen receptor ß is involved in the anorectic action of estrogen. Int J Obes. 2002, 26, 1103–9.
456. Rathor R, Srivastava S, Suryakumar G. A Comparative Biochemical Study Between L-Carnosine and β-Alanine in Amelioration of Hypobaric Hypoxia-Induced Skeletal Muscle Protein Loss. High Alt Med Biol. 2023, 24, 302–11.
457. Pae M, Romeo GR. The multifaceted role of profilin-1 in adipose tissue inflammation and glucose homeostasis. Adipocyte. 2014, 3, 69–74.
458. Khan T, Muise ES, Iyengar P, Wang Z V., Chandalia M, Abate N, et al. Metabolic Dysregulation and Adipose Tissue Fibrosis: Role of Collagen VI. Mol Cell Biol. 2009, 29, 1575–91.
459. Munoz A, Abate N, Chandalia M. Adipose Tissue Collagen and Inflammation in Nonobese Asian Indian Men. J Clin Endocrinol Metab. 2013, 98, E1360–3.
460. Chun TH. Peri-adipocyte ECM remodeling in obesity and adipose tissue fibrosis. Adipocyte. 2012, 1, 89–95.
461. Huang A, Lin Y, Kao L, Chiou Y, Lee G, Lin H, et al. Inflammation-induced macrophage lysyl oxidase in adipose stiffening and dysfunction in obesity. Clin Transl Med. 2021, 11, 2–8.
462. Soták M, Rajan MR, Clark M, Biörserud C, Wallenius V, Hagberg CE, et al. Healthy Subcutaneous and Omental Adipose Tissue Is Associated with High Expression of Extracellular Matrix Components. Int J Mol Sci. 2022, 23, 520.
463. Ren Y, Zhao H, Yin C, Lan X, Wu L, Du X, et al. Adipokines, Hepatokines and Myokines: Focus on Their Role and Molecular Mechanisms in Adipose Tissue Inflammation. Front Endocrinol (Lausanne). 2022, 13, 1–26.
464. Takahashi M, Nagaretani H, Funahashi T, Nishizawa H, Maeda N, Kishida K, et al. The Expression of SPARC in Adipose Tissue and Its Increased Plasma Concentration in Patients with Coronary Artery Disease. Obes Res. 2001, 9, 388–93.
465. Lee SH, Lee JA, Park HS, Song YS, Jang YJ, Kim JH, et al. Associations among SPARC mRNA expression in adipose tissue, serum SPARC concentration and metabolic parameters in Korean women. Obesity. 2013, 21, 2296–302.
466. Shin J, Toyoda S, Okuno Y, Hayashi R, Nishitani S, Onodera T, et al. HSP47 levels determine the degree of body adiposity. Nat Commun. 2023, 14, 7319.
467. Kim J, Lee SK, Shin J min, Jeoun U woo, Jang YJ, Park HS, et al. Enhanced

biglycan gene expression in the adipose tissues of obese women and its association with obesity-related genes and metabolic parameters. Sci Rep. 2016, 6, 30609.

468. Meissburger B, Stachorski L, Röder E, Rudofsky G, Wolfrum C. Tissue inhibitor of matrix metalloproteinase 1 (TIMP1) controls adipogenesis in obesity in mice and in humans. Diabetologia. 2011, 54, 1468–79.
469. Maquoi E, Munaut C, Colige A, Collen D, Lijnen HR. Modulation of Adipose Tissue Expression of Murine Matrix Metalloproteinases and Their Tissue Inhibitors With Obesity. Diabetes. 2002, 51, 1093–101.
470. Roger Lijnen H, Demeulemeester D, Van Hoef B, Collen D, Maquoi E. Deficiency of tissue inhibitor of matrix metalloproteinase-1 (TIMP-1) impairs nutritionally induced obesity in mice. Thromb Haemost. 2003, 89, 249–55.
471. Tiaden AN, Bahrenberg G, Mirsaidi A, Glanz S, Blüher M, Richards PJ. Novel Function of Serine Protease HTRA1 in Inhibiting Adipogenic Differentiation of Human Mesenchymal Stem Cells via MAP Kinase-Mediated MMP Upregulation. Stem Cells. 2016, 34, 1601–14.
472. Ballak DB, Stienstra R, Tack CJ, Dinarello CA, van Diepen JA. IL-1 family members in the pathogenesis and treatment of metabolic disease: Focus on adipose tissue inflammation and insulin resistance. Cytokine. 2015, 75, 280–90.
473. Blüher M, Klöting N, Wueest S, Schoenle EJ, Schön MR, Dietrich A, et al. Fas and FasL Expression in Human Adipose Tissue Is Related to Obesity, Insulin Resistance, and Type 2 Diabetes. J Clin Endocrinol Metab. 2014, 99, E36–44.
474. Rouault C, Pellegrinelli V, Schilch R, Cotillard A, Poitou C, Tordjman J, et al. Roles of chemokine ligand-2 (CXCL2) and neutrophils in influencing endothelial cell function and inflammation of human adipose tissue. Endocrinology. 2013, 154, 1069–79.
475. Hellmann J, Sansbury BE, Holden CR, Tang Y, Wong B, Wysoczynski M, et al. CCR7 Maintains Nonresolving Lymph Node and Adipose Inflammation in Obesity. Diabetes. 2016, 65, 2268–81.
476. Pan Y, Cao S, Tang J, Arroyo JP, Terker AS, Wang Y, et al. Cyclooxygenase-2 in adipose tissue macrophages limits adipose tissue dysfunction in obese mice. J Clin Invest. 2022, 132, e152391.
477. Wang L, Wang Y, Zhang C, Li J, Meng Y, Dou M, et al. Inhibiting Glycogen Synthase Kinase 3 Reverses Obesity-Induced White Adipose Tissue Inflammation by Regulating Apoptosis Inhibitor of Macrophage/CD5L-Mediated Macrophage Migration. Arterioscler Thromb Vasc Biol. 2018, 38, 2103–16.
478. Newling M, Sritharan L, van der Ham AJ, Hoepel W, Fiechter RH, de Boer L, et al. C-Reactive Protein Promotes Inflammation through FcγR-Induced Glycolytic Reprogramming of Human Macrophages. J Immunol. 2019, 203, 225–35.
479. Piacentini L, Chiesa M, Colombo GI. Gene Regulatory Network Analysis of Perivascular Adipose Tissue of Abdominal Aortic Aneurysm Identifies Master Regulators of Key Pathogenetic Pathways. Biomedicines. 2020, 8, 288.
480. Purvis GSD, Collino M, Aranda-Tavio H, Chiazza F, O'Riordan CE, Zeboudj L, et al. Inhibition of Bruton's TK regulates macrophage NF-κB and NLRP3 inflammasome activation in metabolic inflammation. Br J Pharmacol. 2020, 177, 4416–32.

481. Purvis GSD, Collino M, van Dam AD, Einaudi G, Ng Y, Shanmuganathan M, et al. OxPhos in adipose tissue macrophages regulated by BTK enhances their M2-like phenotype and confers a systemic immunometabolic benefit in obesity. Diabetes. 2024, Jan 8, db220275.

482. Morin SO, Poggi M, Alessi MC, Landrier JF, Nunès JA. Modulation of T Cell Activation in Obesity. Antioxid Redox Signal. 2017, 26, 489–500.

483. Schleinitz D, Klöting N, Lindgren CM, Breitfeld J, Dietrich A, Schön MR, et al. Fat depot-specific mRNA expression of novel loci associated with waist–hip ratio. Int J Obes. 2014, 38, 120–5.

484. Cariou B, Capitaine N, Le Marcis V, Vega N, Béréziat V, Kergoat M, et al. Increased adipose tissue expression of Grb14 in several models of insulin resistance. FASEB J. 2004, 18, 965–7.

485. Sun C, Förster F, Gutsmann B, Moulla Y, Stroh C, Dietrich A, et al. Metabolic Effects of the Waist-To-Hip Ratio Associated Locus GRB14/COBLL1 Are Related to GRB14 Expression in Adipose Tissue. Int J Mol Sci. 2022, 23, 8558.

486. Tian J, Dang HN, Yong J, Chui WS, Dizon MPG, Yaw CKY, et al. Oral Treatment with γ-Aminobutyric Acid Improves Glucose Tolerance and Insulin Sensitivity by Inhibiting Inflammation in High Fat Diet-Fed Mice. Zimmer J, editor. PLoS One. 2011, 6, e25338.

487. Heli Z, Hongyu C, Dapeng B, Yee Shin T, Yejun Z, Xi Z, et al. Recent advances of γ-aminobutyric acid: Physiological and immunity function, enrichment, and metabolic pathway. Front Nutr. 2022, 9, 1–16.

488. Charrier A, Xu X, Guan BJ, Ngo J, Wynshaw-Boris A, Hatzoglou M, et al. Adipocyte-specific deletion of zinc finger protein 407 results in lipodystrophy and insulin resistance in mice. Mol Cell Endocrinol. 2021, 521, 111109.

UNIVERSITAT ROVIRA I VIRGILI
NUTRITIONAL STRATEGIES BASED ON THE COMBINED SUPPLEMENTATION OF BIOACTIVE COMPOUNDS TO AMELIORATE OBESITY AND METABOLIC ALTERATIONS OCCURRING AT KEY STAGES OF FEMALE REPRODUCTIVE AGING
Julio Carlos Baudin Luque

VII. LIST OF PUBLICATIONS

Manuscripts included in the thesis:

Baudin J, Hernandez-Baixauli J, Quesada-Vázquez S, Mulero F, Puiggròs F, Arola L, Caimari A (2024). Combined supplementation with hesperidin, phytosterols and curcumin decreases adiposity and improves metabolic health in ovariectomized rats. Food and Function. 15:4905-4924.

Baudin J, Hernandez-Baixauli J, Romero-Giménez J, Yang H, Mulero F, Puiggròs F, Mardinoglu A, Arola L, Caimari A (2024). Combined histidine, carnosine, cysteine and serine consumption reduces adiposity and improves metabolic health and adipose tissue immunometabolic function in ovariectomized rats. Under revision, Biomedicine & Pharmacology.

Baudin J, Fernández-Arroyo S, Del Pino A, Puiggròs F, Arola L, Caimari A (2024). Impact of the Natural Female Reproductive Aging on the Rat Serum Lipidome. Manuscript in preparation.

Baudin J, Komar D, Yang H, Puiggròs F, Mardinoglu A, Arola L, Caimari A (2024). Peripheral blood mononuclear cells capture alterations in bone and inmunometabolic-related metabolisms in ovariectomized rats, a postmenopausal model with oestrogen deficiency. Manuscript in preparation.

Other manuscripts

Quesada-Vázquez S, Castells-Nobau A, Latorre J, Oliveras-Cañellas N, Puig-Parnau I, Tejera N, Tobajas Y, **Baudin J**, Hildebrand F, Beraza N, Burcelin R, Martinez-Gili L, Chilloux J, Dumas ME, Federici M, Hoyles L, Caimari A, Del Bas JM, Escoté X, Fernández-Real JM, Mayneris-Perxachs J (2023). Potential therapeutic implications of histidine catabolism by the gut microbiota in NAFLD patients with morbid obesity. Cell Rep Med, 4:101341.

Conference contributions

Baudin J, Hernandez-Baixauli J, Quesada-Vázquez S, Puiggròs F, Arola L, Caimari A (2022). Combined supplementation with hesperidin, phytosterols and curcumin improve body composition and decrease adiposity and LDL cholesterol in ovariectomized rats. Poster presentation at 18th NuGO week Congress, Tarragona, Spain.

Julio Baudin (2022). Bioactive ingredients for modulating metabolic alterations associated with menopause: studies with ovariectomized rats. Oral presentation at 23rd Metnet Meeting (IBUB), Barcelona Spain.

Patent presented

Pharmaceutical and nutraceutical compositions with a combination of amino acids and its use in diseases characterized by lipid accumulation in tissues. EU patent EP22382390.7. Reference: PCT/EP2023/060827.

VIII. ANNEX

(12) INTERNATIONAL APPLICATION PUBLISHED UNDER THE PATENT COOPERATION TREATY (PCT)

(19) World Intellectual Property Organization
International Bureau

(43) International Publication Date
02 November 2023 (02.11.2023)

WIPO | PCT

(10) International Publication Number
WO 2023/208944 A1

(51) International Patent Classification:
A23L 5/00 (2016.01) *A61P 1/16* (2006.01)
A61K 31/198 (2006.01) *A61P 3/04* (2006.01)
A61K 31/4172 (2006.01) *A61P 9/10* (2006.01)
A61K 38/00 (2006.01)

(21) International Application Number:
PCT/EP2023/060827

(22) International Filing Date:
25 April 2023 (25.04.2023)

(25) Filing Language: English

(26) Publication Language: English

(30) Priority Data:
22382390.7 25 April 2022 (25.04.2022) EP

(71) Applicants: **FUNDACIÓ EURECAT** [ES/ES]; Parc Tecnològic del Vallès, Av. Universitat Autònoma, núm. 23, 08290 CERDANYOLA DEL VALLÈS (ES). **FUNDACIÓ INSTITUT D'INVESTIGACIÓ BIOMÈDICA DE GIRONA DR. JOSEP TRUETA** [ES/ES]; C. Dr. Castany s/n, Edifici de la Mancomunitat 2 - Parc Hospitalari Martí i Julià, 17190 SALT (ES). **CONSORCIO CENTRO DE INVESTIGACIÓN BIOMÉDICA EN RED** [ES/ES]; C. Monforte de Lemos 3-5. Pabellón 11, 28029 MADRID (ES).

(72) Inventors: **DEL BAS PRIOR, Josep Maria**; C. Narcís Oller, 7. Esc A2, 3r 2a, 43007 TARRAGONA (ES). **ESCOTÉ MIRÓ, Xavier**; C. Europa, 22, 43440 L'ESPLUGA DE FRANCOLÍ (ES). **QUESADA VÁZQUEZ, Sergio**; C. Sant Antoni Maria Claret 25 esc. F 2 2, 43002 TARRAGONA (ES). **FERNÁNDEZ-REAL LEMOS, José Manuel**; Pujada Creu de Palau, 33, 17033 GIRONA (ES). **MAYNERIS PERXACHS, Jordi**; C. Pau Casals 6, 17833 FONTCOBERTA (VEÏNAT DE MELIANTA) (ES). **BAUDIN LUQUE, Julio Carlos**; Av. de la Universitat 1, 43204 REUS (ES). **CAIMARI PALOU, Antoni**; Av. de la Universitat 1, 43204 REUS (ES). **PUIGGRÒS LLAVINÉS, Francesc**; Av. de la Universitat 1, 43204 REUS (ES). **CASTELLS NOBAU, Ana**; Institut d'Investigació Biomèdica de Girona Dr. Josep Trueta (IDIBGI), Edifici M2 Parc Hospitalari Martí i Julià de Salt, C. Dr. Castany s/n, 17190 SALT (ES).

(74) Agent: **ZBM PATENTS - ZEA, BARLOCCI & MARKVARDSEN**; Rambla de Catalunya, 123, 08008 Barcelona (ES).

(81) Designated States *(unless otherwise indicated, for every kind of national protection available)*: AE, AG, AL, AM, AO, AT, AU, AZ, BA, BB, BG, BH, BN, BR, BW, BY, BZ, CA, CH, CL, CN, CO, CR, CU, CV, CZ, DE, DJ, DK, DM, DO, DZ, EC, EE, EG, ES, FI, GB, GD, GE, GH, GM, GT, HN, HR, HU, ID, IL, IN, IQ, IR, IS, IT, JM, JO, JP, KE, KG, KH, KN, KP, KR, KW, KZ, LA, LC, LK, LR, LS, LU, LY, MA, MD, MG, MK, MN, MU, MW, MX, MY, MZ, NA, NG, NI, NO, NZ, OM, PA, PE, PG, PH, PL, PT, QA, RO, RS, RU, RW, SA, SC, SD, SE, SG, SK, SL, ST, SV, SY, TH, TJ, TM, TN, TR, TT, TZ, UA, UG, US, UZ, VC, VN, WS, ZA, ZM, ZW.

(84) Designated States *(unless otherwise indicated, for every kind of regional protection available)*: ARIPO (BW, CV, GH, GM, KE, LR, LS, MW, MZ, NA, RW, SC, SD, SL, ST, SZ, TZ, UG, ZM, ZW), Eurasian (AM, AZ, BY, KG, KZ, RU, TJ, TM), European (AL, AT, BE, BG, CH, CY, CZ, DE, DK, EE, ES, FI, FR, GB, GR, HR, HU, IE, IS, IT, LT, LU, LV, MC, ME, MK, MT, NL, NO, PL, PT, RO, RS, SE, SI, SK, SM, TR), OAPI (BF, BJ, CF, CG, CI, CM, GA, GN, GQ, GW, KM, ML, MR, NE, SN, TD, TG).

Declarations under Rule 4.17:
— *as to applicant's entitlement to apply for and be granted a patent (Rule 4.17(ii))*

Published:
— *with international search report (Art. 21(3))*
— *with sequence listing part of description (Rule 5.2(a))*

(54) **Title:** PHARMACEUTICAL AND NUTRACEUTICAL COMPOSITIONS WITH A COMBINATION OF AMINO ACIDS AND ITS USE IN DISEASES CHARACTERIZED BY LIPID ACCUMULATION IN TISSUES

(57) **Abstract:** The invention discloses a pharmaceutical or dietary supplement composition comprising a particular combination of compounds including histidine, serine, cysteine and carnosine. The compositions are proposed as ingredients in food products, and they have been proved effective in the treatment of diseases characterized by accumulation of fat in tissues, such as in fatty liver disease, obesity, and atherosclerosis.

WO 2023/208944 A1

Pharmaceutical and nutraceutical compositions with a combination of amino acids and its use in diseases characterized by lipid accumulation in tissues

This application claims the benefit of European Patent Application 22382390.7 filed April 25th 2022.

Technical Field

Present invention relates to the field of dietetical supplements and pharmaceutical compositions to reduce the risk or to treat diseases related with fat tissue deposition. Thus, it relates to the field of nutrition and medicine.

Background Art

Due to the increased and worldwide extended consumption of a diet know as Western diet, including processed food and food rich in fat, diseases or disorders related with the deposition of fat tissue within several parts of the body, including viscera, blood vessels and subcutaneous tissue, are a trend involving not only high costs for the health system but also and most important health problems in the subjects. Examples of these disorders are the obesity with the associated visceral fat accumulation, atherosclerosis and the fatty liver diseases.

In short, obesity is a condition in which excess body fat has accumulated to such an extent that it may have a negative effect on health.

Atherosclerosis is a pattern of the disease arteriosclerosis in which the wall of the artery develops abnormalities, called lesions. These lesions may lead to narrowing due to the build-up of atheromatous plaque. When severe, it can result in coronary artery disease, stroke, peripheral artery disease, or kidney problems, depending on which arteries are affected.

Fatty liver diseases (FLD), also known generically as hepatic steatosis (HS), is a condition where excess fat builds up in the liver. Fatty liver disease is typified as non-alcoholic fatty liver disease (NAFLD) and alcoholic liver disease. Westernized changes in diet and lifestyle can lead to the progression of some key risk factors, such as obesity, leptin, or insulin resistance (IR), dyslipidaemia and metabolic syndrome, which are associated with the development of NAFLD. NAFLD is one of the human diseases with more prevalence nowadays affecting almost one-third of the world's population. This disease is characterized by an excessive accumulation of fat in the liver and a low-grade inflammation. This abnormal lipid metabolism could affect lipid oxidation disturbing redox homeostasis in more advanced stages. Thus, accumulation of reactive species of oxygen (ROS) and consequently the increase of lipid peroxidation could induce hepatic cellular damage and fibrosis. NAFLD is classified in different grades according to severity and capacity to recover its healthy state: Non-alcoholic fatty liver (NAFL) with a simple steatosis; non-alcoholic steatohepatitis (NASH) with an advanced steatosis and inflammation. Moreover, NASH could end up developing fibrosis in advanced stages

and finally progressing to irreversible stages like cirrhosis or hepatocarcinoma. Treatment of NAFLD is generally carried out by dietary changes and promotion of exercise to reduce body weight, unless a severe evolution makes compulsory a liver transplantation.

Cocktails of certain compounds have been tested in vivo as supplements in diet to boost the oxidation of fat and the synthesis of glutathione (GSH). GSH is required for preventing the accumulation of incomplete products of fatty acids oxidation. An example is the document of Mardinoglu et al., "Personal model-assisted identification of NAD+
and glutathione metabolism as intervention target in NAFLD", Mol Syst Biol-2017, vol. no. 13:916. These authors tested in mice, fed with Western diet, including high levels of fat and sucrose, a cocktail consisting of serine, NAC (N-acetyl-L-cysteine), and nicotinamide riboside (NR). Serine was included into the cocktail since it can be easily converted to glycine whereas NAC was included since cysteine may be the limiting metabolite after the repletion of the glycine in the synthesis of GSH. The aim of this assay was to provide a proof-of-concept of a possible therapeutic strategy based on promoting the synthesis of GSH and NAD+ and resulting from an analysis by personalized genome-scale metabolic modelling of a human cohort with several degrees of hepatic steatosis. The rationale behind was to reduce the oxidative stress in lipid metabolism. From the GEMs analysis of the human cohort, the authors also concluded that the plasma levels of serine and glycine negatively correlated with HS, and that no significant correlation was present between HS and the plasma levels of cysteine and glutamine.

Another document proposing the supplementation of diet for mitigating high fat diet induced hepatic steatosis is the one of Mong et al., "Histidine and carnosine alleviated hepatic steatosis in mice consumed high saturated fat diet", European Journal of Pharmacology 653 (2011) 82–88. The authors propose using histidine and the dipeptide carnosine to reduce hepatic steatosis after having observed that mice fed with these supplements lowered their body weight, the epididymal fat, and hepatic triglyceride and cholesterol levels, at the same time an improved insulin sensitivity and attenuated hyper-insulinemia was observed.

Among others, some of the roles attributed to histidine are those of being an anti-inflammatory and antioxidant, thus acting as a protective agent against liver. Firstly, this anti-inflammatory property of histidine supplementation has been related to a regulation of NF-kB and PPARα-induced pathways decreasing plasma concentrations of TNFα, IL6 and C-reactive protein and hepatic levels as well. Moreover, histidine has an anti-glycation action related to reduced inflammasome activation. In the other hand, the antioxidant characteristic of histidine treatment is due to that this amino acid is a free radical scavenger and it has the capacity to bind divalent metal ions.

Based on this later capacity as a free radical scavenger, some authors propose using a newly synthesized dimeric histidine (H-bihistidine) to treat non-alcoholic liver injury (NLI) and other free-radical-induced diseases (see. Zhao, Z.; Fu, C.; Zhang, Y.; Fu, A. Dimeric Histidine as a Novel Free Radical Scavenger Alleviates Non-Alcoholic Liver Injury. Antioxidants 2021, 10, 1529. https://doi.org/10.3390/antiox10101529). Although this is a

good approach, the complexity of using a synthetic compound is always a drawback.

There is, thus, still a need of alternative approaches to face all these diseases or disorders associated with fat deposition in tissues.

Summary of Invention

Inventors surprisingly found that a particular combination of three or more of histidine, cysteine, serine and carnosine were able to reduce liver injury and liver features of NAFLD, said injury seen macroscopically in terms of liver weight, whitish and fatty liver; and at biochemical level by the analysis of the levels of alanine aminotransferanse (ALT) and aspartate aminotransferase (AST). The combination of the compounds also decreased hepatic lipid content and liver steatosis. The supplementation of a diet with the combination of the compounds reduced hepatic inflammation associated to NAFLD, increased the antioxidant defence and antitumoral activity, and reduced resistance to insulin. In short, the combination of three or more of these compounds allowed reverting the NAFLD symptomatology in an animal model of the disease.

In addition, the inventors have found that the combination of compounds also allows to counteract the fat mass accretion associated to menopause in ovariectomized (OVX) rats and to decrease the loss of lean mass of OVX rats, contributing to a healthier profile of body composition. These compounds also ameliorate insulin resistance in this animal model. Thus, the authors have found that the combination of compounds contribute to revert metabolic changes associated to menopause in ovariectomized (OVX) rats.

Without being bound to any theory, the inventors propose that the combination of these compounds as ingredients in nutraceutical compositions, food supplements or as active ingredients in pharmaceutic compositions finally lead to an increase in the plasma histidine levels, which ultimately and due to a complexity of factors allow decreasing fat accumulation. This supposes a new approach in relation to the proposed used of histidine as radical scavenger or as anti-inflammatory in those disease involving fat accumulation, as previously disclosed. The approach is surprising since, moreover, histidine was only proposed as having a moderate effect on all these diseases, being the treatments in the prior art focused more on the promotion of the oxidation of fat and the synthesis of glutathione (GSH). Moreover, the proposed approach, resulting from the genuine observations made by the inventors, allow to safely face these disorders related with fat accumulation in several body tissue in subjects in which the control of the oxidative capacity of the fat is not jeopardized but that due to other mechanisms, that ultimately reduce histidine circulating levels, do also suffer from the clinical symptomatology.

This rationale could also be behind the reduction of visceral fat in obese subjects and in a reduction of LDL-cholesterol in a model of atherosclerosis.

Thus, a first aspect of the invention is a pharmaceutical or dietary supplement composition comprising, together with one or more pharmaceutically or nutraceutical acceptable excipients or carriers, a therapeutically or nutraceutical effective amount of at least three of histidine or a pharmaceutically or nutraceutical acceptable salt thereof or a solvate of any of both; cysteine or a pharmaceutically or nutraceutical acceptable salt thereof or a solvate of any of both, serine or a pharmaceutically or nutraceutical acceptable salt thereof or a solvate of any of both, and carnosine or a pharmaceutically or nutraceutical acceptable salt thereof or a solvate of any of both; and/or a therapeutically or nutraceutical effective amount of a peptide, said peptide comprising a sequence of amino acids including at least three of the histidine, cysteine, serine and carnosine, particularly, the pharmaceutical or dietary supplement composition comprises, together with one or more pharmaceutically or nutraceutical acceptable excipients or carriers:
(i) a therapeutically or nutraceutical effective amount of cysteine or a pharmaceutically or nutraceutical acceptable salt thereof or a solvate of any of both, and a therapeutically or nutraceutical effective amount of at least two of: histidine or a pharmaceutically or nutraceutical acceptable salt thereof or a solvate of any of both, serine or a pharmaceutically or nutraceutical acceptable salt thereof or a solvate of any of both, and carnosine or a pharmaceutically or nutraceutical acceptable salt thereof or a solvate of any of both; and/or a therapeutically or nutraceutical effective amount of a peptide, said peptide comprising a sequence of amino acids including cysteine and at least two of the histidine, serine and carnosine; or, alternatively,
(ii) a therapeutically or nutraceutical effective amount of N-acetylcysteine (NAC) or a pharmaceutically or nutraceutical acceptable salt thereof or a solvate of any of both, and a therapeutically or nutraceutical effective amount of at least two of: histidine or a pharmaceutically or nutraceutical acceptable salt thereof or a solvate of any of both, serine or a pharmaceutically or nutraceutical acceptable salt thereof or a solvate of any of both, and carnosine or a pharmaceutically or nutraceutical acceptable salt thereof or a solvate of any of both; and/or a therapeutically or nutraceutical effective amount of a peptide, said peptide comprising a sequence of amino acids including NAC and at least two of the histidine, serine and carnosine.

The pharmaceutical or dietary supplement composition can be used as ingredient in food products of common use, such as in beverages (i.e., sodas), dairy products (i.e., yogurts), bakery, etc., together with the common ingredients of these kind of foods. Thus, a second aspect of the invention is a food product in solid or liquid form comprising the pharmaceutical or dietary supplement composition as defined in the first aspect.

As will be illustrated in the examples, and as previously indicated, the composition or food comprising at least three of the listed compounds provided several beneficial effects in an animal model of NAFLD and in a menopause animal model Thus, another aspect of the invention is the composition as defined in the first aspect, or the food product of the second aspect, for use in therapy (i.e., as a medicament).

Brief Description of Drawings

FIG. 1 shows the effects of treatments on (A) liver weight, (B) a representative macroscopic appearance of livers; and the (C) serum ALT (alanine amino-transferase); and (D) serum AST (aspartate amino-transferase).

Claims

1.- A pharmaceutical or dietary supplement composition comprising, together with one or more pharmaceutically or nutraceutical acceptable excipients or carriers:

(i) a therapeutically or nutraceutical effective amount of cysteine or a pharmaceutically or nutraceutical acceptable salt thereof or a solvate of any of both, and a therapeutically or nutraceutical effective amount of at least two of: histidine or a pharmaceutically or nutraceutical acceptable salt thereof or a solvate of any of both, serine or a pharmaceutically or nutraceutical acceptable salt thereof or a solvate of any of both, and carnosine or a pharmaceutically or nutraceutical acceptable salt thereof or a solvate of any of both; and/or a therapeutically or nutraceutical effective amount of a peptide, said peptide comprising a sequence of amino acids including cysteine and at least two of histidine, serine and carnosine; or, alternatively,

(ii) a therapeutically or nutraceutical effective amount of N-acetylcysteine (NAC) or a pharmaceutically or nutraceutical acceptable salt thereof or a solvate of any of both, and a therapeutically or nutraceutical effective amount of at least two of: histidine or a pharmaceutically or nutraceutical acceptable salt thereof or a solvate of any of both, serine or a pharmaceutically or nutraceutical acceptable salt thereof or a solvate of any of both, and carnosine or a pharmaceutically or nutraceutical acceptable salt thereof or a solvate of any of both; and/or a therapeutically or nutraceutical effective amount of a peptide, said peptide comprising a sequence of amino acids including NAC and at least two of histidine, serine and carnosine.

2- The composition according to claim 1, comprising, together with one or more pharmaceutically or nutraceutical acceptable excipients or carriers:

(i) a therapeutically or nutraceutical effective amount of cysteine or a pharmaceutically or nutraceutical acceptable salt thereof or a solvate of any of both, a therapeutically or nutraceutical effective amount of histidine or a pharmaceutically or nutraceutical acceptable salt thereof or a solvate of any of both, a therapeutically or nutraceutical effective amount of serine or a pharmaceutically or nutraceutical acceptable salt thereof or a solvate of any of both and a therapeutically or nutraceutical effective amount carnosine or a pharmaceutically or nutraceutical acceptable salt thereof or a solvate of any of both; and/or a therapeutically or nutraceutical effective amount of a peptide, said peptide comprising a sequence of amino acids including cysteine, histidine, serine and carnosine; or, alternatively,

(ii) a therapeutically or nutraceutical effective amount of NAC or a pharmaceutically or nutraceutical acceptable salt thereof or a solvate of any of both, a therapeutically or nutraceutical effective amount of histidine or a pharmaceutically or nutraceutical acceptable salt thereof or a solvate of any of both, a therapeutically or nutraceutical effective amount of serine or a pharmaceutically or nutraceutical acceptable salt thereof or a solvate of any of both, and a therapeutically or nutraceutical effective amount carnosine or a pharmaceutically or nutraceutical acceptable salt thereof or a solvate of any of both; and/or a therapeutically or nutraceutical effective amount of a peptide, said peptide comprising a sequence of amino acids including NAC, histidine, serine and carnosine.

3- The composition according to claim 1, comprising, together with one or more pharmaceutically or nutraceutical acceptable excipients or carriers:

(i) a therapeutically or nutraceutical effective amount of cysteine or a pharmaceutically or nutraceutical acceptable salt thereof or a solvate of any of both, and a therapeutically or nutraceutical effective amount of at least two of: histidine or a pharmaceutically or nutraceutical acceptable salt thereof or a solvate of any of both;, serine or a pharmaceutically or nutraceutical acceptable salt thereof or a solvate of any of both, and carnosine or a pharmaceutically or nutraceutical acceptable salt thereof or a solvate of any of both; or, alternatively,

(ii) a therapeutically or nutraceutical effective amount of N-acetylcysteine (NAC) or a pharmaceutically or nutraceutical acceptable salt thereof or a solvate of any of both, and a therapeutically or nutraceutical effective amount of at least two of: histidine or a pharmaceutically or nutraceutical acceptable salt thereof or a solvate of any of both, serine or a pharmaceutically or nutraceutical acceptable salt thereof or a solvate of any of both, and carnosine or a pharmaceutically or nutraceutical acceptable salt thereof or a solvate of any of both.

4- The composition according to any of claims 1-3, comprising, together with one or more pharmaceutically or nutraceutical acceptable excipients or carriers:

(i) a therapeutically or nutraceutical effective amount of cysteine or a pharmaceutically or nutraceutical acceptable salt thereof or a solvate of any of both, a therapeutically or nutraceutical effective amount of histidine or a pharmaceutically or nutraceutical acceptable salt thereof or a solvate of any of both, a therapeutically or nutraceutical effective amount of serine or a pharmaceutically or nutraceutical acceptable salt thereof or a solvate of any of both, and a therapeutically or nutraceutical effective amount carnosine or a pharmaceutically or nutraceutical acceptable salt thereof or a solvate of any of both; or, alternatively,

(ii) a therapeutically or nutraceutical effective amount of NAC or a pharmaceutically or nutraceutical acceptable salt thereof or a solvate of any of both, a therapeutically or nutraceutical effective amount of histidine or a pharmaceutically or nutraceutical acceptable salt thereof or a solvate of any of both, a therapeutically or nutraceutical effective amount of serine or a pharmaceutically or nutraceutical acceptable salt thereof or a solvate of any of both, and a therapeutically or nutraceutical effective amount carnosine or a pharmaceutically or nutraceutical acceptable salt thereof or a solvate of any of both.

5- The composition according to any of claims 1 or 3, comprising, together with one or more pharmaceutically or nutraceutical acceptable excipients or carriers, a therapeutically or nutraceutical effective amount of N-acetylcysteine (NAC) or a pharmaceutically or nutraceutical acceptable salt thereof or a solvate of any of both, and a therapeutically or nutraceutical effective amount of at least two of: histidine or a pharmaceutically or nutraceutical acceptable salt thereof or a solvate of any of both, serine or a pharmaceutically or nutraceutical acceptable salt thereof or a solvate of any of both, and carnosine or a pharmaceutically or nutraceutical acceptable salt thereof or a solvate of any of both.

6- The composition according to any of claims 1-5, comprising, together with one or more pharmaceutically or nutraceutical acceptable excipients or carriers, a therapeutically or nutraceutical effective amount of NAC or a pharmaceutically or nutraceutical acceptable salt thereof or a solvate of any of both, a therapeutically or nutraceutical effective amount of histidine or a pharmaceutically or nutraceutical acceptable salt thereof or a

solvate of any of both, a therapeutically or nutraceutical effective amount of serine or a pharmaceutically or nutraceutical acceptable salt thereof or a solvate of any of both, and a therapeutically or nutraceutical effective amount carnosine or a pharmaceutically or nutraceutical acceptable salt thereof or a solvate of any of both.

7- The composition according to any one of claims 1-4, wherein the therapeutically effective amount of cysteine or a pharmaceutically or nutraceutical acceptable salt thereof or a solvate of any of both is that giving a dose from 2 to 550 mg per Kg of the subject; the therapeutically or nutraceutical effective amount of histidine or a pharmaceutically or nutraceutical acceptable salt thereof or a solvate of any of both is that giving a dose from 7.5 mg to 250 mg per Kg of the subject; the therapeutically effective amount of serine or a pharmaceutically or nutraceutical acceptable salt thereof or a solvate of any of both is that giving a dose from 1.3 to 250 mg per Kg of the subject; and the therapeutically effective amount of carnosine or a pharmaceutically or nutraceutical acceptable salt thereof or a solvate of any of both is that giving a dose from 4.5 to 200 mg per Kg of the subject.

8.- The composition according to claim 7, wherein the therapeutically effective amount of cysteine or a pharmaceutically or nutraceutical acceptable salt thereof or a solvate of any of both is that giving a dose from 30 to 550 mg per Kg of the subject; the therapeutically or nutraceutical effective amount of histidine or a pharmaceutically or nutraceutical acceptable salt thereof or a solvate of any of both is that giving a dose from 10 mg to 250 mg per Kg of the subject; the therapeutically effective amount of serine or a pharmaceutically or nutraceutical acceptable salt thereof or a solvate of any of both is that giving a dose from 10 to 250 mg per Kg of the subject; and the therapeutically effective amount of carnosine or a pharmaceutically or nutraceutical acceptable salt thereof or a solvate of any of both is that giving a dose from 10 to 200 mg per Kg of the subject.

9- The composition according to any one of claims 1-6, wherein the therapeutically effective amount of NAC or a pharmaceutically or nutraceutical acceptable salt thereof or a solvate of any of both is that giving a dose from 2 to 550 mg per Kg of the subject; the therapeutically or nutraceutical effective amount of histidine or a pharmaceutically or nutraceutical acceptable salt thereof or a solvate of any of both is that giving a dose from 7.5 mg to 250 mg per Kg of the subject; the therapeutically effective amount of serine or a pharmaceutically or nutraceutical acceptable salt thereof or a solvate of any of both is that giving a dose from 1.3 to 250 mg per Kg of the subject; and the therapeutically effective amount of carnosine or a pharmaceutically or nutraceutical acceptable salt thereof or a solvate of any of both is that giving a dose from 4.5 to 200 mg per Kg of the subject.

10.- The composition according to claim 9, wherein the therapeutically effective amount of NAC or a pharmaceutically or nutraceutical acceptable salt thereof or a solvate of any of both is that giving a dose from 30 to 550 mg per Kg of the subject; the therapeutically or nutraceutical effective amount of histidine or a pharmaceutically or nutraceutical acceptable salt thereof or a solvate of any of both is that giving a dose from 10 mg to 250 mg per Kg of the subject; the therapeutically effective amount of serine or a pharmaceutically or

nutraceutical acceptable salt thereof or a solvate of any of both is that giving a dose from 10 to 250 mg per Kg of the subject; and the therapeutically effective amount of carnosine or a pharmaceutically or nutraceutical acceptable salt thereof or a solvate of any of both is that giving a dose from 10 to 200 mg per Kg of the subject.

11.- The composition according to any one of claims 1-10, wherein the pharmaceutically or nutraceutical acceptable salt of histidine is the hydrochloride salt of L-histidine.

12.- The composition according to any one of claims 1-11, wherein the pharmaceutically acceptable salt of histidine is L-histidine monohydrochloride monohydrate.

13- The composition according to any one of claims 1-4, 7, 8, 11 or 12, wherein the pharmaceutically or nutraceutical acceptable salt of cysteine is the hydrochloride salt of L-cysteine.

14.- The composition according to any of claims 1-6 or 9-12, comprising:
- a therapeutically or nutraceutical effective amount of L-histidine monohydrochloride monohydrate;
- a therapeutically or nutraceutical effective amount of NAC;
- a therapeutically or nutraceutical effective amount of L-serine; and
- a therapeutically or nutraceutical effective amount of L-carnosine,
together with one or more pharmaceutically or nutraceutical acceptable excipients or carriers.

15- The composition according to any of claims 1-4 and 7, 8, 11-13, comprising:
- a therapeutically or nutraceutical effective amount of L-histidine monohydrochloride monohydrate;
- a therapeutically or nutraceutical effective amount of L-cysteine hydrochloride;
- a therapeutically or nutraceutical effective amount of L-serine; and
- a therapeutically or nutraceutical effective amount of L-carnosine,
together with one or more pharmaceutically or nutraceutical acceptable excipients or carriers.

16.- A food product in solid or liquid form comprising the pharmaceutical or dietary supplement composition as defined in any one of claims 1-15.

17.- The food product according to claim 16, which is a beverage.

18.- A pharmaceutical or dietary supplement composition as defined in any one of claims of claims 1-15, or a food product as defined in any of claims 16-17, for use in therapy.

19.- The pharmaceutical or dietary supplement composition or the food product for use according to claim 18, which is for use in the prevention and/or treatment of a disease selected from the group consisting of a fatty liver disease, obesity, overweight, atherosclerosis, dysbiosis, and combinations thereof.

20.- The pharmaceutical or dietary supplement composition or the food product for use according to any one of claims 18-19, which is for use in the prevention and/or treatment of a fatty liver disease selected from non-alcoholic fatty liver disease and alcoholic fatty liver disease.

21.- The pharmaceutical or dietary supplement composition or the food product for use according to claim 20, wherein the non-alcoholic fatty liver disease is selected from non-alcoholic fatty liver (NAFLD) with a simple steatosis and non-alcoholic steatohepatitis (NASH).

22. The pharmaceutical or dietary supplement composition or the food product for use according to claim 18, which is for use in the prevention and/or treatment of menopause-associated symptoms in a female mammal, particularly in a woman.

23. The pharmaceutical or dietary supplement composition or the food product for use according to claim 22, wherein the menopause-associated symptoms are metabolic changes associated to menopause, in a female mammal, particularly in a woman.

UNIVERSITAT ROVIRA I VIRGILI
NUTRITIONAL STRATEGIES BASED ON THE COMBINED SUPPLEMENTATION OF BIOACTIVE COMPOUNDS TO AMELIORATE OBESITY AND METABOLIC ALTERATIONS OCCURRING AT KEY STAGES OF FEMALE REPRODUCTIVE AGING
Julio Carlos Baudin Luque

UNIVERSITAT ROVIRA i VIRGILI

Menopausal transition, known as perimenopause, and later, the postmenopausal state are natural biological phases in a woman's life associated with reproductive aging. These processes are characterized by senescence in the ovarian function accompanied by a decline in oestrogen production, which already occurs in perimenopause with the appearance of irregular menstrual cycles and is exacerbated during the postmenopausal state. This reproductive aging process is often accompanied by various vasomotor symptoms, such as sleep disturbances, night sweats, and hot flashes, and can be associated with an increased risk of osteoporosis and with the appearance of obesity and other cardiovascular risk factors. In this PhD thesis, we hypothesized that two multi-ingredients acting against complementary targets, one containing the natural bioactive compounds curcumin, hesperidin, and phytosterols, and the other composed of the amino acid-related compounds histidine, serine, cysteine, and carnosine can exert beneficial effects against obesity and related cardiometabolic disturbances associated with menopause. We firstly characterized the menopausal transition using ovarian-intact middle-aged rats and analyzed circulating signatures across perimenopause, identifying potential lipidomic-based biomarkers in serum during the menopausal transition. Secondly, we used ovariectomized rats, a postmenopausal model with oestrogen deficiency, and we reported, using a transcriptomics approach, that peripheral blood mononuclear cells reflected the molecular changes associated with oestrogen deficiency in the postmenopausal stage concerning alterations in immune function, stress response, bone metabolism, cholesterol metabolism, and glucose homeostasis. Finally, we revealed that the oral supplementation with the two above commented multi-ingredients ameliorated obesity and related metabolic alterations in ovariectomized rats, being these effects of a similar magnitude to those produced by the administration of oestradiol, a pharmacological treatment that simulates hormone replacement therapy that is sometimes prescribed to women during the post-menopausal state. Our findings can pave the way for using these multi-ingredient-based formulations as alternative therapies to manage menopausal-related disturbances.

eurecat
Centre Tecnològic de Catalunya